SPECIATION DE L'URANIUM(VI), MODELISATION, INCERTITUDE ET IMPLICATION POUR LES MODELES DE BIODISPONIBILITE. APPLICATION A L'ACCUMULATION DANS LES BRANCHIES CHEZ UN BIVALVE D'EAU DOUCE

Francis Denison

UNIVERSITE DE PROVENCE
AIX MARSEILLE 1

Thèse

Présentée **à l'Université d'Aix-Marseille 1**
Pour l'obtention du titre de
Docteur de l'Université de Provence
Mention Sciences

Ecole Doctorale: Sciences De L'environnement

Spécialité : **Biosciences de l'Environnement, Chimie, et Santé.**

URANIUM(VI) SPECIATION: MODELLING, UNCERTAINTY AND RELEVANCE TO BIOAVAILABILITY MODELS.

APPLICATION TO URANIUM UPTAKE BY THE GILLS OF A FRESHWATER BIVALVE

Par

DENISON Francis

Soutenu le 22 juillet devant le jury d'examen composé de :

Mme. GARNIER-LAPLACE, J., H.D.R., IRSN Cadarache, Directrice de Thèse.
Mme. ADAM, C., IRSN Cadarache, Encadrant IRSN.
Mme. MASSIANI, C., Professeur, Université d'Aix-Marseille I.
M. SMITH, J., Centre for Ecology and Hydrology, U.K., Encadrant CEH.
M. VAN DER LEE, J., Professeur, Ecole des Mines de Paris.
M. BLUST, R., Professeur, Université d'Anvers, Belgique.

CONTENTS

LIST OF FIGURES

LIST OF TABLES

ACKNOWLEDGEMENTS

It is a pleasure to thank the many individuals whose participation and support as friends, teachers, and colleagues have made this thesis possible.

First and foremost, Jacqueline Garnier-Laplace has fulfilled many roles, as a supervisor her great insight and sense of perspective has been invaluable in bringing this work to fruition. Always supportive of my approach to research, her enthusiasm, encouragement and willingness to take the risk of allowing me to pursue paths that at times deviated greatly from the original subject, has been invaluable during the development of this work. On the personal side, her friendship and support during some extremely difficult times and the hospitality I received from her, her husband Dominique, and her two daughters Marine and Sophie were priceless. The best mentor I could have wished for, it would be difficult to overstate my gratitude to Jackie.

I thank all those involved in choosing both the research subject and myself, giving me the opportunity to work within a stimulating research group and live in a beautiful region. Mr. Gariel, head of SERLAB, has been supportive throughout my three years working within his group. My thesis supervisors, Jacqueline Garnier-Laplace, Christelle Adam and Jim Smith have all made themselves available for advice and support.

The experimental program was performed with the competent help of Brigitte Ksas, Virginie Camilleri and Gaëla Grasset. The large number of samples were analysed by Marcel Morello and Danielle Poncet-Bonnard who were always pleased to answer my questions, work to short deadlines and most importantly gave me great confidence in their results.

Within the laboratory I was surrounded by knowledgeable and friendly people who helped me daily. It was a great pleasure to work with Claude Fortin, Rodolphe Gilbin, Arnaud Martin-Garin and Laureline Février who provided stimulating discussions, encouragement, inspiration and positive criticism. Many others contributed by providing a stimulating and fun environment in which to work.

I offer both my thanks and apologies to the biologists who have worked with me, notably Damien Tran and Olivier Simon. I fully appreciate that my sometimes

unorthodox approach to ecotoxicology could have been distressing to a physiologist, however they responded with both good humour and sound advice, even after I tried intubating a bivalve.

I would like to thank Jan van der Lee, firstly for providing me with a great piece of software but most importantly for his speedy responses to my questions.

My forays into programming were helped immensely by the availability of GNU free software, particularly Bloodshed Dev-C++ and the GNU Scientific Library.

Thanks also to Claudine Van Crasbeck for her efficiency in protecting me from administration and her great efforts to make me feel very welcome.

Most importantly I want to thank all my friends who were there when I needed them. The past three years have had both high and low points. Although the difficult times were not pleasant, it was a joy to discover how many people were there to pick up the pieces. Alex, Arnaud, Astrid, Dave, Elodie, Graham, Hélène, Jackie, Laetitia, Rodolphe, Toby I thank you all. This thesis is dedicated to them.

1 ABBREVIATIONS, SYMBOLS AND UNITS

BLM	Biotic Ligand Model
DIC	Dissolved Inorganic Carbon
EDTA	EthylenDiamineTetraAcetate
FIAM	Free-Ion Activity Model
GNU	GNU's NOT UNIX
GPL	General Public Licence
GSIM	Gill Surface Interaction Model
GSL	GNU Scientific Library
MC	Monte Carlo
NEA	Nuclear Energy Authority
NTA	NitriloTriAcetate
OECD	Organisation for Economic Co-operation and Development
QMC	Quasi-Monte Carlo

Symbols, terminology and units used	
Pressure	p/ Pa
Volume	V/ dm^{-3}
Mass	m/ kg
Temperature	T/ K
Gas constant (molar)	R/ J K^{-1} mol^{-1}
Gibbs free energy (molar)	G_m/ J mol^{-1}
Enthalpy (molar)	H_m/ J mol^{-1}
Entropy (molar)	S_m/ J mol^{-1} K^{-1}
Heat capacity at constant pressure (molar)	$C_{p,m}$
Chemical potential of substance i	μ_i/ J mol^{-1}
Partial pressure of substance i	p_i
Fugacity of substance i	f_i
Activity of substance i	α_i
Activity coefficient of substance i	γ_i/ mol^{-1} kg
Molal concentration of substance i (amount of i dissolved divided by the mass of solvent)	m_i/ mol kg^{-1}
Molar concentration of substance i (amount of i dissolved divided by the volume of solvent)	c_i, [i]
Equilibrium constant of a reaction	$K_r°$
Stoichiometric coefficient of substance i	ν_I
Charge number of ion i (positive for cations, negative for anions)	z_i
Ionic strength: $I_m = 0.5\Sigma_i m_i z_i^2$ or $I_c = 0.5\Sigma_i c_i z_i^2$	I_c / mol dm^{-3}
Superscript for standard state*	°
Formation of a compound from its constituent elements	Δ_f
General chemical reaction	Δ_r
Pure liquid substance phase designator	(l)
Undissociated, uncharged aqueous species phase designator, e.g. CO_2(aq)	(aq)
Crystalline solid phase designator	(c)
Amorphous solid phase designator	(am)

Symbols, terminology and units used	
Solid phase designator	(s)
Gas phase designator	(g)
Negative logarithm of hydrogen ion activity	pH

*Standard state: the definition of IUPAC (Laffitte 1982) was adopted. The standard state refers to the standard pressure, $p^\circ = 10^5$ Pa and the reference temperature of 298.15 K.

- The standard state for a gaseous substance is the pure substance in a (hypothetical) state in which it exhibits ideal gas behaviour.
- The standard state for a pure liquid is the pure liquid.
- The standard state for a pure solid is the pure solid.
- The standard state for a solute i in a solution is the hypothetical solution in which $m_i = m^\circ = 1$ mol kg^{-1}, and in which the activity coefficient γ_i is unity.

2 ABSTRACT

The effects of varying solution composition on the interactions between uranium(VI) and excised gills of the freshwater bivalve *Corbicula fluminea* have been investigated in well defined solution media. A significant reduction in the uptake of uranium was observed on increasing the concentrations of the uranium complexing ligands citrate and carbonate. Saturation kinetics as a function of uranium concentration at a pH value of 5.0 were observed, indicating that the uptake of uranium is a facilitated process, probably involving one or several trans-membrane transport systems. A relatively small change in the uptake of uranium was found as a function of pH (factor of *ca.* 2), despite the extremely large changes to the solution speciation of uranium within the range of pH investigated (5.0 – 7.5).

A comprehensive review of the thermodynamic data relevant to the solution composition domain employed for this study was performed. Estimates of the uncertainties for the formation constants of aqueous uranium(VI) species were integrated into a thermodynamic database. A computer program was written to predict the equilibrium distribution of uranium(VI) in simple aqueous systems, using thermodynamic parameter mean-values. The program was extended to perform Monte Carlo and Quasi Monte Carlo uncertainty analyses, incorporating the thermodynamic database uncertainty estimates, to quantitatively predict the uncertainties inherent in predicting the solution speciation of uranium.

The use of thermodynamic equilibrium modelling as a tool for interpreting the bioavailability of uranium(VI) was investigated. Observed uranium(VI) uptake behaviour was interpreted as a function of the predicted changes to the solution speciation of uranium. Different steady-state or pre-equilibrium approaches to modelling uranium uptake were tested. Alternative modelling approaches were also tested, considering the potential changes to membrane transport system activity or sorption characteristics on varying solution composition. Finally the effect of uncertainty on the use of thermodynamic equilibrium modelling for interpretation of uranium(VI) bioavailability was assessed.

3 INTRODUCTION

3.1 Uranium: A Freshwater Contaminant

Uranium is a widely distributed naturally occurring element usually present in trace quantities, the average crustal abundance being 2 – 3 mg kg^{-1} (Ragnarsdottir and Charlet 2000). The concentrations found in natural waters are characterised by an extremely large range, from a few ng L^{-1} to over 2 mg L^{-1}, usually reflecting the concentration of uranium in the surrounding rocks (WHO. 2001). The aqueous transport of uranium is dominated by redox conditions, it being sparingly soluble under reducing conditions where the U(IV) species is formed but considerably more soluble under oxic conditions where U(VI) is present as the dioxo cation UO_2^{2+} and various aqueous complexes. In oxic conditions the chemistry of uranium is governed by the hexavalent dioxo cation UO_2^{2+}. In aqueous solution U(VI) forms a large number of inorganic complexes, including monomeric and oligomeric hydrolysis species, carbonato and phosphato species. The distribution of uranium among these species depends upon the solution pH, ligand concentrations and total uranium concentration. Uranium also readily forms organic complexes both with low molecular weight organic ligands and humic and fulvic substances e.g. (Denecke, Reich et al. 1998; Lenhart, Cabaniss et al. 2000; Montavon, Mansel et al. 2000; Crançon and van der Lee 2003). Under reducing conditions uranium is largely immobilised, the solubility being several orders of magnitude smaller than under oxidising conditions. There are many uranium solid phases, the most significant of which contain uranium in the U(IV) state; the principle primary ore minerals are uraninite and pitchblende, both UO_2. Secondary minerals include schoepite ($UO_3 \cdot 2H_2O$) and various phosphate and silicate minerals. Uranium has an atomic number of 92. All isotopes of uranium are radioactive, of which three are naturally occurring: ^{234}U (0.0054 %), ^{235}U (0.711 %) and ^{238}U (99.2836 %) with a specific activity (in equilibrium with daughter nuclides) of $2.6 \cdot 10^4$ Bq kg^{-1}.

Various anthropogenic activities can considerably enhance levels of uranium in the environment, particularly in surface waters, the main industrial sources being related to the nuclear fuel cycle, mainly uranium-mining waste or phosphor-gypsum and oil-scale/sludge. A recent additional source of contamination is from the use of depleted

uranium munitions, for example in the region of 10 tonnes of depleted uranium was used during the 1999 Kosovo conflict (UNEP 2000).

Uranium has a double toxicity, both chemical and radiological. For animals, uranium is mainly present as the most stable form in the biological fluids, i.e. the uranyl ion which has a high affinity for carboxylate and phosphate functional groups, and as is the case for many heavy metals it exerts an oxidative stress at the cellular level. The ability of uranium to be accumulated by aquatic organisms has been demonstrated for a number of wildlife groups, for example see (Ribera, Labrot et al. 1996; Colle, Garnier-Laplace et al. 2001). Precipitation with phosphate to form phosphate granules in certain target organelles such as lysosomes has been observed in both crustaceans and molluscs (Chassard-Bouchaud 1983). The radiological aspect of uranium's toxicity arises from the production of both α and β particles from its radioactive decay, and also the further decay of its daughter nuclides, including thorium, radon, radium and lead. Because of its low specific activity, natural uranium in freshwater is very often considered to be a significant chemical hazard, e.g. see (Cooley, Evans et al. 2000; Khune, Caldwell et al. 2002), although radiological effects cannot be ruled out (Miller, Stewart et al. 2002).

3.2 Biological Model: *Corbicula fluminea*

Bivalves are frequently employed as bioindicator organisms, they are generally sedentary, robust and hence easily maintained under laboratory conditions, of a size and lifespan amenable to experimentation. Most significantly however, their feeding strategy and means of respiration ensures a high throughput of the environmental medium, and allows the concurrent uptake of the contaminant from a range of the available physico-chemical forms. *Corbicula fluminea* was selected as the biological model for this study, it is a benthic species, which places it at the sediment-water interface exposed to three potential contamination sources, namely the dissolved and suspended sediment fractions and also the surfacial sediment. It is an invasive species that is now both ubiquitous and abundant throughout the majority of European freshwaters. This species has been already used for biomonitoring purposes within aquatic ecosystems, to assess early changes in the water/sediment quality by measuring the exposure and/or the induced biological effects, such as the accumulation of the contaminants within the soft bodies (Andres, Baudrimont et al.

1999; Gunther, Davis et al. 1999; Baudrimont, Andres et al. 1999.), biochemical perturbations (Cossu, Doyotte et al. 1997; Doyotte, Cossu et al. 1997) or behavioral changes (Sloff, De Zwart et al. 1983; Kramer, Jenner et al. 1989; Sluyts, Van Hoof et al. 1996).

3.3 Biomonitoring In Ecotoxicology

3.3.1 Concepts

In order to manage aquatic ecosystems it is vital to know the biological status of the system, especially when evaluating the impact of a chemical stressor on the biota. Organisms respond to the totality of their usually complex and dynamic environment, and it is insufficient to define that environment by measuring selected physical and chemical parameters, both for reasons of the impracticability (or impossibility) of sufficiently characterising the system and also due to the limited knowledge of the interaction of toxicants (antagonistic or synergistic effects) and the effect of other stress factors (temperature, water velocity, dissolved oxygen concentration, etc.). Equally it is insufficient to consider the biological status in isolation from a comprehensive physical and chemical characterisation of the system, if a greater understanding of the controlling parameters is to be achieved, and hence the development of a predictive ability that can be applied to different ecosystems. Biomonitoring consists of using live organisms as detectors of changes in the quality of their environment, by measuring one or several effects on the organisms, such as the accumulation of the contaminant/contaminants, behavioural changes or biochemical perturbations. These two complementary approaches lead to a greater understanding of the mechanisms controlling the bioavailability of a contaminant within the natural environment, and hence an improved ability to predict the probable effects to the biota in diverse ecosystems.

3.3.2 Bioaccumulation

There are a number of factors that influence the transfer of contaminants from the environmental medium to the biota, which may be classed in two general categories: the medium specific characteristics such as the physico-chemical conditions and the nature of the contamination and also biological factors such as the behaviour and

physiology of the organisms. These factors are interrelated and must be considered together. Parameters such as the temperature, pH, major ions concentrations, concentration and composition of suspended material and water velocity can exert both a direct effect on the biota, such as behavioural or physiological changes (water processing, filtration and metabolic rates) and also the form of the contaminant (physico-chemical speciation). Both of these effects will impact on the rate and extent of contaminant transfer to the organisms. At the level of an individual organism the important factors that need to be considered are the behaviour, the physiological state of the individual, and the interactions of the contaminant with the biological membrane that controls the transfer of the contaminant to the organism.

For the biological model selected for this study, behavioural effects play a significant role in regulating the transfer rate of the contaminant. Bivalves respire and obtain food in the form of suspended particulate material, by ventilation of water. The water enters via the inhalant siphon, is passed through the branchial filaments that retain suspended particles, and exits via the exhalent siphon. As the ventilation rate required to satisfy the respiratory demand in oxic conditions is small compared to the optimal ventilation rate for feeding (Tran, Boudou et al. 2002), these organisms have the ability to greatly modify their ventilation rate in response to stress factors, effectively isolating themselves from the external environment. This defensive behavioural response has an obvious effect on the transfer rate of the contaminant (Tran 2001). The interactions of the contaminant with the biological membrane are influenced both by the physiological state of the individual, and abiotic factors which both determine the chemical speciation of the contaminant and compete with it for membrane binding sites. Biotic factors are also important at the community level when the processes of bioaccumulation and trophic transfer are considered, where such factors as feeding strategy and assimilation efficiencies of food are important.

The total concentration of a contaminant is generally not a good indicator of its bioavailability; this is especially true for uranium that has a very extensive and complex solution chemistry. The speciation of uranium, i.e. its distribution among various possible species is usefully described by its physical speciation, i.e. the distribution between dissolved, colloidal and particulate species, and its chemical solution speciation.

3.3.3 The biological interface

All living cells are delimited from their environment by a selectively permeable plasma membrane (Simkiss and Taylor 1995). A bimolecular layer of amphipathic lipids, typically 4 to 10 nm thick, forms this membrane with the lipid hydrophobic chains forming the centre of the sheet and the hydrophilic ends oriented outwards to the two surfaces. A variety of embedded proteins occur as important components in these membranes, contributing in the range 1:4 to 4:1 by weight. These proteins perform a number of different roles, including membrane transport and structure. Some of the proteins are relatively loosely associated with the membrane, bound only to the surface (extrinsic or peripheral), while others are very strongly bound and can only be extracted by disruption of the membrane bilayer (intrinsic or integral proteins). The association of membrane proteins with the lipid bilayer is generally governed by hydrophobic interactions. Membrane proteins are generally responsible for the selective ionic permeability of the membrane. Membranes are asymmetric in that the compositions of the two faces differ according to the functions of each surface. Membrane phospholipids contain ionisable groups at the hydrophilic ends, which dissociate to create a net negative charge at the membrane surface. This charge is especially important on the cytoplasmic face of the membrane, generating a trans-membrane potential difference. The negative surface potential of both faces of the membrane results in a near surface ionic environment different to that of the bulk solution, due to the tendency for charge neutralisation. The concentrations of ions in the near surface environment are related to, but different from, their concentrations in the bulk solution, cations having a higher and anions a lower concentration than in the bulk solution. Intrinsic proteins that traverse the lipid bilayer can provide water filled channels through which ions can permeate. Different channel proteins are selective for different ions, some being cation selective and others anion selective. Ion selectivity is performed with respect to both charge and size, solutes generally passing through the channels in their hydrated forms. Channels often have wide, charged mouths that facilitate the entry of ions and specific constrictions that selectively filter the ions that may pass. The permeability of an ion channel is inversely related to its selectivity, i.e. channels of high ionic flux rates are relatively poorly selective and vice versa. Ion channels may be either continuously open, or transiently in response to either a change in membrane potential or a specific cell-surface ligand receptor. These

regulated channels are termed “gated”. Ions may enter a cell by specific or non-specific channels, by permeation by active processes either generally (e.g. membrane electrochemical potential) or specifically (e.g. ATPases).

3.4 Behavioural Factors

The behaviour and physiological state of the organisms during exposure to contaminants is critical in determining the uptake kinetics of the bioavailable forms of the contaminant. Preliminary experiments were performed to assess the importance of the behavioural response of *Corbicula fluminea* to both changes in the physico-chemical conditions in their environment, and exposure to uranium. The behavioural response to varying solution composition was investigated by a valvometry technique. The impedance between two platinum microelectrodes attached to each valve was measured in real-time, allowing the valve gape of each individual to be assessed. This parameter is not directly related to the ventilation rate of the individual, which is most likely to be the factor controlling the uptake capacity of the individual. However it is sufficient to estimate the inter-individual behavioural variability and behavioural differences between different experimental conditions. Experiments were performed after acclimatising individuals to the experimental conditions. The effect of changing pH (with no uranium contamination) was investigated at two pH values of 5.5 and 6.5. A very significant difference in mean duration of valve opening time was found (a factor of approximately two was observed). The effect of uranium contamination on duration of valve opening was also investigated and an important response to increasing uranium concentration was observed (Fournier, Tran et al. 2004). These behavioural modifications in response to the environmental conditions suggest that interpretation of uptake data merely in terms of changes in the solution speciation is a gross oversimplification of the processes involved in the accumulation of a contaminant. Further, the inter-individual variability in duration of valve opening was assessed in non-contaminated systems and found to be extremely high for short-duration monitoring periods. These observations highlight the difficulty of performing short-duration experiments with organisms that have the capability of modifying their behaviour to protect themselves against unfavourable conditions.

3.5 Research Objectives And Adopted Methodology

The two main objectives of this study were to investigate the effects of solution speciation on the chemical bioavailability of uranium(VI) and assess whether a chemical equilibrium based approach is appropriate for modelling the bioavailability of uranium. The importance of behavioural factors in the uptake of contaminants by bivalves has been discussed above. This significantly limits the interpretation of contaminant uptake by bivalves in terms of the physical and chemical processes involved. Indeed, initial experiments performed to assess the uptake kinetics of uranium by *C. fluminea* in well defined conditions, resulted in extreme inter-individual variability due principally to the behavioural responses of the organisms to the exposure conditions. In light of these findings, an *in-vitro* approach was adopted in order to study the physico-chemical processes involved in the uptake of uranium at the level of the biological interface. The gills of bivalve molluscs are known to be critical organs for the uptake and accumulation of metals from the medium (Pentreath 1973; Vercauteren and Blust 1996). The use of excised gill tissues to study exchange processes has previously been adopted as a viable experimental approach for both fish (Pärt and Svanberg 1981; Playle 1998; Taylor, Baker et al. 2002) and bivalves (Winkle 1972; Swinehart, Giannini et al. 1998; Mubiana and Blust 2000). This approach enabled the effects of solution composition on uranium – gill interactions to be studied in well defined and regulated conditions.

3.6 Overview Of Thesis Content

This document firstly considers the modelling of equilibrium chemical speciation (section 4), an overview of the general thermodynamic principles and computational methods is provided. More specifically for this study, the thermodynamic data requirements for modelling the aqueous speciation of uranium(VI) within the solution composition domain space used for the subsequent experiments is discussed, and a critical review of the available thermodynamic data was performed to produce a database integrating uncertainty estimates. Computational methods for calculating the probabilistic uncertainty associated with the predictive modelling of chemical speciation are described and details of the computer program written to perform the modelling are provided.

The different modelling approaches to describe the dependence of a metal's bioavailability on the exposure medium composition is then presented (section 5). The section starts with an overview of the historical development of the modelling framework leading to current methodologies for both uranium bioavailability and more generally metal bioavailability. The assumptions implicit in currently adopted modelling approaches are questioned, and a number of alternative hypotheses are developed.

Section 6 provides details of the experiments performed to measure the uptake of uranium from well-defined and simple exposure media by excised gills of the freshwater bivalve *Corbicula fluminea*. The decisions made regarding the experimental design, the experimental methodologies and the results are presented.

Section 7 describes all of the modelling performed in the study. The section starts with "classical" mean-value speciation modelling relevant to the solution composition domain space used for the uptake experiments and results of probabilistic uncertainty calculations for the same modelling scenarios. The experimental results are then interpreted within the different modelling frameworks described in section 5, as a function of the predicted speciation of uranium using both mean-value and probabilistic approaches to the speciation modelling.

Finally, the principal conclusions of the study, the lessons learnt and the overall research perspectives are discussed in section 8.

4 CHEMICAL SPECIATION MODELLING

4.1 Principles Of Chemical Speciation And Equilibrium Solution Chemistry

Speciation is a general term describing the forms and relative abundances of the different chemical entities that can exist in a system. In environmental chemistry the term covers both the physical speciation, i.e. the distribution through the dissolved, colloidal and particulate forms, as well as the chemical speciation, i.e. the distinct chemical solution species and surface complexes comprising the possible redox states and their complexes with both inorganic and organic ligands.

All chemical reactions are driven by the tendency of the participating atoms, molecules or ions to lower the energetic configuration of their outer shell electrons, i.e. to increase their stability. Two general reaction types that achieve such a reduction in energy can be defined: redox reactions that result in a change of the oxidation states of the participating species and reactions that result in a change in the coordination of the participating species. Coordination changes may be accomplished by either changing the interacting species or by a change in the coordination numbers of the participants. Acid/base reactions, precipitation and complex formation may all be regarded as coordinative reactions.

Many molecules and ions have a tendency to accept or donate an electron pair to form a bond with another species; substances that tend to donate an electron pair are termed Lewis bases which typically have one or more atoms with a lone electron pair and are also referred to as ligands, e.g. H_2O:, $Cl:^-$; substances that accept an electron pair are termed Lewis acids, typically cations or electron deficient molecules. The products of Lewis acid/base pairs are referred to as either complex ions, where the Lewis acid is a cation, or adducts when the Lewis acid is a molecule. The relative affinity between a Lewis acid and base is characteristic for each complex/adduct and can be measured in terms of the change in the standard molar free energy of reaction for the equilibrium between the reacting Lewis acid and base and the product complex/adduct.

Speciation is key to controlling the behaviour of many environmental and biological processes, as it determines the actual concentrations of individual species that may be

more or less reactive with, for example, a surface or a biological transporter site. The total concentration of an element is frequently of lesser significance than the parameters that control its speciation, for example the pH or concentrations of significant ligands. Speciation studies, both analytical and modelling approaches, are central to modern geochemistry and have been successfully applied to a wide range of systems to elucidate the processes underpinning water quality and transport phenomena. The same techniques are being increasingly applied to ecotoxicology to improve the understanding of the processes of bioavailability and toxicity. For metallic elements, consideration of the properties of both the metal and the environmental system is critical to determine the biological reactivity of the metal (Campbell 1995). The interactions at the level of the biological membranes in contact with the environmental medium are directly related to the solution speciation of the metal, frequently the activity of the metal free-ion (Campbell 1995). With a few exceptions, it is generally not possible to directly measure the activities of individual solution species, particularly at the low concentrations of environmental interest, and so the most frequently adopted approach is to employ predictive geochemical speciation models to estimate the distribution of the total metal concentration through its various possible species. Equilibrium solution speciation has been extensively studied, and a robust comprehensive theoretical framework based on thermodynamic principles has been developed.

4.2 Thermodynamic Principles

The application of equilibrium thermodynamics enables the state of a particular system to be calculated if complete chemical equilibrium were to be attained. In natural systems this state is rarely achieved, especially where processes involving the biota are significant. However, the thermodynamic approach is instructive as it is often a reasonable approximation to the actual state, and additionally it predicts the direction in which the system will move towards in the absence of energy input to the system. The equilibrium state is defined as the state of minimum energy of the system, a system not at equilibrium will move towards the equilibrium state by the release of energy. The appropriate measure of the energy of a system is the Gibbs free energy, $G/$ J mol^{-1}, a state variable that provides the criteria for whether any change to the system is favourable. The Gibbs free energy is defined as:

$$G = H - \mathrm{T}S \tag{4-1}$$

where H/ J mol^{-1} is the enthalpy, T/ K is the temperature and S/ J mol^{-1} K^{-1} the entropy. For isothermal and isobaric processes, the change in the Gibbs free energy for the process is:

$$\Delta G = \Delta H - \mathrm{T}\Delta S \tag{4-2}$$

The value of ΔG indicates whether the process is spontaneous or not, negative values of ΔG indicate that the process is spontaneous, positive values that the reverse process is spontaneous and a value of zero indicates that the system is at equilibrium.

A term closely related to the free energy of a system is the chemical potential, μ. Chemical potential is defined as:

$$\mu_i = \left(\frac{\partial G}{\partial n_i} \right)_{T,P,n_j,\ldots} \tag{4-3}$$

The chemical potential of component i is the partial derivative of G with respect to the number of moles of i, n_i, at constant temperature, pressure and amounts of other components n_j,…. i.e. the chemical potential is the partial molar Gibbs free energy, or the change in the free energy of the system on addition of an amount of component i per mole. For a one-component system the chemical potential is simply the molar Gibbs free energy.

To apply the above equations to real (non-ideal) systems, it is necessary to introduce terms to correct for the non-ideal behaviour of real systems. The variables activity, α, and fugacity, f, are used to describe the "effective" concentration and pressure respectively. Activity is defined by the equation:

$$\mu_i = \mu_i^0 + R\mathrm{T}\ln\alpha_i \tag{4-4}$$

where μ°_i is the reference chemical potential referring to an arbitrary chosen reference state, and R is the gas constant (8.31451 J K^{-1} mol^{-1}). In an ideal system the activity of a component is numerically identical to its concentration, in non-ideal systems they are related by the equation:

$$\alpha_i = \gamma_i m_i \tag{4-5}$$

where m_i is the concentration of component i and γ_i is the activity coefficient. For solutes in aqueous solutions, the activity approaches the molal concentration as the concentration approaches zero, i.e. $\gamma_i \rightarrow 1$ as $\Sigma\, m_i \rightarrow 0$.

In a closed system, for practical purposes, the principle of mass conservation can be applied, i.e. in the absence of exchange of matter with the environment the mass of a system remains constant. This fundamental principle underpins chemical modelling. For the modelling of equilibrium chemistry mass conservation is expressed by stoichiometric equations describing the possible reactions in the system, e.g. for the formation of the uranyl hydroxide complex:

$$UO_2^{2+} + OH^- \rightleftharpoons UO_2OH^+ \tag{4-6}$$

These equations merely denote the relevant reactions but do not provide any information about the affinity of the reactions, or the extent of reaction at thermodynamic equilibrium. The affinity of each reaction can be defined in terms of the equations for chemical potential and the Gibbs free energy. For the generalised reaction:

$$aA + bB \rightleftharpoons cC + dD \tag{4-7}$$

the molar Gibbs free energy of reaction, $\Delta_r G$, is given by:

$$\Delta_r G = G_{products} - G_{reactants} \tag{4-8}$$

Which in terms of the chemical potentials of the components may be written:

$$\Delta_r G = c\mu_C + d\mu_D - a\mu_A - b\mu_B \tag{4-9}$$

Substituting $\mu_i = \mu_i^\circ + RT \ln \alpha_i$ gives:

$$\Delta_r G = c\mu^\circ_C + cRT\ln\alpha_C + d\mu^\circ_D + dRT\ln\alpha_D \tag{4-10}$$

$$- a\mu^\circ_A - aRT\ln\alpha_A - b\mu^\circ_B - bRT\ln\alpha_B$$

which on rearranging leads to:

$$\Delta_r G = c\mu_C^0 + d\mu_D^0 - a\mu_A^0 - b\mu_B^0 + R \cdot T \ln\left(\frac{\alpha_C^c \alpha_D^d}{\alpha_A^a \alpha_B^b}\right) \tag{4-11}$$

or the equivalent expression:

$$\Delta_r G = \Delta_r G_m^0 + R \cdot T \ln\left(\frac{\alpha_C^c \alpha_D^d}{\alpha_A^a \alpha_B^b}\right) \tag{4-12}$$

where $\Delta_r G°_m$ is the standard molar free energy of reaction. At equilibrium the Gibbs free energy of reaction, $\Delta_r G = 0$, hence:

$$-\Delta_r G_m^0 = R \cdot T \ln\left(\frac{\alpha_C^c \alpha_D^d}{\alpha_A^a \alpha_B^b}\right) \tag{4-13}$$

or

$$\left(\frac{\alpha_C^c \alpha_D^d}{\alpha_A^a \alpha_B^b}\right) = \exp\left(\frac{-\Delta_r G_m^0}{R \cdot T}\right) = K_r^0 \tag{4-14}$$

where $K°_r$ is the dimensionless equilibrium constant of the reaction. Equilibrium constants are the most common parameters used for expressing the thermodynamic properties of a system. The equilibrium constant of a reaction, $K°_r$, is related to the molar Gibbs energy of the reaction, $\Delta_r G_m°$, by the relation:

$$\log_{10} K_r^o = -\frac{\Delta_r G_m^o \cdot \log_{10}(e)}{R \cdot T} \tag{4-15}$$

The chemical reaction, *r*, involving reactants and products, B, may be described by the equation:

$$\sum_{B=1}^{n} \nu_{r,B} B = 0 \tag{4-16}$$

where $\nu_{r,B}$ is the stoichiometric coefficient of substance B for reaction *r* (positive for products and negative for reactants). Hence the equilibrium constant may be calculated directly from the individual values of $\Delta_f G_m°$(B) by the relation:

$$\log_{10} K_r^o = -\frac{\log_{10}(e)}{R \cdot T} \sum_{B=1}^{n} \nu_{r,B} \Delta_f G_m^o(B) \tag{4-17}$$

4.2.1 Temperature dependencies of thermodynamic data

Usually thermodynamic data is given at a single reference temperature (often 298.15 K, 25.0 °C), however the thermodynamic quantities of enthalpy, entropy, heat capacity and hence the Gibbs free energy are dependant on the temperature of the

system. To apply the thermodynamic data to a system at a temperature other than the reference temperature, the chemical equilibrium data need to be recalculated using appropriate thermodynamic relationships. Ideally, temperature dependence functions for the values of $\Delta_r H_m°$ and $\Delta_r S_m°$ as well as their values at the reference temperature should be used to calculate the value of $\Delta_r G_m°$ at the required temperature. These data are rarely available in complete form so it is necessary to use an approximation method appropriate to the amount of information available. The most commonly used approximations are based on so-called second-law methods; these approximations are generally sufficiently accurate over small temperature ranges. The temperature dependence function of the Gibbs energy of reaction in terms of the enthalpy and heat capacity can be derived from the defining equation of the Gibbs free energy of a reaction at constant temperature:

$$\Delta_r G_m^0 = \Delta_r H_m^0 - T\Delta_r S_m^0 \tag{4-18}$$

and the temperature derivatives of the enthalpy and entropy:

$$\left(\frac{\partial \Delta_r H_m^0}{\partial T}\right)_P = \Delta_r C_{P,m}^0 \;;\; \left(\frac{\partial \Delta_r S_m^0}{\partial T}\right)_P = \frac{\Delta_r C_{P,m}^0}{T} \tag{4-19}$$

where $C°_{P,m}$ is the standard molar heat capacity at constant pressure, which, on integration yield:

$$\Delta_r H_m^0(T) = \Delta_r H_m^0(T_0) + \int_{T_0}^{T} \Delta_r C_{P,m}^0 dT \;;\; \Delta_r S_m^0(T) = \Delta_r S_m^0(T_0) + \int_{T_0}^{T} \frac{\Delta_r C_{P,m}^0}{T} dT \tag{4-20}$$

substitution leads to:

$$\Delta_r G_m^0(T) = \Delta_r H_m^0(T_0) + \int_{T_0}^{T} \Delta_r C_{P,m}^0 dT - T\left(\Delta_r S_m^0(T_0) + \int_{T_0}^{T} \frac{\Delta_r C_{P,m}^0}{T} dT\right) \tag{4-21}$$

or expressed in terms of the equilibrium constant:

$$\log_{10} K_r^0(T) = \log_{10} K_r^0(T_0) - \frac{\log(e)\Delta_r H_m^0(T_0)}{R}\left(\frac{1}{T} - \frac{1}{T_0}\right) - \frac{\log(e)}{RT}\int_{T_0}^{T} C_{P,m}^0 dT + \frac{\log(e)}{R}\int_{T_0}^{T} \frac{C_{P,m}^0}{T} dT \tag{4-22}$$

This equation can be used to calculate the value of the equilibrium constant as a function of the temperature if:

- the value of the equilibrium constant is known at the reference temperature ;
- the value of the standard molar enthalpy of reaction is known at the reference temperature ;
- the temperature dependence of the change in the molar heat capacity of reaction, over the temperature interval required is known.

It is rare that all of this information is available for the reaction and so an appropriate approximation must be used. For reactions for which values of the equilibrium constant (or Gibbs free energy of reaction), the enthalpy of reaction and the molar heat capacity at the reference temperature are available, but the temperature dependence of the heat capacity is not known, the heat capacity may be assumed to be constant over the temperature range required. In this case equation (4-22) reduces to:

$$\log_{10} K_r^0(T) = \log_{10} K_r^0(T_0) - \frac{\log(e)\Delta_r H_m^0(T_0)}{R}\left(\frac{1}{T} - \frac{1}{T_0}\right) \qquad (4\text{-}23)$$

$$- \frac{\log(e)\Delta_r C_{p,m}^0}{R}\left((T_0/T) - 1 + \ln(T/T_0)\right)$$

Use of equation (4-23) is appropriate for most reactions in the temperature range of 273 to 473 K. For reactions for which only the values of the equilibrium constant (or Gibbs free energy of reaction) and the enthalpy of reaction at the reference temperature are available, the enthalpy of reaction may be assumed to be constant. In this case equation (4-22) reduces to:

$$\log_{10} K_r^0(T) = \log_{10} K_r^0(T_0) - \frac{\log(e)\Delta_r H_m^0(T_0)}{R}\left(\frac{1}{T} - \frac{1}{T_0}\right) \qquad (4\text{-}24)$$

This expression, the integrated van't Hoff equation, is the most commonly applied temperature dependence relationship for geochemically relevant equilibrium databases. For small temperature ranges (± 10 K) the approximation is generally well within the uncertainty limits of experimentally determined values. If only the value of the equilibrium constant (or Gibbs free energy of reaction) of the reaction is available, there are various estimation methods for heat capacity and entropy (and hence enthalpy) values available, which are discussed in detail by Allard *et al* (Allard, Banwart et al. 1997).

4.2.2 Correction for non-ideal behaviour

As discussed above thermodynamic data always refer to a selected standard state, by convention for aqueous solutes the standard state is a hypothetical solution in which the molality of the solute is 1 mol kg^{-1} and the activity coefficient is 1 mol^{-1} kg. In ionic solutions the interactions between ions (electrostatic and Van der Waals interactions, osmotic effects and also effects from the relative permittivity of the medium) are significant except in very dilute solutions, and so the activity of an ion is not identical to its concentration. This effect may be accounted for by one of several solution models. The most commonly applied solution models are based on the Debye-Hückel theory of ionic solutions, combined with a description of the medium-specific properties of the system by introducing ion-association reactions between the medium ions and the species involved in equilibrium reactions. The Debye-Hückel theory is based on the premise that Coulombic interactions are the dominant factor in the non-ideality of solutions. Due to the long range and strength of Coulombic interactions the distribution of ions in solution is not uniform, overall the solution is electrically neutral, however averaged over time, near any ion there is an excess of counter ions. This phenomenon results in an ionic atmosphere around each ion, where due to the excess of oppositely charged ions in the sphere surrounding the central ion the energy and hence the chemical potential of the central ion is reduced. The Debye-Hückel limiting law adequately describes the mean ion activity-concentration relationship at very low concentrations:

$$\log \gamma_{\pm} = -\left|z_{+} z_{-}\right| A\sqrt{I} \tag{4-25}$$

where $\gamma_{\pm}$ is the mean ion activity coefficient, z_i is the charge of the ion, A is a parameter dependent on the temperature and the relative permittivity of the solvent and I is the ionic strength of the solution:

$$I = \frac{1}{2}\sum m_i z_i^2 \tag{4-26}$$

Although single-ion activity coefficients are not rigorously defined thermodynamically (it is not experimentally possible to vary the concentration of a single ion without also varying the concentration of some counter-ion), they are convenient to use for dilute solutions, equation (4-25) then becomes:

$$\log \gamma_i = -z_i^2 A\sqrt{I} \tag{4-27}$$

At ionic strengths greater than about 10^{-3} mol dm^{-3} the limiting law fails, due to it not accounting for the finite size of the ions. The equation may be modified to account for this factor leading to the extended Debye-Hückel equation:

$$\log \gamma_i = \frac{-Az_i^2\sqrt{I}}{1+Ba_i\sqrt{I}} \tag{4-28}$$

where B is a parameter dependent on the temperature related to the distance of closest approach of the ions and a_i is the effective diameter of the hydrated ion. This equation extends the validity range of the limiting law to higher ionic strengths; it is reasonably accurate to *ca*. 10^{-1}. A number of modifications to the extended Debye-Hückel equation are commonly used, such as the Güntelberg equation where the product Ba_i is merely set to a value of 1, or an additional term may be introduced such as for the Davies equation:

$$\log \gamma_i = -A \cdot z_i^2\left(\frac{\sqrt{I}}{1+\sqrt{I}} - bI\right) \tag{4-29}$$

where the constant b is fixed at a value between 0.2 and 0.3 for all systems, this is probably the most frequently used equation to describe the activity-concentration relationship and is generally a good approximation to an ionic strength of about 0.3 mol dm^{-3}, although this depends on the exact electrolyte. To improve the approximation at ionic strengths higher than 0.3 mol dm^{-3}, a truncated form of the equation was proposed by Colston and et al (Colston, Chandratillake et al. 1990), where $I = 0.3 \;\forall\; I > 0.3$.

Another modification of the extended Debye-Hückel equation is the "B-dot" equation, which also uses an additional correction term, however in this case it is temperature dependent:

$$\log \gamma_i = \frac{-Az^2\sqrt{I}}{1+Ba_i\sqrt{I}} + \dot{B}I \tag{4-30}$$

This equation provides accurate activity coefficient values to ionic strengths of up to about 1 molal. At higher ionic strengths the specific short-range interactions between

ions become significant, and more precise methods such as the Pitzer or S.I.T. equations (Pitzer 1973) need to be employed.

4.3 Computation Of Aqueous Speciation

Applying the thermodynamic principles outlined above to manually calculate the distribution of species in a solution is impractical for all but the simplest systems, especially so for geochemical systems where the interactions of solution species with solid and gas phases also need to be considered. In response to this a number of specialised computer programs have been developed, all of which are based on the same principles but each with its own specificities, the most commonly used models include MINEQL (Westall, Zachary et al. 1986), PHREEQC (Parkhurst and Appelo 1999) and JCHESS (Van der Lee 1998). Any of these programs are adequate for computing the aqueous speciation of a metal in the simple solution compositions employed for this work, provided that a suitable database is used. However, in order to perform both uncertainty analyses (described in section 4.5) and biological availability model parameter fitting (described in section 5) a new program was written in order to fulfil these additional requirements. To apply mathematical solvers to the problem the system needs to be described in a systematic manner. The basic framework that is used is described in full by Morel (Morel and Herring 1993) and relies on the principle of describing all possible species in the system in terms of the minimum number of basis species (also called master species or principle components). The requirements for choosing the composition of the basis set are quite simple: each element contained in the system must be represented by a member of the basis set; every chemical species must be a reaction product of the basis set; no member of the basis set can be obtained through reactions of the other members of the basis set. There is no unique basis set for a system and so a choice has to be made from the various possibilities.

In principle every set will give the same distribution of species at thermodynamic equilibrium, however, there are a number of factors that must be considered when choosing the basis species. It is desirable that the concentration of the chosen basis species is significant relative to the total concentration of that element for a number of reasons including computational efficiency, to avoid rounding errors and to avoid instability of the numerical method employed and possible convergence problems. For

example, in a solution of pH 1 choosing the species PO_4^{3-} as the phosphate basis species would be inappropriate as its fractional concentration is only *ca.* $2 \cdot 10^{-19}$ of the total phosphate concentration. Obviously it is not feasible to change the basis set for each particular solution (and the required recalculation of the thermodynamic database in terms of the new basis set) and so experience needs to be applied to develop the basis set to be suitable for the majority of conditions to which the database will be applied. For example for geochemical systems of pH 5 – 9 using the above example either HPO_4^{2-} or $H_2PO_4^-$ could be used as the basis species for phosphate.

Using the basis set enables all mass balance relationships to be defined in terms of the chemical elements and the stoichiometric coefficients of the species. Charge balance relationships can also be defined in terms of the charges of the species. All species within the dataset can be related to one or more of the basis species by the associated equilibrium equation and constant, enabling the complete speciation of the system to be calculated in function of the concentrations of the basis species. However, the implementation of such a pure basis set requires the modelled system be in complete equilibrium which is often not the case in reality, for example solutions that are under or over saturated with respect to mineral phases or redox couples in a state of disequilibria. An auxiliary set of basis species is therefore required, which consist primarily of different oxidation states of the strict basis species. These species may be treated as either a basis or secondary species, depending on the modelling scenario.

In some cases it is necessary to impose a basis species, for example if equilibrium with a mineral or gas phase determines the total aqueous concentration of an element, or if the total concentration of an element possessing multiple oxidation states is defined by a single state and redox equilibrium is disallowed. Algorithms have been devised that permit the swapping of basis species for dependent secondary species for these cases.

4.3.1 Equations for speciation modelling

For a system of N_p basis species with concentrations m_i containing N_s derived species (S_j), the concentration of each species may be calculated from the mass-action equation:

$$\left[S_j\right] = K^0_{r,j} \prod_{i=1}^{N_p} \left(\gamma_i m_i\right)^{\nu_{j,i}} \tag{4-31}$$

and the total concentrations are calculated from:

$$\left[m_i\right]_{TOT} = \sum_{j=1}^{N_s} \nu_{j,i} \left[S_j\right] \tag{4-32}$$

rearranging (4-32) yields

$$\left[m_i\right]_{TOT} - \sum_{j=1}^{N_s} \nu_{j,i} K^0_{r,j} \prod_{i=1}^{N_p} \left(\gamma_i m_i\right)^{\nu_{j,i}} = 0 \tag{4-33}$$

defining

$$f_i\left(m_i\right) = \left[m_i\right]_{TOT} - \sum_{j=1}^{N_s} \nu_{j,i} K^0_{r,j} \prod_{i=1}^{N_p} \left(\gamma_i m_i\right)^{\nu_{j,i}} \tag{4-34}$$

where f_i is the nonlinear polynomial function of the ith basis species, permits the application of a multidimensional root finding algorithm to find a solution vector **C** of values m_i (order N_p) to the polynomial function vector **F** of N_p equations f_i, i.e.

$$f_i\left(m_1, \ldots, m_{N_p}\right) = \mathbf{F}\left(\mathbf{C}\right) = 0 \quad \text{for } i = 1 \ \ldots \ N_p. \tag{4-35}$$

In general there are no bracketing methods available for the root finding of n dimensional systems, and no way of knowing whether any solutions exist. Therefore, unlike the one-dimensional case there are no good general methods for solving the system of nonlinear equations i.e. convergence to the solution vector is not guaranteed. All algorithms proceed by iteration from an initial trial vector, hopefully improving the solution until some predetermined convergence criteria is satisfied. Both the success of the algorithm and the number of iterations required depend strongly on having an initial trial vector sufficiently close to the solution. The Newton-Raphson method is most commonly applied to speciation calculations. Close to **C**, each of the functions f_i can be expanded in Taylor series:

$$f_i\left(\mathbf{C} + \delta\mathbf{C}\right) = f_i\left(\mathbf{C}\right) + \sum_{k=1}^{N_p} \frac{\partial f_i}{\partial m_k} \delta c_k + O\left(\delta \mathbf{C}^2\right) \tag{4-36}$$

the matrix of partial derivatives in equation (4-36) is the Jacobian matrix **J**:

$$J_{ik} = \frac{\partial f_i}{\partial m_k} \tag{4-37}$$

In matrix notation equation (4-36) is

$$\mathbf{F}(\mathbf{C} + \delta\mathbf{C}) = \mathbf{F}(\mathbf{C}) + \mathbf{J} \cdot \delta\mathbf{C} + O(\delta\mathbf{C}^2) \tag{4-38}$$

By neglecting terms of order $\delta\mathbf{C}^2$ and higher and setting $\mathbf{F}(\mathbf{C} + \delta\mathbf{C}) = 0$ a set of linear equations for the corrections $\delta\mathbf{C}$ is obtained that move the solution vector closer to zero:

$$\mathbf{J} \cdot \delta\mathbf{C} = -\mathbf{F}(\mathbf{C}) \tag{4-39}$$

Matrix equation (4-39) can be solved by *LU* decomposition and the corrections then added to the trial vector to obtain an improved estimate of the solution vector:

$$\mathbf{C} \rightarrow \mathbf{C}' = \mathbf{C} - \mathbf{J}^{-1}\mathbf{F}(\mathbf{C}) \tag{4-40}$$

The process is iterated to the predetermined convergence criteria. Additional strategies can be used to enlarge the region of convergence. If the initial trial vector is sufficiently close to the solution vector, the Newton-Raphson method converges quadratically to the solution, however there are two significant disadvantages to the method: poor global convergence and the need to evaluate the Jacobian matrix which can be computationally demanding. An alternative method that does not require computation of the Jacobian matrix can also be applied. This method relies on imposing the chemically permitted interval for the values of the basis species, i.e.

$$0 < m_i \leq [m_i]_{TOT} \quad \text{for} \quad [m_i]_{TOT} > 0 \tag{4-41}$$

and proceeds by adjusting the trial vector elements by iteration of:

$$m_i \rightarrow m_i' = m_i \frac{[m_i]_{TOT}}{[m_i]_{TOT} - f_i(m_i)} \tag{4-42}$$

For the chemical systems modelled in this work, this simple ratio method was found to be considerably more robust than the Newton-Raphson method, with a region of convergence generally much greater than that of the Newton-Raphson method. The convergence rate of this method is lower than that of the Newton-Raphson method, however as the Jacobian matrix does not need to be computed the processing time was generally found to be less. The method generally provided a trial vector close to the

solution vector within a few iterations, however in a few cases the convergence to the predetermined convergence criteria then proceeded slowly. The optimal strategy was found to be the application of the ratio method followed by the Newton-Raphson method if convergence was not obtained within a relatively small number of iterations (generally 20).

4.3.2 Organisation of the speciation computer code

Figure 4-1 shows the organisation of the computer code used to perform the speciation calculations. Model input is provided to the program in two keyword structured text files: a database file containing log $K_r°$ values for the equilibrium equations of all derived solution species considered in the model; a file containing basis species total concentrations, solution pH and initial trial values for the ionic strength and basis species activities. As detailed above, the ratio method is applied initially to obtain either the solution vector if convergence is achieved within a few iterations or close starting values for the Newton-Raphson method if convergence is not reached. The Jacobian matrix **J** is calculated analytically rather than numerically to reduce computation time. The GSL (Galassi, Davies et al. 2002) implementations of the Newton-Raphson algorithm and standard linear algebra routines (for example LU-decomposition) were used. For both the ratio and Newton-Raphson methods the ionic strength estimation and hence activity coefficients (calculated from the Davies equation (4-29) with A = 0.5114 and b = 0.3) is updated at each iteration. At each iteration of both the ratio and Newton-Raphson algorithms the error vector **F(C)** is evaluated (equation (4-35)) and used to calculate the error criteria, ε, for stopping the iteration. The error criterion is calculated from the sum of the absolute error bounds normalised with respect to the ionic strength and number of basis components, i.e.

$$\varepsilon = \frac{\sum_{i=1}^{N_p} \left| f_i\left(m_i\right) \right|}{N_p \cdot I} \tag{4-43}$$

Iteration was stopped when $\varepsilon < 10^{-10}$.

Figure 4-1. Organisation of the computer code developed to perform the speciation calculations, see text in sections 4.2.2, 4.3.1 and 4.3.2 for definitions of symbols.

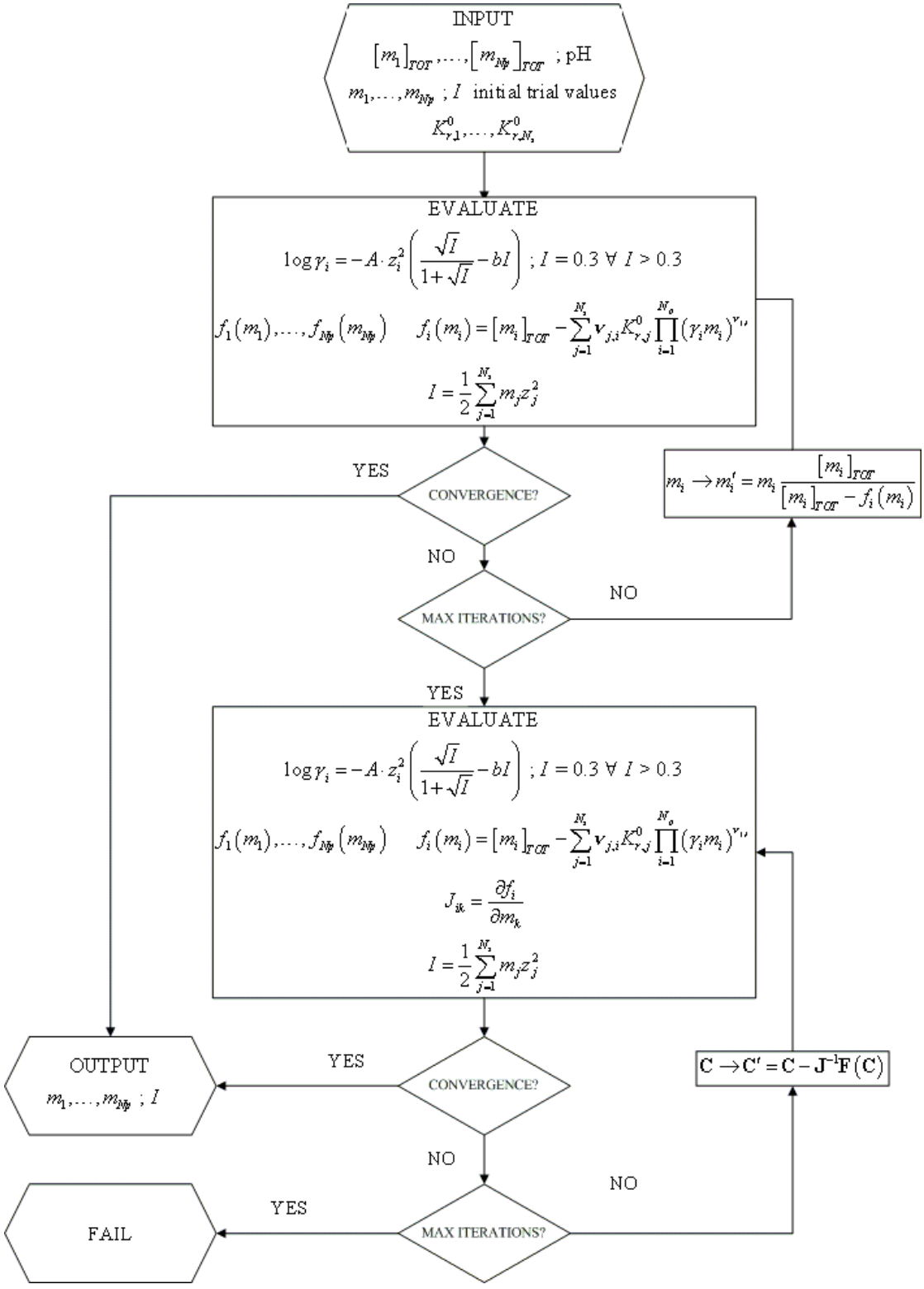

4.3.3 Optimisation issues

Although speciation calculation times are quite short, uncertainty analyses or model parameter optimisation requires large numbers of calculations to be performed. Therefore, in order to reduce computational demands a number of code optimisations were performed. Due to the inefficiency of the standard C library implementation of power functions for small exponent integer values, a different power function was implemented to deal with small integer powers as a special case calculating the power by the minimum number of multiplications.

4.4 Thermodynamic Data

All models of chemical speciation require thermodynamic parameters for the system under consideration. These values are preferably derived from primary experimental data, although estimated values may be used if these are lacking for some species, and are compiled into a database in a format compatible with the model software. Thermodynamic data for aqueous species (of principle interest for the current application) are normally provided in the form of equilibrium or formation constants. The measurements are performed in an ionic medium, usually with an ionic strength higher than environmental fresh waters in order to maintain constant conditions over the range of experimental compositions. For complex equilibrium systems (where several different species may be present in comparable concentrations), the task of interpreting the experimental results in terms of a chemical model is non trivial. A number of different chemical models comprising different component species may describe the results equally well. In these cases a selection between the different models needs to be based on the known properties of the metal and ligand, or preferably on direct observation of the species present (e.g. by Raman spectroscopy).

Irrespective of how well the mathematical constructs of the model represent (or reproduce the behaviour of) the physical system, the quality of the model output is determined by the input parameters. The compilation of high quality databases, relevant to the domain to which the model will be applied, is of primary importance to speciation modelling. There are a number of desirable qualities that a database should possess:

- It should be coherent for the domain to which it is applied, i.e. it should be complete with respect to all possible species that may be formed for the given set of components. Performing calculations with missing species can lead to totally wrong results.
- It should be internally consistent. Thermodynamic parameters all refer to a set of selected reference species and states; literature values are presented in a variety of forms and so need to be reduced to a consistent format. For example by correcting equilibrium constants to infinite dilution, or expressing reaction equations in terms of different component species to be consistent with the chosen basis species set.
- The included data should be transparent and traceable. i.e. the sources of the included data should be cited, data reduction techniques should be defined and data selection procedures should be justified.
- Estimates of the uncertainties associated with each datum when those uncertainties can be estimated.
- The database should be available in a format that can be directly used by the chosen computer model.
- The database should not contain errors, an obvious requirement but difficult to satisfy due to the size and complexity of databases for even simple systems. Most available databases contain errors which arise for a number of reasons, for example simple transcription errors, constants that do not refer to the given reaction equation (for example equilibrium constants defined with the overall formation reaction, see Serkiz *et al.* (Serkiz, Allison et al. 1996)) and also inconsistent application or the absence of methods used to correct to infinite dilution.

4.4.1 Review of available databases

A survey of available thermodynamic databases was performed by the Organisation for Economic Co-operation and Development, Nuclear Energy Authority (OECD-NEA) in 1996 (OECD-NEA 1996) and the current situation has not significantly changed. There are a number of databases apparently suited to the requirements of modelling the solution speciation of uranium in relatively simple solution

compositions, these include databases integrated with computer programs (for example EQ3/6 (Wolery 1992), PHREEQC (Parkhurst and Appelo 1999), WATEQ (Parkhurst and Appelo 1999), MINTEQA2 (Allison, Brown et al. 1991)), critically reviewed databases for restricted systems (e.g. the NEA review series (Grenthe, Fuger et al. 1992; Grenthe, Puigdomenech et al. 1995; Silva, Bidoglio et al. 1995)) and databases of compilations of stability constants (Martell, Smith et al. 2001; Pettit and Powell 2001). A brief comparison of four different databases was performed (1) MINTEQA2 (Allison, Brown et al. 1991), (2) the WATEQ4f database supplied with PHREEQC (Parkhurst and Appelo 1999), (3) the Lawrence Livermore National Laboratory (LLNL) database compiled for EQ3/6 (Wolery 1992) and translated to CHESS format (Van der Lee 1998; Van der Lee 1999) and (4) the NEA database, also compiled for CHESS. Only solution species relevant to the system H_2O-Na-Cl-CO_2-PO_4-UO_2^{2+} were considered, and a number of differences were found between these databases. The most significant differences were due to the number and identity of uranium species included in the different databases, which are summarised in Table 4-1.

Table 4-1. The inorganic uranium aqueous species included in the four selected databases, LLNL (Wolery 1992), MINTEQA2 (Allison, Brown et al. 1991), NEA (Grenthe, Fuger et al. 1992), Wateq4f (Parkhurst and Appelo 1999).

Species	LLNL	MINTEQA2	NEA	Wateq4f
$(UO_2)_{11}(CO_3)_6(OH)_{12}^{2-}$	X		X	
$(UO_2)_2(OH)_2^{2+}$	X	X	X	X
$(UO_2)_2CO_3(OH)_3^-$	X		X	
$(UO_2)_2OH^{3+}$	X		X	X
$(UO_2)_3(CO_3)_6^{6-}$	X		X	X
$(UO_2)_3(OH)_4^{2+}$	X		X	X
$(UO2)3(OH)5^+$	X	X	X	X
$(UO_2)_3(OH)_5CO_2^+$	X			
$(UO_2)_3(OH)_7^-$	X		X	X
$(UO_2)_3O(OH)_2(HCO_3)^+$	X		X	
$(UO_2)_4(OH)_7^+$	X		X	X
$UO_2(CO_3)_2^{2-}$	X	X	X	X
$UO_2(CO_3)_3^{4-}$	X	X	X	X
$UO_2(H_2PO_4)(H_3PO_4)^+$	X		X	
$UO_2(H_2PO_4)_{2\ (aq)}$	X	X	X	X
$UO_2(H_2PO_4)_3^-$		X		X
$UO_2(HPO_4)_2^{2-}$		X		X
$UO_2(OH)_{2\ (aq)}$	X		X	
$UO_2(OH)_3^-$	X		X	X
$UO_2(OH)_4^{2-}$	X		X	X
UO_2^{2+}	X	X	X	X
UO_2Cl^+	X	X	X	X
$UO_2Cl_{2\ (aq)}$	X		X	X
$UO_2CO_{3\ (aq)}$	X	X	X	X
$UO_2H_2PO_4^+$	X	X	X	X
$UO_2H_3PO_4^{2+}$	X		X	X
$UO_2HPO_{4\ (aq)}$	X	X	X	X
UO_2OH^+	X	X	X	X
$UO_2PO_4^-$	X	X	X	X
Total species	27	14	26	29

The LLNL and NEA databases were identical except for the inclusion of the $(UO_2)_3(OH)_5CO_2^+$ species in the LLNL database. This species is in fact a duplicate entry of $(UO_2)_3O(OH)_2(HCO_3)^+$ illustrating the difficulty of maintaining consistency when there are a number of possible ways of formulating the same species. Apart from this error, it is not surprising that the same species are included, as the bulk of the NEA review was inserted into the LLNL database, however there are some differences in the equilibrium constants values between the two databases. The differences between these two databases and the MINTEQA2 and WATEQ4f databases are more marked, both in terms of the number and identity of species, and the formation constants associated with them. In addition to the differences between the uranium species considered, differences in the coherency of the auxiliary dataset and the formation constant values of these species also influence the output of speciation calculations. An example of the differences found modelling a simple solution composition with each of the 4 databases is shown in Figure 4-2. As can be seen from the figures, the differences found are highly significant even for this very simple system, a maximum range of values for the free-ion of close to an order of magnitude is observed.

It is difficult to assess the merits of each database, as little or no documentation is provided. The one notable exception to this is the NEA database, which is provided in conjunction with a series of published reviews for each element or group of elements (Östhols and Wanner 2000). The review of uranium species was published in 1992 (Grenthe, Fuger et al. 1992), and is widely regarded as the most comprehensive single database for uranium species.

Figure 4-2. Differences in output species obtained by modelling a simple solution composition ([NaCl] = 10^{-2} M, [PO_4] = 10^{-5} M, [UO_2] = 5.10^{-6} M, P_{CO2} = $10^{-3.5}$ atm, equilibrium with calcite). LLNL (Wolery 1992), MINTEQA2 (Allison, Brown et al. 1991), NEA (Grenthe, Fuger et al. 1992), Wateq4f (Parkhurst and Appelo 1999)

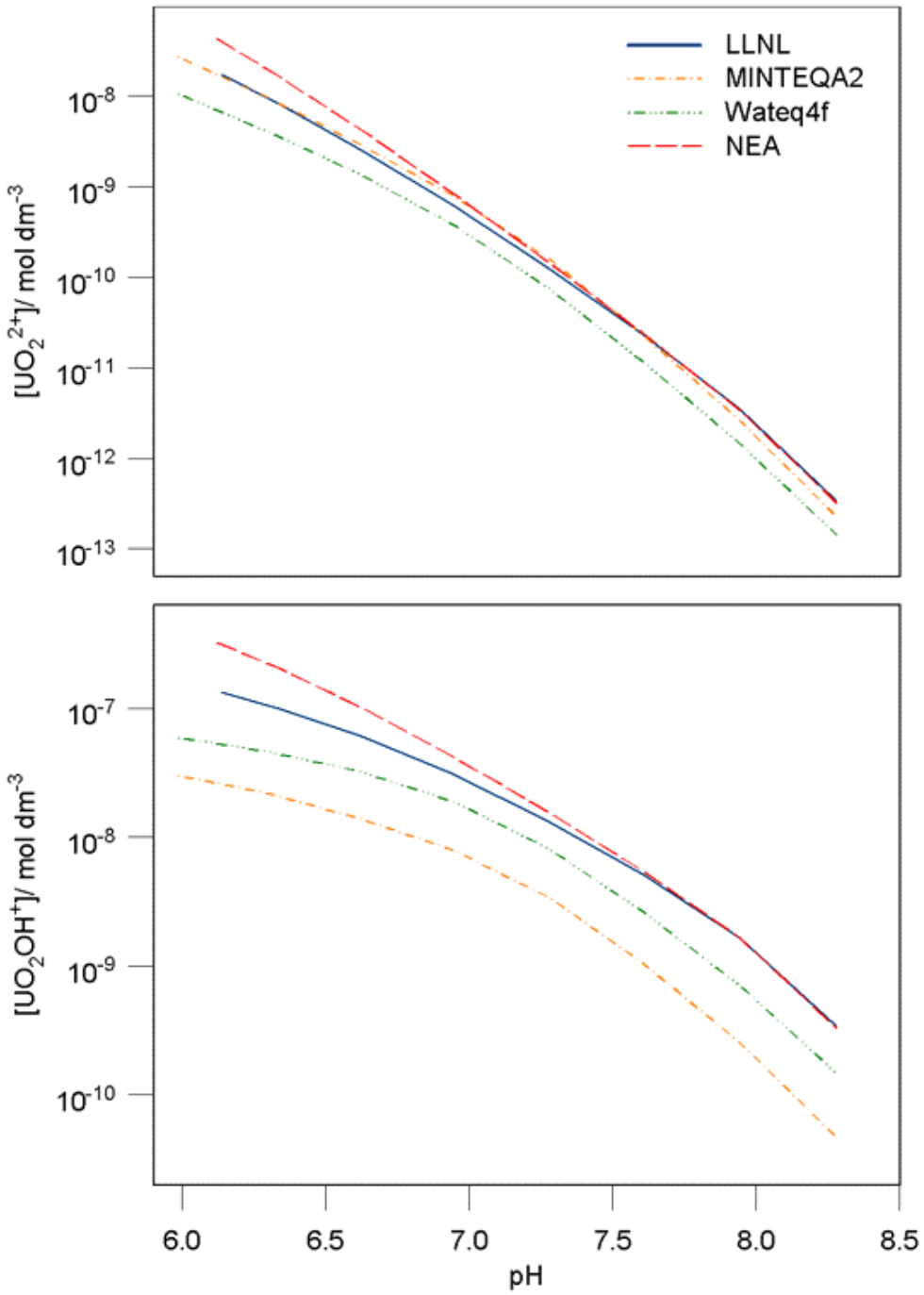

Figure 4-2 (continued). Differences in output species obtained by modelling a simple solution composition ([NaCl] = 10^{-2} M, [PO_4] = 10^{-5} M, [UO_2] = 5.10^{-6} M, P_{CO2} = $10^{-3.5}$ atm, equilibrium with calcite). LLNL (Wolery 1992), MINTEQA2 (Allison, Brown et al. 1991), NEA (Grenthe, Fuger et al. 1992), Wateq4f (Parkhurst and Appelo 1999)

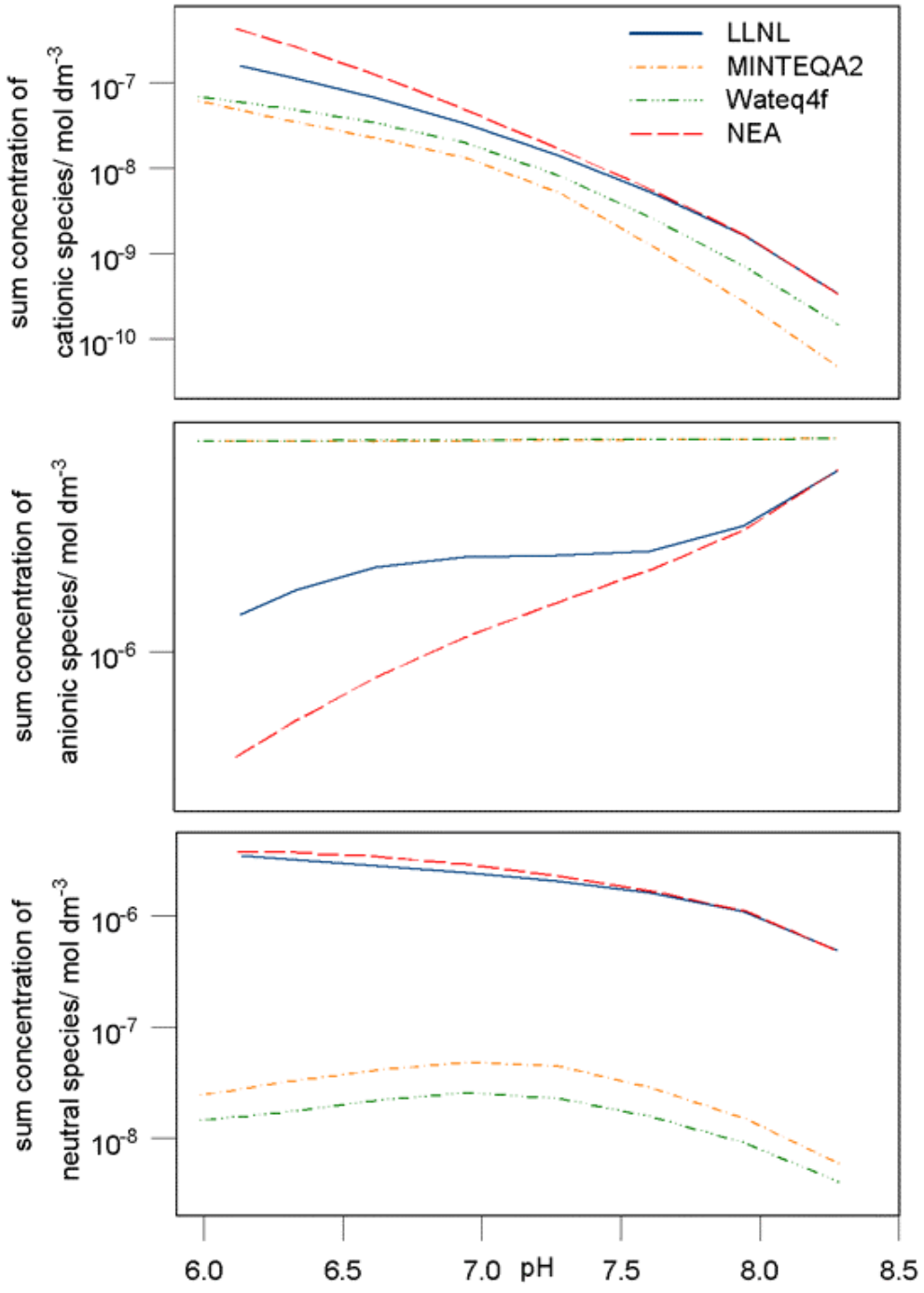

4.4.2 Thermodynamic database compilation

Due to the inadequacy of the available thermodynamic databases a new database was compiled, adapted for the domain of application of these studies. The OECD Nuclear Energy Agency (NEA) database (Östhols and Wanner 2000) was chosen as the foundation for this new compilation, this database project was initiated in 1984 to provide a "comprehensive, internally consistent and internationally recognised thermodynamic database" for the modelling requirements of safety assessments for radioactive waste disposal sites.

4.4.2.1 Overview of the OECD Nuclear Energy Agency (NEA) Thermochemical Database

The NEA thermochemical database project (Östhols and Wanner 2000) was initiated in 1984, in response to the realisation that existing compilations of environmentally relevant thermodynamic databases were insufficient for the modelling of radionuclide migration. To satisfy these objectives the database needs to: contain all relevant elements present in the systems to be modelled; provide data for all aqueous, solid and gaseous forms of those elements at a set of selected and defined reference conditions; be internally consistent, often requiring the reinterpretation of published data; comprehensively document the sources of data used, the procedures adopted to select those data and the methods used for any recalculation of the data. The project is ongoing and far from complete for all systems of interest, however currently, data for the inorganic chemistry of five selected elements relevant to radioactive waste disposal systems have been reviewed (uranium, plutonium, americium, technetium and neptunium), as well as a larger number of auxiliary elements relevant to geologic systems.

The project is devoted to the critical review of selected thermodynamic quantities from published data, rather than the measurement of thermodynamic parameters. The review procedure generally only includes primary experimental data and not estimates, values from previous compilations or calculated values, although there are some exceptions to these criteria if reliable primary data is lacking and analogy with a similar element with reliable data is possible. Where possible, experimental data were re-evaluated using consistent chemical models. The data are consistent with the ICSU

Committee on Data for Science and Technology (CODATA) published values (Cox, Wagman et al. 1989). The IUPAC definitions of standard and reference conditions have been adopted, and also the standard state pressure, $p^\circ = 10^5$ Pa, and reference temperature of 298.15 K.

For gaseous substances the standard state is the pure substance at the standard state pressure in a hypothetical state at which it exhibits ideal gas behaviour. The standard state for a pure liquid substance is the pure liquid at the standard state pressure. The standard state for a pure solid substance is the pure solid at the standard state pressure. For dissolved species the standard state is the hypothetical ideal solution at standard state pressure in which the solute concentration is one molal and the activity coefficient is unity. The activity correction model used to extrapolate data to this ideal reference state was based on the specific ion interaction theory described by Brønsted (Brønsted 1922; Brønsted 1923), Guggenheim (Guggenheim 1966) and Scatchard (Scatchard 1936).

4.4.2.2 Parameters included in the thermochemical database, and conventions used

The data is presented in Fortran-style formatted files; for each species there are a total of thirteen lines of data, containing between three and six parameters separated by blank spaces. Parameters included are the standard molar Gibbs energy of formation ($\Delta_f G_m^\circ$/ kJ mol^{-1}), the standard molar enthalpy of formation ($\Delta_f H_m^\circ$/ kJ mol^{-1}), the standard molar entropy of the species (S_m°/ J K^{-1} mol^{-1}) and the standard molar heat capacity of the species at constant pressure ($C_p^\circ{}_{,m}$/ J K^{-1} mol^{-1}), together with the associated uncertainties at a 95% confidence level and the temperature dependencies of the values where available. As only relative changes in the values of thermodynamic parameters can be determined experimentally, and not their absolute values, all of the parameters refer to the formation reaction of the species in its standard state from the component elements in their reference states. The chosen reference states of the elements are their most stable form under the chosen standard state and are tabulated in Table 4-2, by convention the values of $\Delta_f G_m^\circ$ and $\Delta_f H_m^\circ$ are set to zero. Full details of the standards and conventions used for the database are detailed in the report by Wanner and Östhols (Wanner and Östhols 2000).

Table 4-2. The reference states for elements included in the NEA thermochemical database at the reference standard state pressure and temperature.

Element	State	Element	State
Ag(c)	crystalline, cubic	Li(c)	crystalline, cubic
Al(c)	crystalline, cubic	Mg(c)	crystalline, hexagonal
Am(c)	crystalline, dhcp	N_2(g)	gaseous
Ar(g)	gaseous	Na(c)	crystalline, cubic
As(c)	crystalline, rhombohedral (grey)	Ne(g)	gaseous
B(c)	β, crystalline, rhombohedral	Np(c)	crystalline
Ba(c)	crystalline, cubic	O_2(g)	gaseous
Be(c)	crystalline, hexagonal	P(c)	crystalline, cubic (white)
Bi(c)	crystalline, rhombohedral	Pb(c)	crystalline, cubic
Br_2(l)	liquid	Pu(c)	crystalline
C(c)	crystalline, hexagonal (graphite)	Rb(c)	crystalline, cubic
Ca(c)	crystalline, cubic, fcc	S(c)	crystalline, orthorhombic
Cd(c)	crystalline, hexagonal	Sb(c)	crystalline, rhombohedral
Cl_2(g)	gaseous	Se(c)	crystalline, hexagonal (black)
Cs(c)	crystalline, cubic	Si(c)	crystalline, cubic
Cu(c)	crystalline, cubic	Sn(c)	crystalline, tetragonal (white)
F_2(g)	gaseous	Sr(c)	crystalline, cubic, fcc
Ge(c)	crystalline, cubic	Tc(c)	crystalline, hexagonal
H_2(g)	gaseous	Te(c)	crystalline, hexagonal
H^+	aqueous	Th(c)	crystalline, cubic
He(g)	gaseous	Ti(c)	crystalline, hexagonal
Hg(l)	liquid	U(c)	crystalline, orthorhombic
I_2(c)	crystalline, orthorhombic	Xe(g)	gaseous
K(c)	crystalline, cubic	Zn(c)	crystalline, hexagonal
Kr(g)	gaseous		

4.4.2.3 Conversion of the data to a format compatible with geochemical speciation programmes

As given, it is not possible to directly use the database with any existing geochemical equilibrium computer model; the data must be converted to a compatible format whilst retaining the internal consistency of the database. The various existing software programs (e.g. Chess, Phreeqc, MinteqA2, Mineql+) all use a similar framework to describe the system, which has influenced the manner in which the database has been converted for use with these programs. As described in Section 4.3, a (minimal) pure basis set needs to be defined and then an auxiliary basis set and all other secondary species need to be defined in terms of this pure data set by means of mass-balance equations with associated equilibrium or formation constants. Such a conversion has been performed for the EQ3/6 programme (Wolery 1992), however on comparing a number of species with the original NEA data files several problems and inconsistencies were discovered. A number of species provided in the NEA database were not included in the converted database, several duplicate species entries were found, a number of mass balance equations were wrong and several formation constant values were significantly different from values calculated using NEA values. Finally not all mass balance equations were formulated in terms of consistent oxidation states of the participating elements, this prohibits considering these species for calculations of systems in redox disequilibria.

It was decided to recompile the NEA database for a number of reasons. Firstly verifying the existing database conversion and correcting all errors would be essentially the same amount of work as compiling a new version of the database. It permitted the elimination of the problems detailed above, and also the inclusion of new data released by the NEA subsequent to the previous conversion. Temperature dependencies for a temperature range more suited to the expected domain of application could be calculated, and species for which the temperature dependencies had not been calculated in the previous conversion, but for which sufficient data for the calculations to be performed exist could be included. The new compilation could also be compared with the existing version to find any inconsistencies, which could then be investigated further to try to minimise the risk of introducing new errors.

It also permitted the development of a systematic method to store thermodynamic parameters and calculate appropriate equilibrium/formation constant values in terms of the desired mass balance equations. The temperature dependencies were calculated by the approximation methods detailed in section 4.2.1 depending on the richness of the data for the species and all basis or auxiliary basis species included in the mass balance equation. The format developed was spreadsheet based (using Microsoft Excel) and is extensible, allowing new species to be incorporated (for example to improve the coherency of the database with respect to the domain of interest). Visual Basic Macros were written to export the data in the format required by the chosen speciation program.

Following the principles described in section 4.3 a pure basis species set was chosen, appropriate for oxic surface waters, which are tabulated in appendix A. In nearly all cases these basis species are not the same as the reference states for elements used by the NEA, which would be a very poor choice of basis species for modelling aqueous speciation. Mass balance equations for all auxiliary basis species (redox species) and secondary species (aqueous, gaseous and mineral species) were formulated in terms of the chosen basis species, or for species containing elements in different oxidation states to the basis species set in terms of the appropriate auxiliary basis species.

Stability constants at 298.15 K (given as $\log_{10}$ values) were calculated by equation (4-17), stability constants at other temperatures (273.15, 323.15, 348.15 and 373.15 K) were calculated where sufficient data existed by one of either equations (4-23) or (4-24) according to the extent of the available data (i.e. values of $\Delta_f H_m^o, C_{p,m}^0$ for all the species in the mass balance equation). Uncertainty values nominally at a confidence interval (CI) of 0.95 for the $\log_{10} K°_r$ values are calculated by combination of the individual $\Delta_f G°_m$ uncertainties with their stoichiometric coefficients as described in Wanner and Östhols (Wanner and Östhols 1999). Additionally, hard core diameters of the species taken from the CHESS database are incorporated for use with the B-dot activity coefficient model, references to the specific NEA data files of origin of each species and comments related to the temperature dependence estimation method employed are generated.

The format of the database chosen was CHESS version 3 (Van der Lee 1998). This format offers a number of advantages related to the database format compared to other

available programmes, namely that references and comments can be recorded for each included species, and read by the end-user directly from the associated graphical interface JCHESS. This is a major improvement to the traceability of compiled databases. A screenshot of the information contained in the compiled database for the species UO_2OH^+, presented by the database analyser component of JChess are shown in Figure 4-3. The basic information contained in the compiled database is presented in appendix B.

Figure 4-3 Example of information presented by JChess database analyser.

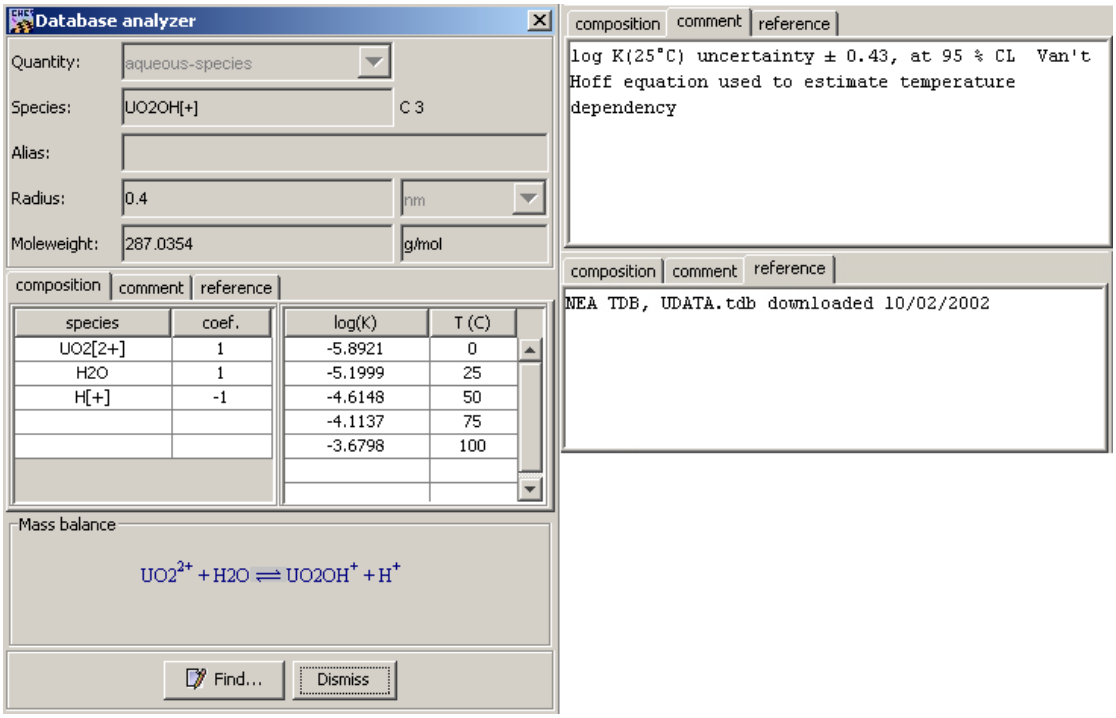

4.4.2.4 Augmentation of the NEA database

The data for species included in the NEA database may be considered to be of high quality, with few exceptions. However, there are relatively few auxiliary species included in the database and on its own it cannot be considered coherent except for particular, very simple systems. To attempt to remedy this problem a domain of modelling application was chosen, and a literature review performed to find experimentally determined stability constants (preferably several independent sources) for all possible aqueous complexes within that domain. The domain was restricted to systems containing the following species: H_2O, Na^+, K^+, Mg^{2+}, Ca^{2+}, Fe^{2+}/Fe^{3+}, UO_2^{2+}, Cl^-, NO_3^-, SO_4^{2-}, CO_3^{2-}, PO_4^{3-} and citrate. Stability constant values were derived from a number of sources, including the NIST and IUPAC searchable databases of published values (Martell, Smith et al. 2001; 2001), original research papers, and data compilations (Nordstrom, Plummer et al. 1990; Shock, Oelkers et al. 1992; Shock, Sassani et al. 1997; Sverjensky, Shock et al. 1997; Markich and Brown 1999; Shock 2000). Unless noted in the tables in appendix B, all data refer to the same standard states as employed by the OECD-NEA database.

The truncated Davies activity coefficient model, equation (4-29) (Colston, Chandratillake et al. 1990), was employed when data was not given at null ionic strength with the value of b set to 0.3. This method is different from that employed for the NEA review, however insufficient data were available to employ the specific ion interaction model used in that work (Grenthe, Wanner et al. 2000), particularly in the case of citrate and EDTA complexes. The majority of the data for citrate complexes was taken from a review by Markich and Brown (Markich and Brown 1999) who also used the truncated form of the Davies equation. The literature data available was presented in a number of different formats, including equilibrium and overall formation constants and also a number of reduced thermodynamic values for the species. All data was reduced to the same format, namely $\Delta_f G°_m$ and $\Delta_f H°_m$ values of the species, by combination of the individual $\Delta_f G°_m$ or $\Delta_f H°_m$ values of the other components of the mass balance equation and the stability constant value according to equation (4-17). Uncertainty values have been calculated for species when sufficient data exists (generally 3 or more independent values for the species). The values are given at a confidence interval of 95 % and are calculated relative to the chosen basis

species set, rather than the NEA reference species. Similarly, uncertainty values for species in the NEA database that have not been amended have been calculated relative to the chosen basis species. Generally the uncertainty values were calculated from the standard deviation of the independent mean $\Delta_f G°_m$ values and the appropriate Student's *t*-probability value for the number of data. Estimates of the uncertainty for an individual datum were generally not considered, these literature values (where given) are often small, but when a number of independently determined values are compared the absurdity of these uncertainty estimates becomes apparent. This indicates that although the precision of the studies is often good, the accuracy is generally poor.

For a number of uranium species included within the NEA database, new experimental data have become available; frequently the authors have taken account of the NEA review for the interpretation of the experimental results. Values for a number of species including UO_2OH^+, $UO_2(OH)_2(aq)$, $UO_2(OH)_3^-$, $UO_2(OH)_4^{2-}$ $(UO_2)_2(OH)_2^{2+}$, $(UO_2)_3(OH)_5^+$, $(UO_2)_3(OH)_7^-$, $UO_2HPO_4(aq)$, $UO_2H_2PO_4^+$, and $UO_2(H_2PO_4)_2(aq)$ have been amended to incorporate these new data. The most significant change for the conditions under which it is envisaged that the database will be applied to has been to the second hydrolysis product, $UO_2(OH)_2(aq)$, for which the NEA value was not considered. In the original NEA review of uranium only a limiting value was defined for this species $\Delta_f G°_m(UO_2(OH)_2(aq), 298.15\ K) \geq -1368\ kJ\ mol^{-1}$. In the appendix to the review of americium "Corrections to the uranium NEA-TDB review"(Grenthe, Puigdomenech et al. 1995) it is remarked that the actual value is approximately 8 kJ mol^{-1} larger than this value, in agreement with the amended value of -1360.1 kJ mol^{-1} derived from three other sources. The NEA database was not itself amended due to the decision to "freeze" the values until the next review.

4.5 Uncertainty Analysis Of Speciation Calculations

Computer simulation has become increasingly popular in many different scientific fields, in many cases replacing experimentation, particularly in areas where experiments are difficult or impossible for reasons of cost, safety or the spatial or temporal scales of interest. Quality assessment should be an integral part of the application of computer modelling to environmental problems, however with few exceptions (Ekberg 1999; Nitzsche, Meinrath et al. 2000), very little attention has

been paid to this important aspect of uranium speciation modelling. The reliability of speciation calculations can be questioned at several levels (Cabaniss 1997), in the simplest case the adequacy of the numerical algorithms may be checked against some error tolerance e.g. equation (4-43). As the algorithms are generally robust and the error tolerance can be small the calculations are reliable in this sense. At the other extreme the veracity of the chemical model limits the reliability of the calculations. For example if species that are present in the system are omitted from the model, if the system is not in thermodynamic equilibrium or if input parameters are in gross error (Serkiz, Allison et al. 1996) then the calculated speciation may be meaningless. At an intermediate level the reliability may be questioned if the chemical model is essentially correct but the input parameters are uncertain, resulting in uncertain model predictions.

All thermodynamic values have a degree of uncertainty associated with them due, amongst other factors, to both random and systematic experimental errors, poor or partial understanding of the underlying mechanisms e.g. misinterpretation of the chemical system and errors introduced by the data. Geochemical speciation models produce deterministic results and provide no estimates for the uncertainties associated with output parameters. Speciation modelling, and its associated applications such as geochemical transport modelling and the various implementations of bioavailability models in the field of ecotoxicology, is currently based on mean value calculations. However, thermodynamic values incorporated into databases used to calculate solution speciation are more properly characterised by their expectation values and quantitative estimates of their uncertainty distributions. It is important to assess the effect of these input uncertainties on the model output. There are two different approaches to calculating the uncertainty propagation in aqueous equilibrium calculations: the derivative approach and sampling based methods (Cabaniss 1999). In the derivative method, uncertainty propagation is estimated by assuming that: (a) the input parameters have Gaussian uncertainty distributions of characteristic mean and standard deviation, (b) the equations relating the calculated concentration to the input are sufficiently linear such that the second and higher order derivatives can be disregarded and (c) the input uncertainties are mutually independent. Sampling based methods such as Monte Carlo analysis involve treating the input parameters as random variables with defined probability distributions and, if required, correlations

(first order interactions). The input parameters are then sampled in some fashion (for example by generation of uniform deviates from random or pseudo-random sequences followed by transformation to the assigned probability) and the model output evaluated repeatedly. The derivative method has the significant advantage of rapid calculation time compared to sampling based methods, however the inherently non-linear nature of solution or solubility equilibria can lead to failure of the assumed linear approximation and hence invalidate the approach.

4.5.1 Sampling based methods of uncertainty calculation

As described above, the derivative method is significantly faster than sampling based methods. However, it can only be applied validly to systems where the output distributions are normally distributed. As can be seen from the results of this work, this is often not the case; hence this method has not been applied. Sampling based uncertainty analysis involves four steps:

1. the selection of a distribution for each input parameter;
2. generation of a sample from these distributions;
3. evaluation of the model for each sample element;
4. uncertainty analysis of model output.

Monte Carlo (MC) analysis involves performing step (2) with random number sequences transformed to the desired distributions. As the numbers are generally machine generated by a deterministic process, they are not random *stricto sensu*, and are more correctly referred to as pseudo-random. From a statistical point of view, random sampling has the advantage of producing unbiased estimates of the model output distributions. A special case of MC analysis is Quasi-Monte Carlo (QMC) analysis where the second step is not performed using random numbers but some other form of non-random sampling.

4.5.1.1 Random sampling

In random sampling for mutually independent input variables, a sample of the required dimension N ($\mathbf{x}_1$, $\mathbf{x}_2$,…,$\mathbf{x}_N$) is generated from their respective distributions. This method depends on the generation of random uniform deviates transformed to the required distribution. As mentioned above a deterministic process generally

generates the numbers and so they are not truly random. The generation of such sequences has been widely discussed (Knuth 1981; Press, Teukolsky et al. 1992; L'Ecuyer 1998) and a good generator will provide sequences that are statistically indistinguishable from truly random sequences. Good generators satisfy both theoretical and statistical properties. Desirable theoretical properties include a long period (the number of calls to the generator before the sequence repeats itself), low serial correlation, and a tendency not to "fall mainly on the planes". Statistical tests are generally performed with numerical simulations to estimate some quantity for which probability theory provides an exact answer; a widely utilised set of statistical tests is the "DIEHARD battery of randomness tests" available from http://stat.fsu.edu/~deo/diehard.html. Many standard implementations of random number generators in widespread use are insufficient (Park and Miller 1988) in some respect, so care needs to be exercised in choosing a generator. For this work the GSL (Galassi, Davies et al. 2002) implementation of the "Mersenne Twister" (MT19937) generator of (Matsumoto and Nishimura 1998) was used to generate uniform deviates. This generator has a period of $2^{19937} - 1$ (about 10^{6000}) and is equi-distributed in 623 dimensions; it has passed all of the DIEHARD tests. For this work, the distributions of all input parameters were assumed to be normal (Gaussian). The probability distribution for Gaussian random variates is:

$$p(x)dx = \frac{1}{\sqrt{2\pi\sigma^2}} e^{\left(\frac{-x^2}{2\sigma^2}\right)} dx \tag{4-44}$$

For x in the range $-\infty$ to $+\infty$ with the transformation $z = \mu + x$ for variates of mean μ. For random sampling uncertainty analysis the Box-Muller algorithm (Box and Muller 1958) was used to generate the random variates with a Gaussian distribution, requiring two calls to the random number generator for each variate.

4.5.1.2 Stratified sampling

The objective of stratified sampling is to improve the efficiency of sampling based uncertainty calculations by improving the characterisation of the input variables sample space over that of random sampling for a given sample size. Briefly, the input parameter space is exhaustively divided into a number of non-overlapping sub-regions

from which samples are then randomly selected. One example of stratified sampling is importance sampling in which the volumes of the selected sub-regions are assigned according to their importance to the final outcome of the analysis. For example, this method can be used to ensure the inclusion of input variables sample space that has low probability but high consequences. This idea is carried further in Latin hypercube sampling to ensure the full coverage of the range of each variable. Specifically, the range of each variable (x_i) is divided into n intervals of equal probability and a value is selected randomly from each interval. The n values obtained for x_1 are then paired at random without replacement with the n values obtained for x_2. These n pairs are then combined randomly without replacement with the n values for x_3 to form n triples and the process continued until a set of n n_x-tuples is formed constituting the Latin hypercube sample. This sampling strategy is more efficient than random sampling when model output is dominated by only a few input parameters or when the output is a monotonic function of each of its arguments. Further, the closer the output function is to being additive in its input variables the greater the improvement over random sampling. However, for non-additive, non-monotonic functions the performance can be equivalent or worse than random sampling.

4.5.1.3 Quasi-random sampling

An alternative sampling strategy to improve efficiency is the use of quasi-random sequences (also referred to as sub-random or low-discrepancy sequences). These are sequences of n-tuples that progressively fill n-space more uniformly than uncorrelated random points; algorithms for the production of quasi-random sequences are crafted to provide sequences of sample points that are "maximally avoiding" of each other. This sampling strategy, while similar to stratified strategies, fits more naturally into the program framework built to perform random sampling and has a number of other advantages, including reduced memory requirements for producing the sequences. A number of quasi-random sequences are available including Faure, Sobol and Niederreiter sequences. For this work the GSL (Galassi, Davies et al. 2002) implementation of the Sobol sequence (Antonov and Saleev 1979) which is valid for up to 40 dimensions was used. The potential advantage of this approach is that the error bound of the mean value has probabilistic order of $O\left(n^{-1}\log^{s} n\right)$ where s is the dimension, which is an improved asymptotic rate for fixed s over that of MC of

$O\left(n^{-1/2}\right)$. Hence if n is sufficiently large a QMC method is expected to approximate the parameter values with a smaller error than MC. However, the dimension s does not need to be very large in order for $n^{-1}\log^{s} n > n^{-1/2}$ for large values of n in which case the superiority of the convergence rate of the QMC error over MC is not of practical use. The Sobol sequence provides uniform variates, which need to be transformed to a required probability distribution (in this case the Gaussian distribution). In order to maintain the low discrepancy characteristics of the n-sequence Moro's algorithm was used to approximate the inversion of the standard Gaussian distribution function (Moro 1995). Figure 4-4 shows the first 10^4 points of a 2 dimensional Sobol sequence transformed to a Gaussian distribution compared with the same number of random variates of the same joint probability distribution ($\mu = 0$, $\sigma = 1$).

Figure 4-4 First 10^4 points of a 2 dimensional Sobol sequence transformed to a Gaussian distribution compared with 10^4 random variates of the same probability distribution.

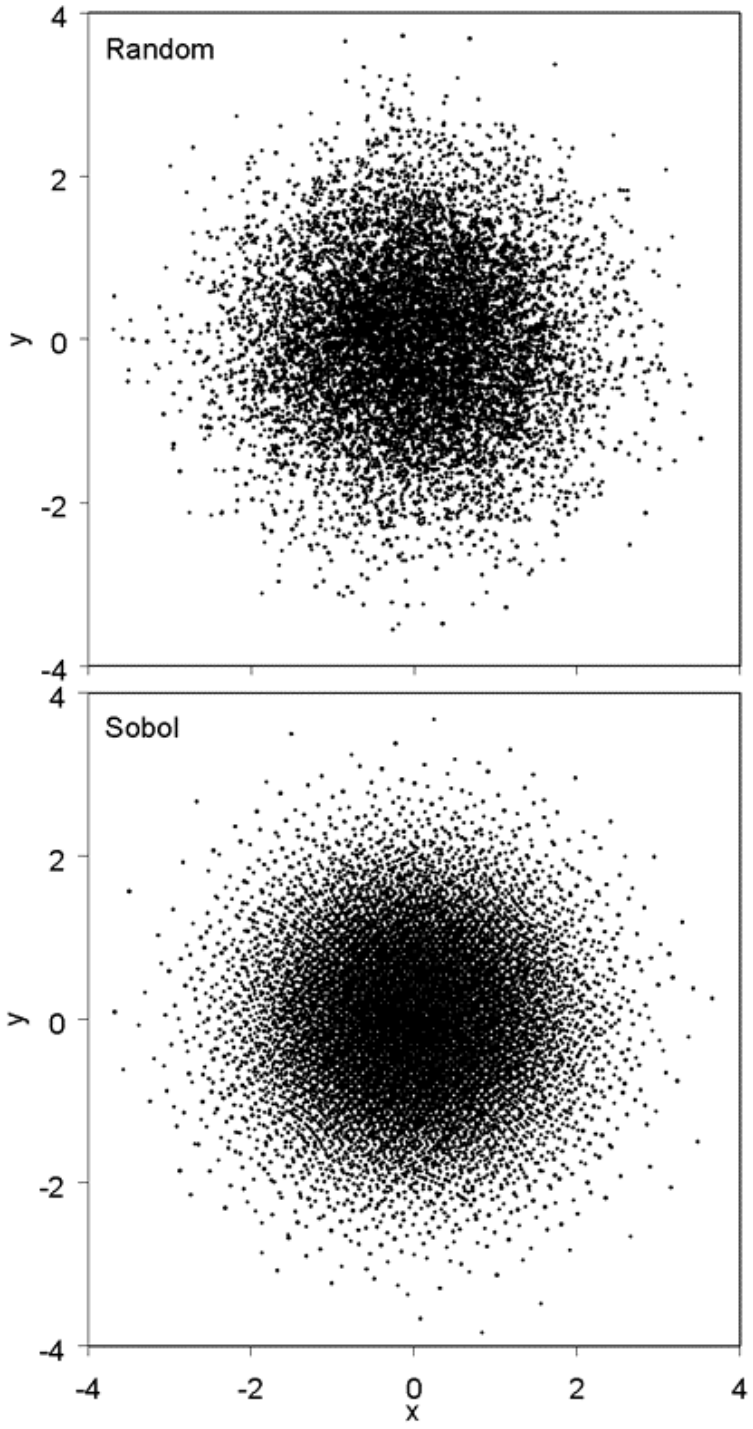

4.5.1.4 Evaluation of model output uncertainty

Using the sample of the input parameter distributions generated by one of the methods detailed above, step 3 of the uncertainty analysis is performed i.e. the model is evaluated for each sample element and the output parameters of interest are stored. These estimates of the output distribution functions are then used for step 4 of the analysis, to calculate a range of descriptive statistical parameters. The statistical parameters calculated by the computer program include: mean, standard deviation, skewness, kurtosis, minimum, maximum, median and a number of distribution quantiles defined in the program input file. Figure 4-5 shows the organisation of the modules of the computer code used to perform the MC and QMC uncertainty calculations. As the output distributions are frequently non-Gaussian, parametric statistical measures of the dispersion are generally not appropriate, and other measures such as inter-quantile ranges are more useful in summarising output uncertainty.

Figure 4-5. Organisation of the computer code developed to perform MC and QMC uncertainty calculations

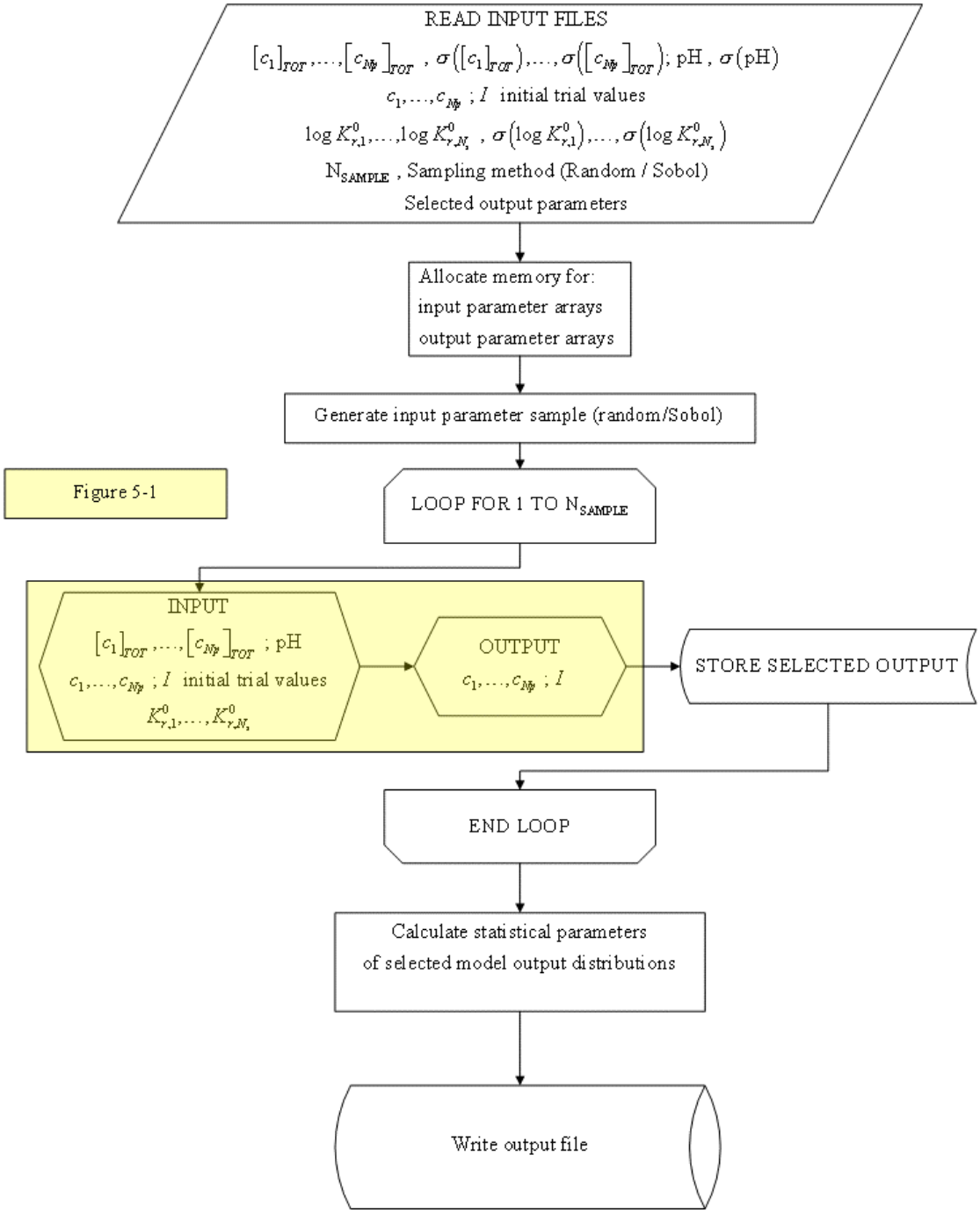

4.5.1.5 Errors of estimated parameters

As the sample size used to perform the uncertainty analysis increases, the estimation of the model output uncertainty distribution improves and hence the probabilistic error of the parameter estimates reduces. For random sampling (MC) the distribution mean values have an error of probabilistic order $O\left(n^{-1/2}\right)$ where n is the number of simulations performed. One of the limitations of MC or QMC analysis is that the sample size required in order to obtain acceptable estimates of the output distributions cannot be calculated a priori. However, the probabilistic uncertainties of statistical parameters of the output distributions can be estimated using a jack-knife resampling procedure. The jack-knife estimate of variance σ^2 for the parameters calculated for the n data ($\overline{p}$) is calculated by recalculating the parameters n times omitting the ith datum (p_i) and is given by:

$$\sigma^2 = \frac{n-1}{n}\sum_{i=1}^{n}\left(p_i - \overline{p}\right)^2 \tag{4-45}$$

This procedure is not overly time consuming for relatively small sample sizes ($< 10^4$), however it is an $O(n^2)$ algorithm and hence for large samples a truncated procedure is preferable.

5 MODELLING BIOLOGICAL AVAILABILITY OF METALS IN AQUATIC SYSTEMS

5.1 Historical Overview Of Modelling Approaches

It is currently well accepted that in order to predict the effects of trace metals on aquatic organisms the effects of the metal's solution speciation need to be accounted for. The fact that the total dissolved concentration of a metal is generally a poor indicator of its toxicity and/or chemical bioavailability has been known for over thirty years. A number of different modelling approaches to relate chemical speciation to toxicity or bioavailability of trace metals have been proposed. Several comprehensive reviews of the development of these different modelling approaches have been published (Tessier, Buffle et al. 1994; Campbell 1995; Paquin, Gorsuch et al. 2002). Early work was oriented mainly towards copper toxicity (due both to the importance of this metal and the availability of sensitive analytical techniques to determine both the free ion and total concentration). These studies included the role of natural organic matter in reducing toxicity to fish e.g. (Zitko, Carson et al. 1973); the effect of complexation by EDTA on algal toxicity (Anderson and Morel 1978); the role of water hardness (as Ca^{2+} and Mg^{2+}) in reducing toxicity e.g. (Zitko 1976; Playle 1998; De Schamphelaere and Janssen 2002; Macdonald, Silk et al. 2002); the role of acidification in modifying toxicity by affecting both the metal's speciation and the metal interactions at biological surfaces e.g. (Campbell and Stokes 1985). Many of the early studies found a correlation between the free ion activity of the metal and the resultant toxicity or bioavailability. These findings were first encoded into models using a chemical equilibrium approach in the early 1980s as the conceptual Free-Ion Activity Model (FIAM) (Morel 1983) or the Gill Surface Interaction Model (GSIM) (Pagenkopf 1983). Both of these models were based on the hypothesis that the metal binds reversibly with some physiologically active surface site, i.e. an equilibrium is rapidly established between the metal free ion in solution and the metal fraction bound to the physiologically active sites. The GSIM was used to successfully describe the acute toxicity of a range of different metals (Cu, Cd, Pb and Zn) in varying water compositions.

Over the past decade, attempts to incorporate these concepts into regulatory water quality standards have resulted in the development of the Biotic Ligand Model (BLM) of acute toxicity. The conceptual basis of the BLM is similar to both the FIAM and GSIM, assuming that the system is at equilibrium to permit the use of thermodynamic and conditional binding constants to calculate the partitioning of the metal between all possible metal species in the system, including the metal bound to the biotic ligand. The model may be considered in terms of three components: the speciation of the metal in the bulk solution, the formation of the metal – biotic ligand complex [M-BL] and the toxic response elicited by the [M-BL]. As for the FIAM or GSIM, the free metal ion is generally considered to be the most toxic metal species, however this concept has been extended within the framework of the BLM to allow for the potential toxicity of other species. A BLM developed for silver toxicity (Paquin, Di Toro et al. 1999) considered both Ag^{+} and $AgCl^{0}$ biotic ligand complexes while a copper BLM (De Schamphelaere and Janssen 2002) included both Cu^{2+} and $CuOH^{+}$ biotic ligand complexes. Similarly, in the case of uranium, an equilibrium model for the valve movement response of an aquatic bivalve (Markich, Brown et al. 2000) considered both UO_2^{2+} and UO_2OH^{+} to be bioreactive.

Biological interfaces such as gill epithelia are characterised by a net negative charge to which cations can bind, due to the dissociation of both the ionisable groups of the membrane phospholipids and the functional groups of membrane embedded proteins. Uptake of metal ions generally occurs via trans-membrane pumps, channels and carriers generically termed transporters. The type of transporter involved in the uptake of a metal determines the nature of the metal-transporter interaction, which can differ significantly. Metal ions transported by trans-membrane channels are conducted through the channel protein without any specific binding to the transporter, or loss of their hydration sphere. However, metal ions transported by carriers (lipid-soluble molecules that bind a metal on one surface of the membrane and migrate to the other surface to release the metal) bind to a specific transport site. The “biotic ligand” is assumed to represent a physiologically active subset of charged membrane surface sites, and the BLM assumes that the metal – biotic ligand interaction can be characterised as a surface adsorption process. Competition for the biotic ligand is assumed to occur between the bioreactive toxic metal species and other cations such as Ca^{2+}, Mg^{2+}, Na^{+} and H^{+}. The modelling requirements to implement a metal BLM

are: knowledge of the solution speciation of the metal (either measured or predicted by a speciation model); values for the binding constants of the bioreactive metal species – biotic ligand complexes (generally these values are conditional on the means used to determine the constants); values for the binding constants of competing cations – biotic ligand complexes. A number of different approaches to the determination of the conditional binding constants of both the toxic metal and competing cations with the biotic ligand have been suggested. These include the direct measurement of the surface adsorbed metal fraction (Playle, Dixon et al. 1993), which is limited by the problem that the biotic ligand represents only the physiologically active subset of the total surface adsorbed metal (with potentially different sorption properties from the non-specific surface sites). Other approaches such as the measurement of physiological end-points (toxic effects, behavioural changes or bioaccumulation of the toxic metal) all require assumptions about the relationship between the fractional coverage of the physiologically active surface sites, and the measured end-point. For example in the case of bioaccumulation the kinetics of the trans-membrane transport of the metal must be assumed to be invariant within the range of conditions to which the model is applied. Similarly in the case of toxicity the dissolved metal LC50, which varies with water chemistry, is assumed to be associated with a fixed critical level of metal accumulation at the biotic ligand (Meyer, Santore et al. 1999).

The equilibrium paradigm has been applied to a wide variety of both experimental and field data and its successes greatly outnumber documented exceptions (Campbell 1995). The approach is very attractive in that it integrates easily with existing and widely used geochemical speciation models. The most convincing experimental evidence for the equilibrium paradigm comes from studies where the concentration of a strong organic chelator is varied and a strong correlation of the free metal ion with metal uptake rate is found. However, for these cases it must be recalled that other composition parameters (e.g. pH, inorganic ligands) are generally kept constant and so all other inorganic metal complexes will co-vary with the free metal ion. Frequently, experimental studies to investigate metal uptake or toxicity are performed in media of constant inorganic ion composition, thus the equilibrium paradigm has not been widely tested with respect to purely inorganic media. Although the equilibrium paradigm has been the favoured approach to modelling metal – organism interactions,

alternatives to this approach exist for cases where the assumption of equilibrium between the bulk solution and the physiologically active surface sites is not valid. Alternative approaches include kinetic models that consider the metal transport and complex association/dissociation kinetics in the diffusion layer of the biological interface (van Leeuwen 1999; van Leeuwen 2001).

There are a number of examples of modelling practice in the literature that should be avoided. In many cases analytical methods to directly measure the speciation of the metal do not exist or are impractical. The speciation of the metal therefore needs to be predicted by a mathematical model as described in section 4. The thermodynamic parameters required for modelling the speciation need to be treated as model constants and not modified in light of the observed biological response behaviour. This is not always the case, for example metal binding affinity constants for a natural dissolved organic matter were treated as adjustable fitting parameters in the development of fish GSIM's for both cobalt (Richards and Playle 1998) and lead (Macdonald, Silk et al. 2002). The development of a model to describe biological response to varying solution composition should be reactive to the observed behaviour, rather than trying to fit the data to a preconceived dogma. An example of modelling practice that does not follow this principle is the study of the effect of magnesium on the accumulation of silver by the rainbow trout *Oncorhynchus mykiss* (Schwartz and Playle 2001). No inhibition of uptake for a range of magnesium concentration of up to 210 mM was observed. The authors however, chose to include a Mg-gill stability constant in their Silver-gill binding model. Another example is a study performed to investigate zinc toxicity mitigation by calcium and magnesium to *Daphnia magna* (Heijerick, De Schamphelaere et al. 2002). In this study a reduction to toxicity on increasing calcium and magnesium concentrations was observed, but only for concentrations of up to 2 mM for magnesium and 3 mM for calcium. The authors used only the lower concentration ranges for determining biotic ligand model affinity constants for these two metals, considering the model to be inapplicable to the higher concentration ranges. It is also important to avoid factors that can potentially confound interpretation of the results. For example, in order to vary the concentration of one solution component, it is necessary to vary the concentration of at least one other component (either a component of same charge whilst maintaining the ionic strength constant, or a component of opposite charge and varying the ionic strength). An

example of the difficulty in interpreting the effects of cation competition when ionic strength is co-varied with the range of cation concentration is discussed in section 6.5.4. The toxicity of copper to *Daphnia magna* (De Schamphelaere and Janssen 2002) was found to be mitigated by calcium, magnesium and sodium, attributed to the antagonistic competition for binding sites by the authors. However, on inspection of these results the interpretation of the dataset is confounded by the fact that ionic strength was not maintained at a constant value, and in fact can be used as a simpler and equally good parameter to explain the changes in observed toxicity.

5.2 Modelling Uranium Accumulation: State Of The Art And Developments

As described in section 5.1 the understanding of how trace metals interact with aquatic organisms has evolved considerably over the past thirty years. Different implementations of equilibrium based metal – organism interaction models have used more or less restrictive assumptions of the underlying physical and physiological processes. Any attempt to relate the physico-chemical properties of the bulk solution to a metal's bioavailability needs to account for (Figure 5-1):

1. the mass transport of the metal from the bulk solution to the biological interface;
2. the speciation of the metal in the micro-environment of the biological interface;
3. the surface complexation of the metal with the physiologically active membrane ligands;
4. the trans-membrane internalisation of the metal-carrier complex.

5.2.1 Pre-equilibrium approaches

Equilibrium or steady-state modelling approaches such as the FIAM, GSIM or BLM all rely on a number of assumptions.

1. the rate-limiting step of the metal bioaccumulation is the internalisation by membrane transporters;

2. the internalisation kinetics are first order or pseudo first order;
3. the mass transport of the metal from the bulk solution to the biological interface is not rate-limiting;
4. the metal speciation in the immediate vicinity of the biological interface is not significantly different from that of the bulk solution;
5. rapid equilibrium is established between the metal species in the immediate vicinity of the interface and the membrane ligands ($\equiv X^{n-}$);
6. for a fixed solution composition the surface activity of the metal – membrane ligand site is constant (the steady state approximation);
7. no significant modification of the biological interface occurs (e.g. both the density and nature of the membrane transporters remains constant for all investigated conditions);
8. no significant changes to biological regulation are induced by either the metal binding to transporter sites or changes to other investigated parameters (e.g. pH, other metal ions concentrations).

Figure 5-1 Processes involved in the bioaccumulation of uranium.

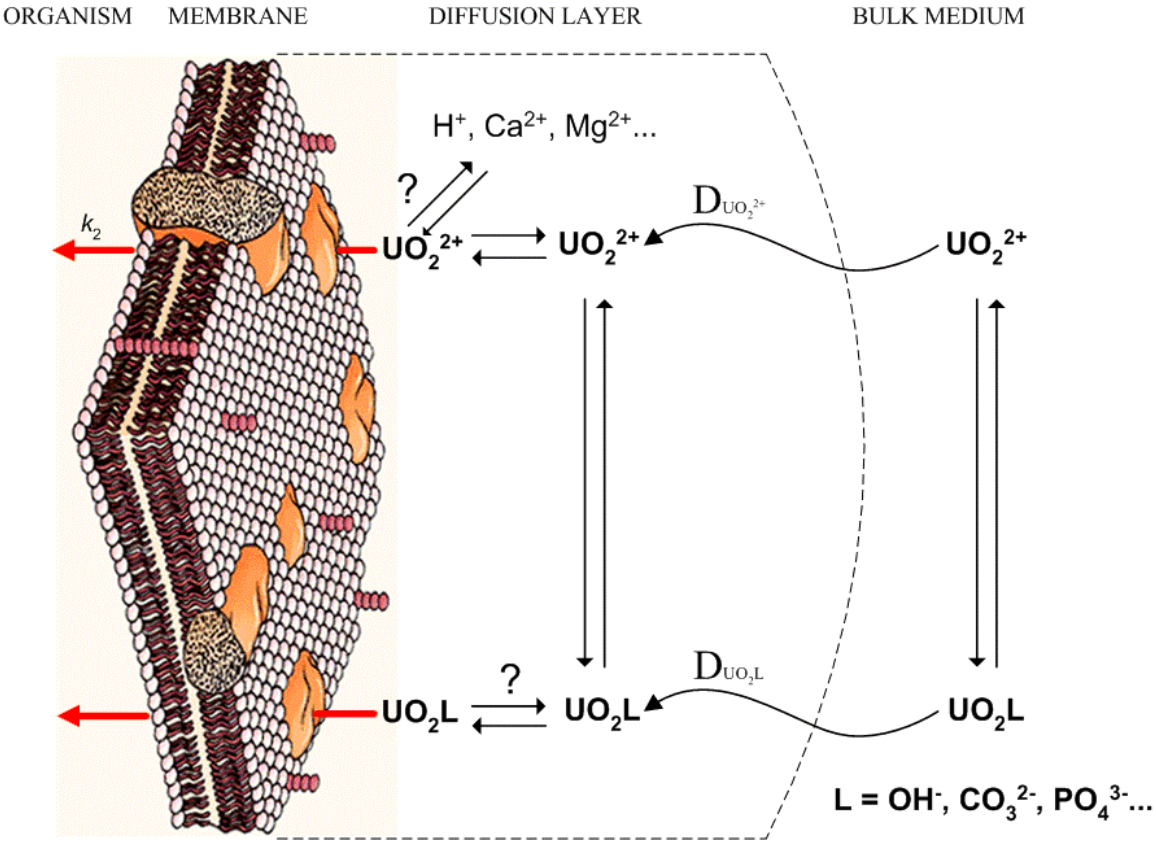

D_M diffusion coefficient of metal ion, M

D_{ML} diffusion coefficient of metal complex, ML

k_2 trans-membrane internalisation kinetic rate constant

Thus the overall bioaccumulation kinetics can be described by:

$$\mathrm{UO_2^{2+}} + \equiv X^{n-} \underset{k_{-1}}{\overset{k_1}{\rightleftharpoons}} \equiv X - \mathrm{UO_2^{2\text{-}n}} \xrightarrow{k_2} \equiv X^{n-} + \left\langle \mathrm{UO_2} \right\rangle_{\mathrm{int}} \tag{5-1}$$

There are no analytical solutions to the rate equations describing the concentration changes of the three components over time, so the steady-state approximation is used, i.e. the activity of the surface complex, $\left\{\equiv X - \mathrm{UO_2^{2\text{-}n}}\right\}$, remains constant.

$$\frac{d\left\{\equiv X - \mathrm{UO_2^{2\text{-}n}}\right\}}{dt} = k_1 \left\{\equiv X^{n-}\right\} \alpha_{\mathrm{UO_2^{2+}}} - \left(k_{-1} + k_2\right) \cdot \left\{\equiv X - \mathrm{UO_2^{2\text{-}n}}\right\} = 0 \tag{5-2}$$

The activity of the surface complex, $\left\{\equiv X - \mathrm{UO_2^{2\text{-}n}}\right\}$, is therefore given by:

$$\left\{\equiv X - \mathrm{UO_2^{2\text{-}n}}\right\} = \frac{k_1}{k_{-1} + k_2} \left\{\equiv X^{n-}\right\} \alpha_{\mathrm{UO_2^{2+}}} \tag{5-3}$$

If $k_{-1} >> k_2$, as assumed by the pre-equilibrium approximation, the activity of the surface complex is therefore:

$$\left\{\equiv X - \mathrm{UO_2^{2\text{-}n}}\right\} \approx \frac{k_1}{k_{-1}} \left\{\equiv X^{n-}\right\} \alpha_{\mathrm{UO_2^{2+}}} \approx K_{\mathrm{UO_2^{2+}}} \left\{\equiv X^{n-}\right\} \alpha_{\mathrm{UO_2^{2+}}} \tag{5-4}$$

where $K_{\mathrm{UO_2^{2+}}}$ is the formation constant of the surface complex and the symbols $\{\ \}$ refer to the activities of the surface species. The affinity of this interaction is assumed to not be dependant on the solution composition.

From equation (5-1) the bioaccumulation flux rate, $\frac{d\left\langle \mathrm{UO_2} \right\rangle_{\mathrm{int}}}{dt}$, is:

$$\frac{d\left\langle \mathrm{UO_2} \right\rangle_{\mathrm{int}}}{dt} = k_2 \cdot \left\{\equiv X - \mathrm{UO_2^{2\text{-}n}}\right\} \tag{5-5}$$

And substituting $\left\{\equiv X - \mathrm{UO_2^{2\text{-}n}}\right\}$ from equation (5-4) yields:

$$\frac{d\left\langle \mathrm{UO_2} \right\rangle_{\mathrm{int}}}{dt} = k_2 \cdot K_{\mathrm{UO_2^{2+}}} \cdot \left\{\equiv X^{n-}\right\} \cdot \alpha_{\mathrm{UO_2^{2+}}} \tag{5-6}$$

All implementations of equilibrium based metal bioaccumulation models are built from this rate equation, using different hypotheses as to the bioreactive metal species

that may form surface complexes and the variation in activity of the free surface sites (for example by competition with other cations).

If the activity of free surface sites, $\left\{\equiv X^{n-}\right\}$ remains nearly constant for the range of metal concentration and solution composition of interest, then the activity of the surface complex $\left\{\equiv X-\mathrm{UO}_2^{2\text{-n}}\right\}$ and hence the bioaccumulation flux rate is simply proportional to the free metal ion activity:

$$\frac{d\left\langle \mathrm{UO}_2\right\rangle_{\mathrm{int}}}{dt}=\text{constant}\cdot\alpha_{\mathrm{UO}_2^{2+}} \tag{5-7}$$

If, however, the fraction of the total surface sites occupied by the metal surface complex becomes significant, the change in activity of free surface sites, $\left\{\equiv X^{n-}\right\}$ needs to be accounted for by the mass action law:

$$\left\{\equiv X\right\}_T=\left\{\equiv X-\mathrm{UO}_2^{2\text{-n}}\right\}+\left\{\equiv X^{n-}\right\} \tag{5-8}$$

Combining equations (5-3) and (5-8) gives an explicit expression for the activity of the surface complex:

$$\left\{\equiv X-\mathrm{UO}_2^{2\text{-n}}\right\}=\frac{K_{\mathrm{UO}_2^{2+}}\cdot\left\{\equiv X\right\}_T\cdot\alpha_{\mathrm{UO}_2^{2+}}}{1+K_{\mathrm{UO}_2^{2+}}\cdot\alpha_{\mathrm{UO}_2^{2+}}} \tag{5-9}$$

Which is a hyperbolic function often termed the occupancy relation, and has the same form as the Langmuir adsorption isotherm. Combining equations (5-5) and (5-9) gives the bioaccumulation flux rate:

$$\frac{d\left\langle \mathrm{UO}_2\right\rangle_{\mathrm{int}}}{dt}=\frac{k_2\cdot K_{\mathrm{UO}_2^{2+}}\cdot\left\{\equiv X\right\}_T\cdot\alpha_{\mathrm{UO}_2^{2+}}}{1+K_{\mathrm{UO}_2^{2+}}\cdot\alpha_{\mathrm{UO}_2^{2+}}} \tag{5-10}$$

This relationship, derived from the most restrictive hypotheses of the chemical equilibrium approach to modelling metal bioavailability, is the simplest relationship between the free metal ion and the bioaccumulation flux rate. The equation reduces to the linear approximation as already described (5-7) with the conditions that the fraction of the total surface sites occupied by the metal surface complex is small, i.e. $\left\{\equiv X-\mathrm{UO}_2^{2\text{-n}}\right\} << \left\{\equiv X^{n-}\right\}$ and no other factors (e.g. pH, $[Ca^{2+}]$, $[Mg^{2+}]$…) influence the activity of the free surface sites.

5.2.1.1 Competitive inhibition by other cations

The potential for other cations to competitively bind to the free surface sites can be introduced into the modelling framework by modifying the mass action equation (5-8) and defining the appropriate pre-equilibrium equation with the same form as (5-2) to (5-4). For the case of H^+ competition equation (5-8) is modified to:

$$\left\{\equiv X\right\}_T = \left\{\equiv X - \mathrm{UO_2^{2\text{-}n}}\right\} + \left\{\equiv X - \mathrm{H}\right\} + \left\{\equiv X^{n-}\right\} \tag{5-11}$$

and the equilibrium equation is:

$$\left\{\equiv X - \mathrm{H}\right\} = K_H \cdot \left\{\equiv X^{n-}\right\} \cdot \alpha_{\mathrm{H^+}} \tag{5-12}$$

where K_H is the formation constant of the proton – surface complex. Combining equations (5-4), (5-11) and (5-12) yields the modified expression for the activity of the surface complex:

$$\left\{\equiv X - \mathrm{UO_2^{2\text{-}n}}\right\} = \frac{K_{\mathrm{UO_2^{2+}}} \cdot \left\{\equiv X\right\}_T \cdot \alpha_{\mathrm{UO_2^{2+}}}}{1 + K_H \cdot \alpha_{\mathrm{H^+}} + K_{\mathrm{UO_2^{2+}}} \cdot \alpha_{\mathrm{UO_2^{2+}}}} \tag{5-13}$$

and substitution into (5-5) gives the competitive bioaccumulation flux rate equation:

$$\frac{d\left\langle \mathrm{UO_2} \right\rangle_{\mathrm{int}}}{dt} = \frac{k_2 \cdot K_{\mathrm{UO_2^{2+}}} \cdot \left\{\equiv X\right\}_T \cdot \alpha_{\mathrm{UO_2^{2+}}}}{1 + K_H \cdot \alpha_{\mathrm{H^+}} + K_{\mathrm{UO_2^{2+}}} \cdot \alpha_{\mathrm{UO_2^{2+}}}} \tag{5-14}$$

5.2.1.2 Internalisation of metal species additional to the free metal ion

The possibility of there being bioreactive metal species other than just the free metal ion, as permitted by the BLM, can be incorporated into the equilibrium modelling framework in two different ways. It can either be assumed that all bioreactive species compete for the same physiologically active membrane ligands, or alternatively that different transport systems are responsible for the accumulation of the different bioreactive species. For the first hypothesis the relevant mass action equation for the addition of a second bioreactive species $\left\{\equiv X - \mathrm{UO_2B}\right\}$ is:

$$\left\{\equiv X\right\}_T = \left\{\equiv X - \mathrm{UO_2^{2\text{-}n}}\right\} + \left\{\equiv X - \mathrm{UO_2B}\right\} + \left\{\equiv X^{n-}\right\} \tag{5-15}$$

and the equilibrium equation is:

$$\{\equiv X-\mathrm{UB}\} = K_{\mathrm{UO_2B}} \cdot \{\equiv X^{n-}\} \cdot \alpha_{\mathrm{UB}} \tag{5-16}$$

where $K_{\mathrm{UO_2B}}$ is the formation constant of the secondary bioreactive uranium species – surface complex. From equations (5-4), (5-15) and (5-16) the activities of the two bioreactive surface complexes are therefore:

$$\{\equiv X-\mathrm{UO_2^{2\text{-}n}}\} = \frac{K_{\mathrm{UO_2^{2+}}} \cdot \{\equiv X\}_T \cdot \alpha_{\mathrm{UO_2^{2+}}}}{1 + K_{\mathrm{UO_2^{2+}}} \cdot \alpha_{\mathrm{UO_2^{2+}}} + K_{\mathrm{UO_2B}} \cdot \alpha_{\mathrm{UO_2B}}} \tag{5-17}$$

$$\{\equiv X-\mathrm{UO_2B}\} = \frac{K_{\mathrm{UO_2B}} \cdot \{\equiv X\}_T \cdot \alpha_{\mathrm{UO_2B}}}{1 + K_{\mathrm{UO_2^{2+}}} \cdot \alpha_{\mathrm{UO_2^{2+}}} + K_{\mathrm{UO_2B}} \cdot \alpha_{\mathrm{UO_2B}}}$$

Assuming that the internalisation rate constant is the same for both bioreactive surface complexes, this leads to a bioaccumulation flux rate equation for two bioreactive metal species of:

$$\frac{d\langle \mathrm{UO_2}\rangle_{\mathrm{int}}}{dt} = k_2\left(\{\equiv X-\mathrm{UO_2^{2\text{-}n}}\} + \{\equiv X-\mathrm{UO_2B}\}\right) \tag{5-18}$$

$$\frac{d\langle \mathrm{UO_2}\rangle_{\mathrm{int}}}{dt} = \frac{k_2 \cdot \{\equiv X\}_T \cdot \left(K_{\mathrm{UO_2^{2+}}} \cdot \alpha_{\mathrm{UO_2^{2+}}} + K_{\mathrm{UO_2B}} \cdot \alpha_{\mathrm{UO_2B}}\right)}{1 + K_{\mathrm{UO_2^{2+}}} \cdot \alpha_{\mathrm{UO_2^{2+}}} + K_{\mathrm{UO_2B}} \cdot \alpha_{\mathrm{UO_2B}}}$$

If the second hypothesis is taken, i.e. that different transport systems are responsible for the accumulation of the different bioreactive species, then equation (5-1) needs to be modified to allow for this parallel accumulation scheme:

$$\mathrm{UO_2^{2+}} + \equiv X^{n-} \overset{K_{\mathrm{UO_2^{2+}}}}{\rightleftharpoons} \equiv X-\mathrm{UO_2^{2\text{-}n}} \overset{k_2}{\rightarrow} \equiv X^{n-} + \langle \mathrm{UO_2}\rangle_{\mathrm{int}} \tag{5-19}$$

$$\mathrm{UO_2B} + \equiv X' \overset{K_{\mathrm{UO_2B}}}{\rightleftharpoons} \equiv X'-\mathrm{UO_2B} \overset{k_3}{\rightarrow} \equiv X' + \langle \mathrm{UO_2}\rangle_{\mathrm{int}}$$

leading to a modification of equation (5-5) to give the new bioaccumulation flux rate equation:

$$\frac{d\langle \mathrm{UO_2}\rangle_{\mathrm{int}}}{dt} = k_2 \cdot \{\equiv X-\mathrm{UO_2^{2\text{-}n}}\} + k_3 \cdot \{\equiv X'-\mathrm{UB}\} \tag{5-20}$$

In this case the activities of the two bioreactive surface complexes are independent of one another:

$$\left\{\equiv X-\mathrm{UO_2^{2\text{-}n}}\right\}=\frac{K_{\mathrm{UO_2^{2+}}}\cdot\left\{\equiv X\right\}_T\cdot\alpha_{\mathrm{UO_2^{2+}}}}{1+K_{\mathrm{UO_2^{2+}}}\cdot\alpha_{\mathrm{UO_2^{2+}}}} \tag{5-21}$$

$$\left\{\equiv X'-\mathrm{UO_2B}\right\}=\frac{K_{\mathrm{UO_2B}}\cdot\left\{\equiv X'\right\}_T\cdot\alpha_{\mathrm{UO_2B}}}{1+K_{\mathrm{UO_2B}}\cdot\alpha_{\mathrm{UO_2B}}}$$

Leading to the bioaccumulation flux rate equation for the two independent bioreactive metal species of:

$$\frac{d\left\langle\mathrm{UO_2}\right\rangle_{\mathrm{int}}}{dt}=\frac{k_2\cdot\left\{\equiv X\right\}_T\cdot K_{\mathrm{UO_2^{2+}}}\cdot\alpha_{\mathrm{UO_2^{2+}}}}{1+K_{\mathrm{UO_2^{2+}}}\cdot\alpha_{\mathrm{UO_2^{2+}}}}+\frac{k_3\cdot\left\{\equiv X'\right\}_T\cdot K_{\mathrm{UO_2B}}\cdot\alpha_{\mathrm{UO_2B}}}{1+K_{\mathrm{UO_2B}}\cdot\alpha_{\mathrm{UO_2B}}} \tag{5-22}$$

5.2.2 Alternatives to the equilibrium paradigm

The list of assumptions required for the development of steady-state models detailed at the start of section 5.2.1 may be questioned in several ways. For convenience these will be addressed under two broad categories: kinetic and metal – transporter stability considerations.

5.2.2.1 Kinetic considerations.

The implications of the assumptions of the equilibrium paradigm for the transport kinetics of metal accumulation need to be addressed at two stages of the transport process: the mass transport of the metal from the bulk solution to the biological interface and the trans-membrane internalisation of the metal-carrier complex. The transport of the metal from the bulk solution to the close vicinity of the biological interface is a diffusion process that, from assumptions 1 and 3 (section 5.2.1), is assumed not to be rate determining for the pre-equilibrium modelling approaches. If diffusion limits the metal flux rate, the kinetics of the ligand exchange reactions in the diffusive boundary layer will be significant in controlling the rate of formation of the metal – transporter complex. If this is the case then the uptake kinetics will depend on the near surface concentrations of kinetically labile species rather than the free metal ion. Distinguishing diffusion limitation from biological transport limitation is potentially difficult if the exchange kinetics of the different complexing ligands investigated and the diffusion rates of the formed metal complexes vary significantly. An observed metal uptake dependence on solution composition may be a function of

the lability of metal – ligand complexes formed rather than the equilibrium control of the formation of the metal – transporter surface complex assumed by the equilibrium paradigm. Non-equilibrium conditions could change the apparent rate-controlling species for metal uptake. Modelling the dynamics of metal flux rates across an uptake determining diffusion boundary layer and the metal complexes association/disassociation kinetics requires knowledge of these complexes diffusion coefficients and ligand exchange rate constants. Except for the simplest systems, these parameters are generally unknown and so a rigorous treatment is impossible.

If however the transport is indeed limited by the trans-membrane internalisation of the metal-carrier complex, the rate constant of this process will be determining for the metal uptake. The equilibrium paradigm assumes that the kinetic rate constant for this process is invariant within the range of physico-chemical conditions to which the model is calibrated and applied. This assumption may be invalid depending on both the different physico-chemical parameters considered by the model and the nature of the uptake process. For example, both pH and ionic strength influence the trans-membrane potential difference and hence the conductance of ion channels (in addition to the pH effects on both the metal's speciation and protonation/deprotonation reactions of the functional groups within the ion transport system). Factors that affect membrane fluidity (such as temperature) will also directly affect membrane proteins involved in ion transport, including both ATPases and particularly carrier molecules. Physiological regulation processes such as changes in ATPase activity resulting from ion homeostasis will also directly influence the internalisation dynamics of the metal, if these transport pathways are implicated in its uptake. If the assumption of pre-equilibrium of the metal – transporter complex is satisfied, but the kinetics of the trans-membrane metal transport depends on an investigated parameter, the accumulation rate equation (5-5) must modified. For example, if the solution pH affects the kinetics of the trans-membrane metal transport, the accumulation rate equation (5-5) is modified by replacing the rate constant k_2 with a parameter dependent on pH:

$$\frac{d\left\langle \mathrm{UO_2} \right\rangle_{\mathrm{int}}}{dt} = k_2^{(pH)} \cdot \left\{ \equiv X - \mathrm{UO_2^{2\text{-}n}} \right\} \tag{5-23}$$

As the assumption of pre-equilibrium is still valid, expressions for the activity of the metal-carrier complex can be derived as previously shown to account for the effects of

the metal's speciation, competition with other cations for the transporter binding site etc.

5.2.2.2 Metal – transporter stability considerations

A number of the assumptions used to develop pre-equilibrium models may be questioned with respect to the stability constant of the metal – transporter complex. In the preceding sections the interaction of the metal with the biosurface is assumed to be a surface complexation process with physiologically active membrane ligands that are equivalent and independent of each other. These transporter binding sites are also assumed to remain constant both in number and nature. Additionally the metal speciation in the immediate vicinity of the biosurface is assumed to be identical to that of the bulk solution. Obviously, any changes to the number of available transporter binding sites will strongly influence the uptake dynamics; such changes may result from the induction of transporter proteins in response to concentration changes of a regulated metal for example. The assumption that the sites are all equivalent and independent may be inadequate if several transport pathways are implicated in the metal uptake. Chemical heterogeneity of binding sites is commonly observed for the sorption behaviour of natural organic matter for example and a number of different modelling approaches are available to describe this behaviour. Adsorption enthalpies typically become less negative as surface coverage increases, as the energetically most favourable sites are occupied first. To describe adsorption where the adsorption enthalpy changes as a function of the fractional coverage of the sites, a number of empirical isotherm models are available, such as the Temkin isotherm (assumes that adsorption enthalpy changes linearly with coverage) or the Freundlich isotherm (which assumes a logarithmic change). These models do not permit the incorporation of competitive binding effects and so are inadequate in this case. Another approach that enables the effects of competitive adsorption to be incorporated is by approximating the distribution of binding site enthalpies with a series of discrete sites of different enthalpies and fractional coverage's. This approach results in a multi-site Langmuir adsorption isotherm (House and Denison 2000) but obviously the number of adjustable parameters in the model are increased significantly.

The assumption that the metal speciation in the immediate vicinity of the biosurface is identical to that of the bulk solution is a simplification that may have significant implications for the model. As is the case for all charged surfaces, the ionic environment in the vicinity of the biological interface is different to that of the bulk solution: an electrical double layer is formed of the charged surface and the diffuse cloud of oppositely charged ions (counterions). In general terms, the layer of counterions consists of ions more or less attached to the surface (the Stern layer) and a more diffuse (Gouy) layer in which the ions are more mobile. Several different mathematical models to describe the structure of the double layer exist including the constant capacitance, diffuse double-layer and triple-layer models. Factors that can influence the ionic environment at the biosurface include the equilibria responsible for the surface charge (e.g. the protonation – deprotonation equilibria of the surface functional groups and surface complexes formed with other ions) and the ionic strength of the solution. The surface charge potential of the membrane is not necessarily related to the charge of the binding site of the transporter due to the much higher site density of non-specific sites e.g. the membrane phospholipids. The structure of the electrical double layer has obvious consequences for the formation of the metal – membrane transporter complex, as the activity of the metal species at the biosurface will differ from that of the bulk solution. Although the biosurface is not homogeneous, i.e. there are a wide variety of surface functional groups, an approaching species will feel the net effect of these point charges as if the surface were electrically homogeneous. The effect of this phenomenon on the process of metal uptake is to modify the apparent affinity of the metal – membrane transporter complex formation in function of parameters that modify the ionic environment at the biosurface. The free energy change for the process of a surface adsorption has components of the chemical free energy change and the Coulombic free energy change, i.e.

$$\Delta G_{ads} = \Delta G_{chem} + \Delta G_{coul} \tag{5-24}$$

The intrinsic formation constant is related to the chemical Gibbs free energy change by the standard relation (4-15):

$$\log_{10} K_{ads} = -\frac{\Delta G_{chem} \cdot \log_{10}(e)}{R \cdot T} \tag{5-25}$$

and the apparent formation constant, K'_{ads}, includes the Coulombic term:

$$\log_{10} K'_{ads} = \log_{10} K_{ads} - \frac{\Delta G_{coul} \cdot \log_{10}(e)}{R \cdot T} \tag{5-26}$$

As the principal factors that influence the structure of the electrical double layer are the pH and ionic strength, the equilibrium constant, $K_{UO_2^{2+}}$ in equation (4-1) now becomes a function of these parameters giving:

$$\frac{d\langle UO_2 \rangle_{int}}{dt} = \frac{k_2 \cdot K_{UO_2^{2+}}^{(pH,I)} \cdot \{\equiv X\}_T \cdot \alpha_{UO_2^{2+}}}{1 + K_{UO_2^{2+}}^{(pH,I)} \cdot \alpha_{UO_2^{2+}}} \tag{5-27}$$

5.2.3 Model hypotheses tested in this study

As described in the previous sections, a number of different plausible hypotheses can be proposed to describe the mechanisms involved in the transfer of metals from the bulk solution, across a biological interface to the interior of an organism. In order to investigate the likelihood of these different hypotheses for the uptake of uranium observed in the experiments performed in this study, a multi-hypotheses approach was adopted. A number of different models were applied to the experimental results in order to assess the likelihood of each of the different hypotheses outlined above. This series of models was developed starting with the most restrictive hypotheses of the pre-equilibrium paradigm, resulting in the simplest "pure" BLM models, progressively relaxing the physical and physiological hypotheses leading to increasingly complex and flexible models. The different hypotheses tested were:

- Free uranyl ion the only bioavailable species
- Free uranyl ion and a second uranyl complex bioavailable
- Free uranyl ion and two other uranyl complexes bioavailable
- Single homogeneous and independent transporter surface site
- Different transporter surface sites specific to each bioavailable species
- Proton / cation competition for binding site(s)
- Pre-equilibrium of metal-transporter complex(es), internalisation rate determining and first order

- Pre-equilibrium of metal-transporter complex(es), internalisation rate determining and dependent on pH
- Pre-equilibrium of metal-transporter complex(es), metal – transporter stability dependent on pH

Full details of all the tested models are given in section 7.3.1.

5.3 Principles Of Data Modelling

There are several possible objectives to fitting a mathematical model to an observed dataset, ranging from simply codifying the data with an entirely empirical model (that fits the data well), to attempts to elucidate the underlying physical processes by fitting mechanistically derived models. For this study the second objective is paramount, i.e. from the obtained dataset of observed behaviour the adjustable parameters of each proposed model need to be optimised in order to obtain the "best-fit" to the data and with these parameter values a statistical measure of "goodness of fit" of the model needs to be calculated. The general approach to fitting a mathematical model to a dataset is to design a merit function that measures the agreement between the data and the model with a particular choice of parameters. Small values of the merit function conventionally indicate close agreement to the data. The model parameters are then adjusted to achieve a minimum in the merit function yielding the best-fit parameters; hence the problem is one of multi-dimensional minimisation.

5.3.1 Chi-square minimisation as a maximum likelihood estimator

The most commonly applied merit function is based on the least squares maximum likelihood estimator. A model with M adjustable parameters a_j, $j = 1,\ldots,M$, is fitted to N data points (x_i,y_i) $i = 1,\ldots,N$, where the model predicts a functional relationship between the measured independent and dependent variables:

$$y(x) = y(x; a_1,..., a_M) \tag{5-28}$$

Assuming that each data point y_i has a normally distributed independently random measurement error around the true model (of standard deviation σ_i), the set of model parameters that give the maximal probability for the obtained data set is obtained by minimising the chi-square function:

$$\chi^2 \equiv \sum_{i=1}^{N} \left[\frac{y_i - y(x_i; a_1, ..., a_M)}{\sigma_i} \right]^2 \tag{5-29}$$

5.3.1.1 Multidimensional nonlinear least-squares parameter fitting

For models that depend nonlinearly on the set of M unknown parameters the minimisation of the chi-square merit function must proceed iteratively from initial trial values for the parameters. The most commonly applied method of parameter optimisation for nonlinear models is the Levenberg-Marquardt method (Marquardt 1963). This method is based on approximating the χ^2 function close to the minimum by a quadratic form (a truncated Taylor series):

$$\chi^2\left(\mathbf{a^{n+1}}\right) \approx \gamma - \mathbf{d}\cdot\mathbf{a^{n+1}} + \frac{1}{2}\mathbf{a^{n+1}}\cdot\mathbf{D}\cdot\mathbf{a^{n+1}} \tag{5-30}$$

$$\gamma \equiv \chi^2\left(\mathbf{a^n}\right) \quad \mathbf{d} \equiv -\nabla\chi^2\,|_{\mathbf{a^n}} \qquad [\mathbf{D}]_{kl} \equiv \left.\frac{\partial^2\chi^2}{\partial a_k \partial a_l}\right|_{\mathbf{a^n}}$$

where **a** is the trial vector (the approximation of the chi-square minimum values of the M parameters), **d** is an M vector and **D** is an $M \times M$ matrix whose components are the second partial derivative matrix of the χ^2 function (the Hessian matrix of the χ^2 function at **a)**. If the approximation is sufficiently close to the solution (and the quadratic approximation is a good one) the trial solution can be improved by iterating:

$$\mathbf{a^{n+1}} = \mathbf{a^n} + \mathbf{D^{-1}}\cdot\left[-\nabla\chi^2\left(\mathbf{a^n}\right)\right] \tag{5-31}$$

However, if the shape of the χ^2 function is poorly approximated by the quadratic form at $\mathbf{a^n}$ then the best approach is to proceed down the gradient, i.e.

$$\mathbf{a^{n+1}} = \mathbf{a^n} - \alpha\cdot\nabla\chi^2\left(\mathbf{a^n}\right) \tag{5-32}$$

Where the constant α is sufficiently small not to exhaust the downhill direction. The gradient of χ^2 with respect to the parameters **a** (zero at the χ^2 minimum), has components:

$$\frac{\partial\chi^2}{\partial a_k} = -2\sum_{i=1}^{N} \frac{\left[y_i - y(x_i;\mathbf{a})\right]}{\sigma_i^2} \frac{\partial y(x_i;\mathbf{a})}{\partial a_k} \quad k = 1, ..., M \tag{5-33}$$

And the second partial derivative gives

$$\frac{\partial^2 \chi^2}{\partial a_k \partial a_l} = 2\sum_{i=1}^{N} \frac{1}{\sigma_i^2}\left[\frac{\partial y(x_i;\mathbf{a})}{\partial a_l}\frac{\partial y(x_i;\mathbf{a})}{\partial a_k} - \left[y_i - y(x_i;\mathbf{a})\right]\frac{\partial^2 y(x_i;\mathbf{a})}{\partial a_k \partial a_l}\right] \tag{5-34}$$

defining:

$$\beta_k \equiv -\frac{1}{2}\frac{\partial \chi^2}{\partial a_k} \qquad \varepsilon_{kl} \equiv \frac{1}{2}\frac{\partial^2 \chi^2}{\partial a_k \partial a_l} \tag{5-35}$$

Making [ε] = ½**D** in equation (5-31), allows (5-31) to be rewritten as the set of linear equations:

$$\mathbf{D}\left(\mathbf{a^{n+1}} - \mathbf{a^n}\right) = -\nabla\chi^2\left(\mathbf{a^n}\right) \tag{5-36}$$

$$\sum_{l=1}^{M} \varepsilon_{kl}\delta a_l = \beta_k$$

This set is solved for the increments δa_l, which added to the current approximation, gives the next. Equation (5-32), the gradient descent, translates to

$$\delta a_l = 2 \cdot \alpha \cdot \beta_l \tag{5-37}$$

The Levenberg-Marquardt method uses the steepest descent method (5-37) when far from the minimum, switching to the inverse-Hessian method (5-36) as the minimum is approached. As is evident from equation (5-29) the quantity χ^2 is dimensionless, however β_k has dimensions of $1/a_k$ and hence the constant of proportionality between β_k and δa_k must have the dimensions of a_k^2. The component $1/\varepsilon_{kk}$, the reciprocal of the diagonal element of [ε], has the same dimensions as a_k^2 and so can be used to set the scale of the constant. Setting the constant $2\cdot\alpha$ in equation (5-37) to this value divided by a scaling parameter λ yields:

$$\delta a_l = \frac{1}{\lambda \cdot \varepsilon_{ll}} \cdot \beta_l \qquad \text{or} \qquad \lambda \cdot \varepsilon_{ll} \cdot \delta a_l = \beta_l \tag{5-38}$$

It is required that ε_{ll} is positive, however the components ε_{kl} of the Hessian matrix (5-34) depend on both the first and second derivatives of the model function with respect to the adjustable parameters. The second derivative term may be ignored when it is negligible compared to the first derivative term. The term multiplying the second derivative in equation (5-34) is $[y_i - y(x_i;\mathbf{a})]$ which, for an ideal model, is just the

random measurement error of each point. Therefore the second derivative terms tend to cancel out when summed over *i*, and can be reasonably neglected:

$$\varepsilon_{kl} \approx \sum_{i=1}^{N} \frac{1}{\sigma_i^2} \left[\frac{\partial y(x_i;\mathbf{a})}{\partial a_l} \frac{\partial y(x_i;\mathbf{a})}{\partial a_k} \right] \tag{5-39}$$

This redefinition of ε_{kl} guarantees that ε_{ll} is positive. Defining a new matrix ε' by:

$$\begin{aligned} \varepsilon'_{jj} &\equiv \varepsilon_{jj}(1+\lambda) \\ \varepsilon'_{jk} &\equiv \varepsilon_{jk} \qquad (j \neq k) \end{aligned} \tag{5-40}$$

allows both equations (5-38) and (5-36) to be replaced with:

$$\sum_{l=1}^{M} \varepsilon'_{kl} \delta a_l = \beta_k \tag{5-41}$$

When λ is very large, the matrix ε' is forced into being diagonally dominant so that equation (5-41) reduces to (5-38), but as λ approaches zero (5-41) becomes (5-36), hence the magnitude of the scaling parameter λ can be used to vary smoothly between the extremes of the inverse-Hessian and steepest descent methods. The method is started with initial trial values for the adjustable parameters **a**, $\chi^2(\mathbf{a})$ and equation (5-41) are evaluated with a small value of λ (say $\lambda = 10^{-3}$) to solve for $\delta\mathbf{a}$, and $\chi^2(\mathbf{a} + \delta\mathbf{a})$ is evaluated. If $\chi^2(\mathbf{a} + \delta\mathbf{a}) \geq \chi^2(\mathbf{a})$ then λ is increased by a selected factor (say 10) and the process repeated, or if $\chi^2(\mathbf{a} + \delta\mathbf{a}) < \chi^2(\mathbf{a})$ then λ is decreased by the selected factor, the trial solution **a** is updated ($\mathbf{a^{n+1}} = \mathbf{a^n} + \delta\mathbf{a}$) and the process repeated. Iteration is continued until a chi-square minimum within specified precision or a specified maximum number of iterations are reached. As was the case for the methods used to calculate speciation (multidimensional root finding of a nonlinear set of equations) there is no guarantee that the global χ^2 minimum will be found, the initial trial solution must be sufficiently close to the minimum and the fitted function must be suitable (i.e. an appropriate model). Once the acceptable chi-squared minimum is obtained, λ is set to zero and the estimated covariance matrix, [*C*], is calculated from (5-41) where

$$[C] \equiv [\varepsilon]^{-1} \tag{5-42}$$

If the chi-squared value obtained with the best-fit parameters is sufficiently small to indicate a good model fit (see section 5.3.1.2), the standard errors on the fitted parameters can be estimated from the square roots of the diagonal elements of [*C*].

5.3.1.2 Model selection: choosing between multiple hypotheses

Once the above fitting procedure has been applied for each of the tested models, and optimal values for each model's parameters have been found, the appropriateness of each different model needs to be assessed; the chi-square merit function residual obtained with the best-fit parameters needs to be tested against some statistical standard. It is not possible to calculate the probability that a particular model is "correct": there is no statistical universe of models from which the parameters are drawn, there is just one correct model, and a statistical universe of data sets that are drawn from it. However, it *is* possible to calculate the probability of obtaining a particular dataset given a particular model and set of parameters. If the probability of obtaining the dataset is small, then either the model or the model's parameters are unlikely to be correct, or the standard deviations of the dataset have been underestimated. For models that are linear in the *a*'s the probability distribution for the minimum χ^2, the chi-squared distribution for $N - M$ degrees of freedom, can be derived analytically from the normalised incomplete gamma function:

$$P\left(\chi^2 \mid \upsilon\right) = \frac{1}{\Gamma\left(\frac{\upsilon}{2}\right)} \int_{\frac{\chi^2}{2}}^{\infty} e^{-t} \cdot t^{\left(\frac{\upsilon}{2}-1\right)} \cdot dt \text{ for } \upsilon > 0 \text{ , } \chi^2 \geq 0 \tag{5-43}$$

$$\lim_{\chi^2 \to 0}\left[P\left(\chi^2 \mid \upsilon\right)\right] = 1 \;\; ; \;\; \lim_{\chi^2 \to \infty}\left[P\left(\chi^2 \mid \upsilon\right)\right] = 0$$

Where υ is the number of degrees of freedom and P is the probability that the observed chi-square should exceed a particular value of χ^2 by chance even for a correct model. This chi-square probability function for several values of υ is shown in Figure 5-2.

Figure 5-2 The chi-square probability function for selected values of υ (number of degrees of freedom).

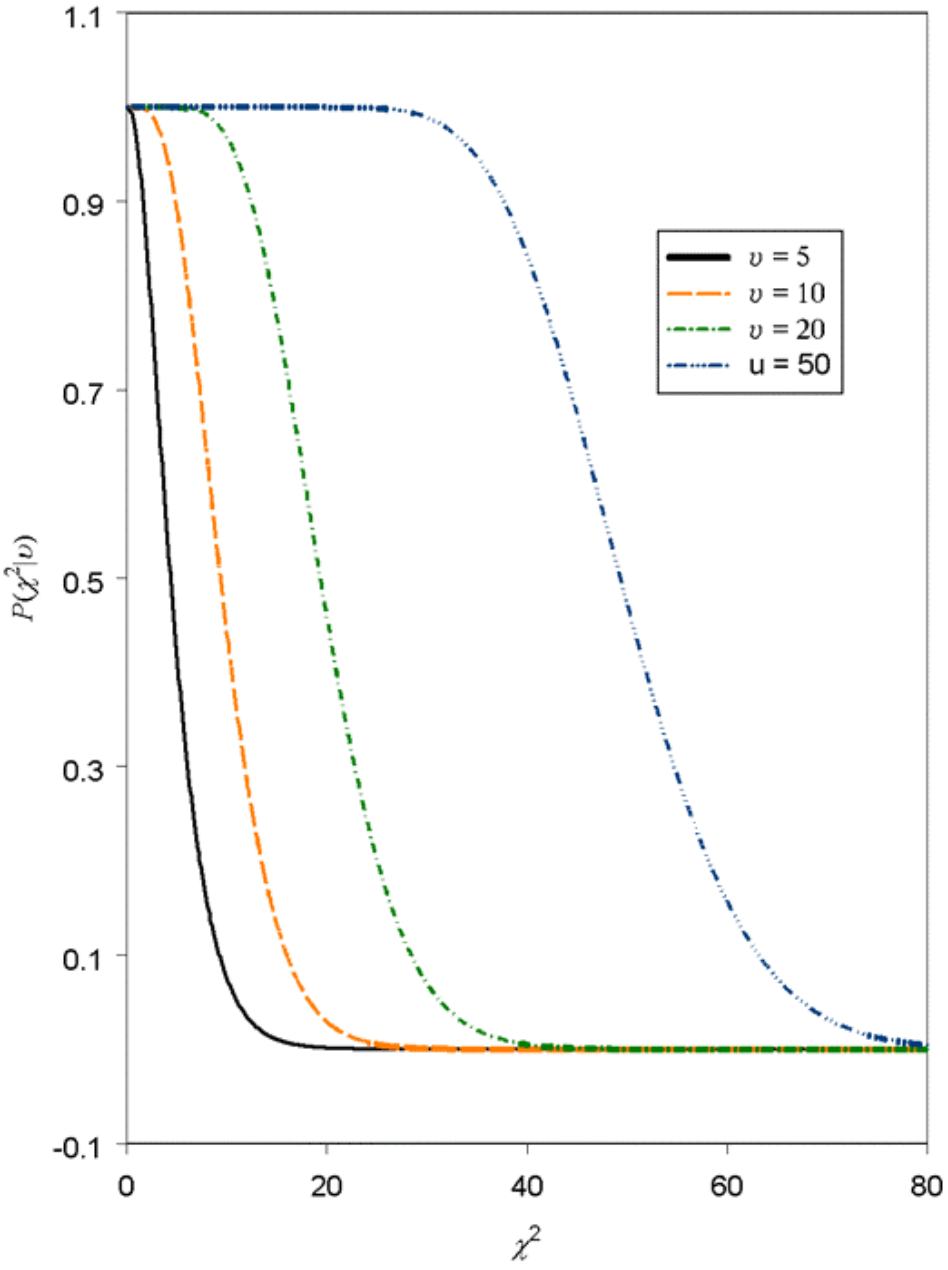

From the chi-square probability function it is now possible to discriminate between different model hypotheses at a given probability threshold, i.e. if the probability of obtaining the observed dataset is less than some threshold value, e.g. $P = 0.001$, the hypotheses assumed to derive the model can be rejected at that probability level. The normalised chi-squared threshold values (χ^2/ν) for several probability values are shown in Figure 5-3. This approach to selecting between different model hypotheses does not enable any particular model to be "proven", however it does enable the falsification of a number of the different working hypotheses at a given likelihood threshold. For the surviving hypotheses of acceptable normalised chi-squared value, the errors on the best-fit parameters can be estimated from the square roots of the diagonal elements of the covariance matrix, **C**, as well as the inter-parameter covariances.

Figure 5-3 Threshold normalised chi-squared values for selected probability values.

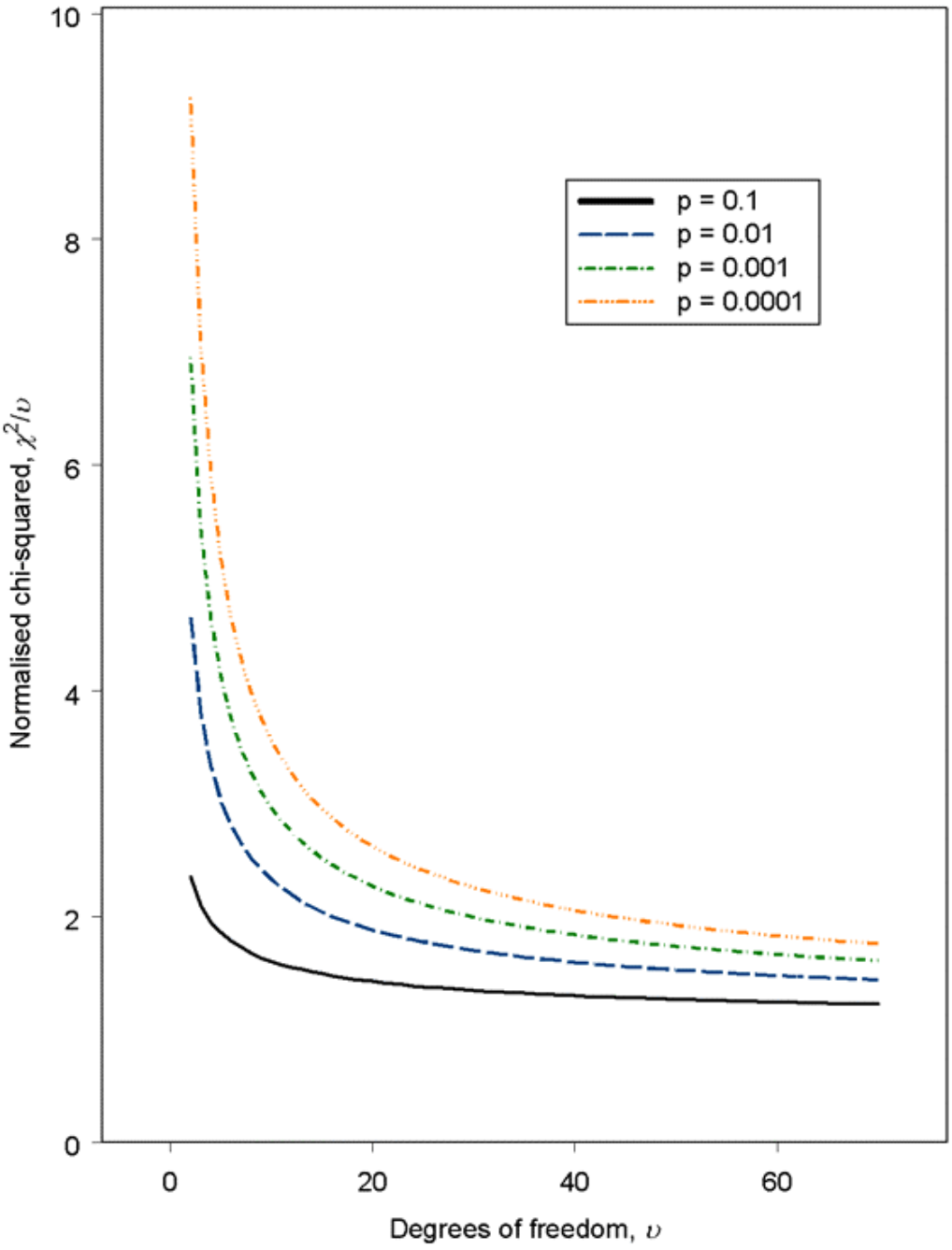

5.3.2 Integrating speciation modelling uncertainty

As discussed in section 4.5, the reliability of uranium speciation modelling depends on both the precision and accuracy of the model's input parameters. The thermodynamic values describing the stability of each uranium species considered in the speciation model are, to some extent, uncertain. Therefore the output (predicted speciation) of the speciation model is also uncertain. All of the uranium accumulation models tested during this study rely on the predicted speciation of uranium in the different exposure media. The use of conventional mean-value based speciation calculations does not permit assessment of the effects of this modelling uncertainty on both the estimation of fitted model parameter values and also the discrimination between different model working hypotheses. As described in section 4.5.1, Monte-Carlo simulation methods can be applied to estimate the probabilistic uncertainty distributions of predicted speciation. This method can be integrated quite simply into the bioaccumulation modelling process with one caveat: the uranium accumulation models fitted to the observed datasets depend on both the absolute concentrations and also the relative changes in concentration, of one or several chemical species, between the different solution compositions studied. The output uncertainty distributions of the predicted concentrations of a species for different solution compositions cannot be considered to be independent of each other. To illustrate this, Figure 5-4 shows the output probability distributions for the concentration of UO_2^{2+} at several different pH values ($[UO_2^{2+}]_T = 10^{-7}$ M, $I = 0.01$, CO_2 free system), and Figure 5-5 shows the correlations of these output distributions between paired pH values. As can be clearly seen the concentrations of UO_2^{2+} calculated at different pH values are strongly correlated (for calculations performed with the same Monte Carlo sample of the input parameter set) for small changes in pH, becoming less correlated as the change in pH increases. It is important to preserve these correlations between output parameters for different solution compositions, which will have the effect of reducing the impact of the modelled speciation uncertainty on the accumulation model fitting compared to treating the uncertainty distributions as mutually independent. In order to achieve this the different steps involved in the data analysis need to be performed in a specific sequence as detailed in the following section.

Figure 5-4 Uncertainty distributions of $[UO_2^{2+}]$ at different pH values ($[UO_2]_T = 10^{-7}$ M, $I = 0.01$, CO_2 free)

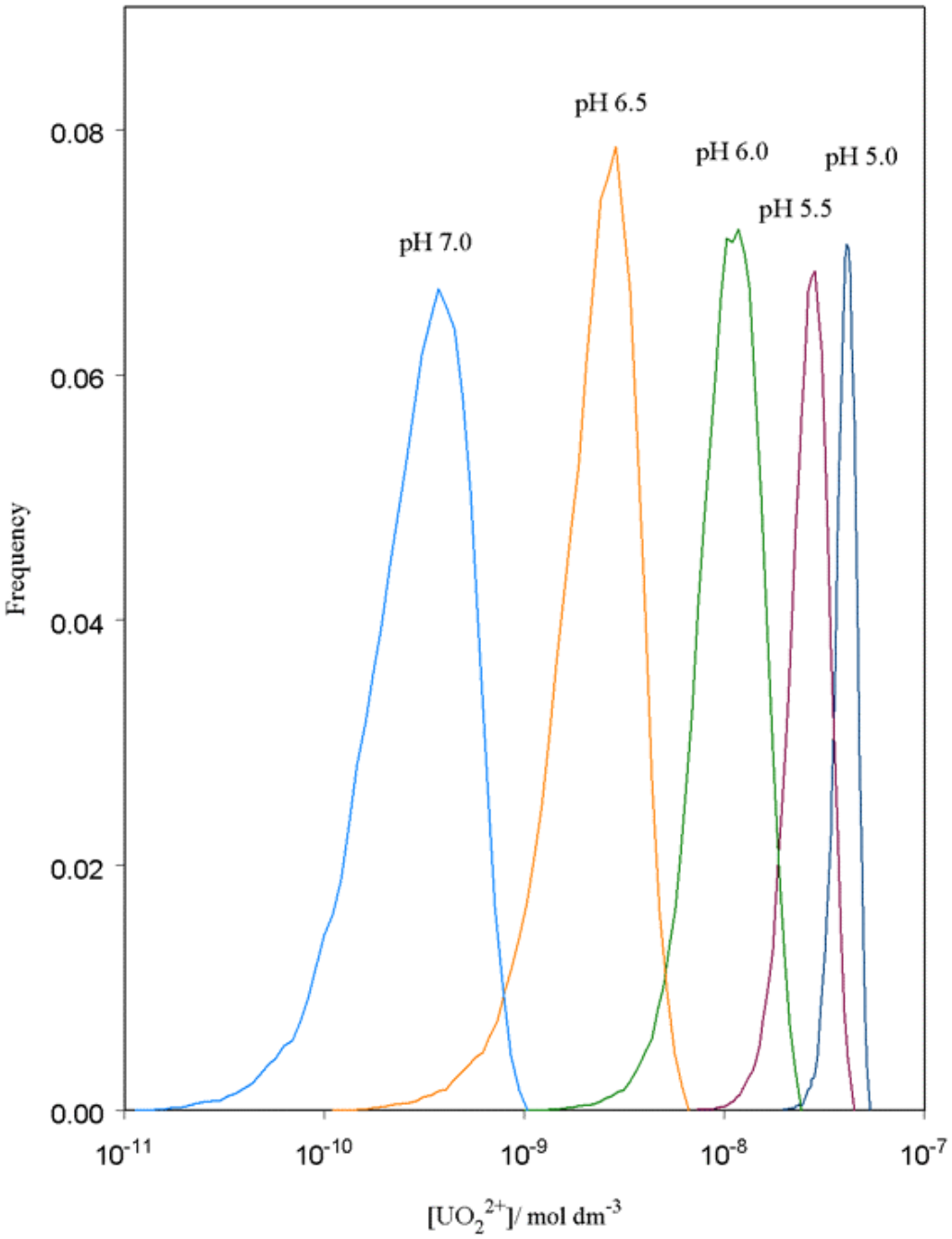

Figure 5-5 Correlations between output uncertainty distributions for paired pH values

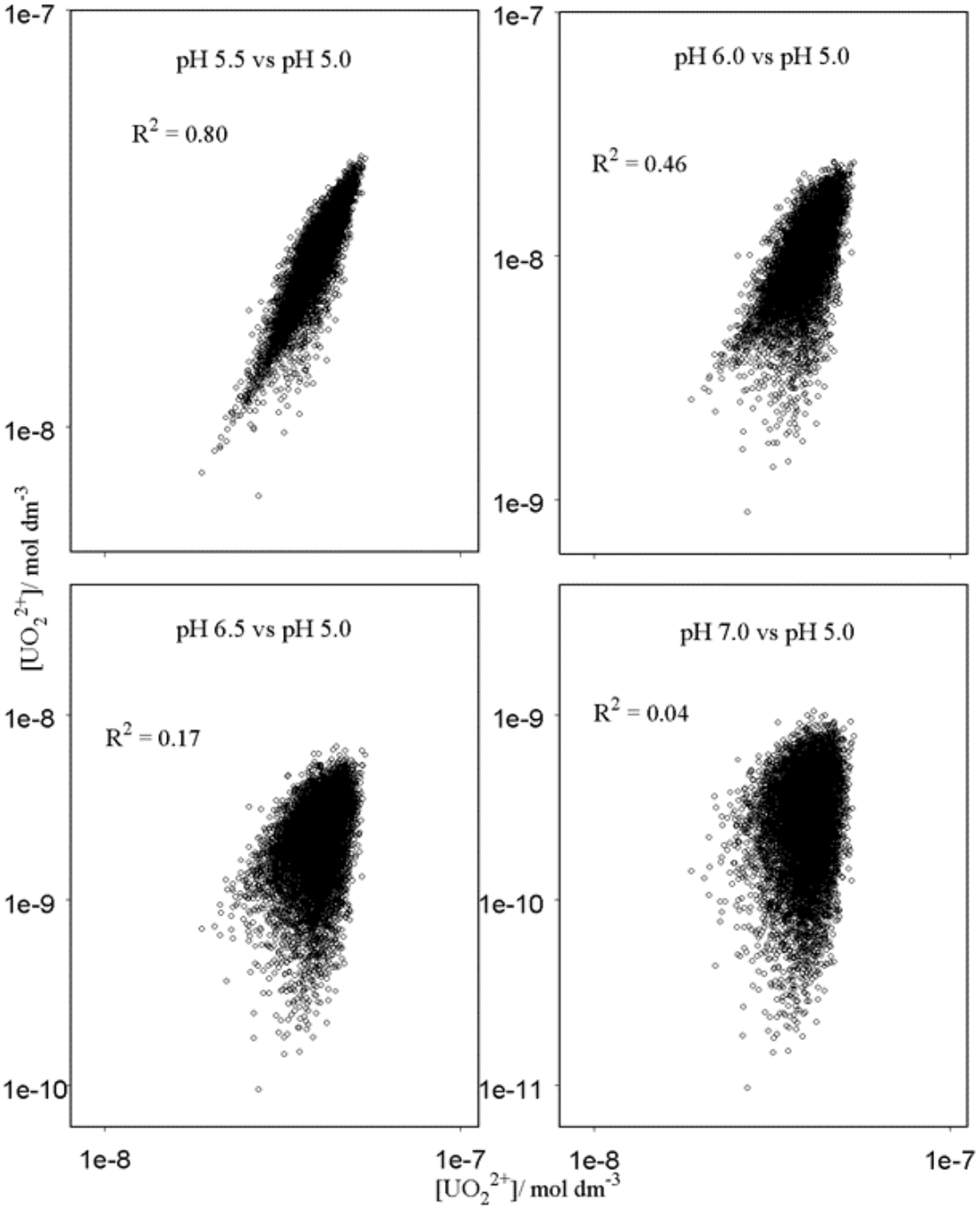

Figure 5-5 Correlations between output uncertainty distributions for paired pH values (cont'd)

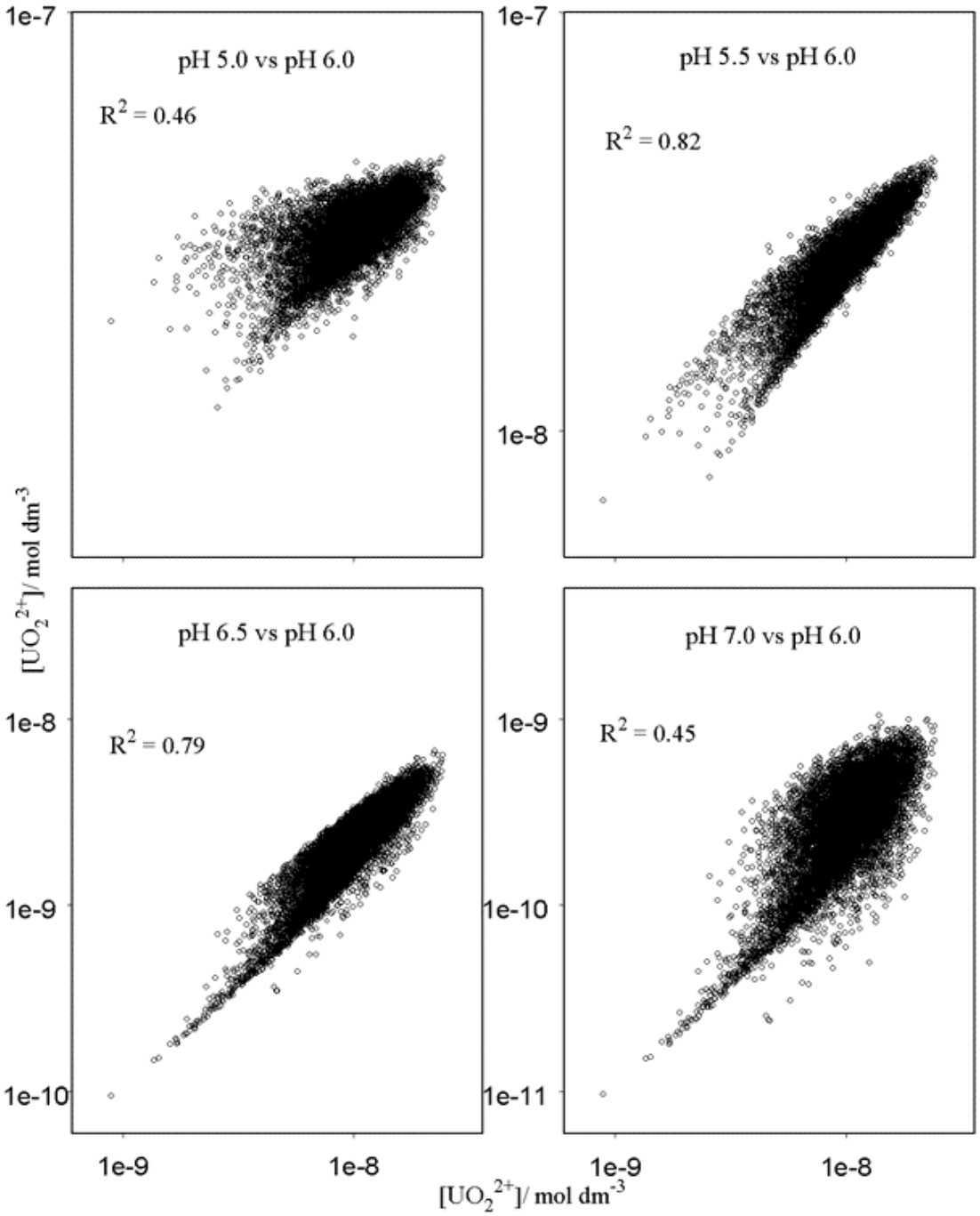

Figure 5-5 Correlations between output uncertainty distributions for paired pH values (cont'd)

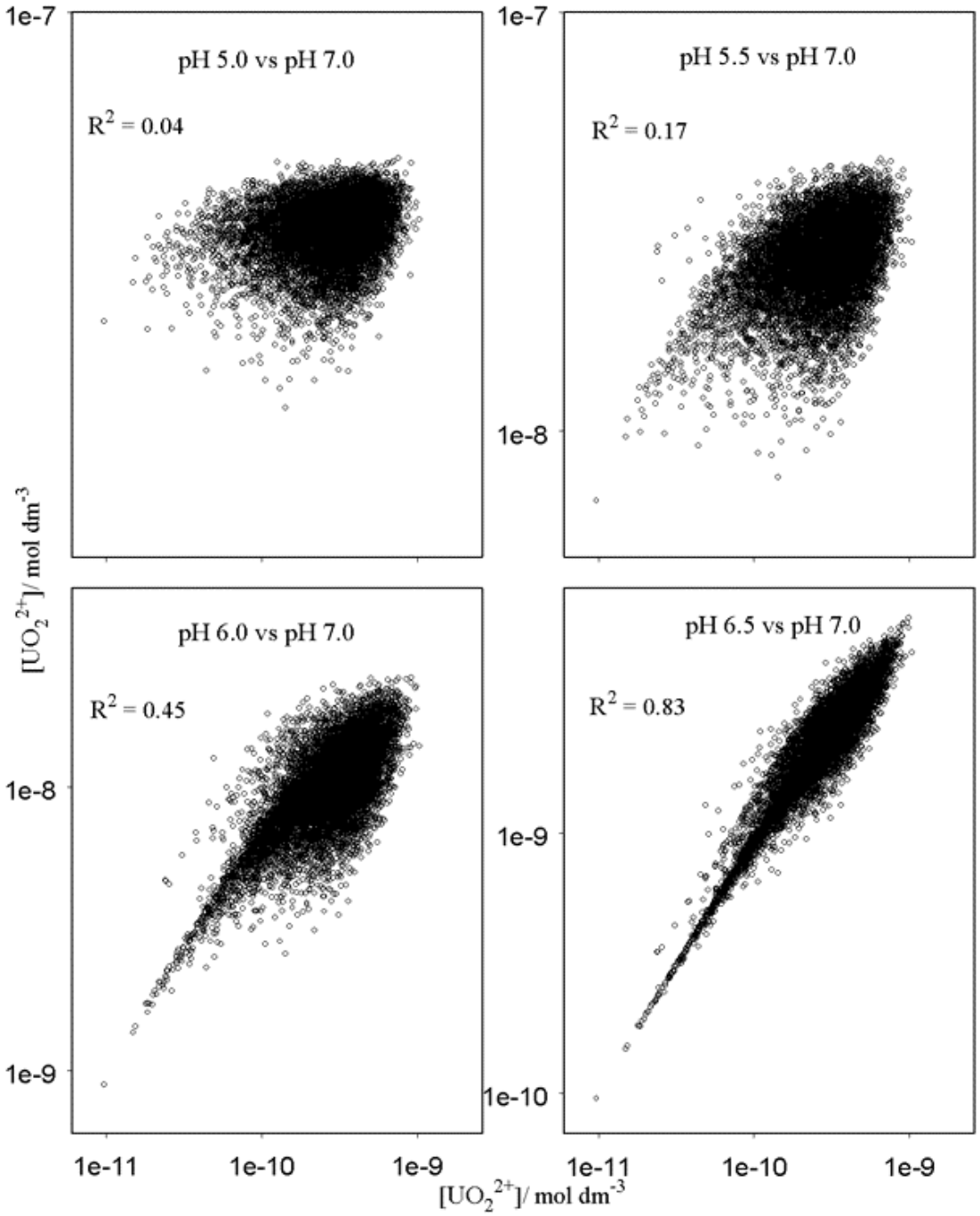

5.3.3 Organisation of the computer code

The computer program written to perform the data-analysis has four different calculation modes:

1. **Calculates thermodynamic equilibrium of solution with gas phase**

   Conventional speciation model where the equilibrium state of a solution defined by the total concentrations or activities of the components is calculated using the mean-values for the input parameters (supplied as a thermodynamic database). Simulation output can be selected for all chemical species as either concentration or activity values and written to a text file.

2. **Calculates probabilistic uncertainty distributions for equilibrium calculations**

   Performs Monte Carlo or Quasi-Monte Carlo analysis for equilibrium calculations by generating N samples of input parameter values drawn from the assigned probability distributions of the model's input constraints (either thermodynamic parameters or concentration/activity constraints). Thermodynamic equilibrium is then calculated for each sample and the output distributions of the selected output parameters are written to a file.

3. **Fits uranium accumulation models**

   An input dataset consisting of X solution compositions (defined by total concentrations or activities of the components) and associated uranium accumulation quantities and their standard deviations is supplied to the model. The equilibrium state of each solution is calculated using the mean-values for the thermodynamic input parameters. The desired uranium accumulation models selected from the list tabulated in Table 7-2 are fitted to the input dataset using the calculated equilibrium activities of the solution species considered in the model. The best-fit parameter values, their associated errors from the covariance matrix and the best-fit chi-squared value for the model are written to a file.

4. **Calculates effect of speciation uncertainty on accumulation model fitting**

N input parameter samples are generated from the probability distributions of the thermodynamic input constraints. For each of the N samples the equilibrium state of each of the *X* input solution compositions is calculated. The uranium accumulation models are then fitted to each of the N samples using the calculated equilibrium activities of the solution species considered in the models. For each of the *N* samples, the best-fit parameter values, their associated errors from the covariance matrix and the best-fit chi-squared value for the model are written to a file.

The organisation of the program is described in Figure 5-6 and an example input file is shown in Table 5-1.

Figure 5-6 Organisation of the program developed to test uranium accumulation models

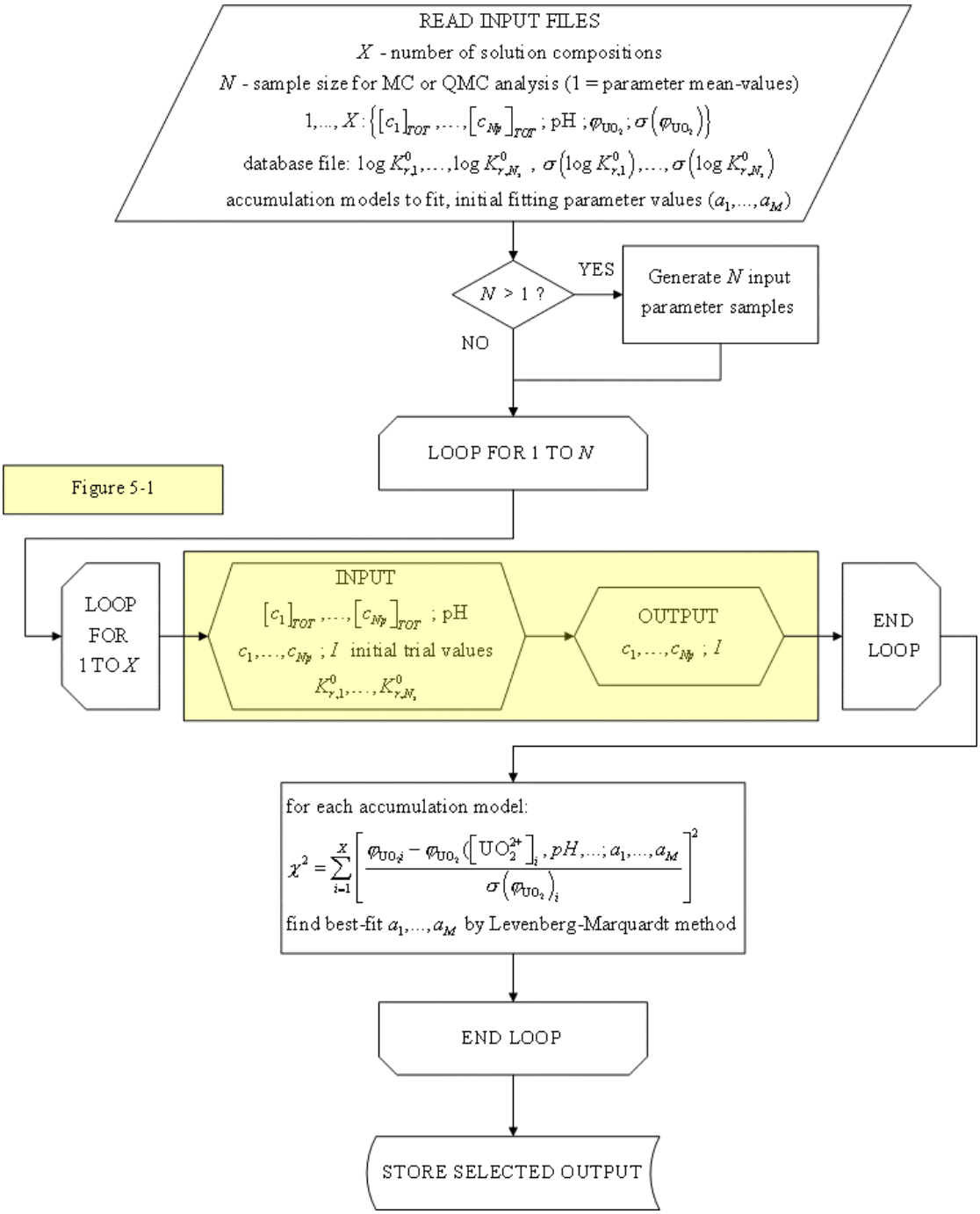

5.3.3.1 Description of data input and example simulation

The input file starts with a keyword (line 1 Table 5-1) to define the program calculation mode for either simple solution speciation calculation (FIT_MODELS OFF) or additionally the evaluation of the uranium bioaccumulation models (FIT_MODELS ON). Lines 3 – 46 then define which of the uranium bioaccumulation models will be applied to the input dataset, and initialises those models' fitting parameters. In the example input file shown, the models L1Sa, L1Sb and 1T1S0H (see section 7.3.1) will be tested and the fitting parameters are initialised on lines 4, 6 and 12. The keyword on line 48 sets the program mode for either a single or multiple input solution compositions and either mean-value or uncertainty calculation mode. The example shown (MULTI_SOLN_SPEC_MEAN 6) defines multiple input solution compositions (6) and mean-value speciation calculation. The keyword RUNS on line 52 defines the sample size to be used for MC analysis, in the example set to 1 as only mean-value speciation calculation is to be performed. Lines 54 – 148 then specify the input constraints for the 6 different solution compositions and the quantity of uranium accumulated from each of those solutions. Each solution composition is initiated by the keyword INPUT_START and terminated by the keyword INPUT_END. The pH value of each solution is specified (with a standard deviation value if required, [9999] denotes zero error) followed by the concentrations of each solution component, initial guess activity values and if required standard deviation values. The name of the output text file to store the calculated concentrations or activities of selected species is assigned after the keyword OUTFILE. The measured quantity of uranium accumulated by the exposed tissue from the defined solution composition is then defined after the keyword U_acc with the associated standard deviation. After the different input solution compositions have been defined, the output species required are selected after the keyword SELECT_OUTPUT, and the input file terminated with the keyword END_OF_INPUTFILE.

Table 5-1 Example of an input file for uranium accumulation modelling program

```
FIT_MODELS ON

MODEL_L1Sa ON
START_VALUES LOG(A) = 5,
MODEL_L1Sb ON
START_VALUES LOG(A) = 5, LOG(B) = -5,
MODEL_L2Soff OFF
START_VALUES
MODEL_L3Soff OFF
START_VALUES
MODEL_1T1S0H ON
START_VALUES LOG(a) = -5, LOG(KU) = 7,
MODEL_1T1S1H OFF
START_VALUES
MODEL_1T1S2H OFF
START_VALUES
MODEL_1T2S0H OFF
START_VALUES
MODEL_1T2S1H OFF
START_VALUES
MODEL_1T3S0H OFF
START_VALUES
MODEL_1T3S1H OFF
START_VALUES
MODEL_2T2S0H OFF
START_VALUES
MODEL_2T2S1HA OFF
START_VALUES
MODEL_2T2S1HB OFF
START_VALUES
MODEL_2T2S2H OFF
START_VALUES
MODEL_3T3S0H OFF
START_VALUES
MODEL_pHkin1T1S OFF
START_VALUES
MODEL_pHkin1T2S OFF
START_VALUES
MODEL_pHkin1T3S OFF
START_VALUES
MODEL_pHUaffinity1T1S OFF
START_VALUES
MODEL_pHUaffinity1T2S OFF
START_VALUES
MODEL_pHUaffinity1T3S OFF
START_VALUES

MULTI_SOLN_SPEC_MEAN 6
LOGFILE ON
RATIO_METHOD ON

RUNS = 1

INPUT_START 1
pH = 5[9999]
Ca_2 = 0.0005(0.0004)[9999]
Mg_2 = 0.0005(0.0004)[9999]
Na_1 = 0.0032(0.0025)[9999]
K_1 = 0.0032(0.0025)[9999]
Cl_1 = 0.0055(0.004)[9999]
NO3_1 = 0.002(0.0015)[9999]
SO4_2 =0.0005(0.0004)[9999]
HCO3_1 = 0.000016(0.00001)[9999]
UO2_2 = 3.8e-8(1e-8)[9999]
OUTFILE = 1.txt
IONIC = 0.01
U_acc = 1.2E-07[4E-08]
INPUT_END

INPUT_START 2
pH = 5[9999]
Ca_2 = 0.0005(0.0004)[9999]
Mg_2 = 0.0005(0.0004)[9999]
Na_1 = 0.0032(0.0025)[9999]
K_1 = 0.0032(0.0025)[9999]
Cl_1 = 0.0055(0.004)[9999]
NO3_1 = 0.002(0.0015)[9999]
SO4_2 =0.0005(0.0004)[9999]
HCO3_1 = 0.000016(0.00001)[9999]
UO2_2 = 7.2e-8(1e-8)[9999]
OUTFILE = 2.txt
IONIC = 0.01
U_acc = 2.8E-07[7E-08]
INPUT_END

INPUT_START 3
pH = 5[9999]
Ca_2 = 0.0005(0.0004)[9999]
Mg_2 = 0.0005(0.0004)[9999]
Na_1 = 0.0032(0.0025)[9999]
K_1 = 0.0032(0.0025)[9999]
Cl_1 = 0.0055(0.004)[9999]
NO3_1 = 0.002(0.0015)[9999]
SO4_2 =0.0005(0.0004)[9999]
HCO3_1 = 0.000016(0.00001)[9999]
UO2_2 = 2.9e-7(1e-7)[9999]
OUTFILE = 3.txt
IONIC = 0.01
U_acc = 9.8E-07[4E-07]
INPUT_END

INPUT_START 4
pH = 5[9999]
Ca_2 = 0.0005(0.0004)[9999]
Mg_2 = 0.0005(0.0004)[9999]
Na_1 = 0.0032(0.0025)[9999]
K_1 = 0.0032(0.0025)[9999]
Cl_1 = 0.0055(0.004)[9999]
NO3_1 = 0.002(0.0015)[9999]
SO4_2 =0.0005(0.0004)[9999]
HCO3_1 = 0.000016(0.00001)[9999]
UO2_2 = 9.3e-7(1e-7)[9999]
OUTFILE = 4.txt
IONIC = 0.01
U_acc = 3.4E-06[1E-06]
INPUT_END

INPUT_START 5
pH = 5[9999]
Ca_2 = 0.0005(0.0004)[9999]
Mg_2 = 0.0005(0.0004)[9999]
Na_1 = 0.0032(0.0025)[9999]
K_1 = 0.0032(0.0025)[9999]
Cl_1 = 0.0055(0.004)[9999]
NO3_1 = 0.002(0.0015)[9999]
SO4_2 =0.0005(0.0004)[9999]
HCO3_1 = 0.000016(0.00001)[9999]
UO2_2 = 3.6e-6(1e-6)[9999]
OUTFILE = 5.txt
IONIC = 0.01
U_acc = 9.0E-06[1E-06]
INPUT_END

INPUT_START 6
pH = 5[9999]
Ca_2 = 0.0005(0.0004)[9999]
Mg_2 = 0.0005(0.0004)[9999]
Na_1 = 0.0032(0.0025)[9999]
K_1 = 0.0032(0.0025)[9999]
Cl_1 = 0.0055(0.004)[9999]
NO3_1 = 0.002(0.0015)[9999]
SO4_2 =0.0005(0.0004)[9999]
HCO3_1 = 0.000016(0.00001)[9999]
UO2_2 = 1.1e-5(1e-6)[9999]
OUTFILE = 6.txt
IONIC = 0.01
U_acc = 1.6E-05[3E-06]
INPUT_END

SELECT_OUTPUT
[UO2[2+]]
END_OF_INPUTFILE
```

For the example shown all input parameters (pH, total concentrations) are kept constant, except for the total uranium concentration. The example accumulation behaviour is shown in Figure 5-7 (data points with error bars corresponding to single standard deviations). Processing this input file creates an output file for each solution composition (1.txt to 6.txt) containing the selected model output, in this case the concentration of UO_2^{2+}. An output file containing the results of the accumulation model fitting is also created, storing values for the best-fit parameters and their estimated errors, the chi-squared value for each model and the final status of the Levenberg-Marquardt algorithm. The results of the example simulation performed using mean-value input thermodynamic parameter values are given in Table 5-2 and the three model fits compared graphically with the data are shown in Figure 5-7. The details of the models and fitting parameters are given in Table 7-2.

Table 5-2 Example model fitting results, model details given in Table 7-2

Model	Log(A)	Log(A) ERR	$Log(B/K_{UO2})$	$Log(B/K_{UO2})$ ERR	χ^2/ν
L1Sa	0.76423	0.037	--	--	2.1
L1Sb	0.74426	0.04	-7.2297	0.27	2.0
1T1S0H	-4.5199	0.15	5.4769	0.2	0.1

Figure 5-7 Example uranium accumulation data for model fitting showing three different model fits. φ_{UO_2} is the uranium uptake rate, details of the fitted models are given in Table 7-2.

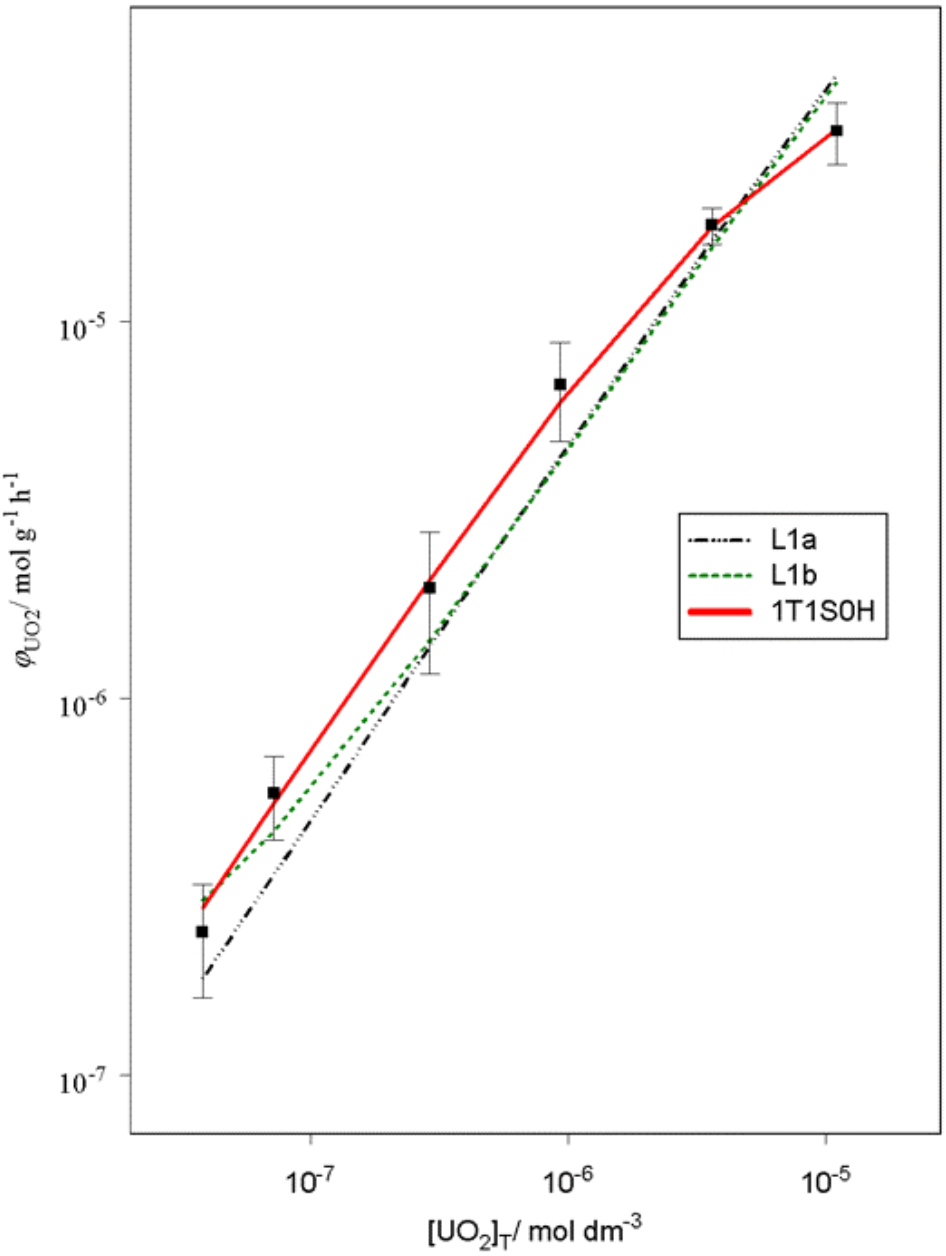

The effect of the thermodynamic input parameter uncertainty on the modelling can be assessed by modifying line 48 of the input file to the keyword MULTI_SOLN_SPEC_DIST, and line 52 to define the sample size for the MC simulation, for this example RUNS = 1000. Processing this input file results in an output file containing the results of the accumulation model fitting for each of the 1000 MC samples, which are summarised in Table 5-3. As can be seen, for this example the effects of uncertain thermodynamic input constraints on the modelling procedure are minimal.

Table 5-3 Results of model fitting example integrating database uncertainty by 10^3 MC samples. Details of the models are provided in Table 7-2.

Model	Log(A) mean	Log(A) S.D.	Log(B/K_{UO2}) mean	Log(B/K_{UO2}) S.D.	χ^2/ν mean	χ^2/ν S.D.
L1Sa	0.78	0.05	--	--	2.5	0.5
L1Sb	0.77	0.05	-7.25	0.05	1.9	0.4
1T1S0H	-4.509	0.03	5.479	0.08	0.110	0.003

6 EXPERIMENTAL SECTION

6.1 Experimental Design

To investigate the effects of varying solution composition, two different approaches were considered: either the concentration of each investigated solution component (with the added counter-ion) may be varied whilst maintaining all other components at constant concentration, or the concentration of the selected component can be inversely co-varied with another component of like charge in order to maintain a constant ionic strength and concentrations of counter-ions for all conditions. The first approach is the most commonly applied and has the advantage of maintaining nearly all concentrations constant with the exception of the varied component, but the disadvantage of varying both the concentration(s) of the counter-ion(s) and the ionic strength of the solution e.g. in (De Schamphelaere and Janssen 2002) ionic strength varied by a maximum factor of *ca.* 12. This could be a potential confounding factor due, for example, to the surface charge modification of the biological interface. The second approach was chosen for this study, it has the disadvantage that two (or more) components of like charge must be varied simultaneously, however if the reference solution composition is designed appropriately, the relative changes to the concentrations of the compensating components can be minimised. The composition of the reference solution is given in Table 6-1, all exposure solutions were based on this reference composition, modifying the concentration of both the component being investigated and the compensating component(s) concentration(s). The pH of the reference solution composition in air equilibrium is approximately 5.67 and the ionic strength 0.01 mol dm^{-3}.

Table 6-1 Reference solution composition for uranium exposures

Component	Concentration/ mol dm^{-3}
$[Ca]_T$	$5 \cdot 10^{-4}$
$[Mg]_T$	$5 \cdot 10^{-4}$
$[Na]_T$	$3.25 \cdot 10^{-3}$
$[K]_T$	$3.25 \cdot 10^{-3}$
$[Cl]_T$	$5.5 \cdot 10^{-3}$
$[NO_3]_T$	$2 \cdot 10^{-3}$
$[SO_4]_T$	$5 \cdot 10^{-4}$

Table 6-2 Concentration ranges of solution components investigated in the study

Investigated factor	Uranyl	Phosphate	Carbonate (DIC)	Citrate	Calcium	Magnesium
Concentration range investigated/ mol dm^{-3}	$2 \cdot 10^{-8}$ – $1 \cdot 10^{-5}$	0 – $1 \cdot 10^{-4}$	$1 \cdot 10^{-5}$ – $5 \cdot 10^{-3}$	0 – $1 \cdot 10^{-5}$	$1 \cdot 10^{-5}$ – $2.5 \cdot 10^{-3}$	$1 \cdot 10^{-5}$ – $2.5 \cdot 10^{-3}$
Compensating ion(s)	Na / K	Cl	Cl	Cl	Na / K	Na / K
pH values investigated	5.0, 5.5, 6.0, 6.5, 7.0, 7.5	5.0, 5.5, 6.0, 6.5, 7.0	5.0, 6.0, 7.0, 7.5	5.0, 6.0	6.0, 7.0	6.0, 7.0
Nominal concentration of $[UO_2]_T$/ mol dm^{-3}	--	$5 \cdot 10^{-8}$	$5 \cdot 10^{-7}$	$5 \cdot 10^{-7}$	$5 \cdot 10^{-8}$	$5 \cdot 10^{-8}$

The factors investigated in this study were: total uranyl concentration; water hardness as calcium and magnesium concentrations; phosphate concentration; carbonate concentration; citrate concentration and finally solution pH. Series of experiments were performed varying each of the investigated parameters and the compensating ion(s) while maintaining all other factors as constant as possible. Due to the importance of pH to the speciation of uranium, its potential effect on the surface charge of the biological interface and the potential for protons to compete for physiological binding sites, each parameter was investigated at several pH values. Changes to the concentrations of calcium, magnesium and hydronium ion were compensated by varying the concentrations of both sodium and potassium in a ratio of 1:1 and changes to the concentrations of phosphate, citrate and carbonate were compensated by varying chloride concentration. The concentration range of sodium and potassium was $2.5 \cdot 10^{-4} – 4 \cdot 10^{-3}$ mol dm^{-3} and for chloride $9 \cdot 10^{-4} – 6 \cdot 10^{-3}$ mol dm^{-3}. The concentration ranges of each of the investigated factors are summarised in Table 6-2. Except for the experimental series varying carbonate concentration, the DIC concentrations were determined by equilibrium with the air.

The solutions were designed to be prepared with the total carbonate concentration, predicted by speciation calculations, to be in equilibrium with a CO_2 partial pressure of $10^{-3.5}$ at the desired pH values. For the series of experiments varying carbonate concentration, the solutions were equilibrated with gas mixtures containing CO_2 partial pressures appropriate to give the desired DIC concentrations for the selected pH values. Full details of all the solution compositions used for the uranium uptake experiments are given in section 6.5.

6.2 Preparation Of The Exposure Solutions

200 mL volumes of each solution composition were prepared by mixing appropriate volumes of stock solutions prepared by dissolving the salts ($CaCl_2$; $MgSO_4$; $NaNO_3$; NaCl; KCl; $Ca(NO_3)_2$; Na_2SO_4; $MgCl_2$; $Mg(NO_3)_2$; $NaHCO_3$; K_2CO_3; $Na_3C_6H_5O_7$) in ultrapure water and adjusting the final volume to 200 mL. Prepared solutions were designed to have the required pH and DIC concentration for air equilibrium. The prepared solutions were transferred to 500 ml LDPE beakers agitated by a magnetic stirrer bar 24-hours before the exposures. Uranium added as the ^{233}U radioisotope ($8.3 \cdot 10^{10}$ Bq mol^{-1} as uranyl nitrate in a nitric acid matrix, CERCA Framatome,

France). The pH of the solution was regulated by additions of either HCl or a mixture of $KOH/K_2CO_3/NaHCO_3$ from a pH-stat (Radiometer PHM290) equipped with a Radiometer GK2401C combination glass electrode calibrated at the same temperature as the experiments with NBS recommended buffer solutions (Garrels and Christ 1965) of 4.002 and 7.429 (at 298 K). Recalibration at the end of the experiments showed a change in response of pH of less than 0.01 units. Gas equilibrium was established by bubbling 2 dm^{-3} min^{-1} of either compressed air for the conditions nominally in atmospheric equilibrium, or a mixture of compressed air and CO_2 regulated by two massic flow meters for the conditions with elevated carbonate concentrations.

6.3 Preparation Of The Excised Gills And Exposure Protocol

Corbicula fluminea specimens (25 ± 5 mm antero-posterior shell length, 6 ± 1 g total wet weight) were collected manually from lake Cazeaux-Sanguinet (Gironde, France). On arrival at the laboratory they were maintained at 20°C, in the synthetic media (pH 6.5 ± 0.5) over washed quartz sand (SILAQ, Mios, France). Weekly water changes were performed in order to minimise any evolution of the chemical composition. Gills were excised by dissection during a 1-hour period before the exposures were performed, and immediately transferred to the exposure medium (without added uranium). This acclimation minimised the effects of the initial shock period of physiological adaptation to the medium (Winkle 1972) and stabilised mucous production. Cillial activity was observed to continue for periods of at least 4-hours after dissection. Immediately prior to the exposures the acclimation solution was removed, excess water was removed from the gills by blotting with tissue paper and the gills were transferred to the exposure solutions. The solutions were gently agitated by gas bubbling during the exposure periods to maintain a homogeneous solution, and pH was regulated as previously described. At the end of the exposure periods the gills were recovered on a 5-µm polycarbonate filter membrane (Poretics, Minnetonka, MN, USA) using vacuum pressure. Surface-bound (adsorbed) uranium was removed by rapid washing with an EDTA solution (1 mM, pH 5.0). The extraction efficiency of the EDTA rinsing was assessed by washing gills contaminated by flash exposures to uranium (< 15 s) and was found to efficiently remove uranium. Filtered (0.45 µm) water samples were retained for subsequent ^{233}U, major ions and DIC analyses. The

gills were acid-digested with a mixture of concentrated HNO_3 and 30 % v/v H_2O_2 in glass vials, slowly evaporated on a heated sand bed.

6.4 Analytical Methods

All chemicals were reagent grade unless specified otherwise, and analytical quality ultrapure water (18 MΩ cm^{-1}) was used throughout

Uranium was measured by liquid scintillation counting. Digested or aqueous samples were evaporated to dryness in 25 mL glass tubes on a heated sand bed. The samples were re-dissolved with 1 mL of 0.1 M nitric acid and 19 mL of Instagel® scintillation cocktail (Packard Instruments, Rungis, France) was added. ^{233}U activities were measured using a low-background spectrometer (Quantulus 1220, Wallac Oy, Turku, Finland; detection limit: 30 mBq). Molar concentrations of uranium were determined from the specific activity of ^{233}U ($8.3 \cdot 10^{10}$ Bq mol^{-1}).

Cation concentrations (Ca^{2+}, Mg^{2+}, Na^{+}, K^{+}) were measured by ion-exchange chromatography (Dionex DX-120). 25 µL samples were injected into an eluent steam (20 mM methanesulfonic acid, 1.0 mL min^{-1}), passed through an IonPac CS12A cation exchange column and the separated cations measured by conductivity after suppression of the eluent conductivity by a CSRS-ULTRA cation self-regenerating suppressor.

Anion concentrations (Cl^{-}, NO_3^{-}, SO_4^{2-}, PO_4^{3-}) were measured by ion-exchange chromatography (Dionex DX-120). 100 µL samples were injected into an eluent steam (1 mM $NaHCO_3$/ 3.5 mM Na_2CO_3, 2.0 mL min^{-1}), passed through an IonPac AS14 cation exchange column and the separated anions measured by conductivity after suppression of the eluent conductivity by a ASRS-ULTRA anion self-regenerating suppressor.

Dissolved Inorganic Carbon (DIC) concentrations were measured by a Shimatzu 5000A carbon analyser. Samples of 200 – 2000 µL were acidified (25 % H_3PO_4) and sparged by a stream of O_2, the liberated CO_2 being detected by infra-red absorption.

For samples of pH values ≥ 6.0 the DIC concentrations were verified by performing alkalinity titrations. Solutions in equilibrium with atmospheric P_{CO_2} values ≥ $3.2 \cdot 10^{-3}$ atm. were immediately diluted with freshly prepared 10^{-2} M KCl to minimise CO_2

out-gassing. Samples of 50 – 100 mL were titrated with 10^{-2} M HCl (the same ionic strength as the samples) by a Radiometer Titralab 90 equipped with a Radiometer GK2401C combination glass electrode calibrated at the same temperature as the experiments with NBS recommended buffer solutions. Titrations were performed using the continuous inflection point predictive addition algorithm. End points of the titration curves were located by linear regression of the Gran function (Stumm and Morgan 1996) in the pH range 3.5 – 4.2. Although the approximation of equating titrable alkalinity to bicarbonate concentration is adequate for pH values of 7 – 7.5 in the absence of other weak acids, at lower pH values and in the presence of phosphate this approximation can introduce significant error. The sample DIC concentrations were therefore calculated from the following equation:

$$\mathrm{DIC} = \left(\begin{array}{l} V_T \cdot 10^{-2} + \dfrac{(V_S + V_T) \cdot 10^{-14}}{10^{-pH_e} \cdot \gamma_1} + \dfrac{(V_S + V_T) \cdot \Sigma PO_4}{\left(1 + 10^{7.21} \cdot 10^{-pH_e} \, \gamma_2 / \gamma_1\right)} \\ + \dfrac{V_S \cdot 10^{-pH_i}}{\gamma_1} - \dfrac{V_S \cdot 10^{-14}}{10^{-pH_i} \cdot \gamma_1} - \dfrac{V_s \cdot \Sigma PO_4}{\left(1 + 10^{7.21} \cdot 10^{-pH_i} \, \gamma_2 / \gamma_1\right)} \end{array} \right) \cdot \left(\frac{\left(1 + 10^{6.35} \cdot 10^{-pH_i} \cdot \gamma_1\right)}{V_S} \right)$$

Where:

V_S/ dm^3 is the sample volume, V_T/ dm^{-3} is the volume of 10^{-2} M HCl to attain the Gran plot end-point ($[H^+] = [HCO_3^-]$), ΣPO_4 is the total phosphate concentration, pH_i is the pH of the sample, pH_e is the pH of the Gran plot end-point and γ_x is the single ion activity coefficient of charge x.

Using the approximations:

$\mathrm{DIC} = [CO_{2(aq)}] + [HCO_3^-]$, $\Sigma PO_4 = [HPO_4^{2-}] + [H_2PO_4^-]$ $(4 < \mathrm{pH} < 8)$.

6.5 Experimental Results And Discussion

6.5.1 Uranium uptake kinetics by isolated gills

Exposures were performed at pH values of 5, 6 and 7, at several time intervals up to a two-hour period, in order to assess the uranium uptake kinetics. All major ion concentrations were nominally as given in Table 6-1 (not measured) and the solutions were pre-equilibrated with air bubbling as detailed in section 6.2. The results of these experiments are given in Table 6-3. Figure 6-1 shows the internalised uranium concentrations as a function of exposure time for 10^{-7} mol dm^{-3} $[UO_2]_T$ and the calculated uranium uptake flux rates for the same exposure periods. As can be seen, the internalised concentration of uranium increased linearly with time for all exposure pH values during the first hour of exposure, the flux rates decreasing after this period. As the flux rates determined at each time interval up to 45 minutes were constant, it was decided to perform all further uptake experiments at a constant time interval of 30 minutes.

Table 6-3 Results of uranium uptake kinetics by excised gills

Time/ h	pH	$[UO_2]_T$/ nmol dm^{-3}	$\overline{\varphi}_{UO_2}$ / nmol g^{-1} h^{-1}	$\sigma_{\varphi_{UO_2}}$ / nmol g^{-1} h^{-1}
0.25	5.00	74	984	368
0.5	5.00	81	982	262
0.75	5.00	91	1069	312
1	5.00	92	951	316
2	5.00	68	622	135
0.25	6.00	67	1148	316
0.5	6.00	80	1126	330
0.75	6.00	78	1220	309
1	6.00	82	1156	424
2	6.00	79	659	247
0.25	7.00	96	1816	364
0.5	7.00	90	2044	604
0.75	7.00	89	1984	576
1	7.00	81	1770	492
2	7.00	65	1182	450

Figure 6-1 Uranium uptake kinetics for 10^{-7} mol dm^{-3} $[UO_2]_T$. a) internalised uranium concentrations as a function of exposure time, b) uranium uptake flux rates, error bars show ± 1 S.D.

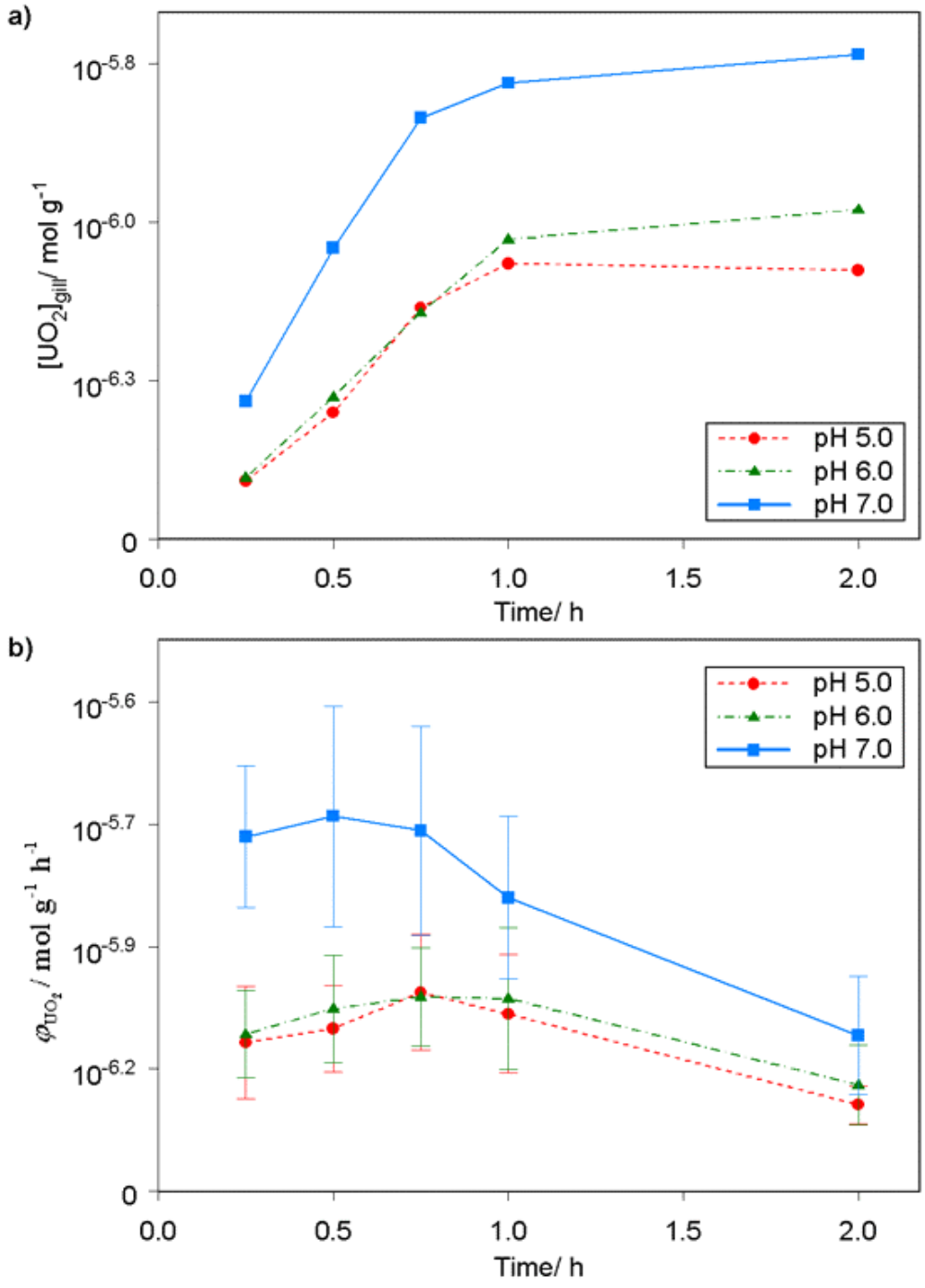

6.5.2 Effect of citrate

The series of experiments designed to assess the effect of citrate complexation were performed at pH values of 5.0 and 6.0 for a citrate concentration range of 0 – 10 µmol dm^{-3} and a total uranium concentration of $5 \cdot 10^{-7}$ mol dm^{-3} after exposure periods of 30 minutes. The results of these experiments are given in Table 6-4, the normalised uptake fluxes as a function of citrate concentration for a total uranium concentration of $5 \cdot 10^{-7}$ mol dm^{-3} are shown in Figure 6-2 a) and the uptake fluxes in function of the predicted free uranyl ion concentration (mean-value speciation calculations) are shown in Figure 6-2 b). It can be seen that the presence of citrate strongly reduces the uptake of uranium due to complexation in solution. The uptake flux rate was found to be approximately proportional to the predicted concentration of the free uranyl ion at both pH values, consistent with the assumptions of the equilibrium paradigm for the accumulation of the free ion. Linear regression of the log transformed accumulation data as a function of predicted free uranyl ion concentration gave gradients of 0.87 for the dataset at pH 5.0, and 1.12 for the data at pH 6.0, compared to the expected value of 1.0 if only the free uranyl ion was chemically bioavailable (or any combination of covariant uranyl species). These discrepancies are within the predicted uncertainty of the speciation modelling, and so improving the model fits by proposing alternative accumulation models was not attempted. However, it must be stressed that the proportional relationship found with the predicted free ion concentration does not preclude the accumulation of other solution species that are covariant with the free ion for these conditions at constant pH (for example UO_2OH^+, $UO_2CO_3^0$…). The uptake of anionic metal-ligand organic complexes has been previously suggested to explain metal accumulation results in the presence of low molecular weight assimilable organic metabolites. For example the toxicity of copper, cadmium and zinc towards the green alga *P. subcapitata* exceeded that predicted on the basis of the free-metal ion in the presence of citrate, that can be internalised and metabolised by the alga (Guy and Kean 1980; Errecalde, Seidl et al. 1998). Uptake of cadmium by the common carp, *Cyprinus carpio*, in the presence of citrate, glycine and histidine was also higher than expected from predicted free ion concentrations (van Ginneken, Chowdhury et al. 1999). The authors proposed that cadmium complexes of these low molecular weight organic ligands were available for direct uptake.

Table 6-4 Experimental conditions used to assess the effect of citrate on uranium uptake by excised gills

pH	**5.00**	**5.00**	**5.00**	**5.00**	**5.00**	**6.00**	**6.00**	**6.00**	**6.00**	**6.00**
$[Ca]_T$/ µmol dm^{-3}	517	508	506	533	510	494	495	502	517	509
$[Mg]_T$/ µmol dm^{-3}	520	513	513	542	521	503	504	511	524	515
$[Na]_T$/ µmol dm^{-3}	3420	3378	3331	3516	3321	3227	3221	3264	3408	3271
$[K]_T$/ µmol dm^{-3}	3358	3325	3364	3504	3360	3218	3316	3287	3422	3419
$[Cl]_T$/ µmol dm^{-3}	5612	5509	5896	5888	5806	5237	5395	5512	5597	5388
$[NO_3]_T$/ µmol dm^{-3}	2112	2132	2068	2295	2281	2128	2038	2145	2158	2427
$[SO_4]_T$/ µmol dm^{-3}	540	516	532	532	521	505	528	501	516	523
[DIC]/ µmol dm^{-3}	16	11	14	15	16	32	21	12	20	17
$[PO_4]_T$/ µmol dm^{-3}	0	0	0	0	0	0	0	0	0	0
$[UO_2]_T$/ nmol dm^{-3}	291	554	628	632	674	299	578	634	670	685
$[Citrate]_T$/ µmol dm^{-3}	**0**	**1***	**2.5***	**5***	**10***	**0**	**1***	**2. 5***	**5***	**10***
$\bar{\varphi}_{UO_2}$/ nmol g^{-1} h^{-1}	1952	1151	635	285	170	2949	2540	1313	509	391
$\sigma_{\varphi_{UO_2}}$/ nmol g^{-1} h^{-1}	828	260	166	51	43	847	746	324	134	188
$\alpha_{UO_2^{2+}}$	1.2E-07	6.4E-08	2.8E-08	1.4E-08	6.9E-09	2.1E-08	2.1E-08	1.2E-08	6.7E-09	3.3E-09
f_{CO_2}	4.6E-04	3.3E-04	3.9E-04	4.2E-04	4.6E-04	6.4E-04	4.2E-04	2.5E-04	4.0E-04	3.4E-04
I	1.0E-02	1.0E-02	1.0E-02	1.1E-02	1.0E-02	9.7E-03	9.8E-03	9.9E-03	1.0E-02	1.0E-02

* nominal concentrations

Figure 6-2 Effect of citrate concentration on uranium uptake by excised gills, a) uptake flux rate as a function of citrate concentration ($[UO_2]_T = 5{\cdot}10^{-7}$ mol dm^{-3}), b) uptake flux rate as a function of predicted free uranyl concentration. Error bars show ± 1 S.D.

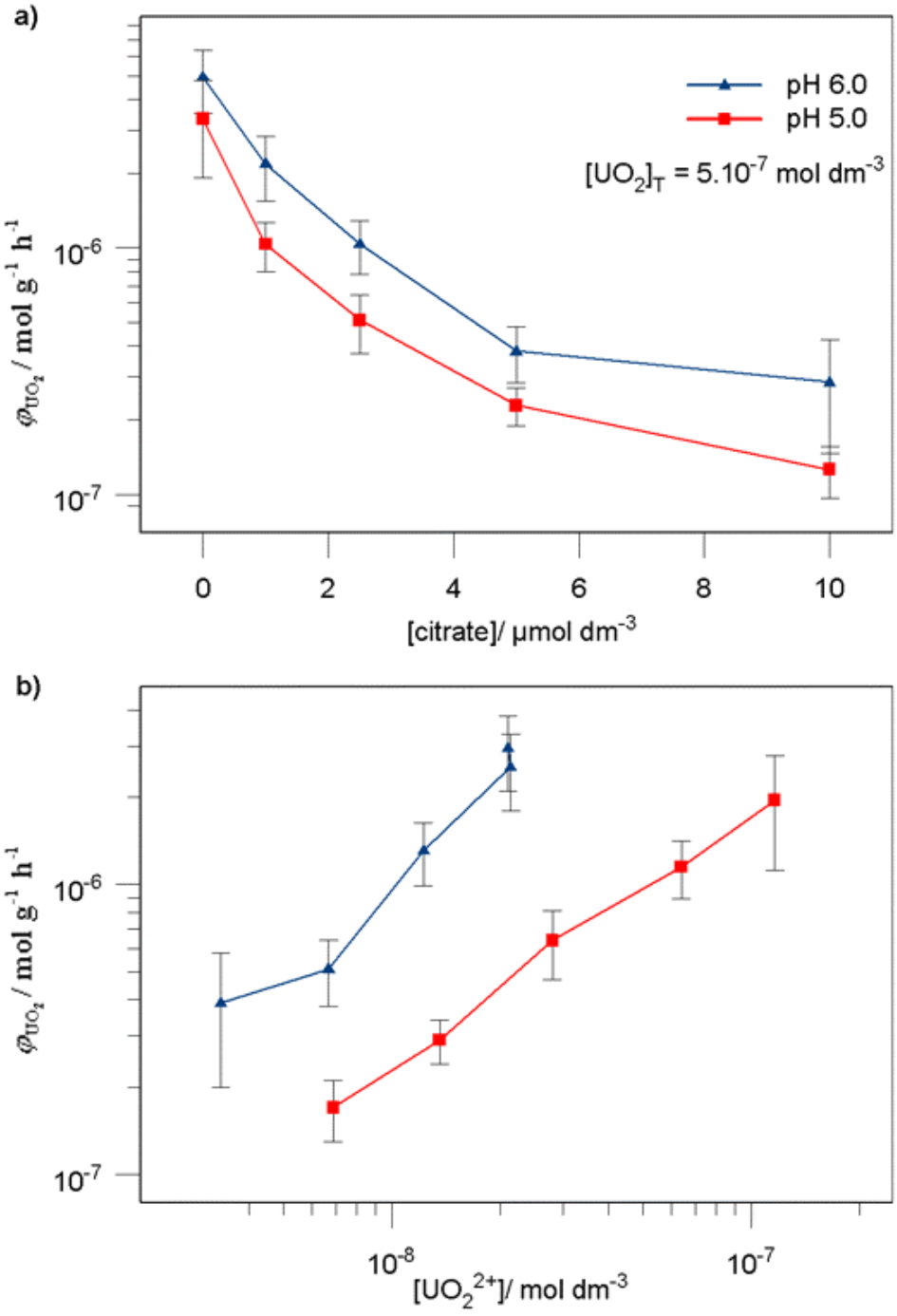

6.5.3 Effect of pH and uranium concentration

Bioaccumulation experiments were performed in the pH range 5 – 7.5 and total uranium concentration range of approximately 10^{-8} – 10^{-5} mol dm^{-3} for exposure periods of 30 minutes. The distribution of uranyl through its major species predicted by mean-value speciation calculations for this pH range and in air equilibrium (P_{CO_2} = $10^{-3.5}$) for total uranium concentrations of 10^{-8} and 10^{-6} mol dm^{-3} is shown in Figure 7-2. As can be seen, the concentration of the free uranyl ion decreases very significantly as pH increases, changing from being the predominant species in the pH range 5 – 5.5 to contributing only 0.01 % of the total concentration at pH 7.5. As discussed in section 5.2, one of the assumptions of equilibrium based approaches to modelling bioavailability, is that the internalisation flux is proportional to the concentration(s) of the metal – membrane ligand site complex(es). For the data series at constant pH values of 5, 6 and 7, but varying total uranium concentration shown in Figure 6-3 a), the calculated uptake flux rates are proportional to total uranium concentration in the concentration range 10^{-8} – 10^{-6} mol dm^{-3}. This is consistent with a first-order relationship with either the free uranyl ion concentration or a combination of several mono-nuclear uranyl species, which for these conditions at constant pH are approximately proportional to the free uranyl ion concentration as a function of total uranium concentration. However, when the uptake flux rates are expressed in terms of the predicted free uranyl ion concentrations, Figure 6-3 b), it is evident that the accumulation of uranium cannot be described simply in terms of the free ion concentration. As discussed in section 5.2 a number of hypotheses may be forwarded to explain the pH dependence of metal uptake, both within the pre-equilibrium framework (e.g. section 5.2.1) or by alternatives to the equilibrium paradigm (section 5.2.2). A number of these alternative modelling approaches will be tested in section 7.3. The uptake of uranium at pH 5.0 as a function of dissolved uranium concentration was linear up to *ca*. 10^{-6} M after which the uptake flux started to level off. At other pH values it was not possible to extend the uranium concentration range investigated due to the solubility boundary of schoepite. These saturable uptake kinetics indicate that the uptake of uranium is a facilitated process, implicating some membrane transport system i.e. a channel, carrier or pump, in uranium uptake.

Studies of metal bioaccumulation or toxicity that have investigated the effects of varying pH have presented a number of different hypotheses to explain observed pH dependencies. Interpretation of pH variable bioaccumulation or toxicity data is frequently difficult as many metals exhibit large speciation changes in function of pH; separating the effects to a metal's speciation and the potential competition for binding sites by protons is often difficult. Additional confounding factors include the fact that the pH in the microenvironment of the biological interface may differ from that of the bulk solution, that pH can directly modulate the activity of ion transport systems and also that pH may affect physiological processes which directly or indirectly influence the uptake of metals, e.g. trans-membrane electrical potential or acid-base homeostasis. The effect of pH at the biological interface differing from that of the bulk solution has been demonstrated for the gills of fathead minnows (Playle, Gensemer et al. 1992) where gas exchange by the release of CO_2 was found to buffer the pH of the exposure solution, increasing the pH of acidic waters and decreasing the pH of basic waters, thus regulating the pH at the gill surface within a relatively narrow range.

Acute toxicity of copper to *Daphnia magna* (De Schamphelaere and Janssen 2002) in the pH range 6 – 8 observed 48-h EC50 values ranging from 88 to 820 nM total copper concentration. The range in EC50 was significantly reduced when expressed as the predicted free-ion concentration (17 to 33 nM), suggesting that the variation in EC50 can be at least partially explained by changes to copper speciation. The authors considered the possibilities of both proton competition and the co-toxicity of copper hydroxide to explain the observed pH dependence. The co-toxicity of the copper hydroxide species was favoured in order to explain the observed behaviour, but the possibility of proton competition (either separately or in concert with the co-toxicity of copper hydroxide) could not be excluded.

The uptake of strontium by carp (Chowdhury and Blust 2001) was found to be inhibited by protons in a partially non-competitive manner and the effect of pH was found to be dependent on the pH of acclimation. The authors suggested that the inhibition by protons did not occur by direct competition with strontium for the transporter binding site, but reduced the transport rate of strontium by acting indirectly on the transport system, for example by inducing conformational changes to the transporter protein or altering trans-membrane potential. The authors proposed

that the significant acclimation effect indicated chronic changes to the transport characteristics of the Sr^{2+}/Ca^{2+} transport system, in addition to the potential effects of pH at the time of exposure such as the competitive protonation equilibria of transporter binding sites or conformational changes to transporter proteins. The acclimation pH effect was opposite to that of the exposure effect indicating that the two effects were fundamentally different in nature.

A number of studies have investigated the effect of pH on zinc toxicity, but the findings are sometimes contradictory. For some biological model organisms increasing toxicity with increasing pH was observed (Cusimano, Brakke et al. 1986) whereas other studies have found an inverse relationship between pH and toxicity (Belanger and Cherry 1990; Heijerick, De Schamphelaere et al. 2002). In zinc toxicity studies for *Daphnia magna* (Heijerick, De Schamphelaere et al. 2002) acute toxicity expressed as 48h-EC50 values, increased significantly in terms of the total dissolved zinc concentration, however when expressed in terms of the predicted free ion concentration the EC50 values were constant as a function of pH. The authors concluded that for the domain of solution composition studied that changes to zinc speciation were sufficient to explain the toxicity pH dependence, and that neither proton competition for binding sites, nor the bioavailability of zinc species other than the free ion (for example $ZnOH^+$) needed to be considered.

The accumulation of both iron and manganese by the unicellular green alga *Chlamydomonas variabilis* was found to decrease strongly on decreasing pH, although the surface bound fraction of these metals remained constant (Schenck, Tessier et al. 1988).

The toxicity of uranium to the green alga *Chlorella sp.* (Franklin, Stauber et al. 2000) was greater at pH 6.5 relative to 5.7, with 72-h EC50 values of 44 and 78 $\mu g\ l^{-1}$ respectively and accumulated intracellular uranium concentrations significantly higher at pH 6.5 relative to 5.7. These results are consistent with either proton competition with the free uranyl ion for binding sites, or the bioavailability of uranium species other than the free ion, for example UO_2OH^+.

A careful study of the effect of pH on lead bioaccumulation by the unicellular alga *Chlorella kesslerii* (Slaveykova and Wilkinson 2003) found that both uptake fluxes and surface bound lead increased with pH in the interval 4 to 5, were relatively stable

in the interval 5 to 6.5 and again increased up to a pH of 8. The authors proposed that protons affected both adsorption and uptake fluxes by either direct competition for binding sites, modification of the surface charge potential of the membrane and also by modifying lead solution speciation. Simple steady-state or pre-equilibrium approaches to modelling bioavailability, considering only the free-ion as chemically bioavailable and including proton competition for binding sites, were found to be adequate to describe the observed pH dependence only within the pH range of 5.0 to 6.0. Below pH 5.0 the decrease in both uptake flux and surface bound lead was greater than could be predicted by considering only the changes in speciation and proton competition. Above pH 7.0, the observed increased flux and surface bound concentration was opposite to what would be expected by these simple modelling approaches. The authors proposed a number of hypotheses to account for these discrepancies. The pH induced changes to the surface charge potential which modifies the affinity of cations for the anionic binding sites, i.e. equation (5-26) was found to be potentially sufficient to explain the discrepancies observed below pH 5.0, however at pH values above 5.5 modification of the surface charge was not a plausible explanation to the observed discrepancy. pH induced changes to transporter protein conformation were also considered, but thought to be insufficient to explain the observed discrepancy. The hypothesis proposed as most likely to explain the observed pH behaviour at elevated pH values was that lead species other than just the free-ion were chemically bioavailable, potentially the $PbOH^+$ or $PbCO_3^0$ complexes.

Sub-lethal toxicity of uranium to the freshwater bivalve *Velesunio angasi*, as measured by the valve movement responses of immobilised individuals, decreased with increasing pH (Brown and Markich 2000; Markich, Brown et al. 2000). Changes to the solution speciation of uranium were predicted to be insufficient to explain this decrease in terms of the free uranyl-ion concentration. Both mitigation of toxicity by proton competition and the co-toxicity of the uranyl species UO_2OH^+ were considered as mechanisms to explain the observed behaviour, the second of these hypotheses being preferred by the authors.

As can be seen from the large number of different hypotheses proposed to explain the widely varying pH dependencies of the uptake or toxicity of different metals, there is little general consensus about how to best approach the modelling of the effects of pH. This is somewhat surprising due to the crucial role of pH in determining a wide range

of physico-chemical phenomena in the environment. As discussed in section 5.2, a number of alternative approaches to modelling the effect of pH can be proposed, and a number of these will be tested in section 7.3.

Table 6-5 Experimental conditions used to assess the effect of pH and uranyl concentration on uranium uptake by excised gills

pH	**5.00**	**5.00**	**5.00**	**5.00**	**5.00**	**5.00**	**5.50**	**5.50**	**6.00**	**6.00**	**6.00**	**6.00**
$[Ca]_T$/ µmol dm^{-3}	501	496	517	509	524	530	497	491	496	491	494	484
$[Mg]_T$/ µmol dm^{-3}	505	500	520	516	529	536	504	499	505	497	503	495
$[Na]_T$/ µmol dm^{-3}	3244	3178	3420	3289	3461	3607	3218	3242	3209	3156	3227	3170
$[K]_T$/ µmol dm^{-3}	3259	3218	3358	3291	3653	3442	3221	3241	3241	3186	3218	3203
$[Cl]_T$/ µmol dm^{-3}	5451	5405	5612	5322	5405	4481	5421	5587	5391	5382	5237	5261
$[NO_3]_T$/ µmol dm^{-3}	1993	1989	2112	2133	2618	3473	2001	2040	1974	1983	2128	1987
$[SO_4]_T$/ µmol dm^{-3}	517	512	540	509	532	539	509	505	509	506	505	496
[DIC]/ µmol dm^{-3}	16	16	16	16	16	16	19	19	39	32	32	32
$[PO_4]_T$/ µmol dm^{-3}	0	0	0	0	0	0	0	0	0	0	0	0
$[UO_2]_T$/ nmol dm^{-3}	**38**	**72**	**291**	**929**	**3591**	**10744**	**30**	**592**	**18**	**24**	**299**	**981**
$[Citrate]_T$/ µmol dm^{-3}	0	0	0	0	0	0	0	0	0	0	0	0
$\overline{\varphi}_{UO_2}$/ nmol g^{-1} h^{-1}	231	564	1952	6782	17965	31273	218	4915	199	238	2949	10172
$\sigma_{\varphi_{UO_2}}$/ nmol g^{-1} h^{-1}	80	143	828	2118	3255	6209	60	1599	62	49	847	3088
$\alpha_{UO_2^{2+}}$	1.5E-08	2.9E-08	1.2E-07	3.7E-07	1.4E-06	3.7E-06	7.9E-09	1.5E-07	1.5E-09	2.2E-09	2.1E-08	4.9E-08
f_{CO_2}	4.6E-04	4.6E-04	4.6E-04	4.6E-04	4.6E-04	4.6E-04	5.0E-04	4.8E-04	7.7E-04	6.4E-04	6.4E-04	6.4E-04
I	9.8E-03	9.7E-03	1.0E-02	9.9E-03	1.1E-02	1.1E-02	9.7E-03	9.8E-03	9.7E-03	9.6E-03	9.7E-03	9.6E-03

Table 6-5 Experimental conditions used to assess the effect of pH and uranyl concentration on uranium uptake by excised gills(continued)

pH	**6.50**	**6.50**	**7.00**	**7.00**	**7.00**	**7.00**	**7.50**	**7.50**
$[Ca]_T$/ µmol dm^{-3}	500	502	510	481	518	522	498	489
$[Mg]_T$/ µmol dm^{-3}	507	513	520	490	527	531	507	499
$[Na]_T$/ µmol dm^{-3}	3221	3218	3376	3263	3443	3485	3358	3238
$[K]_T$/ µmol dm^{-3}	3226	3233	3347	3234	3452	3445	3245	3174
$[Cl]_T$/ µmol dm^{-3}	5409	5642	5465	5383	5577	5525	5252	5112
$[NO_3]_T$/ µmol dm^{-3}	2014	2267	2024	2010	2139	2273	2003	2427
$[SO_4]_T$/ µmol dm^{-3}	510	523	525	512	539	544	511	502
[DIC]/ µmol dm^{-3}	49	33	127	114	131	120	319	198
$[PO_4]_T$/ µmol dm^{-3}	0	0	0	0	0	0	0	0
$[UO_2]_T$/ nmol dm^{-3}	**31**	**658**	**28**	**60**	**372**	**822**	**123**	**726**
$[Citrate]_T$/ µmol dm^{-3}	0	0	0	0	0	0	0	0
$\overline{\varphi}_{UO_2}$/ nmol g^{-1} h^{-1}	465	8457	782	1462	7364	13259	2621	11584
$\sigma_{\varphi_{UO_2}}$/ nmol g^{-1} h^{-1}	169	1565	366	469	2501	4456	580	4433
$\alpha_{UO_2^{2+}}$	4.2E-10	4.1E-09	2.5E-11	4.8E-11	1.4E-10	2.3E-10	2.9E-12	1.5E-11
f_{CO_2}	5.7E-04	3.8E-04	6.4E-04	5.7E-04	6.5E-04	6.0E-04	5.7E-04	3.5E-04
I	9.8E-03	1.0E-02	1.0E-02	9.8E-03	1.0E-02	1.0E-02	9.9E-03	9.8E-03

Figure 6-3 Effect of pH and uranium concentration on uranium uptake by excised gills. a) uranium accumulation fluxes in function of total uranium concentration, b) fluxes in function of the predicted free uranyl ion concentration. Error bars show ± 1 S.D.

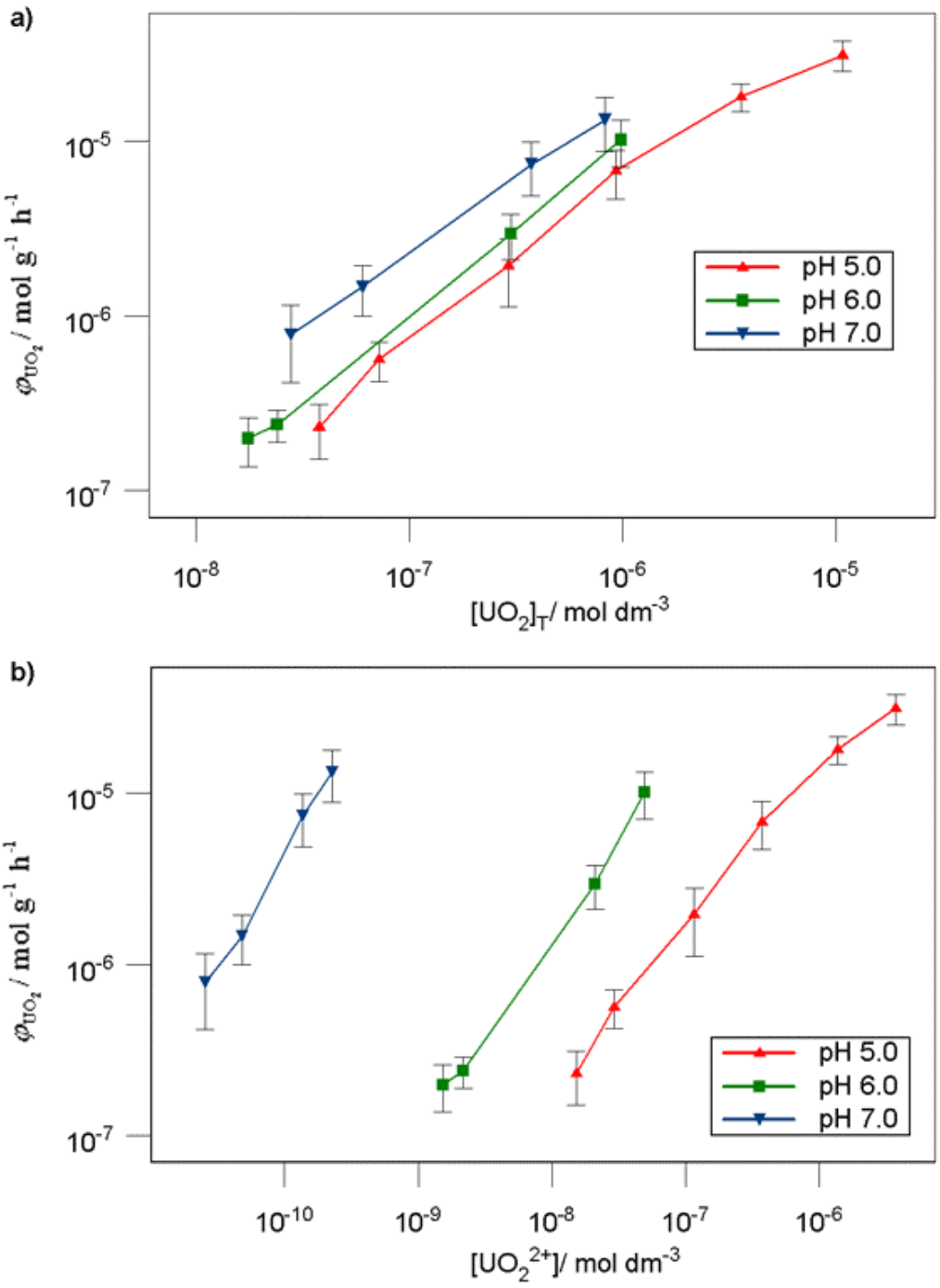

6.5.4 Effect of water hardness

Bioaccumulation experiments to assess the effect of water hardness were performed by varying the concentrations of either calcium or magnesium in the range 10^{-4} – $2.5 \cdot 10^{-3}$ mol dm^{-3}, whilst keeping the concentration of the other hardness ion constant (0.5 mmol dm^{-3}). Ionic strength was maintained at a constant 0.01 mol dm^{-3} by co-varying the concentrations of sodium and potassium in a 1:1 ratio. Anion concentrations were maintained constant, and experiments were performed at pH values of 6 and 7 for an exposure duration of 30 minutes. For constant pH, the variation in the concentrations of the hardness cations is predicted to have virtually no effect on the distribution of uranyl solution species. The results of these experiments for varying calcium concentration are shown in Table 6-6, and for varying magnesium concentration in Table 6-7. Graphs of the normalised accumulation flux rates at a total uranium concentration of $5 \cdot 10^{-8}$ mol dm^{-3} as a function of either calcium or magnesium concentration at each of the two selected pH values are shown in Figure 6-4. As can be seen the accumulation of uranium was not affected by varying either calcium or magnesium concentration, i.e. no antagonistic competition for physiologically active membrane carrier sites by either calcium or magnesium was observed.

The lack of effect of either calcium or magnesium concentration on the accumulation of uranium found in this study appears to be contrary to the proposed BLM framework. However, the results of previous studies that have investigated the effects of varying water hardness are mixed, some studies finding that increasing concentrations of hardness cations reduce toxicity or accumulation of other metals and others finding no effect. Often the interpretation of accumulation or toxicity studies is confounded by the fact that it is not possible to vary the concentration of a single cation without changing other solution composition parameters as discussed in section 6.1. Changes to the concentration of a hardness cation must be accompanied by the concomitant change of either the concentration of another cation at constant ionic strength, or the concentration of a counter-anion at variable ionic strength.

The binding of copper to rainbow trout gills (Taylor, Baker et al. 2002), measured by a similar experimental approach to this study employing short duration in-vitro exposures of isolated gill tissues, was found to be unaffected by varying calcium

concentration in the exposure media. However, an effect on the accumulation of copper after acclimation in waters of different calcium concentrations was observed. Gills of fish which had been fully acclimated to either hard water or soft water bound similar amounts of copper in the exposure medium. However, gills of fish which had been acclimated to a hard water and then acutely transferred to a soft water for periods of 3 – 24 hours immediately prior to the copper exposures bound increasingly larger amounts of copper. The authors ascribed this to ionoregulatory homeostatic upset due to the important role that calcium plays in regulating membrane permeability and stabilising membrane proteins, and also potentially regulating the number and affinity of membrane carriers.

A study of the effect of magnesium on the accumulation of silver by the rainbow trout *Oncorhynchus mykiss* found no inhibition of uptake for a range of magnesium concentration of up to 210 mM (Schwartz and Playle 2001). The authors however, chose to include a Mg-gill stability constant in their Silver-gill binding model.

The accumulation of cobalt in the gills of rainbow trout (2 – 3 hr exposures) was found to be inhibited by increasing calcium concentration (Richards and Playle 1998), attributed by the authors to the antagonistic competition of calcium for metal binding sites. Similarly, the uptake of strontium by carp (Chowdhury and Blust 2001) was found to be inhibited by increasing calcium concentration.

The toxicity of uranium to the freshwater hydra *Hydra viridissima* decreased on increasing calcium hardness at constant pH (6.0) and alkalinity (4 mg-$CaCO_3$ l^{-1}), the EC50 value increasing by 92 % for a 50 fold increase in water hardness (Riethmuller, Markich et al. 2001).

Acute toxicity of copper to *Daphnia magna* (De Schamphelaere and Janssen 2002) was found to be mitigated by calcium, magnesium and sodium, attributed to the antagonistic competition for binding sites by the authors, but no effect was found for potassium. However, on inspection of these results the interpretation of the dataset is confounded by the fact that ionic strength was not maintained at a constant value, and in fact can be used as a simpler and equally good parameter to explain the changes in observed toxicity. The much smaller concentration range employed to study the effect of potassium compared to the other cations can explain the lack of observed effect. Figure 6-5 shows the acute toxicity values expressed as the predicted free copper ion

concentrations (calculated by the authors of the study) as a function of calcium, magnesium, sodium and potassium concentrations and ionic strength. Whether the mitigation of toxicity observed was due to the direct effect of increased cation concentrations or the indirect effect of varying ionic strength leading to surface charge modification of the biological interface cannot be determined from this study. A further study performed to investigate the toxicity of zinc to *Daphnia magna* (Heijerick, De Schamphelaere et al. 2002) found the same mitigating effects on toxicity from calcium, magnesium and sodium, but not potassium. However, in this study the reduction in toxicity on increasing calcium and magnesium concentrations was only observed up to concentrations of 2 mM for magnesium and 3 mM for calcium. The authors used only the lower concentration ranges for determining biotic ligand model affinity constants for these two metals, considering the model to be inapplicable to the higher concentration ranges. This study also suffers from the same confounding factors as the previous study as the ionic strength of the exposure solutions was not maintained at a constant value.

Table 6-6 Experimental conditions used to assess the effect of calcium on uranium uptake by excised gills

pH	**6.00**	**6.00**	**6.00**	**6.00**	**6.00**	**6.00**	**7.00**	**7.00**	**7.00**	**7.00**	**7.00**	**7.00**
$[Ca]_T$/ µmol dm^{-3}	**20**	**59**	**102**	**491**	**1014**	**2652**	**22**	**60**	**103**	**481**	**1028**	**2620**
$[Mg]_T$/ µmol dm^{-3}	514	512	521	497	519	535	542	532	537	490	522	524
$[Na]_T$/ µmol dm^{-3}	3999	3932	3905	3156	2560	280	4268	4149	4051	3263	2606	308
$[K]_T$/ µmol dm^{-3}	3998	3934	3891	3186	2562	290	4266	4118	4004	3234	2600	278
$[Cl]_T$/ µmol dm^{-3}	5875	5853	5815	5382	5036	3647	6198	6060	5997	5383	5075	3541
$[NO_3]_T$/ µmol dm^{-3}	1998	2005	2007	1983	2026	2034	2118	2079	2078	2010	2035	2025
$[SO_4]_T$/ µmol dm^{-3}	513	512	512	506	519	534	543	532	530	512	525	525
[DIC]/ µmol dm^{-3}	35	38	38	32	36	36	121	120	123	114	121	111
$[PO_4]_T$/ µmol dm^{-3}	0	0	0	0	0	0	0	0	0	0	0	0
$[UO_2]_T$/ nmol dm^{-3}	23	23	18	24	22	43	35	42	48	60	49	54
$[Citrate]_T$/ µmol dm^{-3}	0	0	0	0	0	0	0	0	0	0	0	0
$\bar{\varphi}_{UO_2}$/ nmol g^{-1} h^{-1}	199	156	182	238	186	390	956	1211	1337	1462	1401	1242
$\sigma_{\varphi_{UO_2}}$/ nmol g^{-1} h^{-1}	51	30	40	49	33	132	224	290	389	469	295	150
$\alpha_{UO_2^{2+}}$	2.0E-09	2.0E-09	1.6E-09	2.2E-09	1.9E-09	3.7E-09	3.1E-11	3.6E-11	3.9E-11	4.8E-11	3.9E-11	4.3E-11
f_{CO_2}	7.0E-04	7.7E-04	7.6E-04	6.4E-04	7.2E-04	7.2E-04	6.1E-04	6.0E-04	6.2E-04	5.7E-04	6.0E-04	5.5E-04
I	9.9E-03	9.9E-03	9.9E-03	9.6E-03	9.9E-03	1.0E-02	1.1E-02	1.0E-02	1.0E-02	9.8E-03	1.0E-02	1.0E-02

Table 6-7 Experimental conditions used to assess the effect of magnesium on uranium uptake by excised gills

pH	**6.00**	**6.00**	**6.00**	**6.00**	**6.00**	**6.00**	**7.00**	**7.00**	**7.00**	**7.00**	**7.00**	**7.00**
$[Ca]_T$/ µmol dm^{-3}	496	492	501	491	505	505	516	529	526	481	518	507
$[Mg]_T$/ µmol dm^{-3}	**14**	**51**	**103**	**497**	**1011**	**2579**	**21**	**55**	**107**	**490**	**1044**	**2606**
$[Na]_T$/ µmol dm^{-3}	3991	3905	3889	3156	2525	285	4219	4238	4125	3263	2640	331
$[K]_T$/ µmol dm^{-3}	3982	3908	3888	3186	2535	290	4178	4194	4078	3234	2614	295
$[Cl]_T$/ µmol dm^{-3}	5950	5970	5896	5382	5001	3597	6189	6269	6190	5383	5135	3579
$[NO_3]_T$/ µmol dm^{-3}	2003	2014	2032	1983	2037	2102	2112	2141	2139	2010	2103	2125
$[SO_4]_T$/ µmol dm^{-3}	506	508	510	506	516	530	531	545	539	512	535	538
[DIC]/ µmol dm^{-3}	42	45	44	32	43	40	135	126	125	114	132	125
$[PO_4]_T$/ µmol dm^{-3}	0	0	0	0	0	0	0	0	0	0	0	0
$[UO_2]_T$/ nmol dm^{-3}	29	32	24	24	44	30	48	40	42	60	51	50
$[Citrate]_T$/ µmol dm^{-3}	0	0	0	0	0	0	0	0	0	0	0	0
$\overline{\varphi}_{UO_2}$/ nmol g^{-1} h^{-1}	230	316	205	238	406	462	1528	1127	1224	1462	1553	1834
$\sigma_{\varphi_{UO_2}}$/ nmol g^{-1} h^{-1}	73	83	36	49	99	204	472	283	301	469	420	939
$\alpha_{UO_2^{2+}}$	2.4E-09	2.6E-09	2.0E-09	2.2E-09	3.6E-09	2.6E-09	3.6E-11	3.4E-11	3.5E-11	4.8E-11	3.9E-11	4.0E-11
f_{CO_2}	8.4E-04	9.0E-04	8.9E-04	6.4E-04	8.7E-04	8.0E-04	6.8E-04	6.3E-04	6.3E-04	5.7E-04	6.6E-04	6.2E-04
I	9.9E-03	9.9E-03	9.9E-03	9.6E-03	9.8E-03	9.9E-03	1.0E-02	1.1E-02	1.0E-02	9.8E-03	1.0E-02	1.0E-02

Figure 6-4 Effect of water hardness as calcium and magnesium concentration on uranium uptake by excised gills. Error bars show ± 1 S.D.

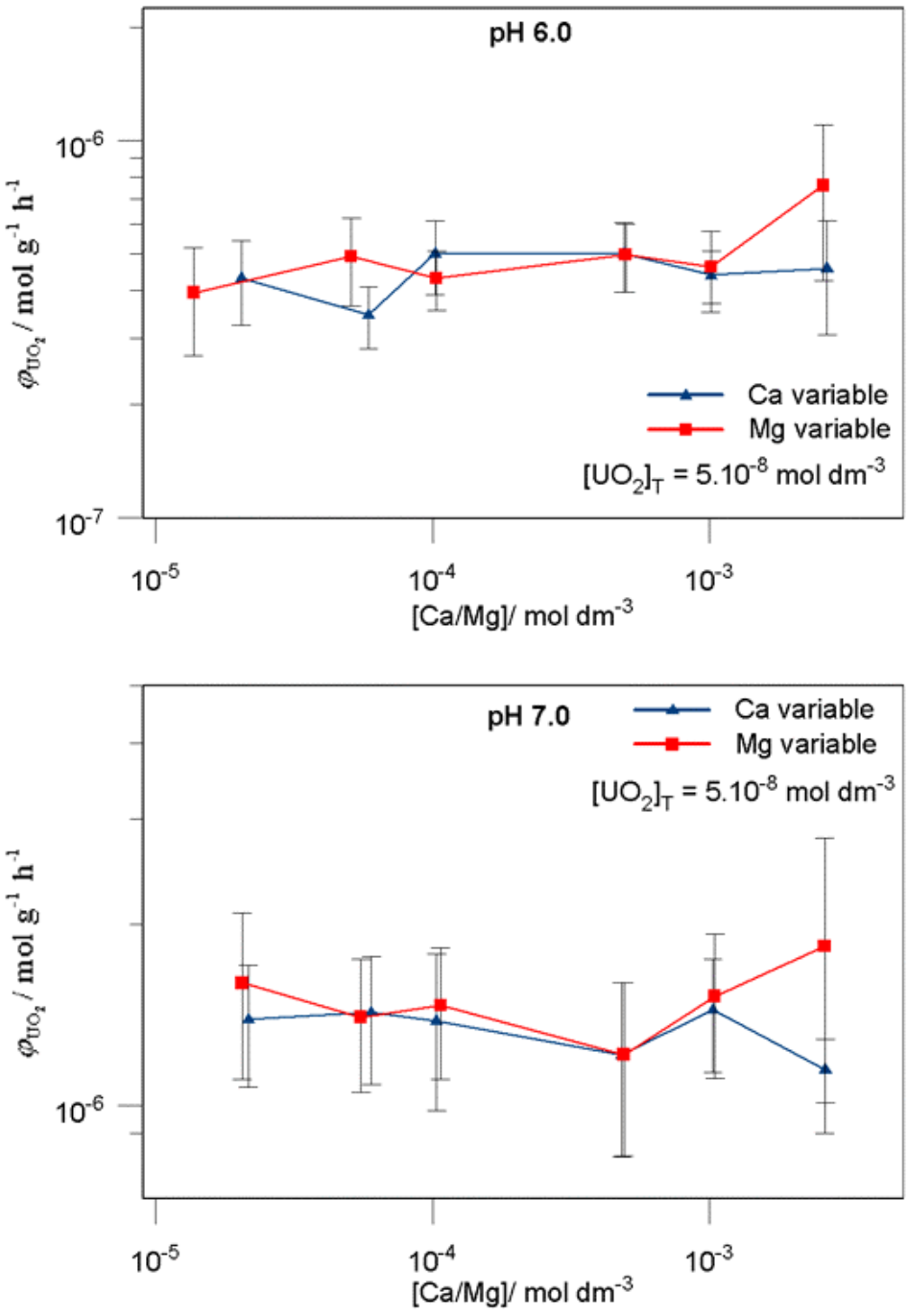

Figure 6-5 48-hour copper toxicities in function of a) calcium concentration, b) magnesium concentration, c) sodium concentration, d) potassium concentration and e) ionic strength. Data reinterpreted from tabulated values provided in article (De Schamphelaere and Janssen 2002).

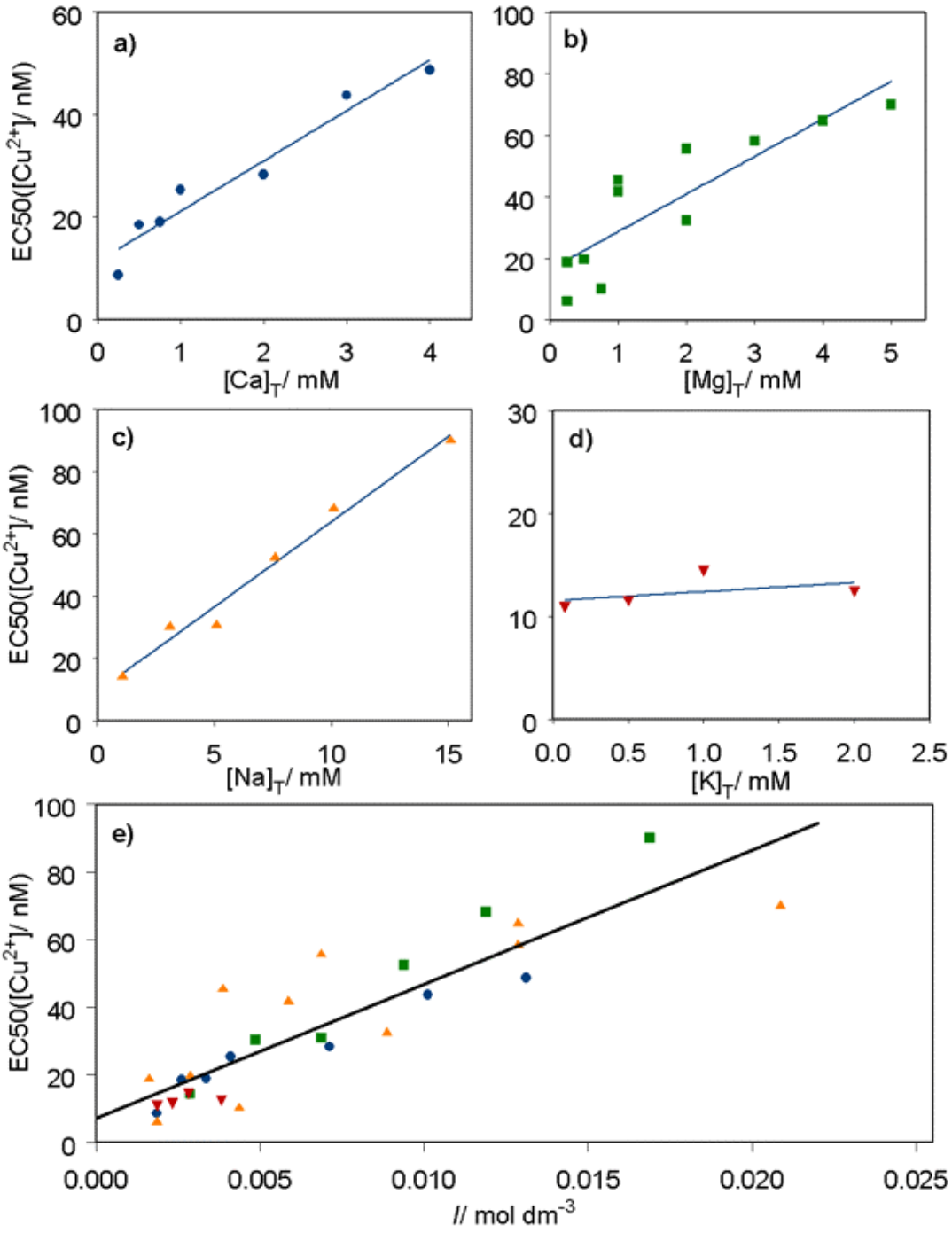

6.5.5 Effect of carbonate

Bioaccumulation experiments were performed at a uranium concentration of $5 \cdot 10^{-7}$ mol dm^{-3}, a pH range 5.0 – 7.5 and a range of DIC concentration of 10^{-5} – $5 \cdot 10^{-3}$ mol dm^{-3}. The partial pressures of carbon dioxide in the gas mixtures used to regulate DIC concentration were in the range $3 \cdot 10^{-4}$ – $3 \cdot 10^{-2}$ atm. The effects of pH and carbonate on uranium speciation are discussed in section 7.1.5. Details of the precise experimental conditions and results of these exposure experiments are given in Table 6-8, all exposures were of 30 minutes duration. For the experiments performed at elevated pH (7.0 and 7.5), increasing carbonate concentration significantly reduced the observed accumulation flux of uranium, as shown in Figure 6-6 a) for a total uranium concentration of $5 \cdot 10^{-7}$ mol dm^{-3}. However, the accumulation flux of uranium was not proportional to the predicted concentration of the free uranyl ion, as shown in Figure 6-6 b). In contrast, at lower pH values (5.0 and 6.0), increasing carbonate concentration increased the observed accumulation flux of uranium, as shown in Figure 6-7 contrary to the expected decrease in chemical bioavailability due to increasing carbonate complexation. A possible mechanism to explain these results is the formation of a ternary uranyl carbonate complex with a physiologically active carrier site. As can be seen in section 7.1.5, the only uranyl carbonate species that is significant at low pH, but relatively unimportant at elevated pH is the 1:1 $UO_2CO_3^0$ complex, suggesting the same stoichiometry for the surface complex, i.e. the formation and subsequent internalisation of $\{\equiv X - UO_2CO_3\}$. This hypothesis will be tested in section 7.3.

Studies of the effect of carbonate that have been performed using well defined conditions and varying carbonate concentrations independent of pH and hardness, and at several values of pH, are rare. Studies that have varied alkalinity at constant pH have generally not regulated the gas atmosphere in contact with the solutions in order to maintain the equilibrium with respect to CO_2 (Riethmuller, Markich et al. 2001; Taylor, Baker et al. 2002). This may not be a great problem for very short duration exposures, such as the 5-minute exposure periods of the second study. However for longer exposures such as the 96 hours of the first study (water renewal every 24 hours), the composition of the medium can be expected to evolve over time as equilibrium with respect to the atmosphere is approached. Results of these two studies

were similar, in that increasing carbonate concentration at constant pH and water hardness did not significantly change the measured chemical bioavailability of the metal. In the first study the toxicity of uranium to the freshwater hydra *Hydra viridissima* was unaffected by a 25-fold increase of alkalinity at constant pH (6.0) and hardness (165 mg-$CaCO_3$ l^{-1}) and in the second study the accumulation of copper by isolated fish gill tissues. This is despite significant changes to the free ion concentrations, in both cases increasing complexation of the metal by carbonate decreased the free ion concentration with increasing carbonate concentration. These results are consistent with the hypothesis that metal carbonate complexes may be bioavailable, although the authors of the two studies did not propose this as a possible mechanism. In a study of the pH dependence of lead uptake by the freshwater alga *Chlorella kesslerii* (Slaveykova and Wilkinson 2003), $PbOH^+$ or $PbCO_3^0$ species were proposed as potentially chemically bioavailable to explain the observed uptake behaviour.

Table 6-8 Experimental conditions used to assess the effect of carbonate

pH	**5.00**	**5.00**	**5.00**	**6.00**	**6.00**	**6.00**	**6.00**	**7.00**	**7.00**	**7.00**	**7.00**	**7.50**	**7.50**	**7.50**	**7.50**
$[Ca]_T$/ µmol dm^{-3}	517	649	490	494	503	512	572	518	506	493	526	489	512	525	501
$[Mg]_T$/ µmol dm^{-3}	520	591	494	503	507	514	541	527	509	509	537	499	518	529	511
$[Na]_T$/ µmol dm^{-3}	3420	3783	3215	3227	3246	3286	3463	3443	3260	3678	3785	3238	3407	3491	3281
$[K]_T$/ µmol dm^{-3}	3358	3833	3289	3218	3273	3316	3487	3452	3283	3286	3216	3174	3361	3515	3237
$[Cl]_T$/ µmol dm^{-3}	5612	6762	5728	5237	5527	5381	5614	5577	5036	3377	1570	5112	3804	2154	897
$[NO_3]_T$/ µmol dm^{-3}	2112	2377	2097	2128	2094	2129	2195	2139	2090	2111	2190	2427	2009	2216	2015
$[SO_4]_T$/ µmol dm^{-3}	540	607	539	505	522	528	571	539	524	522	573	502	549	518	530
[DIC]/ µmol dm^{-3}	**16**	**1071**	**662**	**32**	**142**	**563**	**1167**	**131**	**634**	**2870**	**5301**	**198**	**1805**	**3669**	**5318**
$[PO_4]_T$/ µmol dm^{-3}	0	0	0	0	0	0	0	0	0	0	0	0	0	0	0
$[UO_2]_T$/ nmol dm^{-3}	291	233	616	299	354	312	236	372	484	615	616	726	662	632	656
$[Citrate]_T$/ µmol dm^{-3}	0	0	0	0	0	0	0	0	0	0	0	0	0	0	0
$\bar{\varphi}_{UO_2}$/ nmol g^{-1} h^{-1}	1952	4235	8071	2949	5563	5172	5382	7364	10478	4391	2675	11584	2396	1359	243
$\sigma_{\varphi_{UO_2}}$/ nmol g^{-1} h^{-1}	828	1201	1903	847	1389	1359	1695	2501	3613	1900	717	4433	940	343	62
$\alpha_{UO_2^{2+}}$	1.2E-07	6.5E-08	2.0E-07	2.1E-08	1.3E-08	4.7E-09	1.8E-09	1.4E-10	4.1E-11	2.6E-12	5.6E-13	1.5E-11	3.6E-13	5.1E-14	2.0E-14
f_{CO_2}	4.6E-04	3.1E-02	1.9E-02	6.4E-04	2.8E-03	1.1E-02	2.3E-02	6.5E-04	3.2E-03	1.4E-02	2.7E-02	3.5E-04	3.2E-03	6.5E-03	9.5E-03
I	1.0E-02	1.2E-02	1.0E-02	9.7E-03	9.9E-03	1.0E-02	1.1E-02	1.0E-02	1.0E-02	1.0E-02	1.1E-02	9.8E-03	1.0E-02	1.0E-02	1.0E-02

Figure 6-6 Effect of carbonate concentration on uranium uptake by excised gills, pH 7 & 7.5, a) normalised accumulation flux as a function of DIC at $[UO_2]_T = 5 \cdot 10^{-7}$ mol dm^{-3}, b) accumulation flux as a function of predicted free uranyl ion concentration. Error bars show ± 1 S.D.

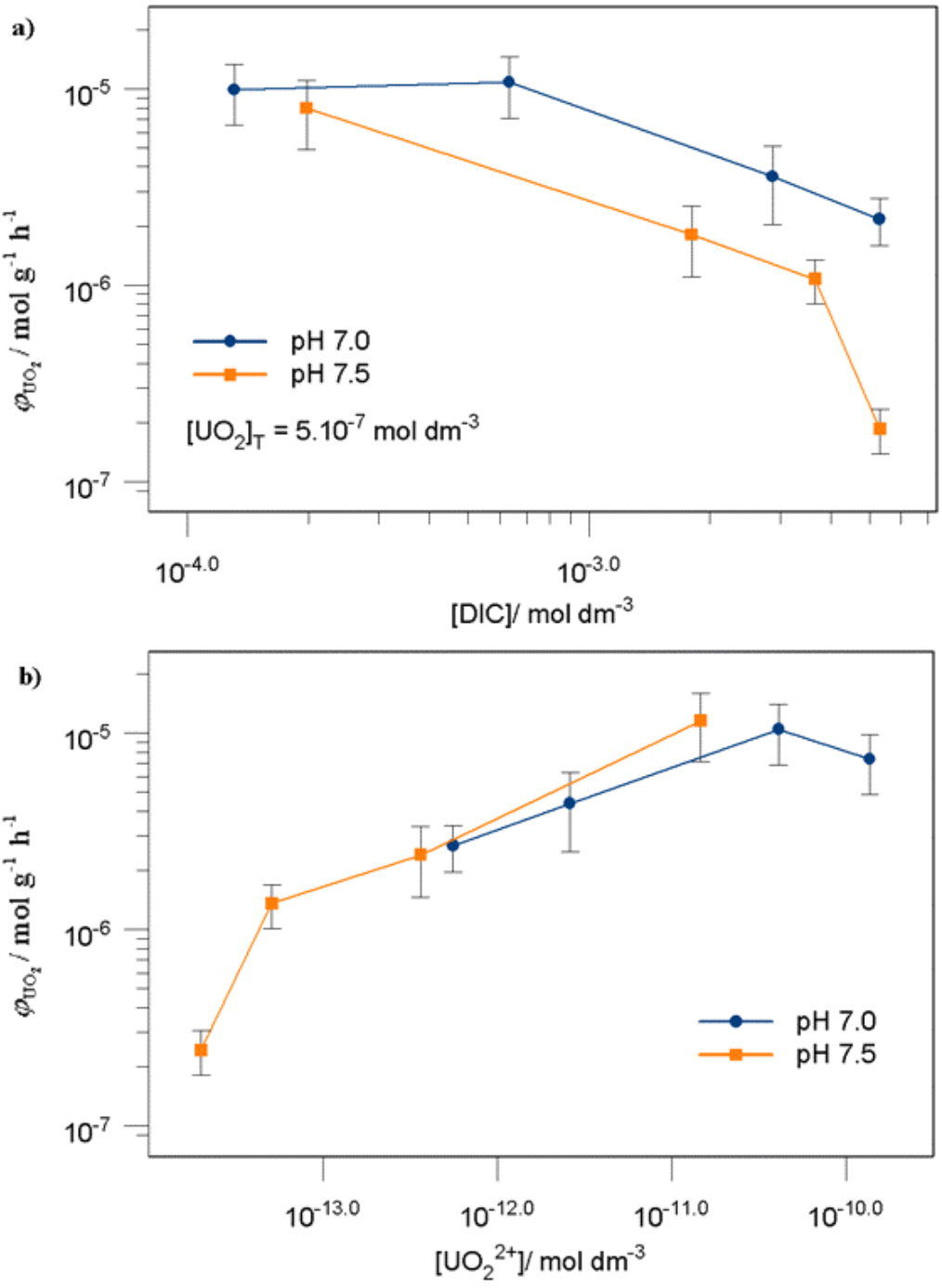

Figure 6-7 Effect of carbonate concentration on uranium uptake by excised gills, pH 5 & 6. Error bars show ± 1 S.D.

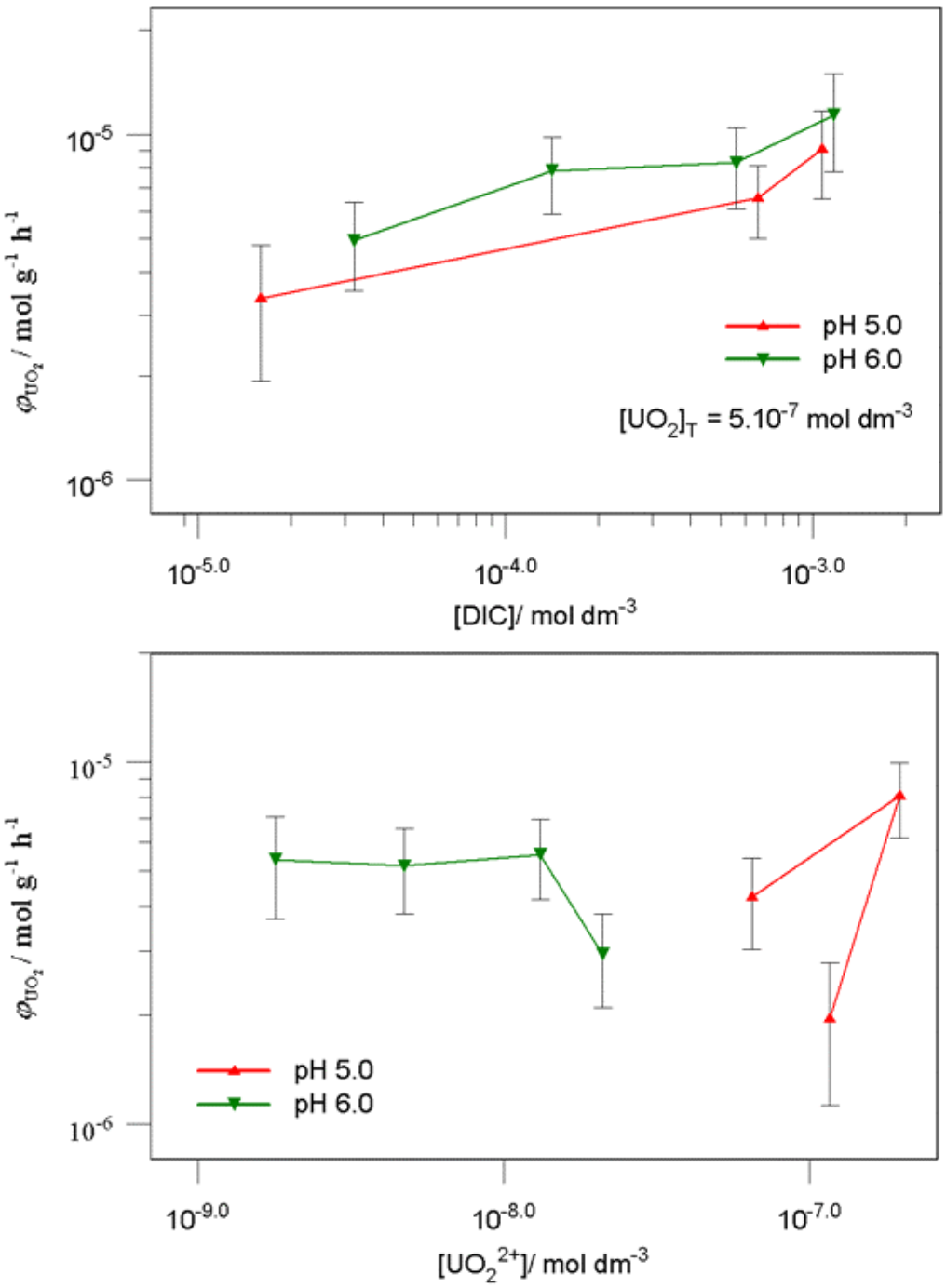

6.5.6 Effect of phosphate

Bioaccumulation experiments were performed at a uranium concentration of $5 \cdot 10^{-8}$ mol dm^{-3}, a pH range 5 – 7 and a range of phosphate concentration of 0 – 10^{-4} mol dm^{-3}. The DIC concentrations were determined by equilibrium with the air. The predicted speciation of uranium for these conditions is discussed in section 7.1.6. Details of the precise experimental conditions and results of these exposure experiments are given in Table 6-9, all exposures were of 30 minutes duration. Normalised accumulation fluxes as a function of phosphate concentration at a total uranium concentration of $5 \cdot 10^{-8}$ mol dm^{-3} are shown for pH values of 5.0, 5.5 and 6.0 in Figure 6-8 a) and pH values of 6.5 and 7.0 in Figure 6-8 b). A slight increase in uranium accumulation can be seen in function of phosphate concentration at pH 5.0, whereas at the other pH values there is no significant effect of phosphate concentration. This is in contrast to the predicted reduction in free uranyl ion concentration predicted for all of the pH values investigated, due to the complexation of uranium by phosphate. As was the case for the effect of carbonate, it is possible that these results may be explained by the uptake of uranyl phosphate species, and this hypothesis will be investigated further in section 7.3.

Table 6-9 Experimental conditions used to assess the effect of phosphate

pH	**5.00**	**5.00**	**5.00**	**5.00**	**5.50**	**5.50**	**5.50**	**6.00**	**6.00**	**6.00**	**6.00**	**6.50**	**6.50**	**6.50**	**7.00**	**7.00**	**7.00**
$[Ca]_T$/ µmol dm^{-3}	501	498	493	495	497	498	500	491	499	504	503	500	501	502	481	511	500
$[Mg]_T$/ µmol dm^{-3}	505	505	502	501	504	508	508	497	507	515	511	507	512	510	490	518	507
$[Na]_T$/ µmol dm^{-3}	3244	3225	3208	3206	3218	3244	3216	3156	3238	3279	3250	3221	3294	3276	3263	3365	3293
$[K]_T$/ µmol dm^{-3}	3259	3228	3223	3301	3221	3268	3356	3186	3269	3307	3373	3226	3315	3368	3234	3349	3336
$[Cl]_T$/ µmol dm^{-3}	5451	5493	5485	5459	5421	5527	5531	5382	5526	5599	5545	5409	5548	5527	5383	5576	5504
$[NO_3]_T$/ µmol dm^{-3}	1993	2009	2009	1998	2001	2026	2033	1983	2030	2060	2033	2014	2042	2040	2010	2066	2057
$[SO_4]_T$/ µmol dm^{-3}	517	510	512	508	509	516	517	506	522	532	526	510	521	523	512	529	526
[DIC]/ µmol dm^{-3}	16	16	16	16	19	25	25	32	53	55	65	49	49	49	114	91	91
$[PO_4]_T$/ µmol dm^{-3}	**0**	**8**	**24**	**99**	**0**	**9**	**99**	**0**	**9**	**13**	**100**	**0**	**25**	**99**	**0**	**26**	**99**
$[UO_2]_T$/ nmol dm^{-3}	38	61	88	66	30	62	68	24	67	63	57	31	37	50	60	59	37
$[Citrate]_T$/ µmol dm^{-3}	0	0	0	0	0	0	0	0	0	0	0	0	0	0	0	0	0
$\bar{\varphi}_{UO_2}$/ nmol g^{-1} h^{-1}	231	516	1192	1942	218	429	703	238	570	517	532	465	226	485	1462	974	369
$\sigma_{\varphi_{UO_2}}$/ nmol g^{-1} h^{-1}	80	196	670	419	60	100	225	49	347	155	160	169	98	138	469	297	97
$\alpha_{UO_2^{2+}}$	1.5E-08	1.8E-08	1.7E-08	4.8E-09	7.9E-09	8.4E-09	1.6E-09	2.2E-09	2.6E-09	2.0E-09	3.7E-10	4.2E-10	1.7E-10	7.6E-11	4.8E-11	3.7E-11	1.1E-11
f_{CO_2}	4.6E-04	4.6E-04	4.6E-04	4.6E-04	5.0E-04	6.5E-04	6.5E-04	6.4E-04	1.1E-03	1.1E-03	1.3E-03	5.7E-04	5.7E-04	5.7E-04	5.7E-04	4.6E-04	4.6E-04
I	9.8E-03	9.8E-03	9.8E-03	9.8E-03	9.7E-03	9.9E-03	1.0E-02	9.6E-03	9.9E-03	1.0E-02	1.0E-02	9.8E-03	1.0E-02	1.0E-02	9.8E-03	1.0E-02	1.0E-02

Figure 6-8 Effect of phosphate concentration on uranium uptake by excised gills. Error bars show ± 1 S.D.

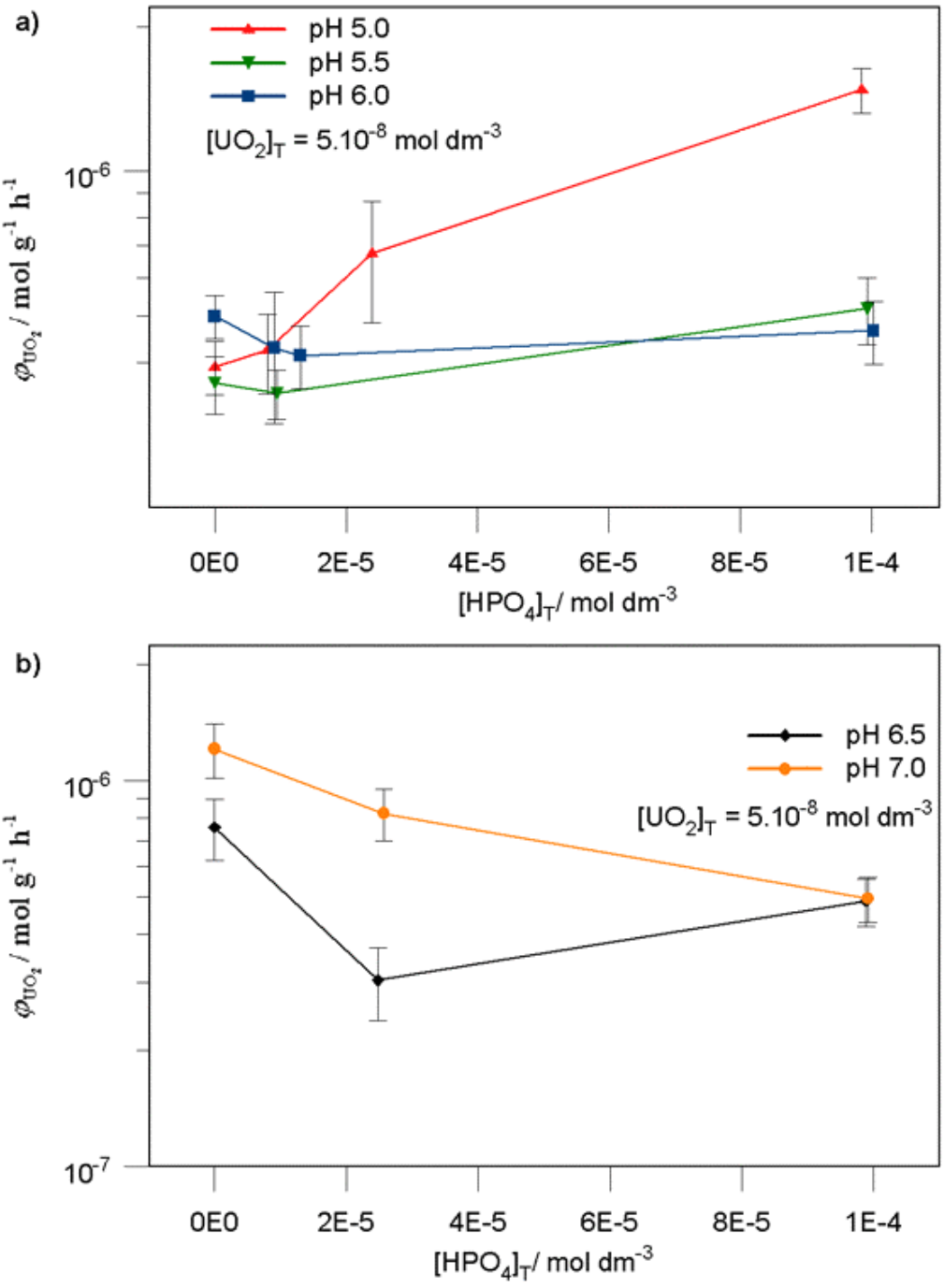

6.6 Summary Of The Experimental Results

The effect of citrate on the accumulation of uranium is consistent with the equilibrium paradigm at both pH values studied. Although the uptake was not exactly proportional to predicted free uranyl ion concentrations at either pH value and regression gradients were different for the two pH values, the observed uptake was within uncertainty estimates for the predicted concentration changes of the free ion. However, as a range of different mononuclear inorganic solution species were covariant with the free ion for these conditions it is not possible to identify the free ion as the *only* bioavailable uranium species. The uptake behaviour as a function of uranium concentration at pH 5.0 showed saturable uptake kinetics, indicating that accumulation is a facilitated process. The uptake dependence on pH demonstrated that the predicted free ion concentration is not a good indicator of the chemical bioavailability of uranium, in fact it is considerably worse than the total concentration for this range of conditions. A number of different hypotheses may be proposed to account for this behaviour, including the competition for binding sites by protons, the accumulation of uranium species other than the free ion and the modulation of the activity of the transport systems by pH. All of these hypotheses will be assessed in section 7.3. The lack of any inhibitory effect from increasing calcium or magnesium concentration may be unexpected in the light of the BLM modelling framework, indicating that cation competition for transporter binding sites is relatively unimportant for uranium accumulation. In light of these results, competitive effects were not tested in the subsequent modelling, with the exception of the possibility of protonation - deprotonation reactions of the transporter binding site. The contrasting effects of carbonate complexation at different pH values provide evidence for the potential chemical bioavailability of some uranyl carbonate species, but not others. The increased uptake at low pH values (5.0 and 6.0) contrary to the expected decrease in free ion concentration provides evidence for the uptake of a carbonate species important at these low pH values ($UO_2CO_3^0$ being the most likely candidate). At elevated pH values (7.0 and 7.5) the significant reduction in accumulation points towards the non-availability of the complexes dominant in this pH range (including $(UO_2)_2CO_3(OH)_3^-$, $UO_2(CO_3)_2^{2-}$ and $UO_2(CO_3)_3^{4-}$), however the fluxes are not proportional to predicted free ion concentrations, again pointing towards the co-

availability of other uranium species. The hypothesis that some metal complexes may be chemically bioavailable in addition to the free ion has been proposed by many workers, including:

The uptake of $SrNTA^-$ and $CaNTA^-$ complexes by the common carp proposed by (Chowdhury and Blust 2002).

In acute copper toxicity studies with *Daphnia magna* (De Schamphelaere and Janssen 2002) the co-toxicity of copper hydroxide was proposed to explain the observed pH dependence. Subsequent studies by the same workers resulted in $CuCO_3^0$ also being proposed as a bioavailable species (De Schamphelaere, Heijerick et al. 2002).

The uptake of dissolved zinc by the mussel *Mytilus edulis* was enhanced by the presence of histidine (Vercauteren and Blust 1996) and the complex $ZnHis^+$ was suggested as a potentially bioavailable species by the authors.

Uptake of cadmium by the common carp, *Cyprinus carpio*, in the presence of citrate, glycine and histidine was higher than expected from predicted free ion concentrations (van Ginneken, Chowdhury et al. 1999). The authors proposed that cadmium complexes of these low molecular weight organic ligands were available for direct uptake.

The accidental anion transport of the silver thiosulfate complex was proposed as a mechanism for silver uptake by the unicellular green algae *C. reinhardtii* (Fortin and Campbell 2001).

The uptake of anionic metal-ligand complexes has been suggested to explain metal accumulation results in the presence of low molecular weight assimilable organic metabolites. For example the toxicity of copper, cadmium and zinc towards the green alga *P. subcapitata* exceeded that predicted on the basis of the free-metal ion in the presence of citrate that can be internalised and metabolised by the alga (Guy and Kean 1980; Errecalde, Seidl et al. 1998).

$PbOH^+$ or $PbCO_3^0$ were proposed as potentially chemically bioavailable for the freshwater alga *Chlorella kesslerii* (Slaveykova and Wilkinson 2003).

7 MODELLING RESULTS

7.1 Aqueous Speciation Modelling

In order to interpret the results of the uranium uptake experiments, the solution speciation of uranium in the composition domain studied needs to be predicted. This was achieved by performing both "classical" speciation modelling, employing mean-values of all thermodynamic parameters used to describe the chemical system as described in section 4.3, and also probabilistic uncertainty modelling as described in section 4.5 to account for the thermodynamic parameter uncertainty.

7.1.1 Effects of database uncertainty on aqueous uranyl speciation calculations and selection of calculation methods

In order to assess the effect of thermodynamic parameter uncertainty on the aqueous speciation calculations performed within this study, uncertainty calculations were performed for the same chemical composition domain as used for the uranium bioaccumulation experiments. The composition domain investigated may be divided into a number of paired variable factors for convenience, namely:

- pH and uranium concentration
- pH and citrate concentration
- pH and water hardness (as calcium and magnesium)
- pH and carbonate concentration
- pH and phosphate concentration

Sampling based methods of uncertainty calculation provide an estimation of the true probabilistic output distribution of the parameters of interest, the estimation improving, and tending towards, the true distribution as the sample size N used to perform the calculations increases. It is therefore important to assess the likely errors of the output parameters investigated, for the sample size used to perform the calculations. A number of descriptive statistical parameters to characterise the output distributions were selected, and the fractional errors for a number of different solution

compositions and uranyl species were calculated from the jack-knife estimate of variance (equation (4-45)) normalised by the output parameters. This approach also permits a comparison of the different sampling methods available, in this case random sampling (section 4.5.1.1) for the MC method and Quasi-random sampling by the Sobol low-discrepancy sequence (section 4.5.1.3) for the QMC method. Selected results from these calculations are presented in Figure 7-1 for solutions of pH 5.0 and 7.5, $[UO_2]_T$ of 10^{-8} and 10^{-5} mol dm^{-3} in equilibrium with a CO_2 partial pressure of $10^{-3.5}$ atm, other ion concentrations using the reference composition given in Table 6-1.

As can be seen from the graphs, as the sample size increases, the probabilistic error of the parameter estimates reduces. The results generally show the expected convergence behaviour for the MC method, the distribution mean value has an error of probabilistic order $O\left(N^{-1/2}\right)$ and the other parameters have a lower convergence rate.

For these simulations, the theoretical advantage of the QMC sampling method is not realised, and no significant advantage over the MC method was found, the convergence rates and fractional errors being generally very similar for the two methods. It is possible that for larger simulation numbers the theoretical advantage of the QMC method would become more apparent. It is evident that for some species and some scenarios, a very large number of simulations need to be performed in order to reduce the probabilistic error of the estimated parameters to an acceptable level. This is most notable for parameters that are sensitive to extreme values, such as quantile values, and species that have highly skewed distributions. It was for this reason that the distribution inter-decile interval, corresponding to a confidence interval of 0.8, was chosen to represent the relative uncertainty of the output distribution. More conventional but higher confidence intervals, such as 0.95, were found to have unacceptably high probabilistic errors even for very large sample sizes. For the solution compositions, uranyl species and output parameters shown, the maximum fractional probabilistic error for the MC method was 0.13 for $N = 10^3$, decreasing to 0.04 and 0.02 for $N = 10^4$ and 10^5 respectively. For the QMC method the corresponding values were 0.10, 0.07 and 0.01 respectively.

Figure 7-1 The fractional errors of a number of output parameters for different uranyl species in function of the sample size, *N* for the MC method (left) or the QMC method (right). pH = 5.0, $PCO_2 = 10^{-3.5}$, $[UO_2]_T = 10^{-8}$ mol dm^{-3}. Relative uncertainty is the inter-decile interval normalised by the distribution mean.

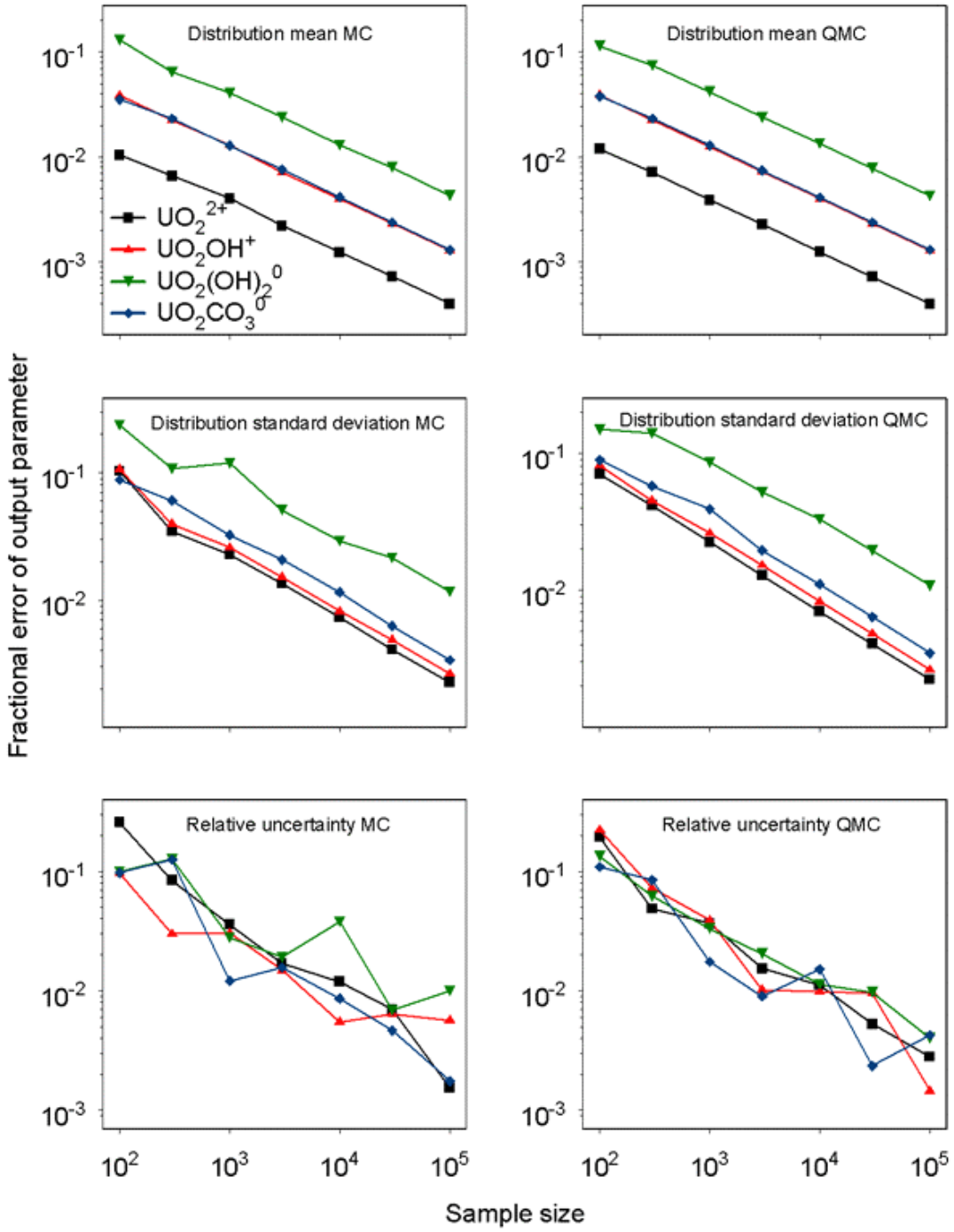

Figure 7-1 The fractional errors of a number of output parameters for different uranyl species in function of the sample size, *N* for the MC method (left) or the QMC method (right). pH = 5.0, $PCO_2 = 10^{-3.5}$, $[UO_2]_T = 10^{-5}$ mol dm^{-3}. Relative uncertainty is the inter-decile interval normalised by the distribution mean.

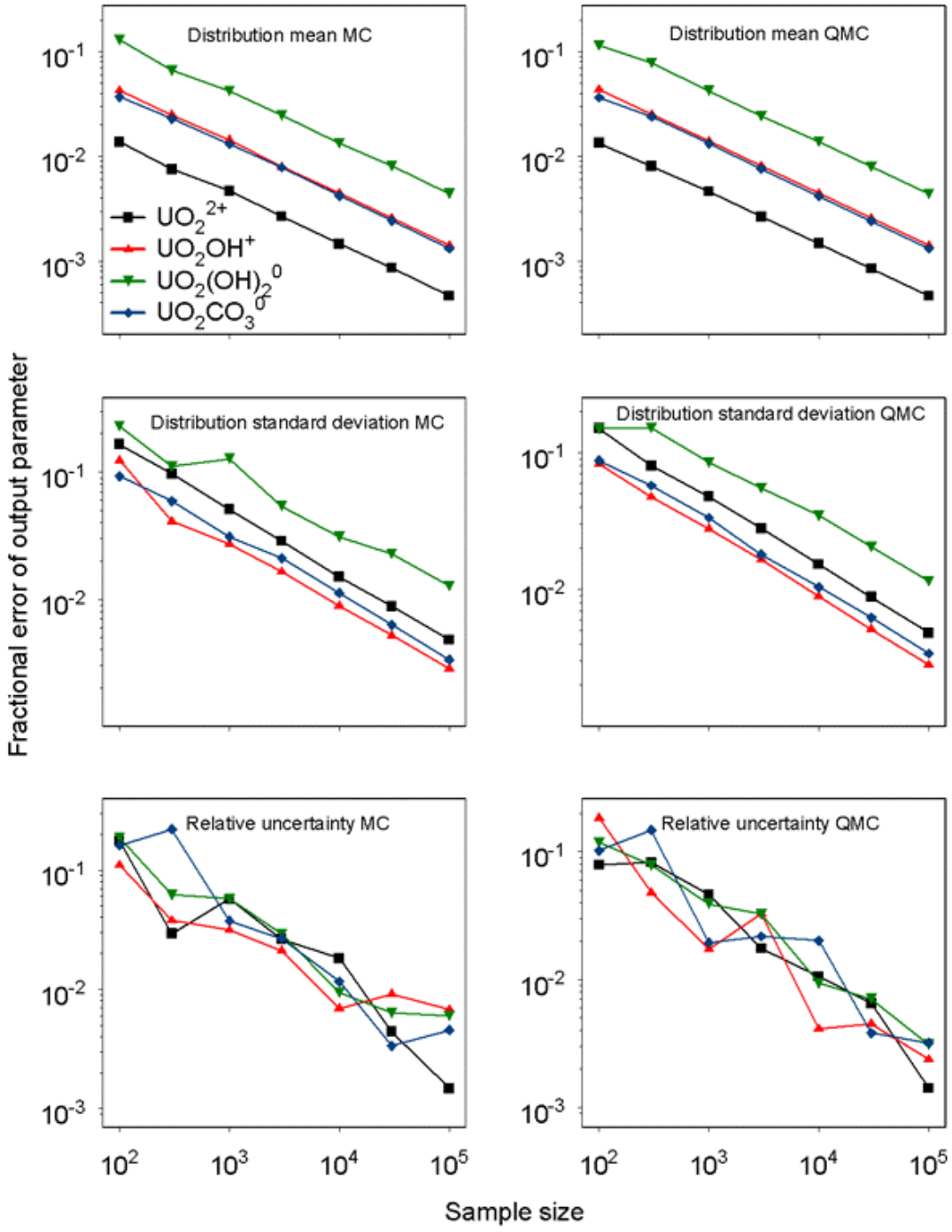

Figure 7-1 The fractional errors of a number of output parameters for different uranyl species in function of the sample size, *N* for the MC method (left) or the QMC method (right). pH = 7.5, $PCO_2 = 10^{-3.5}$, $[UO_2]_T = 10^{-8}$ mol dm^{-3}. Relative uncertainty is the inter-decile interval normalised by the distribution mean.

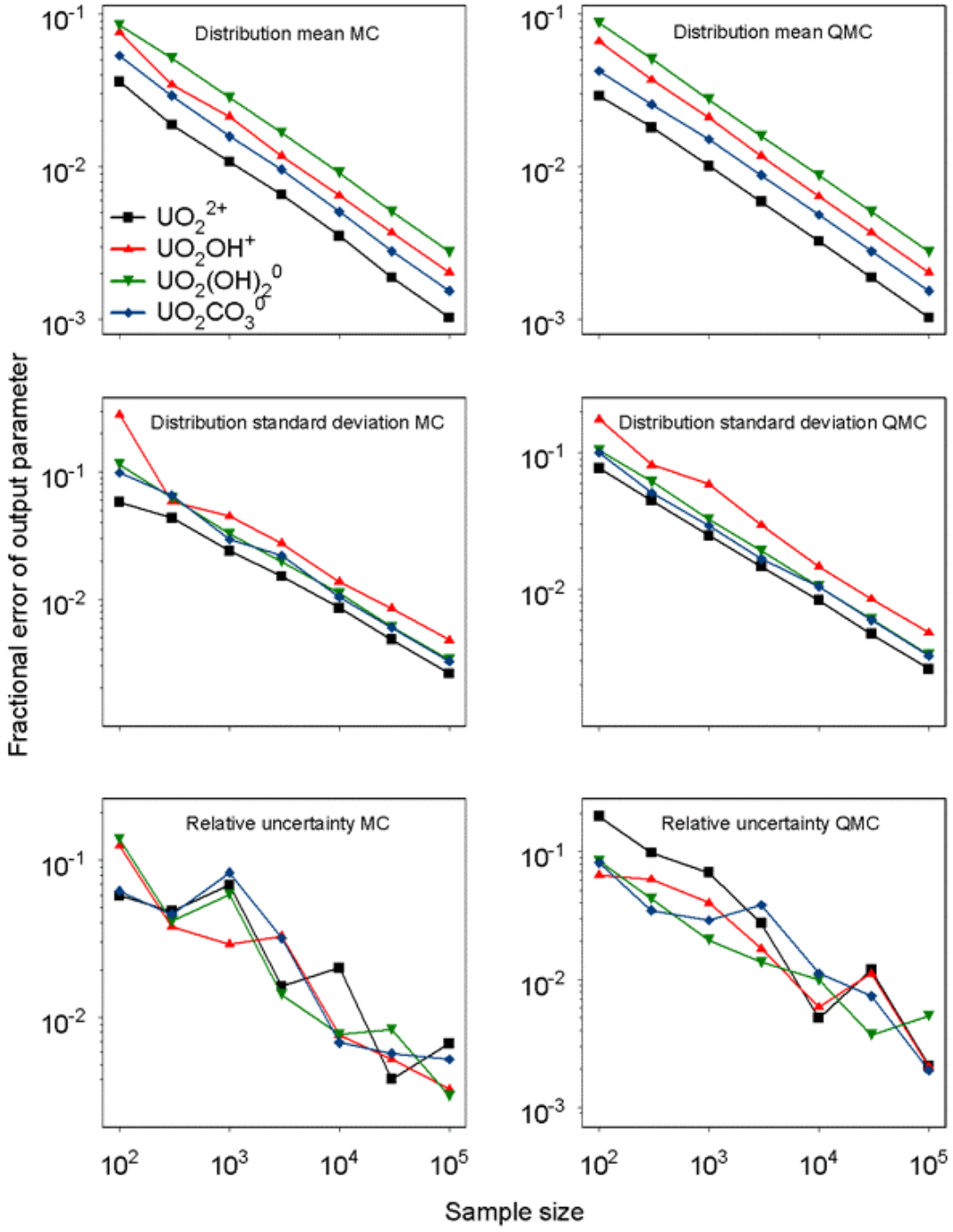

Figure 7-1 The fractional errors of a number of output parameters for different uranyl species in function of the sample size, *N* for the MC method (left) or the QMC method (right). pH = 7.5, $PCO_2 = 10^{-3.5}$, $[UO_2]_T = 10^{-5}$ mol dm^{-3}. Relative uncertainty is the inter-decile interval normalised by the distribution mean.

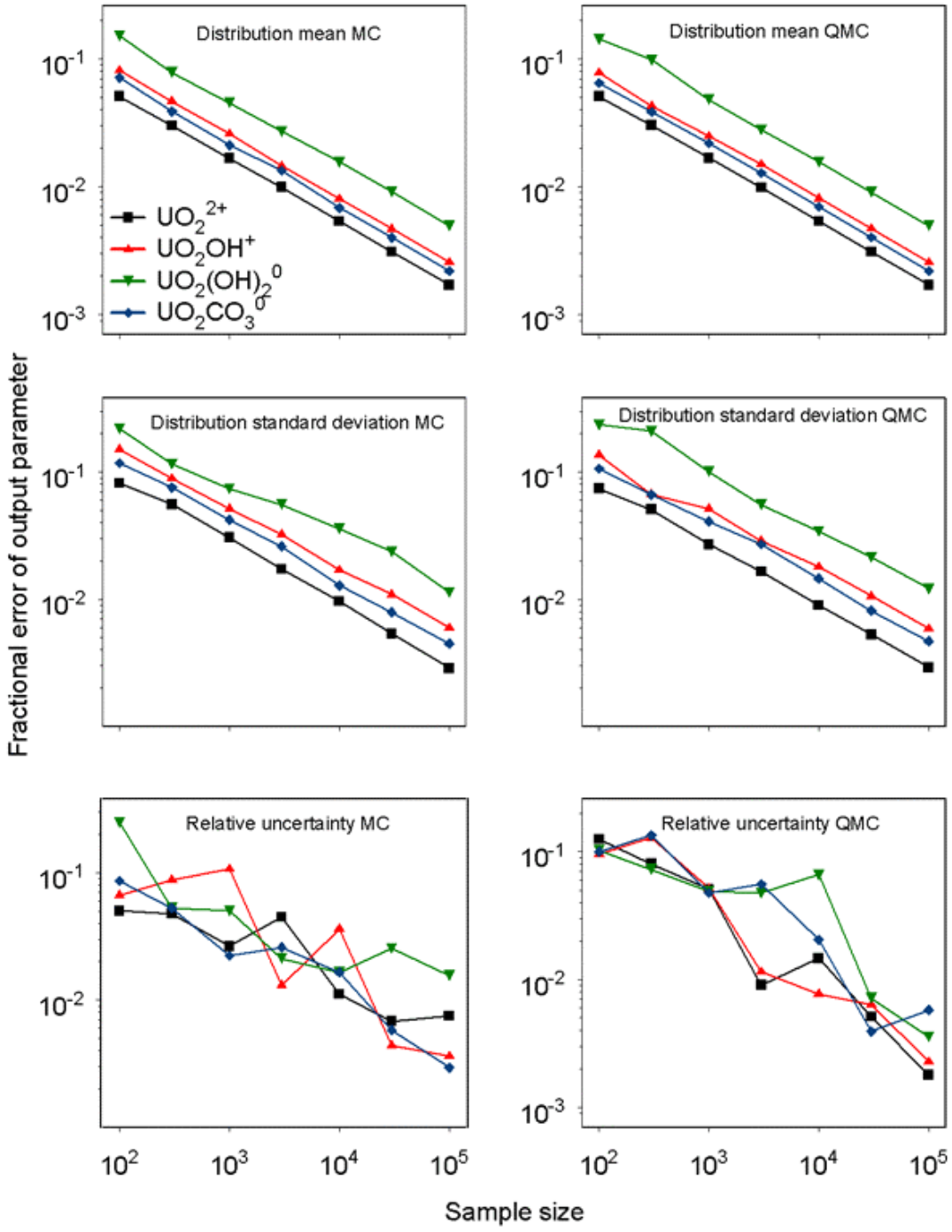

As no significant advantage was found to using the QMC method and there being a number of disadvantages to the method (principally the dimensional limitation of the Sobol sequence), all uncertainty calculations were performed using the MC method with a sample size of 10^4, which was found to provide generally adequate estimations of the output distributions. The mean-values and standard deviations of the input formation constants used are tabulated in appendix B. Except where stated in the text, the reference compositions tabulated in Table 6-1 were used for all calculations, giving an ionic strength of 0.01 mol dm^{-3}.

7.1.2 Effect of pH and uranium concentration

Bioaccumulation experiments were performed in the pH range 5 – 7.5 and total uranium concentration range of approximately 10^{-8} – 10^{-5} mol dm^{-3}. The distribution of uranyl through its major species predicted by mean-value speciation calculations for this pH range and in air equilibrium (P_{CO_2} = $10^{-3.5}$) for total uranium concentrations of 10^{-8} and 10^{-6} mol dm^{-3} are shown in Figure 7-2. As can be seen, the concentration of the free uranyl ion decreases very significantly as pH increases, changing from being the predominant species in the pH range 5 – 5.5 to contributing only 0.01 % of the total concentration at pH 7.5. The predominant species in the pH range 5.5 – 7.5 in air equilibrium depends on the total uranium concentration. At low concentration (10^{-8} mol dm^{-3}) the first and second uranyl hydrolysis products (UO_2OH^+ and $UO_2(OH)_2^0$) are predominant in the pH range 5.5 – 7, followed by the carbonate species $UO_2(CO_3)_2^{2-}$ up to pH 7.5. At higher uranium concentrations (10^{-6} mol dm^{-3}) the bi-nuclear species $(UO_2)_2CO_3(OH)_3^-$ is predicted to be predominant in the pH interval 6 – 7.5. The uranium species considered in the models applied to the accumulation data relevant to this composition domain were: UO_2^{2+}, UO_2OH^+, $UO_2(OH)_2^0$ and $UO_2CO_3^0$. Output distribution histograms of the four relevant uranyl species at pH values of 5, 6 and 7 for a total uranium concentration of 10^{-6} mol dm^{-3} at equilibrium with a CO_2 partial pressure of $10^{-3.5}$ are shown in Figure 7-3. Figure 7-4 shows the variation of the output distributions as a function of pH for the same species and solution composition domain. The variation of the relative uncertainties of the predicted concentrations for the four output species, defined as the inter-decile intervals expressed as percentages of distribution means, are shown for the relevant composition domain in Figure 7-5. As can be clearly seen, the probabilistic output

distributions vary considerably in function of the solution composition and the species of interest. The relative uncertainty of the predicted concentrations of these species varies greatly within this solution composition domain, for example the inter-decile confidence interval of the concentration of the free uranyl ion varies from 30 to 140 % of the distribution mean value.

Figure 7-2 Predicted distribution of major uranyl species in function of pH ($[UO_2]_T = 10^{-6}$ and 10^{-8} mol dm^{-3}, air equilibrium), calculated using mean-value database.

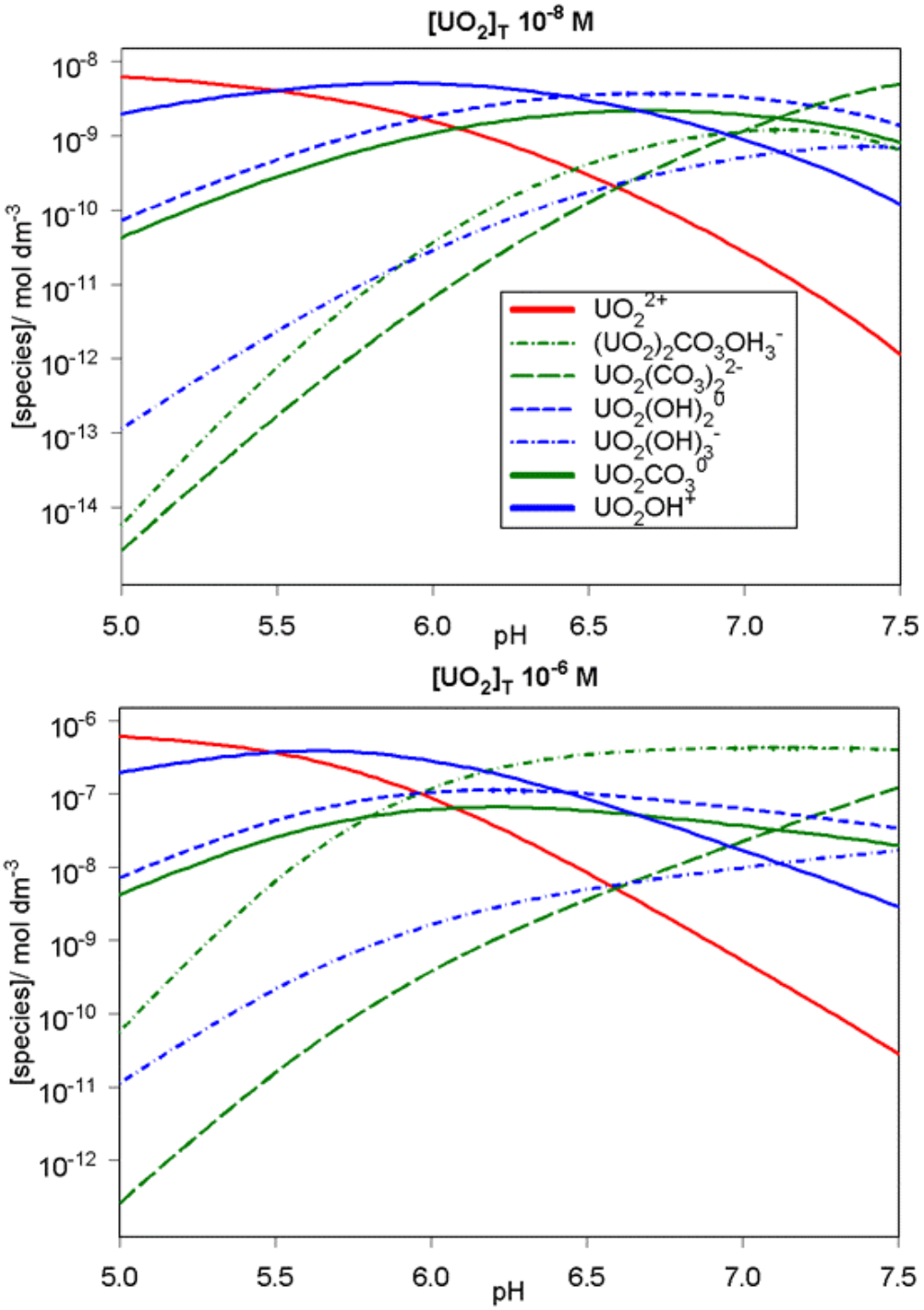

Figure 7-3 Histograms of uncertainty output distributions for different uranyl species at selected pH values ($[UO_2]_T = 10^{-6}$ M, air equilibrium).

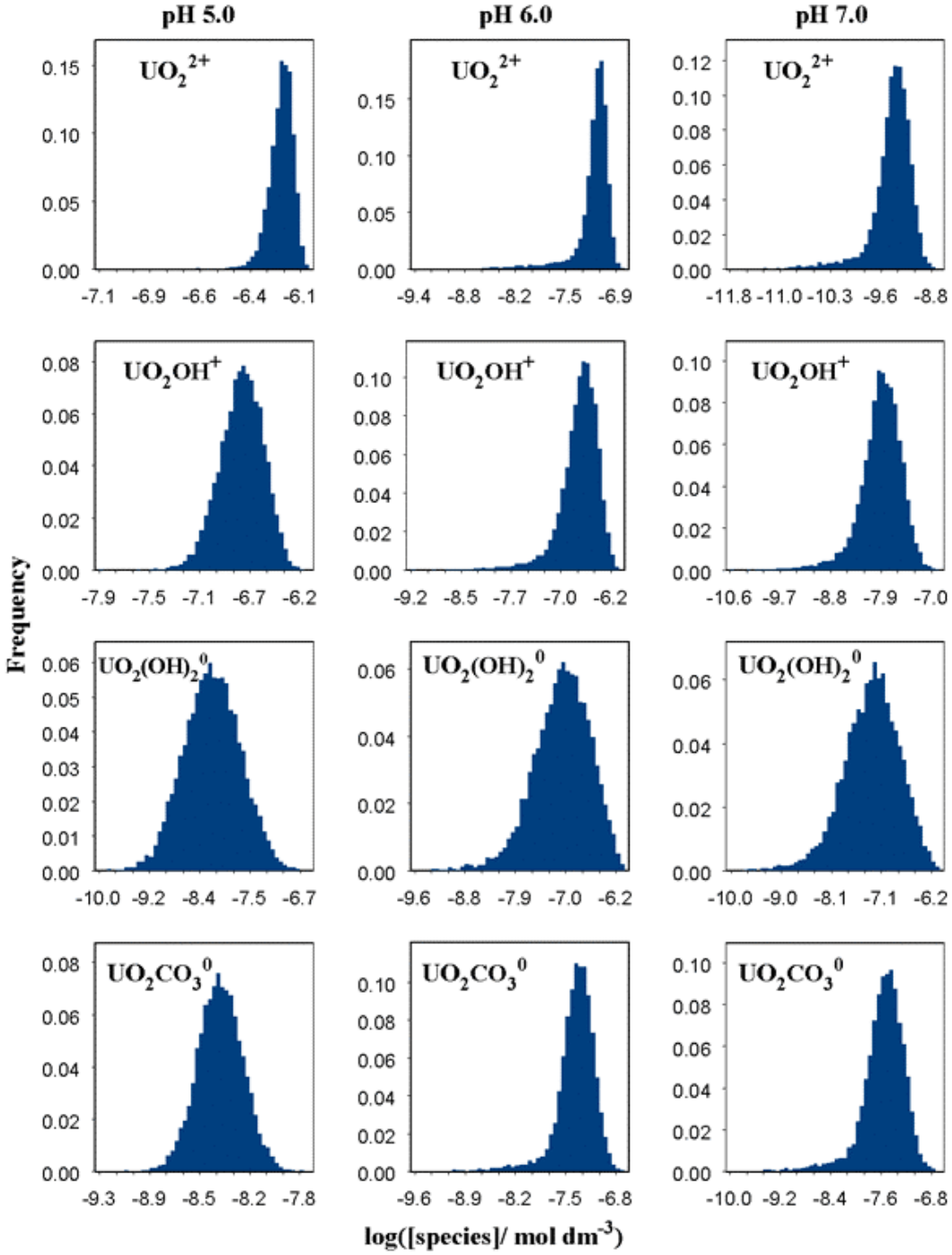

Figure 7-4 Uncertainty output distributions for different uranyl species in function of pH ($[UO_2]_T = 10^{-6}$ M, air equilibrium).

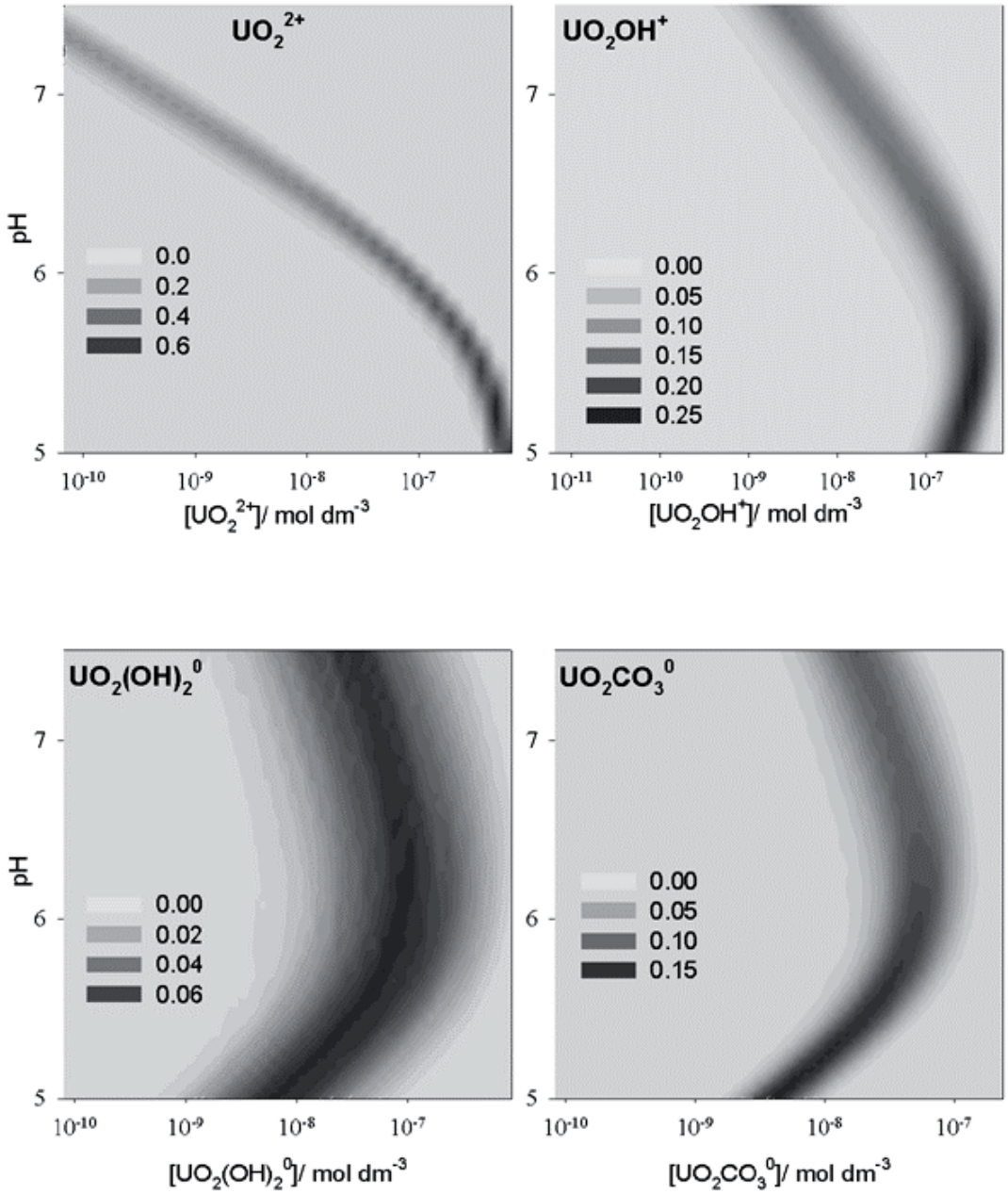

Figure 7-5 Relative uncertainties of selected uranyl species in function of pH and total uranium concentration (uncertainty distribution inter-decile intervals expressed as % of mean values)

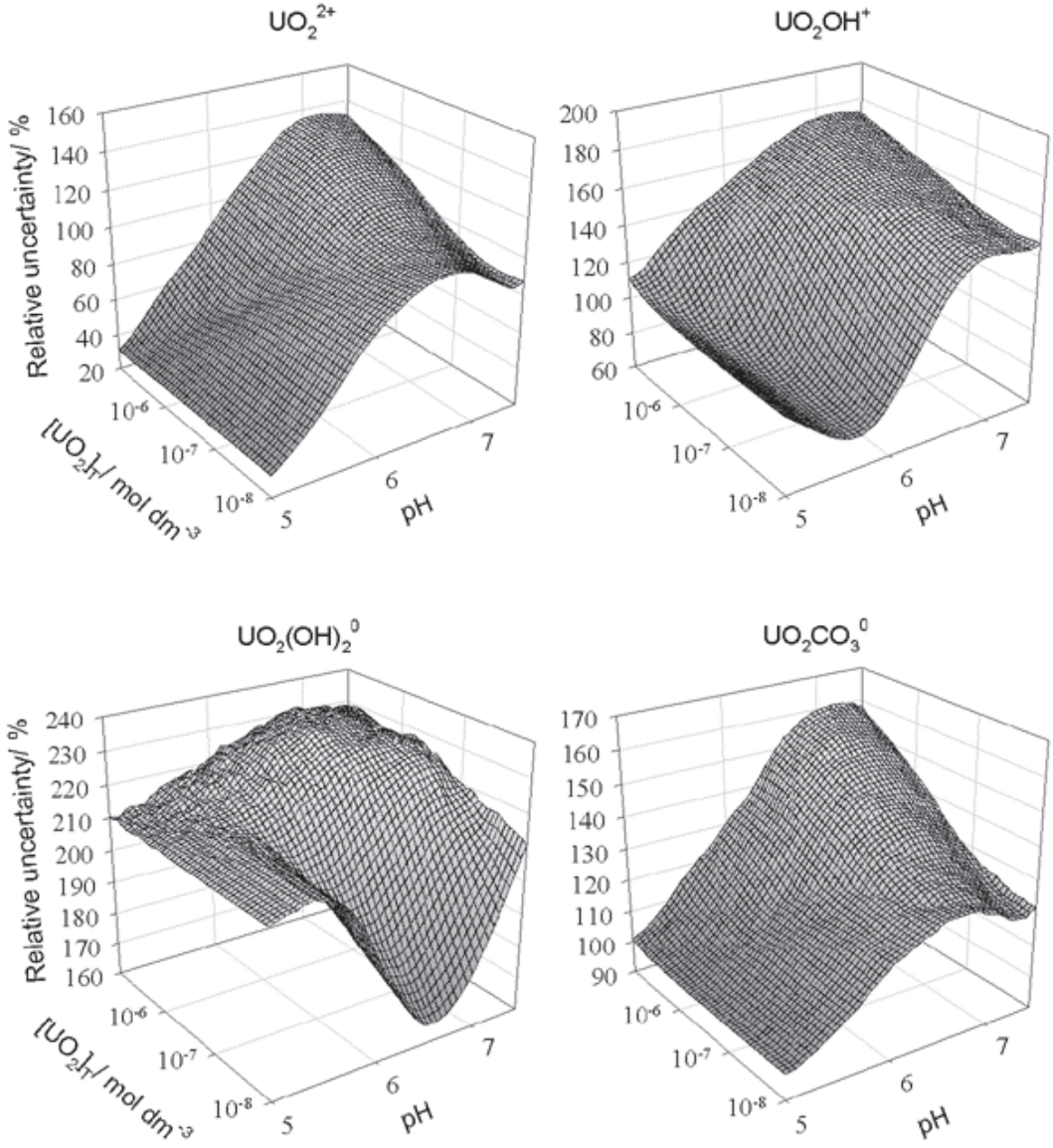

7.1.3 Effect of pH and citrate concentration

The series of experiments designed to assess the effect of citrate complexation were performed at pH values of 5.0 and 6.0 for a citrate concentration range of 0 – 10^{-5} mol dm^{-3} and a total uranium concentration of $5 \cdot 10^{-7}$ mol dm^{-3}. The concentration changes to the major solution species predicted by mean-value speciation calculations are shown in Figure 7-6 in function of total citrate concentration at each of the two pH values. As can be seen the effect of citrate complexation on the concentration of the free uranyl ion is predicted to be very significant at both of the two pH values, decreasing over one order of magnitude for the range of citrate concentration considered. The changes to the relative uncertainties of the predicted free uranyl ion concentrations in the same range of conditions is shown in Figure 7-7, the inter-decile interval of the probability distribution ranges from 30 to 140 % of the distribution mean value.

Figure 7-6 Predicted distribution of major uranyl species in function of citrate concentration at two pH values ($[UO_2]_T = 5.10^{-7}$ mol dm^{-3}, air equilibrium), calculated using mean-value database.

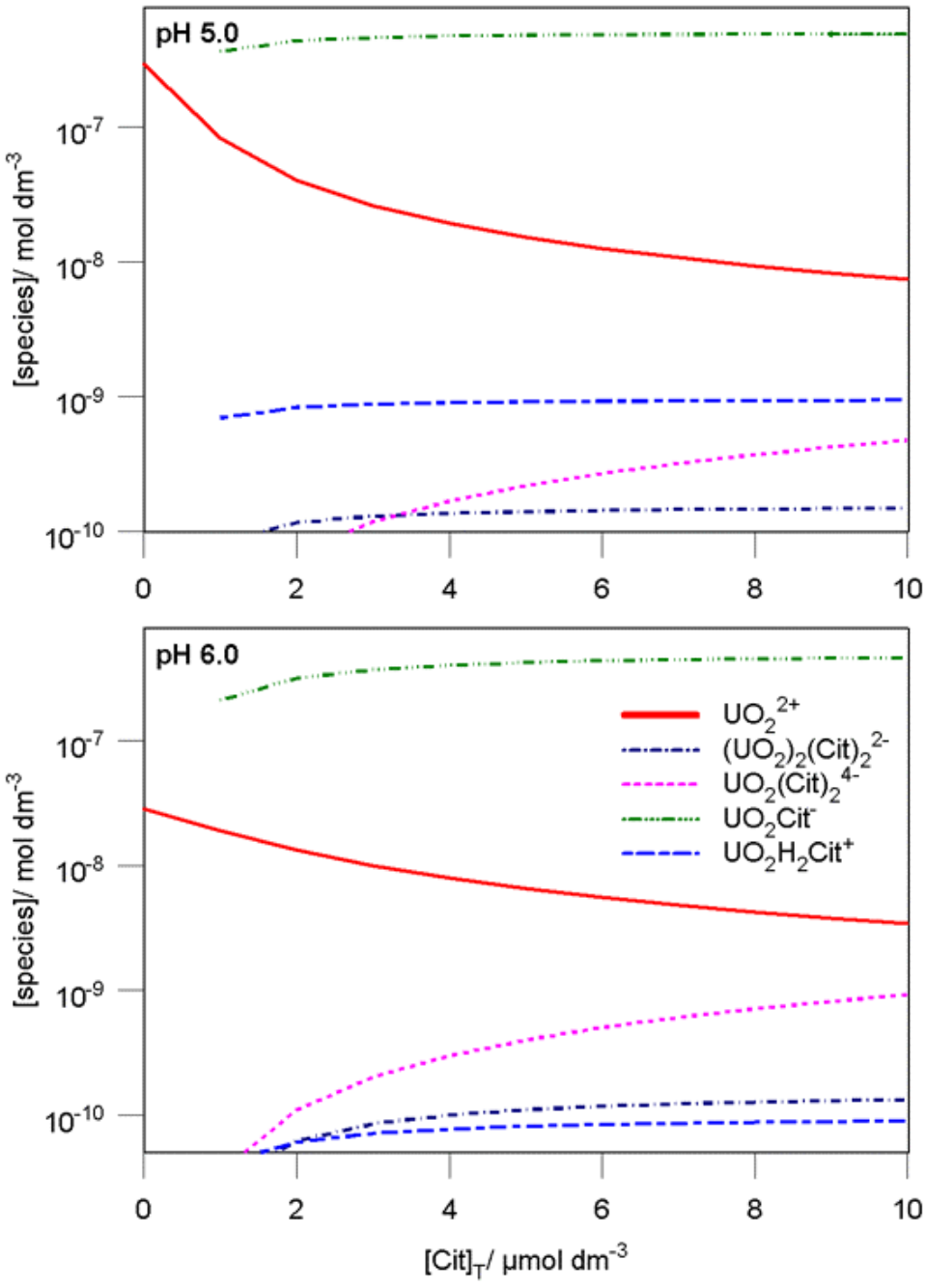

Figure 7-7 Relative uncertainties of UO_2^{2+} in function of citrate concentration at pH 5 and 6 ($[UO_2]_T$ 5.10^{-7} mol dm^{-3}, air equilibrium, uncertainty distribution inter-decile intervals expressed as % of mean values)

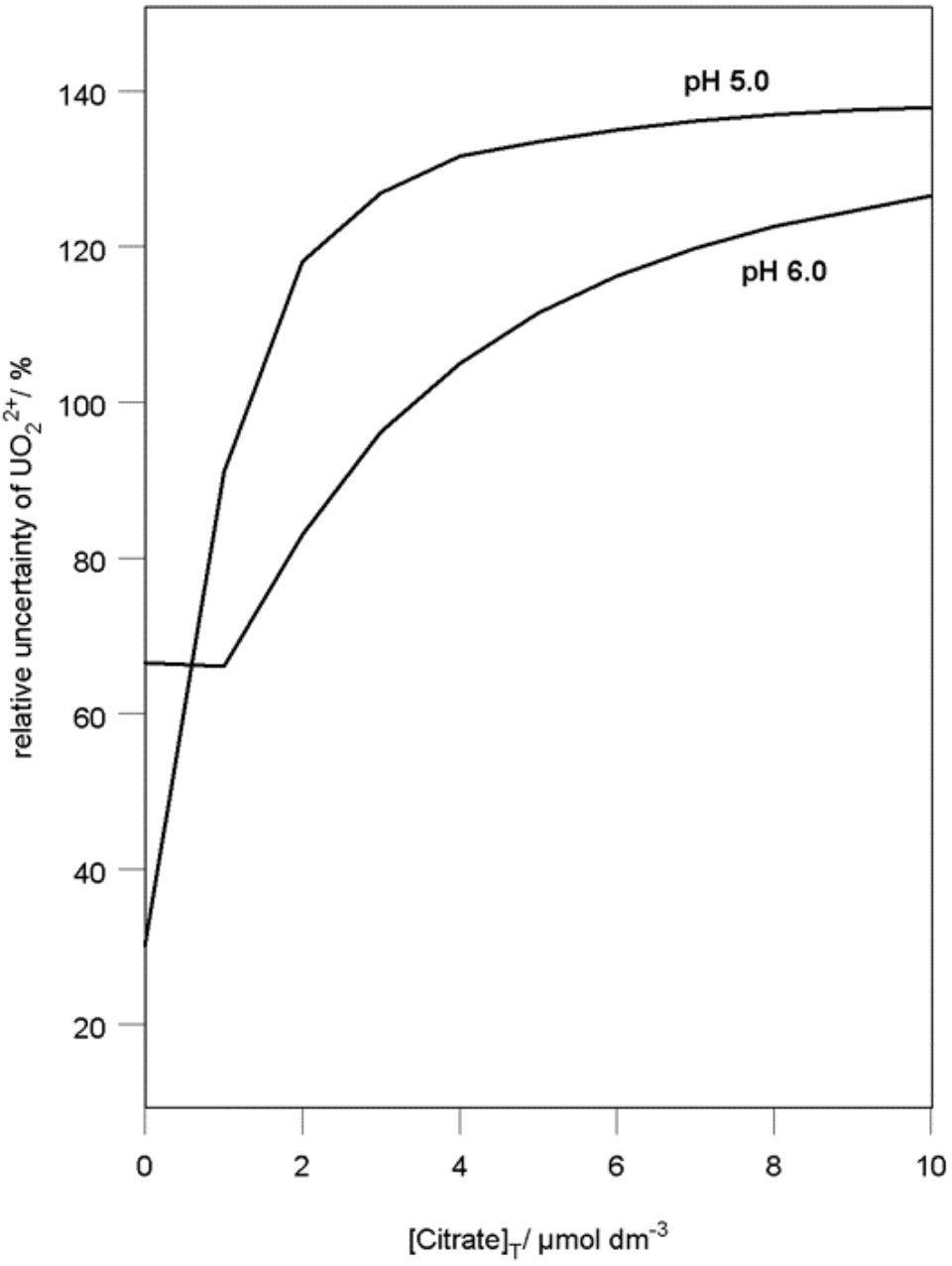

7.1.4 Effect of water hardness and pH

Bioaccumulation experiments to assess the effect of water hardness were performed by varying the concentrations of either calcium or magnesium in the range 10^{-4} – $2.5 \cdot 10^{-3}$ mol dm^{-3}, whilst keeping the concentration of the other hardness ion constant ($5 \cdot 10^{-4}$ mol dm^{-3}). Ionic strength was maintained at a constant 0.01 mol dm^{-3} by co-varying the concentrations of sodium and potassium in a 1:1 ratio. Anion concentrations were maintained constant, and experimental series were performed at pH values of 6 and 7. The predicted major solution species in this solution composition domain in function of the varied hardness ion, at both pH values, are shown in Figure 7-8 in function of magnesium concentration and Figure 7-9 in function of calcium concentration. As can be seen, there is predicted to be virtually no change with respect to the speciation of uranium, the only significant changes being to the minority ternary calcium uranyl carbonate species. Similarly, there is virtually no change to the predicted uncertainty of the major uranyl species. For example the relative uncertainty of the free uranyl ion is constant in function of both calcium and magnesium at both pH values, the inter-decile interval for this species is 66 % of the distribution mean at pH 6 and 95 % at pH 7.

Figure 7-8 Predicted distribution of major uranyl species in function of magnesium concentration at pH 6.0 and 7.0 ($[UO_2]_T = 5.10^{-7}$ mol dm^{-3}, air equilibrium), calculated using mean-value database.

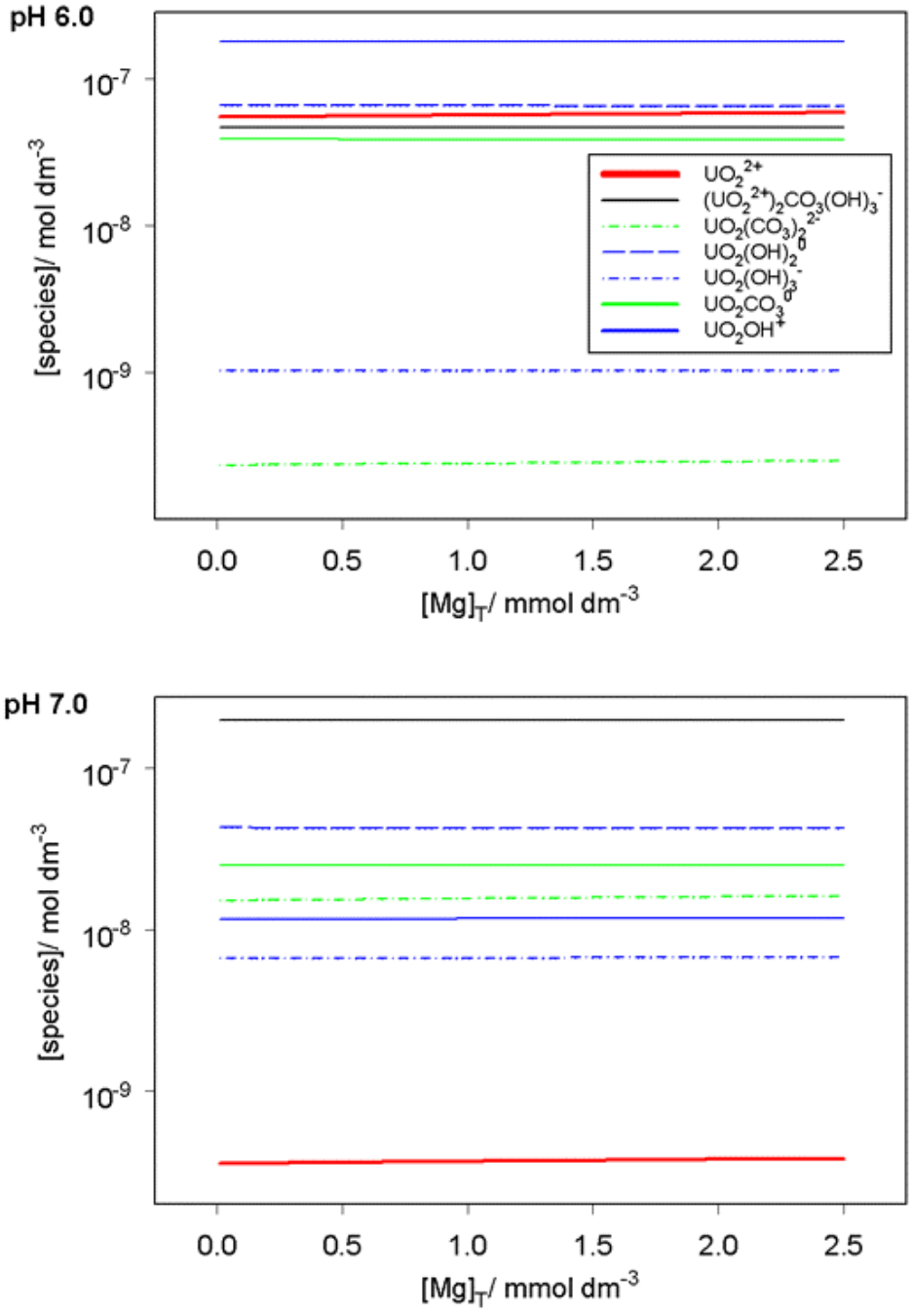

Figure 7-9 Predicted distribution of major uranyl species in function of calcium concentration at pH 6.0 and 7.0 ($[UO_2]_T = 5.10^{-7}$ mol dm^{-3}, air equilibrium), calculated using mean-value database.

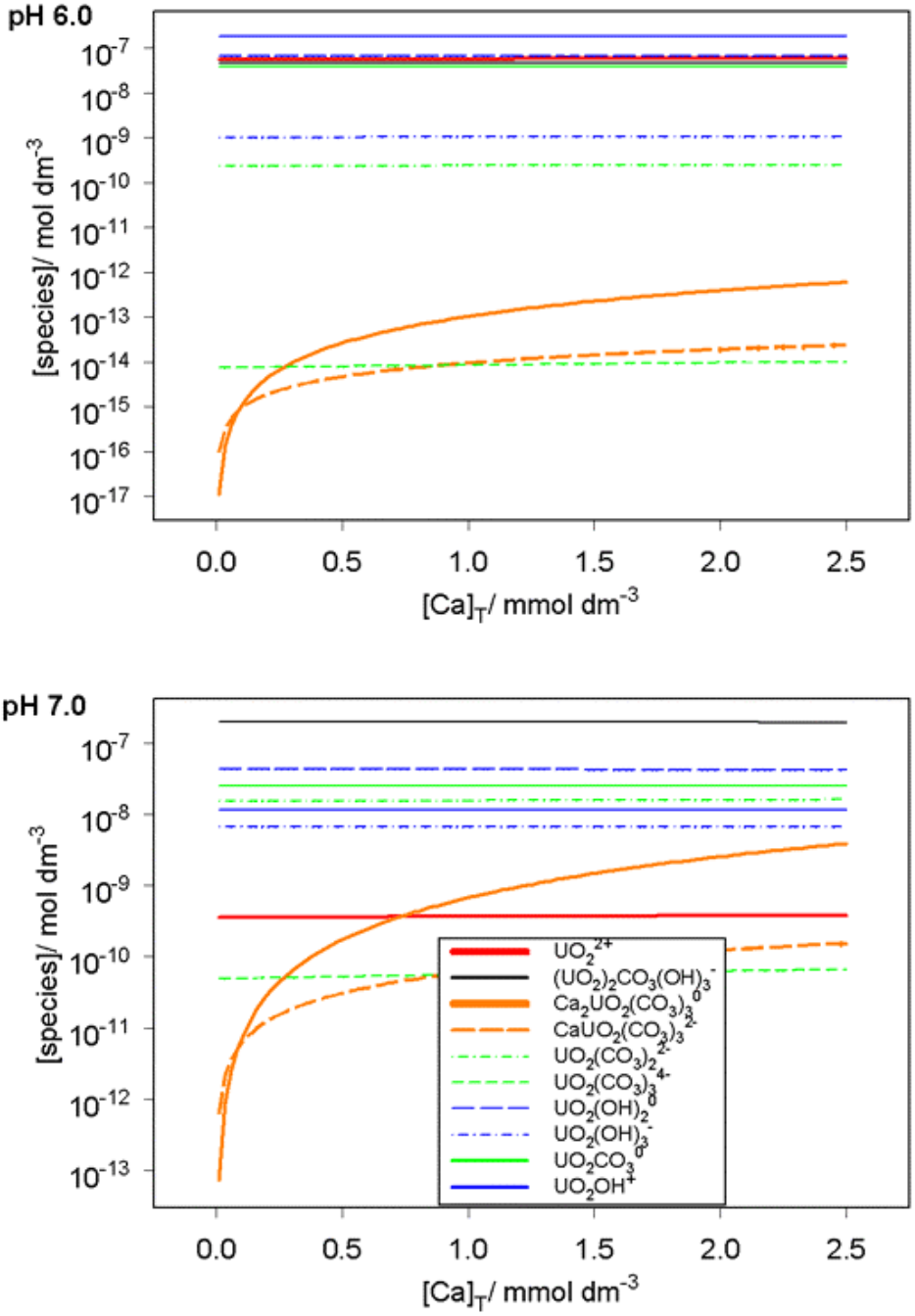

7.1.5 Effect of pH and carbonate concentration

Bioaccumulation experiments were performed at a uranium concentration of $5 \cdot 10^{-7}$ mol dm^{-3}, a pH range 5 – 7.5 and a range of DIC concentration of 10^{-5} – $5 \cdot 10^{-3}$ mol dm^{-3}. The partial pressures of carbon dioxide in the gas mixtures used to regulate DIC concentration were in the range $3 \cdot 10^{-4}$ – $3 \cdot 10^{-2}$ atm. The distributions of uranyl through its major species predicted by mean-value speciation calculations for this range of pH and DIC concentration are shown at selected pH values in function of DIC concentration in Figure 7-10, and at selected DIC concentrations in function of pH in Figure 7-11. At low pH the DIC concentration has a limited effect on uranyl speciation, for example at pH 5 carbonate complexation in the range of DIC studied only decreases the concentration of the free uranyl ion by a factor of two. At higher pH values the effect is much more pronounced, at pH 6 the same range of DIC decreases uranyl ion concentration by two orders of magnitude increasing to three orders of magnitude at pH 7. The effect of pH at constant DIC concentration is important even at low DIC concentration, due to the hydrolysis behaviour of uranyl. At the lowest DIC concentration studied, the concentration of the uranyl ion decreases by almost four orders of magnitude for the pH range of interest, but at higher DIC concentrations the effect is much more pronounced: the concentration of uranyl ion decreasing by over six orders of magnitude. The predicted predominant solution species depends on the exact pH and DIC concentration, being one of UO_2^{2+}, UO_2OH^+, $UO_2CO_3^0$, $(UO_2)_2CO_3(OH)_3^-$, $UO_2(CO_3)_2^{2-}$ or $Ca_2UO_2(CO_3)_3^0$ for the solution composition domain of interest. The uranium species considered in the models applied to the accumulation data relevant to this composition domain were UO_2^{2+} and $UO_2CO_3^0$. Output distribution histograms of these uranyl species at pH values of 5, 6 and 7 and DIC concentrations of 10^{-5}, 10^{-4} and 10^{-3} mol dm^{-3} are shown in Figure 7-12. The probabilistic uncertainty distributions are summarised as frequency contour plots in function of DIC concentration at selected pH values in Figure 7-13. The relative uncertainties expressed as the inter-decile intervals of the probability distributions of the concentrations of these two species are shown in function of both pH and DIC concentration as a percentage of the distribution means in Figure 7-14. Again, the relative uncertainties of the predicted concentrations vary greatly in function of the solution composition parameters.

Figure 7-10 Predicted distribution of major uranyl species in function of total carbonate concentration at selected pH values ($[UO_2]_T = 5.10^{-7}$ M), calculated using mean-value database.

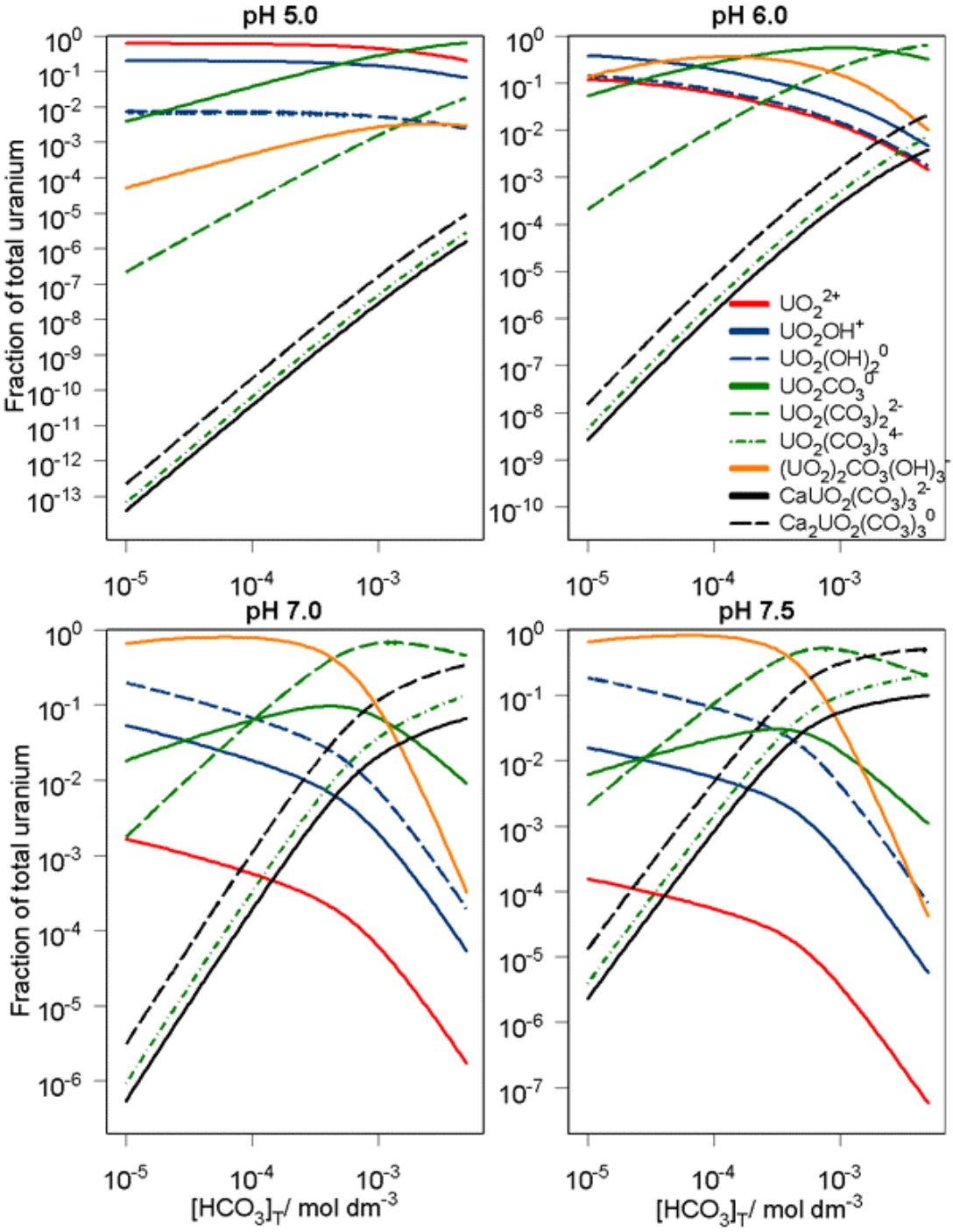

Figure 7-11 Predicted distribution of major uranyl species in function of pH at selected total carbonate concentration values ($[UO_2]_T = 5.10^{-7}$ M) , calculated using mean-value database.

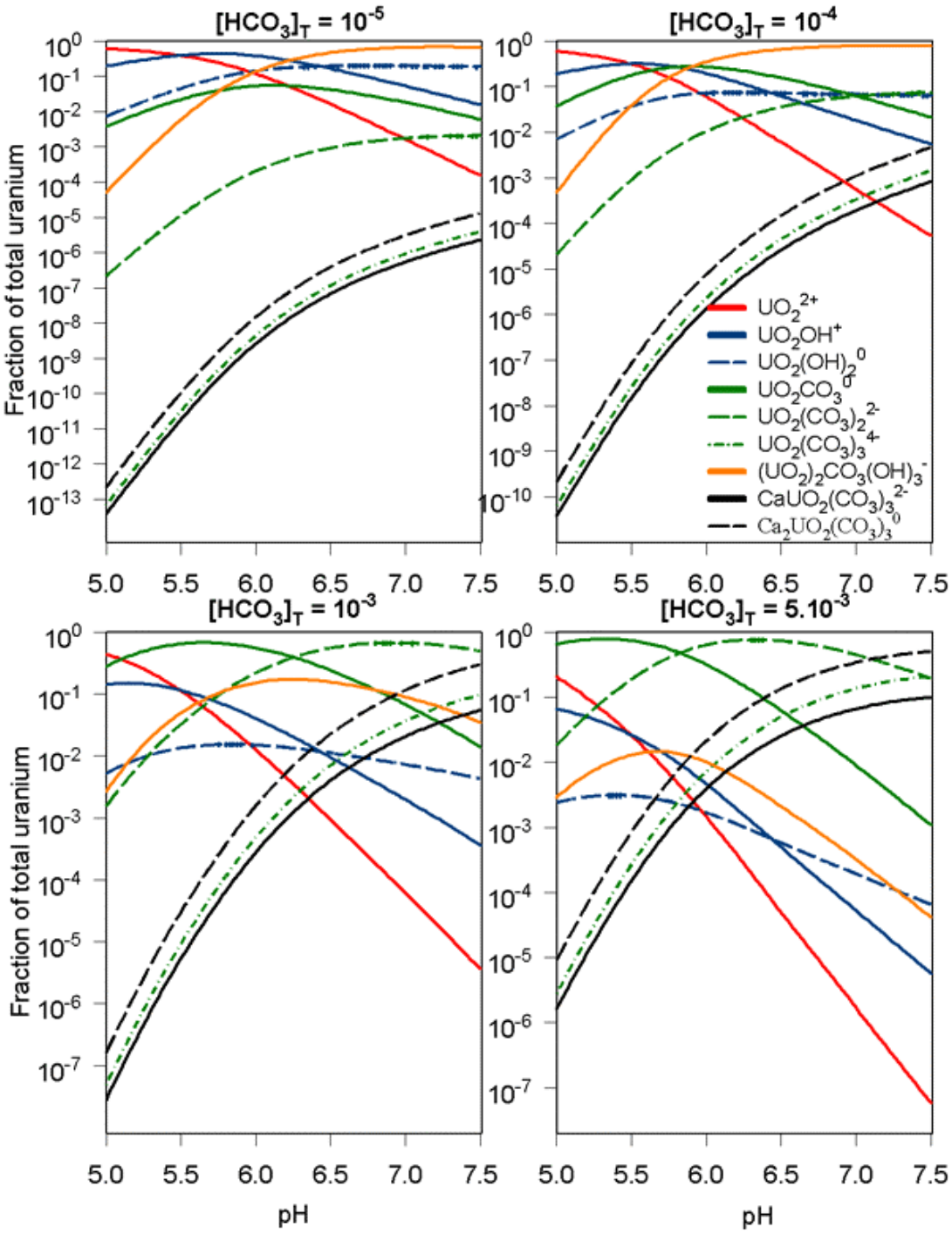

Figure 7-12 Histograms of uncertainty output distributions for the uranyl ion at different pH values and total carbonate concentrations ($[UO_2]_T = 5.10^{-7}$ M).

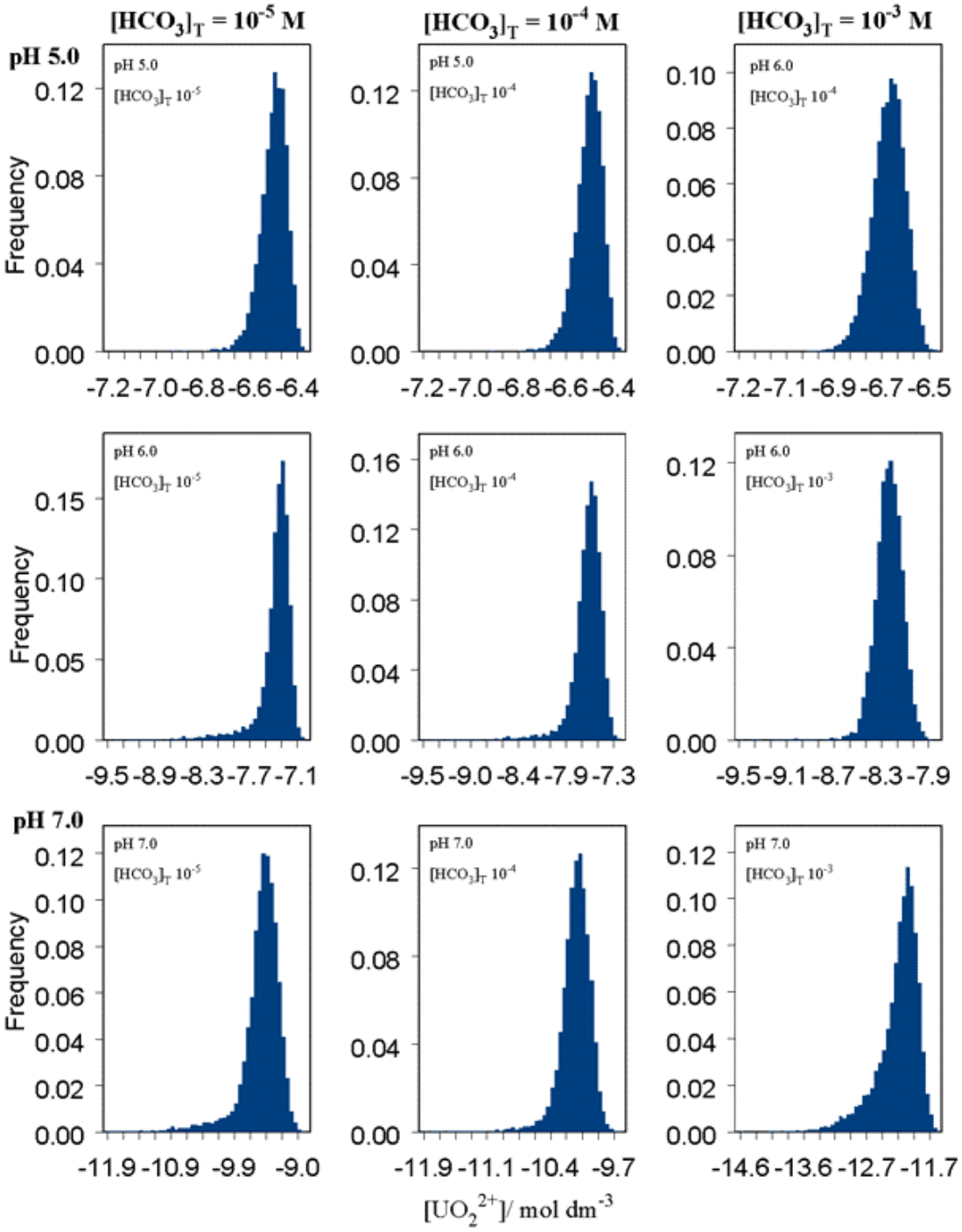

Figure 7-12 Histograms of uncertainty output distributions of uranyl carbonate ($UO_2CO_3^0$) at different pH values and total carbonate concentrations ($[UO_2]_T = 5.10^{-7}$ M).

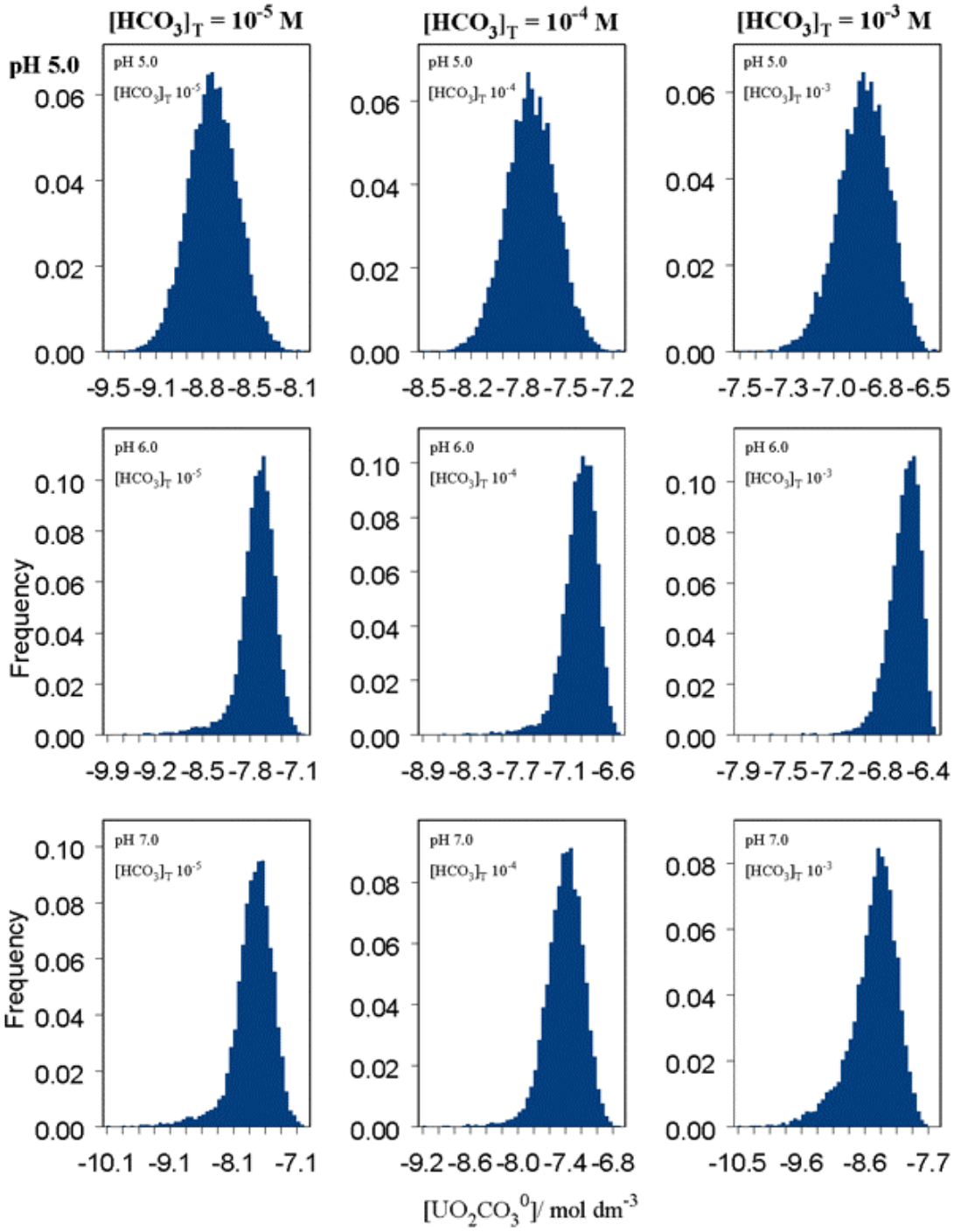

Figure 7-13 Uncertainty output distributions of UO_2^{2+} and $UO_2CO_3^0$ in function of total carbonate concentration at different pH values ($[UO_2]_T = 5.10^{-7}$ M).

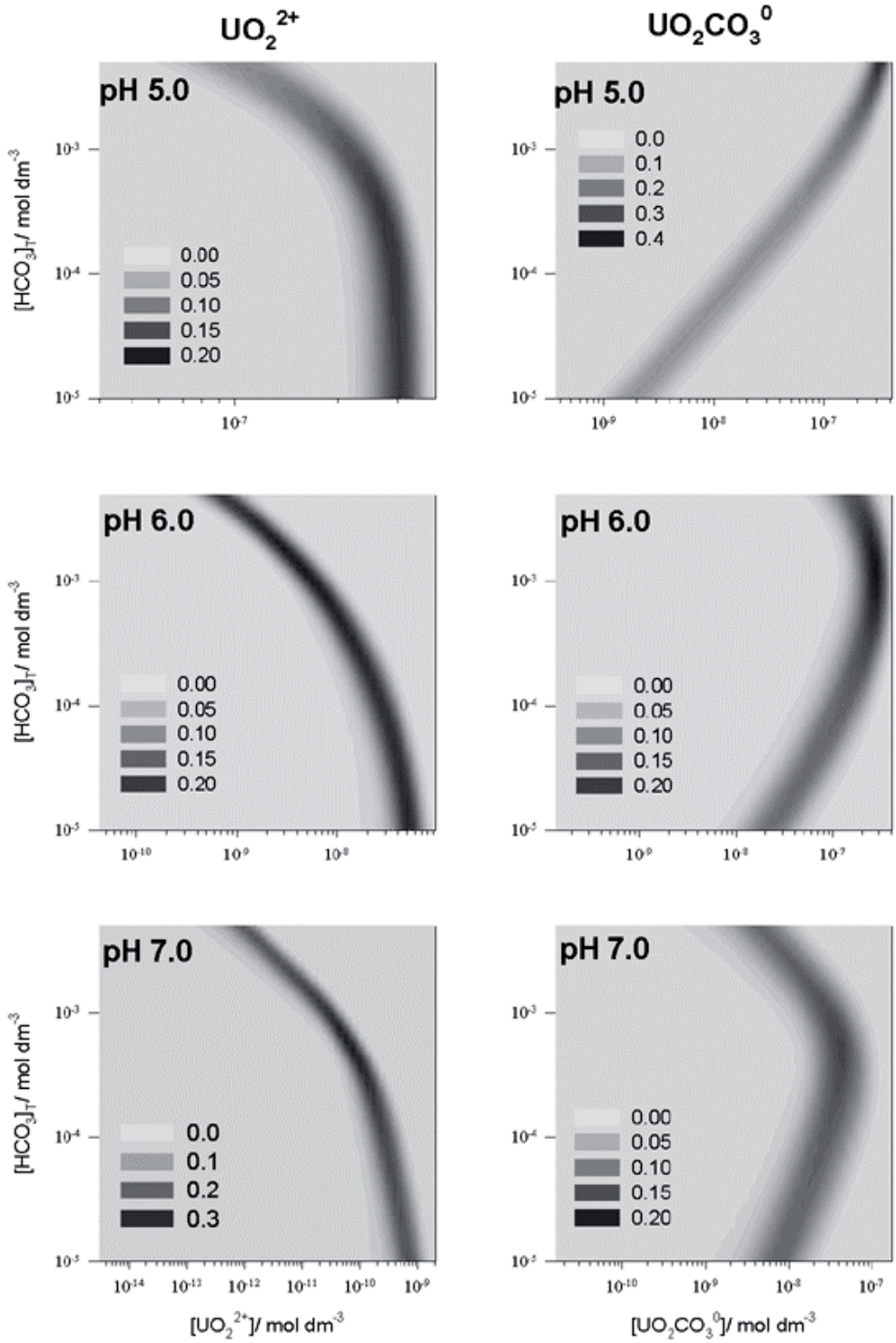

Figure 7-14 Relative uncertainties of selected uranyl species in function of pH and total carbonate concentration ($[UO_2]_T = 5.10^{-7}$, uncertainty distribution inter-decile intervals expressed as % of mean values).

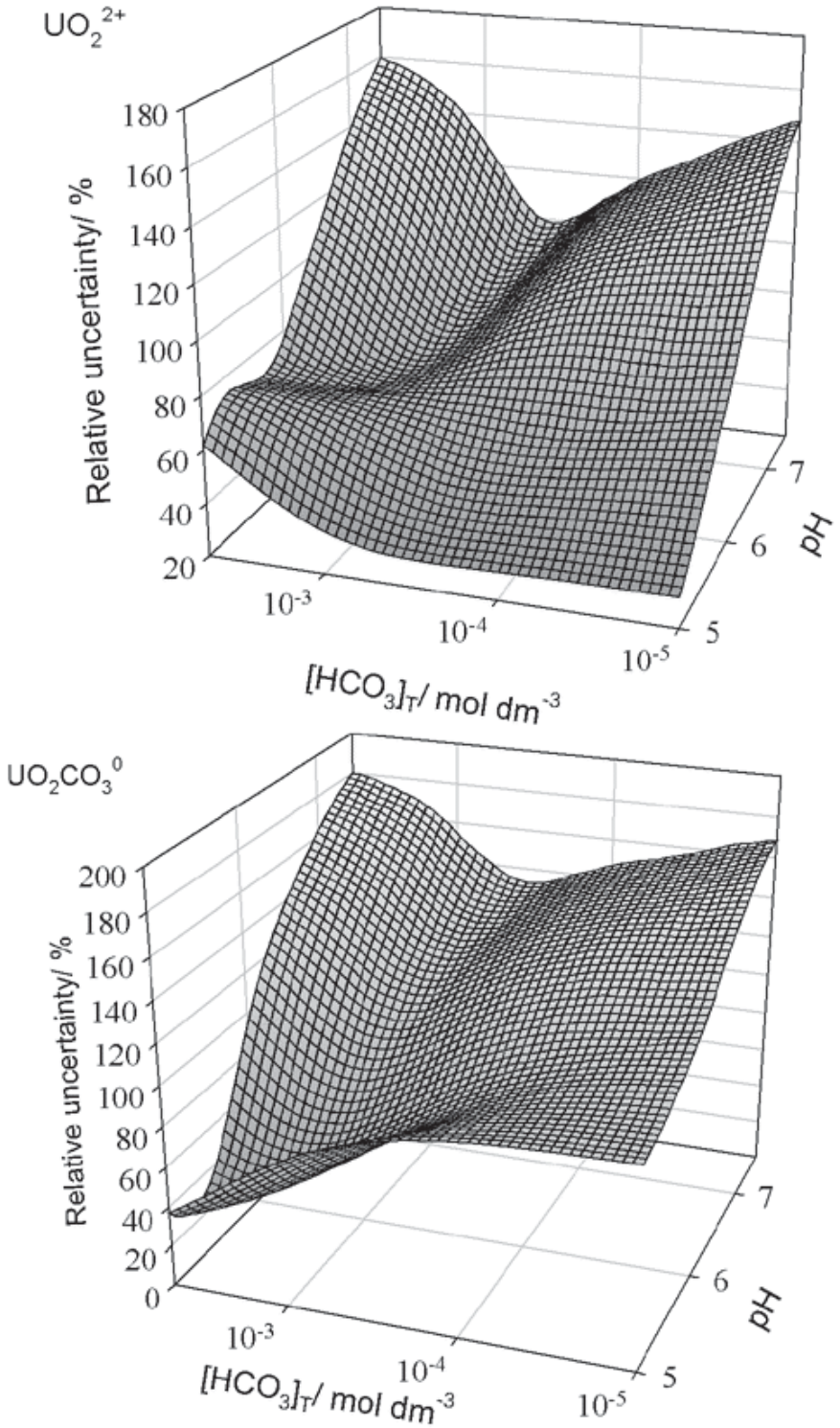

7.1.6 Effect of pH and phosphate concentration

Bioaccumulation experiments were performed at a uranium concentration of $5 \cdot 10^{-8}$ mol dm^{-3}, a pH range 5 – 7 and a range of phosphate concentration of 0 – 10^{-4} mol dm^{-3}. The DIC concentrations were determined by equilibrium with the air. The distributions of uranyl through its major species predicted by mean-value speciation calculations for this domain of pH and phosphate concentration are shown at selected phosphate concentrations in function of pH in Figure 7-15 and at selected pH values in function of phosphate concentration in Figure 7-16. As can be seen, phosphate complexation is very significant at all pH values studied, significantly reducing the concentration of the uranyl ion in the range of phosphate concentration studied. The most significant uranyl phosphate complexes are predicted to be $UO_2HPO_4^0$ (low pH) and $UO_2PO_4^-$ (high pH). The uranium species considered in the models applied to the accumulation data relevant to this composition domain were UO_2^{2+} and $UO_2HPO_4^0$ and $UO_2H_2PO_4^+$. Output distribution histograms of these uranyl species at pH values of 5, 6 and 7 and phosphate concentrations of 10^{-6}, 10^{-5} and 10^{-4} mol dm^{-3} are shown in Figure 7-17. The probabilistic uncertainty distributions are summarised as frequency contour plots in function of phosphate concentration at selected pH values in Figure 7-18. The relative uncertainties expressed as the inter-decile intervals of the probability distributions of the concentrations of these species are shown in function of both pH and phosphate concentration as a percentage of the distributions means in Figure 7-19. Again, the relative uncertainties of the predicted concentrations vary greatly in function of the solution composition parameters.

Figure 7-15 Predicted distribution of major uranyl species in function of pH at selected total phosphate concentration values ($[UO_2]_T = 10^{-7}$ M, air equilibrium), calculated using mean-value database.

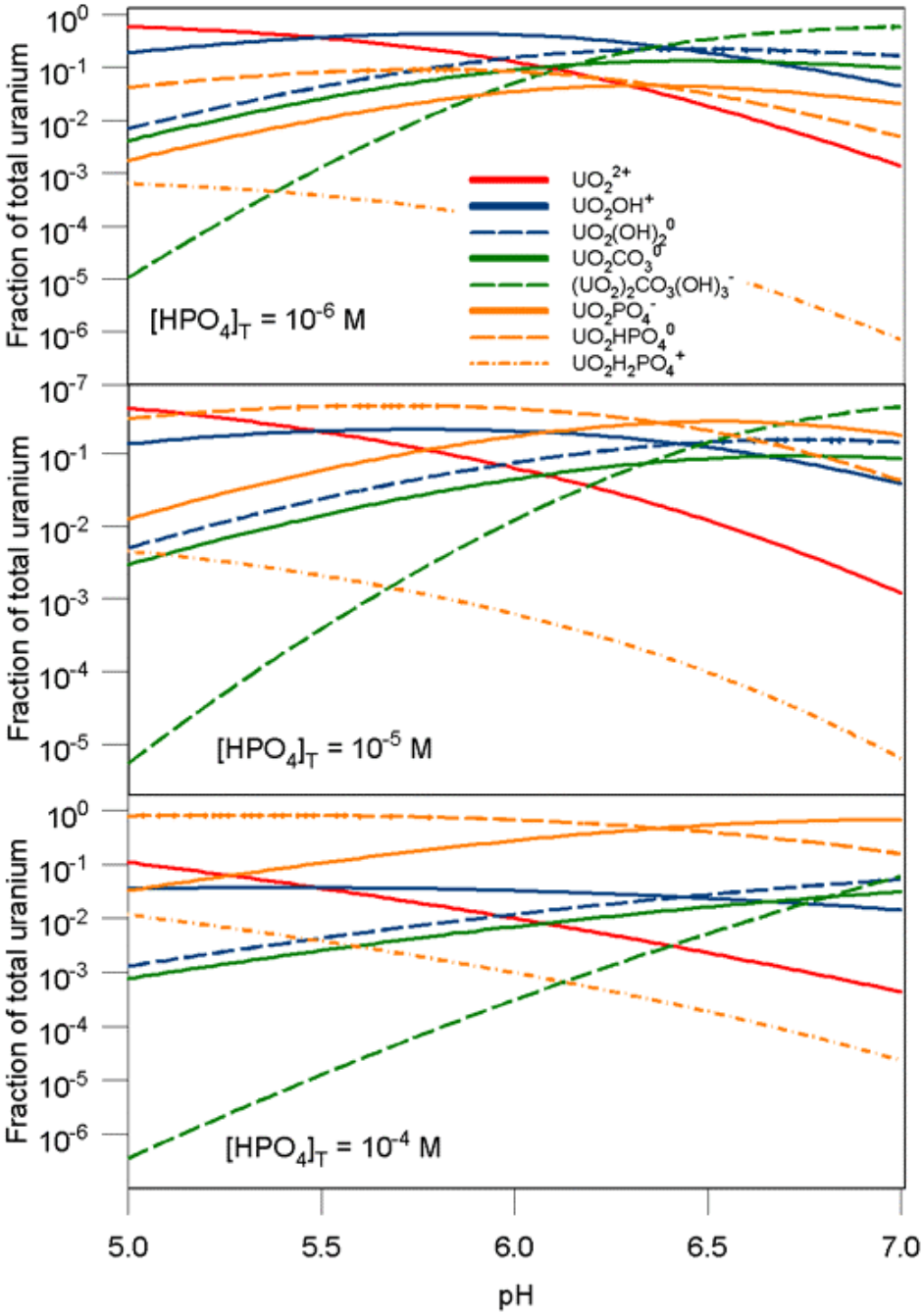

Figure 7-16 Predicted distribution of major uranyl species in function of total phosphate concentration at selected pH values ($[UO_2]_T = 10^{-7}$ M, air equilibrium), calculated using mean-value database.

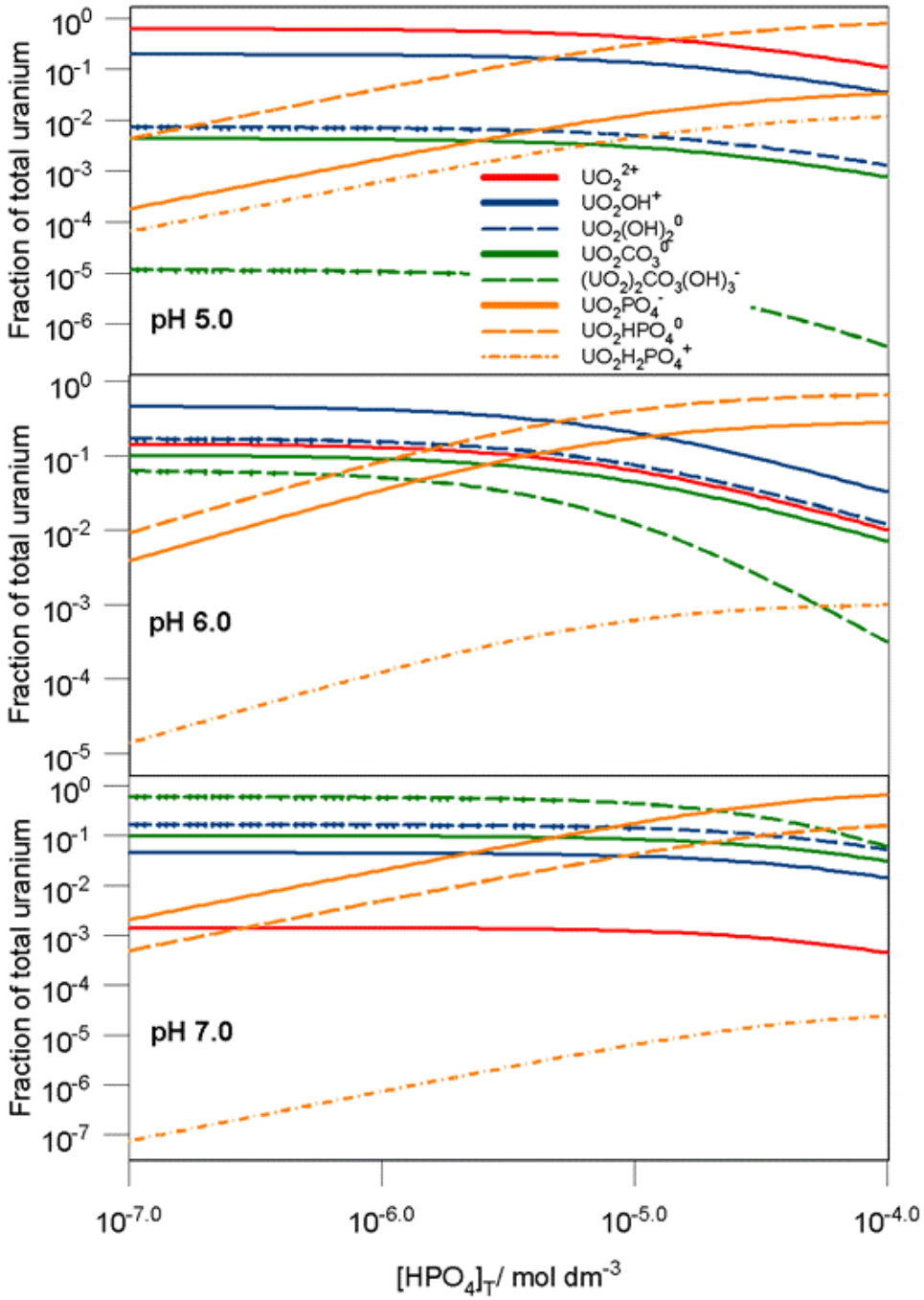

Figure 7-17 Histograms of uncertainty output distributions of selected uranyl species at different total phosphate concentration values ($[UO_2]_T = 10^{-7}$ M, pH 5.0, air equilibrium).

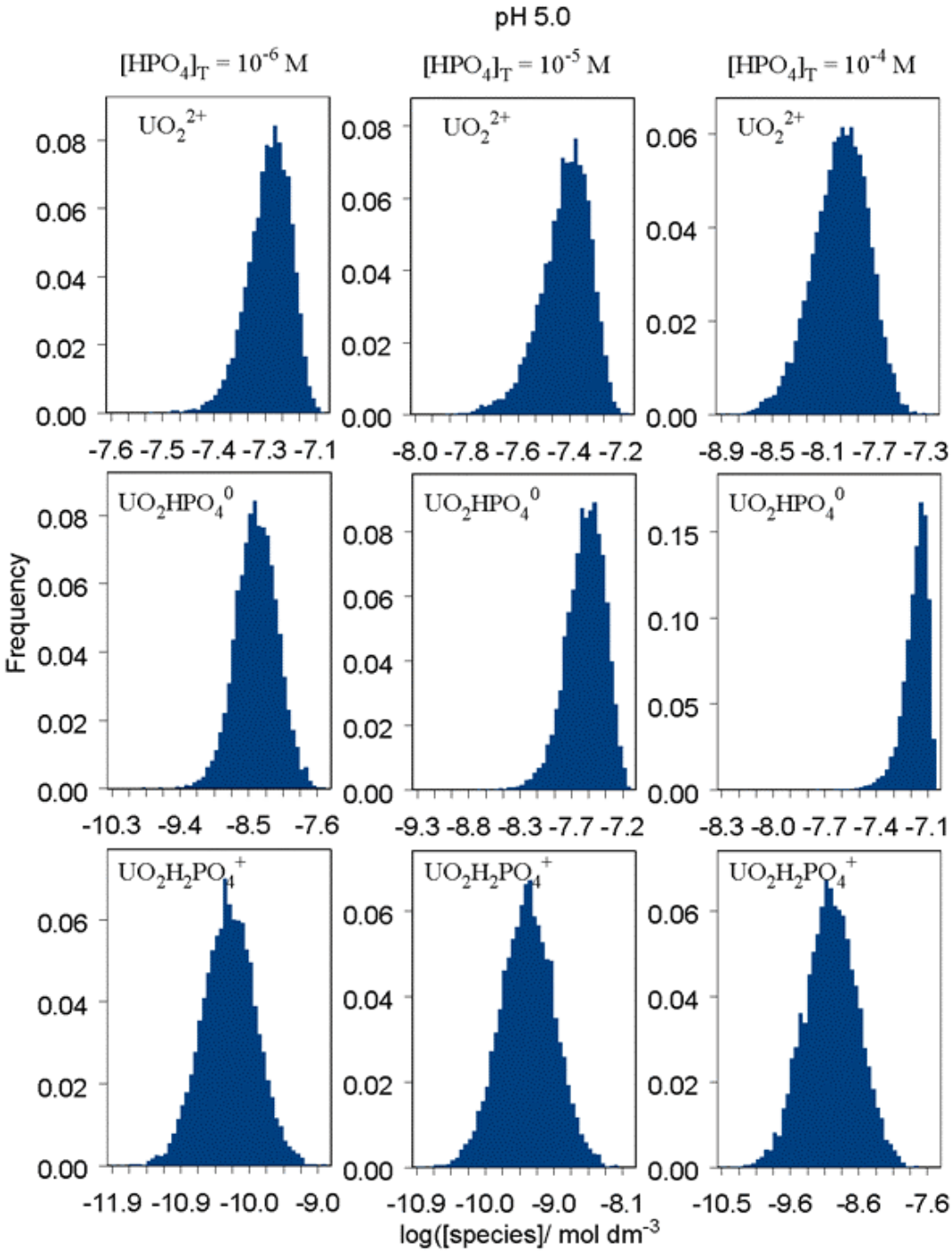

Figure 7-17 Histograms of uncertainty output distributions of selected uranyl species at different total phosphate concentration values ($[UO_2]_T = 10^{-7}$ M, pH 6.0, air equilibrium).

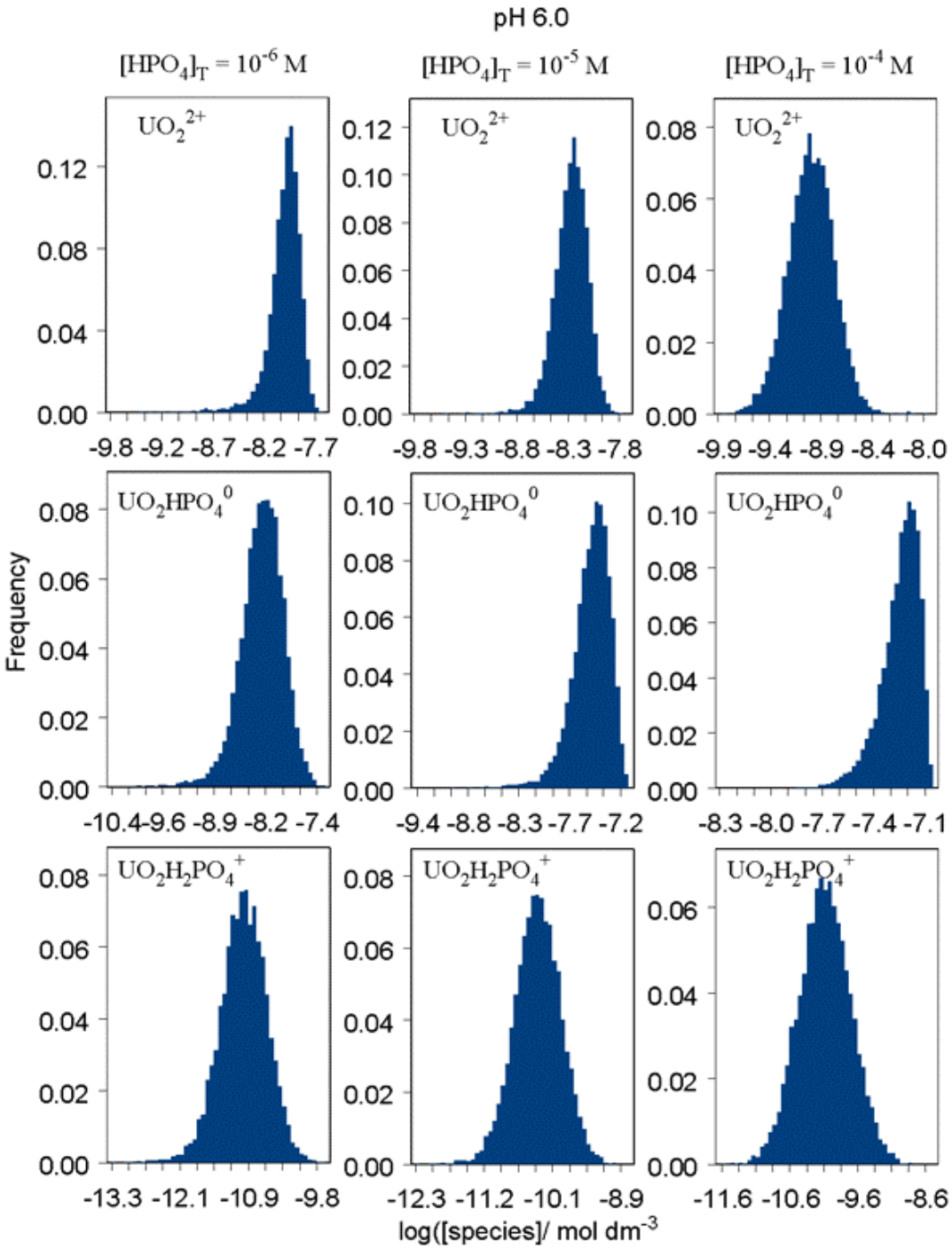

Figure 7-17 Histograms of uncertainty output distributions of selected uranyl species at different total phosphate concentration values ($[UO_2]_T = 10^{-7}$ M, pH 7.0, air equilibrium).

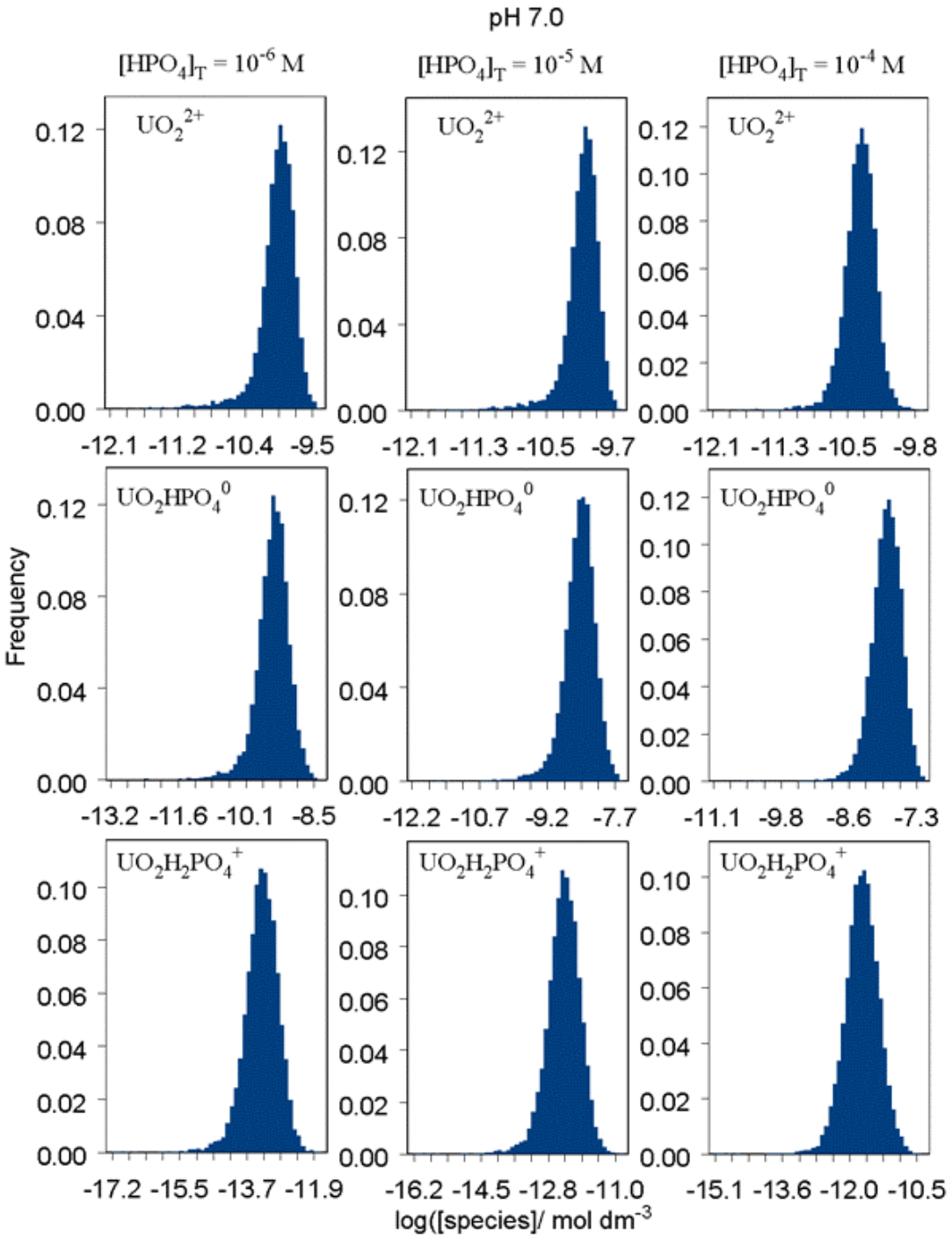

Figure 7-18 Uncertainty output distributions of selected uranyl species in function of total phosphate concentration at different pH values ($[UO_2]_T = 5.10^{-7}$ M, air equilibrium).

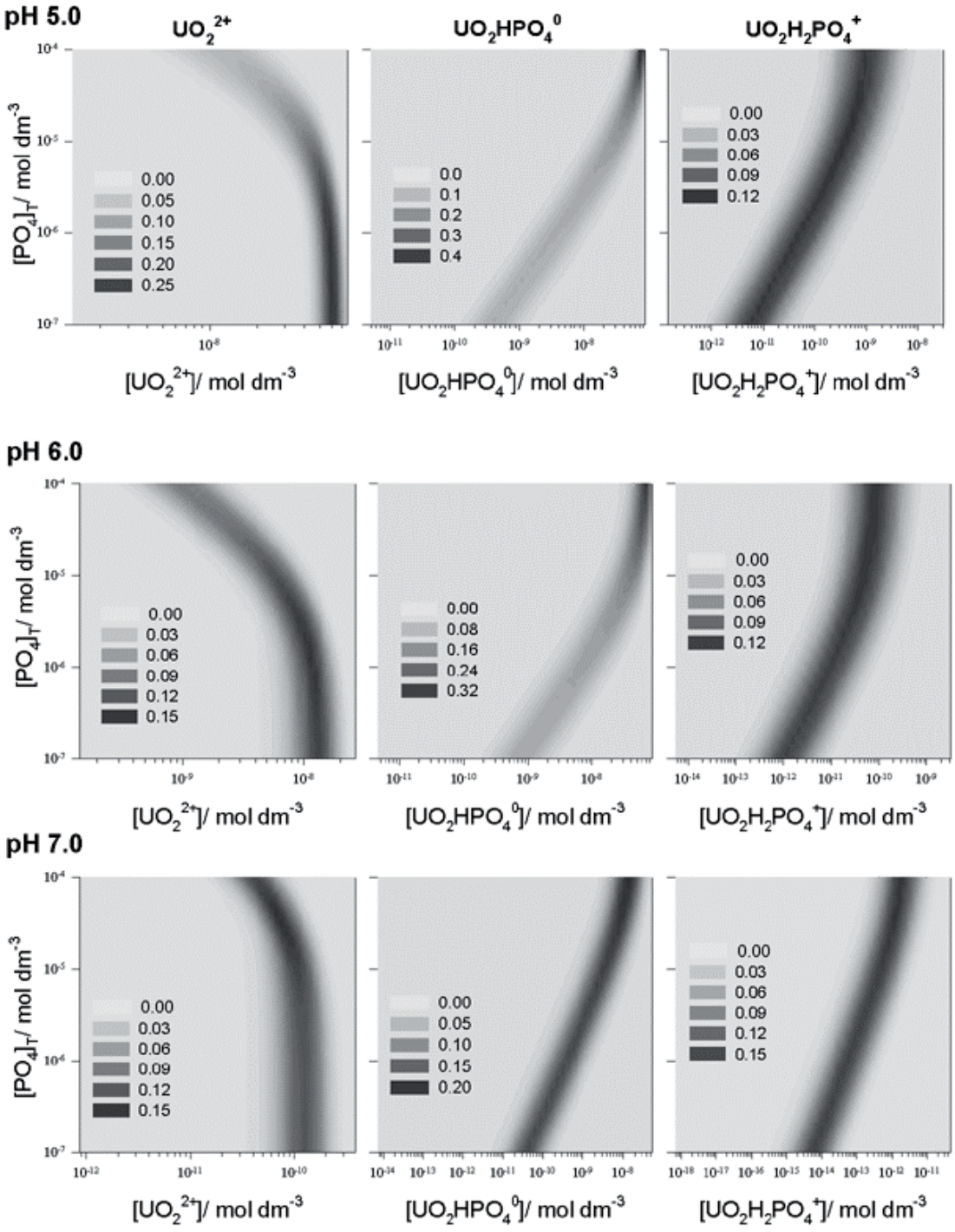

Figure 7-19 Relative uncertainties of selected uranyl species in function of pH and total phosphate concentration ($[UO_2]_T = 5.10^{-7}$, uncertainty distribution inter-decile intervals expressed as % of mean values).

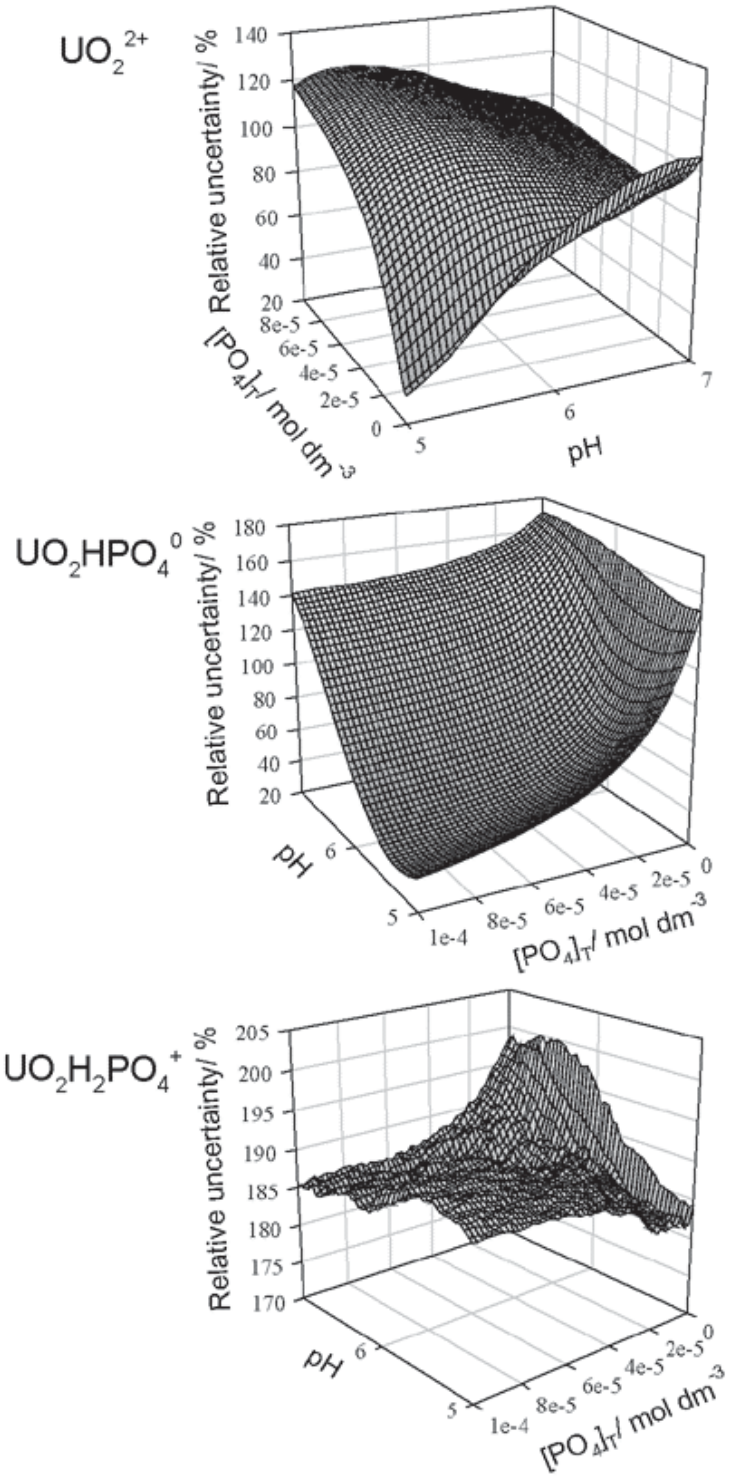

7.2 Discussion Of The Effects Of Database Uncertainty

A number of generally applicable observations can be made. The distributions of the output species are often not normally (or log normally) distributed despite the assumed normal distributions of the input constraints. Additionally the distributions vary according to the exact solution composition of the scenario that is run. A consequence of this is that the mean values calculated from the output distributions are frequently significantly different from the values calculated using the mean-value database. From these results it is obvious that there are very significant uncertainties in aqueous speciation calculations due to database parameter uncertainty. The potential uncertainties due to the input uncertainty of the solution composition, the model coherency (whether all relevant chemical species are considered) or the conceptual model formulation (whether the system is truly at equilibrium, the adequacy of models for ionic strength correction etc.) have not been considered. These additional sources of uncertainty are undoubtedly also important.

The impact of database parameter uncertainty depends very much on the application for which the results of the speciation calculations are used. The absolute uncertainty of the concentration of a particular solution species for a particular solution composition is often not of great importance to the application. Frequently the relative change of a species' concentration in function of one or several parameters is of much greater interest. In this case the magnitude of change over the range of conditions of interest as well as the relative uncertainties over the same range need to be considered together. For example, if a system property (such as the total fraction adsorbed to a surface) can be well described by the calculated concentration of the species UO_2^{2+} in function of the pH, the uncertainties are of little practical importance, as the magnitude of change is very considerable for a reasonable change in pH. However, if a number of different species need to be considered in the model formulation in order to adequately describe the system properties (for example in the case of competitive sorption), both the magnitude of change and relative uncertainties of all these species need to be considered as well as their weighting in the model. Due to the cumulative uncertainties of these parameters, application of a model that requires a large number of species to be considered is likely to be less precise outside the exact validity field

for which the model was parameterised than a model that requires a smaller number of species.

A further problem is that there is no universally accepted "standard" thermodynamic database. This creates the situation where different workers use different databases to calculate new or amended thermodynamic data, whether for solution or surface complexes, mineral solubility data or parameters for biotic ligand type models. These data are then frequently used to augment other, often different, databases, to attempt to improve their coherency, but without amending the "new" data to be consistent with the new database. Recalculation of the data to be consistent with another database is frequently impossible without the original experimental results, and even if these are available it is very time consuming and prone to introducing further errors. Further, some models are often constructed by inferring the composition of surface complexes from the aqueous speciation calculations rather than direct measurement of the composition (for example by various spectroscopic techniques). This is a particular problem of biotic ligand type models, as even if it is possible to directly determine the composition of surface complexes (as is sometimes the case for bacteria or unicellular algae) the fraction of the total surface sites that are physiologically active is likely to be very small. It is of course also possible that the surface complexes that may form at these particular sites are different from the complexes that may form at non-specific surface sites. Models of this type are likely to be more sensitive to the particular database used for the model parameterisation than models developed with direct determination of the surface complexes, and hence model predictions outside the precise validity field of the experimental data is likely to be uncertain.

The presented study is of limited scope, only investigating the effects of database uncertainty for a narrow range of solution compositions and a single simplified application. There are a number of known limitations of the employed methods, including the assumption of independent Gaussian probability distributions for the input parameter uncertainty (parameter independence is for example a simplification for the successive uranyl hydrolysis products), and of course the values selected for the parameters and their uncertainties, which are to some extent subjective. It is probable that the mean and uncertainty values that might be obtained from an "ideal" database compilation, reinterpreting all available literature data in a rigorously

consistent manner with respect to the coherency of the system and the activity-concentration model, may be slightly different. However, such high quality reviews are rare (the NEA-TDB project is probably the best series of reviews available), are very time consuming undertakings, become rapidly dated as new studies are performed, are generally of limited coherency and are of course dependent on the quality of the available literature. The chosen values are probably more representative of databases in common usage, as generally the resources and expertise required to perform a very high quality review are not available. Notwithstanding these possible limitations it is obvious that uncertainties in database parameters have a very significant effect on the predicted distributions of uranyl species in very simple conditions.

7.3 Uranium Accumulation Modelling Results

7.3.1 Tested model hypotheses

As discussed in section 5.2 a number of different mechanistic hypotheses have been proposed in the literature, or in this work, to describe the physical and physiological processes involved in metal bioaccumulation. For this study a multi-hypotheses approach was adopted to test a number of these hypotheses or combinations of hypotheses. Different mathematical models were derived, starting with the most restrictive hypotheses (giving the simplest models) and progressively modifying the hypotheses to give more complex and hence flexible models. The development of this set of models is summarised in Table 7-1. Hypotheses 3 and 4 from section 5.2.1 were assumed to be correct for all the models applied, i.e. that mass transport of the metal from the bulk solution was not rate-limiting and that no significant modification to the metal's speciation in the immediate vicinity of the biological interface occurred. The resulting mathematical models are presented in Table 7-2. The set of different models tested were not intended to be exhaustive with respect to the different mechanistic hypotheses (or combinations thereof) previously discussed, but to represent a set of structurally similar models of increasing complexity and hence flexibility. For the models that considered more then one species to be bioavailable, the uranyl species considered in this study are listed in Table 7-3.

Table 7-1 Overview of tested hypotheses and mathematical models

Hypothesis	Transporter characteristics	Competition	Chemically available species	Transporter kinetics	Adjustable parameters (equation)	Model codes
1	Single type, homogeneous and independent	None	UO_2^{2+}	rate determining and first order	$K_{UO_2^{2+}}; k_2; \{\equiv X\}_T$ (5-10)	L1Sa*, L1Sb*, 1T1S0H
2	Single type, homogeneous and independent	H^+	UO_2^{2+}	rate determining and first order	$K_{UO_2^{2+}}; K_{H^+}; k_2; \{\equiv X\}_T$ (5-13)	1T1S1H
3	Single type, bidentate, homogeneous and independent	H^+	UO_2^{2+}	rate determining and first order	$K_{UO_2^{2+}}; K_{H^+}; K'_{H^+}; k_2; \{\equiv X\}_T$ (5-13)	1T1S2H
4	Single type, homogeneous and independent	None	UO_2^{2+} & UO_2B	rate determining and first order	$K_{UO_2^{2+}}; K_{UO_2B}; k_2; \{\equiv X\}_T$ (5-18)	1T2S0H
5	Single type, homogeneous and independent	H^+	UO_2^{2+} & UO_2B	rate determining and first order	$K_{UO_2^{2+}}; K_{UO_2B}; K_{H^+}; k_2; \{\equiv X\}_T$ (5-13)(5-18)	1T2S1H
6	Single type, homogeneous and independent	None	UO_2^{2+}, UO_2B & UO_2C	rate determining and first order	$K_{UO_2^{2+}}; K_{UO_2B}; K_{UO_2C}; k_2; \{\equiv X\}_T$ (5-18)	1T3S0H
7	Single type, homogeneous and independent	H^+	UO_2^{2+}, UO_2B & UO_2C	rate determining and first order	$K_{UO_2^{2+}}; K_{UO_2B}; K_{UO_2C}; K_{H^+}; k_2; \{\equiv X\}_T$ (5-13)(5-18)	1T3S1H
8	Two types, specific to uranyl species	None	UO_2^{2+} & UO_2B	rate determining and first order for each transporter	$K_{UO_2^{2+}}; K_{UO_2B}; k_2; k_3; \{\equiv X\}_T; \{\equiv X'\}_T$ (5-22)	2T2S0H

*Linear approximation

Table 7-1 Overview of tested hypotheses and mathematical models (cont.)

Hypothesis	Transporter characteristics	Competition	Chemically available species	Transporter kinetics	Adjustable parameters (equation)	Model codes
9	Two types, specific to uranyl species	H^+/UO_2^{2+}	UO_2^{2+} & UO_2B	rate determining and first order for each transporter	$K_{UO_2^{2+}}; K_{UO_2B}; K_{H^+};$ $k_2; k_3; \{\equiv X\}_T; \{\equiv X'\}_T$ (5-13)(5-22)	2T2S1HA
10	Two types, specific to uranyl species	H^+/UO_2B	UO_2^{2+} & UO_2B	rate determining and first order for each transporter	$K_{UO_2^{2+}}; K_{UO_2B}; K_{H^+}$ $k_2; k_3; \{\equiv X\}_T; \{\equiv X'\}_T$ (5-13)(5-22)	2T2S1HB
11	Two types, specific to uranyl species	H^+/UO_2^{2+} H^+/UO_2B	UO_2^{2+} & UO_2B	rate determining and first order for each transporter	$K_{UO_2^{2+}}; K_{UO_2B}; K_{H^+}; K'_{H^+}$ $k_2; k_3; \{\equiv X\}_T; \{\equiv X'\}_T$ (5-13)(5-22)	2T2S2H
12	Three types, specific to uranyl species	None	UO_2^{2+}, UO_2B & UO_2C	rate determining and first order for each transporter	$K_{UO_2^{2+}}; K_{UO_2B}; K_{UO_2C}; k_2; k_3; k_4;$ $\{\equiv X\}_T; \{\equiv X'\}_T; \{\equiv X''\}_T$ (5-22)	3T3S0H
13	Single type, homogeneous and independent	None	UO_2^{2+}	rate determining, dependent on pH	$K_{UO_2^{2+}}; k_2^{(pH)}; \{\equiv X\}_T$ (5-9)(5-23)	kin1T1S
14	Single type, homogeneous and independent	None	UO_2^{2+} & UO_2B	rate determining, dependent on pH	$K_{UO_2^{2+}}; K_{UO_2B}; k_2^{(pH)}; \{\equiv X\}_T$ (5-18)(5-23)	kin1T2S
15	Single type, homogeneous and independent	None	UO_2^{2+}, UO_2B & UO_2C	rate determining, dependent on pH	$K_{UO_2^{2+}}; K_{UO_2B}; K_{UO_2C}; k_2^{(pH)}; \{\equiv X\}_T$ (5-18)(5-23)	kin1T3S

Table 7-1 Overview of tested hypotheses and mathematical models (cont.)

Hypothesis	Transporter characteristics	Competition	Chemically available species	Transporter kinetics	Adjustable parameters (equation)	Model codes
16	Single type, stability of metal – transporter complex dependent on pH	None	UO_2^{2+}	rate determining and first order	$K_{UO_2^{2+}}^{(pH)}; k_2; \{\equiv X\}_T$ (5-18)(5-27)	affin1T1S
17	Single type, stability of metal – transporter complex dependent on pH	None	UO_2^{2+} & UO_2B	rate determining and first order	$K_{UO_2^{2+}}^{(pH)}; K_{UO_2B}; k_2; \{\equiv X\}_T$ (5-18)(5-27)	affin1T2S
18	Single type, stability of metal – transporter complex dependent on pH	None	UO_2^{2+}, UO_2B & UO_2C	rate determining and first order	$K_{UO_2^{2+}}^{(pH)}; K_{UO_2B}; K_{UO_2C}; k_2; \{\equiv X\}_T$ (5-18)(5-27)	affin1T3S

$K_{UO_2^{2+}}; K_{UO_2B}; K_{UO_2C}$ formation constants of the surface complexes

$k_2; k_3; k_4$ rate constants for trans-membrane internalisation kinetics

$\{\equiv X\}_T; \{\equiv X'\}_T; \{\equiv X''\}_T$ total number of surface sites

$K_{UO_2^{2+}}^{(pH)}$ conditional formation constant of the surface complex, dependent on pH

$k_2^{(pH)}$ conditional rate constant for trans-membrane internalisation kinetics, dependent on pH

Table 7-2 Mathematical models tested in this work φ_{UO_2} expressed in mol g^{-1} h^{-1}

Code	Model with adjustable parameters of regrouped constants
L1Sa	$\varphi_{UO_2} = a \cdot \alpha_{UO_2^{2+}}$
L1Sb	$\varphi_{UO_2} = a \cdot \alpha_{UO_2^{2+}} + b$
L2S	$\varphi_{UO_2} = a \cdot \alpha_{UO_2^{2+}} + b \cdot \alpha_{UB} + c$
L3S	$\varphi_{UO_2} = a \cdot \alpha_{UO_2^{2+}} + b \cdot \alpha_{UB} + c \cdot \alpha_{UC} + d$
1T1S0H	$\varphi_{UO_2} = \frac{a \cdot K_{UO_2^{2+}} \cdot \alpha_{UO_2^{2+}}}{1 + K_{UO_2^{2+}} \cdot \alpha_{UO_2^{2+}}}$
1T1S1H	$\varphi_{UO_2} = \frac{a \cdot K_{UO_2^{2+}} \cdot \alpha_{UO_2^{2+}}}{1 + K_{H^+} \cdot \alpha_{H^+} + K_{UO_2^{2+}} \cdot \alpha_{UO_2^{2+}}}$
1T1S2H	$\varphi_{UO_2} = \frac{a \cdot K_{UO_2^{2+}} \cdot \alpha_{UO_2^{2+}}}{1 + K_{H^+} \cdot \alpha_{H^+} + K'_{H^+} \cdot \alpha^2_{H^+} + K_{UO_2^{2+}} \cdot \alpha_{UO_2^{2+}}}$
1T2S0H	$\varphi_{UO_2} = \frac{a \cdot \left(K_{UO_2^{2+}} \cdot \alpha_{UO_2^{2+}} + K_{UO_2B} \cdot \alpha_{UO_2B} \right)}{1 + K_{UO_2^{2+}} \cdot \alpha_{UO_2^{2+}} + K_{UO_2B} \cdot \alpha_{UO_2B}}$
1T2S1H	$\varphi_{UO_2} = \frac{a \cdot \left(K_{UO_2^{2+}} \cdot \alpha_{UO_2^{2+}} + K_{UO_2B} \cdot \alpha_{UO_2B} \right)}{1 + K_{H^+} \cdot \alpha_{H^+} + K_{UO_2^{2+}} \cdot \alpha_{UO_2^{2+}} + K_{UO_2B} \cdot \alpha_{UO_2B}}$
1T3S0H	$\varphi_{UO_2} = \frac{a \cdot \left(K_{UO_2^{2+}} \cdot \alpha_{UO_2^{2+}} + K_{UO_2B} \cdot \alpha_{UO_2B} + K_{UO_2C} \cdot \alpha_{UO_2C} \right)}{1 + K_{UO_2^{2+}} \cdot \alpha_{UO_2^{2+}} + K_{UO_2B} \cdot \alpha_{UO_2B} + K_{UO_2C} \cdot \alpha_{UO_2C}}$
1T3S1H	$\varphi_{UO_2} = \frac{a \cdot \left(K_{UO_2^{2+}} \cdot \alpha_{UO_2^{2+}} + K_{UO_2B} \cdot \alpha_{UO_2B} + K_{UO_2C} \cdot \alpha_{UO_2C} \right)}{1 + K_{H^+} \cdot \alpha_{H^+} + K_{UO_2^{2+}} \cdot \alpha_{UO_2^{2+}} + K_{UO_2B} \cdot \alpha_{UO_2B} + K_{UO_2C} \cdot \alpha_{UO_2C}}$
2T2S0H	$\varphi_{UO_2} = \frac{a_1 \cdot K_{UO_2^{2+}} \cdot \alpha_{UO_2^{2+}}}{1 + K_{UO_2^{2+}} \cdot \alpha_{UO_2^{2+}}} + \frac{a_2 \cdot K_{UO_2B} \cdot \alpha_{UO_2B}}{1 + K_{UO_2B} \cdot \alpha_{UO_2B}}$
2T2S1HA	$\varphi_{UO_2} = \frac{a_1 \cdot K_{UO_2^{2+}} \cdot \alpha_{UO_2^{2+}}}{1 + K_{H^+} \cdot \alpha_{H^+} + K_{UO_2^{2+}} \cdot \alpha_{UO_2^{2+}}} + \frac{a_2 \cdot K_{UO_2B} \cdot \alpha_{UO_2B}}{1 + K_{UO_2B} \cdot \alpha_{UO_2B}}$
2T2S1HB	$\varphi_{UO_2} = \frac{a_1 \cdot K_{UO_2^{2+}} \cdot \alpha_{UO_2^{2+}}}{1 + K_{UO_2^{2+}} \cdot \alpha_{UO_2^{2+}}} + \frac{a_2 \cdot K_{UO_2B} \cdot \alpha_{UO_2B}}{1 + K_{H^+} \cdot \alpha_{H^+} + K_{UO_2B} \cdot \alpha_{UO_2B}}$
2T2S2H	$\varphi_{UO_2} = \frac{a_1 \cdot K_{UO_2^{2+}} \cdot \alpha_{UO_2^{2+}}}{1 + K_{H^+} \cdot \alpha_{H^+} + K_{UO_2^{2+}} \cdot \alpha_{UO_2^{2+}}} + \frac{a_2 \cdot K_{UO_2B} \cdot \alpha_{UO_2B}}{1 + K'_{H^+} \cdot \alpha_{H^+} + K_{UO_2B} \cdot \alpha_{UO_2B}}$
3T3S0H	$\varphi_{UO_2} = \frac{a_1 \cdot K_{UO_2^{2+}} \cdot \alpha_{UO_2^{2+}}}{1 + K_{UO_2^{2+}} \cdot \alpha_{UO_2^{2+}}} + \frac{a_2 \cdot K_{UO_2B} \cdot \alpha_{UO_2B}}{1 + K_{UO_2B} \cdot \alpha_{UO_2B}} + \frac{a_3 \cdot K_{UO_2C} \cdot \alpha_{UO_2C}}{1 + K_{UO_2C} \cdot \alpha_{UO_2C}}$

Table 7-2 Mathematical models tested in this work φ_{UO_2} expressed in mol g^{-1} h^{-1} (cont.)

Code	Model with adjustable parameters of regrouped constants
kin1T1S	$\varphi_{UO_2} = \frac{a^{(pH)} \cdot K_{UO_2^{2+}} \cdot \alpha_{UO_2^{2+}}}{1 + K_{UO_2^{2+}} \cdot \alpha_{UO_2^{2+}}}$
kin1T2S	$\varphi_{UO_2} = \frac{a^{(pH)} \cdot \left(K_{UO_2^{2+}} \cdot \alpha_{UO_2^{2+}} + K_{UO_2B} \cdot \alpha_{UO_2B} \right)}{1 + K_{UO_2^{2+}} \cdot \alpha_{UO_2^{2+}} + K_{UO_2B} \cdot \alpha_{UO_2B}}$
kin1T3S	$\varphi_{UO_2} = \frac{a^{(pH)} \cdot \left(K_{UO_2^{2+}} \cdot \alpha_{UO_2^{2+}} + K_{UO_2B} \cdot \alpha_{UO_2B} + K_{UO_2C} \cdot \alpha_{UO_2C} \right)}{1 + K_{UO_2^{2+}} \cdot \alpha_{UO_2^{2+}} + K_{UO_2B} \cdot \alpha_{UO_2B} + K_{UO_2C} \cdot \alpha_{UO_2C}}$
affin1T1S	$\varphi_{UO_2} = \frac{a \cdot K_{UO_2^{2+}}^{(pH)} \cdot \alpha_{UO_2^{2+}}}{1 + K_{UO_2^{2+}}^{(pH)} \cdot \alpha_{UO_2^{2+}}}$
affin1T2S	$\varphi_{UO_2} = \frac{a \cdot \left(K_{UO_2^{2+}}^{(pH)} \cdot \alpha_{UO_2^{2+}} + K_{UO_2B} \cdot \alpha_{UO_2B} \right)}{1 + K_{UO_2^{2+}}^{(pH)} \cdot \alpha_{UO_2^{2+}} + K_{UO_2B} \cdot \alpha_{UO_2B}}$
affin1T3S	$\varphi_{UO_2} = \frac{a \cdot \left(K_{UO_2^{2+}}^{(pH)} \cdot \alpha_{UO_2^{2+}} + K_{UO_2B} \cdot \alpha_{UO_2B} + K_{UO_2C} \cdot \alpha_{UO_2C} \right)}{1 + K_{UO_2^{2+}}^{(pH)} \cdot \alpha_{UO_2^{2+}} + K_{UO_2B} \cdot \alpha_{UO_2B} + K_{UO_2C} \cdot \alpha_{UO_2C}}$

$$\varphi_{UO_2} = \frac{d\left\langle UO_2 \right\rangle_{int}}{dt}$$

Table 7-3 Chemically available uranium species considered in this study

Model code	UO_2B	UO_2C	Model code	UO_2B	UO_2C
L2Sa	UO_2OH^+	--	2T2S1HBa	UO_2OH^+	--
L2Sb	$UO_2(OH)_2^0$	--	2T2S1HBb	$UO_2(OH)_2^0$	--
L2Sc	$UO_2CO_3^0$	--	2T2S1HBc	$UO_2CO_3^0$	--
L2Sd	$UO_2HPO_4^0$	--	2T2S1HBd	$UO_2HPO_4^0$	--
L2Se	$UO_2H_2PO_4^+$	--	2T2S1HBe	$UO_2H_2PO_4^+$	--
L3Sa	$UO_2CO_3^0$	UO_2OH^+	2T2S2Ha	UO_2OH^+	--
L3Sb	$UO_2CO_3^0$	$UO_2(OH)_2^0$	2T2S2Hb	$UO_2(OH)_2^0$	--
L3Sc	$UO_2CO_3^0$	$UO_2HPO_4^0$	2T2S2Hc	$UO_2CO_3^0$	--
L3Sd	$UO_2CO_3^0$	$UO_2H_2PO_4^+$	2T2S2Hd	$UO_2HPO_4^0$	--
1T2S0Ha	UO_2OH^+	--	2T2S2He	$UO_2H_2PO_4^+$	--
1T2S0Hb	$UO_2(OH)_2^0$	--	3T3S0Ha	UO_2OH^+	$UO_2(OH)_2^0$
1T2S0Hc	$UO_2CO_3^0$	--	3T3S0Hb	UO_2OH^+	$UO_2CO_3^0$
1T2S0Hd	$UO_2HPO_4^0$	--	3T3S0Hc	UO_2OH^+	$UO_2HPO_4^0$
1T2S0He	$UO_2H_2PO_4^+$	--	3T3S0Hd	UO_2OH^+	$UO_2H_2PO_4^+$
1T2S1Ha	UO_2OH^+	--	3T3S0He	$UO_2(OH)_2^0$	$UO_2CO_3^0$
1T2S1Hb	$UO_2(OH)_2^0$	--	3T3S0Hf	$UO_2(OH)_2^0$	$UO_2HPO_4^0$
1T2S1Hc	$UO_2CO_3^0$	--	3T3S0Hg	$UO_2(OH)_2^0$	$UO_2H_2PO_4^+$
1T2S1Hd	$UO_2HPO_4^0$	--	3T3S0Hh	$UO_2CO_3^0$	$UO_2HPO_4^0$
1T2S1He	$UO_2H_2PO_4^+$	--	3T3S0Hi	$UO_2CO_3^0$	$UO_2H_2PO_4^+$
1T3S0Ha	$UO_2CO_3^0$	UO_2OH^+	3T3S0Hj	$UO_2HPO_4^0$	$UO_2H_2PO_4^+$
1T3S0Hb	$UO_2CO_3^0$	$UO_2(OH)_2^0$	kin1T2Sa	UO_2OH^+	--
1T3S0Hc	$UO_2CO_3^0$	$UO_2HPO_4^0$	kin1T2Sb	$UO_2(OH)_2^0$	--
1T3S0Hd	$UO_2CO_3^0$	$UO_2H_2PO_4^+$	kin1T2Sc	$UO_2CO_3^0$	--
1T3S1Ha	$UO_2CO_3^0$	UO_2OH^+	kin1T2Sd	$UO_2HPO_4^0$	--
1T3S1Hb	$UO_2CO_3^0$	$UO_2(OH)_2^0$	kin1T2Se	$UO_2H_2PO_4^+$	--
1T3S1Hc	$UO_2CO_3^0$	$UO_2HPO_4^0$	kin1T3Sa	$UO_2CO_3^0$	UO_2OH^+
1T3S1Hd	$UO_2CO_3^0$	$UO_2H_2PO_4^+$	kin1T3Sb	$UO_2CO_3^0$	$UO_2(OH)_2^0$
2T2S0Ha	UO_2OH^+	--	kin1T3Sc	$UO_2CO_3^0$	$UO_2HPO_4^0$
2T2S0Hb	$UO_2(OH)_2^0$	--	kin1T3Sd	$UO_2CO_3^0$	$UO_2H_2PO_4^+$
2T2S0Hc	$UO_2CO_3^0$	--	affin1T2Sa	UO_2OH^+	--
2T2S0Hd	$UO_2HPO_4^0$	--	affin1T2Sb	$UO_2(OH)_2^0$	--
2T2S0He	$UO_2H_2PO_4^+$	--	affin1T2Sc	$UO_2CO_3^0$	--
2T2S1HAa	UO_2OH^+	--	affin1T2Sd	$UO_2HPO_4^0$	--
2T2S1HAb	$UO_2(OH)_2^0$	--	affin1T2Se	$UO_2H_2PO_4^+$	--
2T2S1HAc	$UO_2CO_3^0$	--	affin1T3Sa	$UO_2CO_3^0$	UO_2OH^+
2T2S1HAd	$UO_2HPO_4^0$	--	affin1T3Sb	$UO_2CO_3^0$	$UO_2(OH)_2^0$
2T2S1HAe	$UO_2H_2PO_4^+$	--	affin1T3Sc	$UO_2CO_3^0$	$UO_2HPO_4^0$
			affin1T3Sd	$UO_2CO_3^0$	$UO_2H_2PO_4^+$

7.3.2 Tested solution composition domains

The domain of chemical composition studied can strongly influence both the choice of model adopted as adequate to describe the observed behaviour, and also the best-fit values of the adjustable parameters for a given model. As the domain of chemical composition used to formulate and parameterise a model is increased, it can be assumed that the domain to which the developed model can be reasonably applied also increases. In the best case the model will be applicable to the full volume of parameter space studied in order to develop the model. In the worst case, if the adopted model poorly describes the underlying mechanisms, the model may only be applicable to the exact chemical compositions used to develop the model. In order to assess the effect of varying chemical composition domain on model selection, the full domain studied was divided in to a number of sub-domains, and the tested models were fitted to all of these sub-domains. The factors that were investigated in this study were: pH, calcium and magnesium concentration, citrate concentration, phosphate concentration and carbonate concentration. Sub-domains of increasing chemical composition domain for both constant pH values (5, 6 and 7) and variable pH are presented in Table 7-4 with the number of data included in each sub-domain.

Table 7-4 Chemical composition sub-domains considered for modelling

domain code	pH	carbonate concentration	phosphate concentration	citrate concentration	Ca/Mg concentration	number of data
pH5(1)	5	air equilibrium	0	0	0.5 mM	6
pH5(2)	5	air equilibrium	0	variable	0.5 mM	10
pH5(3)	5	air equilibrium	variable	0	0.5 mM	9
pH5(4)	5	variable	0	0	0.5 mM	8
pH5(5)	5	air equilibrium	variable	variable	0.5 mM	13
pH5(6)	5	variable	0	variable	0.5 mM	12
pH5(7)	5	variable	variable	0	0.5 mM	11
pH5(8)	5	variable	variable	variable	0.5 mM	15
pH6(1)	6	air equilibrium	0	0	0.5 mM	4
pH6(2)	6	air equilibrium	0	0	variable	14
pH6(3)	6	air equilibrium	0	variable	0.5 mM	8
pH6(4)	6	air equilibrium	variable	0	0.5 mM	7
pH6(5)	6	variable	0	0	0.5 mM	7
pH6(6)	6	air equilibrium	0	variable	variable	18
pH6(7)	6	air equilibrium	variable	0	variable	17
pH6(8)	6	variable	0	0	variable	17
pH6(9)	6	air equilibrium	variable	variable	0.5 mM	11
pH6(10)	6	variable	0	variable	0.5 mM	11
pH6(11)	6	variable	variable	0	0.5 mM	10
pH6(12)	6	variable	variable	variable	0.5 mM	14
pH6(13)	6	variable	variable	0	variable	20
pH6(14)	6	variable	0	variable	variable	21
pH6(15)	6	air equilibrium	variable	variable	variable	21
pH6(16)	6	variable	variable	variable	variable	24
pH7(1)	7	air equilibrium	0	0	0.5 mM	4
pH7(2)	7	air equilibrium	0	0	variable	14
pH7(3)	7	air equilibrium	variable	0	0.5 mM	6
pH7(4)	7	variable	0	0	0.5 mM	7
pH7(5)	7	air equilibrium	variable	0	variable	16
pH7(6)	7	variable	0	0	variable	17
pH7(7)	7	variable	variable	0	0.5 mM	9
pH7(8)	7	variable	variable	0	variable	19

Table 7-4 Chemical composition sub-domains considered for modelling (cont.)

domain code	pH	carbonate concentration	phosphate concentration	citrate concentration	Ca/Mg concentration	number of data
allpH(1)	variable	air equilibrium	0	0	0.5 mM	20
allpH(2)	variable	air equilibrium	0	0	variable	40
allpH(3)	variable	air equilibrium	0	variable	0.5 mM	28
allpH(4)	variable	air equilibrium	variable	0	0.5 mM	32
allpH(5)	variable	variable	0	0	0.5 mM	31
allpH(6)	variable	air equilibrium	0	variable	variable	48
allpH(7)	variable	air equilibrium	variable	0	variable	52
allpH(8)	variable	variable	0	0	variable	51
allpH(9)	variable	air equilibrium	variable	variable	0.5 mM	40
allpH(10)	variable	variable	0	variable	0.5 mM	39
allpH(11)	variable	variable	variable	0	0.5 mM	43
allpH(12)	variable	air equilibrium	variable	variable	variable	60
allpH(13)	variable	variable	0	variable	variable	59
allpH(14)	variable	variable	variable	0	variable	63
allpH(15)	variable	variable	variable	variable	0.5 mM	51
allpH(16)	variable	variable	variable	variable	variable	71

7.3.3 Applicability of different model hypothesis

The models presented in Table 7-2 are not all applicable to each of the chemical composition domains presented in Table 7-4. In a number of cases there are insufficient data points contained in a chemical composition sub-domain to enable models with an equal or greater number of adjustable parameters to be fitted. Additionally, for models that consider two or three uranyl species to be chemically available for uptake, it is required that these different species are not simply co-varied for all data points contained within the sub-domain. For example, models that consider both the free uranyl ion and a hydrolysis species to be chemically available cannot be applied to a chemical composition sub-domain at constant pH, as the two species are not varied independently within the composition sub-domain.

7.3.4 Results of model fitting using mean-value database calculations

The results of the model fitting for the selected chemical composition domains and proposed accumulation models performed using uranium speciation predicted by mean-value calculations are presented in Table 7-5 for composition sub-domains at

constant pH values of 5 and 7, Table 7-6 for pH 6 and Table 7-7 for variable pH. The values shown are the normalised best-fit chi-squared values (χ^2/ν). The colours show whether the models are applicable to the composition domains (black signifying that the model is not applicable) and whether the best-fit chi-squared value is inferior to one of several selected chi-squared distribution threshold values allowing model hypotheses to be falsified at a given probability level. Red squares signify that the corresponding model hypothesis can be rejected for that chemical composition domain with a probability of 99.99 %, i.e. assuming that the model is "correct" and that the dataset standard deviations have not been underestimated, the chance of obtaining the dataset is less than 0.01 %. Similarly, orange squares signify that the model hypotheses may be rejected with a probability of 99.9 %, yellow with a probability of 99 % and blue with a probability of 90 %. The green squares show models that may not be falsified at the lowest selected probability level. As can be seen there are only a relatively small number of models that can be applied to composition domains of constant pH compared to the number applicable to composition domains of variable pH. For chemical composition domains of constant pH, relatively simple models are adequate to explain the observed behaviour. For the three pH values investigated, the simplest models that cannot be falsified at a 99 % probability for all sub-domains contain three adjustable parameters. As the composition domain is increased from left to right in the tables (and the size of the dataset increases) an increasing number of hypotheses may be rejected. For the most restrictive solution composition domain (constant Ca^{2+} and Mg^{2+}, no citrate or phosphate and air equilibrium) none of the three simplest models (L1Sa, L1Sb and 1T1S0H) may be rejected at the lowest selected probability level for the three pH values, i.e. the data at each pH value can be represented by models considering just the free-ion. Extending the composition domain to include variable calcium and magnesium concentrations does not enable rejection of these simplest models. Further extension of the composition domain to include the presence of citrate enables the rejection of the L1Sa model at a 99 % confidence level for the data set at pH 5.0, but not at pH 6.0, i.e. simple proportionality with the free ion is not observed and saturable uptake kinetics needs to be considered in the model (or a linear approximation). Including the effects of variable carbonate concentrations at each pH value results in these simplest modelling approaches being rejected for all pH values

at a minimum of a 90 % probability, the simplest applicable model hypotheses that can be retained considers the co-accumulation of both the free-ion and the carbonate complex $UO_2CO_3^0$. If the largest solution compositions domains are considered for each pH value (variable Ca^{2+}, Mg^{2+}, citrate, carbonate and phosphate concentrations) there is only one model that cannot be rejected at a probability of 90 % that is applicable to all pH values, the 1T2S0Hc model. However, at each individual pH value there are at least two models that cannot be rejected at a 90 % probability. For the datasets at constant pH the pre-equilibrium or steady state approach to modelling is largely sufficient to explain the observed behaviour.

The results for the composition domains of varying pH are rather different. For the most restricted composition domain where all factors apart from pH are kept constant, the simplest model that cannot be falsified at a 90 % probability contains four fitting parameters and considers the co-accumulation of the free-ion and a hydroxide species, as well as proton competition for the binding site. Thus a pre-equilibrium or steady state based model is sufficient to explain the observed pH behaviour as long as other solution composition parameters are kept constant. As the composition domain is increased the complexity and hence flexibility of the models required to explain the observed behaviour also increases. Extending the composition domain to include variable calcium, magnesium and citrate concentrations results in all models with less than 5 fitting parameters being rejected at a minimum 99 % probability. Further extending the domain results in all models with less than 6 fitting parameters being rejected at a minimum 90 % probability. The only model flexible enough to represent the complete solution composition domain retained as a hypothesis at the lowest probability level considers the accumulation of 3 different uranium species and non-competitive pH dependent modulation of the transport system. For the level of model complexity considered in this study, the pre-equilibrium or steady state framework is not sufficient to explain the observed uptake rate behaviour for the complete solution composition domain space studied. It is probable that the extension of the model to consider further or different available uranium species would eventually provide an adequate fit to the data, however it is doubtful that such a complex model would be useful for predictive modelling purposes due to its increased sensitivity. It seems more probable that the observed pH effect is due to non-competitive effects of varying proton concentration.

Table 7-5 Results of model fitting using mean-value speciation calculations, pH 5 and 7 solution composition domains, goodness of fit values expressed as χ^2/ν. Model details are listed in Table 7-2 and chemical domain spaces are listed in Table 7-4. *N* is the number of data-points in the composition domain. For composition domain rows: 0 signifies that the parameter was constant, 1 signifies that the parameter was variable for the composition sub-domain.

model code		Fitting parameters	pH5 (1)	pH5 (2)	pH5 (3)	pH5 (4)	pH5 (5)	pH5 (6)	pH5 (7)	pH5 (8)		pH7 (1)	pH7 (2)	pH7 (3)	pH7 (4)	pH7 (5)	pH7 (6)	pH7 (7)	pH7 (8)
		N	6	10	9	8	13	12	11	15		4	14	6	7	16	17	9	19
domain	[carbonate]		0	0	0	1	0	1	1	1		0	0	0	1	0	1	1	1
	[phosphate]		0	0	1	0	1	0	1	1		0	0	1	0	1	0	1	1
	[citrate]		0	1	0	0	1	1	0	1		0	0	0	0	0	0	0	0
	[Ca/Mg]		0	0	0	0	0	0	0	0		0	1	0	0	1	1	0	1
L1Sa		1	1.8	2.5	4.2	3.8	3.9	3.5	5.1	4.5		0.9	0.5	0.7	4.6	0.4	2.0	3.6	1.8
L1Sb		2	1.6	1.2	3.7	3.9	2.7	2.7	4.7	3.6		1.3	0.5	0.9	4.8	0.5	1.9	4.1	1.8
1T1S0H		2	0.1	0.2	3.2	2.1	2.1	1.3	3.7	2.7		1.3	0.5	0.9	5.5	0.5	2.1	4.1	1.9
L2Sc		3				1.3		1.1	3.2	2.5					456		1075	496	987.1
L2Sd		3			1.4		1.2		3.3	2.4				1.3		0.5		4.8	2.0
L2Se		3			1.4		1.2		3.3	2.4				1.2		0.5		4.8	20.5
1T2S0Hc		3				0.1		0.2	2.8	2.0					2.2		0.9	1.6	0.8
1T2S0Hd		3			0.5		0.5		2.0	1.4				1.2		0.5		4.8	2.0
1T2S0He		3			0.5		0.5		2.0	1.4				1.2		0.5		4.8	2.0
2T2S0Hc		4				0.1		1.6	3.2	3.1					3.0		1.0	1.9	0.9
2T2S0Hd		4			0.6		0.6		2.2	1.5				1.9		0.5		5.8	2.1
2T2S0He		4			0.6		0.6		2.2	1.5				1.9		0.5		5.8	2.1

model inapplicable	$P(\chi^2\|\nu) < 0.0001$	$0.0001 < P(\chi^2\|\nu) < 0.001$	$0.001 < P(\chi^2\|\nu) < 0.01$	$0.01 < P(\chi^2\|\nu) < 0.1$	$0.1 < P(\chi^2\|\nu)$

Table 7-6 Results of model fitting using mean-value speciation calculations, pH 6 solution composition domains, goodness of fit values expressed as χ^2/ν. Model details are listed in Table 7-2 and chemical domain spaces are listed in Table 7-4. *N* is the number of data-points in the composition domain. For composition domain rows: 0 signifies that the parameter was constant, 1 signifies that the parameter was variable for the composition sub-domain.

model code	Fitting parameters	pH6 (1)	pH6 (2)	pH6 (3)	pH6 (4)	pH6 (5)	pH6 (6)	pH6 (7)	pH6 (8)	pH6 (9)	pH6 (10)	pH6 (11)	pH6 (12)	pH6 (13)	pH6 (14)	pH6 (15)	pH6 (16)
	N	4	14	8	7	7	18	17	17	11	11	10	14	20	21	21	24
domain	[carbonate]	0	0	0	0	1	0	0	1	0	1	1	1	1	1	0	1
	[phosphate]	0	0	0	1	0	0	1	0	1	0	1	1	1	0	1	1
	[citrate]	0	0	1	0	0	1	0	0	1	1	0	1	0	1	1	1
	[Ca/Mg]	0	1	0	0	0	1	1	1	0	0	0	0	1	1	1	1
L1Sa	1	0.8	0.7	0.9	2.4	5.0	0.6	1.4	2.5	2.0	3.6	4.6	3.8	2.8	2.1	1.3	2.4
L1Sb	2	1.1	0.7	1.0	2.9	6.1	0.7	1.5	2.6	2.0	4.0	5.2	4.0	3.0	2.2	1.3	2.5
1T1S0H	2	1.1	0.7	1.0	2.9	6.1	0.7	1.5	2.6	2.2	4.0	5.2	4.1	3.0	2.2	1.3	2.5
L2Sc	3					4.0			6.4		2.9	1.8	1.4	1.5	5.5		5.3
L2Sd	3				9.5			0.8		0.8		9.5	3.3	2.4		0.6	2.0
L2Se	3				0.6			0.6		0.8		4.4	3.3	2.3		0.6	2.0
1T2S0Hc	3					0.8			0.9		0.7	1.8	1.4	1.4	1.0		1.4
1T2S0Hd	3				0.6			0.6		0.8		4.4	3.3	2.3		0.6	2.0
1T2S0He	3				0.6			0.6		0.8		4.4	3.3	2.3		0.6	2.0
2T2S0Hc	4					1.1			1.0		0.8	2.1	1.5	1.5	1.1		1.5
2T2S0Hd	4				0.8			0.7		0.9		5.1	3.6	2.5		0.6	2.1
2T2S0He	4				0.8			0.7		0.9		5.1	3.6	2.5		0.6	2.1

model inapplicable	$P(\chi^2\|\nu) < 0.0001$	$0.0001 < P(\chi^2\|\nu) < 0.001$	$0.001 < P(\chi^2\|\nu) < 0.01$	$0.01 < P(\chi^2\|\nu) < 0.1$	$0.1 < P(\chi^2\|\nu)$

Table 7-7 Results of model fitting using mean-value speciation calculations, all pH solution composition domains, goodness of fit values expressed as χ^2/ν. Model details are listed in Table 7-2 and chemical domain spaces are listed in Table 7-4. *N* is the number of data-points in the composition domain. For composition domain rows: 0 signifies that the parameter was constant, 1 signifies that the parameter was variable for the composition sub-domain.

model code	Fitting parameters	allpH (1)	allpH (2)	allpH (3)	allpH (4)	allpH (5)	allpH (6)	allpH (7)	allpH (8)	allpH (9)	allpH (10)	allpH (11)	allpH (12)	allpH (13)	allpH (14)	allpH (15)	allpH (16)
	N	20	40	28	32	31	48	52	51	40	39	43	60	59	63	51	71
Domain	[carbonate]	0	0	0	0	1	0	0	1	0	1	1	0	1	1	1	1
	[phosphate]	0	0	0	1	0	0	1	0	1	0	1	1	0	1	1	1
	[citrate]	0	0	1	0	0	1	0	0	1	1	0	1	1	0	1	1
	[Ca/Mg]	0	1	0	0	0	1	1	1	0	0	0	1	1	1	0	1
L1Sa	1	8.4	12.7	7.6	8.7	9.3	11.3	11.8	12.3	8.0	8.5	9.3	10.8	11.2	11.6	8.6	10.8
L1Sb	2	6.2	7.0	5.4	5.0	7.1	6.4	6.2	7.4	4.9	6.4	5.9	5.9	6.9	6.6	5.7	6.3
1T1S0H	2	7.7	11.4	6.4	7.9	8.7	10.2	10.5	11.0	7.0	7.6	8.5	9.7	10.2	10.3	7.7	9.8
L2Sa	3	5.4	7.1	4.0	5.0	6.8	6.1	6.3	7.5	4.2	5.5	5.9	5.8	6.7	6.7	5.1	6.3
L2Sb	3	4.3	4.3	2.7	3.6	5.5	4.0	5.1	5.6	3.2	4.6	4.9	4.3	5.1	5.6	4.4	5.1
L2Sc	3	3.7	5.4	3.1	4.0	4.2	4.9	5.6	5.4	3.4	3.5	4.0	5.1	4.9	5.4	3.5	5.0
L2Sd	3				4.5			5.8		4.3		5.6	5.5		6.3	5.3	6.0
L2Se	3				4.5			5.8		4.4		5.6	5.6		6.3	5.4	6.1
1T1S1H	3	5.2	7.7	4.3	5.8	7.0	6.8	7.6	8.3	5.1	6.0	6.9	6.9	7.4	8.1	6.2	7.4
1T2S0Ha	3	5.1	7.6	3.7	5.8	6.9	6.4	7.4	8.1	4.7	5.6	6.8	6.5	7.0	7.9	5.9	7.0
1T2S0Hb	3	2.6	4.2	2.3	7.5	10.1	3.7	4.5	5.4	3.3	4.5	5.0	7.4	8.6	8.0	4.7	7.8
1T2S0Hc	3	3.2	5.3	2.4	7.5	4.1	8.4	5.4	5.2	3.2	3.3	4.4	4.8	4.7	8.0	3.8	7.7
1T2S0Hd	3				5.8			7.7		5.3		7.0	7.4		9.6	6.5	7.8
1T2S0He	3				6.8			10.1		6.2		7.8	9.3		10.1	7.1	9.4
L3Sa	4	5.2	5.6	3.2	4.2	4.3	5.1	5.7	5.5	3.5	3.6	4.1	5.1	5.0	5.5	3.6	5.0
L3Sb	4	3.2	67.5	2.9	3.8	4.1	4.1	4.7	16.8	3.3	3.4	4.0	4.4	4.7	5.3	3.5	4.8
L3Sc	4				3.1			4.7		2.8		3.5	4.4		4.7	3.1	4.4
L3Sd	4				3.0			4.8		2.7		3.4	4.5		4.8	3.1	4.5

model inapplicable	$P(\chi^2\|\nu) < 0.0001$	$0.0001 < P(\chi^2\|\nu) < 0.001$	$0.001 < P(\chi^2\|\nu) < 0.01$	$0.01 < P(\chi^2\|\nu) < 0.1$	$0.1 < P(\chi^2\|\nu)$

Table 7-7 Results of model fitting using mean-value speciation calculations, all pH solution composition domains, goodness of fit values expressed as χ^2/ν. Model details are listed in Table 7-2 and chemical domain spaces are listed in Table 7-4. *N* is the number of data-points in the composition domain. For composition domain rows: 0 signifies that the parameter was constant, 1 signifies that the parameter was variable for the composition sub-domain. (cont.)

model code	Fitting parameters	allpH (1)	allpH (2)	allpH (3)	allpH (4)	allpH (5)	allpH (6)	allpH (7)	allpH (8)	allpH (9)	allpH (10)	allpH (11)	allpH (12)	allpH (13)	allpH (14)	allpH (15)	allpH (16)
N		20	40	28	32	31	48	52	51	40	39	43	60	59	63	51	71
Domain	[carbonate]	0	0	0	0	1	0	0	1	0	1	1	0	1	1	1	1
	[phosphate]	0	0	0	1	0	0	1	0	1	0	1	1	0	1	1	1
	[citrate]	0	0	1	0	0	1	0	0	1	1	0	1	1	0	1	1
	[Ca/Mg]	0	1	0	0	0	1	1	1	0	0	0	1	1	1	0	1
1T1S2H	4	5.5	7.9	4.4	6.0	7.3	7.0	7.7	8.5	5.3	6.1	7.0	7.0	7.6	8.2	6.3	7.5
1T2S1Ha	4	4.3	5.9	3.9	4.7	6.6	6.5	7.9	8.3	4.9	5.7	6.2	6.6	7.2	8.2	6.0	7.1
1T2S1Hb	4	1.2	1.1	2.4	2.6	5.4	3.8	2.1	3.1	3.4	4.6	5.2	4.1	3.3	3.5	4.8	3.6
1T2S1Hc	4	3.4	1.3	2.5	2.7	4.2	1.8	2.3	2.0	3.3	3.4	4.5	2.5	2.3	2.6	3.8	4.9
1T2S1Hd	4				7.7			7.9		3.9		5.9	7.6		8.2	5.3	6.7
1T2S1He	4				4.4			6.6		4.0		6.0	6.1		7.3	7.8	7.9
1T3S0Ha	4	3.4	5.4	2.5	4.1	4.2	4.7	5.6	5.4	3.3	3.4	4.5	4.9	4.8	5.5	3.8	4.9
1T3S0Hb	4	2.8	4.3	2.3	3.7	3.9	3.8	4.6	5.1	3.2	3.2	4.2	4.1	4.5	5.2	3.6	4.7
1T3S0Hc	4				2.9			4.6		2.4		3.6	4.1		4.7	3.1	4.3
1T3S0Hd	4				2.9			4.7		2.4		3.7	4.3		4.8	3.2	4.4
2T2S0Ha	4	5.5	7.8	3.9	6.0	7.2	6.5	7.6	8.3	4.9	5.7	7.0	6.6	7.2	8.0	6.0	7.1
2T2S0Hb	4	2.7	4.3	2.3	3.6	5.4	3.7	4.6	5.5	3.3	4.6	5.1	4.1	4.9	5.5	4.7	5.0
2T2S0Hc	4	3.4	5.4	2.5	4.0	4.0	4.6	5.5	5.4	3.3	3.3	4.3	4.9	4.7	5.5	3.7	4.9
2T2S0Hd	4				5.9			9.6		5.4		7.1	8.9		9.7	6.5	9.1
2T2S0He	4				8.6			10.3		7.4		7.1	8.9		10.2	6.5	9.6

model inapplicable	$P(\chi^2\|\nu) < 0.0001$	$0.0001 < P(\chi^2\|\nu) < 0.001$	$0.001 < P(\chi^2\|\nu) < 0.01$	$0.01 < P(\chi^2\|\nu) < 0.1$	$0.1 < P(\chi^2\|\nu)$

Table 7-7 Results of model fitting using mean-value speciation calculations, all pH solution composition domains, goodness of fit values expressed as χ^2/ν. Model details are listed in Table 7-2 and chemical domain spaces are listed in Table 7-4. *N* is the number of data-points in the composition domain. For composition domain rows: 0 signifies that the parameter was constant, 1 signifies that the parameter was variable for the composition sub-domain. (cont.)

model code	Fitting parameters	allpH (1)	allpH (2)	allpH (3)	allpH (4)	allpH (5)	allpH (6)	allpH (7)	allpH (8)	allpH (9)	allpH (10)	allpH (11)	allpH (12)	allpH (13)	allpH (14)	allpH (15)	allpH (16)
	N	20	40	28	32	31	48	52	51	40	39	43	60	59	63	51	71
Domain	[carbonate]	0	0	0	0	1	0	0	1	0	1	1	0	1	1	1	1
	[phosphate]	0	0	0	1	0	0	1	0	1	0	1	1	0	1	1	1
	[citrate]	0	0	1	0	0	1	0	0	1	1	0	1	1	0	1	1
	[Ca/Mg]	0	1	0	0	0	1	1	1	0	0	0	1	1	1	0	1
1T3S1Ha	5	1.6	1.3	2.6	2.8	2.2	1.9	2.3	2.0	3.4	3.5	2.9	2.5	2.3	2.6	3.9	2.8
1T3S1Hb	5	1.3	1.1	2.4	2.7	2.2	1.7	2.1	2.0	3.3	3.3	2.9	2.4	2.3	2.6	3.7	2.8
1T3S1Hc	5				3.0			2.0		2.5		2.7	2.3		2.4	3.2	2.6
1T3S1Hd	5				3.0			1.3		2.5		2.1	1.7		1.9	3.2	2.1
2T2S1HAa	5	5.8	8.0	4.1	6.2	7.5	6.7	7.8	8.5	5.0	5.9	7.2	6.7	7.3	8.1	6.1	7.2
2T2S1HAb	5	2.9	4.4	2.4	3.7	5.6	3.8	4.7	5.6	3.4	4.7	5.3	4.2	5.0	5.6	4.8	5.1
2T2S1HAc	5	3.6	5.6	2.6	4.2	4.2	4.7	5.6	5.5	3.4	3.4	4.4	5.0	4.8	5.6	3.8	5.0
2T2S1HAd	5				4.6			6.7		4.0		6.1	6.2		7.4	7.5	7.6
2T2S1HAe	5				5.0			7.1		4.4		6.4	6.6		7.7	5.8	7.1
2T2S1HBa	5	2.9	4.4	2.4	3.7	5.6	3.8	4.7	5.6	3.4	4.7	5.3	4.2	5.0	5.6	4.8	5.1
2T2S1HBb	5	1.2	0.8	0.9	2.9	4.5	0.7	1.8	2.8	2.3	3.6	4.7	1.6	2.5	3.2	3.9	2.9
2T2S1HBc	5	1.4	1.0	1.2	2.8	1.7	1.0	1.9	1.4	2.3	1.5	2.6	1.8	1.4	2.0	2.3	1.9
2T2S1HBd	5				6.0			9.7		5.5		7.3	9.0		9.7	6.6	9.2
2T2S1HBe	5				6.1			9.8		5.5		7.3	9.0		9.8	6.7	9.2

model inapplicable	$P(\chi^2\|\nu) < 0.0001$	$0.0001 < P(\chi^2\|\nu) < 0.001$	$0.001 < P(\chi^2\|\nu) < 0.01$	$0.01 < P(\chi^2\|\nu) < 0.1$	$0.1 < P(\chi^2\|\nu)$

Table 7-7 Results of model fitting using mean-value speciation calculations, all pH solution composition domains, goodness of fit values expressed as χ^2/ν. Model details are listed in Table 7-2 and chemical domain spaces are listed in Table 7-4. *N* is the number of data-points in the composition domain. For composition domain rows: 0 signifies that the parameter was constant, 1 signifies that the parameter was variable for the composition sub-domain. (cont.)

model code	Fitting parameters	allpH (1)	allpH (2)	allpH (3)	allpH (4)	allpH (5)	allpH (6)	allpH (7)	allpH (8)	allpH (9)	allpH (10)	allpH (11)	allpH (12)	allpH (13)	allpH (14)	allpH (15)	allpH (16)
	N	20	40	28	32	31	48	52	51	40	39	43	60	59	63	51	71
domain	[carbonate]	0	0	0	0	1	0	0	1	0	1	1	0	1	1	1	1
	[phosphate]	0	0	0	1	0	0	1	0	1	0	1	1	0	1	1	1
	[citrate]	0	0	1	0	0	1	0	0	1	1	0	1	1	0	1	1
	[Ca/Mg]	0	1	0	0	0	1	1	1	0	0	0	1	1	1	0	1
2T2S2Ha	6	3.1	4.5	2.6	3.9	5.8	3.9	4.8	5.8	3.5	4.8	5.4	4.3	5.1	5.7	4.9	5.1
2T2S2Hb	6	0.8	0.7	0.7	2.6	8.2	0.6	1.7	5.8	2.1	3.5	4.5	1.5	2.4	3.1	3.8	2.8
2T2S2Hc	6	1.2	0.8	1.0	2.6	1.6	0.8	1.8	1.3	2.1	1.4	2.4	1.6	1.2	2.0	2.1	1.8
2T2S2Hd	6				4.6			6.8		7.7		6.2	7.8		7.5	7.7	7.8
2T2S2He	6				5.2			7.2		4.6		6.3	6.7		7.6	5.9	7.2
3T3S0Ha	6	3.1	4.5	2.6	3.9	5.8	3.9	4.8	5.8	3.5	4.8	5.4	4.3	5.1	5.7	4.9	5.1
3T3S0Hb	6	3.8	5.7	2.7	4.3	4.4	4.9	5.8	5.6	3.5	3.5	4.5	5.1	4.9	5.7	3.8	5.1
3T3S0Hc	6				4.7			6.8		3.7		6.2	5.9		7.4	5.2	6.6
3T3S0Hd	6				5.2			7.2		4.2		6.6	6.2		7.7	5.6	6.8
3T3S0He	6	3.1	4.5	2.5	3.9	4.2	3.9	4.8	5.3	3.4	3.5	5.4	4.3	4.7	5.4	4.4	4.8
3T3S0Hf	6				2.4			3.8		2.3		4.5	3.4		4.9	4.3	4.4
3T3S0Hg	6				2.5			3.9		2.5		4.5	3.6		5.0	4.2	4.6
3T3S0Hh	6				3.2			4.7		2.7		3.6	4.2		4.8	3.1	4.4
3T3S0Hi	6				3.1			4.9		2.5		3.6	4.4		5.0	3.1	4.5
3T3S0Hj	6				6.1			10.0		5.6		7.4	9.1		10.0	6.7	9.3

model inapplicable	$P(\chi^2\|\nu) < 0.0001$	$0.0001 < P(\chi^2\|\nu) < 0.001$	$0.001 < P(\chi^2\|\nu) < 0.01$	$0.01 < P(\chi^2\|\nu) < 0.1$	$0.1 < P(\chi^2\|\nu)$

Table 7-7 Results of model fitting using mean-value speciation calculations, all pH solution composition domains, goodness of fit values expressed as χ^2/ν. Model details are listed in Table 7-2 and chemical domain spaces are listed in Table 7-4. *N* is the number of data-points in the composition domain. For composition domain rows: 0 signifies that the parameter was constant, 1 signifies that the parameter was variable for the composition sub-domain. (cont.)

model code	Fitting parameters	allpH (1)	allpH (2)	allpH (3)	allpH (4)	allpH (5)	allpH (6)	allpH (7)	allpH (8)	allpH (9)	allpH (10)	allpH (11)	allpH (12)	allpH (13)	allpH (14)	allpH (15)	allpH (16)
	N	20	40	28	32	31	48	52	51	40	39	43	60	59	63	51	71
domain	[carbonate]	0	0	0	0	1	0	0	1	0	1	1	0	1	1	1	1
	[phosphate]	0	0	0	1	0	0	1	0	1	0	1	1	0	1	1	1
	[citrate]	0	0	1	0	0	1	0	0	1	1	0	1	1	0	1	1
	[Ca/Mg]	0	1	0	0	0	1	1	1	0	0	0	1	1	1	0	1
kin1T1S	7	0.7	0.6	0.7	2.5	4.4	0.5	1.6	2.7	2.1	3.5	4.4	1.5	2.3	3.1	3.8	2.8
affin1T1S	7	0.8	0.6	0.8	2.6	4.5	0.6	1.7	2.7	2.1	3.6	4.5	1.5	2.4	3.1	3.8	2.8
kin1T2Sa	8	0.7	0.6	0.7	2.6	4.6	0.6	1.7	2.8	2.1	3.6	4.5	1.5	2.4	3.1	3.9	2.8
kin1T2Sb	8	0.7	0.6	0.7	2.6	4.6	0.6	1.7	2.8	2.1	3.6	4.5	1.5	2.4	3.1	3.9	2.8
kin1T2Sc	8	0.7	0.6	0.7	2.6	1.4	0.5	1.6	1.0	2.1	1.2	2.3	1.5	1.1	1.7	2.0	1.7
kin1T2Sd	8				2.6			1.7		3.0		4.5	1.5		3.1	4.6	2.8
kin1T2Se	8				1.9			1.5		1.7		4.1	1.4		3.0	3.5	2.7
affin1T2Sa	8	18.5	17.7	16.0	14.3	15.4	16.6	15.6	16.2	13.8	14.6	13.6	15.1	15.6	14.9	13.3	14.5
affin1T2Sb	8	19.7	18.6	17.2	14.9	16.1	17.6	16.3	16.9	14.6	15.4	4.6	15.9	16.4	15.5	14.0	15.2
affin1T2Sc	8	0.9	0.6	0.8	2.6	2.7	0.6	1.7	1.8	2.1	2.2	3.2	1.5	1.7	2.3	2.7	2.2
affin1T2Sd	8				1.1			0.8		1.0		3.6	0.8		2.5	3.1	2.2
affin1T2Se	8				1.2			0.9		1.1		3.6	0.9		2.6	3.1	2.3

model inapplicable	$P(\chi^2\|\nu) < 0.0001$	$0.0001 < P(\chi^2\|\nu) < 0.001$	$0.001 < P(\chi^2\|\nu) < 0.01$	$0.01 < P(\chi^2\|\nu) < 0.1$	$0.1 < P(\chi^2\|\nu)$

Table 7-7 Results of model fitting using mean-value speciation calculations, all pH solution composition domains, goodness of fit values expressed as χ^2/ν. Model details are listed in Table 7-2 and chemical domain spaces are listed in Table 7-4. *N* is the number of data-points in the composition domain. For composition domain rows: 0 signifies that the parameter was constant, 1 signifies that the parameter was variable for the composition sub-domain. (cont.)

model code	Fitting parameters	allpH (1)	allpH (2)	allpH (3)	allpH (4)	allpH (5)	allpH (6)	allpH (7)	allpH (8)	allpH (9)	allpH (10)	allpH (11)	allpH (12)	allpH (13)	allpH (14)	allpH (15)	allpH (16)
	N	20	40	28	32	31	48	52	51	40	39	43	60	59	63	51	71
domain	[carbonate]	0	0	0	0	1	0	0	1	0	1	1	0	1	1	1	1
	[phosphate]	0	0	0	1	0	0	1	0	1	0	1	1	0	1	1	1
	[citrate]	0	0	1	0	0	1	0	0	1	1	0	1	1	0	1	1
	[Ca/Mg]	0	1	0	0	0	1	1	1	0	0	0	1	1	1	0	1
kin1T3Sa	9	0.8	0.6	0.7	2.7	1.3	0.5	1.7	1.0	2.1	1.1	2.3	1.5	1.0	1.8	2.0	1.7
kin1T3Sb	9	0.8	0.6	0.7	2.7	1.4	0.5	1.7	1.0	2.1	1.2	2.3	1.5	1.1	1.8	2.0	1.7
kin1T3Sc	9				1.3			1.0		1.3		1.6	11.3		10.6	1.4	1.2
kin1T3Sd	9				12.6			11.3		12.3		11.1	11.3		10.6	10.0	10.7
affin1T3Sa	9	19.7	17.4	16.4	14.5	15.5	16.3	15.3	15.8	13.9	14.6	13.5	14.8	15.2	14.5	13.2	14.2
affin1T3Sb	9	20.9	18.2	17.1	15.2	16.2	17.2	16.0	16.5	14.7	15.4	14.0	15.5	16.0	15.1	13.9	14.8
affin1T3Sc	9				1.2			0.9		1.0		2.4	0.8		1.7	2.0	1.7
affin1T3Sd	9				1.2			0.9		1.1		2.3	0.9		1.7	2.0	1.7

model inapplicable	$P(\chi^2\|\nu) < 0.0001$	$0.0001 < P(\chi^2\|\nu) < 0.001$	$0.001 < P(\chi^2\|\nu) < 0.01$	$0.01 < P(\chi^2\|\nu) < 0.1$	$0.1 < P(\chi^2\|\nu)$

7.3.5 Results of model fitting integrating the effect of speciation calculation uncertainty

The results of the model fitting for the same chemical composition domains and accumulation models as for the mean-value speciation based calculations, but integrating the effect of speciation calculation uncertainty, are presented in Table 7-8 to Table 7-16. The values shown in the boxes for each composition domain and fitted model correspond to the percentage of MC samples that gave best-fit chi-squared values inferior to the selected probability threshold from the chi-squared distribution. Table 7-8 to Table 7-10 show the results for a probability threshold of 0.1, Table 7-11 to Table 7-13 for a probability threshold of 0.01 and Table 7-14 to Table 7-16 for a probability threshold of 0.0001. For a given composition domain and proposed model, the smaller the number of samples that pass the probability threshold and the smaller the selected probability threshold value the less likely it is that the proposed model is correct, i.e. the greater the confidence in rejecting the hypothesis. The colour code used to aid interpretation of the results table signifies the percentage of MC samples that pass the appropriate threshold value. Black indicates that the corresponding model is inapplicable to that composition domain, red that less than 1 % of the MC samples provided best-fit chi-squared values inferior to the selected probability threshold from the chi-squared distribution and similarly yellow less than 10 %, blue less than 50 % and green over 50 %.

If the results of the model fitting performed with mean-value speciation calculations are compared with the results of the MC simulation model fitting with the selected chi-squared distribution threshold value of 0.1, it can be seen that virtually all model and composition domain pairs that gave good ($0.1 < P(\chi^2|\upsilon)$) model fits with the mean-value speciation calculations also give high percentage values of MC simulations resulting in an acceptable best-fit chi-squared value. However, there are a number of composition domain and model pairs that are rejected with a relatively high confidence based on the mean-value speciation calculations, which give a relatively high proportion of MC simulations that have acceptable best-fit chi-squared values. For example the L2Sc model can be rejected at a 99.99 % confidence level for mean-value speciation calculations, but MC analysis results in 45 % of samples giving a $P(\chi^2|\upsilon) > 0.1$. The results of the MC simulation model fitting with the selected chi-

squared distribution threshold value of 0.01, i.e. the percentage of simulations that result in a best-fit chi-squared value that cannot be rejected at a 90 % probability, show the same trends as remarked earlier; as the chemical composition domain is extended, the complexity of the models required to describe the uptake behaviour increases, i.e. simpler models can be rejected as plausible hypotheses. As the selected probability threshold from the chi-squared distribution decreases, so does the number of modelling hypotheses that can be confidently falsified. As was the case for the model fitting performed using the mean-value thermodynamic database, the solution composition domain spaces at constant pH values can be adequately represented by the pre-equilibrium or steady-state modelling framework, at each pH value there are a number of candidate models that cannot be rejected at a 90 % probability for greater than 50 % of the MC samples. There is no single candidate model that meets these requirements for each of the three pH values, however the 1T2S0Hc model performs reasonably well: a minimum of 45 % of the MC samples cannot be rejected at a 90 % probability.

Similarly to the model fitting performed using the mean-value thermodynamic database, the pre-equilibrium or steady state modelling framework was sufficient to describe the observed uptake behaviour for composition domain spaces of variable pH but a restricted number of other variable parameters. For example four different pre-equilibrium models cannot be rejected at a 90 % probability for more than 50 % of the MC samples for a composition domain space of variable pH, citrate concentration and water hardness. Similarly for a composition domain space of variable pH, carbonate concentration and water hardness two different pre-equilibrium models cannot be rejected at a 90 % probability for more than 50 % of the MC samples. However, for the largest composition domain space considered in this study, pre-equilibrium models up to the degree of complexity considered are not adequate to describe the observed uptake behaviour: all of the models can be rejected at a 99.99 % for a minimum of 83 % of the MC samples. A number of the model candidates that consider a non-competitive effect of proton concentration cannot be rejected at a 99.99 % probability for over 10 % of MC samples and are therefore retained as plausible model hypotheses.

Table 7-8 Results of model fitting incorporating speciation uncertainty, pH 5 and 7 solution composition domains, % of samples greater than $P\left(\chi^2 \mid \nu\right) = 0.1$.

Model details are listed in Table 7-2 and chemical domain spaces are listed in Table 7-4. *N* is the number of data-points in the composition domain. For composition domain rows: 0 signifies that the parameter was constant, 1 signifies that the parameter was variable for the composition sub-domain.

model code	Fitting parameters	pH5 (1)	pH5 (2)	pH5 (3)	pH5 (4)	pH5 (5)	pH5 (6)	pH5 (7)	pH5 (8)		pH7 (1)	pH7 (2)	pH7 (3)	pH7 (4)	pH7 (5)	pH7 (6)	pH7 (7)	pH7 (8)
	N	6	10	9	8	13	12	11	15		4	14	6	7	16	17	9	19
domain	[carbonate]	0	0	0	1	0	1	1	1		0	0	0	1	0	1	1	1
	[phosphate]	0	0	1	0	1	0	1	1		0	0	1	0	1	0	1	1
	[citrate]	0	1	0	0	1	1	0	1		0	0	0	0	0	0	0	0
	[Ca/Mg]	0	0	0	0	0	0	0	0		0	1	0	0	1	1	0	1
L1Sa	1	65	32	0	0	0	0	0	0		100	97	93	0	93	0	0	0
L1Sb	2	99	75	0	0	0	0	0	0		99	100	89	0	92	1	0	0
1T1S0H	2	100	81	0	4	0	44	0	0		99	97	88	0	92	0	0	0
L2Sc	3				100		80	0	0					8		11	15	27
L2Sd	3			92		74		0	0				50		87		0	0
L2Se	3			92		74		0	0				74		59		0	0
1T2S0Hc	3				100		83	0	0					41		88	46	85
1T2S0Hd	3			100		80		9	35				81		91		0	0
1T2S0He	3			96		76		8	32				82		91		0	0
2T2S0Hc	4				72		57	0	0					30		87	36	84
2T2S0Hd	4			100		77		1	25				64		90		0	0
2T2S0He	4			97		74		1	25				65		90		0	0

inapplicable	< 1% of samples > *P*	1 - 10% of samples > *P*	10 - 50% of samples > *P*	>50% of samples > *P*

Table 7-9 Results of model fitting incorporating speciation uncertainty, pH 6 solution composition domains, % of samples greater than $P\left(\chi^2 \mid \nu\right) = 0.1$. Model details are listed in Table 7-2 and chemical domain spaces are listed in Table 7-4. *N* is the number of data-points in the composition domain. For composition domain rows: 0 signifies that the parameter was constant, 1 signifies that the parameter was variable for the composition sub-domain.

model code	Fitting parameters	pH6 (1)	pH6 (2)	pH6 (3)	pH6 (4)	pH6 (5)	pH6 (6)	pH6 (7)	pH6 (8)	pH6 (9)	pH6 (10)	pH6 (11)	pH6 (12)	pH6 (13)	pH6 (14)	pH6 (15)	pH6 (16)
	N	4	14	8	7	7	18	17	17	11	11	10	14	20	21	21	24
domain	[carbonate]	0	0	0	0	1	0	0	1	0	1	1	1	1	1	0	1
	[phosphate]	0	0	0	1	0	0	1	0	1	0	1	1	1	0	1	1
	[citrate]	0	0	1	0	0	1	0	0	1	1	0	1	0	1	1	1
	[Ca/Mg]	0	1	0	0	0	1	1	1	0	0	0	0	1	1	1	1
L1Sa	1	96	100	61	18	0	71	56	0	16	0	0	0	0	0	37	0
L1Sb	2	86	100	60	10	0	82	45	0	13	0	0	0	0	0	34	0
1T1S0H	2	86	100	56	9	0	70	45	0	10	0	0	0	0	0	30	0
L2Sc	3					41			48		45	44	35	43	45		27
L2Sd	3				58			91		56		0	0	0		81	0
L2Se	3				98			100		71		0	0	0		87	0
1T2S0Hc	3					94			97		69	44	35	57	67		32
1T2S0Hd	3				99			100		65		0	0	0		74	0
1T2S0He	3				99			100		65		0	0	0		76	0
2T2S0Hc	4					85			95		60	29	25	46	62		26
2T2S0Hd	4				95			100		61		0	0	0		71	0
2T2S0He	4				95			98		60		0	0	0		70	0

inapplicable	< 1% of samples > *P*	1 - 10% of samples > *P*	10 - 50% of samples > *P*	>50% of samples > *P*

Table 7-10 Results of model fitting incorporating speciation uncertainty, all pH solution composition domains, % of samples greater than $P\left(\chi^2 \mid \nu\right) = 0.1$. Model details are listed in Table 7-2 and chemical domain spaces are listed in Table 7-4. *N* is the number of data-points in the composition domain. For composition domain rows: 0 signifies that the parameter was constant, 1 signifies that the parameter was variable for the composition sub-domain.

model code	Fitting parameters	allpH (1)	allpH (2)	allpH (3)	allpH (4)	allpH (5)	allpH (6)	allpH (7)	allpH (8)	allpH (9)	allpH (10)	allpH (11)	allpH (12)	allpH (13)	allpH (14)	allpH (15)	allpH (16)
	N	20	40	28	32	31	48	52	51	40	39	43	60	59	63	51	71
domain	[carbonate]	0	0	0	0	1	0	0	1	0	1	1	0	1	1	1	1
	[phosphate]	0	0	0	1	0	0	1	0	1	0	1	1	0	1	1	1
	[citrate]	0	0	1	0	0	1	0	0	1	1	0	1	1	0	1	1
	[Ca/Mg]	0	1	0	0	0	1	1	1	0	0	0	1	1	1	0	1
L1Sa	1	0	0	0	0	0	0	0	0	0	0	0	0	0	0	0	0
L1Sb	2	0	0	0	0	0	0	0	0	0	0	0	0	0	0	0	0
1T1S0H	2	0	0	0	0	0	0	0	0	0	0	0	0	0	0	0	0
L2Sa	3	0	0	0	0	0	0	0	0	0	0	0	0	0	0	0	0
L2Sb	3	0	0	0	0	0	0	0	0	0	0	0	0	0	0	0	0
L2Sc	3	0	0	0	0	0	0	0	0	0	0	0	0	0	0	0	0
L2Sd	3				0			0		0		0	0		0	0	0
L2Se	3				0			0		0		0	0		0	0	0
1T1S1H	3	0	0	0	0	0	0	0	0	0	0	0	0	0	0	0	0
1T2S0Ha	3	0	0	0	0	0	0	0	0	0	0	0	0	0	0	0	0
1T2S0Hb	3	3	0	0	0	0	0	0	0	0	0	0	0	0	0	0	0
1T2S0Hc	3	0	0	0	0	0	0	0	0	0	0	0	0	0	0	0	0
1T2S0Hd	3				0			0		0		0	0		0	0	0
1T2S0He	3				0			0		0		0	0		0	0	0
L3Sa	4	0	0	0	0	0	0	0	0	0	0	0	0	0	0	0	0
L3Sb	4	0	0	0	0	0	0	0	0	0	0	0	0	0	0	0	0
L3Sc	4				0			0		0		0	0		0	0	0
L3Sd	4				0			0		0		0	0		0	0	0

inapplicable	< 1% of samples > *P*	1 - 10% of samples > *P*	10 - 50% of samples > *P*	>50% of samples > *P*

Table 7-10 Results of model fitting incorporating speciation uncertainty, all pH solution composition domains, % of samples greater than $P\left(\chi^2 \mid \nu\right) = 0.1$. Model details are listed in Table 7-2 and chemical domain spaces are listed in Table 7-4. *N* is the number of data-points in the composition domain. For composition domain rows: 0 signifies that the parameter was constant, 1 signifies that the parameter was variable for the composition sub-domain. (cont.)

model code	Fitting parameters	allpH (1)	allpH (2)	allpH (3)	allpH (4)	allpH (5)	allpH (6)	allpH (7)	allpH (8)	allpH (9)	allpH (10)	allpH (11)	allpH (12)	allpH (13)	allpH (14)	allpH (15)	allpH (16)
	N	20	40	28	32	31	48	52	51	40	39	43	60	59	63	51	71
domain	[carbonate]	0	0	0	0	1	0	0	1	0	1	1	0	1	1	1	1
	[phosphate]	0	0	0	1	0	0	1	0	1	0	1	1	0	1	1	1
	[citrate]	0	0	1	0	0	1	0	0	1	1	0	1	1	0	1	1
	[Ca/Mg]	0	1	0	0	0	1	1	1	0	0	0	1	1	1	0	1
1T1S2H	4	0	0	0	0	0	0	0	0	0	0	0	0	0	0	0	0
1T2S1Ha	4	0	0	0	0	0	0	0	0	0	0	0	0	0	0	0	0
1T2S1Hb	4	53	67	0	0	0	6	1	0	0	0	0	0	0	0	0	0
1T2S1Hc	4	48	50	1	0	2	6	1	3	0	0	0	0	0	0	0	0
1T2S1Hd	4				0			0		0		0	0		0	0	0
1T2S1He	4				0			0		0		0	0		0	0	0
1T3S0Ha	4	0	0	0	0	0	0	0	0	0	0	0	0	0	0	0	0
1T3S0Hb	4	2	0	0	0	0	0	0	0	0	0	0	0	0	0	0	0
1T3S0Hc	4				0			0		0		0	0		0	0	0
1T3S0Hd	4				0			0		0		0	0		0	0	0
2T2S0Ha	4	0	0	0	0	0	0	0	0	0	0	0	0	0	0	0	0
2T2S0Hb	4	2	0	0	0	0	0	0	0	0	0	0	0	0	0	0	0
2T2S0Hc	4	0	0	0	0	0	0	0	0	0	0	0	0	0	0	0	0
2T2S0Hd	4				0			0		0		0	0		0	0	0
2T2S0He	4				0			0		0		0	0		0	0	0

inapplicable	< 1% of samples > *P*	1 - 10% of samples > *P*	10 - 50% of samples > *P*	>50% of samples > *P*

Table 7-10 Results of model fitting incorporating speciation uncertainty, all pH solution composition domains, % of samples greater than $P\left(\chi^2 \mid \nu\right) = 0.1$. Model details are listed in Table 7-2 and chemical domain spaces are listed in Table 7-4. *N* is the number of data-points in the composition domain. For composition domain rows: 0 signifies that the parameter was constant, 1 signifies that the parameter was variable for the composition sub-domain. (cont.)

model code	Fitting parameters	allpH (1)	allpH (2)	allpH (3)	allpH (4)	allpH (5)	allpH (6)	allpH (7)	allpH (8)	allpH (9)	allpH (10)	allpH (11)	allpH (12)	allpH (13)	allpH (14)	allpH (15)	allpH (16)
	N	20	40	28	32	31	48	52	51	40	39	43	60	59	63	51	71
domain	[carbonate]	0	0	0	0	1	0	0	1	0	1	1	0	1	1	1	1
	[phosphate]	0	0	0	1	0	0	1	0	1	0	1	1	0	1	1	1
	[citrate]	0	0	1	0	0	1	0	0	1	1	0	1	1	0	1	1
	[Ca/Mg]	0	1	0	0	0	1	1	1	0	0	0	1	1	1	0	1
1T3S1Ha	5	48	48	1	0	1	6	1	3	0	0	0	0	0	0	0	0
1T3S1Hb	5	62	67	1	0	3	8	1	5	0	0	0	0	0	0	0	0
1T3S1Hc	5				0			4		0		0	0		0	0	0
1T3S1Hd	5				22			41		0		0	4		2	0	0
2T2S1HAa	5	0	0	0	0	0	0	0	0	0	0	0	0	0	0	0	0
2T2S1HAb	5	2	0	0	0	0	0	0	0	0	0	0	0	0	0	0	0
2T2S1HAc	5	0	0	0	0	0	0	0	0	0	0	0	0	0	0	0	0
2T2S1HAd	5				0			0		0		0	0		0	0	0
2T2S1HAe	5				0			0		0		0	0		0	0	0
2T2S1HBa	5	2	0	0	0	0	0	0	0	0	0	0	0	0	0	0	0
2T2S1HBb	5	74	95	52	0	0	68	0	0	0	0	0	0	0	0	0	0
2T2S1HBc	5	50	94	31	0	1	62	0	20	0	1	0	0	9	0	0	0
2T2S1HBd	5				0			0		0		0	0		0	0	0
2T2S1HBe	5				0			0		0		0	0		0	0	0

inapplicable	< 1% of samples > *P*	1 - 10% of samples > *P*	10 - 50% of samples > *P*	>50% of samples > *P*

Table 7-10 Results of model fitting incorporating speciation uncertainty, all pH solution composition domains, % of samples greater than $P\left(\chi^2 \mid \nu\right) = 0.1$. Model details are listed in Table 7-2 and chemical domain spaces are listed in Table 7-4. *N* is the number of data-points in the composition domain. For composition domain rows: 0 signifies that the parameter was constant, 1 signifies that the parameter was variable for the composition sub-domain. (cont.)

model code	Fitting parameters	allpH (1)	allpH (2)	allpH (3)	allpH (4)	allpH (5)	allpH (6)	allpH (7)	allpH (8)	allpH (9)	allpH (10)	allpH (11)	allpH (12)	allpH (13)	allpH (14)	allpH (15)	allpH (16)
	N	20	40	28	32	31	48	52	51	40	39	43	60	59	63	51	71
domain	[carbonate]	0	0	0	0	1	0	0	1	0	1	1	0	1	1	1	1
	[phosphate]	0	0	0	1	0	0	1	0	1	0	1	1	0	1	1	1
	[citrate]	0	0	1	0	0	1	0	0	1	1	0	1	1	0	1	1
	[Ca/Mg]	0	1	0	0	0	1	1	1	0	0	0	1	1	1	0	1
2T2S2Ha	6	1	0	0	0	0	0	0	0	0	0	0	0	0	0	0	0
2T2S2Hb	6	91	92	62	0	0	71	2	0	0	0	0	1	0	0	0	0
2T2S2Hc	6	77	89	54	0	4	67	2	28	0	5	0	1	19	0	0	0
2T2S2Hd	6				0			0		0		0	0		0	0	0
2T2S2He	6				0			0		0		0	0		0	0	0
3T3S0Ha	6	1	0	0	0	0	0	0	0	0	0	0	0	0	0	0	0
3T3S0Hb	6	0	0	0	0	0	0	0	0	0	0	0	0	0	0	0	0
3T3S0Hc	6				0			0		0		0	0		0	0	0
3T3S0Hd	6				0			0		0		0	0		0	0	0
3T3S0He	6	1	0	0	0	0	0	0	0	0	0	0	0	0	0	0	0
3T3S0Hf	6				0			0		0		0	0		0	0	0
3T3S0Hg	6				1			0		0		0	0		0	0	0
3T3S0Hh	6				0			0		0		0	0		0	0	0
3T3S0Hi	6				0			0		0		0	0		0	0	0
3T3S0Hj	6				0			0		0		0	0		0	0	0

inapplicable	< 1% of samples > *P*	1 - 10% of samples > *P*	10 - 50% of samples > *P*	>50% of samples > *P*

Table 7-10 Results of model fitting incorporating speciation uncertainty, all pH solution composition domains, % of samples greater than $P\left(\chi^2 \mid \nu\right) = 0.1$. Model details are listed in Table 7-2 and chemical domain spaces are listed in Table 7-4. *N* is the number of data-points in the composition domain. For composition domain rows: 0 signifies that the parameter was constant, 1 signifies that the parameter was variable for the composition sub-domain. (cont.)

model code	Fitting parameters	allpH (1)	allpH (2)	allpH (3)	allpH (4)	allpH (5)	allpH (6)	allpH (7)	allpH (8)	allpH (9)	allpH (10)	allpH (11)	allpH (12)	allpH (13)	allpH (14)	allpH (15)	allpH (16)
	N	20	40	28	32	31	48	52	51	40	39	43	60	59	63	51	71
domain	[carbonate]	0	0	0	0	1	0	0	1	0	1	1	0	1	1	1	1
	[phosphate]	0	0	0	1	0	0	1	0	1	0	1	1	0	1	1	1
	[citrate]	0	0	1	0	0	1	0	0	1	1	0	1	1	0	1	1
	[Ca/Mg]	0	1	0	0	0	1	1	1	0	0	0	1	1	1	0	1
kin1T1S	7	97	98	68	0	0	77	3	0	0	0	0	2	0	0	0	0
affin1T1S	7	95	98	65	0	0	75	2	0	0	0	0	2	0	0	0	0
kin1T2Sa	8	96	98	66	0	0	75	2	0	0	0	0	2	0	0	0	0
kin1T2Sb	8	96	98	66	0	0	76	2	0	0	0	0	2	0	0	0	0
kin1T2Sc	8	97	98	70	0	25	87	5	74	0	21	0	5	46	0	0	0
kin1T2Sd	8				0			2		0		0	2		0	0	0
kin1T2Se	8				9			14		6		0	9		0	0	0
affin1T2Sa	8	0	0	0	0	0	0	0	0	0	0	0	0	0	0	0	0
affin1T2Sb	8	10	17	4	0	0	7	0	0	0	0	0	0	0	0	0	0
affin1T2Sc	8	92	98	71	0	0	86	2	3	0	0	0	2	1	0	0	0
affin1T2Sd	8				72			88		47		0	62		0	0	0
affin1T2Se	8				64			89		34		0	58		0	0	0

inapplicable	< 1% of samples > *P*	1 - 10% of samples > *P*	10 - 50% of samples > *P*	>50% of samples > *P*

Table 7-10 Results of model fitting incorporating speciation uncertainty, all pH solution composition domains, % of samples greater than $P\left(\chi^2 \mid \nu\right) = 0.1$. Model details are listed in Table 7-2 and chemical domain spaces are listed in Table 7-4. *N* is the number of data-points in the composition domain. For composition domain rows: 0 signifies that the parameter was constant, 1 signifies that the parameter was variable for the composition sub-domain. (cont.)

model code	Fitting parameters	allpH (1)	allpH (2)	allpH (3)	allpH (4)	allpH (5)	allpH (6)	allpH (7)	allpH (8)	allpH (9)	allpH (10)	allpH (11)	allpH (12)	allpH (13)	allpH (14)	allpH (15)	allpH (16)
	N	20	40	28	32	31	48	52	51	40	39	43	60	59	63	51	71
domain	[carbonate]	0	0	0	0	1	0	0	1	0	1	1	0	1	1	1	1
	[phosphate]	0	0	0	1	0	0	1	0	1	0	1	1	0	1	1	1
	[citrate]	0	0	1	0	0	1	0	0	1	1	0	1	1	0	1	1
	[Ca/Mg]	0	1	0	0	0	1	1	1	0	0	0	1	1	1	0	1
kin1T3Sa	9	94	98	68	0	35	85	4	71	0	27	0	4	47	1	0	1
kin1T3Sb	9	85	93	64	0	28	82	4	67	0	23	0	4	45	0	0	0
kin1T3Sc	9				42			67		27		3	35		27	1	13
kin1T3Sd	9				0			0		0		0	0		0	0	0
affin1T3Sa	9	0	0	0	0	0	0	0	0	0	0	0	0	0	0	0	0
affin1T3Sb	9	10	17	4	0	0	9	0	1	0	0	0	0	0	0	0	0
affin1T3Sc	9				67			87		50		0	72		1	0	0
affin1T3Sd	9				62			88		48		0	71		1	0	1

inapplicable	< 1% of samples > *P*	1 - 10% of samples > *P*	10 - 50% of samples > *P*	>50% of samples > *P*

Table 7-11 Results of model fitting incorporating speciation uncertainty, pH 5 and 7 solution composition domains, % of samples greater than $P\left(\chi^2 \mid \nu\right) = 0.01$.

Model details are listed in Table 7-2 and chemical domain spaces are listed in Table 7-4. *N* is the number of data-points in the composition domain. For composition domain rows: 0 signifies that the parameter was constant, 1 signifies that the parameter was variable for the composition sub-domain.

model code	Fitting parameters	pH5 (1)	pH5 (2)	pH5 (3)	pH5 (4)	pH5 (5)	pH5 (6)	pH5 (7)	pH5 (8)		pH7 (1)	pH7 (2)	pH7 (3)	pH7 (4)	pH7 (5)	pH7 (6)	pH7 (7)	pH7 (8)
	N	6	10	9	8	13	12	11	15		4	14	6	7	16	17	9	19
domain	[carbonate]	0	0	0	1	0	1	1	1		0	0	0	1	0	1	1	1
	[phosphate]	0	0	1	0	1	0	1	1		0	0	1	0	1	0	1	1
	[citrate]	0	1	0	0	1	1	0	1		0	0	0	0	0	0	0	0
	[Ca/Mg]	0	0	0	0	0	0	0	0		0	1	0	0	1	1	0	1
L1Sa	1	100	51	0	0	0	4	0	0		100	99	99	0	97	68	0	66
L1Sb	2	100	93	0	0	0	9	0	0		100	100	99	0	96	98	0	63
1T1S0H	2	100	90	3	100	33	74	0	0		100	99	99	0	96	37	0	52
L2Sc	3				100		95	0	2					18		17	26	29
L2Sd	3			100		93		1	13				67		94		0	50
L2Se	3			100		93		1	13				85		65		0	25
1T2S0Hc	3				100		91	11	45					74		94	78	94
1T2S0Hd	3			100		89		99	73				97		96		0	38
1T2S0He	3			96		85		92	68				98		96		0	39
2T2S0Hc	4				100		85	2	14					65		94	71	93
2T2S0Hd	4			100		88		93	68				92		95		0	19
2T2S0He	4			97		86		93	68				94		95		0	19

inapplicable	< 1% of samples > *P*	1 - 10% of samples > *P*	10 - 50% of samples > *P*	>50% of samples > *P*

Table 7-12 Results of model fitting incorporating speciation uncertainty, pH 6 solution composition domains, % of samples greater than $P\left(\chi^2 \mid \nu\right) = 0.01$. Model details are listed in Table 7-2 and chemical domain spaces are listed in Table 7-4. *N* is the number of data-points in the composition domain. For composition domain rows: 0 signifies that the parameter was constant, 1 signifies that the parameter was variable for the composition sub-domain.

model code	Fitting parameters	pH6 (1)	pH6 (2)	pH6 (3)	pH6 (4)	pH6 (5)	pH6 (6)	pH6 (7)	pH6 (8)	pH6 (9)	pH6 (10)	pH6 (11)	pH6 (12)	pH6 (13)	pH6 (14)	pH6 (15)	pH6 (16)
	N	4	14	8	7	7	18	17	17	11	11	10	14	20	21	21	24
domain	[carbonate]	0	0	0	0	1	0	0	1	0	1	1	1	1	1	0	1
	[phosphate]	0	0	0	1	0	0	1	0	1	0	1	1	1	0	1	1
	[citrate]	0	0	1	0	0	1	0	0	1	1	0	1	0	1	1	1
	[Ca/Mg]	0	1	0	0	0	1	1	1	0	0	0	0	1	1	1	1
L1Sa	1	100	100	78	74	0	81	98	5	51	0	0	0	1	6	66	0
L1Sb	2	100	100	85	62	0	97	97	3	58	0	0	0	1	3	80	0
1T1S0H	2	100	100	73	57	0	91	97	3	43	0	0	0	1	3	65	0
L2Sc	3					60			48		68	90	74	78	54		54
L2Sd	3				60			91		78		0	0	6		92	8
L2Se	3				100			100		93		0	0	9		98	10
1T2S0Hc	3					100			100		90	90	76	96	87		72
1T2S0Hd	3				100			100		81		0	0	9		94	9
1T2S0He	3				100			100		81		0	0	9		98	9
2T2S0Hc	4					97			100		83	78	66	94	85		68
2T2S0Hd	4				100			100		78		0	0	5		96	6
2T2S0He	4				100			98		77		0	0	5		94	6

inapplicable	< 1% of samples > *P*	1 - 10% of samples > *P*	10 - 50% of samples > *P*	>50% of samples > *P*

Table 7-13 Results of model fitting incorporating speciation uncertainty, all pH solution composition domains, % of samples greater than $P\left(\chi^2 \mid \nu\right) = 0.01$. Model details are listed in Table 7-2 and chemical domain spaces are listed in Table 7-4. *N* is the number of data-points in the composition domain. For composition domain rows: 0 signifies that the parameter was constant, 1 signifies that the parameter was variable for the composition sub-domain.

model code	Fitting parameters	allpH (1)	allpH (2)	allpH (3)	allpH (4)	allpH (5)	allpH (6)	allpH (7)	allpH (8)	allpH (9)	allpH (10)	allpH (11)	allpH (12)	allpH (13)	allpH (14)	allpH (15)	allpH (16)
	N	20	40	28	32	31	48	52	51	40	39	43	60	59	63	51	71
domain	[carbonate]	0	0	0	0	1	0	0	1	0	1	1	0	1	1	1	1
	[phosphate]	0	0	0	1	0	0	1	0	1	0	1	1	0	1	1	1
	[citrate]	0	0	1	0	0	1	0	0	1	1	0	1	1	0	1	1
	[Ca/Mg]	0	1	0	0	0	1	1	1	0	0	0	1	1	1	0	1
L1Sa	1	0	0	0	0	0	0	0	0	0	0	0	0	0	0	0	0
L1Sb	2	0	0	0	0	0	0	0	0	0	0	0	0	0	0	0	0
1T1S0H	2	0	0	0	0	0	0	0	0	0	0	0	0	0	0	0	0
L2Sa	3	0	0	0	0	0	0	0	0	0	0	0	0	0	0	0	0
L2Sb	3	3	0	0	0	0	0	0	0	0	0	0	0	0	0	0	0
L2Sc	3	0	0	0	0	0	0	0	0	0	0	0	0	0	0	0	0
L2Sd	3				0			0		0		0	0		0	0	0
L2Se	3				0			0		0		0	0		0	0	0
1T1S1H	3	0	0	0	0	0	0	0	0	0	0	0	0	0	0	0	0
1T2S0Ha	3	0	0	0	0	0	0	0	0	0	0	0	0	0	0	0	0
1T2S0Hb	3	15	1	4	0	0	0	0	0	0	0	0	0	0	0	0	0
1T2S0Hc	3	3	0	2	0	0	0	0	0	0	0	0	0	0	0	0	0
1T2S0Hd	3				0			0		0		0	0		0	0	0
1T2S0He	3				0			0		0		0	0		0	0	0

inapplicable	< 1% of samples > *P*	1 - 10% of samples > *P*	10 - 50% of samples > *P*	>50% of samples > *P*

Table 7-13 Results of model fitting incorporating speciation uncertainty, all pH solution composition domains, % of samples greater than $P\left(\chi^2 \mid \nu\right) = 0.01$. Model details are listed in Table 7-2 and chemical domain spaces are listed in Table 7-4. *N* is the number of data-points in the composition domain. For composition domain rows: 0 signifies that the parameter was constant, 1 signifies that the parameter was variable for the composition sub-domain. (cont.)

model code	Fitting parameters	allpH (1)	allpH (2)	allpH (3)	allpH (4)	allpH (5)	allpH (6)	allpH (7)	allpH (8)	allpH (9)	allpH (10)	allpH (11)	allpH (12)	allpH (13)	allpH (14)	allpH (15)	allpH (16)
	N	20	40	28	32	31	48	52	51	40	39	43	60	59	63	51	71
domain	[carbonate]	0	0	0	0	1	0	0	1	0	1	1	0	1	1	1	1
	[phosphate]	0	0	0	1	0	0	1	0	1	0	1	1	0	1	1	1
	[citrate]	0	0	1	0	0	1	0	0	1	1	0	1	1	0	1	1
	[Ca/Mg]	0	1	0	0	0	1	1	1	0	0	0	1	1	1	0	1
L3Sa	4	0	0	0	0	0	0	0	0	0	0	0	0	0	0	0	0
L3Sb	4	2	0	0	0	0	0	0	0	0	0	0	0	0	0	0	0
L3Sc	4				0			0		0		0	0		0	0	0
L3Sd	4				0			0		0		0	0		0	0	0
1T1S2H	4	0	0	0	0	0	0	0	0	0	0	0	0	0	0	0	0
1T2S1Ha	4	0	0	0	0	0	0	0	0	0	0	0	0	0	0	0	0
1T2S1Hb	4	63	83	5	1	0	20	7	0	0	0	0	0	0	0	0	0
1T2S1Hc	4	70	69	3	1	11	19	6	12	0	0	0	1	1	0	0	0
1T2S1Hd	4				0			0		0		0	0		0	0	0
1T2S1He	4				0			0		0		0	0		0	0	0
1T3S0Ha	4	3	0	2	0	0	0	0	0	0	0	0	0	0	0	0	0
1T3S0Hb	4	14	1	5	0	0	0	0	0	0	0	0	0	0	0	0	0
1T3S0Hc	4				0			0		0		0	0		0	0	0
1T3S0Hd	4				1			0		0		0	0		0	0	0

inapplicable	< 1% of samples > *P*	1 - 10% of samples > *P*	10 - 50% of samples > *P*	>50% of samples > *P*

Table 7-13 Results of model fitting incorporating speciation uncertainty, all pH solution composition domains, % of samples greater than $P\left(\chi^2 \mid \nu\right) = 0.01$. Model details are listed in Table 7-2 and chemical domain spaces are listed in Table 7-4. *N* is the number of data-points in the composition domain. For composition domain rows: 0 signifies that the parameter was constant, 1 signifies that the parameter was variable for the composition sub-domain. (cont.)

model code	Fitting parameters	allpH (1)	allpH (2)	allpH (3)	allpH (4)	allpH (5)	allpH (6)	allpH (7)	allpH (8)	allpH (9)	allpH (10)	allpH (11)	allpH (12)	allpH (13)	allpH (14)	allpH (15)	allpH (16)
	N	20	40	28	32	31	48	52	51	40	39	43	60	59	63	51	71
domain	[carbonate]	0	0	0	0	1	0	0	1	0	1	1	0	1	1	1	1
	[phosphate]	0	0	0	1	0	0	1	0	1	0	1	1	0	1	1	1
	[citrate]	0	0	1	0	0	1	0	0	1	1	0	1	1	0	1	1
	[Ca/Mg]	0	1	0	0	0	1	1	1	0	0	0	1	1	1	0	1
2T2S0Ha	4	0	0	0	0	0	0	0	0	0	0	0	0	0	0	0	0
2T2S0Hb	4	15	1	5	0	0	0	0	0	0	0	0	0	0	0	0	0
2T2S0Hc	4	4	0	3	0	0	0	0	0	0	0	0	0	0	0	0	0
2T2S0Hd	4				0			0		0		0	0		0	0	0
2T2S0He	4				0			0		0		0	0		0	0	0
1T3S1Ha	5	77	67	4	1	9	17	5	11	0	0	0	0	1	0	0	0
1T3S1Hb	5	83	85	6	1	11	25	7	12	0	0	0	0	1	1	0	0
1T3S1Hc	5				5			15		0		0	1		1	0	0
1T3S1Hd	5				49			64		1		4	15		9	0	1
2T2S1HAa	5	0	0	0	0	0	0	0	0	0	0	0	0	0	0	0	0
2T2S1HAb	5	13	1	4	0	0	0	0	0	0	0	0	0	0	0	0	0
2T2S1HAc	5	3	0	2	0	0	0	0	0	0	0	0	0	0	0	0	0
2T2S1HAd	5				0			0		0		0	0		0	0	0
2T2S1HAe	5				0			0		0		0	0		0	0	0

inapplicable	< 1% of samples > *P*	1 - 10% of samples > *P*	10 - 50% of samples > *P*	>50% of samples > *P*

Table 7-13 Results of model fitting incorporating speciation uncertainty, all pH solution composition domains, % of samples greater than $P\left(\chi^2 \mid \nu\right) = 0.01$. Model details are listed in Table 7-2 and chemical domain spaces are listed in Table 7-4. *N* is the number of data-points in the composition domain. For composition domain rows: 0 signifies that the parameter was constant, 1 signifies that the parameter was variable for the composition sub-domain. (cont.)

model code	Fitting parameters	allpH (1)	allpH (2)	allpH (3)	allpH (4)	allpH (5)	allpH (6)	allpH (7)	allpH (8)	allpH (9)	allpH (10)	allpH (11)	allpH (12)	allpH (13)	allpH (14)	allpH (15)	allpH (16)
	N	20	40	28	32	31	48	52	51	40	39	43	60	59	63	51	71
domain	[carbonate]	0	0	0	0	1	0	0	1	0	1	1	0	1	1	1	1
	[phosphate]	0	0	0	1	0	0	1	0	1	0	1	1	0	1	1	1
	[citrate]	0	0	1	0	0	1	0	0	1	1	0	1	1	0	1	1
	[Ca/Mg]	0	1	0	0	0	1	1	1	0	0	0	1	1	1	0	1
2T2S1HBa	5	13	1	4	0	0	0	0	0	0	0	0	0	0	0	0	0
2T2S1HBb	5	95	97	72	0	0	78	2	0	0	0	0	2	0	0	0	0
2T2S1HBc	5	96	97	65	0	27	82	7	60	0	17	0	3	34	0	0	0
2T2S1HBd	5				0			0		0		0	0		0	0	0
2T2S1HBe	5				0			0		0		0	0		0	0	0
2T2S2Ha	6	10	1	3	0	0	0	0	0	0	0	0	0	0	0	0	0
2T2S2Hb	6	94	93	75	0	0	80	17	0	0	0	0	13	0	0	0	0
2T2S2Hc	6	96	91	73	1	40	77	18	67	1	31	0	14	48	2	0	1
2T2S2Hd	6				0			0		0		0	0		0	0	0
2T2S2He	6				0			0		0		0	0		0	0	0
3T3S0Ha	6	10	0	3	0	0	0	0	0	0	0	0	0	0	0	0	0
3T3S0Hb	6	2	0	2	0	0	0	0	0	0	0	0	0	0	0	0	0
3T3S0Hc	6				0			0		0		0	0		0	0	0
3T3S0Hd	6				0			0		0		0	0		0	0	0

inapplicable	< 1% of samples > *P*	1 - 10% of samples > *P*	10 - 50% of samples > *P*	>50% of samples > *P*

Table 7-13 Results of model fitting incorporating speciation uncertainty, all pH solution composition domains, % of samples greater than $P\left(\chi^2 \mid \nu\right) = 0.01$. Model details are listed in Table 7-2 and chemical domain spaces are listed in Table 7-4. *N* is the number of data-points in the composition domain. For composition domain rows: 0 signifies that the parameter was constant, 1 signifies that the parameter was variable for the composition sub-domain. (cont.)

model code	Fitting parameters	allpH (1)	allpH (2)	allpH (3)	allpH (4)	allpH (5)	allpH (6)	allpH (7)	allpH (8)	allpH (9)	allpH (10)	allpH (11)	allpH (12)	allpH (13)	allpH (14)	allpH (15)	allpH (16)
	N	20	40	28	32	31	48	52	51	40	39	43	60	59	63	51	71
domain	[carbonate]	0	0	0	0	1	0	0	1	0	1	1	0	1	1	1	1
	[phosphate]	0	0	0	1	0	0	1	0	1	0	1	1	0	1	1	1
	[citrate]	0	0	1	0	0	1	0	0	1	1	0	1	1	0	1	1
	[Ca/Mg]	0	1	0	0	0	1	1	1	0	0	0	1	1	1	0	1
3T3S0He	6	10	1	4	0	0	0	0	0	0	0	0	0	0	0	0	0
3T3S0Hf	6				7			0		1		0	0		0	0	0
3T3S0Hg	6				8			0		1		0	0		0	0	0
3T3S0Hh	6				0			0		0		0	0		0	0	0
3T3S0Hi	6				1			0		1		0	0		0	0	0
3T3S0Hj	6				0			0		0		0	0		0	0	0
kin1T1S	7	100	99	83	2	0	85	25	0	2	0	0	18	0	0	0	0
affin1T1S	7	100	99	82	1	0	84	21	0	1	0	0	16	0	0	0	0
kin1T2Sa	8	100	99	81	1	0	84	21	0	1	0	0	16	0	0	0	0
kin1T2Sb	8	100	99	81	1	0	85	21	0	1	0	0	16	0	0	0	0
kin1T2Sc	8	100	99	86	2	73	93	31	89	3	55	0	28	69	7	0	5
kin1T2Sd	8				1			25		2		0	17		0	0	0
kin1T2Se	8				32			44		21		0	29		0	0	0

inapplicable	< 1% of samples > *P*	1 - 10% of samples > *P*	10 - 50% of samples > *P*	>50% of samples > *P*

Table 7-13 Results of model fitting incorporating speciation uncertainty, all pH solution composition domains, % of samples greater than $P\left(\chi^2 \mid \nu\right) = 0.01$. Model details are listed in Table 7-2 and chemical domain spaces are listed in Table 7-4. *N* is the number of data-points in the composition domain. For composition domain rows: 0 signifies that the parameter was constant, 1 signifies that the parameter was variable for the composition sub-domain. (cont.)

model code	Fitting parameters	allpH (1)	allpH (2)	allpH (3)	allpH (4)	allpH (5)	allpH (6)	allpH (7)	allpH (8)	allpH (9)	allpH (10)	allpH (11)	allpH (12)	allpH (13)	allpH (14)	allpH (15)	allpH (16)
	N	20	40	28	32	31	48	52	51	40	39	43	60	59	63	51	71
domain	[carbonate]	0	0	0	0	1	0	0	1	0	1	1	0	1	1	1	1
	[phosphate]	0	0	0	1	0	0	1	0	1	0	1	1	0	1	1	1
	[citrate]	0	0	1	0	0	1	0	0	1	1	0	1	1	0	1	1
	[Ca/Mg]	0	1	0	0	0	1	1	1	0	0	0	1	1	1	0	1
affin1T2Sa	8	0	0	0	0	0	0	0	0	0	0	0	0	0	0	0	0
affin1T2Sb	8	10	17	5	0	0	9	3	0	0	0	0	0	0	0	0	0
affin1T2Sc	8	100	99	86	1	2	93	21	19	2	2	0	22	13	0	0	0
affin1T2Sd	8				95			96		72		0	77		0	0	0
affin1T2Se	8				93			96		67		0	76		0	0	0
kin1T3Sa	9	99	99	85	2	73	93	27	90	2	57	0	25	70	9	1	5
kin1T3Sb	9	90	93	79	2	65	89	26	85	2	53	0	24	67	7	0	4
kin1T3Sc	9				69			79		55		23	56		52	16	36
kin1T3Sd	9				0			0		0		0	0		0	0	0
affin1T3Sa	9	0	0	0	0	0	0	0	0	0	0	0	0	0	0	0	0
affin1T3Sb	9	10	17	5	0	1	9	2	4	0	0	0	2	2	0	0	0
affin1T3Sc	9				93			95		77		1	86		9	0	6
affin1T3Sd	9				92			96		77		2	87		12	1	7

inapplicable	< 1% of samples > *P*	1 - 10% of samples > *P*	10 - 50% of samples > *P*	>50% of samples > *P*

Table 7-14 Results of model fitting incorporating speciation uncertainty, pH 5 and 7 solution composition domains, % of greater than $P\left(\chi^2 \mid \nu\right) = 0.0001$. Model details are listed in Table 7-2 and chemical domain spaces are listed in Table 7-4. *N* is the number of data-points in the composition domain. For composition domain rows: 0 signifies that the parameter was constant, 1 signifies that the parameter was variable for the composition sub-domain.

model code	Fitting parameters	pH5 (1)	pH5 (2)	pH5 (3)	pH5 (4)	pH5 (5)	pH5 (6)	pH5 (7)	pH5 (8)		pH7 (1)	pH7 (2)	pH7 (3)	pH7 (4)	pH7 (5)	pH7 (6)	pH7 (7)	pH7 (8)
	N	6	10	9	8	13	12	11	15		4	14	6	7	16	17	9	19
domain	[carbonate]	0	0	0	1	0	1	1	1		0	0	0	1	0	1	1	1
	[phosphate]	0	0	1	0	1	0	1	1		0	0	1	0	1	0	1	1
	[citrate]	0	1	0	0	1	1	0	1		0	0	0	0	0	0	0	0
	[Ca/Mg]	0	0	0	0	0	0	0	0		0	1	0	0	1	1	0	1
L1Sa	1	100	74	26	98	33	50	0	0		100	99	100	70	98	97	81	94
L1Sb	2	100	96	100	100	91	89	0	1		100	100	100	99	99	100	65	94
1T1S0H	2	100	97	100	100	85	93	57	62		100	99	100	13	98	97	59	93
L2Sc	3				100		97	100	93					31		19	34	31
L2Sd	3			100		96		100	90				72		96		38	92
L2Se	3			100		96		100	90				89		68		17	41
1T2S0Hc	3				100		97	87	86					98		97	97	96
1T2S0Hd	3			100		97		100	93				100		98		26	91
1T2S0He	3			96		92		93	88				100		98		27	91
2T2S0Hc	4				100		97	58	70					96		97	96	97
2T2S0Hd	4			100		96		100	91				98		98		5	90
2T2S0He	4			97		94		100	90				100		98		5	90

inapplicable	< 1% of samples > *P*	1 - 10% of samples > *P*	10 - 50% of samples > *P*	>50% of samples > *P*

Table 7-15 Results of model fitting incorporating speciation uncertainty, pH 6 solution composition domains, % of greater than $P\left(\chi^2 \mid \nu\right) = 0.0001$. Model details are listed in Table 7-2 and chemical domain spaces are listed in Table 7-4. *N* is the number of data-points in the composition domain. For composition domain rows: 0 signifies that the parameter was constant, 1 signifies that the parameter was variable for the composition sub-domain.

model code	Fitting parameters	pH6 (1)	pH6 (2)	pH6 (3)	pH6 (4)	pH6 (5)	pH6 (6)	pH6 (7)	pH6 (8)	pH6 (9)	pH6 (10)	pH6 (11)	pH6 (12)	pH6 (13)	pH6 (14)	pH6 (15)	pH6 (16)
	N	4	14	8	7	7	18	17	17	11	11	10	14	20	21	21	24
domain	[carbonate]	0	0	0	0	1	0	0	1	0	1	1	1	1	1	0	1
	[phosphate]	0	0	0	1	0	0	1	0	1	0	1	1	1	0	1	1
	[citrate]	0	0	1	0	0	1	0	0	1	1	0	1	0	1	1	1
	[Ca/Mg]	0	1	0	0	0	1	1	1	0	0	0	0	1	1	1	1
L1Sa	1	100	100	93	100	29	90	100	93	79	31	12	10	36	62	85	29
L1Sb	2	100	100	100	100	15	100	100	85	99	25	6	7	28	62	99	24
1T1S0H	2	100	100	94	100	15	100	100	86	76	24	6	6	28	58	99	23
L2Sc	3					77			48		84	99	94	90	57		63
L2Sd	3				69			92		89		16	25	70		95	65
L2Se	3				100			100		100		46	39	95		100	73
1T2S0Hc	3					100			100		99	97	95	100	99		96
1T2S0Hd	3				100			100		99		46	39	96		96	67
1T2S0He	3				100			100		99		46	39	96		100	67
2T2S0Hc	4					99			100		94	91	89	100	98		94
2T2S0Hd	4				100			100		97		26	30	93		100	62
2T2S0He	4				100			98		97		26	30	93		98	62

inapplicable	< 1% of samples > *P*	1 - 10% of samples > *P*	10 - 50% of samples > *P*	>50% of samples > *P*

Table 7-16 Results of model fitting incorporating speciation uncertainty, all pH solution composition domains, % of greater than $P\left(\chi^2 \mid \nu\right) = 0.0001$. Model details are listed in Table 7-2 and chemical domain spaces are listed in Table 7-4. *N* is the number of data-points in the composition domain. For composition domain rows: 0 signifies that the parameter was constant, 1 signifies that the parameter was variable for the composition sub-domain.

model code	Fitting parameters	allpH (1)	allpH (2)	allpH (3)	allpH (4)	allpH (5)	allpH (6)	allpH (7)	allpH (8)	allpH (9)	allpH (10)	allpH (11)	allpH (12)	allpH (13)	allpH (14)	allpH (15)	allpH (16)
	N	20	40	28	32	31	48	52	51	40	39	43	60	59	63	51	71
domain	[carbonate]	0	0	0	0	1	0	0	1	0	1	1	0	1	1	1	1
	[phosphate]	0	0	0	1	0	0	1	0	1	0	1	1	0	1	1	1
	[citrate]	0	0	1	0	0	1	0	0	1	1	0	1	1	0	1	1
	[Ca/Mg]	0	1	0	0	0	1	1	1	0	0	0	1	1	1	0	1
L1Sa	1	0	0	0	0	0	0	0	0	0	0	0	0	0	0	0	0
L1Sb	2	0	0	0	0	0	0	0	0	0	0	0	0	0	0	0	0
1T1S0H	2	0	0	0	0	0	0	0	0	0	0	0	0	0	0	0	0
L2Sa	3	0	0	0	0	0	0	0	0	0	0	0	0	0	0	0	0
L2Sb	3	28	1	10	0	0	0	0	0	0	0	0	0	0	0	0	0
L2Sc	3	7	0	4	0	0	0	0	0	0	0	0	0	0	0	0	0
L2Sd	3				0			0		0		0	0		0	0	0
L2Se	3				0			0		0		0	0		0	0	0
1T1S1H	3	0	0	0	0	0	0	0	0	0	0	0	0	0	0	0	0
1T2S0Ha	3	0	0	0	0	0	0	0	0	0	0	0	0	0	0	0	0
1T2S0Hb	3	56	2	27	1	0	1	0	0	0	0	0	0	0	0	0	0
1T2S0Hc	3	26	0	21	0	0	0	0	0	0	0	0	0	0	0	0	0
1T2S0Hd	3				0			0		0		0	0		0	0	0
1T2S0He	3				0			0		0		0	0		0	0	0

inapplicable	< 1% of samples > *P*	1 - 10% of samples > *P*	10 - 50% of samples > *P*	>50% of samples > *P*

Table 7-16 Results of model fitting incorporating speciation uncertainty, all pH solution composition domains, % of greater than $P\left(\chi^2 \mid \nu\right) = 0.0001$. Model details are listed in Table 7-2 and chemical domain spaces are listed in Table 7-4. *N* is the number of data-points in the composition domain. For composition domain rows: 0 signifies that the parameter was constant, 1 signifies that the parameter was variable for the composition sub-domain. (cont.)

model code	Fitting parameters	allpH (1)	allpH (2)	allpH (3)	allpH (4)	allpH (5)	allpH (6)	allpH (7)	allpH (8)	allpH (9)	allpH (10)	allpH (11)	allpH (12)	allpH (13)	allpH (14)	allpH (15)	allpH (16)
	N	20	40	28	32	31	48	52	51	40	39	43	60	59	63	51	71
domain	[carbonate]	0	0	0	0	1	0	0	1	0	1	1	0	1	1	1	1
	[phosphate]	0	0	0	1	0	0	1	0	1	0	1	1	0	1	1	1
	[citrate]	0	0	1	0	0	1	0	0	1	1	0	1	1	0	1	1
	[Ca/Mg]	0	1	0	0	0	1	1	1	0	0	0	1	1	1	0	1
L3Sa	4	8	0	3	0	0	0	0	0	0	0	0	0	0	0	0	0
L3Sb	4	34	1	10	0	0	0	0	0	0	0	0	0	0	0	0	0
L3Sc	4				2			0		1		0	0		0	0	0
L3Sd	4				9			0		3		0	0		0	0	0
1T1S2H	4	0	0	0	0	0	0	0	0	0	0	0	0	0	0	0	0
1T2S1Ha	4	6	0	0	0	0	0	0	0	0	0	0	0	0	0	0	0
1T2S1Hb	4	79	93	29	16	0	40	34	0	1	0	0	2	0	0	0	0
1T2S1Hc	4	85	88	20	18	40	45	24	39	0	3	2	4	7	3	0	0
1T2S1Hd	4				0			0		0		0	0		0	0	0
1T2S1He	4				0			0		0		0	0		0	0	0
1T3S0Ha	4	24	0	18	0	0	0	0	0	0	0	0	0	0	0	0	0
1T3S0Hb	4	56	2	32	1	1	1	0	0	1	0	0	0	0	0	0	0
1T3S0Hc	4				10			0		7		0	0		0	0	0
1T3S0Hd	4				14			0		9		0	0		0	0	0

inapplicable	< 1% of samples > *P*	1 - 10% of samples > *P*	10 - 50% of samples > *P*	>50% of samples > *P*

Table 7-16 Results of model fitting incorporating speciation uncertainty, all pH solution composition domains, % of greater than $P\left(\chi^2 \mid \nu\right) = 0.0001$. Model details are listed in Table 7-2 and chemical domain spaces are listed in Table 7-4. *N* is the number of data-points in the composition domain. For composition domain rows: 0 signifies that the parameter was constant, 1 signifies that the parameter was variable for the composition sub-domain. (cont.)

model code	Fitting parameters	allpH (1)	allpH (2)	allpH (3)	allpH (4)	allpH (5)	allpH (6)	allpH (7)	allpH (8)	allpH (9)	allpH (10)	allpH (11)	allpH (12)	allpH (13)	allpH (14)	allpH (15)	allpH (16)
	N	20	40	28	32	31	48	52	51	40	39	43	60	59	63	51	71
domain	[carbonate]	0	0	0	0	1	0	0	1	0	1	1	0	1	1	1	1
	[phosphate]	0	0	0	1	0	0	1	0	1	0	1	1	0	1	1	1
	[citrate]	0	0	1	0	0	1	0	0	1	1	0	1	1	0	1	1
	[Ca/Mg]	0	1	0	0	0	1	1	1	0	0	0	1	1	1	0	1
2T2S0Ha	4	0	0	0	0	0	0	0	0	0	0	0	0	0	0	0	0
2T2S0Hb	4	60	2	30	1	0	1	0	0	1	0	0	0	0	0	0	0
2T2S0Hc	4	28	0	22	0	0	0	0	0	0	0	0	0	0	0	0	0
2T2S0Hd	4				0			0		0		0	0		0	0	0
2T2S0He	4				0			0		0		0	0		0	0	0
1T3S1Ha	5	95	88	20	18	45	45	23	36	1	5	1	3	7	3	0	0
1T3S1Hb	5	93	97	31	19	39	55	33	38	1	3	2	4	7	5	0	0
1T3S1Hc	5				34			46		6		4	10		7	0	0
1T3S1Hd	5				68			87		8		31	43		34	2	6
2T2S1HAa	5	0	0	0	0	0	0	0	0	0	0	0	0	0	0	0	0
2T2S1HAb	5	56	2	26	1	0	1	0	0	0	0	0	0	0	0	0	0
2T2S1HAc	5	23	0	19	0	0	0	0	0	0	0	0	0	0	0	0	0
2T2S1HAd	5				0			0		0		0	0		0	0	0
2T2S1HAe	5				0			0		0		0	0		0	0	0

inapplicable	< 1% of samples > *P*	1 - 10% of samples > *P*	10 - 50% of samples > *P*	>50% of samples > *P*

Table 7-16 Results of model fitting incorporating speciation uncertainty, all pH solution composition domains, % of greater than $P\left(\chi^2 \mid \nu\right) = 0.0001$. Model details are listed in Table 7-2 and chemical domain spaces are listed in Table 7-4. *N* is the number of data-points in the composition domain. For composition domain rows: 0 signifies that the parameter was constant, 1 signifies that the parameter was variable for the composition sub-domain. (cont.)

model code	Fitting parameters	allpH (1)	allpH (2)	allpH (3)	allpH (4)	allpH (5)	allpH (6)	allpH (7)	allpH (8)	allpH (9)	allpH (10)	allpH (11)	allpH (12)	allpH (13)	allpH (14)	allpH (15)	allpH (16)
	N	20	40	28	32	31	48	52	51	40	39	43	60	59	63	51	71
domain	[carbonate]	0	0	0	0	1	0	0	1	0	1	1	0	1	1	1	1
	[phosphate]	0	0	0	1	0	0	1	0	1	0	1	1	0	1	1	1
	[citrate]	0	0	1	0	0	1	0	0	1	1	0	1	1	0	1	1
	[Ca/Mg]	0	1	0	0	0	1	1	1	0	0	0	1	1	1	0	1
2T2S1HBa	5	56	2	26	1	0	1	0	0	0	0	0	0	0	0	0	0
2T2S1HBb	5	99	98	89	3	0	87	57	0	4	0	0	39	0	0	0	0
2T2S1HBc	5	100	99	85	8	79	93	57	87	7	58	0	36	71	15	1	7
2T2S1HBd	5				0			0		0		0	0		0	0	0
2T2S1HBe	5				0			0		0		0	0		0	0	0
2T2S2Ha	6	48	2	22	1	0	1	0	0	0	0	0	0	0	0	0	0
2T2S2Hb	6	95	94	87	20	0	88	67	0	17	0	0	52	0	0	0	0
2T2S2Hc	6	98	92	88	25	83	86	72	89	23	66	4	53	77	23	4	17
2T2S2Hd	6				0			0		0		0	0		0	0	0
2T2S2He	6				0			0		0		0	0		0	0	0
3T3S0Ha	6	48	2	23	1	0	1	0	0	0	0	0	0	0	0	0	0
3T3S0Hb	6	19	0	16	0	0	0	0	0	0	0	0	0	0	0	0	0
3T3S0Hc	6				0			0		0		0	0		0	0	0
3T3S0Hd	6				0			0		0		0	0		0	0	0

inapplicable	< 1% of samples > *P*	1 - 10% of samples > *P*	10 - 50% of samples > *P*	>50% of samples > *P*

Table 7-16 Results of model fitting incorporating speciation uncertainty, all pH solution composition domains, % of greater than $P\left(\chi^2 \mid \nu\right) = 0.0001$. Model details are listed in Table 7-2 and chemical domain spaces are listed in Table 7-4. *N* is the number of data-points in the composition domain. For composition domain rows: 0 signifies that the parameter was constant, 1 signifies that the parameter was variable for the composition sub-domain. (cont.)

model code	Fitting parameters	allpH (1)	allpH (2)	allpH (3)	allpH (4)	allpH (5)	allpH (6)	allpH (7)	allpH (8)	allpH (9)	allpH (10)	allpH (11)	allpH (12)	allpH (13)	allpH (14)	allpH (15)	allpH (16)
	N	20	40	28	32	31	48	52	51	40	39	43	60	59	63	51	71
domain	[carbonate]	0	0	0	0	1	0	0	1	0	1	1	0	1	1	1	1
	[phosphate]	0	0	0	1	0	0	1	0	1	0	1	1	0	1	1	1
	[citrate]	0	0	1	0	0	1	0	0	1	1	0	1	1	0	1	1
	[Ca/Mg]	0	1	0	0	0	1	1	1	0	0	0	1	1	1	0	1
3T3S0He	6	49	2	27	1	1	1	0	0	0	0	0	0	0	0	0	0
3T3S0Hf	6				44			1		19		0	0		0	0	0
3T3S0Hg	6				38			2		12		0	1		0	0	0
3T3S0Hh	6				7			0		5		0	0		0	0	0
3T3S0Hi	6				12			0		8		0	0		0	0	0
3T3S0Hj	6				0			0		0		0	0		0	0	0
kin1T1S	7	100	100	93	37	0	92	82	0	27	0	0	59	0	0	0	0
affin1T1S	7	100	100	93	32	0	92	80	0	23	0	0	57	0	0	0	0
kin1T2Sa	8	100	100	93	31	0	92	80	0	23	0	0	57	0	0	0	0
kin1T2Sb	8	100	100	93	31	0	93	80	0	23	0	0	56	0	0	0	0
kin1T2Sc	8	100	100	95	35	92	97	85	96	37	82	13	73	87	54	14	37
kin1T2Sd	8				33			80		21		0	54		0	0	0
kin1T2Se	8				83			88		60		0	66		0	0	0

inapplicable	< 1% of samples > *P*	1 - 10% of samples > *P*	10 - 50% of samples > *P*	>50% of samples > *P*

Table 7-16 Results of model fitting incorporating speciation uncertainty, all pH solution composition domains, % of greater than $P\left(\chi^2 \mid \nu\right) = 0.0001$. Model details are listed in Table 7-2 and chemical domain spaces are listed in Table 7-4. *N* is the number of data-points in the composition domain. For composition domain rows: 0 signifies that the parameter was constant, 1 signifies that the parameter was variable for the composition sub-domain. (cont.)

model code	Fitting parameters	allpH (1)	allpH (2)	allpH (3)	allpH (4)	allpH (5)	allpH (6)	allpH (7)	allpH (8)	allpH (9)	allpH (10)	allpH (11)	allpH (12)	allpH (13)	allpH (14)	allpH (15)	allpH (16)
	N	20	40	28	32	31	48	52	51	40	39	43	60	59	63	51	71
domain	[carbonate]	0	0	0	0	1	0	0	1	0	1	1	0	1	1	1	1
	[phosphate]	0	0	0	1	0	0	1	0	1	0	1	1	0	1	1	1
	[citrate]	0	0	1	0	0	1	0	0	1	1	0	1	1	0	1	1
	[Ca/Mg]	0	1	0	0	0	1	1	1	0	0	0	1	1	1	0	1
affin1T2Sa	8	0	0	0	0	0	0	0	0	0	0	0	0	0	0	0	0
affin1T2Sb	8	10	17	7	1	0	10	8	0	0	0	0	5	0	0	0	0
affin1T2Sc	8	100	100	95	35	28	97	79	84	36	32	0	69	58	4	0	2
affin1T2Sd	8				100			99		91		0	89		0	0	0
affin1T2Se	8				100			99		90		0	89		0	0	0
kin1T3Sa	9	100	100	94	31	93	97	82	96	33	82	17	71	87	52	16	38
kin1T3Sb	9	90	94	88	28	83	93	79	92	32	77	12	69	84	50	14	36
kin1T3Sc	9				77			83		74		60	70		70	48	61
kin1T3Sd	9				0			0		0		0	0		0	0	0
affin1T3Sa	9	0	0	0	0	0	0	0	0	0	0	0	0	0	0	0	0
affin1T3Sb	9	10	17	5	3	5	9	8	15	3	3	0	8	10	0	0	0
affin1T3Sc	9				100			99		93		18	95		69	20	46
affin1T3Sd	9				100			99		93		24	95		68	25	46

inapplicable	< 1% of samples > *P*	1 - 10% of samples > *P*	10 - 50% of samples > *P*	>50% of samples > *P*

8 CONCLUSIONS AND PERSPECTIVES

This study has encompassed two different fields of study: the predictive modelling of chemical speciation in equilibrium conditions and the effect of solution composition on the short-term uptake rate of uranium(VI) by the gills of *C. fluminea*. The application of the first subject to the interpretation of the second has also been exhaustively studied.

With regards to the modelling of chemical speciation, the most significant findings of this work are that the uncertainties inherent in the thermodynamic input constraints required by the model can severely limit the predictive ability of equilibrium speciation modelling. Calculation methods permitting quantitative prediction of the uncertainties associated with a particular modelling scenario have rarely been applied previous to this study. This work demonstrates that it is currently feasible to integrate probabilistic uncertainty calculations, in both simple solution speciation modelling and also the application of those calculations to the interpretation of solution composition dependent phenomena such as a metal's chemical bioavailability. Calculation time is no longer too restrictive for performing sampling based uncertainty analyses for simple modelling scenarios. For example, the program written to perform the modelling described in this study can perform a 10^4 sample MC uncertainty analysis of the equilibrium speciation of a single solution composition in less than five seconds. Modelling applications that require a large number of speciation calculations to be performed (such as the uranium uptake modelling described in this work or reactive transport modelling) can still be limited by computation time. For example, the model fitting described in section 7.3 required approximately one week of processing time. More complex studies could require prohibitive processing times.

The effects of varying solution composition on the short-term uptake rate of uranium by the gills of *C. fluminea* have been studied for a relatively large solution composition domain space. The magnitude of the effect on uptake rate on varying each of the solution composition parameters varies considerably as a function of the parameter being studied. For example, varying group II cation concentrations at a constant ionic strength had no measurable effect on the uranium uptake rate. pH was found to have a significant effect, but much smaller than would be expected from the

predicted magnitude of change to the equilibrium solution speciation. The clearest effect of solution composition on the uptake rate of uranium was observed for varying the concentration of the organic ligand, citrate. At each of the two pH values studied, the uptake rate was found to be approximately proportional to the predicted concentration of the free uranyl ion. At elevated pH values, the effect of increasing carbonate concentration was to significantly reduce the uptake rate of uranium. However, the uptake rate was not found to be proportional to the predicted free ion concentration. This fact, coupled with the results obtained at lower pH values, where an increase in uranium uptake rate on increasing carbonate concentration was observed, suggested that one or several uranyl carbonate species were chemically bioavailable. Models considering the co-accumulation of the free ion UO_2^{2+} and the carbonate species $UO_2CO_3^0$ were quite successful at representing the observed behaviour at constant pH values. Another mechanistic possibility that was not considered in this study is that the uptake of uranium is limited by the diffusional mass flux of uranium from the bulk solution towards the biological interface and the subsequent dissociation of labile metal complexes. Modelling approaches based on this hypothesis have been advocated for a number of relatively simple situations, for examples see (van Leeuwen 1999; van Leeuwen 2000; van Leeuwen 2001; van Leeuwen and Pinheiro 2001; Jansen, Blust et al. 2002). This hypothesis is consistent with the observed uptake rate behaviour of this study. However due to the complexity of uranium speciation and hence the large number of parameters required for a model implementation of the hypothesis (e.g. the diffusion coefficients and ligand exchange kinetic rate constants for each uranyl solution species) it was not feasible to attempt such a modelling approach.

The pre-equilibrium approach to modelling a metal's bioavailability has evolved over the years from the quite restrictive hypotheses of the FIAM to the much more flexible BLM approach. The current state of the pre-equilibrium modelling framework allows for not only the metal's solution speciation to be considered, but also competitive interactions with other cations and the potential for the co-accumulation of solution species in concert with the metal free ion. This flexibility provides many different candidate model structures available for a particular composition domain space that need to be assessed. The increased flexibility of the BLM approach has the advantage that results that would be considered an exception to the FIAM can potentially be

described by a BLM implementation. There are of course a number of disadvantages to the approach. Although the increased structural flexibility of the BLM may allow bioavailability behaviour that is not compliant with the FIAM to be described for an increased composition domain space, there is no guarantee that it is valid for a larger domain space than that used for the study. Additionally, the consideration of several potentially bioavailable metal solution species renders the model more sensitive to thermodynamic parameter uncertainty.

The equilibrium paradigm has proven to be historically useful, and in light of bioaccumulation or toxicity data that depend on solution composition, is an obvious modelling approach. The early development of such modelling approaches generally arose from experimental results that demonstrated the important effects of complexation by synthetic ligands such as EDTA or NTA. However, it must be recalled that a biological response that apparently depends on the free metal ion concentration, for chemical composition domain spaces of varying strong chelating ligand concentrations such as EDTA, does not necessarily preclude the bioavailability of other inorganic metal complexes that are covariant with the free ion for that composition domain space. A number of studies have found apparent exceptions to the equilibrium paradigm; these studies were grouped into four categories in the exhaustive review by (Campbell 1995):

1. organic ligands forming lipophilic metal complexes
2. inorganic anions
3. low molecular weight organic ligands forming hydrophilic metal complexes
4. miscellaneous unexplained examples

For the results of this study, the second category is the most relevant. Previous exceptions to the equilibrium paradigm have been observed for experiments where inorganic anions were important in determining the metal speciation. These observations were explained by either the accumulation of neutral metal anion complexes due to their lipophilicity, or alternatively that ternary metal-ligand-transporter complexes were formed and subsequently contributed to the biological response. The second of these hypotheses is the only possible way to reconcile the uptake behaviour observed in this study with the equilibrium paradigm, a considerable portion of the results can indeed be successfully modelled by considering the

formation of ternary uranyl-ligand-transporter complexes. However, ternary complexes involving hydroxide, carbonate and phosphate ligands need to be considered to successfully encompass a large portion of the chemical composition domain space considered in this study. It seems more plausible that this apparent uptake multi-dependence on the concentrations of several inorganic solution species indicates that the uptake process is in fact controlled by the diffusional mass flux of uranium from the bulk solution towards the biological interface and the subsequent dissociation of labile metal complexes. As discussed earlier it is not feasible to develop such a model due to its calibration requirements. Further, this hypothesis alone is not sufficient to explain the observed uptake behaviour; the increase in uptake with increasing pH could only be explained by a higher diffusion rate of hydroxide or carbonate uranyl complexes than that of the free uranyl ion. Again, several of the tenets of the steady-state dogma may be questioned: that no significant modification of the biological interface occurs (the constancy of the density and nature of membrane transporters) and that no changes to biological regulation are induced by either the metal's binding to transporter sites or changes to other investigated parameters such as pH. A non-competitive modulation of the transporter system by proton concentration can successfully explain the observed pH dependence.

Models cannot be proven to be correct, they can however be falsified at a defined probability level, thus permitting the elimination of a number of candidate models. Studies generally propose a single candidate model, providing no information about any other hypotheses that were considered during the modelling process, or the probability with which they were rejected. A systematic multi-hypotheses approach to modelling a metal's bioavailability has, to the author's knowledge, not been performed prior to this study. The multi-hypotheses modelling approach adopted for this study, and the application of the set of different models derived from these different hypotheses, to different solution composition domain spaces, illustrates the difficulty of choosing a single model based on a dataset drawn from a particular domain space. Additionally, the increased sensitivity of increasingly complex models to the particular realisation of the mean-value thermodynamic database employed to perform the speciation calculations has been evidenced by the model fitting performed incorporating the probabilistic speciation uncertainty. There are several consequences of this sensitivity: models fitted using mean-value speciation calculations may be

rejected when, in fact, the model provides an acceptable fit within the parameter uncertainty of the thermodynamic parameters; conversely models may be retained as plausible when in fact there is a low probability of them being correct when the thermodynamic parameter uncertainty is considered; models derived using a particular set of thermodynamic parameters are dependent on using those precise values for predictive modelling, changes to one or several of the thermodynamic parameters may significantly impact the predictive ability of the model, complex models are much more susceptible to this phenomenon than simple models.

The principal lessons learnt from this study are:

- For uranium (and metals generally) the thermodynamic data used for predictive speciation modelling is critical. Both the quality, and coherency with respect to the application domain, are vital to ensure reliable speciation modelling. In environmental systems this requirement is challenging with regard to, for example, natural organic matter such as humic and fulvic substances, which are heterogeneous in nature.
- Even in cases where the thermodynamic properties of a metal's speciation are well known, and uranium is by a large margin the most studied element of the actinide series, the effect of the uncertainties of the thermodynamic parameters on the predictive ability of speciation modelling can be very significant. Consideration of the effects of uncertainty propagation in speciation modelling needs to be an integral part of the modelling process.
- Where possible, analytical techniques should be used to validate the modelling of a metal's speciation. In the case of uranium, analytical techniques are not yet available that would permit measurement of the solution speciation in a wide range of environmentally relevant conditions. The development of such analytical techniques is of great importance to the future study of the effects of speciation on environmental phenomena.
- The equilibrium paradigm has gained widespread acceptance in ecotoxicological studies. It should not however be accepted as dogma. The flexibility of this modelling approach can enable phenomena, not conforming to the hypotheses used to develop equilibrium models, to be adequately represented within the equilibrium modelling framework. Obtaining datasets

relevant to a chemical composition domain space sufficiently large to reliably test the hypotheses of the equilibrium modelling framework is not trivial, and there exist many possibilities for the experimental design to confound interpretation of the observed biological response.

9 REFERENCES

Allard, B., S. A. Banwart, et al. (1997). Modelling in Aquatic Chemistry. Paris, OECD Nuclear Energy Authority.

Allison, J. D., D. S. Brown, et al. (1991). MINTEQA2/PRODEFA2, A Geochemical Assessment Model for Environmental Systems: Version 3.0 User's Manual. Athens, GA., U.S. Environmental Protection Agency.

Anderson, D. M. and F. M. M. Morel (1978). "Copper sensitivity of Gonyaulax tamarensis." Limnol. Oceanogr. **23**: 283-295.

Andres, S., M. Baudrimont, et al. (1999). "Field transplantation of the freshwater bivalve Corbicula fluminea along a polymetallic contamination gradient (River Lot, France) : I. Geochemical characteristics of the sampling sites and cadmium and zinc bioaccumulation kinetics." Environ. Toxicol. Chem. **18**: 2462-2471.

Antonov, I. A. and V. M. Saleev (1979). U.S.S.R Comput. Math. and Math. Phys. **19**(1): 252-256.

Baudrimont, M., S. Andres, et al. (1999.). "Field transplantation of the freshwater bivalve Corbicula fluminea along a polymetalllic contamination gradient (River Lot, France) : II. Metallothionein response to metal exposure." Environ. Toxicol. Chem. **18**: 2472-2477.

Belanger, S. E. and D. S. Cherry (1990). "Interacting effects of pH acclimation, pH and heavy metals on acute and chronic toxicity to *Ceriodaphnia dubia* (Cladocera)." J. Crustac. Biol. **10**: 225-235.

Box, G. E. P. and M. E. Muller (1958). "A note on the generation of random normal deviates." Ann. Math, Stat. **29**: 610-611.

Brønsted, J. N. (1922). "Studies of solubility: IV. The principle of specific interaction of ions." Journal of the American Chemical Society **44**: 877-898.

Brønsted, J. N. (1923). "The individual thermodynamic properties of ions." Journal of the American Chemical Society **45**: 2898-2910.

Brown, P. L. and S. J. Markich (2000). "Evaluation of the free ion activity model of metal-organism interaction: extension of the conceptual model." Aquatic Toxicology **51**(2): 177-194.

Cabaniss, S. E. (1997). "Propagation of uncertainty in aqueous equilibrium calculations: non-gaussian output distribution." Anal.Chem. **69**: 3658-3664.

Cabaniss, S. E. (1999). "Uncertainty propagation in geochemical calculations: non-linearity in solubility equilibria." Applied Geochemistry **14**: 255-262.

Campbell, P. G. C. (1995). Interactions between trace metals and aquatic organisms : A critique of the free-ion activity model. Metal speciation and bioavailability in aquatic systems. A. Tessier and D. R. Turner. Chichester, Wiley & Sons**:** 45-101.

Campbell, P. G. C. and P. M. Stokes (1985). "Acidification and toxicity of metals to aquatic biota." Can. J. Fish. Aquat. Sci. **42**: 2034-2049.

Chassard-Bouchaud, C. (1983). "Cellular and sub-cellular localization of uranium in the crab *Carcinus maenas :* a microanalytical study." Mar. Pol. Bull. **14**(4): 133-136.

Chowdhury, M. J. and R. Blust (2001). "A mechanistic model for the uptake of waterborne strontium in the common carp (Cyprinus carpio L.)." Environmental Science & Technology **35**(4): 669-675.

Chowdhury, M. J. and R. Blust (2002). "Bioavailability of waterborne strontium to the common carp, Cyprinus carpio, in complexing environments." Aquatic Toxicology **58**(3-4): 215-227.
Colle, C., J. Garnier-Laplace, et al. (2001). Comportement do l'uranium dans l'environnement. L'Uranium, de l'environnement à l'homme, EDP Sciences, Les Ulis (France).
Colston, B., M. Chandratillake, et al. (1990). Correction for ionic strength effects in modelling aqueous systems. Manchester, Department of Chemistry, Manchester University.
Cooley, H. M., R. E. Evans, et al. (2000). "Toxicology of dietary uranium in lake whitefish (Coregonus clupeaformis)." Aquat. Toxicol. **48**: 495-515.
Cossu, C., A. Doyotte, et al. (1997). "Glutathione reductase, selenium-dependent glutathione peroxidase, glutathione levels, and lipid peroxidation in freshwater bivalves, Unio tumidus, as biomarkers of aquatic contamination in field studies." Ecotoxicol. Environ. Safe. **38**: 122-131.
Cox, J. D., D. D. Wagman, et al. (1989). CODATA Key Values for Thermodynamics, New York: Hemisphere Publishing Corporation. New York, Hemisphere Publishing Corporation.
Crançon, P. and J. van der Lee (2003). "Speciation and mobility of uranium(VI) in humic-containing soils." Radiochimica Acta. **91**: 673-679.
Cusimano, R. F., D. F. Brakke, et al. (1986). "Effects of pH on the Toxicities of Cadmium, Copper, and Zinc to Steelhead Trout (Salmo gairdneri)." Can. J. Fish. Aquat. Sci. **43**: 1497-1503.
De Schamphelaere, K. A. C., D. G. Heijerick, et al. (2002). "Refinement and field validation of a biotic ligand model predicting acute copper toxicity to Daphnia magna." Comparative Biochemistry and Physiology Part C: Toxicology & Pharmacology **133**(1-2): 243-258.
De Schamphelaere, K. A. C. and C. R. Janssen (2002). "A biotic ligand model predicting acute copper toxicity for Daphnia magna: The effects of calcium, magnesium, sodium, potassium, and pH." Environmental Science & Technology **36**(1): 48-54.
Denecke, M. A., T. Reich, et al. (1998). "Determination of structural parameters of uranyl ions complexed with organic acids using EXAFS." Journal of Alloys and Compounds **271-273**: 123-127.
Doyotte, A., C. Cossu, et al. (1997). "Antioxydant enzymes, glutathione and lipid peroxidation as relevant biomarkers of experimental or field exposure in the gills and the digestive gland of the freshwater bivalve Unio tumidus." Aquat. Toxicol. **39**: 93-110.
Ekberg, C. (1999). "Sensitivity analysis and simulation uncertainties in predictive geochemical modelling." Freiberg on-line geoscience http://www.geo.tu-freiberg.de/fog **2**.
Errecalde, O., M. Seidl, et al. (1998). "Influence of low molecular weight metabolite (citrate) on the toxicity of cadmium and zinc to the unicellular green alga Selenastrum capricornatum: an exception to the free-ion model." Wat. Res. **32**(2): 419-429.
Fortin, C. and P. G. C. Campbell (2001). "Thiosulfate enhances silver uptake by a green alga: Role of anion transporters in metal uptake." Environmental Science & Technology **35**(11): 2214-2218.
Fournier, E., D. Tran, et al. (2004). "Valve closure response to uranium exposure for a freshwater bivalve Corbicula fluminea :

quantification of the influence of pH." Envirom. Toxicol. Chem. **23**(5): 1108-1114.
Franklin, N. M., J. L. Stauber, et al. (2000). "pH-dependent toxicity of copper and uranium to a tropical freshwater alga (Chlorella sp.)." Aquatic Toxicology **48**(2-3): 275-289.
Galassi, M., J. Davies, et al. (2002). GNU Scientific Library. Cambridge, MA, USA, Free Software Foundation.
Garrels, R. and C. L. Christ (1965). Solutions, Minerals, and Equilibria. New York, Harper and Row.
Grenthe, I., J. Fuger, et al. (1992). Chemical Thermodynamics of Uranium. Amsterdam, North-Holland.
Grenthe, I., I. Puigdomenech, et al. (1995). Corrections to the Uranium NEA-TDB review. Chemical Thermodynamics of Americium. e. al. Amsterdam, North-Holland**:** 347-374.
Grenthe, I., H. Wanner, et al. (2000). Guidelines for the extrapolation to zero ionic strength. Issy-les-Moulineaux, France, OECD-NEA**:** 34.
Guggenheim, E. A. (1966). Applications of statistical mechanics. Oxford, Clarendon Press.
Gunther, A. J., J. A. Davis, et al. (1999). "Long-term bioaccumulation monitoring with transplanted bivalves in the San Francisco estuary." Mar. Pollut. Bull. **38**: 170-181.
Guy, R. D. and A. R. Kean (1980). "Algae as a chemical speciation monitor - I a comparison of algal growth and computer calculated speciation." Water Research **14**: 891-899.
Heijerick, D. G., K. A. C. De Schamphelaere, et al. (2002). "Predicting acute zinc toxicity for Daphnia magna as a function of key water chemistry characteristics: Development and validation of a biotic ligand model." Environmental Toxicology and Chemistry **21**(6): 1309-1315.
House, W. A. and F. H. Denison (2000). "Factors influencing the measurement of equilibrium phosphate concentrations in river sediments." Water Research **34**(4): 1187-1200.
Jansen, S., R. Blust, et al. (2002). "Metal speciation dynamics and bioavailability: Zn(II) and Cd(II) uptake by mussel (Mytilus edulis) and carp (Cyprinus carpio)." Environmental Science & Technology **36**(10): 2164-2170.
Khune, W. W., C. A. Caldwell, et al. (2002). "Effects of depleted uranium on the health and survival of Ceriodaphnia Dubia and Hyalella Azteca." Envirom. Toxicol. Chem. **21**: 2198-2203.
Knuth, D. E. (1981). Seminumerical Algorithms, 2nd ed., vol 2 of The Art of Computer Programming. Reading, MA. USA., Addison-Wesley.
Kramer, K. J. M., H. A. Jenner, et al. (1989). "The valve movement response of mussels : a tool in biological monitoring." Hydrobiologia **188/189**: 433-443.
Laffitte, M. (1982). "A report of IUPAC commission I.2 on thermodynamics: Notation for states and processes, significance of the word "standard" in chemical thermodynamics, and remarks on commonly tabulated forms of thermodynamic functions." Journal of Chemical Thermodynamics **14**: 805-815.
L'Ecuyer, P. (1998). Random number generation. Handbook of Simulation. J. Banks. NY, Wiley**:** 93-137.
Lenhart, J. J., S. E. Cabaniss, et al. (2000). "Uranium(VI) complexation with citric, humic and fulvic acids." Radiochimica Acta **88**(6): 345-353.

Macdonald, A., L. Silk, et al. (2002). "A lead-gill binding model to predict acute lead toxicity to rainbow trout (Oncorhynchus mykiss)." Comparative Biochemistry and Physiology Part C: Toxicology & Pharmacology **133**(1-2): 227-242.
Markich, S. J. and P. L. Brown (1999). Thermochemical data (log K) for environmentally-relevent elements. Menai, NSW, Australia, ANSTO Environment Division**:** 131.
Markich, S. J., P. L. Brown, et al. (2000). "Valve movement responses of Velesunio angasi (Bivalvia : Hyriidae) to manganese and uranium: An exception to the free ion activity model." Aquatic Toxicology **51**(2): 155-175.
Marquardt, D. W. (1963). Journal of the Society for Industrial and Applied Mathematics **11**: 431-441.
Martell, A. E., R. M. Smith, et al. (2001). NIST Critically Selected Stability Constants of Metal Complexes. Gaithersburg, MD. USA, NIST Standard Reference Data.
Matsumoto, M. and T. Nishimura (1998). "Mersenne Twister. A 623-dimensionally equidistributed uniform pseudo-random number generator." ACM Transactions on Modelling and Computer Simulation, Special issue on Uniform Random Number Generation.
Meyer, J. S., R. C. Santore, et al. (1999). "Binding of nickel and copper to fish gills predicts toxicity when water hardness varies, but free-ion activity does not." Environ. Sci. Technol. **33**: 913-916.
Miller, A. C., M. Stewart, et al. (2002). "Depleted uranium-catalyzed oxidative DNA damage: absence of significant alpha particle decay." J. Inorg. Biochem **91**(1): 246-252.
Montavon, G., A. Mansel, et al. (2000). "Complexation studies of UO22+ with humic acid at low metal ion concentrations by indirect speciation methods." Radiochimica Acta **88**(1): 17-24.
Morel, F. M. M. (1983). Principles of aquatic chemistry. New York, Wiley-Interscience.
Morel, F. M. M. and J. G. Herring (1993). Principles and applications of aquatic chemistry. New York, John Wiley and sons Inc.
Moro, B. (1995). "The Full Monte". Over the Rainbow. Developments in Exotic Options and Complex Swaps. R. Jarrow, RISK Publications.
Mubiana, V. K. and R. Blust (2000). "Uptake of heavy metals in isolated gills of the marine bivalve *Mytilus edulis*." Comp. Biochem. Physiol. Part A. **126**: 108.
Nitzsche, O., G. Meinrath, et al. (2000). "Database uncertainty as a limiting factor in reactive transport prognosis." Journal of Contaminant Hydrology **44**: 223-237.
Nordstrom, D. K., L. N. Plummer, et al. (1990). Revised chemical equilibrium data for major water-mineral reactions and their limitations. Chemical Modelling of Aqueous Systems II. R. L. Bassett. Washington D.C., American Chemical Society**:** 398-413.
OECD-NEA (1996). Survey of Thermodynamic and Kinetic Databases. Paris, Organisation for Economic Co-operation and Development, Nuclear Energy Authority**:** 39.
Östhols, E. and H. Wanner (2000). The NEA Thermochemical Data Base Project. Issy-les-Moulineaux, France, OECD-NEA**:** 21.
Pagenkopf, G. K. (1983). "Gill surface interaction model for trace-metal toxicity to fishes: role of complexation, pH and water hardness." Environ. Sci. Technol. **17**: 342-347.

Paquin, P. R., D. M. Di Toro, et al. (1999). A biotic ligand model of the acute toxicity of metals. III.Application to fish and Daphnia exposure to silver. Integrated approach to Assessing the Bioavailability and Toxicity of Metals in Surface Waters and Sediments. Washington, DC., EPA Science Advisory Board, Office of Water. Office of Research and Development.

Paquin, P. R., J. W. Gorsuch, et al. (2002). "The biotic ligand model: a historical overview." Comparative Biochemistry and Physiology Part C: Toxicology & Pharmacology **133**(1-2): 3-35.

Park, S. K. and K. W. Miller (1988). "Random number generators: good ones are hard to find." Communications of the ACM **31**(10): 1192-1201.

Parkhurst, D. L. and C. A. J. Appelo (1999). Users guide to Phreeqc (version 2) - a computer program for speciation, batch-reaction, one-dimensional transport, and inverse geochemical calculations. Denver, Colorado, U.S. Department of the interior, U.S. Geological survey**:** 312.

Pärt, P. and O. Svanberg (1981). "Uptake of cadmium in perfused rainbow trout (Salmo gairdneri) gills." Can. J. Fish. Aquat. Sci. **38**: 917-924.

Pentreath, R. J. (1973). "The accumulation from water of ^{65}Zn, ^{54}Mn, ^{58}Co, and ^{59}Fe by the mussel *Mytilus edulis*." J.Mar.Biol.Ass.UK **53**: 127-143.

Pettit, D. and K. Powell (2001). IUPAC Stability constants database, Academic Software and the Royal Society of Chemistry.

Pitzer, K. S. (1973). "Thermodynamics of electrolytes: I. Theoretical basis and general equations." Journal of Physical Chemistry **77**: 268-277.

Playle, R. C. (1998). "Modelling metal interactions at fish gills." Sci. Tot. Environ. **219**(2-3): 147-163.

Playle, R. C., D. G. Dixon, et al. (1993). "Copper and cadmium binding to fish gills: Estimates of metal-gill stability constants and modelling of metal accumulation." Can. J. Fish. Aquat. Sci. **50**: 2678-2686.

Playle, R. C., R. W. Gensemer, et al. (1992). Environ. Toxicol. Chem. **11**: 381-391.

Press, W. H., S. A. Teukolsky, et al. (1992). Numerical Recipies in C: The art of scientific computing. Cambridge, Cambridge University Press.

Ragnarsdottir, K. V. R. and L. Charlet (2000). Uranium behaviour in natural environments. Environmental Mineralogy: Microbial interactions, Anthropogenic Influences, Contaminated Land and Waste Management, Mineralogical Society of Great Britain & Ireland. **9:** 333-377.

Ribera, D., F. Labrot, et al. (1996). "Uranium in the environment: occurrence, transfer, and biological effects." Rev. Environ. Contam. Toxicol. **146**: 53-89.

Richards, J. G. and R. C. Playle (1998). "Cobalt Binding to Gills of Rainbow Trout (Oncorhynchus mykiss) : An Equilibrium Model." Comp. Biochem. Physiol. **119C**(2): 185-197.

Riethmuller, N., S. J. Markich, et al. (2001). "Effects of water hardness and alkalinity on the toxicity of uranium to a tropical freshwater hydra (Hydra viridissima)." Biomarkers **6**(1): 45-51.

Scatchard, G. (1936). "Concentrated solutions of strong electrolytes." Chem. Rev. **19**: 309-327.

Schenck, R. C., A. Tessier, et al. (1988). "The effect of pH on iron and manganese uptake by a green alga." Limnol Oceanogr **33**(4): 538-550.

Schwartz, M. L. and R. C. Playle (2001). "Adding magnesium to the silver-gill binding model for rainbow trout (Oncorhynchus mykiss)." Environmental Toxicology and Chemistry **20**(3): 467-472.

Serkiz, S. M., J. D. Allison, et al. (1996). "Correcting errors in the thermodynamic database for the equilibrium speciation model MINTEQA2." Water Research **30**(8): 1930-1933.
Shock, E. L., E. H. Oelkers, et al. (1992). J. Chem. Soc. Faraday Trans. **88**: 803-826.
Shock, E. L., D. C. Sassani, et al. (1997). Geochimica et Cosmochimica Acta. **61**(5): 907-950.
Silva, R. J., G. Bidoglio, et al. (1995). Chemical Thermodynamics of Americium. Amsterdam, North-Holland.
Simkiss, K. and M. G. Taylor (1995). Transport of Metals Across Membranes. Metal Speciation and Bioavailability in Aquatic Systems. A. Tessier and D. Turner. Chichester, UK, John Wiley & Sons Ltd.
Slaveykova, V. I. and K. J. Wilkinson (2003). "Effect of pH on Pb biouptake by the freshwater alga *Chlorella kesslerii*." Environ. Chem. Lett. **1**(3): 185-189.
Sloff, W., D. De Zwart, et al. (1983). "Detection limits of a biological monitoring system for chemical water pollution based on mussel activity." Bull. Environ. Contam. Toxicol. **30**: 400-405.
Sluyts, H., F. Van Hoof, et al. (1996). "A dynamic new alarm system for use in biological early warning systems." Environ. Toxicol. Chem. **15**: 1317-1323.
Stumm, W. and J. J. Morgan (1996). Aquatic Chemistry, Chemical Equilibria and Rates in Natural Waters. New York, John Wiley & Sons, Inc.
Sverjensky, D. A., E. L. Shock, et al. (1997). Geochimica et Cosmochimica Acta **61**(7): 1359-1412.
Swinehart, J. H., A. P. Giannini, et al. (1998). "Effects of divalent cations on amino acid and divalent cation losses from and glycine influx into gills of freshwater bivalve molluscs *Anodonta californiensis* and *Corbicula manilensis*." Colloids and surfaces A: Physicochemical and engineering aspects **144**: 19-25.
Taylor, L. N., D. W. Baker, et al. (2002). "An in vitro approach for modelling branchial copper binding in rainbow trout." Comparative Biochemistry and Physiology Part C: Toxicology & Pharmacology **133**(1-2): 111-124.
Tessier, A., J. Buffle, et al. (1994). Uptake of trace metals by aquatic organisms. Chemical and Biological Regulation of Aquatic Systems. J. Buffle and R. R. DeVitre. Boca Raton, FL, USA, Lewis**:** 197-230.
Tran, D. (2001). Etude des méchanismes de régulation de la ventilation chez le bivalve filtreur *Corbicula fluminea*. Influence de l'oxygène et de l'apport trophique. Application aux problèmes de bioaccumulation et de biodétection du cadmium. Sciences du vivant, Géosciences et Sciences de l'Environment. Bordeaux, L'Universite Bordeaux 1**:** 140.
Tran, D., A. Boudou, et al. (2002). "Relationship between feeding-induced ventilatory activity and bioaccumulation of dissolved and algal-bound cadmium in the asiatic clam Corbicula fluminea." Environmental Toxicology and Chemistry **21**(2): 327-333.
UNEP (2000). UN considers new data on depleted uranium in Kosovo. Geneva, UNEP.
Van der Lee, J. (1998). Thermodynamic and mathematical concepts of Chess. Paris, École des Mines de Paris**:** 103.
Van der Lee, J. (1999). CHESS database.
van Ginneken, L., M. J. Chowdhury, et al. (1999). "Bioavailability of Cd and zinc to the common carp, Cyprinus carpio, in complexing environments: A test for the validity of the free ion activity model." Environmental Toxicology and Chemistry **18**(10): 2295-2304.

van Leeuwen, H. P. (1999). "Metal speciation dynamics and bioavailability: inert and labile complexes." Environ. Sci. Technol. **33**: 3743-3748.
van Leeuwen, H. P. (2000). "Speciation dynamics and bioavailability of metals." Journal of Radioanalytical and Nuclear Chemistry **246**(3): 487-492.
van Leeuwen, H. P. (2001). "Revisited: The conception of lability of metal complexes." Electroanalysis **13**(10): 826-830.
van Leeuwen, H. P. and J. P. Pinheiro (2001). "Speciation dynamics and bioavailability of metals. Exploration of the case of two uptake routes." Pure and Applied Chemistry **73**(1): 39-44.
Vercauteren, K. and R. Blust (1996). "Bioavailability of dissolved zinc to the common mussel Mytilus edulis in complexing environments." Marine Ecology Progress Series **137**(1-3): 123-132.
Wanner, H. and E. Östhols (1999). Guidelines for the Assignment of uncertainties. Issy-les-Moulineaux, France, OECD-NEA**:** 17.
Wanner, H. and E. Östhols (2000). Standards and Conventions for TDB Publications. Issy-les-Moulineaux, France, OECD-NEA**:** 40.
Westall, J., J. Zachary, et al. (1986). MINEQL - A computer program for the calculation of the chemical equilibrium composition of aqueous systems., Department of chemistry, Oregon State University.
WHO. (2001). Depleted uranium, sources, exposurer and health effects. Geneva, Switzerland, World Health Organisation.
Winkle, W. V. (1972). "Cillary activity and oxygen consumption of excised bivalve gill tissue." Comp. Biochem. Physiol. **42A**: 473-485.
Wolery, T. J. (1992). EQ3/6, A Software Package for Geochemical Modeling of Aqueous Systems: Package Overview and Installation Guide. Livermore, California, University of California**:** 74.
Zitko, V. (1976). Structure-activity relationships and the toxicity of trace elements to aquatic biota., Proceedings of Toxicity to Biota of Metal Forms in Natural Water. International Joint Commission**:** 9-32.
Zitko, V., W. V. Carson, et al. (1973). "Prediction of incipient lethal levels of copper to juvenile Atlantic salmon in the presence of humic acid by copper electrode." Bull. Environ. Contam. Toxicol. **10**: 265-271.

Appendix A Conversion of the OECD-NEA database to Chess format

Basis species	$\Delta_f G_m^0$ / kJ mol^{-1}	log K	log K uncertainty	Temperature dependency estimation
Ag^{+}	77.1			
Al^{3+}	-491.51			
Am^{3+}	-598.7			
$B(OH)_{3\ (aq)}$	-969.27			
Ba^{2+}	-557.66			
Br^{-}	-103.85			
Ca^{2+}	-552.81			
Cd^{2+}	-77.73			
Cl^{-}	-131.22			
Cs^{+}	-291.46			
Cu^{2+}	65.04			
F^{-}	-281.52			
H^{+}	0			
$H_2AsO_4^{-}$	-753.2			
H2O	-237.14			
HCO_3^{-}	-586.85			
Hg^{2+}	164.67			
HPO_4^{2-}	-1095.99			
I^{-}	-51.72			
K^{+}	-282.51			
Li^{+}	-292.92			
Mg^{2+}	-455.38			
Na^{+}	-261.95			
NO_3^{-}	-110.79			
NpO_2^{+}	-907.77			
$O_{2\ (aq)}$	16.36			
Pb^{2+}	-24.24			
Pu^{4+}	-477.99			
Rb^{+}	-284.01			
SeO_3^{2-}	-361.6			
$Si(OH)_{4\ (aq)}$	-1307.74			
Sn^{2+}	-27.62			

Appendix A Conversion of the OECD-NEA database to Chess format

Basis species	$\Delta_f G_m^0$ / kJ mol^{-1}	log K	log K uncertainty	Temperature dependency estimation
SO_4^{2-}	-744			
Sr^{2+}	-563.86			
TcO_4^-	-637.41			
Tl^+	-32.4			
UO_2^{2+}	-952.55			
Zn^{2+}	-147.2			

Redox species	Equilibrium equation	$\Delta_f G_m^0$ / kJ mol^{-1}	log K	log K uncertainty	Temperature dependency estimation
Am^{2+}	1 Am^{3+} + 0.5 H_2O ⇌ 1 Am^{2+} + 1 H^+ + 0.25 $O_{2\,(aq)}$	-376.78	-60.37	2.67	Van't Hoff
Am^{4+}	1 Am^{3+} + 1 H^+ + 0.25 $O_{2\,(aq)}$ ⇌ 1 Am^{4+} + 0.5 H_2O	-346.36	-22.72	1.52	Van't Hoff
AmO_2^+	1 Am^{3+} + 0.5 $O_{2\,(aq)}$ + 1 H_2O ⇌ 1 AmO_2^+ + 2 H^+	-739.8	-15.39	1.09	Van't Hoff
AmO_2^{2+}	1 Am^{3+} + 0.75 $O_{2\,(aq)}$ + 0.5 H_2O ⇌ 1 AmO_2^{2+} + 1 H^+	-585.8	-20.88	1.00	Van't Hoff
$Br_{2\,(aq)}$	2 Br^- + 2 H^+ + 0.5 $O_{2\,(aq)}$ ⇌ 1 $Br_{2\,(aq)}$ + 1 H_2O	4.9	5.73	0.18	None
BrO^-	1 Br^- + 0.5 $O_{2\,(aq)}$ ⇌ 1 BrO^-	-32.1	-11.14	0.27	None
BrO_3^-	1 Br^- + 1.5 $O_{2\,(aq)}$ ⇌ 1 BrO_3^-	19.07	-17.24	0.11	Van't Hoff
ClO^-	1 Cl^- + 0.5 $O_{2\,(aq)}$ ⇌ 1 ClO^-	-37.67	-14.96	0.17	None
ClO_2^-	1 Cl^- + 1 $O_{2\,(aq)}$ ⇌ 1 ClO_2^-	10.25	-21.92	0.71	None
ClO_3^-	1 Cl^- + 1.5 $O_{2\,(aq)}$ ⇌ 1 ClO_3^-	-7.9	-17.3	0.24	Van't Hoff
ClO_4^-	1 Cl^- + 2 $O_{2\,(aq)}$ ⇌ 1 ClO_4^-	-7.89	-15.87	0.11	Van't Hoff
$H_2AsO_3^-$	1 $H_2AsO_4^-$ ⇌ 1 $H_2AsO_3^-$ + 0.5 $O_{2\,(aq)}$	-587.08	-30.54	0.70	Van't Hoff
Hg_2^{2+}	2 Hg^{2+} + 1 H_2O ⇌ 1 Hg_2^{2+} + 0.5 $O_{2\,(aq)}$ + 2 H^+	153.57	-12.19	0.10	Van't Hoff
HS^-	1 H^+ + 1 SO_4^{2-} ⇌ 1 HS^- + 2 $O_{2\,(aq)}$	12.24	-138.22	0.37	Van't Hoff
IO_3^-	1 I^- + 1.5 $O_{2\,(aq)}$ ⇌ 1 IO_3^-	-126.34	17.37	0.14	Van't Hoff
N_3^-	3 NO_3^- + 2 H^+ ⇌ 1 N_3^- + 1 H_2O + 4 $O_{2\,(aq)}$	348.2	-89.15	0.35	Van't Hoff
$NH_{3\,(aq)}$	1 NO_3^- + 1 H_2O + 1 H^+ ⇌ 1 $NH_{3\,(aq)}$ + 2 $O_{2\,(aq)}$	-26.67	-62.01	0.05	Van't Hoff
Np^{3+}	1 NpO_2^+ + 2 H^+ ⇌ 1 Np^{3+} + 1 H_2O + 0.5 $O_{2\,(aq)}$	-512.87	-29.07	0.99	Van't Hoff
Np^{4+}	1 NpO_2^+ + 3 H^+ ⇌ 1 Np^{4+} + 1.5 H_2O + 0.25 $O_{2\,(aq)}$	-491.77	-11.28	0.98	Van't Hoff
NpO_2^{2+}	1 NpO_2^+ + 1 H^+ + 0.25 $O_{2\,(aq)}$ ⇌ 1 NpO_2^{2+} + 0.5 H_2O	-795.94	1.9	0.98	Van't Hoff
Pu^{3+}	1 Pu^{4+} + 0.5 H_2O ⇌ 1 Pu^{3+} + 1 H^+ + 0.25 $O_{2\,(aq)}$	-578.98	-3.8	0.47	Van't Hoff
PuO_2^+	1 Pu^{4+} + 1.5 H_2O + 0.25 $O_{2\,(aq)}$ ⇌ 1 PuO_2^+ + 3 H^+	-852.65	4.04	0.50	Van't Hoff
PuO_2^{2+}	1 Pu^{4+} + 1 H_2O + 0.5 $O_{2\,(aq)}$ ⇌ 1 PuO_2^{2+} + 2 H^+	-762.35	9.71	0.49	Van't Hoff
$S_2O_3^{2-}$	2 H^+ + 2 SO_4^{2-} ⇌ 1 $S_2O_3^{2-}$ + 1 H_2O + 2 $O_{2\,(aq)}$	-519.29	-133.9	1.99	None

Appendix A Conversion of the OECD-NEA database to Chess format

Redox species	Equilibrium equation	$\Delta_f G_m^0$ / kJ mol^{-1}	log K	log K uncertainty	Temperature dependency estimation
SCN^-	1 SO_4^{2-} + 1 HCO_3^- + 1 NO_3^- + 3 H^+ ⇌ 1 SCN^- + 1.5 H_2O + 4.25 $O_{2\,(aq)}$	92.7	-218.67	0.70	Van't Hoff
SO_3^{2-}	1 SO_4^{2-} ⇌ 1 SO_3^{2-} + 0.5 $O_{2\,(aq)}$	-487.47	-46.38	0.70	None
TcO^{2+}	1 TcO_4^- + 3 H^+ ⇌ 1 TcO^{2+} + 0.75 $O_{2\,(aq)}$ + 1.5 H_2O	-116.8	-31.04	-	None
TcO_4^{2-}	1 TcO_4^- + 0.5 H_2O ⇌ 1 TcO_4^{2-} + 1 H^+ + 0.25 $O_{2\,(aq)}$	-575.76	-32.29	1.56	None
U^{3+}	1 UO_2^{2+} + 1 H^+ ⇌ 1 U^{3+} + 0.75 $O_{2\,(aq)}$ + 0.5 H_2O	-476.47	-64.78	0.32	Constant heat capacity
U^{4+}	1 UO_2^{2+} + 2 H^+ ⇌ 1 U^{4+} + 1 H_2O + 0.5 $O_{2\,(aq)}$	-529.86	-33.94	0.31	Constant heat capacity
UO_2^+	1 UO_2^{2+} + 0.5 H_2O ⇌ 1 UO_2^+ + 1 H^+ + 0.25 $O_{2\,(aq)}$	-961.02	-20.01	0.31	Van't Hoff
Aqueous species	Equilibrium equation	$\Delta_f G_m^0$ / kJ mol^{-1}	log K	log K uncertainty	Temperature dependency estimation
$(NpO_2)_2(OH)_2^{2+}$	2 NpO_2^{2+} + 2 H_2O ⇌ 1 $(NpO_2)_2(OH)_2^{2+}$ + 2 H^+	-2030.37	-6.27	2.79	None
$(NpO_2)_2CO_3(OH)_3^-$	2 NpO_2^{2+} + 1 HCO_3^- + 3 H_2O ⇌ 1 $(NpO_2)_2CO_3(OH)_3^-$ + 4 H^+	-2814.91	-13.18	3.24	None
$(NpO_2)_3(CO_3)_6^{6-}$	3 NpO_2^{2+} + 6 HCO_3^- ⇌ 1 $(NpO_2)_3(CO_3)_6^{6-}$ + 6 H^+	-5839.71	-12.12	4.47	None
$(NpO_2)_3(OH)_5^+$	3 NpO_2^{2+} + 5 H_2O ⇌ 1 $(NpO_2)_3(OH)_5^+$ + 5 H^+	-3475.8	-17.12	4.18	None
$(PuO_2)_2(OH)_2^{2+}$	2 PuO_2^{2+} + 2 H_2O ⇌ 1 $(PuO_2)_2(OH)_2^{2+}$ + 2 H^+	-1956.18	-7.5	1.72	None
$(PuO_2)_3(CO_3)_6^{6-}$	3 PuO_2^{2+} + 6 HCO_3^- ⇌ 1 $(PuO_2)_3(CO_3)_6^{6-}$ + 6 H^+	-5740.43	-11.86	3.29	None
$(UO_2)_{11}(CO_3)_6(OH)_{12}^{2-}$	11 UO_2^{2+} + 6 HCO_3^- + 12 H_2O ⇌ 1 $(UO_2)_{11}(CO_3)_6(OH)_{12}^{2-}$ + 18 H^+	-16699	-25.54	3.92	None
$(UO_2)_2(OH)_2^{2+}$	2 UO_2^{2+} + 2 H_2O ⇌ 1 $(UO_2)_2(OH)_2^{2+}$ + 2 H^+	-2347.3	-5.62	0.61	Van't Hoff
$(UO_2)_2(PuO_2)(CO_3)_6^{6-}$	2 UO_2^{2+} + 1 PuO_2^{2+} + 6 HCO_3^- ⇌ 1 $(UO_2)_2(PuO_2)(CO_3)_6^{6-}$ + 6 H^+	-6135.67	-9.26	1.90	None
$(UO_2)_2CO_3(OH)_3^-$	2 UO_2^{2+} + 1 HCO_3^- + 3 H_2O ⇌ 1 $(UO_2)_2CO_3(OH)_3^-$ + 4 H^+	-3139.53	-11.18	0.79	None
$(UO_2)_2NpO_2(CO_3)_6^{6-}$	2 UO_2^{2+} + 1 NpO_2^{2+} + 6 HCO_3^- ⇌ 1 $(UO_2)_2NpO_2(CO_3)_6^{6-}$ + 6 H^+	-6174.31	-8.37	3.13	None
$(UO_2)_2OH^{3+}$	2 UO_2^{2+} + 1 H_2O ⇌ 1 $(UO_2)_2OH^{3+}$ + 1 H^+	-2126.83	-2.7	1.17	None
$(UO_2)_3(CO_3)_6^{6-}$	3 UO_2^{2+} + 6 HCO_3^- ⇌ 1 $(UO_2)_3(CO_3)_6^{6-}$ + 6 H^+	-6333.29	-7.96	1.42	Van't Hoff
$(UO_2)_3(OH)_4^{2+}$	3 UO_2^{2+} + 4 H_2O ⇌ 1 $(UO_2)_3(OH)_4^{2+}$ + 4 H^+	-3738.29	-11.9	0.97	None
$(UO_2)_3(OH)_5^+$	3 UO_2^{2+} + 5 H_2O ⇌ 1 $(UO_2)_3(OH)_5^+$ + 5 H^+	-3954.59	-15.55	0.93	Van't Hoff
$(UO_2)_3(OH)_7^-$	3 UO_2^{2+} + 7 H_2O ⇌ 1 $(UO_2)_3(OH)_7^-$ + 7 H^+	-4340.69	-31	2.20	None
$(UO_2)_3O(OH)_2(HCO_3)^+$	3 UO_2^{2+} + 1 HCO_3^- + 3 H_2O ⇌ 1 $(UO_2)_3O(OH)_2(HCO_3)^+$ + 4 H^+	-4100.7	-9.67	1.05	None
$(UO_2)_4(OH)_7^+$	4 UO_2^{2+} + 7 H_2O ⇌ 1 $(UO_2)_4(OH)_7^+$ + 7 H^+	-5345.18	-21.9	1.58	None
$Am(CO_3)_2^-$	1 Am^{3+} + 2 HCO_3^- ⇌ 1 $Am(CO_3)_2^-$ + 2 H^+	-1724.71	-8.35	0.93	None
$Am(CO_3)_3^{3-}$	1 Am^{3+} + 3 HCO_3^- ⇌ 1 $Am(CO_3)_3^{3-}$ + 3 H^+	-2269.16	-15.78	1.05	None
$Am(CO_3)_5^{6-}$	1 Am^{4+} + 5 HCO_3^- ⇌ 1 $Am(CO_3)_5^{6-}$ + 5 H^+	-3210.23	-12.33	2.06	None
$Am(OH)_2^+$	1 Am^{3+} + 2 H_2O ⇌ 1 $Am(OH)_2^+$ + 2 H^+	-992.5	-14.1	1.03	None
$Am(OH)_{3\,(aq)}$	1 Am^{3+} + 3 H_2O ⇌ 1 $Am(OH)_{3\,(aq)}$ + 3 H^+	-1163.42	-25.7	0.97	None

Appendix A Conversion of the OECD-NEA database to Chess format

Aqueous species	Equilibrium equation	$\Delta_f G_m^0$ / kJ mol^{-1}	log K	log K uncertainty	Temperature dependency estimation
$Am(SO_4)_2^-$	1 Am^{3+} + 2 SO_4^{2-} ⇌ 1 $Am(SO_4)_2^-$	-2117.53	5.4	1.10	None
$AmCl^{2+}$	1 Am^{3+} + 1 Cl^- ⇌ 1 $AmCl^{2+}$	-735.91	1.05	0.84	None
$AmCO_3^+$	1 Am^{3+} + 1 HCO_3^- ⇌ 1 $AmCO_3^+$ + 1 H^+	-1171.12	-2.53	0.89	None
AmF^{2+}	1 Am^{3+} + 1 F^- ⇌ 1 AmF^{2+}	-899.63	3.4	0.93	None
AmF_2^+	1 Am^{3+} + 2 F^- ⇌ 1 AmF_2^+	-1194.85	5.8	0.89	None
$AmH_2PO_4^{2+}$	1 Am^{3+} + 1 HPO_4^{2-} + 1 H^+ ⇌ 1 $AmH_2PO_4^{2+}$	-1752.97	10.21	1.01	None
AmN_3^{2+}	1 Am^{3+} + 1 N_3^- ⇌ 1 AmN_3^{2+}	-260.03	1.67	0.97	None
$AmNO_3^{2+}$	1 Am^{3+} + 1 NO_3^- ⇌ 1 $AmNO_3^{2+}$	-717.08	1.33	0.86	None
$AmOH^{2+}$	1 Am^{3+} + 1 H_2O ⇌ 1 $AmOH^{2+}$ + 1 H^+	-799.31	-6.4	1.09	None
$AmSCN^{2+}$	1 Am^{3+} + 1 SCN^- ⇌ 1 $AmSCN^{2+}$	-513.42	1.3	1.33	None
$AmSO_4^+$	1 Am^{3+} + 1 SO_4^{2-} ⇌ 1 $AmSO_4^+$	-1364.68	3.85	0.84	None
AsO_2^-	1 $H_2AsO_3^-$ ⇌ 1 AsO_2^- + 1 H_2O	-350.02	0.01	0.99	Van't Hoff
AsO_4^{3-}	1 $H_2AsO_4^-$ ⇌ 1 AsO_4^{3-} + 2 H^+	-648.36	-18.37	0.70	Van't Hoff
$CO_{2\ (aq)}$	1 HCO_3^- + 1 H^+ ⇌ 1 $CO_{2\ (aq)}$ + 1 H_2O	-385.97	6.35	0.05	Van't Hoff
CO_3^{2-}	1 HCO_3^- ⇌ 1 CO_3^{2-} + 1 H^+	-527.9	-10.33	0.07	Van't Hoff
$H_2P_2O_7^{2-}$	2 HPO_4^{2-} + 2 H^+ ⇌ 1 $H_2P_2O_7^{2-}$ + 1 H_2O	-2027.12	12.66	0.78	None
$H_2PO_4^-$	1 HPO_4^{2-} + 1 H^+ ⇌ 1 $H_2PO_4^-$	-1137.15	7.21	0.27	Van't Hoff
$H_2S_{(aq)}$	1 H^+ + 1 HS^- ⇌ 1 $H_2S_{(aq)}$	-27.65	6.99	0.52	Van't Hoff
$H_2SeO_{3\ (aq)}$	2 H^+ + 1 SeO_3^{2-} ⇌ 1 $H_2SeO_{3\ (aq)}$	-425.53	11.2	0.13	None
$H_2SO_{3\ (aq)}$	1 SO_3^{2-} + 2 H^+ ⇌ 1 $H_2SO_{3\ (aq)}$	-539.19	9.06	1.00	None
$H_3AsO_{3\ (aq)}$	1 $H_2AsO_3^-$ + 1 H^+ ⇌ 1 $H_3AsO_{3\ (aq)}$	-639.68	9.22	0.99	Van't Hoff
$H_3AsO_{4\ (aq)}$	1 H^+ + 1 $H_2AsO_4^-$ ⇌ 1 $H_3AsO_{4\ (aq)}$	-766.12	2.26	0.70	Van't Hoff
$H_3P_2O_7^-$	2 HPO_4^{2-} + 3 H^+ ⇌ 1 $H_3P_2O_7^-$ + 1 H_2O	-2039.96	14.91	0.76	None
$H_3PO_{4\ (aq)}$	1 HPO_4^{2-} + 2 H^+ ⇌ 1 $H_3PO_{4\ (aq)}$	-1149.37	9.35	0.28	Van't Hoff
$H_4P_2O_{7\ (aq)}$	2 HPO_4^{2-} + 4 H^+ ⇌ 1 $H_4P_2O_{7\ (aq)}$ + 1 H_2O	-2045.67	15.91	0.58	Van't Hoff
$HAsO_{2\ (aq)}$	1 H^+ + 1 $H_2AsO_3^-$ ⇌ 1 $HAsO_{2\ (aq)}$ + 1 H_2O	-402.93	9.28	0.99	Van't Hoff
$HAsO_4^{2-}$	1 $H_2AsO_4^-$ ⇌ 1 $HAsO_4^{2-}$ + 1 H^+	-714.59	-6.76	0.70	Van't Hoff
$HBrO_{(aq)}$	1 H^+ + 1 BrO^- ⇌ 1 $HBrO_{(aq)}$	-81.36	8.63	0.38	None
$HClO_{(aq)}$	1 H^+ + 1 ClO^- ⇌ 1 $HClO_{(aq)}$	-80.02	7.42	0.20	None
$HClO_{2\ (aq)}$	1 H^+ + 1 ClO_2^- ⇌ 1 $HClO_{2\ (aq)}$	-0.94	1.96	1.00	None
$HF_{(aq)}$	1 H^+ + 1 F^- ⇌ 1 $HF_{(aq)}$	-299.68	3.18	0.12	Van't Hoff
HF_2^-	1 H^+ + 2 F^- ⇌ 1 HF_2^-	-583.71	3.62	0.21	Van't Hoff

Appendix A Conversion of the OECD-NEA database to Chess format

Aqueous species	Equilibrium equation	$\Delta_f G_m^0$ / kJ mol^{-1}	log K	log K uncertainty	Temperature dependency estimation
$HIO_{3\ (aq)}$	1 H^+ + 1 IO_3^- ⇌ 1 $HIO_{3\ (aq)}$	-130.84	0.79	0.20	None
$HN_{3\ (aq)}$	1 H^+ + 1 N_3^- ⇌ 1 $HN_{3\ (aq)}$	321.37	4.7	0.50	Van't Hoff
$HP_2O_7^{3-}$	2 HPO_4^{2-} + 1 H^+ ⇌ 1 $HP_2O_7^{3-}$ + 1 H_2O	-1989.16	6.01	0.79	None
$HS_2O_3^-$	1 H^+ + 1 $S_2O_3^{2-}$ ⇌ 1 $HS_2O_3^-$	-528.37	1.59	2.81	None
$HSeO_3^-$	1 H^+ + 1 SeO_3^{2-} ⇌ 1 $HSeO_3^-$	-409.54	8.4	0.24	None
HSO_3^-	1 H^+ + 1 SO_3^{2-} ⇌ 1 HSO_3^-	-528.68	7.22	1.00	None
HSO_4^-	1 H^+ + 1 SO_4^{2-} ⇌ 1 HSO_4^-	-755.32	1.98	0.24	Van't Hoff
NH_4^+	1 H^+ + 1 $NH_{3\ (aq)}$ ⇌ 1 NH_4^+	-79.4	9.24	0.07	Van't Hoff
$Np(CO_3)_3^{3-}$	1 Np^{3+} + 3 HCO_3^- ⇌ 1 $Np(CO_3)_3^{3-}$ + 3 H^+	-2185.95	-15.32	2.88	None
$Np(CO_3)_4^{4-}$	1 Np^{4+} + 4 HCO_3^- ⇌ 1 $Np(CO_3)_4^{4-}$ + 4 H^+	-2812.77	-4.62	1.74	None
$Np(CO_3)_5^{6-}$	1 Np^{4+} + 5 HCO_3^- ⇌ 1 $Np(CO_3)_5^{6-}$ + 5 H^+	-3334.57	-16.02	1.77	None
$Np(OH)_{4\ (aq)}$	1 Np^{4+} + 4 H_2O ⇌ 1 $Np(OH)_{4\ (aq)}$ + 4 H^+	-1384.22	-9.83	1.78	None
$Np(SCN)^{3+}$	1 Np^{4+} + 1 SCN^- ⇌ 1 $Np(SCN)^{3+}$	-416.2	3	1.73	Van't Hoff
$Np(SCN)_2^{2+}$	1 Np^{4+} + 2 SCN^- ⇌ 1 $Np(SCN)_2^{2+}$	-329.78	4.1	2.47	Van't Hoff
$Np(SCN)_3^+$	1 Np^{4+} + 3 SCN^- ⇌ 1 $Np(SCN)_3^+$	-241.07	4.8	3.32	Van't Hoff
$Np(SO_4)_{2\ (aq)}$	1 Np^{4+} + 2 SO_4^{2-} ⇌ 1 $Np(SO_4)_{2\ (aq)}$	-2042.87	11.05	1.48	Van't Hoff
$NpCl^{3+}$	1 Np^{4+} + 1 Cl^- ⇌ 1 $NpCl^{3+}$	-631.55	1.5	1.42	None
NpF^{3+}	1 Np^{4+} + 1 F^- ⇌ 1 NpF^{3+}	-824.44	8.96	1.40	Van't Hoff
NpF_2^{2+}	1 Np^{4+} + 2 F^- ⇌ 1 NpF_2^{2+}	-1144.44	15.7	1.44	None
NpI^{3+}	1 Np^{4+} + 1 I^- ⇌ 1 NpI^{3+}	-552.06	1.5	1.44	None
$NpNO_3^{3+}$	1 Np^{4+} + 1 NO_3^- ⇌ 1 $NpNO_3^{3+}$	-613.41	1.9	1.39	None
$NpO_2(CO_3)_2^{2-}$	1 NpO_2^{2+} + 2 HCO_3^- ⇌ 1 $NpO_2(CO_3)_2^{2-}$ + 2 H^+	-1946.01	-4.14	1.58	None
$NpO_2(CO_3)_2^{3-}$	1 NpO_2^+ + 2 HCO_3^- ⇌ 1 $NpO_2(CO_3)_2^{3-}$ + 2 H^+	-2000.86	-14.12	1.00	None
$NpO_2(CO_3)_2OH^{4-}$	1 NpO_2^+ + 2 HCO_3^- + 1 H_2O ⇌ 1 $NpO_2(CO_3)_2OH^{4-}$ + 3 H^+	-2170.42	-25.96	1.54	None
$NpO_2(CO_3)_3^{4-}$	1 NpO_2^{2+} + 3 HCO_3^- ⇌ 1 $NpO_2(CO_3)_3^{4-}$ + 3 H^+	-2490.21	-11.61	1.41	Van't Hoff
$NpO_2(CO_3)_3^{5-}$	1 NpO_2^+ + 3 HCO_3^- ⇌ 1 $NpO_2(CO_3)_3^{5-}$ + 3 H^+	-2522.86	-25.48	1.00	Van't Hoff
$NpO_2(HPO_4)_2^{2-}$	1 NpO_2^{2+} + 2 HPO_4^{2-} ⇌ 1 $NpO_2(HPO_4)_2^{2-}$	-3042.14	9.5	1.80	None
$NpO_2(OH)_2^-$	1 NpO_2^+ + 2 H_2O ⇌ 1 $NpO_2(OH)_2^-$ + 2 H^+	-1247.34	-23.6	1.11	Van't Hoff
$NpO_2(SO_4)_2^{2-}$	1 NpO_2^{2+} + 2 SO_4^{2-} ⇌ 1 $NpO_2(SO_4)_2^{2-}$	-2310.78	4.7	1.40	Van't Hoff
NpO_2Cl^+	1 NpO_2^{2+} + 1 Cl^- ⇌ 1 NpO_2Cl^+	-929.44	0.4	1.40	None
$NpO_2CO_3^-$	1 NpO_2^+ + 1 HCO_3^- ⇌ 1 $NpO_2CO_3^-$ + 1 H^+	-1463.99	-5.36	0.99	None
$NpO_2CO_{3\ (aq)}$	1 NpO_2^{2+} + 1 HCO_3^- ⇌ 1 $NpO_2CO_{3\ (aq)}$ + 1 H^+	-1377.04	-1.01	1.52	None

Appendix A Conversion of the OECD-NEA database to Chess format

Aqueous species	Equilibrium equation	$\Delta_f G_m^0$ / kJ mol^{-1}	log K	log K uncertainty	Temperature dependency estimation
$NpO_2F_{(aq)}$	1 NpO_2^+ + 1 F^- ⇌ 1 $NpO_2F_{(aq)}$	-1196.14	1.2	1.04	None
NpO_2F^+	1 NpO_2^{2+} + 1 F^- ⇌ 1 NpO_2F^+	-1103.55	4.57	1.40	None
$NpO_2F_{2\,(aq)}$	1 NpO_2^{2+} + 2 F^- ⇌ 1 $NpO_2F_{2\,(aq)}$	-1402.37	7.6	1.41	None
$NpO_2H_2PO_4^+$	1 NpO_2^{2+} + 1 HPO_4^{2-} + 1 H^+ ⇌ 1 $NpO_2H_2PO_4^+$	-1952.04	10.53	1.50	None
$NpO_2HPO_4^-$	1 NpO_2^+ + 1 HPO_4^{2-} ⇌ 1 $NpO_2HPO_4^-$	-2020.59	2.95	1.03	None
$NpO_2HPO_{4\,(aq)}$	1 NpO_2^{2+} + 1 HPO_4^{2-} ⇌ 1 $NpO_2HPO_{4\,(aq)}$	-1927.31	6.2	1.58	None
$NpO_2IO_{3\,(aq)}$	1 NpO_2^+ + 1 IO_3^- ⇌ 1 $NpO_2IO_{3\,(aq)}$	-1036.96	0.5	1.05	None
$NpO_2IO_3^+$	1 NpO_2^{2+} + 1 IO_3^- ⇌ 1 $NpO_2IO_3^+$	-929.13	1.2	1.44	None
$NpO_2OH_{(aq)}$	1 NpO_2^+ + 1 H_2O ⇌ 1 $NpO_2OH_{(aq)}$ + 1 H^+	-1080.4	-11.3	1.21	Van't Hoff
NpO_2OH^+	1 NpO_2^{2+} + 1 H_2O ⇌ 1 NpO_2OH^+ + 1 H^+	-1003.97	-5.1	1.45	None
$NpO_2SO_4^-$	1 NpO_2^+ + 1 SO_4^{2-} ⇌ 1 $NpO_2SO_4^-$	-1654.28	0.44	1.02	Van't Hoff
$NpO_2SO_{4\,(aq)}$	1 NpO_2^{2+} + 1 SO_4^{2-} ⇌ 1 $NpO_2SO_{4\,(aq)}$	-1558.67	3.28	1.39	Van't Hoff
$NpOH^{2+}$	1 Np^{3+} + 1 H_2O ⇌ 1 $NpOH^{2+}$ + 1 H^+	-711.19	-6.8	1.44	None
$NpOH^{3+}$	1 Np^{4+} + 1 H_2O ⇌ 1 $NpOH^{3+}$ + 1 H^+	-727.26	-0.29	1.71	None
$NpSO_4^{2+}$	1 Np^{4+} + 1 SO_4^{2-} ⇌ 1 $NpSO_4^{2+}$	-1274.89	6.85	1.41	Van't Hoff
OH^-	1 H_2O ⇌ 1 OH^- + 1 H^+	-157.22	-14	0.01	Van't Hoff
$P_2O_7^{4-}$	2 HPO_4^{2-} ⇌ 1 $P_2O_7^{4-}$ + 1 H_2O	-1935.5	-3.39	0.80	None
PO_4^{3-}	1 HPO_4^{2-} ⇌ 1 PO_4^{3-} + 1 H^+	-1025.49	-12.35	0.28	Van't Hoff
$Pu(SO_4)_2^-$	1 Pu^{3+} + 2 SO_4^{2-} ⇌ 1 $Pu(SO_4)_2^-$	-2099.55	5.7	1.11	Van't Hoff
$Pu(SO_4)_{2\,(aq)}$	1 Pu^{4+} + 2 SO_4^{2-} ⇌ 1 $Pu(SO_4)_{2\,(aq)}$	-2029.6	11.14	0.74	None
$PuBr^{3+}$	1 Pu^{4+} + 1 Br^- ⇌ 1 $PuBr^{3+}$	-590.97	1.6	0.56	None
$PuCl^{2+}$	1 Pu^{3+} + 1 Cl^- ⇌ 1 $PuCl^{2+}$	-717.05	1.2	0.70	None
$PuCl^{3+}$	1 Pu^{4+} + 1 Cl^- ⇌ 1 $PuCl^{3+}$	-619.48	1.8	0.56	None
PuF^{3+}	1 Pu^{4+} + 1 F^- ⇌ 1 PuF^{3+}	-809.97	8.84	0.50	Van't Hoff
PuF_2^{2+}	1 Pu^{4+} + 2 F^- ⇌ 1 PuF_2^{2+}	-1130.65	15.7	0.57	Van't Hoff
$PuH_3PO_4^{4+}$	1 Pu^{4+} + 1 HPO_4^{2-} + 2 H^+ ⇌ 1 $PuH_3PO_4^{4+}$	-1641.05	11.75	0.63	None
PuI^{2+}	1 Pu^{3+} + 1 I^- ⇌ 1 PuI^{2+}	-636.99	1.1	0.78	None
$PuNO_3^{3+}$	1 Pu^{4+} + 1 NO_3^- ⇌ 1 $PuNO_3^{3+}$	-599.91	1.95	0.50	None
$PuO_2(CO_3)_2^{2-}$	1 PuO_2^{2+} + 2 HCO_3^- ⇌ 1 $PuO_2(CO_3)_2^{2-}$ + 2 H^+	-1900.92	-6.15	2.70	Van't Hoff
$PuO_2(CO_3)_3^{4-}$	1 PuO_2^{2+} + 3 HCO_3^- ⇌ 1 $PuO_2(CO_3)_3^{4-}$ + 3 H^+	-2447.08	-13.28	1.16	Van't Hoff
$PuO_2(CO_3)_3^{5-}$	1 PuO_2^+ + 3 HCO_3^- ⇌ 1 $PuO_2(CO_3)_3^{5-}$ + 3 H^+	-2465.03	-25.95	1.18	Van't Hoff
$PuO_2(OH)_{2\,(aq)}$	1 PuO_2^{2+} + 2 H_2O ⇌ 1 $PuO_2(OH)_{2\,(aq)}$ + 2 H^+	-1161.29	-13.2	1.65	None

Appendix A Conversion of the OECD-NEA database to Chess format

Aqueous species	Equilibrium equation	$\Delta_f G_m^0$ / kJ mol^{-1}	log K	log K uncertainty	Temperature dependency estimation
$PuO_2(SO_4)_2^{2-}$	1 PuO_2^{2+} + 2 SO_4^{2-} ⇌ 1 $PuO_2(SO_4)_2^{2-}$	-2275.48	4.4	0.74	Van't Hoff
PuO_2Cl^+	1 PuO_2^{2+} + 1 Cl^- ⇌ 1 PuO_2Cl^+	-897.57	0.7	0.71	None
$PuO_2Cl_{2\ (aq)}$	1 PuO_2^{2+} + 2 Cl^- ⇌ 1 $PuO_2Cl_{2\ (aq)}$	-1021.36	-0.6	0.73	None
$PuO_2CO_3^-$	1 PuO_2^+ + 1 HCO_3^- ⇌ 1 $PuO_2CO_3^-$ + 1 H^+	-1409.77	-5.21	0.73	None
$PuO_2CO_{3\ (aq)}$	1 PuO_2^{2+} + 1 HCO_3^- ⇌ 1 $PuO_2CO_{3\ (aq)}$ + 1 H^+	-1356.47	1.27	3.08	None
PuO_2F^+	1 PuO_2^{2+} + 1 F^- ⇌ 1 PuO_2F^+	-1069.9	4.56	0.74	None
$PuO_2F_{2\ (aq)}$	1 PuO_2^{2+} + 2 F^- ⇌ 1 $PuO_2F_{2\ (aq)}$	-1366.78	7.25	0.87	None
$PuO_2OH_{\ (aq)BOUND}$	1 PuO_2^+ + 1 H_2O ⇌ 1 $PuO_2OH_{\ (aq)BOUND}$ + 1 H^+	-1034.25	-9.73	-	None
PuO_2OH^+	1 PuO_2^{2+} + 1 H_2O ⇌ 1 PuO_2OH^+ + 1 H^+	-968.1	-5.5	0.86	Van't Hoff
$PuO_2SO_{4\ (aq)}$	1 PuO_2^{2+} + 1 SO_4^{2-} ⇌ 1 $PuO_2SO_{4\ (aq)}$	-1525.65	3.38	0.73	Van't Hoff
$PuOH^{2+}$	1 Pu^{3+} + 1 H_2O ⇌ 1 $PuOH^{2+}$ + 1 H^+	-776.74	-6.9	0.73	None
$PuOH^{3+}$	1 Pu^{4+} + 1 H_2O ⇌ 1 $PuOH^{3+}$ + 1 H^+	-710.68	-0.78	0.76	Van't Hoff
$PuSCN^{2+}$	1 Pu^{3+} + 1 SCN^- ⇌ 1 $PuSCN^{2+}$	-493.7	1.3	1.26	Van't Hoff
$PuSO_4^+$	1 Pu^{3+} + 1 SO_4^{2-} ⇌ 1 $PuSO_4^+$	-1345.32	3.91	0.93	Van't Hoff
$PuSO_4^{2+}$	1 Pu^{4+} + 1 SO_4^{2-} ⇌ 1 $PuSO_4^{2+}$	-1261.33	6.89	0.57	None
S^{2-}	1 HS^- ⇌ 1 S^{2-} + 1 H^+	120.7	-19	2.07	None
$Si_2O_2(OH)_5^-$	2 $Si(OH)_{4\ (aq)}$ ⇌ 1 $Si_2O_2(OH)_5^-$ + 1 H_2O + 1 H^+	-2332.1	-8.1	0.50	None
$Si_2O_3(OH)_4^{2-}$	2 $Si(OH)_{4\ (aq)}$ ⇌ 1 $Si_2O_3(OH)_4^{2-}$ + 1 H_2O + 2 H^+	-2269.88	-19	0.50	None
$Si_3O_5(OH)_5^{3-}$	3 $Si(OH)_{4\ (aq)}$ ⇌ 1 $Si_3O_5(OH)_5^{3-}$ + 2 H_2O + 3 H^+	-3291.96	-27.5	0.68	None
$Si_3O_6(OH)_3^{3-}$	3 $Si(OH)_{4\ (aq)}$ ⇌ 1 $Si_3O_6(OH)_3^{3-}$ + 3 H_2O + 3 H^+	-3048.54	-28.6	0.68	None
$Si_4O_7(OH)_5^{3-}$	4 $Si(OH)_{4\ (aq)}$ ⇌ 1 $Si_4O_7(OH)_5^{3-}$ + 4 H_2O + 3 H^+	-4136.83	-25.5	0.86	None
$Si_4O_8(OH)_4^{4-}$	4 $Si(OH)_{4\ (aq)}$ ⇌ 1 $Si_4O_8(OH)_4^{4-}$ + 4 H_2O + 4 H^+	-4075.18	-36.3	0.95	None
$SiO(OH)_3^-$	1 $Si(OH)_{4\ (aq)}$ ⇌ 1 $SiO(OH)_3^-$ + 1 H^+	-1251.74	-9.81	0.20	Van't Hoff
$SiO_2(OH)_2^{2-}$	1 $Si(OH)_{4\ (aq)}$ ⇌ 1 $SiO_2(OH)_2^{2-}$ + 2 H^+	-1175.65	-23.14	0.22	Van't Hoff
$TcCO_3(OH)_{2\ (aq)}$	1 TcO^{2+} + 1 H_2O + 1 HCO_3^- ⇌ 1 $TcCO_3(OH)_{2\ (aq)}$ + 1 H^+	-968.9	4.93	-	None
$TcCO_3(OH)_3^-$	1 TcO^{2+} + 2 H_2O + 1 HCO_3^- ⇌ 1 $TcCO_3(OH)_3^-$ + 2 H^+	-1158.66	-3.38	-	None
$TcO(OH)^+$	1 TcO^{2+} + 1 H_2O ⇌ 1 $TcO(OH)^+$ + 1 H^+	-345.38	-1.5	-	None
$TcO(OH)_{2\ (aq)}$	1 TcO^{2+} + 2 H_2O ⇌ 1 $TcO(OH)_{2\ (aq)}$ + 2 H^+	-568.25	-4	-	None
$TcO(OH)_3^-$	1 TcO^{2+} + 3 H_2O ⇌ 1 $TcO(OH)_3^-$ + 3 H^+	-743.17	-14.9	-	None
$U(CO_3)_4^{4-}$	1 U^{4+} + 4 HCO_3^- ⇌ 1 $U(CO_3)_4^{4-}$ + 4 H^+	-2841.93	-6.19	1.09	None
$U(CO_3)_5^{6-}$	1 U^{4+} + 5 HCO_3^- ⇌ 1 $U(CO_3)_5^{6-}$ + 5 H^+	-3363.43	-17.63	1.06	Van't Hoff
$U(NO_3)_2^{2+}$	1 U^{4+} + 2 NO_3^- ⇌ 1 $U(NO_3)_2^{2+}$	-764.58	2.3	0.58	None

Appendix A Conversion of the OECD-NEA database to Chess format

Aqueous species	Equilibrium equation	$\Delta_f G_m^0$ / kJ mol^{-1}	log K	log K uncertainty	Temperature dependency estimation
$U(OH)_{4\ (aq)}$	$1\ U^{4+} + 4\ H_2O \rightleftharpoons 1\ U(OH)_{4\ (aq)} + 4\ H^+$	-1452.5	-4.54	1.44	Constant heat capacity
$U(OH)_5^-$	$1\ U^{4+} + 5\ H_2O \rightleftharpoons 1\ U(OH)_5^- + 5\ H^+$	-1621.14	-16.54	-	None
$U(SCN)_2^{2+}$	$1\ U^{4+} + 2\ SCN^- \rightleftharpoons 1\ U(SCN)_2^{2+}$	-368.78	4.26	2.04	Van't Hoff
$U(SO_4)_{2\ (aq)}$	$1\ U^{4+} + 2\ SO_4^{2-} \rightleftharpoons 1\ U(SO_4)_{2\ (aq)}$	-2077.86	10.51	0.50	Van't Hoff
UBr^{3+}	$1\ U^{4+} + 1\ Br^- \rightleftharpoons 1\ UBr^{3+}$	-642.04	1.46	0.48	None
UCl^{3+}	$1\ U^{4+} + 1\ Cl^- \rightleftharpoons 1\ UCl^{3+}$	-670.9	1.72	0.46	Van't Hoff
UF^{3+}	$1\ U^{4+} + 1\ F^- \rightleftharpoons 1\ UF^{3+}$	-864.35	9.28	0.46	Van't Hoff
UF_2^{2+}	$1\ U^{4+} + 2\ F^- \rightleftharpoons 1\ UF_2^{2+}$	-1185.55	16.23	0.52	Van't Hoff
UF_3^+	$1\ U^{4+} + 3\ F^- \rightleftharpoons 1\ UF_3^+$	-1497.72	21.6	1.15	Van't Hoff
$UF_{4\ (aq)}$	$1\ U^{4+} + 4\ F^- \rightleftharpoons 1\ UF_{4\ (aq)}$	-1802.08	25.6	1.19	Van't Hoff
UF_5^-	$1\ U^{4+} + 5\ F^- \rightleftharpoons 1\ UF_5^-$	-2091.65	27.01	0.81	None
UF_6^{2-}	$1\ U^{4+} + 6\ F^- \rightleftharpoons 1\ UF_6^{2-}$	-2384.99	29.08	0.87	None
UI^{3+}	$1\ U^{4+} + 1\ I^- \rightleftharpoons 1\ UI^{3+}$	-588.72	1.25	0.53	None
UNO_3^{3+}	$1\ U^{4+} + 1\ NO_3^- \rightleftharpoons 1\ UNO_3^{3+}$	-649.05	1.47	0.46	None
$UO_2(CO_3)_2^{2-}$	$1\ UO_2^{2+} + 2\ HCO_3^- \rightleftharpoons 1\ UO_2(CO_3)_2^{2-} + 2\ H^+$	-2105.04	-3.71	0.36	Van't Hoff
$UO_2(CO_3)_3^{4-}$	$1\ UO_2^{2+} + 3\ HCO_3^- \rightleftharpoons 1\ UO_2(CO_3)_3^{4-} + 3\ H^+$	-2659.54	-9.38	0.37	Van't Hoff
$UO_2(CO_3)_3^{5-}$	$1\ UO_2^+ + 3\ HCO_3^- \rightleftharpoons 1\ UO_2(CO_3)_3^{5-} + 3\ H^+$	-2586.99	-23.57	0.55	None
$UO_2(H_2PO_4)(H_3PO_4)^+$	$1\ UO_2^{2+} + 2\ HPO_4^{2-} + 3\ H^+ \rightleftharpoons 1\ UO_2(H_2PO_4)(H_3PO_4)^+$	-3260.7	20.35	0.64	None
$UO_2(H_2PO_4)_{2\ (aq)}$	$1\ UO_2^{2+} + 2\ HPO_4^{2-} + 2\ H^+ \rightleftharpoons 1\ UO_2(H_2PO_4)_{2\ (aq)}$	-3254.94	19.34	0.64	None
$UO_2(IO_3)_{2\ (aq)}$	$1\ UO_2^{2+} + 2\ IO_3^- \rightleftharpoons 1\ UO_2(IO_3)_{2\ (aq)}$	-1225.72	3.59	0.52	None
$UO_2(N_3)_{2\ (aq)}$	$1\ UO_2^{2+} + 2\ N_3^- \rightleftharpoons 1\ UO_2(N_3)_{2\ (aq)}$	-280.87	4.33	1.06	None
$UO_2(N_3)_3^-$	$1\ UO_2^{2+} + 3\ N_3^- \rightleftharpoons 1\ UO_2(N_3)_3^-$	59.29	5.74	1.53	None
$UO_2(N_3)_4^{2-}$	$1\ UO_2^{2+} + 4\ N_3^- \rightleftharpoons 1\ UO_2(N_3)_4^{2-}$	412.17	4.92	2.02	None
$UO_2(OH)_{2\ (aq)}$	$1\ UO_2^{2+} + 2\ H_2O \rightleftharpoons 1\ UO_2(OH)_{2\ (aq)} + 2\ H^+$	-1368.04	-10.3	-	None
$UO_2(OH)_3^-$	$1\ UO_2^{2+} + 3\ H_2O \rightleftharpoons 1\ UO_2(OH)_3^- + 3\ H^+$	-1554.38	-19.2	0.50	None
$UO_2(OH)_4^{2-}$	$1\ UO_2^{2+} + 4\ H_2O \rightleftharpoons 1\ UO_2(OH)_4^{2-} + 4\ H^+$	-1712.75	-33	2.02	None
$UO_2(SCN)_{2\ (aq)}$	$1\ UO_2^{2+} + 2\ SCN^- \rightleftharpoons 1\ UO_2(SCN)_{2\ (aq)}$	-774.23	1.24	2.08	Van't Hoff
$UO_2(SCN)_3^-$	$1\ UO_2^{2+} + 3\ SCN^- \rightleftharpoons 1\ UO_2(SCN)_3^-$	-686.44	2.1	3.03	Van't Hoff
$UO_2(SO_4)_2^{2-}$	$1\ UO_2^{2+} + 2\ SO_4^{2-} \rightleftharpoons 1\ UO_2(SO_4)_2^{2-}$	-2464.19	4.14	0.35	Van't Hoff
UO_2Br^+	$1\ UO_2^{2+} + 1\ Br^- \rightleftharpoons 1\ UO_2Br^+$	-1057.66	0.22	0.31	None
$UO_2BrO_3^+$	$1\ UO_2^{2+} + 1\ BrO_3^- \rightleftharpoons 1\ UO_2BrO_3^+$	-937.08	0.63	0.35	Van't Hoff
UO_2Cl^+	$1\ UO_2^{2+} + 1\ Cl^- \rightleftharpoons 1\ UO_2Cl^+$	-1084.74	0.17	0.31	Van't Hoff

Appendix A Conversion of the OECD-NEA database to Chess format

Aqueous species	Equilibrium equation	$\Delta_f G_m^0$ / kJ mol^{-1}	log K	log K uncertainty	Temperature dependency estimation
$UO_2Cl_{2\ (aq)}$	1 UO_2^{2+} + 2 Cl^- ⇌ 1 $UO_2Cl_{2\ (aq)}$	-1208.71	-1.1	0.51	Van't Hoff
$UO_2ClO_3^+$	1 UO_2^{2+} + 1 ClO_3^- ⇌ 1 $UO_2ClO_3^+$	-963.31	0.5	0.46	Van't Hoff
$UO_2CO_{3\ (aq)}$	1 UO_2^{2+} + 1 HCO_3^- ⇌ 1 $UO_2CO_{3\ (aq)}$ + 1 H^+	-1535.7	-0.65	0.32	Van't Hoff
UO_2F^+	1 UO_2^{2+} + 1 F^- ⇌ 1 UO_2F^+	-1263.13	5.09	0.35	Van't Hoff
$UO_2F_{2\ (aq)}$	1 UO_2^{2+} + 2 F^- ⇌ 1 $UO_2F_{2\ (aq)}$	-1564.8	8.62	0.39	Van't Hoff
$UO_2F_3^-$	1 UO_2^{2+} + 3 F^- ⇌ 1 $UO_2F_3^-$	-1859.34	10.9	0.62	Van't Hoff
$UO_2F_4^{2-}$	1 UO_2^{2+} + 4 F^- ⇌ 1 $UO_2F_4^{2-}$	-2145.43	11.7	0.91	Van't Hoff
$UO_2H_2PO_4^+$	1 UO_2^{2+} + 1 HPO_4^{2-} + 1 H^+ ⇌ 1 $UO_2H_2PO_4^+$	-2108.31	10.47	0.42	None
$UO_2H_3PO_4^{2+}$	1 UO_2^{2+} + 1 HPO_4^{2-} + 2 H^+ ⇌ 1 $UO_2H_3PO_4^{2+}$	-2106.26	10.11	0.44	None
$UO_2HPO_{4\ (aq)}$	1 UO_2^{2+} + 1 HPO_4^{2-} ⇌ 1 $UO_2HPO_{4\ (aq)}$	-2089.86	7.24	0.49	None
$UO_2IO_3^+$	1 UO_2^{2+} + 1 IO_3^- ⇌ 1 $UO_2IO_3^+$	-1090.3	2	0.36	Van't Hoff
$UO_2N_3^+$	1 UO_2^{2+} + 1 N_3^- ⇌ 1 $UO_2N_3^+$	-619.08	2.58	0.59	None
$UO_2NO_3^+$	1 UO_2^{2+} + 1 NO_3^- ⇌ 1 $UO_2NO_3^+$	-1065.06	0.3	0.35	None
UO_2OH^+	1 UO_2^{2+} + 1 H_2O ⇌ 1 UO_2OH^+ + 1 H^+	-1160.01	-5.2	0.43	Van't Hoff
$UO_2PO_4^-$	1 UO_2^{2+} + 1 HPO_4^{2-} ⇌ 1 $UO_2PO_4^-$ + 1 H^+	-2053.56	0.88	0.44	None
$UO_2S_2O_{3\ (aq)}$	1 UO_2^{2+} + 1 $S_2O_3^{2-}$ ⇌ 1 $UO_2S_2O_{3\ (aq)}$	-1487.82	2.8	2.84	None
UO_2SCN^+	1 UO_2^{2+} + 1 SCN^- ⇌ 1 UO_2SCN^+	-867.84	1.4	1.06	Van't Hoff
$UO_2SO_{3\ (aq)}$	1 UO_2^{2+} + 1 SO_3^{2-} ⇌ 1 $UO_2SO_{3\ (aq)}$	-1477.7	6.6	1.20	None
$UO_2SO_{4\ (aq)}$	1 UO_2^{2+} + 1 SO_4^{2-} ⇌ 1 $UO_2SO_{4\ (aq)}$	-1714.54	3.15	0.32	Van't Hoff
UOH^{3+}	1 U^{4+} + 1 H_2O ⇌ 1 UOH^{3+} + 1 H^+	-763.92	-0.54	0.44	Van't Hoff
$USCN^{3+}$	1 U^{4+} + 1 SCN^- ⇌ 1 $USCN^{3+}$	-454.11	2.97	1.08	Van't Hoff
USO_4^{2+}	1 U^{4+} + 1 SO_4^{2-} ⇌ 1 USO_4^{2+}	-1311.42	6.58	0.48	Van't Hoff
Gaseous species	**Equilibrium equation**	$\Delta_f G_m^0$ / kJ mol^{-1}	**log K**	**log K uncertainty**	**Temperature dependency estimation**
$Ag_{(g)}$	1 Ag^+ + 0.5 H_2O ⇌ 1 $Ag_{(g)}$ + 1 H^+ + 0.25 $O_{2\ (aq)}$	246.01	-51.08	0.14	Van't Hoff
$Al_{(g)}$	1 Al^{3+} + 1.5 H_2O ⇌ 1 $Al_{(g)}$ + 3 H^+ + 0.75 $O_{2\ (aq)}$	289.38	-201.27	0.70	Van't Hoff
$Am_{(g)}$	1 Am^{3+} + 1.5 H_2O ⇌ 1 $Am_{(g)}$ + 3 H^+ + 0.75 $O_{2\ (aq)}$	242	-211.75	0.30	Van't Hoff
$AmF_{3\ (g)}$	1 Am^{3+} + 3 F^- ⇌ 1 $AmF_{3\ (g)}$	-1159.33	-49.74	2.65	Van't Hoff
$B_{(g)}$	1 $B(OH)_{3\ (aq)}$ ⇌ 1 $B_{(g)}$ + 1.5 H_2O + 0.75 $O_{2\ (aq)}$	521.01	-200.92	0.88	Van't Hoff
$BF_{3\ (g)}$	1 $B(OH)_{3\ (aq)}$ + 3 H^+ + 3 F^- ⇌ 1 $BF_{3\ (g)}$ + 3 H_2O	-1119.4	2.98	0.14	Van't Hoff
$Br_{(g)}$	1 Br^- + 1 H^+ + 0.25 $O_{2\ (aq)}$ ⇌ 1 $Br_{(g)}$ + 0.5 H_2O	82.38	-11.14	0.02	Van't Hoff
$Br_{2\ (g)}$	2 Br^- + 2 H^+ + 0.5 $O_{2\ (aq)}$ ⇌ 1 $Br_{2\ (g)}$ + 1 H_2O	3.11	6.05	0.02	Van't Hoff

Appendix A Conversion of the OECD-NEA database to Chess format

Gaseous species	Equilibrium equation	$\Delta_f G_m^0$ / kJ mol^{-1}	log K	log K uncertainty	Temperature dependency estimation
$C_{(g)}$	$1\ HCO_3^- + 1\ H^+ \rightleftharpoons 1\ C_{(g)} + 1\ H_2O + 1\ O_{2\,(aq)}$	671.25	-181.73	0.08	Van't Hoff
$Ca_{(g)}$	$1\ Ca^{2+} + 1\ H_2O \rightleftharpoons 1\ Ca_{(g)} + 2\ H^+ + 0.5\ O_{2\,(aq)}$	144.02	-165.06	0.14	Van't Hoff
$Cd_{(g)}$	$1\ Cd^{2+} + 1\ H_2O \rightleftharpoons 1\ Cd_{(g)} + 2\ H^+ + 0.5\ O_{2\,(aq)}$	77.23	-70.13	0.04	Van't Hoff
$Cl_{(g)}$	$1\ Cl^- + 1\ H^+ + 0.25\ O_{2\,(aq)} \rightleftharpoons 1\ Cl_{(g)} + 0.5\ H_2O$	105.31	-19.95	0.00	Van't Hoff
$Cl_{2\,(g)}$	$2\ Cl^- + 2\ H^+ + 0.5\ O_{2\,(aq)} \rightleftharpoons 1\ Cl_{2\,(g)} + 1\ H_2O$	0	-3	-	Van't Hoff
$CO_{(g)}$	$1\ HCO_3^- + 1\ H^+ \rightleftharpoons 1\ CO_{(g)} + 1\ H_2O + 0.5\ O_{2\,(aq)}$	-137.17	-38.67	0.03	Van't Hoff
$CO_{2\,(g)}$	$1\ HCO_3^- + 1\ H^+ \rightleftharpoons 1\ CO_{2\,(g)} + 1\ H_2O$	-394.37	7.83	0.02	Van't Hoff
$Cs_{(g)}$	$1\ Cs^+ + 0.5\ H_2O \rightleftharpoons 1\ Cs_{(g)} + 1\ H^+ + 0.25\ O_{2\,(aq)}$	49.56	-81.23	0.18	Van't Hoff
$Cu_{(g)}$	$1\ Cu^{2+} + 1\ H_2O \rightleftharpoons 1\ Cu_{(g)} + 2\ H^+ + 0.5\ O_{2\,(aq)}$	297.67	-83.73	0.21	Van't Hoff
$F_{(g)}$	$1\ F^- + 1\ H^+ + 0.25\ O_{2\,(aq)} \rightleftharpoons 1\ F_{(g)} + 0.5\ H_2O$	62.28	-38.74	0.05	Van't Hoff
$F_{2\,(g)}$	$2\ F^- + 2\ H^+ + 0.5\ O_{2\,(aq)} \rightleftharpoons 1\ F_{2\,(g)} + 1\ H_2O$	0	-55.66	-	Van't Hoff
$H_{(g)}$	$0.5\ H_2O \rightleftharpoons 1\ H_{(g)} + 0.25\ O_{2\,(aq)}$	203.28	-57.1	0.00	Constant heat capacity
$H_{2\,(g)}$	$1\ H_2O \rightleftharpoons 1\ H_{2\,(g)} + 0.5\ O_{2\,(aq)}$	0	-42.98	-	Constant heat capacity
$H_2O_{(g)}$	$1\ H_2O \rightleftharpoons 1\ H_2O_{(g)}$	-228.58	-1.5	0.01	Constant heat capacity
$H_2S_{(g)}$	$1\ HS^- + 1\ H^+ \rightleftharpoons 1\ H_2S_{(g)}$	-33.44	8	0.38	Van't Hoff
$HBr_{(g)}$	$1\ H^+ + 1\ Br^- \rightleftharpoons 1\ HBr_{(g)}$	-53.36	-8.85	0.03	Van't Hoff
$HCl_{(g)}$	$1\ H^+ + 1\ Cl^- \rightleftharpoons 1\ HCl_{(g)}$	-95.3	-6.29	0.02	Van't Hoff
$HF_{(g)}$	$1\ H^+ + 1\ F^- \rightleftharpoons 1\ HF_{(g)}$	-275.4	-1.07	0.12	Van't Hoff
$Hg_{(g)}$	$1\ Hg^{2+} + 1\ H_2O \rightleftharpoons 1\ Hg_{(g)} + 2\ H^+ + 0.5\ O_{2\,(aq)}$	31.84	-19.71	0.01	Van't Hoff
$HI_{(g)}$	$1\ H^+ + 1\ I^- \rightleftharpoons 1\ HI_{(g)}$	1.7	-9.36	0.02	Van't Hoff
$I_{(g)}$	$1\ H^+ + 1\ I^- + 0.25\ O_{2\,(aq)} \rightleftharpoons 1\ I_{(g)} + 0.5\ H_2O$	70.17	0.13	0.01	Van't Hoff
$I_{2\,(g)}$	$2\ H^+ + 2\ I^- + 0.5\ O_{2\,(aq)} \rightleftharpoons 1\ I_{2\,(g)} + 1\ H_2O$	19.32	21.47	0.02	Van't Hoff
$K_{(g)}$	$1\ K^+ + 0.5\ H_2O \rightleftharpoons 1\ K_{(g)} + 1\ H^+ + 0.25\ O_{2\,(aq)}$	60.48	-81.58	0.14	Van't Hoff
$Li_{(g)}$	$1\ Li^+ + 0.5\ H_2O \rightleftharpoons 1\ Li_{(g)} + 1\ H^+ + 0.25\ O_{2\,(aq)}$	126.6	-94.99	0.18	Van't Hoff
$Mg_{(g)}$	$1\ Mg^{2+} + 1\ H_2O \rightleftharpoons 1\ Mg_{(g)} + 2\ H^+ + 0.5\ O_{2\,(aq)}$	112.52	-142.47	0.14	Van't Hoff
$N_{(g)}$	$1\ NH_{3\,(aq)} + 0.75\ O_{2\,(aq)} \rightleftharpoons 1\ N_{(g)} + 1.5\ H_2O$	455.54	-20.01	0.09	Van't Hoff
$N_{2\,(g)}$	$2\ NH_{3\,(aq)} + 1.5\ O_{2\,(aq)} \rightleftharpoons 1\ N_{2\,(g)} + 3\ H_2O$	0	119.59	0.11	Van't Hoff
$Na_{(g)}$	$1\ Na^+ + 0.5\ H_2O \rightleftharpoons 1\ Na_{(g)} + 1\ H^+ + 0.25\ O_{2\,(aq)}$	76.96	-80.86	0.12	Van't Hoff
$NH_{3\,(g)}$	$1\ NH_{3\,(aq)} \rightleftharpoons 1\ NH_{3\,(g)}$	-16.41	-1.8	0.08	Van't Hoff
$Np_{(g)}$	$1\ Np^{3+} + 1.5\ H_2O \rightleftharpoons 1\ Np_{(g)} + 3\ H^+ + 0.75\ O_{2\,(aq)}$	421.2	-228.11	1.12	Van't Hoff
$NpCl_{3\,(g)}$	$1\ Np^{3+} + 3\ Cl^- \rightleftharpoons 1\ NpCl_{3\,(g)}$	-582.36	-56.79	2.14	Van't Hoff
$NpCl_{4\,(g)}$	$1\ Np^{4+} + 4\ Cl^- \rightleftharpoons 1\ NpCl_{4\,(g)}$	-765.05	-44.08	1.37	Van't Hoff

Appendix A Conversion of the OECD-NEA database to Chess format

Gaseous species	Equilibrium equation	$\Delta_f G_m^0$ / kJ mol^{-1}	log K	log K uncertainty	Temperature dependency estimation
$NpF_{(g)}$	$1\ Np^{3+} + 1\ F^- + 1\ H_2O \rightleftharpoons 1\ NpF_{(g)} + 2\ H^+ + 0.5\ O_{2\,(aq)}$	-111.56	-162.6	5.36	Van't Hoff
$NpF_{2\,(g)}$	$1\ Np^{3+} + 2\ F^- + 0.5\ H_2O \rightleftharpoons 1\ NpF_{2\,(g)} + 1\ H^+ + 0.25\ O_{2\,(aq)}$	-585.13	-107.47	8.83	Van't Hoff
$NpF_{3\,(g)}$	$1\ Np^{3+} + 3\ F^- \rightleftharpoons 1\ NpF_{3\,(g)}$	-1104.8	-44.26	3.68	Van't Hoff
$NpF_{4\,(g)}$	$1\ Np^{4+} + 4\ F^- \rightleftharpoons 1\ NpF_{4\,(g)}$	-1535.29	-14.47	4.01	Van't Hoff
$NpF_{6\,(g)}$	$1\ NpO_2^{2+} + 6\ F^- + 4\ H^+ \rightleftharpoons 1\ NpF_{6\,(g)} + 2\ H_2O$	-1837.53	-30.35	3.64	Van't Hoff
$O_{(g)}$	$0.5\ O_{2\,(aq)} \rightleftharpoons 1\ O_{(g)}$	231.74	-39.17	0.02	Constant heat capacity
$O_{2\,(g)}$	$1\ O_{2\,(aq)} \rightleftharpoons 1\ O_{2\,(g)}$	0	2.87	-	Constant heat capacity
$P_{(g)}$	$1\ HPO_4^{2-} + 2\ H^+ \rightleftharpoons 1\ P_{(g)} + 1.5\ H_2O + 1.25\ O_{2\,(aq)}$	280.09	-182.34	0.18	Van't Hoff
$P_{2\,(g)}$	$2\ HPO_4^{2-} + 4\ H^+ \rightleftharpoons 1\ P_{2\,(g)} + 3\ H_2O + 2.5\ O_{2\,(aq)}$	103.47	-284.67	0.35	Van't Hoff
$P_{4\,(g)}$	$4\ HPO_4^{2-} + 8\ H^+ \rightleftharpoons 1\ P_{4\,(g)} + 6\ H_2O + 5\ O_{2\,(aq)}$	24.42	-537.37	0.08	Van't Hoff
$Pb_{(g)}$	$1\ Pb^{2+} + 1\ H_2O \rightleftharpoons 1\ Pb_{(g)} + 2\ H^+ + 0.5\ O_{2\,(aq)}$	162.23	-75.65	0.14	Van't Hoff
$Pu_{(g)}$	$1\ Pu^{3+} + 1.5\ H_2O \rightleftharpoons 1\ Pu_{(g)} + 3\ H^+ + 0.75\ O_{2\,(aq)}$	312.42	-220.63	0.71	Van't Hoff
$PuBr_{3\,(g)}$	$1\ Pu^{3+} + 3\ Br^- \rightleftharpoons 1\ PuBr_{3\,(g)}$	-529.81	-63.2	2.78	Van't Hoff
$PuCl_{3\,(g)}$	$1\ Pu^{3+} + 3\ Cl^- \rightleftharpoons 1\ PuCl_{3\,(g)}$	-641.3	-58.05	0.79	Van't Hoff
$PuCl_{4\,(g)}$	$1\ Pu^{4+} + 4\ Cl^- \rightleftharpoons 1\ PuCl_{4\,(g)}$	-764.68	-41.73	1.83	Van't Hoff
$PuF_{(g)}$	$1\ Pu^{3+} + 1\ F^- + 1\ H_2O \rightleftharpoons 1\ PuF_{(g)} + 2\ H^+ + 0.5\ O_{2\,(aq)}$	-140.97	-169.04	1.83	Van't Hoff
$PuF_{2\,(g)}$	$1\ Pu^{3+} + 2\ F^- + 0.5\ H_2O \rightleftharpoons 1\ PuF_{2\,(g)} + 1\ H^+ + 0.25\ O_{2\,(aq)}$	-626.15	-111.87	1.27	Van't Hoff
$PuF_{3\,(g)}$	$1\ Pu^{3+} + 3\ F^- \rightleftharpoons 1\ PuF_{3\,(g)}$	-1161.08	-45.98	0.96	Van't Hoff
$PuF_{4\,(g)}$	$1\ Pu^{4+} + 4\ F^- \rightleftharpoons 1\ PuF_{4\,(g)}$	-1517.87	-15.1	3.89	Van't Hoff
$PuF_{6\,(g)}$	$1\ PuO_2^{2+} + 6\ F^- + 4\ H^+ \rightleftharpoons 1\ PuF_{6\,(g)} + 2\ H_2O$	-1725.06	-44.17	3.56	Van't Hoff
$PuI_{3\,(g)}$	$1\ Pu^{3+} + 3\ I^- \rightleftharpoons 1\ PuI_{3\,(g)}$	-366.52	-64.41	2.78	Van't Hoff
$Rb_{(g)}$	$1\ Rb^+ + 0.5\ H_2O \rightleftharpoons 1\ Rb_{(g)} + 1\ H^+ + 0.25\ O_{2\,(aq)}$	53.08	-80.54	0.14	Van't Hoff
$S_{(g)}$	$1\ HS^- + 1\ H^+ + 0.5\ O_{2\,(aq)} \rightleftharpoons 1\ S_{(g)} + 1\ H_2O$	236.69	3.66	0.37	Van't Hoff
$S_{2\,(g)}$	$2\ HS^- + 2\ H^+ + 1\ O_{2\,(aq)} \rightleftharpoons 1\ S_{2\,(g)} + 2\ H_2O$	79.69	76.29	0.74	Van't Hoff
$Si_{(g)}$	$1\ Si(OH)_{4\,(aq)} \rightleftharpoons 1\ Si_{(g)} + 2\ H_2O + 1\ O_{2\,(aq)}$	405.53	-219.93	1.40	Van't Hoff
$SiF_{4\,(g)}$	$1\ Si(OH)_{4\,(aq)} + 4\ F^- + 4\ H^+ \rightleftharpoons 1\ SiF_{4\,(g)} + 4\ H_2O$	-1572.77	15.33	0.14	Van't Hoff
$Sn_{(g)}$	$1\ Sn^{2+} + 1\ H_2O \rightleftharpoons 1\ Sn_{(g)} + 2\ H^+ + 0.5\ O_{2\,(aq)}$	266.22	-94.46	0.26	Van't Hoff
$SO_{2\,(g)}$	$1\ SO_3^{2-} + 2\ H^+ \rightleftharpoons 1\ SO_{2\,(g)} + 1\ H_2O$	-300.1	8.72	0.71	None
$Tc_{(g)}$	$1\ TcO^{2+} + 1\ H_2O \rightleftharpoons 1\ Tc_{(g)} + 2\ H^+ + 1\ O_{2\,(aq)}$	630.71	-175.37	-	None
$Tc_2O_{7\,(g)}$	$2\ TcO_4^- + 2\ H^+ \rightleftharpoons 1\ Tc_2O_{7\,(g)} + 1\ H_2O$	-904.82	-23.27	2.88	Constant heat capacity
$TcC_{(g)}$	$1\ TcO^{2+} + 1\ HCO_3^- \rightleftharpoons 1\ TcC_{(g)} + 1\ H^+ + 2\ O_{2\,(aq)}$	765.6	-263.13	-	None
$TcO_{(g)}$	$1\ TcO^{2+} + 1\ H_2O \rightleftharpoons 1\ TcO_{(g)} + 2\ H^+ + 0.5\ O_{2\,(aq)}$	357.49	-126.07	-	None

Appendix A Conversion of the OECD-NEA database to Chess format

Gaseous species	Equilibrium equation	$\Delta_f G_m^0$ / kJ mol^{-1}	log K	log K uncertainty	Temperature dependency estimation
$TcS_{(g)}$	$1\ TcO^{2+} + 1\ HS^- \rightleftharpoons 1\ TcS_{(g)} + 1\ H^+ + 0.5\ O_{2(aq)}$	491.92	-105.93	-	None
$U_{(g)}$	$1\ U^{3+} + 1.5\ H_2O \rightleftharpoons 1\ U_{(g)} + 3\ H^+ + 0.75\ O_{2(aq)}$	488.4	-233.5	1.44	Constant heat capacity
$U_2Cl_{10(g)}$	$2\ UO_2^+ + 10\ Cl^- + 8\ H^+ \rightleftharpoons 1\ U_2Cl_{10(g)} + 4\ H_2O$	-1813.81	-82.66	1.94	Van't Hoff
$U_2Cl_{8(g)}$	$2\ U^{4+} + 8\ Cl^- \rightleftharpoons 1\ U_2Cl_{8(g)}$	-1639.66	-82.3	3.00	Van't Hoff
$U_2F_{10(g)}$	$2\ UO_2^+ + 10\ F^- + 8\ H^+ \rightleftharpoons 1\ U_2F_{10(g)} + 4\ H_2O$	-3860.97	12.66	5.32	Van't Hoff
$UBr_{(g)}$	$1\ U^{3+} + 1\ Br^- + 1\ H_2O \rightleftharpoons 1\ UBr_{(g)} + 2\ H^+ + 0.5\ O_{2(aq)}$	201.77	-179.99	3.04	Van't Hoff
$UBr_{2(g)}$	$1\ U^{3+} + 2\ Br^- + 0.5\ H_2O \rightleftharpoons 1\ UBr_{2(g)} + 1\ H^+ + 0.25\ O_{2(aq)}$	-77.69	-127.74	4.42	Van't Hoff
$UBr_{3(g)}$	$1\ U^{3+} + 3\ Br^- \rightleftharpoons 1\ UBr_{3(g)}$	-401.12	-67.78	6.51	Van't Hoff
$UBr_{4(g)}$	$1\ U^{4+} + 4\ Br^- \rightleftharpoons 1\ UBr_{4(g)}$	-636.18	-54.15	1.52	Van't Hoff
$UBr_{5(g)}$	$1\ UO_2^+ + 5\ Br^- + 4\ H^+ \rightleftharpoons 1\ UBr_{5(g)} + 2\ H_2O$	-656.31	-61.26	3.07	Van't Hoff
$UCl_{(g)}$	$1\ U^{3+} + 1\ Cl^- + 1\ H_2O \rightleftharpoons 1\ UCl_{(g)} + 2\ H^+ + 0.5\ O_{2(aq)}$	157.12	-176.97	3.95	Van't Hoff
$UCl_{2(g)}$	$1\ U^{3+} + 2\ Cl^- + 0.5\ H_2O \rightleftharpoons 1\ UCl_{2(g)} + 1\ H^+ + 0.25\ O_{2(aq)}$	-182.59	-118.95	3.95	Van't Hoff
$UCl_{3(g)}$	$1\ U^{3+} + 3\ Cl^- \rightleftharpoons 1\ UCl_{3(g)}$	-535.66	-58.59	2.83	Van't Hoff
$UCl_{4(g)}$	$1\ U^{4+} + 4\ Cl^- \rightleftharpoons 1\ UCl_{4(g)}$	-790.17	-46.35	1.04	Van't Hoff
$UCl_{5(g)}$	$1\ UO_2^+ + 5\ Cl^- + 4\ H^+ \rightleftharpoons 1\ UCl_{5(g)} + 2\ H_2O$	-831.84	-54.48	2.70	Van't Hoff
$UCl_{6(g)}$	$1\ UO_2^{2+} + 6\ Cl^- + 4\ H^+ \rightleftharpoons 1\ UCl_{6(g)} + 2\ H_2O$	-903.59	-63.42	1.52	Van't Hoff
$UF_{(g)}$	$1\ U^{3+} + 1\ F^- + 1\ H_2O \rightleftharpoons 1\ UF_{(g)} + 2\ H^+ + 0.5\ O_{2(aq)}$	-81.94	-161.42	5.29	Van't Hoff
$UF_{2(g)}$	$1\ U^{3+} + 2\ F^- + 0.5\ H_2O \rightleftharpoons 1\ UF_{2(g)} + 1\ H^+ + 0.25\ O_{2(aq)}$	-548.79	-107.46	5.29	Van't Hoff
$UF_{3(g)}$	$1\ U^{3+} + 3\ F^- \rightleftharpoons 1\ UF_{3(g)}$	-1052	-47.13	2.82	Van't Hoff
$UF_{4(g)}$	$1\ U^{4+} + 4\ F^- \rightleftharpoons 1\ UF_{4(g)}$	-1573.54	-14.44	1.63	Van't Hoff
$UF_{5(g)}$	$1\ UO_2^+ + 5\ F^- + 4\ H^+ \rightleftharpoons 1\ UF_{5(g)} + 2\ H_2O$	-1858.99	-6.2	2.70	Van't Hoff
$UF_{6(g)}$	$1\ UO_2^{2+} + 6\ F^- + 4\ H^+ \rightleftharpoons 1\ UF_{6(g)} + 2\ H_2O$	-2064.5	-18.03	0.33	Van't Hoff
$UI_{(g)}$	$1\ U^{3+} + 1\ I^- + 1\ H_2O \rightleftharpoons 1\ UI_{(g)} + 2\ H^+ + 0.5\ O_{2(aq)}$	288.01	-185.97	4.42	Van't Hoff
$UI_{2(g)}$	$1\ U^{3+} + 2\ I^- + 0.5\ H_2O \rightleftharpoons 1\ UI_{2(g)} + 1\ H^+ + 0.25\ O_{2(aq)}$	37.49	-129.65	4.42	Van't Hoff
$UI_{3(g)}$	$1\ U^{3+} + 3\ I^- \rightleftharpoons 1\ UI_{3(g)}$	-200.7	-75.5	4.42	Van't Hoff
$UI_{4(g)}$	$1\ U^{4+} + 4\ I^- \rightleftharpoons 1\ UI_{4(g)}$	-370.37	-64.19	1.18	Van't Hoff
$UO_{(g)}$	$1\ U^{3+} + 1.5\ H_2O \rightleftharpoons 1\ UO_{(g)} + 3\ H^+ + 0.25\ O_{2(aq)}$	1.87	-146.84	3.00	Constant heat capacity
$UO_{2(g)}$	$1\ U^{4+} + 2\ H_2O \rightleftharpoons 1\ UO_{2(g)} + 4\ H^+$	-481.06	-91.64	3.52	Constant heat capacity
$UO_2Cl_{2(g)}$	$1\ UO_2^{2+} + 2\ Cl^- \rightleftharpoons 1\ UO_2Cl_{2(g)}$	-941.36	-47.94	2.68	Van't Hoff
$UO2F2_{(g)}$	$1\ UO2^{2+} + 2\ F^- \rightleftharpoons 1\ UO2F2_{(g)}$	-1318.17	-34.59	2.69	Van't Hoff
$UO_{3(g)}$	$1\ UO_2^{2+} + 1\ H_2O \rightleftharpoons 1\ UO_{3(g)} + 2\ H^+$	-784.76	-70.94	2.63	Constant heat capacity
$UOF_{4(g)}$	$1\ UO_2^{2+} + 4\ F^- + 2\ H^+ \rightleftharpoons 1\ UOF_{4(g)} + 1\ H_2O$	-1703.75	-24.13	3.54	Van't Hoff

Appendix A Conversion of the OECD-NEA database to Chess format

Gaseous species	Equilibrium equation	$\Delta_f G_m^0$ / kJ mol^{-1}	log K	log K uncertainty	Temperature dependency estimation
$Zn_{(g)}$	1 Zn^{2+} + 1 H_2O ⇌ 1 $Zn_{(g)}$ + 2 H^+ + 0.5 $O_{2(aq)}$	94.81	-85.38	0.07	Van't Hoff
Mineral species	**Equilibrium equation**	$\Delta_f G_m^0$ / kJ mol^{-1}	**log K**	**log K uncertainty**	**Temperature dependency estimation**
$(NH_4)_4NpO_2(CO_3)_{3(s)}$	4 $NH_{3(aq)}$ + 1 NpO_2^{2+} + 3 HCO_3^- + 1 H^+ ⇌ 1 $(NH_4)_4NpO_2(CO_3)_{3(s)}$	-2850.28	32.78	1.47	None
$(UO2)2As2O7_{(c)}$	2 $UO2^{2+}$ + 2 $H2AsO4^-$ ⇌ 1 $(UO2)2As2O7_{(c)}$ + 1 H2O + 2 H^+	-3130.25	-7.73	2.10	Van't Hoff
$(UO_2)_2Cl_{3(c)}$	1 UO_2^{2+} + 1 UO_2^+ + 3 Cl^- ⇌ 1 $(UO_2)_2Cl_{3(c)}$	-2234.76	-12.69	0.60	Van't Hoff
$(UO_2)_2P_2O_{7(c)}$	2 UO_2^{2+} + 2 HPO_4^{2-} ⇌ 1 $(UO_2)_2P_2O_{7(c)}$ + 1 H_2O	-3930	12.27	1.20	Van't Hoff
$(UO_2)_3(AsO_4)_{2(c)}$	3 UO_2^{2+} + 2 $H_2AsO_4^-$ ⇌ 1 $(UO_2)_3(AsO_4)_{2(c)}$ + 4 H^+	-4310.79	-9.33	2.10	Van't Hoff
$(UO_2)_3(PO_4)_{2(c)}$	3 UO_2^{2+} + 2 HPO_4^{2-} ⇌ 1 $(UO_2)_3(PO_4)_{2(c)}$ + 2 H^+	-5115.97	11.62	0.96	Van't Hoff
$(UO_2)_3(PO_4)_2{\cdot}4H_2O_{(c)}$	3 UO_2^{2+} + 2 HPO_4^{2-} + 4 H_2O ⇌ 1 $(UO_2)_3(PO_4)_2{\cdot}4H_2O_{(c)}$ + 2 H^+	-6138.97	24.66	1.11	Van't Hoff
$(UO_2)_3(PO_4)_2{\cdot}6H_2O_{(c)}$	3 UO_2^{2+} + 2 HPO_4^{2-} + 6 H_2O ⇌ 1 $(UO_2)_3(PO_4)_2{\cdot}6H_2O_{(c)}$ + 2 H^+	-6618	25.5	1.23	None
$Ag_{(c)}$	1 Ag^+ + 0.5 H_2O ⇌ 1 $Ag_{(c)}$ + 1 H^+ + 0.25 $O_{2(aq)}$	0	-7.98	-	Van't Hoff
$AgCl_{(c)}$	1 Ag^+ + 1 Cl^- ⇌ 1 $AgCl_{(c)}$	-109.77	9.75	0.02	Van't Hoff
$AgTcO_{4(c)}$	1 Ag^+ + 1 TcO_4^- ⇌ 1 $AgTcO_{4(c)}$	-578.98	3.27	1.34	None
$Al_{(c)}$	1 Al^{3+} + 1.5 H_2O ⇌ 1 $Al_{(c)}$ + 3 H^+ + 0.75 $O_{2(aq)}$	0	-150.57	-	Van't Hoff
Al_2O_3(coru)	2 Al^{3+} + 3 H_2O ⇌ 1 Al_2O_3(coru) + 6 H^+	-1582.26	-19.65	0.23	Van't Hoff
$AlF_{3(c)}$	1 Al^{3+} + 3 F^- ⇌ 1 $AlF_{3(c)}$	-1431.1	16.65	0.23	Van't Hoff
$Am_{(c)}$	1 Am^{3+} + 1.5 H_2O ⇌ 1 $Am_{(c)}$ + 3 H^+ + 0.75 $O_{2(aq)}$	0	-169.35	-	Van't Hoff
$Am(OH)_{3(am)}$	1 Am^{3+} + 3 H_2O ⇌ 1 $Am(OH)_{3(am)}$ + 3 H^+	-1213.08	-17	1.03	None
$Am(OH)_{3(c)}$	1 Am^{3+} + 3 H_2O ⇌ 1 $Am(OH)_{3(c)}$ + 3 H^+	-1223.36	-15.2	1.03	None
$Am_2(CO_3)_{3(c)}$	2 Am^{3+} + 3 HCO_3^- ⇌ 1 $Am_2(CO_3)_{3(c)}$ + 3 H^+	-2971.74	2.42	2.77	None
$Am_2C_{3(c)}$	2 Am^{3+} + 3 HCO_3^- ⇌ 1 $Am_2C_{3(c)}$ + 4.5 $O_{2(aq)}$ + 3 H^+	-156.06	-503.76	7.43	Van't Hoff
$Am_2O_{3(c)}$	2 Am^{3+} + 3 H_2O ⇌ 1 $Am_2O_{3(c)}$ + 6 H^+	-1613.32	-51.77	1.62	Van't Hoff
$AmBr_{3(c)}$	1 Am^{3+} + 3 Br^- ⇌ 1 $AmBr_{3(c)}$	-786.53	-21.67	1.97	Van't Hoff
$AmCl_{3(c)}$	1 Am^{3+} + 3 Cl^- ⇌ 1 $AmCl_{3(c)}$	-910.65	-14.31	0.40	Van't Hoff
$AmCO_3OH_{(c)}$	1 Am^{3+} + 1 HCO_3^- + 1 H_2O ⇌ 1 $AmCO_3OH_{(c)}$ + 2 H^+	-1404.83	-3.13	1.63	None
$AmF_{3(c)}$	1 Am^{3+} + 3 F^- ⇌ 1 $AmF_{3(c)}$	-1518.83	13.24	2.29	Van't Hoff
$AmF_{4(c)}$	1 Am^{4+} + 4 F^- ⇌ 1 $AmF_{4(c)}$	-1616.83	25.29	3.83	Van't Hoff
$AmH_{2(c)}$	1 Am^{2+} + 2 H_2O ⇌ 1 $AmH_{2(c)}$ + 1 $O_{2(aq)}$ + 2 H^+	-134.66	-128.37	3.75	Van't Hoff
$AmI_{3(c)}$	1 Am^{3+} + 3 I^- ⇌ 1 $AmI_{3(c)}$	-613.31	-24.62	1.61	Van't Hoff
$AmO_{2(c)}$	1 Am^{4+} + 2 H_2O ⇌ 1 $AmO_{2(c)}$ + 4 H^+	-874.49	9.43	1.70	Van't Hoff
$AmOBr_{(c)}$	1 Am^{3+} + 1 Br^- + 1 H_2O ⇌ 1 $AmOBr_{(c)}$ + 2 H^+	-861.37	-13.72	2.35	Van't Hoff

Appendix A Conversion of the OECD-NEA database to Chess format

Mineral species	Equilibrium equation	$\Delta_f G_m^0$ / kJ mol^{-1}	log K	log K uncertainty	Temperature dependency estimation
$AmOCl_{(c)}$	$1\ Am^{3+} + 1\ Cl^- + 1\ H_2O \rightleftharpoons 1\ AmOCl_{(c)} + 2\ H^+$	-902.54	-11.3	1.18	Van't Hoff
$As_{(c)}$	$1\ H_2AsO_4^- + 1\ H^+ \rightleftharpoons 1\ As_{(c)} + 1.25\ O_{2\,(aq)} + 1.5\ H_2O$	0	-73.22	0.00	Van't Hoff
$As_2O_{5\,(c)}$	$2\ H_2AsO_4^- + 2\ H^+ \rightleftharpoons 1\ As_2O_{5\,(c)} + 3\ H_2O$	-782.45	-2.2	1.40	Van't Hoff
$As_4O_{6\,(cubi)}$	$4\ H_2AsO_3^- + 4\ H^+ \rightleftharpoons 1\ As_4O_{6\,(cubi)} + 6\ H_2O$	-1152.44	39.76	3.97	Van't Hoff
$As_4O_{6\,(mono)}$	$4\ H_2AsO_3^- + 4\ H^+ \rightleftharpoons 1\ As_4O_{6\,(mono)} + 6\ H_2O$	-1154.01	40.04	3.97	Van't Hoff
$B_{(c)}$	$1\ B(OH)_{3\,(aq)} \rightleftharpoons 1\ B_{(c)} + 0.75\ O_{2\,(aq)} + 1.5\ H_2O$	0	-109.64	-	Van't Hoff
$B(OH)_{3\,(c)}$	$1\ B(OH)_{3\,(aq)} \rightleftharpoons 1\ B(OH)_{3\,(c)}$	-969.67	0.07	0.14	Van't Hoff
$B_2O_{3\,(c)}$	$2\ B(OH)_{3\,(aq)} \rightleftharpoons 1\ B_2O_{3\,(c)} + 3\ H_2O$	-1194.32	-5.75	0.25	Van't Hoff
$Ba_{(c)}$	$1\ Ba^{2+} + 1\ H_2O \rightleftharpoons 1\ Ba_{(c)} + 2\ H^+ + 0.5\ O_{2\,(aq)}$	0	-140.67	0.00	Van't Hoff
$Ba_2U_2O_{7\,(c)}$	$2\ Ba^{2+} + 2\ UO_2^+ + 3\ H_2O \rightleftharpoons 1\ Ba_2U_2O_{7\,(c)} + 6\ H^+$	-3547.02	-35.35	1.49	Van't Hoff
$Ba_3UO_{6\,(c)}$	$3\ Ba^{2+} + 1\ UO_2^{2+} + 4\ H_2O \rightleftharpoons 1\ Ba_3UO_{6\,(c)} + 8\ H^+$	-3044.95	-92.7	1.61	Van't Hoff
$BaCl_{2\,(c)}$	$1\ Ba^{2+} + 2\ Cl^- \rightleftharpoons 1\ BaCl_{2\,(c)}$	-806.95	-2.3	0.44	Van't Hoff
$BaO_{(c)}$	$1\ Ba^{2+} + 1\ H_2O \rightleftharpoons 1\ BaO_{(c)} + 2\ H^+$	-520.39	-48.07	0.44	Van't Hoff
$BaU_2O_{7\,(c)}$	$1\ Ba^{2+} + 2\ UO_2^{2+} + 3\ H_2O \rightleftharpoons 1\ BaU_2O_{7\,(c)} + 6\ H^+$	-3052.09	-21.39	1.18	Van't Hoff
$BaUO_{4\,(c)}$	$1\ Ba^{2+} + 1\ UO_2^{2+} + 2\ H_2O \rightleftharpoons 1\ BaUO_{4\,(c)} + 4\ H^+$	-1883.81	-17.64	0.59	Van't Hoff
$Br_2(l)$	$2\ Br^- + 2\ H^+ + 0.5\ O_{2\,(aq)} \rightleftharpoons 1\ Br_2(l) + 1\ H_2O$	0	6.59	0.00	Van't Hoff
$C_{(c)}$	$1\ HCO_3^- + 1\ H^+ \rightleftharpoons 1\ C_{(c)} + 1\ H_2O + 1\ O_{2\,(aq)}$	0	-64.13	0.00	Van't Hoff
$Ca_{(c)}$	$1\ Ca^{2+} + 1\ H_2O \rightleftharpoons 1\ Ca_{(c)} + 2\ H^+ + 0.5\ O_{2\,(aq)}$	0	-139.82	-	Van't Hoff
$CaO_{(c)}$	$1\ Ca^{2+} + 1\ H_2O \rightleftharpoons 1\ CaO_{(c)} + 2\ H^+$	-603.3	-32.7	0.16	Van't Hoff
$CaUO_{4\,(c)}$	$1\ Ca^{2+} + 1\ UO_2^{2+} + 2\ H_2O \rightleftharpoons 1\ CaUO_{4\,(c)} + 4\ H^+$	-1888.71	-15.93	0.42	Van't Hoff
$Cd_{(c)}$	$1\ Cd^{2+} + 1\ H_2O \rightleftharpoons 1\ Cd_{(c)} + 2\ H^+ + 0.5\ O_{2\,(aq)}$	0	-56.6	-	Van't Hoff
$CdO_{(c)}$	$1\ Cd^{2+} + 1\ H_2O \rightleftharpoons 1\ CdO_{(c)} + 2\ H^+$	-228.66	-15.1	0.11	Van't Hoff
$CdSO_4{\cdot}2.667H_2O_{(c)}$	$1\ Cd^{2+} + 1\ SO_4^{2-} + 2.667\ H_2O \rightleftharpoons 1\ CdSO_4{\cdot}2.667H_2O_{(c)}$	-1464.96	1.89	0.14	Van't Hoff
$Cs_{(c)}$	$1\ Cs^+ + 0.5\ H_2O \rightleftharpoons 1\ Cs_{(c)} + 1\ H^+ + 0.25\ O_{2\,(aq)}$	0	-72.55	-	Van't Hoff
$Cs_2NaAmCl_{6\,(c)}$	$1\ Am^{3+} + 2\ Cs^+ + 1\ Na^+ + 6\ Cl^- \rightleftharpoons 1\ Cs_2NaAmCl_{6\,(c)}$	-2164.82	-11.57	0.85	Van't Hoff
$Cs_2NaPuCl_{6\,(c)}$	$2\ Cs^+ + 1\ Na^+ + 1\ Pu^{3+} + 6\ Cl^- \rightleftharpoons 1\ Cs_2NaPuCl_{6\,(c)}$	-2143.5	-11.85	1.02	Van't Hoff
$Cs_2NpBr_{6\,(c)}$	$2\ Cs^+ + 1\ Np^{4+} + 6\ Br^- \rightleftharpoons 1\ Cs_2NpBr_{6\,(c)}$	-1620.12	-13.61	1.17	Van't Hoff
$Cs_2NpCl_{6\,(c)}$	$2\ Cs^+ + 1\ Np^{4+} + 6\ Cl^- \rightleftharpoons 1\ Cs_2NpCl_{6\,(c)}$	-1833.04	-5.07	1.30	Van't Hoff
$Cs_2PuBr_{6\,(c)}$	$2\ Cs^+ + 1\ Pu^{4+} + 6\ Br^- \rightleftharpoons 1\ Cs_2PuBr_{6\,(c)}$	-1634.33	-8.7	1.08	Van't Hoff
$Cs_2PuCl_{6\,(c)}$	$2\ Cs^+ + 1\ Pu^{4+} + 6\ Cl^- \rightleftharpoons 1\ Cs_2PuCl_{6\,(c)}$	-1838.24	-1.75	1.18	Van't Hoff
$Cs_2U_2O_{7\,(c)}$	$2\ Cs^+ + 3\ H_2O + 2\ UO_2^{2+} \rightleftharpoons 1\ Cs_2U_2O_{7\,(c)} + 6\ H^+$	-3022.88	-30.93	1.75	Van't Hoff
$Cs_2U_4O_{12\,(c)}$	$2\ Cs^+ + 2\ UO_2^+ + 2\ UO_2^{2+} + 4\ H_2O \rightleftharpoons 1\ Cs_2U_4O_{12\,(c)} + 8\ H^+$	-5251.06	-18.84	0.88	Van't Hoff

Appendix A Conversion of the OECD-NEA database to Chess format

Mineral species	Equilibrium equation	$\Delta_f G_m^0$ / kJ mol^{-1}	log K	log K uncertainty	Temperature dependency estimation
$Cs_2UO_{4\,(c)}$	$2\ Cs^+ + 1\ UO_2^{2+} + 2\ H_2O \rightleftharpoons 1\ Cs_2UO_{4\,(c)} + 4\ H^+$	-1805.37	-35.8	0.22	Van't Hoff
$Cs_3PuCl_{6\,(c)}$	$3\ Cs^+ + 1\ Pu^{3+} + 6\ Cl^- \rightleftharpoons 1\ Cs_3PuCl_{6\,(c)}$	-2208.04	-5.71	1.73	Van't Hoff
$CsBr_{\,(c)}$	$1\ Cs^+ + 1\ Br^- \rightleftharpoons 1\ CsBr_{\,(c)}$	-391.17	-0.72	0.05	Van't Hoff
$CsCl_{\,(c)}$	$1\ Cs^+ + 1\ Cl^- \rightleftharpoons 1\ CsCl_{\,(c)}$	-413.81	-1.55	0.04	Van't Hoff
$CsPu_2Cl_{7\,(c)}$	$1\ Cs^+ + 2\ Pu^{3+} + 7\ Cl^- \rightleftharpoons 1\ CsPu_2Cl_{7\,(c)}$	-2235.12	-23.27	1.32	Van't Hoff
$CsTcO_{4\,(c)}$	$1\ Cs^+ + 1\ TcO_4^- \rightleftharpoons 1\ CsTcO_{4\,(c)}$	-949.7	3.65	1.34	None
$Cu_{\,(c)}$	$1\ Cu^{2+} + 1\ H_2O \rightleftharpoons 1\ Cu_{\,(c)} + 2\ H^+ + 0.5\ O_{2\,(aq)}$	0	-31.58	-	Van't Hoff
$CuSO_{4\,(c)}$	$1\ Cu^{2+} + 1\ SO_4^{2-} \rightleftharpoons 1\ CuSO_{4\,(c)}$	-662.19	-2.94	0.21	Van't Hoff
Hg(l)	$1\ Hg^{2+} + 1\ H_2O \rightleftharpoons 1\ Hg(l) + 2\ H^+ + 0.5\ O_{2\,(aq)}$	0	-14.13	0.00	Van't Hoff
$Hg_2Cl_{2\,(c)}$	$1\ Hg_2^{2+} + 2\ Cl^- \rightleftharpoons 1\ Hg_2Cl_{2\,(c)}$	-210.73	17.84	0.13	Van't Hoff
$Hg_2SO_{4\,(c)}$	$1\ Hg_2^{2+} + 1\ SO_4^{2-} \rightleftharpoons 1\ Hg_2SO_{4\,(c)}$	-625.78	6.19	0.12	Van't Hoff
HgO(mont)	$1\ Hg^{2+} + 1\ H_2O \rightleftharpoons 1\ HgO(mont) + 2\ H^+$	-58.52	-2.44	0.03	Van't Hoff
$I_{2\,(c)}$	$2\ I^- + 2\ H^+ + 0.5\ O_{2\,(aq)} \rightleftharpoons 1\ I_{2\,(c)} + 1\ H_2O$	0	24.85	0.00	Van't Hoff
$K_{\,(c)}$	$1\ K^+ + 0.5\ H_2O \rightleftharpoons 1\ K_{\,(c)} + 1\ H^+ + 0.25\ O_{2\,(aq)}$	0	-70.98	-	Van't Hoff
$K_2UO_{4\,(c)}$	$2\ K^+ + 1\ UO_2^{2+} + 2\ H_2O \rightleftharpoons 1\ K_2UO_{4\,(c)} + 4\ H^+$	-1798.5	-33.87	0.57	Van't Hoff
$K_4NpO_2(CO_3)_{3\,(s)}$	$4\ K^+ + 1\ NpO_2^{2+} + 3\ HCO_3^- \rightleftharpoons 1\ K_4NpO_2(CO_3)_{3\,(s)} + 3\ H^+$	-3660.4	-4.57	1.66	None
$KTcO_{4\,(c)}$	$1\ K^+ + 1\ TcO_4^- \rightleftharpoons 1\ KTcO_{4\,(c)}$	-932.92	2.28	1.33	Van't Hoff
$Li_{\,(c)}$	$1\ Li^+ + 0.5\ H_2O \rightleftharpoons 1\ Li_{\,(c)} + 1\ H^+ + 0.25\ O_{2\,(aq)}$	0	-72.81	-	Van't Hoff
$Li_2UO_{4\,(c)}$	$2\ Li^+ + 1\ UO_2^{2+} + 2\ H_2O \rightleftharpoons 1\ Li_2UO_{4\,(c)} + 4\ H^+$	-1853.19	-27.94	0.39	Van't Hoff
$Mg_{\,(c)}$	$1\ Mg^{2+} + 1\ H_2O \rightleftharpoons 1\ Mg_{\,(c)} + 2\ H^+ + 0.5\ O_{2\,(aq)}$	0	-122.76	-	Van't Hoff
$MgF_{2\,(c)}$	$1\ Mg^{2+} + 2\ F^- \rightleftharpoons 1\ MgF_{2\,(c)}$	-1071.05	9.22	0.21	Van't Hoff
$MgO_{\,(c)}$	$1\ Mg^{2+} + 1\ H_2O \rightleftharpoons 1\ MgO_{\,(c)} + 2\ H^+$	-569.31	-21.58	0.05	Van't Hoff
$MgUO_{4\,(c)}$	$1\ Mg^{2+} + 1\ UO_2^{2+} + 2\ H_2O \rightleftharpoons 1\ MgUO_{4\,(c)} + 4\ H^+$	-1749.6	-23.23	0.26	Van't Hoff
$Na_{\,(c)}$	$1\ Na^+ + 0.5\ H_2O \rightleftharpoons 1\ Na_{\,(c)} + 1\ H^+ + 0.25\ O_{2\,(aq)}$	0	-67.38	-	Van't Hoff
$Na_2U_2O_{7\,(c)}$	$2\ Na^+ + 2\ UO_2^{2+} + 3\ H_2O \rightleftharpoons 1\ Na_2U_2O_{7\,(c)} + 6\ H^+$	-3011.45	-22.6	0.70	Van't Hoff
$Na_2UO_{4\,(alpha)}$	$2\ Na^+ + 1\ UO_2^{2+} + 2\ H_2O \rightleftharpoons 1\ Na_2UO_{4\,(alpha)} + 4\ H^+$	-1779.3	-30.03	0.61	Van't Hoff
$Na_3NpF_{8\,(c)}$	$3\ Na^+ + 1\ NpO_2^+ + 8\ F^- + 4\ H^+ \rightleftharpoons 1\ Na_3NpF_{8\,(c)} + 2\ H_2O$	-3521.24	8.71	3.73	Van't Hoff
$Na_3NpO_2(CO_3)_{2\,(s)}$	$3\ Na^+ + 2\ HCO_3^- + 1\ NpO_2^+ \rightleftharpoons 1\ Na_3NpO_2(CO_3)_{2\,(s)} + 2\ H^+$	-2833.33	-5.95	1.20	None
$Na_3UO_{4\,(c)}$	$3\ Na^+ + 1\ UO_2^+ + 2\ H_2O \rightleftharpoons 1\ Na_3UO_{4\,(c)} + 4\ H^+$	-1899.91	-56.28	1.44	Van't Hoff
$Na_4UO_2(CO_3)_{3\,(c)}$	$4\ Na^+ + 1\ UO_2^{2+} + 3\ HCO_3^- \rightleftharpoons 1\ Na_4UO_2(CO_3)_{3\,(c)} + 3\ H^+$	-3737.84	-4.04	0.41	None
$NaNpO_2CO_{3\,(s,aged)}$	$1\ Na^+ + 1\ NpO_2^+ + 1\ HCO_3^- \rightleftharpoons 1\ NaNpO_2CO_{3\,(s,aged)} + 1\ H^+$	-1764.16	1.33	1.11	None
$NaNpO_2CO_3{\cdot}3.5H_2O_{\,(s)}$	$1\ Na^+ + 1\ NpO_2^+ + 1\ HCO_3^- + 3.5\ H_2O \rightleftharpoons 1\ NaNpO_2CO_3{\cdot}3.5H_2O_{\,(s)} + 1\ H^+$	-2591.29	0.83	1.05	None

Appendix A Conversion of the OECD-NEA database to Chess format

Mineral species	Equilibrium equation	$\Delta_f G_m^0$ / kJ mol^{-1}	log K	log K uncertainty	Temperature dependency estimation
$NaTcO_4{\cdot}4H_2O_{(s)}$	$1\ Na^+ + 1\ TcO_4^- + 4\ H_2O \rightleftharpoons 1\ NaTcO_4{\cdot}4H_2O_{(s)}$	-1843.41	-0.79	1.34	None
$NaUO_{3\ (c)}$	$1\ UO_2^+ + 1\ Na^+ + 1\ H_2O \rightleftharpoons 1\ NaUO_{3\ (c)} + 2\ H^+$	-1412.49	-8.34	0.42	Van't Hoff
$NH_4TcO_{4\ (c)}$	$1\ H^+ + 1\ NH_{3\ (aq)} + 1\ TcO_4^- \rightleftharpoons 1\ NH_4TcO_{4\ (c)}$	-722	10.15	1.34	None
$Np_{(c)}$	$1\ Np^{3+} + 1.5\ H_2O \rightleftharpoons 1\ Np_{(c)} + 3\ H^+ + 0.75\ O_{2\ (aq)}$	0	-154.32	-	Van't Hoff
$Np_2C_{3\ (c)}$	$2\ Np^{3+} + 3\ HCO_3^- \rightleftharpoons 1\ Np_2C_{3\ (c)} + 3\ H^+ + 4.5\ O_{2\ (aq)}$	-192.43	-467.32	3.94	Van't Hoff
$Np_2O_{5\ (c)}$	$2\ NpO_2^+ + 1\ H_2O \rightleftharpoons 1\ Np_2O_{5\ (c)} + 2\ H^+$	-2031.57	-3.7	1.97	Constant heat capacity
$NpBr_{3\ (c)}$	$1\ Np^{3+} + 3\ Br^- \rightleftharpoons 1\ NpBr_{3\ (c)}$	-705.52	-20.83	1.19	Van't Hoff
$NpBr_{4\ (c)}$	$1\ Np^{4+} + 4\ Br^- \rightleftharpoons 1\ NpBr_{4\ (c)}$	-737.84	-29.67	1.15	Van't Hoff
$NpC_{0.91\ (c)}$	$1\ Np^{3+} + 0.91\ HCO_3^- + 0.59\ H_2O \rightleftharpoons 1\ NpC_{0.91\ (c)} + 2.09\ H^+ + 1.66\ O_{2\ (aq)}$	-76.02	-199.36	2.02	Van't Hoff
$NpCl_{3\ (c)}$	$1\ Np^{3+} + 3\ Cl^- \rightleftharpoons 1\ NpCl_{3\ (c)}$	-829.81	-13.44	1.14	Van't Hoff
$NpCl_{4\ (c)}$	$1\ Np^{4+} + 4\ Cl^- \rightleftharpoons 1\ NpCl_{4\ (c)}$	-895.56	-21.21	1.11	Van't Hoff
$NpF_{3\ (c)}$	$1\ Np^{3+} + 3\ F^- \rightleftharpoons 1\ NpF_{3\ (c)}$	-1460.5	18.06	1.76	Van't Hoff
$NpF_{4\ (c)}$	$1\ Np^{4+} + 4\ F^- \rightleftharpoons 1\ NpF_{4\ (c)}$	-1783.8	29.07	2.98	Van't Hoff
$NpF_{5\ (c)}$	$1\ NpO_2^+ + 5\ F^- + 4\ H^+ \rightleftharpoons 1\ NpF_{5\ (c)} + 2\ H_2O$	-1834.43	-1.17	4.45	Van't Hoff
$NpF_{6\ (c)}$	$1\ NpO_2^{2+} + 6\ F^- + 4\ H^+ \rightleftharpoons 1\ NpF_{6\ (c)} + 2\ H_2O$	-1841.87	-29.59	3.64	Van't Hoff
$NpI_{3\ (c)}$	$1\ Np^{3+} + 3\ I^- \rightleftharpoons 1\ NpI_{3\ (c)}$	-512.5	-27.25	1.19	Van't Hoff
$NpN_{(c)}$	$1\ Np^{3+} + 1\ NH_{3\ (aq)} \rightleftharpoons 1\ NpN_{(c)} + 3\ H^+$	-270.04	-47.21	1.33	Van't Hoff
$NpO_{2\ (am,hyd)}$	$1\ Np^{4+} + 2\ H_2O \rightleftharpoons 1\ NpO_{2\ (am,hyd)} + 4\ H^+$	-957.32	-1.53	1.71	None
$NpO_{2\ (c)}$	$1\ Np^{4+} + 2\ H_2O \rightleftharpoons 1\ NpO_{2\ (c)} + 4\ H^+$	-1021.73	9.75	1.07	Van't Hoff
$NpO_2(NO_3)_2{\cdot}6H_2O_{(s)}$	$1\ NpO_2^{2+} + 2\ NO_3^- + 6\ H_2O \rightleftharpoons 1\ NpO_2(NO_3)_2{\cdot}6H_2O_{(s)}$	-2428.07	-2.15	1.38	Van't Hoff
$NpO_2(OH)_{2\ (c)}$	$1\ NpO_2^{2+} + 2\ H_2O \rightleftharpoons 1\ NpO_2(OH)_{2\ (c)} + 2\ H^+$	-1239	-5.47	1.49	Van't Hoff
$NpO_2CO_{3\ (s)}$	$1\ NpO_2^{2+} + 1\ HCO_3^- \rightleftharpoons 1\ NpO_2CO_{3\ (s)} + 1\ H^+$	-1407.16	4.27	1.47	None
$NpO_2OH_{(am,aged)}$	$1\ NpO_2^+ + 1\ H_2O \rightleftharpoons 1\ NpO_2OH_{(am,aged)} + 1\ H^+$	-1118.08	-4.7	1.11	Constant heat capacity
$NpO_2OH_{(am,fresh)}$	$1\ NpO_2^+ + 1\ H_2O \rightleftharpoons 1\ NpO_2OH_{(am,fresh)} + 1\ H^+$	-1114.65	-5.3	1.01	Constant heat capacity
$NpO_3{\cdot}H_2O_{(c)}$	$1\ NpO_2^{2+} + 2\ H_2O \rightleftharpoons 1\ NpO_3{\cdot}H_2O_{(c)} + 2\ H^+$	-1239	-5.47	1.45	None
$NpOBr_{2\ (c)}$	$1\ Np^{4+} + 2\ Br^- + 1\ H_2O \rightleftharpoons 1\ NpOBr_{2\ (c)} + 2\ H^+$	-906.93	-5.2	2.17	Van't Hoff
$NpOCl_{2\ (c)}$	$1\ Np^{4+} + 2\ Cl^- + 1\ H_2O \rightleftharpoons 1\ NpOCl_{2\ (c)} + 2\ H^+$	-960.65	-5.38	1.73	Van't Hoff
$P_{(c)}$	$1\ HPO_4^{2-} + 2\ H^+ \rightleftharpoons 1\ P_{(c)} + 1.5\ H_2O + 1.25\ O_{2\ (aq)}$	0	-133.27	-	Van't Hoff
$Pb_{(c)}$	$1\ Pb^{2+} + 1\ H_2O \rightleftharpoons 1\ Pb_{(c)} + 2\ H^+ + 0.5\ O_{2\ (aq)}$	0	-47.22	-	Van't Hoff
$PbSO_{4\ (c)}$	$1\ Pb^{2+} + 1\ SO_4^{2-} \rightleftharpoons 1\ PbSO_{4\ (c)}$	-813.04	7.85	0.08	Van't Hoff
$Pu_{(c)}$	$1\ Pu^{3+} + 1.5\ H_2O \rightleftharpoons 1\ Pu_{(c)} + 3\ H^+ + 0.75\ O_{2\ (aq)}$	0	-165.9	-	Van't Hoff
$Pu(HPO_4)_{2\ (am,hyd)}$	$1\ Pu^{4+} + 2\ HPO_4^{2-} \rightleftharpoons 1\ Pu(HPO_4)_{2\ (am,hyd)}$	-2843.77	30.45	0.89	None

Appendix A Conversion of the OECD-NEA database to Chess format

Mineral species	Equilibrium equation	$\Delta_f G_m^0$ / kJ mol^{-1}	log K	log K uncertainty	Temperature dependency estimation
$Pu(OH)_{3\,(c)}$	$1\ Pu^{3+} + 3\ H_2O \rightleftharpoons 1\ Pu(OH)_{3\,(c)} + 3\ H^+$	-1200.22	-15.8	1.64	None
$Pu_2C_{3\,(c)}$	$2\ Pu^{3+} + 3\ HCO_3^- \rightleftharpoons 1\ Pu_2C_{3\,(c)} + 3\ H^+ + 4.5\ O_{2\,(aq)}$	-156.51	-496.77	3.08	Van't Hoff
$Pu_2O_{3\,(c)}$	$2\ Pu^{3+} + 3\ H_2O \rightleftharpoons 1\ Pu_2O_{3\,(c)} + 6\ H^+$	-1580.37	-50.63	1.99	Van't Hoff
$Pu_3C_{2\,(c)}$	$3\ Pu^{3+} + 2\ HCO_3^- + 2.5\ H_2O \rightleftharpoons 1\ Pu_3C_{2\,(c)} + 7\ H^+ + 4.25\ O_{2\,(aq)}$	-123.48	-604.33	5.45	Van't Hoff
$PuAs_{\,(c)}$	$1\ Pu^{3+} + 1\ H_2AsO_3^- \rightleftharpoons 1\ PuAs_{\,(c)} + 2\ H^+ + 1.5\ O_{2\,(aq)}$	-241.41	-166.29	3.62	Van't Hoff
$PuBr_{3\,(c)}$	$1\ Pu^{3+} + 3\ Br^- \rightleftharpoons 1\ PuBr_{3\,(c)}$	-767.32	-21.59	0.67	Van't Hoff
$PuC_{0.84\,(c)}$	$1\ Pu^{3+} + 0.84\ HCO_3^- + 0.66\ H_2O \rightleftharpoons 1\ PuC_{0.84\,(c)} + 2.16\ H^+ + 1.59\ O_{2\,(aq)}$	-49.83	-211.04	1.48	Van't Hoff
$PuCl_{3\,(c)}$	$1\ Pu^{3+} + 3\ Cl^- \rightleftharpoons 1\ PuCl_{3\,(c)}$	-891.81	-14.16	0.59	Van't Hoff
$PuCl_3{\cdot}6H_2O_{\,(c)}$	$1\ Pu^{3+} + 3\ Cl^- + 6\ H_2O \rightleftharpoons 1\ PuCl_3{\cdot}6H_2O_{\,(c)}$	-2365.35	-5.28	0.65	Van't Hoff
$PuCl_{4\,(c)}$	$1\ Pu^{4+} + 4\ Cl^- \rightleftharpoons 1\ PuCl_{4\,(c)}$	-879.37	-21.63	1.02	Van't Hoff
$PuF_{3\,(c)}$	$1\ Pu^{3+} + 3\ F^- \rightleftharpoons 1\ PuF_{3\,(c)}$	-1517.37	16.44	0.80	Van't Hoff
$PuF_{4\,(c)}$	$1\ Pu^{4+} + 4\ F^- \rightleftharpoons 1\ PuF_{4\,(c)}$	-1756.74	26.74	3.50	Van't Hoff
$PuF_{6\,(c)}$	$1\ PuO_2^{2+} + 6\ F^- + 4\ H^+ \rightleftharpoons 1\ PuF_{6\,(c)} + 2\ H_2O$	-1729.86	-43.33	3.57	Van't Hoff
$PuI_{3\,(c)}$	$1\ Pu^{3+} + 3\ I^- \rightleftharpoons 1\ PuI_{3\,(c)}$	-579	-27.18	0.93	Van't Hoff
$PuN_{\,(c)}$	$1\ Pu^{3+} + 1\ NH_{3\,(aq)} \rightleftharpoons 1\ PuN_{\,(c)} + 3\ H^+$	-273.72	-58.15	0.65	Van't Hoff
$PuO_{1.61\,(bcc)}$	$0.78\ Pu^{3+} + 0.22\ Pu^{4+} + 1.61\ H_2O \rightleftharpoons 1\ PuO_{1.61\,(bcc)} + 3.22\ H^+$	-834.77	-18.18	1.81	Van't Hoff
$PuO_{2\,(c)}$	$1\ Pu^{4+} + 2\ H_2O \rightleftharpoons 1\ PuO_{2\,(c)} + 4\ H^+$	-998.11	8.03	0.18	Van't Hoff
$PuO_{2\,(hyd,aged)}$	$1\ Pu^{4+} + 2\ H_2O \rightleftharpoons 1\ PuO_{2\,(hyd,aged)} + 4\ H^+$	-963.65	1.99	1.11	None
$PuO_2(NO_3)_2{\cdot}6H_2O_{\,(c)}$	$1\ PuO_2^{2+} + 2\ NO_3^- + 6\ H_2O \rightleftharpoons 1\ PuO_2(NO_3)_2{\cdot}6H_2O_{\,(c)}$	-2393.3	-2.36	0.75	None
$PuO_2(OH)_2{\cdot}H_2O_{\,(c)}$	$1\ PuO_2^{2+} + 3\ H_2O \rightleftharpoons 1\ PuO_2(OH)_2{\cdot}H_2O_{\,(c)} + 2\ H^+$	-1442.38	-5.5	1.22	Van't Hoff
$PuO_2CO_{3\,(s)}$	$1\ PuO_2^{2+} + 1\ HCO_3^- \rightleftharpoons 1\ PuO_2CO_{3\,(s)} + 1\ H^+$	-1371.31	3.87	0.76	None
$PuO_2OH_{\,(am)}$	$1\ PuO_2^{+} + 1\ H_2O \rightleftharpoons 1\ PuO_2OH_{\,(am)} + 1\ H^+$	-1061.25	-5	0.87	Van't Hoff
$PuOBr_{\,(c)}$	$1\ Pu^{3+} + 1\ Br^- + 1\ H_2O \rightleftharpoons 1\ PuOBr_{\,(c)} + 2\ H^+$	-838.35	-14.3	1.57	Van't Hoff
$PuOCl_{\,(c)}$	$1\ Pu^{3+} + 1\ Cl^- + 1\ H_2O \rightleftharpoons 1\ PuOCl_{\,(c)} + 2\ H^+$	-882.41	-11.38	0.58	Van't Hoff
$PuOF_{\,(c)}$	$1\ Pu^{3+} + 1\ F^- + 1\ H_2O \rightleftharpoons 1\ PuOF_{\,(c)} + 2\ H^+$	-1091.57	-1.06	3.57	Van't Hoff
$PuOI_{\,(c)}$	$1\ Pu^{3+} + 1\ I^- + 1\ H_2O \rightleftharpoons 1\ PuOI_{\,(c)} + 2\ H^+$	-776.63	-15.98	3.62	Van't Hoff
$PuP_{\,(c)}$	$1\ Pu^{3+} + 1\ HPO_4^{2-} \rightleftharpoons 1\ PuP_{\,(c)} + 1\ H^+ + 2\ O_{2\,(aq)}$	-313.76	-244.21	3.72	Van't Hoff
$PuPO_{4\,(s,hyd)}$	$1\ Pu^{3+} + 1\ HPO_4^{2-} \rightleftharpoons 1\ PuPO_{4\,(s,hyd)} + 1\ H^+$	-1744.89	12.25	1.08	None
$Rb_{\,(c)}$	$1\ Rb^+ + 0.5\ H_2O \rightleftharpoons 1\ Rb_{\,(c)} + 1\ H^+ + 0.25\ O_{2\,(aq)}$	0	-71.24	-	Van't Hoff
$Rb_2UO_{4\,(c)}$	$2\ Rb^+ + 1\ UO_2^{2+} + 2\ H_2O \rightleftharpoons 1\ Rb_2UO_{4\,(c)} + 4\ H^+$	-1800.14	-34.11	0.57	Van't Hoff
$S_{\,(c)}$	$1\ SO_4^{2-} + 2\ H^+ \rightleftharpoons 1\ S_{\,(c)} + 1\ H_2O + 1.5\ O_{2\,(aq)}$	0	-93.1	0.00	Van't Hoff
$Se_{\,(c)}$	$1\ SeO_3^{2-} + 2\ H^+ \rightleftharpoons 1\ Se_{\,(c)} + 1\ H_2O + 1\ O_{2\,(aq)}$	0	-24.67	0.00	None

Appendix A Conversion of the OECD-NEA database to Chess format

Mineral species	Equilibrium equation	$\Delta_f G_m^0$ / kJ mol^{-1}	log K	log K uncertainty	Temperature dependency estimation
$Si_{(c)}$	$1\ Si(OH)_{4\ (aq)} \rightleftharpoons 1\ Si_{(c)} + 2\ H_2O + 1\ O_{2\ (aq)}$	0	-148.88	-	Van't Hoff
$SiO_{2\ (quar)}$	$1\ Si(OH)_{4\ (aq)} \rightleftharpoons 1\ SiO_{2\ (quar)} + 2\ H_2O$	-856.29	4	0.18	Van't Hoff
$Sn_{(c)}$	$1\ Sn^{2+} + 1\ H_2O \rightleftharpoons 1\ Sn_{(c)} + 2\ H^+ + 0.5\ O_{2\ (aq)}$	0	-47.82	-	Van't Hoff
$SnO_{(tetr)}$	$1\ Sn^{2+} + 1\ H_2O \rightleftharpoons 1\ SnO_{(tetr)} + 2\ H^+$	-251.91	-2.25	0.04	Van't Hoff
$SnO_{2\ (cass)}$	$1\ Sn^{2+} + 1\ H_2O + 0.5\ O_{2\ (aq)} \rightleftharpoons 1\ SnO_{2\ (cass)} + 2\ H^+$	-515.83	45.42	0.04	Van't Hoff
$Sr_{(c)}$	$1\ Sr^{2+} + 1\ H_2O \rightleftharpoons 1\ Sr_{(c)} + 2\ H^+ + 0.5\ O_{2\ (aq)}$	0	-141.76	0.00	Van't Hoff
$Sr(NO_3)_{2\ (c)}$	$1\ Sr^{2+} + 2\ NO_3^- \rightleftharpoons 1\ Sr(NO_3)_{2\ (c)}$	-783.15	-0.4	0.18	Van't Hoff
$SrCl_{2\ (c)}$	$1\ Sr^{2+} + 2\ Cl^- \rightleftharpoons 1\ SrCl_{2\ (c)}$	-784.97	-7.24	0.13	Van't Hoff
$SrO_{(c)}$	$1\ Sr^{2+} + 1\ H_2O \rightleftharpoons 1\ SrO_{(c)} + 2\ H^+$	-559.94	-42.23	0.16	Van't Hoff
$SrUO_{4\ (alpha)}$	$1\ Sr^{2+} + 1\ UO_2^{2+} + 2\ H_2O \rightleftharpoons 1\ SrUO_{4\ (alpha)} + 4\ H^+$	-1881.36	-19.15	0.49	Van't Hoff
$Tc_{(c)}$	$1\ TcO_4^- + 1\ H^+ \rightleftharpoons 1\ Tc_{(c)} + 0.5\ H_2O + 1.75\ O_{2\ (aq)}$	0	-95.91	-	Constant heat capacity
$Tc_2O_{7\ (c)}$	$2\ TcO_4^- + 2\ H^+ \rightleftharpoons 1\ Tc_2O_{7\ (c)} + 1\ H_2O$	-950.28	-15.31	2.73	Constant heat capacity
$Tc_2O_7{\cdot}H_2O_{(s)}$	$2\ TcO_4^- + 2\ H^+ \rightleftharpoons 1\ Tc_2O_7{\cdot}H_2O_{(s)}$	-1194.3	-14.11	2.72	Van't Hoff
$TcO_{2\ (c)}$	$1\ TcO^{2+} + 1\ H_2O \rightleftharpoons 1\ TcO_{2\ (c)} + 2\ H^+$	-401.85	8.39	-	None
$TcO_{2.1}{\cdot}6H_2O_{(s)}$	$1\ TcO^{2+} + 2.6\ H_2O \rightleftharpoons 1\ TcO_{2.1}{\cdot}6H_2O_{(s)} + 2\ H^+$	-758.48	4.4	-	None
$TlTcO_{4\ (c)}$	$1\ Tl^+ + 1\ TcO_4^- \rightleftharpoons 1\ TlTcO_{4\ (c)}$	-700.17	5.32	1.34	None
$U_{(c)}$	$1\ UO_2^{2+} + 1\ H_2O \rightleftharpoons 1\ U_{(c)} + 2\ H^+ + 1.5\ O_{2\ (aq)}$	0	-212.72	0.00	Constant heat capacity
$U(HPO_4)_2{\cdot}4H_2O_{(c)}$	$1\ U^{4+} + 2\ HPO_4^{2-} + 4\ H_2O \rightleftharpoons 1\ U(HPO_4)_2{\cdot}4H_2O_{(c)}$	-3844.45	30.49	0.72	Van't Hoff
$U(OH)_2SO_{4\ (c)}$	$1\ U^{4+} + 1\ SO_4^{2-} + 2\ H_2O \rightleftharpoons 1\ U(OH)_2SO_{4\ (c)} + 2\ H^+$	-1766.22	3.17	0.67	None
$U(SO_3)_{2\ (c)}$	$1\ U^{4+} + 2\ SO_3^{2-} \rightleftharpoons 1\ U(SO_3)_{2\ (c)}$	-1712.83	36.44	3.98	None
$U(SO_4)_{2\ (c)}$	$1\ U^{4+} + 2\ SO_4^{2-} \rightleftharpoons 1\ U(SO_4)_{2\ (c)}$	-2084.52	11.68	2.48	Van't Hoff
$U(SO_4)_2{\cdot}4H_2O_{(c)}$	$1\ U^{4+} + 2\ SO_4^{2-} + 4\ H_2O \rightleftharpoons 1\ U(SO_4)_2{\cdot}4H_2O_{(c)}$	-3033.31	11.72	2.03	Van't Hoff
$U(SO_4)_2{\cdot}8H_2O_{(c)}$	$1\ U^{4+} + 2\ SO_4^{2-} + 8\ H_2O \rightleftharpoons 1\ U(SO_4)_2{\cdot}8H_2O_{(c)}$	-3987.9	12.77	2.95	Van't Hoff
$U_2C_{3\ (c)}$	$2\ U^{3+} + 3\ HCO_3^- \rightleftharpoons 1\ U_2C_{3\ (c)} + 3\ H^+ + 4.5\ O_{2\ (aq)}$	-189.32	-455.11	1.86	Van't Hoff
$U_2F_{9\ (c)}$	$1\ U^{4+} + 1\ UO_2^+ + 9\ F^- + 4\ H^+ \rightleftharpoons 1\ U_2F_{9\ (c)} + 2\ H_2O$	-3812	45.85	3.01	Van't Hoff
$U_2O_2Cl_{5\ (c)}$	$1\ U^{4+} + 1\ UO_2^+ + 5\ Cl^- \rightleftharpoons 1\ U_2O_2Cl_{5\ (c)}$	-2037.31	-19.21	0.96	Van't Hoff
$U_2O_3F_{6\ (c)}$	$2\ UO_2^{2+} + 6\ F^- + 2\ H^+ \rightleftharpoons 1\ U_2O_3F_{6\ (c)} + 1\ H_2O$	-3372.73	2.74	2.59	Van't Hoff
$U_2S_{3\ (c)}$	$2\ U^{3+} + 3\ HS^- \rightleftharpoons 1\ U_2S_{3\ (c)} + 3\ H^+$	-879.79	-6.38	11.81	Van't Hoff
$U_2Se_{3\ (c)}$	$2\ U^{3+} + 3\ SeO_3^{2-} \rightleftharpoons 1\ U_2Se_{3\ (c)} + 4.5\ O_{2\ (aq)}$	-721.19	-243.54	13.15	None
$U_3As_{4\ l}$	$3\ U^{3+} + 4\ H_2AsO_3^- \rightleftharpoons 1\ U_3As_{4\ l} + 5\ H^+ + 1.5\ H_2O + 5.25\ O_{2\ (aq)}$	-725.39	-487.47	4.33	Van't Hoff
$U_3O_5F_{8\ l}$	$3\ UO_2^{2+} + 8\ F^- + 2\ H^+ \rightleftharpoons 1\ U_3O_5F_{8\ l} + 1\ H_2O$	-4890.13	3.05	1.71	Van't Hoff
$U_3O_{8\ l}$	$2\ UO_2^+ + 1\ UO_2^{2+} + 2\ H_2O \rightleftharpoons 1\ U_3O_{8\ l} + 4\ H^+$	-3369.48	3.61	0.76	Van't Hoff

Appendix A Conversion of the OECD-NEA database to Chess format

Mineral species	Equilibrium equation	$\Delta_f G_m^0$ / kJ mol^{-1}	log K	log K uncertainty	Temperature dependency estimation
$U_3P_{4\ (c)}$	$3\ U^{3+} + 4\ HPO_4^{2-} \rightleftharpoons 1\ U_3P_{4\ (c)} + 1\ H^+ + 1.5\ H_2O + 7.25\ O_{2\ (aq)}$	-826.44	-832.13	4.66	Van't Hoff
$U_3S_{5\ (c)}$	$2\ U^{3+} + 1\ U^{4+} + 5\ HS^- \rightleftharpoons 1\ U_3S_{5\ (c)} + 5\ H^+$	-1425.08	0.61	17.68	Van't Hoff
$U_3Se_{4\ (c)}$	$3\ U^{3+} + 4\ SeO_3^{2-} + 0.5\ H_2O \rightleftharpoons 1\ U_3Se_{4\ (c)} + 1\ H^+ + 6.25\ O_{2\ (aq)}$	-988.76	-369.28	15.05	None
$U_3Se_{5\ (c)}$	$3\ U^{3+} + 5\ SeO_3^{2-} + 1\ H^+ \rightleftharpoons 1\ U_3Se_{5\ (c)} + 0.5\ H_2O + 7.25\ O_{2\ (aq)}$	-1130.61	-369.1	19.92	None
$U_4F_{17\ (c)}$	$1\ UO_2^+ + 3\ U^{4+} + 17\ F^- + 4\ H^+ \rightleftharpoons 1\ U_4F_{17\ (c)} + 2\ H_2O$	-7464	105.43	5.35	Van't Hoff
$U_5O_{12}Cl_{\ (c)}$	$5\ UO_2^+ + 1\ Cl^- + 2\ H_2O \rightleftharpoons 1\ U_5O_{12}Cl_{\ (c)} + 4\ H^+$	-5517.95	18.81	2.66	Van't Hoff
$UAs_{\ (c)}$	$1\ U^{3+} + 1\ H_2AsO_3^- \rightleftharpoons 1\ UAs_{\ (c)} + 2\ H^+ + 1.5\ O_{2\ (aq)}$	-237.91	-148.94	1.60	Van't Hoff
$UAs_{2\ (c)}$	$1\ U^{3+} + 2\ H_2AsO_3^- \rightleftharpoons 1\ UAs_{2\ (c)} + 1\ H^+ + 1.5\ H_2O + 2.25\ O_{2\ (aq)}$	-252.79	-189.02	2.70	Van't Hoff
$UBr_2Cl_{\ (c)}$	$1\ U^{3+} + 2\ Br^- + 1\ Cl^- \rightleftharpoons 1\ UBr_2Cl_{\ (c)}$	-714.39	-17.69	1.74	Van't Hoff
$UBr_2Cl_{2\ (c)}$	$1\ U^{4+} + 2\ Br^- + 2\ Cl^- \rightleftharpoons 1\ UBr_2Cl_{2\ (c)}$	-850.9	-26.12	1.74	Van't Hoff
$UBr_{3\ (c)}$	$1\ U^{3+} + 3\ Br^- \rightleftharpoons 1\ UBr_{3\ (c)}$	-673.2	-20.12	0.80	Van't Hoff
$UBr_3Cl_{\ (c)}$	$1\ U^{4+} + 1\ Cl^- + 3\ Br^- \rightleftharpoons 1\ UBr_3Cl_{\ (c)}$	-807.11	-29	1.74	Van't Hoff
$UBr_{4\ (c)}$	$1\ U^{4+} + 4\ Br^- \rightleftharpoons 1\ UBr_{4\ (c)}$	-767.48	-31.15	0.69	Van't Hoff
$UBr_{5\ (c)}$	$1\ UO_2^+ + 5\ Br^- + 4\ H^+ \rightleftharpoons 1\ UBr_{5\ (c)} + 2\ H_2O$	-769.31	-41.47	1.64	Van't Hoff
$UBrCl_{2\ (c)}$	$1\ U^{3+} + 1\ Br^- + 2\ Cl^- \rightleftharpoons 1\ UBrCl_{2\ (c)}$	-760.32	-14.44	1.74	Van't Hoff
$UBrCl_{3\ (c)}$	$1\ U^{4+} + 1\ Br^- + 3\ Cl^- \rightleftharpoons 1\ UBrCl_{3\ (c)}$	-893.5	-23.45	1.64	Van't Hoff
$UC_{\ (c)}$	$1\ U^{3+} + 1\ HCO_3^- + 0.5\ H_2O \rightleftharpoons 1\ UC_{\ (c)} + 2\ H^+ + 1.75\ O_{2\ (aq)}$	-98.9	-194.75	0.61	Van't Hoff
$UC_{1.94\ (alpha)}$	$1\ U^{3+} + 1.94\ HCO_3^- \rightleftharpoons 1\ UC_{1.94}\ (alpha) + 1.06\ H^+ + 0.44\ H_2O + 2.69\ O_{2\ (aq)}$	-87.4	-257.04	0.49	Van't Hoff
$UCl_2F_{2\ (c)}$	$1\ U^{4+} + 2\ Cl^- + 2\ F^- \rightleftharpoons 1\ UCl_2F_{2\ (c)}$	-1375.97	3.61	1.03	Van't Hoff
$UCl_2I_{2\ (c)}$	$1\ U^{4+} + 2\ Cl^- + 2\ I^- \rightleftharpoons 1\ UCl_2I_{2\ (c)}$	-723.36	-30.2	2.01	Van't Hoff
$UCl_{3\ (c)}$	$1\ U^{3+} + 3\ Cl^- \rightleftharpoons 1\ UCl_{3\ (c)}$	-796.1	-12.97	0.47	Van't Hoff
$UCl_3F_{\ (c)}$	$1\ U^{4+} + 3\ Cl^- + 1\ F^- \rightleftharpoons 1\ UCl_3F_{\ (c)}$	-1146.57	-10.24	0.95	Van't Hoff
$UCl_3I_{\ (c)}$	$1\ U^{4+} + 3\ Cl^- + 1\ I^- \rightleftharpoons 1\ UCl_3I_{\ (c)}$	-829.88	-25.47	1.57	Van't Hoff
$UCl_{4\ (c)}$	$1\ U^{4+} + 4\ Cl^- \rightleftharpoons 1\ UCl_{4\ (c)}$	-929.58	-21.93	0.54	Van't Hoff
$UCl_{5\ (c)}$	$1\ UO_2^+ + 5\ Cl^- + 4\ H^+ \rightleftharpoons 1\ UCl_{5\ (c)} + 2\ H_2O$	-930.12	-37.27	0.75	Van't Hoff
$UCl_{6\ (c)}$	$1\ UO_2^{2+} + 6\ Cl^- + 4\ H^+ \rightleftharpoons 1\ UCl_{6\ (c)} + 2\ H_2O$	-937.21	-57.53	0.53	Van't Hoff
$UClF_{3\ (c)}$	$1\ U^{4+} + 1\ Cl^- + 3\ F^- \rightleftharpoons 1\ UClF_{3\ (c)}$	-1606.36	17.64	0.95	Van't Hoff
$UClI_{3\ (c)}$	$1\ U^{4+} + 1\ Cl^- + 3\ I^- \rightleftharpoons 1\ UClI_{3\ (c)}$	-615.79	-35.12	2.01	Van't Hoff
$UF_{3\ (c)}$	$1\ U^{3+} + 3\ F^- \rightleftharpoons 1\ UF_{3\ (c)}$	-1432.53	19.53	0.88	Van't Hoff
$UF_{4\ (c)}$	$1\ U^{4+} + 4\ F^- \rightleftharpoons 1\ UF_{4\ (c)}$	-1823.54	29.36	0.80	Van't Hoff
$UF_{4.2}{\cdot}5H_2O_{\ (c)}$	$1\ U^{4+} + 4\ F^- + 2.5\ H_2O \rightleftharpoons 1\ UF_{4.2}{\cdot}5H_2O_{\ (c)}$	-2440.28	33.55	1.13	Van't Hoff
$UF_{5\ (alpha)}$	$1\ UO_2^+ + 5\ F^- + 4\ H^+ \rightleftharpoons 1\ UF_{5\ (alpha)} + 2\ H_2O$	-1968.69	13.02	1.26	Van't Hoff

Appendix A Conversion of the OECD-NEA database to Chess format

Mineral species	Equilibrium equation	$\Delta_f G_m^0$ / kJ mol^{-1}	log K	log K uncertainty	Temperature dependency estimation
$UF_{5\ (beta)}$	$1\ UO_2^{+} + 5\ F^{-} + 4\ H^{+} \rightleftharpoons 1\ UF_{5\ (beta)} + 2\ H_2O$	-1970.59	13.36	1.03	Van't Hoff
$UF_{6\ (c)}$	$1\ UO_2^{2+} + 6\ F^{-} + 4\ H^{+} \rightleftharpoons 1\ UF_{6\ (c)} + 2\ H_2O$	-2069.21	-17.2	0.32	Van't Hoff
$UH_{3\ (beta)}$	$1\ U^{3+} + 3\ H_2O \rightleftharpoons 1\ UH_{3\ (beta)} + 3\ H^{+} + 1.5\ O_{2\ (aq)}$	-72.56	-199.7	0.32	Constant heat capacity
$UI_{3\ (c)}$	$1\ U^{3+} + 3\ I^{-} \rightleftharpoons 1\ UI_{3\ (c)}$	-466.62	-28.91	0.91	Van't Hoff
$UI_{4\ (c)}$	$1\ U^{4+} + 4\ I^{-} \rightleftharpoons 1\ UI_{4\ (c)}$	-513.17	-39.17	0.74	Van't Hoff
$UN_{(c)}$	$1\ U^{3+} + 1\ NH_{3\ (aq)} \rightleftharpoons 1\ UN_{(c)} + 3\ H^{+}$	-265.08	-41.71	0.62	Van't Hoff
$UN_{1.59\ (alpha)}$	$1\ UO_2^{+} + 1.59\ NH_{3\ (aq)} \rightleftharpoons 1\ UN_{1.59\ (alpha)} + 1\ H^{+} + 1.885\ H_2O + 0.0575\ O_{2\ (aq)}$	-338.2	-38.39	0.97	Van't Hoff
$UN_{1.73\ (alpha)}$	$1\ UO_2^{+} + 1.73\ NH_{3\ (aq)} + 0.0475\ O_{2\ (aq)} \rightleftharpoons 1\ UN_{1.73\ (alpha)} + 1\ H^{+} + 2.095\ H_2O$	-353.75	-27.3	1.35	Van't Hoff
$UO_2(AsO_3)_{2\ (c)}$	$1\ UO_2^{2+} + 2\ H_2AsO_4^{-} \rightleftharpoons 1\ UO_2(AsO_3)_{2\ (c)} + 2\ H_2O$	-1944.91	-6.97	2.10	Van't Hoff
$UO_{2\ (c)}$	$1\ U^{4+} + 2\ H_2O \rightleftharpoons 1\ UO_{2\ (c)} + 4\ H^{+}$	-1031.83	4.85	0.36	Constant heat capacity
$UO_2(IO_3)_{2\ (c)}$	$1\ UO_2^{2+} + 2\ IO_3^{-} \rightleftharpoons 1\ UO_2(IO_3)_{2\ (c)}$	-1250.21	7.88	0.50	Van't Hoff
$UO_2(NO_3)_{2\ (c)}$	$1\ UO_2^{2+} + 2\ NO_3^{-} \rightleftharpoons 1\ UO_2(NO_3)_{2\ (c)}$	-1106.09	-11.92	0.99	Van't Hoff
$UO_2(NO_3)_2{\cdot}2H_2O_{\ (c)}$	$1\ UO_2^{2+} + 2\ NO_3^{-} + 2\ H_2O \rightleftharpoons 1\ UO_2(NO_3)_2{\cdot}2H_2O_{\ (c)}$	-1620.5	-4.89	0.35	Van't Hoff
$UO_2(NO_3)_2{\cdot}3H_2O_{\ (c)}$	$1\ UO_2^{2+} + 2\ NO_3^{-} + 3\ H_2O \rightleftharpoons 1\ UO_2(NO_3)_2{\cdot}3H_2O_{\ (c)}$	-1864.69	-3.66	0.34	Van't Hoff
$UO_2(NO_3)_2{\cdot}6H_2O_{\ (c)}$	$1\ UO_2^{2+} + 2\ NO_3^{-} + 6\ H_2O \rightleftharpoons 1\ UO_2(NO_3)_2{\cdot}6H_2O_{\ (c)}$	-2584.21	-2.24	0.28	Van't Hoff
$UO_2(NO_3)_2{\cdot}H_2O_{\ (c)}$	$1\ UO_2^{2+} + 2\ NO_3^{-} + 1\ H_2O \rightleftharpoons 1\ UO_2(NO_3)_2{\cdot}H_2O_{\ (c)}$	-1362.97	-8.46	1.84	Van't Hoff
$UO_2(OH)_{2\ (beta)}$	$1\ UO_2^{2+} + 2\ H_2O \rightleftharpoons 1\ UO_2(OH)_{2\ (beta)} + 2\ H^{+}$	-1398.68	-4.93	0.31	Constant heat capacity
$UO_{2.25\ (beta)}$	$0.5\ U^{4+} + 0.5\ UO_2^{+} + 1.25\ H_2O \rightleftharpoons 1\ UO_{2.25\ (beta)} + 2.5\ H^{+}$	-1069.08	4.77	0.37	Van't Hoff
$UO_{2.25\ (c)}$	$0.5\ U^{4+} + 0.5\ UO_2^{+} + 1.25\ H_2O \rightleftharpoons 1\ UO_{2.25\ (c)} + 2.5\ H^{+}$	-1069.13	4.78	0.37	Van't Hoff
$UO_{2.3333\ (beta)}$	$0.3334\ U^{4+} + 0.6666\ UO_2^{+} + 1.0001\ H_2O \rightleftharpoons 1\ UO_{2.3333\ (beta)} + 2.0002\ H^{+}$	-1080.57	4.58	0.34	Van't Hoff
$UO_{2.6667\ (c)}$	$0.6666\ UO_2^{+} + 0.3334\ UO_2^{2+} + 0.6667\ H_2O \rightleftharpoons 1\ UO_{2.6667\ (c)} + 1.3334\ H^{+}$	-1123.16	1.2	0.25	Van't Hoff
$UO_2Br_{2\ (c)}$	$1\ UO_2^{2+} + 2\ Br^{-} \rightleftharpoons 1\ UO_2Br_{2\ (c)}$	-1066.42	-16.44	0.32	Van't Hoff
$UO_2Br_2{\cdot}3H_2O_{\ (c)}$	$1\ UO_2^{2+} + 2\ Br^{-} + 3\ H_2O \rightleftharpoons 1\ UO_2Br_2{\cdot}3H_2O_{\ (c)}$	-1818.49	-9.32	0.98	Van't Hoff
$UO_2Br_2{\cdot}H_2O_{\ (c)}$	$1\ UO_2^{2+} + 2\ Br^{-} + 1\ H_2O \rightleftharpoons 1\ UO_2Br_2{\cdot}H_2O_{\ (c)}$	-1328.64	-12.04	0.44	Van't Hoff
$UO_2BrOH{\cdot}2H_2O_{\ (c)}$	$1\ UO_2^{2+} + 1\ Br^{-} + 3\ H_2O \rightleftharpoons 1\ UO_2BrOH{\cdot}2H_2O_{\ (c)} + 1\ H^{+}$	-1744.16	-4.15	0.77	Van't Hoff
$UO_2Cl_{\ (c)}$	$1\ UO_2^{+} + 1\ Cl^{-} \rightleftharpoons 1\ UO_2Cl_{\ (c)}$	-1095.25	0.53	1.50	Van't Hoff
$UO_2Cl_{2\ (c)}$	$1\ UO_2^{2+} + 2\ Cl^{-} \rightleftharpoons 1\ UO_2Cl_{2\ (c)}$	-1145.84	-12.11	0.23	Van't Hoff
$UO_2Cl_2{\cdot}3H_2O_{\ (c)}$	$1\ UO_2^{2+} + 2\ Cl^{-} + 3\ H_2O \rightleftharpoons 1\ UO_2Cl_2{\cdot}3H_2O_{\ (c)}$	-1894.62	-5.57	0.53	Van't Hoff
$UO_2Cl_2{\cdot}H_2O_{\ (c)}$	$1\ UO_2^{2+} + 2\ Cl^{-} + 1\ H_2O \rightleftharpoons 1\ UO_2Cl_2{\cdot}H_2O_{\ (c)}$	-1405	-8.26	0.57	Van't Hoff
$UO_2ClOH{\cdot}2H_2O_{\ (c)}$	$1\ UO_2^{2+} + 1\ Cl^{-} + 3\ H_2O \rightleftharpoons 1\ UO_2ClOH{\cdot}2H_2O_{\ (c)} + 1\ H^{+}$	-1782.22	-2.27	0.79	Van't Hoff
$UO_2CO_{3\ (c)}$	$1\ UO_2^{2+} + 1\ HCO_3^{-} \rightleftharpoons 1\ UO_2CO_{3\ (c)} + 1\ H^{+}$	-1563.16	4.16	0.32	Van't Hoff
$UO_2F_{2\ (c)}$	$1\ UO_2^{2+} + 2\ F^{-} \rightleftharpoons 1\ UO_2F_{2\ (c)}$	-1557.32	7.31	0.23	Van't Hoff

Appendix A Conversion of the OECD-NEA database to Chess format

Mineral species	Equilibrium equation	$\Delta_f G_m^0$ / kJ mol^{-1}	log K	log K uncertainty	Temperature dependency estimation
$UO_2F_2{\cdot}3H_2O_{(c)}$	$1\ UO_2^{2+} + 2\ F^- + 3\ H_2O \rightleftharpoons 1\ UO_2F_2{\cdot}3H_2O_{(c)}$	-2269.66	7.47	1.22	Van't Hoff
$UO_2FOH{\cdot}2H_2O_{(c)}$	$1\ UO_2^{2+} + 1\ F^- + 3\ H_2O \rightleftharpoons 1\ UO_2FOH{\cdot}2H_2O_{(c)} + 1\ H^+$	-1961.03	2.72	1.47	Van't Hoff
$UO_2FOH{\cdot}H_2O_{(c)}$	$1\ UO_2^{2+} + 1\ F^- + 2\ H_2O \rightleftharpoons 1\ UO_2FOH{\cdot}H_2O_{(c)} + 1\ H^+$	-1721.7	2.34	1.31	Van't Hoff
$UO_2HPO_4{\cdot}4H_2O_{(c)}$	$1\ UO_2^{2+} + 1\ HPO_4^{2-} + 4\ H_2O \rightleftharpoons 1\ UO_2HPO_4{\cdot}4H_2O_{(c)}$	-3064.75	11.85	0.42	Van't Hoff
$UO_2SO_{3\ (c)}$	$1\ UO_2^{2+} + 1\ SO_3^{2-} \rightleftharpoons 1\ UO_2SO_{3\ (c)}$	-1530.37	15.83	2.34	None
$UO_2SO_{4\ (c)}$	$1\ UO_2^{2+} + 1\ SO_4^{2-} \rightleftharpoons 1\ UO_2SO_{4\ (c)}$	-1685.78	-1.89	0.46	Van't Hoff
$UO_2SO_4{\cdot}2.5H_2O_{(c)}$	$1\ UO_2^{2+} + 1\ SO_4^{2-} + 2.5\ H_2O \rightleftharpoons 1\ UO_2SO_4{\cdot}2.5H_2O_{(c)}$	-2298.48	1.59	0.32	Van't Hoff
$UO_2SO_4{\cdot}3.5H_2O_{(c)}$	$1\ UO_2^{2+} + 1\ SO_4^{2-} + 3.5\ H_2O \rightleftharpoons 1\ UO_2SO_4{\cdot}3.5H_2O_{(c)}$	-2535.6	1.59	0.32	Van't Hoff
$UO_2SO_4{\cdot}3H_2O_{(c)}$	$1\ UO_2^{2+} + 1\ SO_4^{2-} + 3\ H_2O \rightleftharpoons 1\ UO_2SO_4{\cdot}3H_2O_{(c)}$	-2416.56	1.5	0.32	Van't Hoff
$UO_{3\ (alpha)}$	$1\ UO_2^{2+} + 1\ H_2O \rightleftharpoons 1\ UO_{3\ (alpha)} + 2\ H^+$	-1140.42	-8.63	0.53	Constant heat capacity
$UO_{3\ (beta)}$	$1\ UO_2^{2+} + 1\ H_2O \rightleftharpoons 1\ UO_{3\ (beta)} + 2\ H^+$	-1142.3	-8.3	0.23	Constant heat capacity
$UO_{3\ (gamma)}$	$1\ UO_2^{2+} + 1\ H_2O \rightleftharpoons 1\ UO_{3\ (gamma)} + 2\ H^+$	-1145.74	-7.7	0.21	Constant heat capacity
$UO_3{\cdot}0.9H_2O_{(alpha)}$	$1\ UO_2^{2+} + 1.9\ H_2O \rightleftharpoons 1\ UO_3{\cdot}0.9H_2O_{(alpha)} + 2\ H^+$	-1374.56	-5	0.43	Constant heat capacity
$UO_3{\cdot}2H_2O_{(c)}$	$1\ UO_2^{2+} + 3\ H_2O \rightleftharpoons 1\ UO_3{\cdot}2H_2O_{(c)} + 2\ H^+$	-1636.51	-4.81	0.30	Constant heat capacity
$UOBr_{2\ (c)}$	$1\ U^{4+} + 2\ Br^- + 1\ H_2O \rightleftharpoons 1\ UOBr_{2\ (c)} + 2\ H^+$	-929.65	-7.89	1.50	Van't Hoff
$UOBr_{3\ (c)}$	$1\ UO_2^{+} + 3\ Br^- + 2\ H^+ \rightleftharpoons 1\ UOBr_{3\ (c)} + 1\ H_2O$	-901.5	-23.46	3.75	Van't Hoff
$UOCl_{(c)}$	$1\ U^{3+} + 1\ Cl^- + 1\ H_2O \rightleftharpoons 1\ UOCl_{(c)} + 2\ H^+$	-785.65	-10.37	0.91	Van't Hoff
$UOCl_{2\ (c)}$	$1\ U^{4+} + 2\ Cl^- + 1\ H_2O \rightleftharpoons 1\ UOCl_{2\ (c)} + 2\ H^+$	-998.48	-5.42	0.57	Van't Hoff
$UOCl_{3\ (c)}$	$1\ UO_2^{+} + 3\ Cl^- + 2\ H^+ \rightleftharpoons 1\ UOCl_{3\ (c)} + 1\ H_2O$	-1045.58	-12.61	1.50	Van't Hoff
$UOF_{2\ (c)}$	$1\ U^{4+} + 2\ F^- + 1\ H_2O \rightleftharpoons 1\ UOF_{2\ (c)} + 2\ H^+$	-1434.13	18.23	1.17	Van't Hoff
$UOF_2{\cdot}H_2O_{(c)}$	$1\ U^{4+} + 2\ F^- + 2\ H_2O \rightleftharpoons 1\ UOF_2{\cdot}H_2O_{(c)} + 2\ H^+$	-1674.47	18.8	0.79	Van't Hoff
$UOF_{4\ (c)}$	$1\ UO_2^{2+} + 4\ F^- + 2\ H^+ \rightleftharpoons 1\ UOF_{4\ (c)} + 1\ H_2O$	-1816.26	-4.42	0.75	Van't Hoff
$UOFOH_{(c)}$	$1\ U^{4+} + 1\ F^- + 2\ H_2O \rightleftharpoons 1\ UOFOH_{(c)} + 3\ H^+$	-1336.93	8.98	2.29	Van't Hoff
$UOFOH{\cdot}0.5H_2O_{(c)}$	$1\ U^{4+} + 1\ F^- + 2.5\ H_2O \rightleftharpoons 1\ UOFOH{\cdot}0.5H_2O_{(c)} + 3\ H^+$	-1458.12	9.44	1.26	Van't Hoff
$UP_{(c)}$	$1\ U^{3+} + 1\ HPO_4^{2-} \rightleftharpoons 1\ UP_{(c)} + 1\ H^+ + 2\ O_{2\ (aq)}$	-265.92	-234.63	1.97	Van't Hoff
$UP_{2\ (c)}$	$1\ U^{3+} + 2\ HPO_4^{2-} + 1\ H^+ \rightleftharpoons 1\ UP_{2\ (c)} + 1.5\ H_2O + 3.25\ O_{2\ (aq)}$	-294.56	-362.88	2.65	Van't Hoff
$UP_2O_{7\ (c)}$	$1\ U^{4+} + 2\ HPO_4^{2-} \rightleftharpoons 1\ UP_2O_{7\ (c)} + 1\ H_2O$	-2659.27	30.58	0.99	Van't Hoff
$UPO_{5\ (c)}$	$1\ UO_2^{+} + 1\ HPO_4^{2-} + 1\ H^+ \rightleftharpoons 1\ UPO_{5\ (c)} + 1\ H_2O$	-1924.71	18.37	0.93	Van't Hoff
$US_{(c)}$	$1\ U^{3+} + 1\ HS^- + 0.5\ H_2O \rightleftharpoons 1\ US_{(c)} + 2\ H^+ + 0.25\ O_{2\ (aq)}$	-320.93	-46.59	2.26	Van't Hoff
$US_{1.90\ (c)}$	$0.2\ U^{3+} + 0.8\ U^{4+} + 1.9\ HS^- \rightleftharpoons 1\ US_{1.90\ (c)} + 1.9\ H^+$	-509.47	2.37	3.74	Van't Hoff
$US_{2\ (c)}$	$1\ U^{4+} + 2\ HS^- \rightleftharpoons 1\ US_{2\ (c)} + 2\ H^+$	-519.24	2.43	1.62	Van't Hoff
$US_{3\ (c)}$	$1\ UO_2^{2+} + 3\ HS^- + 1\ H^+ \rightleftharpoons 1\ US_{3\ (c)} + 2\ H_2O$	-537.25	16.77	2.47	Van't Hoff

Appendix A Conversion of the OECD-NEA database to Chess format

Mineral species	Equilibrium equation	$\Delta_f G_m^0$ / kJ mol^{-1}	log K	log K uncertainty	Temperature dependency estimation
$USe_{(c)}$	$1\ U^{3+} + 1\ SeO_3^{2-} + 0.5\ H_2O \rightleftharpoons 1\ USe_{(c)} + 1\ H^+ + 1.75\ O_{2(aq)}$	-276.91	-124.1	2.58	None
$USe_{2(alpha)}$	$1\ U^{3+} + 2\ SeO_3^{2-} + 1\ H^+ \rightleftharpoons 1\ USe_{2(alpha)} + 0.5\ H_2O + 2.75\ O_{2(aq)}$	-427.07	-122.46	7.36	None
$USe_{2(beta)}$	$1\ U^{3+} + 2\ SeO_3^{2-} + 1\ H^+ \rightleftharpoons 1\ USe_{2(beta)} + 0.5\ H_2O + 2.75\ O_{2(aq)}$	-427.97	-122.3	7.40	None
$USe_{3(c)}$	$1\ U^{3+} + 3\ SeO_3^{2-} + 3\ H^+ \rightleftharpoons 1\ USe_{3(c)} + 1.5\ H_2O + 3.75\ O_{2(aq)}$	-452	-142.76	7.42	None
$USiO_{4(c)}$	$1\ U^{4+} + 1\ Si(OH)_{4(aq)} \rightleftharpoons 1\ USiO_{4(c)} + 4\ H^+$	-1883.6	8.06	0.77	Van't Hoff
$Zn_{(c)}$	$1\ Zn^{2+} + 1\ H_2O \rightleftharpoons 1\ Zn_{(c)} + 2\ H^+ + 0.5\ O_{2(aq)}$	0	-68.77	-	Van't Hoff
$ZnO_{(c)}$	$1\ Zn^{2+} + 1\ H_2O \rightleftharpoons 1\ ZnO_{(c)} + 2\ H^+$	-320.48	-11.19	0.05	Van't Hoff

Appendix B IRSN-LRE database, species modified and added to OECD-NEA database

Species	Equilibrium equation	$\Delta_f G_m^0$ / kJ mol^{-1}	log K	log K uncertainty	Reference
H_2Cit^-	1 Cit_3^- + 2 H^+ ⇌ 1 H_2Cit^-	-63.21	11.07	0.15	Appendix C
H_2EDTA^{2-}	1 $EDTA^{4-}$ + 2 H^+ ⇌ 1 H_2EDTA^{2-}	-100.67	17.64	0.28	Appendix C
H_2SO_4(aq)	2 H^+ + 1 SO_4^{2-} ⇌ 1 H_2SO_4(aq)	-731.7	-2.16	-	Appendix C
H_3Cit(aq)	1 Cit^{3-} + 3 H^+ ⇌ 1 H_3Cit(aq)	-81.14	14.21	0.14	Appendix C
H_3EDTA^-	1 $EDTA^{4-}$ + 3 H^+ ⇌ 1 H_3EDTA^-	-118.24	20.71	0.38	Appendix C
H_4EDTA(aq)	1 $EDTA^{4-}$ + 4 H^+ ⇌ 1 H_4EDTA(aq)	-131.21	22.99	0.26	Appendix C
H_5EDTA^+	1 $EDTA^{4-}$ + 5 H^+ ⇌ 1 H_5EDTA^+	-139.04	24.36	0.94	Appendix C
H_6EDTA^{2+}	1 $EDTA^{4-}$ + 6 H^+ ⇌ 1 H_6EDTA^{2+}	-141.4	24.77	-	Appendix C
$HCit^{2-}$	1 Cit^{3-} + 1 H^+ ⇌ 1 $HCit^{2-}$	-36.11	6.33	0.46	Appendix C
HCl(aq)	1 H^+ + 1 Cl^- ⇌ 1 HCl(aq)	-95.97	-6.18	1.35	Appendix C
$HEDTA^{3-}$	1 $EDTA^{4-}$ + 1 H^+ ⇌ 1 $HEDTA^{3-}$	-62.18	10.89	0.58	Appendix C
HNO_3(aq)	1 H^+ + 1 NO_3^- ⇌ 1 HNO_3(aq)	-101.32	-1.66	1.1	Appendix C
Na_2Cit^-	2 Na^+ + 1 Cit^{3-} ⇌ 1 Na_2Cit^-	-538.00	2.47	0.37	Appendix C
Na_2EDTA^{2-}	2 Na^+ + 1 $EDTA^{4-}$ ⇌ 1 Na_2EDTA^{2-}	-545.75	3.83	-	[1]
Na_2HCit(aq)	2 Na^+ + 1 Cit^{3-} + 1 H^+ ⇌ 1 Na_2HCit(aq)	-563.86	7.00	-	[2]
Na_2HPO_4(aq)	2 Na^+ + 1 HPO_4^{2-} ⇌ 1 Na_2HPO_4(aq)	-1625.43	0.97	-	Appendix C
$Na_2PO_4^-$	2 Na^+ + 1 HPO_4^{2-} ⇌ 1 $Na_2PO_4^-$ + 1 H^+	-1564.18	-9.76	-	Appendix C
Na_2SO_4(aq)	2 Na^+ + 1 SO_4^{2-} ⇌ 1 Na_2SO_4(aq)	-1272.53	0.81	-	[3]
$NaCit^{2-}$	1 Na^+ + 1 Cit^{3-} ⇌ 1 $NaCit^{2-}$	-270.38	1.48	0.30	Appendix C
NaCl(aq)	1 Na^+ + 1 Cl^- ⇌ 1 NaCl(aq)	-389.19	-0.70	0.95	Appendix C
$NaCO_3^-$	1 Na^+ + 1 HCO_3^- ⇌ 1 $NaCO_3^-$ + 1 H^+	-795.44	-9.35	1.14	Appendix C
$NaEDTA^{3-}$	1 Na^+ + 1 $EDTA^{4-}$ ⇌ 1 $NaEDTA^{3-}$	-277.54	2.73	0.60	Appendix C
NaH_2Cit(aq)	1 Na^+ + 1 Cit^{3-} + 2 H^+ ⇌ 1 NaH_2Cit(aq)	-328.05	11.58	-	Appendix C
NaH_2EDTA^-	1 Na^+ + 1 $EDTA^{4-}$ + 2 H^+ ⇌ 1 NaH_2EDTA^-	-379.57	20.61	-	[4]
NaH_2PO_4(aq)	1 Na^+ + 1 HPO_4^{2-} + 1 H^+ ⇌ 1 NaH_2PO_4(aq)	-1399.92	7.35	0.98	Appendix C
$NaHCit^-$	1 Na^+ + 1 Cit^{3-} + 1 H^+ ⇌ 1 $NaHCit^-$	-303.84	7.34	0.81	Appendix C
$NaHCO_3$(aq)	1 Na^+ + 1 HCO_3^- ⇌ 1 $NaHCO_3$(aq)	-848.72	-0.01	0.60	Appendix C
$NaHEDTA^{2-}$	1 Na^+ + 1 $EDTA^{4-}$ + 1 H^+ ⇌ 1 $NaHEDTA^{2-}$	-332.56	12.37	3.36	Appendix C
$NaHPO_4^-$	1 Na^+ + 1 HPO_4^{2-} ⇌ 1 $NaHPO_4^-$	-1363.49	0.97	0.33	Appendix C
$NaHSO_4$(aq)	1 Na^+ + 1 SO_4^{2-} + 1 H^+ ⇌ 1 $NaHSO_4$(aq)	-1013.32	1.29	-	[5]
$NaKCit^-$	1 Na^+ + 1 Cit^{3-} + 1 K^+ ⇌ 1 $NaKCit^-$	-558.56	2.47	-	[2]
$NaKHCit$(aq)	1 Na^+ + 1 Cit^{3-} + 1 K^+ + 1 H^+ ⇌ 1 $NaKHCit$(aq)	-586.13	7.30	-	[2]
$NaKPO_4^-$	1 K^+ + 1 Na^+ + 1 HPO_4^{2-} ⇌ 1 $NaKPO_4^-$ + 1 H^+	-1585.65	-9.60	-	[6]

Appendix B IRSN-LRE database, species modified and added to OECD-NEA database

Species	Equilibrium equation	$\Delta_f G_m^0$ / kJ mol^{-1}	log K	log K uncertainty	Reference
$NaNO_3(aq)$	$1\ Na^+ + 1\ NO_3^- \rightleftharpoons 1\ NaNO_3(aq)$	-368.48	-0.75	0.81	Appendix C
$NaOH(aq)$	$1\ Na^+ + 1\ H_2O \rightleftharpoons 1\ NaOH(aq) + 1\ H^+$	-416.79	-14.42	0.89	Appendix C
$NaPO_4^{2-}$	$1\ Na^+ + 1\ HPO_4^{2-} \rightleftharpoons 1\ NaPO_4^{2-} + 1\ H^+$	-1295.61	-10.92	-	Appendix C
$NaSO_4^-$	$1\ Na^+ + 1\ SO_4^{2-} \rightleftharpoons 1\ NaSO_4^-$	-1010.61	0.81	0.33	Appendix C
K_2Cit^-	$2\ K^+ + 1\ Cit^{3-} \rightleftharpoons 1\ K_2Cit^-$	-576.74	2.05	0.46	Appendix C
$K_2HCit(aq)$	$2\ K^+ + 1\ Cit^{3-} + 1\ H^+ \rightleftharpoons 1\ K_2HCit(aq)$	-604.98	7.00	-	[2]
$K_2HPO_4(aq)$	$2\ K^+ + 1\ HPO_4^{2-} \rightleftharpoons 1\ K_2HPO_4(aq)$	-1667.24	1.09	0.02	Appendix C
$K_2PO_4^-$	$2\ K^+ + 1\ HPO_4^{2-} \rightleftharpoons 1\ K_2PO_4^- + 1\ H^+$	-1603.11	-10.14	0.05	Appendix C
$K_2SO_4(aq)$	$2\ K^+ + 1\ SO_4^{2-} \rightleftharpoons 1\ K_2SO_4(aq)$	-1314.50	0.96	-	[7]
$KCit^{2-}$	$1\ K^+ + 1\ Cit^{3-} \rightleftharpoons 1\ KCit^{2-}$	-290.08	1.33	0.38	Appendix C
$KCl(aq)$	$1\ K^+ + 1\ Cl^- \rightleftharpoons 1\ KCl(aq)$	-411.11	-0.46	0.66	Appendix C
$KEDTA^{3-}$	$1\ K^+ + 1\ EDTA^{4-} \rightleftharpoons 1\ KEDTA^{3-}$	-292.71	1.79	1.01	Appendix C
$KH_2Cit(aq)$	$1\ K^+ + 1\ Cit^{3-} + 2\ H^+ \rightleftharpoons 1\ KH_2Cit(aq)$	-346.53	11.22	-	Appendix C
KH_2EDTA^-	$1\ K^+ + 1\ EDTA^{4-} + 2\ H^+ \rightleftharpoons 1\ KH_2EDTA^-$	-382.73	17.56	9.57	Appendix C
$KH_2PO_4(aq)$	$1\ K^+ + 1\ HPO_4^{2-} + 1\ H^+ \rightleftharpoons 1\ KH_2PO_4(aq)$	-1421.10	7.46	0.18	Appendix C
$KHCit^-$	$1\ K^+ + 1\ Cit^{3-} + 1\ H^+ \rightleftharpoons 1\ KHCit^-$	-322.47	7.00	1.01	Appendix C
$KHEDTA^{2-}$	$1\ K^+ + 1\ EDTA^{4-} + 1\ H^+ \rightleftharpoons 1\ KHEDTA^{2-}$	-350.79	11.96	-	Appendix C
$KHPO_4^-$	$1\ K^+ + 1\ HPO_4^{2-} \rightleftharpoons 1\ KHPO_4^-$	-1383.35	0.85	0.15	Appendix C
$KHSO_4(aq)$	$1\ K^+ + 1\ H^+ + 1\ SO_4^{2-} \rightleftharpoons 1\ KHSO_4(aq)$	-1019.07	-1.30	-	[8]
$KOH(aq)$	$1\ K^+ + 1\ H_2O \rightleftharpoons 1\ KOH(aq) + 1\ H^+$	-437.52	-14.39	-	[9]
KPO_4^{2-}	$1\ K^+ + 1\ HPO_4^{2-} \rightleftharpoons 1\ KPO_4^{2-} + 1\ H^+$	-1315.93	-10.96	0.15	Appendix C
KSO_4^-	$1\ K^+ + 1\ SO_4^{2-} \rightleftharpoons 1\ KSO_4^-$	-1031.57	0.89	0.25	Appendix C
$NaKCit^-$	$1\ Na^+ + 1\ Cit^{3-} + 1\ K^+ \rightleftharpoons 1\ NaKCit^-$	-558.56	2.47	-	[2]
$NaKHCit(aq)$	$1\ Na^+ + 1\ Cit^{3-} + 1\ K^+ + 1\ H^+ \rightleftharpoons 1\ NaKHCit(aq)$	-586.13	7.30	-	[2]
$NaKPO_4^-$	$1\ K^+ + 1\ Na^+ + 1\ HPO_4^{2-} \rightleftharpoons 1\ NaKPO_4^- + 1\ H^+$	-1585.65	-9.60	-	[6]
$Mg(Cit)_2^{4-}$	$1\ Mg^{2+} + 2\ Cit^{3-} \rightleftharpoons 1\ Mg(Cit)_2^{4-}$	-488.82	5.86	-	[10]
$Mg(H_2PO_4)_2(aq)$	$1\ Mg^{2+} + 2\ HPO_4^{2-} + 2\ H^+ \rightleftharpoons 1\ Mg(H_2PO_4)_2(aq)$	-2738.41	15.95	-	[11]
$Mg(HPO_4)(H_2PO_4)^-$	$1\ Mg^{2+} + 2\ HPO_4^{2-} + 1\ H^+ \rightleftharpoons 1\ Mg(HPO_4)(H_2PO_4)^-$	-2708.55	10.72	-	[11]
$Mg(HPO_4)_2^{2-}$	$1\ Mg^{2+} + 2\ HPO_4^{2-} \rightleftharpoons 1\ Mg(HPO_4)_2^{2-}$	-2664.7	3.04	-	[12]
$Mg(OH)_2Cit^{3-}$	$1\ Mg^{2+} + 1\ Cit^{3-} + 2\ H_2O \rightleftharpoons 1\ Mg(OH)_2Cit^{3-} + 2\ H^+$	-825.6	-18.23	-	[10]
$Mg_2(OH)_2(Cit)_2^{4-}$	$2\ Mg^{2+} + 2\ Cit^{3-} + 2\ H_2O \rightleftharpoons 1\ Mg_2(OH)_2(Cit)_2^{4-} + 2\ H^+$	-1318.42	-11.67	-	[10]

Appendix B IRSN-LRE database, species modified and added to OECD-NEA database

Species	Equilibrium equation	$\Delta_f G_m^0$ / kJ mol^{-1}	log K	log K uncertainty	Reference
$MgCit^-$	1 Mg^{2+} + 1 Cit^{3-} ⇌ 1 $MgCit^-$	-482.92	4.83	0.31	Appendix C
$MgCl^+$	1 Mg^{2+} + 1 Cl^- ⇌ 1 $MgCl^+$	-588.36	0.31	1.06	Appendix C
$MgCO_3(aq)$	1 Mg^{2+} + 1 HCO_3^- ⇌ 1 $MgCO_3(aq)$ + 1 H^+	-1000.76	-7.26	0.46	Appendix C
$MgEDTA^{2-}$	1 Mg^{2+} + 1 $EDTA^{4-}$ ⇌ 1 $MgEDTA^{2-}$	-513.59	10.2	1.8	Appendix C
$MgH(Cit)_2^{3-}$	1 Mg^{2+} + 2 Cit^{3-} + 1 H^+ ⇌ 1 $MgH(Cit)_2^{3-}$	-524.5	12.11	-	[10]
MgH_2Cit^+	1 Mg^{2+} + 1 Cit^{3-} + 2 H^+ ⇌ 1 MgH_2Cit^+	-526.58	12.48	0.71	Appendix C
$MgH_2PO_4^+$	1 Mg^{2+} + 1 HPO_4^{2-} + 1 H^+ ⇌ 1 $MgH_2PO_4^+$	-1600.5	8.61	1.93	Appendix C
MgHCit(aq)	1 Mg^{2+} + 1 Cit^{3-} + 1 H^+ ⇌ 1 MgHCit(aq)	-506.86	9.02	0.3	Appendix C
$MgHCO_3^+$	1 Mg^{2+} + 1 HCO_3^- ⇌ 1 $MgHCO_3^+$	-1048.4	1.08	0.26	Appendix C
$MgHEDTA^-$	1 Mg^{2+} + 1 $EDTA^{4-}$ + 1 H^+ ⇌ 1 $MgHEDTA^-$	-541.73	15.13	2.05	Appendix C
$MgHPO_4(aq)$	1 Mg^{2+} + 1 HPO_4^{2-} ⇌ 1 $MgHPO_4(aq)$	-1567.69	2.86	0.4	Appendix C
$MgOH^+$	1 Mg^{2+} + 1 H_2O ⇌ 1 $MgOH^+$ + 1 H^+	-625.28	-11.78	0.89	Appendix C
$MgPO_4^-$	1 Mg^{2+} + 1 HPO_4^{2-} ⇌ 1 $MgPO_4^-$ + 1 H^+	-1508.75	-7.47	4.29	Appendix C
$MgSO_4(aq)$	1 Mg^{2+} + 1 SO_4^{2-} ⇌ 1 $MgSO_4(aq)$	-1212.33	2.27	0.2	Appendix C
$Ca(Cit)_2^{4-}$	1 Ca^{2+} + 2 Cit^{3-} ⇌ 1 $Ca(Cit)_2^{4-}$	-585.86	5.79	-	Appendix C
$Ca(H_2PO_4)(HPO_4)^-$	1 Ca^{2+} + 2 HPO_4^{2-} + 1 H^+ ⇌ 1 $Ca(H_2PO_4)(HPO_4)^-$	-2804.10	10.39	-	[13]
$Ca(H_2PO_4)_2(aq)$	1 Ca^{2+} + 2 HPO_4^{2-} + 2 H^+ ⇌ 1 $Ca(H_2PO_4)_2(aq)$	-2834.87	15.78	-	[13]
$Ca(HCit)_2^{2-}$	1 Ca^{2+} + 2 Cit^{3-} + 2 H^+ ⇌ 1 $Ca(HCit)_2^{2-}$	-661.17	18.99	-	Appendix C
$Ca(HPO_4)_2^{2-}$	1 Ca^{2+} + 2 HPO_4^{2-} ⇌ 1 $Ca(HPO_4)_2^{2-}$	-2762.13	3.04	-	[12]
$Ca(NO_3)_2(aq)$	1 Ca^{2+} + 2 NO_3^- ⇌ 1 $Ca(NO_3)_2(aq)$	-775.66	0.22	-	[14]
$Ca(OH)_2(aq)$	1 Ca^{2+} + 2 H_2O ⇌ 1 $Ca(OH)_2(aq)$ + 2 H^+	-878.61	-26.01	-	[15]
$Ca(OH)_2(Cit)_2^{6-}$	1 Ca^{2+} + 2 Cit^{3-} + 2 H_2O ⇌ 1 $Ca(OH)_2(Cit)_2^{6-}$ + 2 H^+	-963.50	-11.14	-	[10]
$Ca(PO_4)_2^{4-}$	1 Ca^{2+} + 2 HPO_4^{2-} ⇌ 1 $Ca(PO_4)_2^{4-}$ + 2 H^+	-2636.08	-19.04	-	[16]
$Ca_2EDTA(aq)$	2 Ca^{2+} + 1 $EDTA^{4-}$ ⇌ 1 $Ca_2EDTA(aq)$	-1188.94	14.60	-	Appendix C
$Ca_2UO_2(CO_3)_3(aq)$	2 Ca^{2+} + 1 UO_2^{2+} + 3 HCO_3^- ⇌ 1 $Ca_2UO_2(CO_3)_3(aq)$ + 3 H^+	-3812.11	-1.15	1.42	[17]
Ca_3EDTA^{2+}	3 Ca^{2+} + 1 $EDTA^{4-}$ ⇌ 1 Ca_3EDTA^{2+}	-1739.46	14.20	-	[18]
$CaCit^-$	1 Ca^{2+} + 1 Cit^{3-} ⇌ 1 $CaCit^-$	-580.04	4.77	0.24	Appendix C
$CaCitHPO_4^{3-}$	1 Ca^{2+} + 1 Cit^{3-} + 1 HPO_4^{2-} ⇌ 1 $CaCitHPO_4^{3-}$	-1714.89	11.58	-	[19]
$CaCl^+$	1 Ca^{2+} + 1 Cl^- ⇌ 1 $CaCl^+$	-684.69	0.12	1.53	Appendix C
$CaCl_2(aq)$	1 Ca^{2+} + 2 Cl^- ⇌ 1 $CaCl_2(aq)$	-812.24	-0.53	-	[8]
$CaCO_3(aq)$	1 Ca^{2+} + 1 HCO_3^- ⇌ 1 $CaCO_3(aq)$ + 1 H^+	-1100.72	-6.82	1.27	Appendix C
$CaEDTA^{2-}$	1 Ca^{2+} + 1 $EDTA^{4-}$ ⇌ 1 $CaEDTA^{2-}$	-622.62	12.23	1.12	Appendix C

Appendix B IRSN-LRE database, species modified and added to OECD-NEA database

Species	Equilibrium equation	$\Delta_f G_m^0$ / kJ mol^{-1}	log K	log K uncertainty	Reference
$CaH(Cit)_2^{3-}$	1 Ca^{2+} + 2 Cit^{3-} + 1 H^+ ⇌ 1 $CaH(Cit)_2^{3-}$	-621.93	12.11	-	[10]
CaH_2Cit^+	1 Ca^{2+} + 1 Cit^{3-} + 2 H^+ ⇌ 1 CaH_2Cit^+	-624.94	12.64	0.18	Appendix C
$CaH_2PO_4^+$	1 Ca^{2+} + 1 HPO_4^{2-} + 1 H^+ ⇌ 1 $CaH_2PO_4^+$	-1696.76	8.40	1.26	Appendix C
CaHCit(aq)	1 Ca^{2+} + 1 Cit^{3-} + 1 H^+ ⇌ 1 CaHCit(aq)	-606.38	9.39	0.42	Appendix C
$CaHCO_3^+$	1 Ca^{2+} + 1 HCO_3^- ⇌ 1 $CaHCO_3^+$	-1146.24	1.15	0.27	Appendix C
$CaHEDTA^-$	1 Ca^{2+} + 1 $EDTA^{4-}$ + 1 H^+ ⇌ 1 $CaHEDTA^-$	-641.67	15.57	0.62	Appendix C
$CaHPO_4$(aq)	1 Ca^{2+} + 1 HPO_4^{2-} ⇌ 1 $CaHPO_4$(aq)	-1663.78	2.62	0.30	Appendix C
$CaNO_3^+$	1 Ca^{2+} + 1 NO_3^- ⇌ 1 $CaNO_3^+$	-666.70	0.54	0.39	Appendix C
$CaOH^+$	1 Ca^{2+} + 1 H_2O ⇌ 1 $CaOH^+$ + 1 H^+	-717.29	-12.73	0.27	Appendix C
$CaOHCit^{2-}$	1 Ca^{2+} + 1 Cit^{3-} + 1 H_2O ⇌ 1 $CaOHCit^{2-}$ + 1 H^+	-747.54	-7.43	-	[10]
$CaPO_4^-$	1 Ca^{2+} + 1 HPO_4^{2-} ⇌ 1 $CaPO_4^-$ + 1 H^+	-1606.42	-7.42	1.05	Appendix C
$CaSO_4$(aq)	1 Ca^{2+} + 1 SO_4^{2-} ⇌ 1 $CaSO_4$(aq)	-1310.04	2.32	0.24	Appendix C
$CaUO_2(CO_3)_3^{2-}$	1 Ca^{2+} + 1 UO_2^{2+} + 3 HCO_3^- ⇌ 1 $CaUO_2(CO_3)_3^{2-}$ + 3 H^+	-3234.04	-5.58	0.28	[17]
$(UO_2)_2(Cit)_2^{2-}$	2 UO_2^{2+} + 2 Cit^{3-} ⇌ 1 $(UO_2)_2(Cit)_2^{2-}$	-2023.21	20.69	2.75	Appendix C
$(UO_2)_2(OH)_2(SO_4)_2^{2-}$	2 UO_2^{2+} + 2 H_2O + 2 SO_4^{2-} ⇌ 1 $(UO_2)_2(OH)_2(SO_4)_2^{2-}$ + 2 H^+	-3863.43	-0.69	-	[20]
$(UO_2)_2(OH)_2^{2+}$	2 UO_2^{2+} + 2 H_2O ⇌ 1 $(UO_2)_2(OH)_2^{2+}$ + 2 H^+	-2346.82	-5.70	0.57	Appendix C
$(UO_2)_2$EDTA(aq)	2 UO_2^{2+} + 1 $EDTA^{4-}$ ⇌ 1 $(UO_2)_2$EDTA(aq)	-2018.96	19.95	3.38	Appendix C
$(UO_2)_3(OH)_{10}^{4-}$	3 UO_2^{2+} + 10 H_2O ⇌ 1 $(UO_2)_3(OH)_{10}^{4-}$ + 10 H^+	-4872.87	-62.40	0.30	[21]
$(UO_2)_3(OH)_4(SO_4)_4^{6-}$	3 UO_2^{2+} + 4 H_2O + 4 SO_4^{2-} ⇌ 1 $(UO_2)_3(OH)_4(SO_4)_4^{6-}$ + 4 H^+	-6748.00	-6.00	-	[20]
$(UO_2)_3(OH)_5^+$	3 UO_2^{2+} + 5 H_2O ⇌ 1 $(UO_2)_3(OH)_5^+$ + 5 H^+	-3954.36	-15.59	0.78	Appendix C
$(UO_2)_3(OH)_7^-$	3 UO_2^{2+} + 7 H_2O ⇌ 1 $(UO_2)_3(OH)_7^-$ + 7 H^+	-4345.35	-30.18	5.94	Appendix C
$(UO_2)_3(OH)_8^{2-}$	3 UO_2^{2+} + 8 H_2O ⇌ 1 $(UO_2)_3(OH)_8^{2-}$ + 8 H^+	-4539.87	-37.65	0.14	[21]
$(UO_2)_4(OH)_7(SO_4)_4^{7-}$	4 UO_2^{2+} + 7 H_2O + 4 SO_4^{2-} ⇌ 1 $(UO_2)_4(OH)_7(SO_4)_4^{7-}$ + 7 H^+	-8337.70	-19.01	-	[20]
$Ca_2UO_2(CO_3)_3$(aq)	2 Ca^{2+} + 1 UO_2^{2+} + 3 HCO_3^- ⇌ 1 $Ca_2UO_2(CO_3)_3$(aq) + 3 H^+	-3812.11	-1.15	1.42	[17]
$CaUO_2(CO_3)_3^{2-}$	1 Ca^{2+} + 1 UO_2^{2+} + 3 HCO_3^- ⇌ 1 $CaUO_2(CO_3)_3^{2-}$ + 3 H^+	-3234.04	-5.58	0.28	[17]
$UO_2(Cit)_2^{4-}$	1 UO_2^{2+} + 2 Cit^{3-} ⇌ 1 $UO_2(Cit)_2^{4-}$	-1023.09	12.36	-	[22]
$UO_2(H_2PO_4)_2$(aq)	1 UO_2^{2+} + 2 HPO_4^{2-} + 2 H^+ ⇌ 1 $UO_2(H_2PO_4)_2$(aq)	-3259.82	20.20	1.72	Appendix C
$UO_2(OH)_2$(aq)	1 UO_2^{2+} + 2 H_2O ⇌ 1 $UO_2(OH)_2$(aq) + 2 H^+	-1359.79	-11.75	0.91	Appendix C
$UO_2(OH)_3^-$	1 UO_2^{2+} + 3 H_2O ⇌ 1 $UO_2(OH)_3^-$ + 3 H^+	-1552.10	-19.60	0.91	Appendix C
$UO_2(OH)_4^{2-}$	1 UO_2^{2+} + 4 H_2O ⇌ 1 $UO_2(OH)_4^{2-}$ + 4 H^+	-1705.72	-34.23	3.26	Appendix C
UO_2(OH)HEDTA^{2-}	1 UO_2^{2+} + 1 $EDTA^{4-}$ + 1 H_2O ⇌ 1 UO_2(OH)HEDTA^{2-}	-1264.63	13.13	2.09	Appendix C
$UO_2(SO_4)_3^{4-}$	1 UO_2^{2+} + 3 SO_4^{2-} ⇌ 1 $UO_2(SO_4)_3^{4-}$	-3199.51	2.62	-	[23]
UO_2Cit^-	1 UO_2^{2+} + 1 Cit^{3-} ⇌ 1 UO_2Cit^-	-1003.88	8.99	1.67	Appendix C

Appendix B IRSN-LRE database, species modified and added to OECD-NEA database

Species	Equilibrium equation	$\Delta_f G_m^0$ / kJ mol^{-1}	log K	log K uncertainty	Reference
UO_2EDTA^{2-}	1 UO_2^{2+} + 1 $EDTA^{4-}$ ⇌ 1 UO_2EDTA^{2-}	-1025.43	12.77	1.58	Appendix C
$UO_2H_2Cit^+$	1 UO_2^{2+} + 1 Cit^{3-} + 2 H^+ ⇌ 1 $UO_2H_2Cit^+$	-1030.20	13.60	-	Appendix C
$UO_2H_2PO_4^+$	1 UO_2^{2+} + 1 HPO_4^{2-} + 1 H^+ ⇌ 1 $UO_2H_2PO_4^+$	-2108.07	10.43	0.66	Appendix C
$UO_2HCit(aq)$	1 UO_2^{2+} + 1 Cit^{3-} + 1 H^+ ⇌ 1 $UO_2HCit(aq)$	-1017.15	11.32	-	Appendix C
UO_2HEDTA^-	1 UO_2^{2+} + 1 $EDTA^{4-}$ + 1 H^+ ⇌ 1 UO_2HEDTA^-	-1064.27	19.57	1.17	Appendix C
$UO_2HPO_4(aq)$	1 UO_2^{2+} + 1 HPO_4^{2-} ⇌ 1 $UO_2HPO_4(aq)$	-2090.23	7.30	0.47	Appendix C
UO_2OH^+	1 UO_2^{2+} + 1 H_2O ⇌ 1 UO_2OH^+ + 1 H^+	-1159.09	-5.36	0.43	Appendix C
Fe^{3+}	1 Fe^{2+} + 1 H^+ + 0.25 $O_2(aq)$ ⇌ 1 Fe^{3+} + 0.5 H_2O	-17.25	8.47	0.09	[9]
$Fe(Cit)_2^{3-}$	1 Fe^{3+} + 2 Cit^{3-} ⇌ 1 $Fe(Cit)_2^{3-}$	-126.33	19.11	3.22	Appendix C
$Fe(Cit)_2^{4-}$	1 Fe^{2+} + 2 Cit^{3-} ⇌ 1 $Fe(Cit)_2^{4-}$	-129.98	6.73	-	[12]
$Fe(CO_3)_2^-$	1 Fe^{3+} + 2 HCO_3^- ⇌ 1 $Fe(CO_3)_2^-$ + 2 H^+	-1126.92	-11.22	-	[24]
$Fe(CO_3)_2^{2-}$	1 Fe^{2+} + 2 HCO_3^- ⇌ 1 $Fe(CO_3)_2^{2-}$ + 2 H^+	-1188.26	-13.49	-	[24]
$Fe(EDTA)_2^{5-}$	1 Fe^{3+} + 2 $EDTA^{4-}$ ⇌ 1 $Fe(EDTA)_2^{5-}$	-137.46	21.06	-	[25]
$Fe(H_2PO_4)(H_3PO_4)^{2+}$	1 Fe^{3+} + 2 HPO_4^{2-} + 3 H^+ ⇌ 1 $Fe(H_2PO_4)(H_3PO_4)^{2+}$	-2330.54	21.25	-	[26]
$Fe(H_2PO_4)_2(aq)$	1 Fe^{2+} + 2 HPO_4^{2-} + 2 H^+ ⇌ 1 $Fe(H_2PO_4)_2(aq)$	-2380.45	16.98	-	Appendix C
$Fe(H_2PO_4)_2(H_3PO_4)^+$	1 Fe^{3+} + 3 HPO_4^{2-} + 4 H^+ ⇌ 1 $Fe(H_2PO_4)_2(H_3PO_4)^+$	-3488.64	32.13	-	[26]
$Fe(H_2PO_4)_2^+$	1 Fe^{3+} + 2 HPO_4^{2-} + 2 H^+ ⇌ 1 $Fe(H_2PO_4)_2^+$	-2333.96	21.85	-	[26]
$Fe(H_2PO_4)_3(aq)$	1 Fe^{3+} + 3 HPO_4^{2-} + 3 H^+ ⇌ 1 $Fe(H_2PO_4)_3(aq)$	-3484.75	31.45	-	[26]
$Fe(HCit)_2^-$	1 Fe^{3+} + 2 Cit^{3-} + 2 H^+ ⇌ 1 $Fe(HCit)_2^-$	-167.77	26.37	-	Appendix C
$Fe(HPO_4)(H_2PO_4)(aq)$	1 Fe^{3+} + 2 HPO_4^{2-} + 1 H^+ ⇌ 1 $Fe(HPO_4)(H_2PO_4)(aq)$	-2317.97	19.05	-	[26]
$Fe(HPO_4)(H_2PO_4)^-$	1 Fe^{2+} + 2 HPO_4^{2-} + 1 H^+ ⇌ 1 $Fe(HPO_4)(H_2PO_4)^-$	-2349.71	11.59	-	[27]
$Fe(HPO_4)_2^-$	1 Fe^{3+} + 2 HPO_4^{2-} ⇌ 1 $Fe(HPO_4)_2^-$	-2247.46	6.70	-	[12]
$Fe(HPO_4)_2^{2-}$	1 Fe^{2+} + 2 HPO_4^{2-} ⇌ 1 $Fe(HPO_4)_2^{2-}$	-2304.82	3.73	-	[12]
$Fe(HPO_4)Cit^{2-}$	1 Fe^{3+} + 1 HPO_4^{2-} + 1 Cit^{3-} ⇌ 1 $Fe(HPO_4)Cit^{2-}$	-1235.36	21.40	-	[28]
$Fe(OH)(HPO_4)_2^{2-}$	1 Fe^{3+} + 2 HPO_4^{2-} + 1 H_2O ⇌ 1 $Fe(OH)(HPO_4)_2^{2-}$ + 1 H^+	-2509.99	11.15	-	[29]
$Fe(OH)_2(aq)$	1 Fe^{2+} + 2 H_2O ⇌ 1 $Fe(OH)_2(aq)$ + 2 H^+	-448.73	-20.52	0.45	Appendix C
$Fe(OH)_2^+$	1 Fe^{3+} + 2 H_2O ⇌ 1 $Fe(OH)_2^+$ + 2 H^+	-458.89	-5.72	1.30	Appendix C
$Fe(OH)_2Cit^{2-}$	1 Fe^{3+} + 2 H_2O + 1 Cit^{3-} ⇌ 1 $Fe(OH)_2Cit^{2-}$ + 2 H^+	-508.59	2.99	-	Appendix C
$Fe(OH)_2EDTA^{3-}$	1 Fe^{3+} + 1 $EDTA^{4-}$ + 2 H_2O ⇌ 1 $Fe(OH)_2EDTA^{3-}$ + 2 H^+	-547.90	9.88	0.40	Appendix C
$Fe(OH)_2EDTA^{4-}$	1 Fe^{2+} + 1 $EDTA^{4-}$ + 2 H_2O ⇌ 1 $Fe(OH)_2EDTA^{4-}$ + 2 H^+	-542.36	-4.12	-	Appendix C

Appendix B IRSN-LRE database, species modified and added to OECD-NEA database

Species	Equilibrium equation	$\Delta_f G_m^0$ / kJ mol^{-1}	log K	log K uncertainty	Reference
$Fe(OH)_2SO_4^-$	$1\ Fe^{3+} + 2\ H_2O + 1\ SO_4^{2-} \rightleftharpoons 1\ Fe(OH)_2SO_4^- + 2\ H^+$	-1207.56	-4.90	-	[30]
$Fe(OH)_3(aq)$	$1\ Fe^{3+} + 3\ H_2O \rightleftharpoons 1\ Fe(OH)_3(aq) + 3\ H^+$	-657.69	-12.43	1.99	Appendix C
$Fe(OH)_3^-$	$1\ Fe^{2+} + 3\ H_2O \rightleftharpoons 1\ Fe(OH)_3^- + 3\ H^+$	-623.01	-31.53	9.70	Appendix C
$Fe(OH)_3EDTA^{4-}$	$1\ Fe^{3+} + 1\ EDTA^{4-} + 3\ H_2O \rightleftharpoons 1\ Fe(OH)_3EDTA^{4-} + 3\ H^+$	-711.22	-3.06	-	[31]
$Fe(OH)_4^-$	$1\ Fe^{3+} + 4\ H_2O \rightleftharpoons 1\ Fe(OH)_4^- + 4\ H^+$	-840.50	-21.95	2.25	Appendix C
$Fe(OH)_4^{2-}$	$1\ Fe^{2+} + 4\ H_2O \rightleftharpoons 1\ Fe(OH)_4^{2-} + 4\ H^+$	-778.54	-45.83	2.49	Appendix C
$Fe(OH)CO_3(aq)$	$1\ Fe^{3+} + 1\ H_2O + 1\ HCO_3^- \rightleftharpoons 1\ Fe(OH)CO_3(aq) + 2\ H^+$	-803.09	-6.68	-	[24]
$Fe(OH)EDTA^{2-}$	$1\ Fe^{3+} + 1\ EDTA^{4-} + 1\ H_2O \rightleftharpoons 1\ Fe(OH)EDTA^{2-} + 1\ H^+$	-367.55	19.82	3.20	Appendix C
$Fe(OH)EDTA^{3-}$	$1\ Fe^{2+} + 1\ EDTA^{4-} + 1\ H_2O \rightleftharpoons 1\ Fe(OH)EDTA^{3-} + 1\ H^+$	-365.74	6.49	0.43	Appendix C
$Fe(OH)PO_4^-$	$1\ Fe^{3+} + 1\ H_2O + 1\ HPO_4^{2-} \rightleftharpoons 1\ Fe(OH)PO_4^- + 2\ H^+$	-1371.74	3.74	-	[29]
$Fe(OH)SO_4(aq)$	$1\ Fe^{3+} + 1\ H_2O + 1\ SO_4^{2-} \rightleftharpoons 1\ Fe(OH)SO_4(aq) + 1\ H^+$	-999.02	0.11	-	[30]
$Fe(PO_4)_2^{3-}$	$1\ Fe^{3+} + 2\ HPO_4^{2-} \rightleftharpoons 1\ Fe(PO_4)_2^{3-} + 2\ H^+$	-2267.27	10.17	-	[29]
$Fe(SO_4)_2^-$	$1\ Fe^{3+} + 2\ SO_4^{2-} \rightleftharpoons 1\ Fe(SO_4)_2^-$	-1537.67	5.68	-	Appendix C
$Fe_2(Cit)_2(aq)$	$2\ Fe^{3+} + 2\ Cit^{3-} \rightleftharpoons 1\ Fe_2(Cit)_2(aq)$	-191.69	27.54	-	[32]
$Fe_2(HCit)_2(aq)$	$2\ Fe^{2+} + 2\ Cit^{3-} + 2\ H^+ \rightleftharpoons 1\ Fe_2(HCit)_2(aq)$	-171.45	-2.05	-	[33]
$Fe_2(OH)_2(Cit)_2^{2-}$	$2\ Fe^{3+} + 2\ Cit^{3-} + 2\ H_2O \rightleftharpoons 1\ Fe_2(OH)_2(Cit)_2^{2-} + 2\ H^+$	-640.97	23.16	0.55	Appendix C
$Fe_2(OH)_2(Cit)_2^{4-}$	$2\ Fe^{2+} + 2\ Cit^{3-} + 2\ H_2O \rightleftharpoons 1\ Fe_2(OH)_2(Cit)_2^{4-} + 2\ H^+$	-632.12	-4.43	-	[33]
$Fe_2(OH)_2^{4+}$	$2\ Fe^{3+} + 2\ H_2O \rightleftharpoons 1\ Fe_2(OH)_2^{4+} + 2\ H^+$	-492.64	-2.83	1.36	Appendix C
$Fe_2(OH)_3(Cit)_2^{3-}$	$2\ Fe^{3+} + 3\ H_2O + 2\ Cit^{3-} \rightleftharpoons 1\ Fe_2(OH)_3(Cit)_2^{3-} + 3\ H^+$	-850.31	18.29	-	Appendix C
$Fe_2HPO_4^{4+}$	$2\ Fe^{3+} + 1\ HPO_4^{2-} \rightleftharpoons 1\ Fe_2HPO_4^{4+}$	-1217.81	15.30	-	[28]
$Fe_2OH(Cit)_2^-$	$2\ Fe^{3+} + 1\ H_2O + 2\ Cit^{3-} \rightleftharpoons 1\ Fe_2OH(Cit)_2^- + 1\ H^+$	-418.73	25.77	-	[34]
$Fe_3(OH)_4^{5+}$	$3\ Fe^{3+} + 4\ H_2O \rightleftharpoons 1\ Fe_3(OH)_4^{5+} + 4\ H^+$	-964.33	-6.30	0.26	Appendix C
$Fe_3(OH)_4SO_4^{3+}$	$3\ Fe^{3+} + 4\ H_2O + 1\ SO_4^{2-} \rightleftharpoons 1\ Fe_3(OH)_4SO_4^{3+} + 4\ H^+$	-1723.70	-3.61	-	[35]
$Fe_4(OH)_{12}(aq)$	$4\ Fe^{3+} + 12\ H_2O \rightleftharpoons 1\ Fe_4(OH)_{12}(aq) + 12\ H^+$	-2805.52	-19.12	-	[36]
FeCit(aq)	$1\ Fe^{3+} + 1\ Cit^{3-} \rightleftharpoons 1\ FeCit(aq)$	-92.68	13.21	1.03	Appendix C
$FeCit^-$	$1\ Fe^{2+} + 1\ Cit^{3-} \rightleftharpoons 1\ FeCit^-$	-125.03	5.86	0.68	Appendix C
$FeCl^+$	$1\ Fe^{2+} + 1\ Cl^- \rightleftharpoons 1\ FeCl^+$	-222.20	-0.10	0.38	Appendix C
$FeCl^{2+}$	$1\ Fe^{3+} + 1\ Cl^- \rightleftharpoons 1\ FeCl^{2+}$	-155.80	1.28	0.92	Appendix C
$FeCl_2(aq)$	$1\ Fe^{2+} + 2\ Cl^- \rightleftharpoons 1\ FeCl_2(aq)$	-323.82	-5.29	-	Appendix C

Appendix B IRSN-LRE database, species modified and added to OECD-NEA database

Species	Equilibrium equation	$\Delta_f G_m^0$ / kJ mol^{-1}	log K	log K uncertainty	Reference
$FeCl_2^+$	1 Fe^{3+} + 2 Cl^- ⇌ 1 $FeCl_2^+$	-289.11	1.65	1.77	Appendix C
$FeCl_3$(aq)	1 Fe^{3+} + 3 Cl^- ⇌ 1 $FeCl_3$(aq)	-415.84	0.87	1.01	Appendix C
$FeCl_4^-$	1 Fe^{3+} + 4 Cl^- ⇌ 1 $FeCl_4^-$	-537.67	-0.78	0.15	Appendix C
$FeCO_3$(aq)	1 Fe^{2+} + 1 HCO_3^- ⇌ 1 $FeCO_3$(aq) + 1 H^+	-648.02	-5.32	1.71	Appendix C
$FeEDTA^-$	1 Fe^{3+} + 1 $EDTA^{4-}$ ⇌ 1 $FeEDTA^-$	-172.17	27.14	3.07	Appendix C
$FeEDTA^{2-}$	1 Fe^{2+} + 1 $EDTA^{4-}$ ⇌ 1 $FeEDTA^{2-}$	-183.39	16.09	0.63	Appendix C
$FeH(Cit)_2^{2-}$	1 Fe^{3+} + 2 Cit^{3-} + 1 H^+ ⇌ 1 $FeH(Cit)_2^{2-}$	-150.99	23.43	-	[37]
$FeH(Cit)_2^{3-}$	1 Fe^{2+} + 2 Cit^{3-} + 1 H^+ ⇌ 1 $FeH(Cit)_2^{3-}$	-170.77	13.88	-	[33]
FeH_2Cit^+	1 Fe^{2+} + 1 Cit^{3-} + 2 H^+ ⇌ 1 FeH_2Cit^+	-164.43	12.77	0.38	Appendix C
FeH_2EDTA(aq)	1 Fe^{2+} + 1 $EDTA^{4-}$ + 2 H^+ ⇌ 1 FeH_2EDTA(aq)	-225.72	23.50	-	[38]
FeH_2EDTA^+	1 Fe^{3+} + 1 $EDTA^{4-}$ + 2 H^+ ⇌ 1 FeH_2EDTA^+	-167.69	26.36	-	[39]
$FeH_2PO_4^+$	1 Fe^{2+} + 1 HPO_4^{2-} + 1 H^+ ⇌ 1 $FeH_2PO_4^+$	-1239.30	9.07	-	Appendix C
$FeH_2PO_4^{2+}$	1 Fe^{3+} + 1 HPO_4^{2-} + 1 H^+ ⇌ 1 $FeH_2PO_4^{2+}$	-1177.45	11.25	0.13	Appendix C
$FeH_3PO_4^{3+}$	1 Fe^{3+} + 1 HPO_4^{2-} + 2 H^+ ⇌ 1 $FeH_3PO_4^{3+}$	-1165.48	9.15	-	[26]
FeHCit(aq)	1 Fe^{2+} + 1 Cit^{3-} + 1 H^+ ⇌ 1 FeHCit(aq)	-148.54	9.98	0.66	Appendix C
$FeHCit^+$	1 Fe^{3+} + 1 Cit^{3-} + 1 H^+ ⇌ 1 $FeHCit^+$	-97.85	14.12	0.92	Appendix C
$FeHCO_3^+$	1 Fe^{2+} + 1 HCO_3^- ⇌ 1 $FeHCO_3^+$	-687.99	1.68	1.91	Appendix C
FeHEDTA(aq)	1 Fe^{3+} + 1 $EDTA^{4-}$ + 1 H^+ ⇌ 1 FeHEDTA(aq)	-177.52	28.08	2.80	Appendix C
$FeHEDTA^-$	1 Fe^{2+} + 1 $EDTA^{4-}$ + 1 H^+ ⇌ 1 $FeHEDTA^-$	-202.14	19.37	1.70	Appendix C
$FeHPO_4$(aq)	1 Fe^{2+} + 1 HPO_4^{2-} ⇌ 1 $FeHPO_4$(aq)	-1212.28	4.33	6.42	Appendix C
$FeHPO_4^+$	1 Fe^{3+} + 1 HPO_4^{2-} ⇌ 1 $FeHPO_4^+$	-1169.03	9.77	1.31	Appendix C
$FeHSO_4^+$	1 Fe^{2+} + 1 SO_4^{2-} + 1 H^+ ⇌ 1 $FeHSO_4^+$	-853.09	3.07	-	[40]
$FeHSO_4^{2+}$	1 Fe^{3+} + 1 SO_4^{2-} + 1 H^+ ⇌ 1 $FeHSO_4^{2+}$	-786.77	4.47	-	[40]
$FeNO_3^{2+}$	1 Fe^{3+} + 1 NO_3^- ⇌ 1 $FeNO_3^{2+}$	-132.75	0.82	0.72	Appendix C
$FeO(HPO_4)_2^{3-}$	1 Fe^{3+} + 2 HPO_4^{2-} + 1 H_2O ⇌ 1 $FeO(HPO_4)_2^{3-}$ + 2 H^+	-2504.02	10.10	-	[29]
$FeOH(Cit)_2^{4-}$	1 Fe^{3+} + 2 Cit^{3-} + 1 H_2O ⇌ 1 $FeOH(Cit)_2^{4-}$ + 1 H^+	-331.56	13.52	-	[37]
$FeOH^+$	1 Fe^{2+} + 1 H_2O ⇌ 1 $FeOH^+$ + 1 H^+	-274.48	-9.50	0.58	Appendix C
$FeOH^{2+}$	1 Fe^{3+} + 1 H_2O ⇌ 1 $FeOH^{2+}$ + 1 H^+	-241.63	-2.24	0.30	Appendix C
$FeOHCit^-$	1 Fe^{3+} + 1 Cit^{3-} + 1 H_2O ⇌ 1 $FeOHCit^-$ + 1 H^+	-314.44	10.52	1.01	Appendix C
$FePO_4$(aq)	1 Fe^{3+} + 1 HPO_4^{2-} ⇌ 1 $FePO_4$(aq) + 1 H^+	-1112.24	-0.18	-	[28]
$FeSO_4$(aq)	1 Fe^{2+} + 1 SO_4^{2-} ⇌ 1 $FeSO_4$(aq)	-850.26	2.57	1.88	Appendix C
$FeSO_4^+$	1 Fe^{3+} + 1 SO_4^{2-} ⇌ 1 $FeSO_4^+$	-783.79	3.95	1.02	Appendix C
$Fe(OH)_2$(s)	1 Fe^{2+} + 2 H_2O ⇌ 1 $Fe(OH)_2$(s) + 2 H^+	-489.21	-13.43	0.79	Appendix C

Appendix B IRSN-LRE database, species modified and added to OECD-NEA database

Species	Equilibrium equation	$\Delta_f G_m^0$ / kJ mol^{-1}	log K	log K uncertainty	Reference
$Fe(OH)_3$, ferrihydrite	1 Fe^{3+} + 3 H_2O ⇌ 1 $Fe(OH)_3$, ferrihydrite + 3 H^+	-702.38	-4.61	2.82	Appendix C
Fe_2O_3, hematite	2 Fe^{3+} + 3 H_2O ⇌ 1 Fe_2O_3, hematite + 6 H^+	-743.57	-0.41	0.46	Appendix C
Fe_3O_4, magnetite	1 Fe^{2+} + 2 Fe^{3+} + 4 H_2O ⇌ 1 Fe_3O_4, magnetite + 8 H^+	-1013.32	-10.74	0.47	Appendix C
$FeCO_3$, siderite	1 Fe^{2+} + 1 HCO_3^- ⇌ 1 $FeCO_3$, siderite + 1 H^+	-676.80	-0.28	2.52	Appendix C
FeOOH, goethite	1 Fe^{3+} + 2 H_2O ⇌ 1 FeOOH, goethite + 3 H^+	-488.10	-0.60	0.54	Appendix C
$Ca(OH)_2$, Portlandite	1 Ca^{2+} + 2 H_2O ⇌ 1 $Ca(OH)_2$, Portlandite + 2 H^+	-874.32	-26.76	15.55	Appendix C
$Ca_4H(PO_4)_3{\cdot}3H_2O$	4 Ca^{2+} + 3 HPO_4^{2-} + 3 H_2O ⇌ 1 $Ca_4H(PO_4)_3{\cdot}3H_2O$ + 2 H^+	-6267.32	9.93	0.39	Appendix C
$Ca_5(PO_4)_3OH$, hydroxyapatite	5 Ca^{2+} + 3 HPO_4^{2-} + 1 H_2O ⇌ 1 $Ca_5(PO_4)_3OH$, hydroxyapatite + 4 H^+	-6328.63	6.92	5.01	Appendix C
$CaCO_3$, Aragonite	1 Ca^{2+} + 1 HCO_3^- ⇌ 1 $CaCO_3$, Aragonite + 1 H^+	-1127.80	-2.08	0.24	Appendix C
$CaCO_3$, Calcite	1 Ca^{2+} + 1 HCO_3^- ⇌ 1 $CaCO_3$, Calcite + 1 H^+	-1128.61	-1.94	0.20	Appendix C
$CaHPO_4{\cdot}2H_2O$, brushite	1 Ca^{2+} + 1 HPO_4^{2-} + 2 H_2O ⇌ 1 $CaHPO_4{\cdot}2H_2O$, brushite	-2160.63	6.58	0.11	Appendix C
$CaMg(CO_3)_2$, Dolomite(Ordered)	1 Ca^{2+} + 1 Mg^{2+} + 2 HCO_3^- ⇌ 1 $CaMg(CO_3)_2$, Dolomite(Ordered) + 2 H^+	-2162.20	-3.45	0.45	Appendix C
$CaSO_4$, anhydrite	1 Ca^{2+} + 1 SO_4^{2-} ⇌ 1 $CaSO_4$, anhydrite	-1321.47	4.32	0.16	Appendix C
$CaSO_4{\cdot}2H_2O$, gypsum	1 Ca^{2+} + 1 SO_4^{2-} + 2 H_2O ⇌ 1 $CaSO_4{\cdot}2H_2O$, gypsum	-1797.17	4.57	0.11	Appendix C
$Mg(OH)_2$, Brucite	1 Mg^{2+} + 2 H_2O ⇌ 1 $Mg(OH)_2$, Brucite + 2 H^+	-834.43	-16.68	0.55	Appendix C
$MgCO_3$, magnesite	1 Mg^{2+} + 1 HCO_3^- ⇌ 1 $MgCO_3$, magnesite + 1 H^+	-1026.55	-2.75	2.81	Appendix C
$MgSO_4$(s)	1 Mg^{2+} + 1 SO_4^{2-} ⇌ 1 $MgSO_4$(s)	-1171.53	-4.88	-	[41]

Appendix C. Data considered in the review of solution complex and mineral thermodynamic constants. Only species with more than one datum considered listed

Species	Equilibrium equation	T/ ºC	I	Corrected logK	$\Delta_f G_m^0$ / kJ mol^{-1}	Ref
$HCit^{2-}$	1 Cit^{3-} + 1 H^+ ⇌ 1 $HCit^{2-}$	25	0	6.40	-36.53	[42]
$HCit^{2-}$	1 Cit^{3-} + 1 H^+ ⇌ 1 $HCit^{2-}$	25	0	6.37	-36.36	[43]
$HCit^{2-}$	1 Cit^{3-} + 1 H^+ ⇌ 1 $HCit^{2-}$	25	0	6.40	-36.53	[44]
$HCit^{2-}$	1 Cit^{3-} + 1 H^+ ⇌ 1 $HCit^{2-}$	25	0.3	5.96	-34.04	[45]
$HCit^{2-}$	1 Cit^{3-} + 1 H^+ ⇌ 1 $HCit^{2-}$	25	0	6.40	-36.53	[46]
$HCit^{2-}$	1 Cit^{3-} + 1 H^+ ⇌ 1 $HCit^{2-}$	25	0.1	6.42	-36.64	[47]
				mean	-36.11	
H_2Cit^-	1 $HCit^{2-}$ + 1 H^+ ⇌ 1 H_2Cit^-	25	0	4.76	-63.28	[42]
H_2Cit^-	1 $HCit^{2-}$ + 1 H^+ ⇌ 1 H_2Cit^-	25	0	4.79	-63.45	[43].
H_2Cit^-	1 $HCit^{2-}$ + 1 H^+ ⇌ 1 H_2Cit^-	25	0	4.76	-63.28	[44]
H_2Cit^-	1 $HCit^{2-}$ + 1 H^+ ⇌ 1 H_2Cit^-	25	0.3	4.64	-62.57	[45]
H_2Cit^-	1 $HCit^{2-}$ + 1 H^+ ⇌ 1 H_2Cit^-	25	0	4.76	-63.28	[46]
H_2Cit^-	1 $HCit^{2-}$ + 1 H^+ ⇌ 1 H_2Cit^-	25	0.1	4.78	-63.41	[47]
				mean	-63.21	
$H_3Cit(aq)$	1 H_2Cit^- + 1 H^+ ⇌ 1 $H_3Cit(aq)$	25	0	3.13	-81.08	[42]
$H_3Cit(aq)$	1 H_2Cit^- + 1 H^+ ⇌ 1 $H_3Cit(aq)$	25	0	3.24	-81.70	[43].
$H_3Cit(aq)$	1 H_2Cit^- + 1 H^+ ⇌ 1 $H_3Cit(aq)$	25	0	3.13	-81.08	[44]
$H_3Cit(aq)$	1 H_2Cit^- + 1 H^+ ⇌ 1 $H_3Cit(aq)$	25	0.3	3.08	-80.76	[45]
$H_3Cit(aq)$	1 H_2Cit^- + 1 H^+ ⇌ 1 $H_3Cit(aq)$	25	0	3.13	-81.08	[46]
$H_3Cit(aq)$	1 H_2Cit^- + 1 H^+ ⇌ 1 $H_3Cit(aq)$	25	0.1	3.14	-81.12	[47]
				mean	-81.14	
$H_2SO_4(aq)$	2 H^+ + 1 SO_4^{2-} ⇌ 1 $H_2SO_4(aq)$	25	0	-3.29	-725.22	[48]
$H_2SO_4(aq)$	2 H^+ + 1 SO_4^{2-} ⇌ 1 $H_2SO_4(aq)$	25	0	-1.02	-738.18	[41]
				mean	-731.70	
HCl(aq)	1 H^+ + 1 Cl^- ⇌ 1 HCl(aq)	25	0	-6.25	-95.54	[49]
HCl(aq)	1 H^+ + 1 Cl^- ⇌ 1 HCl(aq)	25	0	-6.10	-96.40	[50]
				mean	-95.97	

Appendix C. Data considered in the review of solution complex and mineral thermodynamic constants. Only species with more than one datum considered listed

Species	Equilibrium equation	T/ ºC	I	Corrected logK	$\Delta_f G_m^0$ / kJ mol^{-1}	Ref
HNO_3(aq)	1 H^+ + 1 NO_3^- ⇌ 1 HNO_3(aq)	25	0	-2.19	-98.29	[48]
HNO_3(aq)	1 H^+ + 1 NO_3^- ⇌ 1 HNO_3(aq)	25	0	-1.43	-102.63	[51]
HNO_3(aq)	1 H^+ + 1 NO_3^- ⇌ 1 HNO_3(aq)	25	0	-2.23	-98.07	[52]
HNO_3(aq)	1 H^+ + 1 NO_3^- ⇌ 1 HNO_3(aq)	25	0	-1.44	-102.57	[53]
HNO_3(aq)	1 H^+ + 1 NO_3^- ⇌ 1 HNO_3(aq)	25	0	-1.37	-102.97	[54]
HNO_3(aq)	1 H^+ + 1 NO_3^- ⇌ 1 HNO_3(aq)	25	0	-1.30	-103.36	[41]
				mean	-101.32	
$HEDTA^{3-}$	1 $EDTA^{4-}$ + 1 H^+ ⇌ 1 $HEDTA^{3-}$	25	0.10	10.27	-58.64	[55]
$HEDTA^{3-}$	1 $EDTA^{4-}$ + 1 H^+ ⇌ 1 $HEDTA^{3-}$	25	0.10	10.71	-61.11	[56]
$HEDTA^{3-}$	1 $EDTA^{4-}$ + 1 H^+ ⇌ 1 $HEDTA^{3-}$	25	0.10	10.99	-62.71	[57]
$HEDTA^{3-}$	1 $EDTA^{4-}$ + 1 H^+ ⇌ 1 $HEDTA^{3-}$	25	0.10	11.05	-63.05	[58]
$HEDTA^{3-}$	1 $EDTA^{4-}$ + 1 H^+ ⇌ 1 $HEDTA^{3-}$	25	0.10	10.93	-62.36	[59]
$HEDTA^{3-}$	1 $EDTA^{4-}$ + 1 H^+ ⇌ 1 $HEDTA^{3-}$	25	0.10	11.03	-62.93	[60]
$HEDTA^{3-}$	1 $EDTA^{4-}$ + 1 H^+ ⇌ 1 $HEDTA^{3-}$	25	0.10	11.05	-63.05	[61]
$HEDTA^{3-}$	1 $EDTA^{4-}$ + 1 H^+ ⇌ 1 $HEDTA^{3-}$	25	0.10	10.95	-62.48	[62]
$HEDTA^{3-}$	1 $EDTA^{4-}$ + 1 H^+ ⇌ 1 $HEDTA^{3-}$	25	0.10	11.12	-63.45	[63]
$HEDTA^{3-}$	1 $EDTA^{4-}$ + 1 H^+ ⇌ 1 $HEDTA^{3-}$	25	0.10	11.04	-62.99	[64]
$HEDTA^{3-}$	1 $EDTA^{4-}$ + 1 H^+ ⇌ 1 $HEDTA^{3-}$	25	0.10	11.04	-62.99	[65]
$HEDTA^{3-}$	1 $EDTA^{4-}$ + 1 H^+ ⇌ 1 $HEDTA^{3-}$	25	0.12	10.30	-58.77	[66]
$HEDTA^{3-}$	1 $EDTA^{4-}$ + 1 H^+ ⇌ 1 $HEDTA^{3-}$	25	0.15	10.66	-60.82	[67]
$HEDTA^{3-}$	1 $EDTA^{4-}$ + 1 H^+ ⇌ 1 $HEDTA^{3-}$	25	0.20	10.72	-61.19	[68]
$HEDTA^{3-}$	1 $EDTA^{4-}$ + 1 H^+ ⇌ 1 $HEDTA^{3-}$	20	0.1	11.04	-62.99	[69]
$HEDTA^{3-}$	1 $EDTA^{4-}$ + 1 H^+ ⇌ 1 $HEDTA^{3-}$	20	0.1	11.04	-62.99	[70]
$HEDTA^{3-}$	1 $EDTA^{4-}$ + 1 H^+ ⇌ 1 $HEDTA^{3-}$	25	0	11.00	-62.79	[71]
$HEDTA^{3-}$	1 $EDTA^{4-}$ + 1 H^+ ⇌ 1 $HEDTA^{3-}$	25	0.1	10.97	-62.62	[72]
$HEDTA^{3-}$	1 $EDTA^{4-}$ + 1 H^+ ⇌ 1 $HEDTA^{3-}$	25	0.1	10.28	-58.68	[72]
$HEDTA^{3-}$	1 $EDTA^{4-}$ + 1 H^+ ⇌ 1 $HEDTA^{3-}$	25	0.1	10.94	-62.45	[72]
$HEDTA^{3-}$	1 $EDTA^{4-}$ + 1 H^+ ⇌ 1 $HEDTA^{3-}$	25	0.15	11.31	-64.55	[4]
$HEDTA^{3-}$	1 $EDTA^{4-}$ + 1 H^+ ⇌ 1 $HEDTA^{3-}$	RT	0.1	10.98	-62.68	[73]
$HEDTA^{3-}$	1 $EDTA^{4-}$ + 1 H^+ ⇌ 1 $HEDTA^{3-}$	25	0.1	11.25	-64.22	[74]

Appendix C. Data considered in the review of solution complex and mineral thermodynamic constants. Only species with more than one datum considered listed

Species	Equilibrium equation	T/ ºC	I	Corrected logK	$\Delta_f G_m^0$ / kJ mol^{-1}	Ref
$HEDTA^{3-}$	1 $EDTA^{4-}$ + 1 H^+ ⇌ 1 $HEDTA^{3-}$	25	0	10.95	-62.49	[75]
$HEDTA^{3-}$	1 $EDTA^{4-}$ + 1 H^+ ⇌ 1 $HEDTA^{3-}$	25	0.1	11.08	-63.25	[76]
$HEDTA^{3-}$		25	0		-60.34	[77]
				mean	-62.18	
H_2EDTA^{2-}	1 $HEDTA^{3-}$ + 1 H^+ ⇌ 1 H_2EDTA^{2-}	25	0.10	6.74	-100.66	[55]
H_2EDTA^{2-}	1 $HEDTA^{3-}$ + 1 H^+ ⇌ 1 H_2EDTA^{2-}	25	0.10	6.63	-100.03	[56]
H_2EDTA^{2-}	1 $HEDTA^{3-}$ + 1 H^+ ⇌ 1 H_2EDTA^{2-}	25	0.10	6.69	-100.37	[57]
H_2EDTA^{2-}	1 $HEDTA^{3-}$ + 1 H^+ ⇌ 1 H_2EDTA^{2-}	25	0.10	6.74	-100.66	[58]
H_2EDTA^{2-}	1 $HEDTA^{3-}$ + 1 H^+ ⇌ 1 H_2EDTA^{2-}	25	0.10	6.76	-100.77	[59]
H_2EDTA^{2-}	1 $HEDTA^{3-}$ + 1 H^+ ⇌ 1 H_2EDTA^{2-}	25	0.10	6.84	-101.23	[60]
H_2EDTA^{2-}	1 $HEDTA^{3-}$ + 1 H^+ ⇌ 1 H_2EDTA^{2-}	25	0.10	6.77	-100.83	[61]
H_2EDTA^{2-}	1 $HEDTA^{3-}$ + 1 H^+ ⇌ 1 H_2EDTA^{2-}	25	0.10	6.69	-100.37	[62]
H_2EDTA^{2-}	1 $HEDTA^{3-}$ + 1 H^+ ⇌ 1 H_2EDTA^{2-}	25	0.10	6.82	-101.11	[63]
H_2EDTA^{2-}	1 $HEDTA^{3-}$ + 1 H^+ ⇌ 1 H_2EDTA^{2-}	25	0.10	6.72	-100.54	[64]
H_2EDTA^{2-}	1 $HEDTA^{3-}$ + 1 H^+ ⇌ 1 H_2EDTA^{2-}	25	0.10	6.76	-100.77	[65]
H_2EDTA^{2-}	1 $HEDTA^{3-}$ + 1 H^+ ⇌ 1 H_2EDTA^{2-}	25	0.12	6.72	-100.54	[66]
H_2EDTA^{2-}	1 $HEDTA^{3-}$ + 1 H^+ ⇌ 1 H_2EDTA^{2-}	25	0.15	6.78	-100.89	[67]
H_2EDTA^{2-}	1 $HEDTA^{3-}$ + 1 H^+ ⇌ 1 H_2EDTA^{2-}	25	0.20	6.73	-100.60	[68]
H_2EDTA^{2-}	1 $HEDTA^{3-}$ + 1 H^+ ⇌ 1 H_2EDTA^{2-}	20	0.1	6.74	-100.66	[69]
H_2EDTA^{2-}	1 $HEDTA^{3-}$ + 1 H^+ ⇌ 1 H_2EDTA^{2-}	20	0.1	6.74	-100.66	[70]
H_2EDTA^{2-}	1 $HEDTA^{3-}$ + 1 H^+ ⇌ 1 H_2EDTA^{2-}	25	0.1	6.84	-101.19	[72]
H_2EDTA^{2-}	1 $HEDTA^{3-}$ + 1 H^+ ⇌ 1 H_2EDTA^{2-}	25	0.1	6.87	-101.36	[72]
H_2EDTA^{2-}	1 $HEDTA^{3-}$ + 1 H^+ ⇌ 1 H_2EDTA^{2-}	25	0.1	7.07	-102.50	[72]
H_2EDTA^{2-}	1 $HEDTA^{3-}$ + 1 H^+ ⇌ 1 H_2EDTA^{2-}	25	0.15	6.83	-101.15	[4]
H_2EDTA^{2-}	1 $HEDTA^{3-}$ + 1 H^+ ⇌ 1 H_2EDTA^{2-}	RT	0.1	6.78	-100.85	[73]
H_2EDTA^{2-}	1 $HEDTA^{3-}$ + 1 H^+ ⇌ 1 H_2EDTA^{2-}	25	0.1	6.84	-101.19	[74]
H_2EDTA^{2-}	1 $HEDTA^{3-}$ + 1 H^+ ⇌ 1 H_2EDTA^{2-}	25	0	6.70	-100.42	[71]
H_2EDTA^{2-}	1 $HEDTA^{3-}$ + 1 H^+ ⇌ 1 H_2EDTA^{2-}	25	0	6.27	-97.98	[75]
H_2EDTA^{2-}	1 $HEDTA^{3-}$ + 1 H^+ ⇌ 1 H_2EDTA^{2-}	25	0.1	6.70	-100.39	[76]
H_2EDTA^{2-}		25	0		-99.61	[77]

Appendix C. Data considered in the review of solution complex and mineral thermodynamic constants. Only species with more than one datum considered listed

Species	Equilibrium equation	T/ ºC	I	Corrected logK	$\Delta_f G_m^0$ / kJ mol^{-1}	Ref
				mean	-100.67	
H_3EDTA^-	1 H_2EDTA^{2-} + 1 H^+ ⇌ 1 H_3EDTA^-	25	0.10	2.89	-117.17	[57]
H_3EDTA^-	1 H_2EDTA^{2-} + 1 H^+ ⇌ 1 H_3EDTA^-	25	0.10	3.06	-118.14	[60]
H_3EDTA^-	1 H_2EDTA^{2-} + 1 H^+ ⇌ 1 H_3EDTA^-	25	0.10	3.08	-118.25	[61]
H_3EDTA^-	1 H_2EDTA^{2-} + 1 H^+ ⇌ 1 H_3EDTA^-	25	0.10	2.97	-117.62	[62]
H_3EDTA^-	1 H_2EDTA^{2-} + 1 H^+ ⇌ 1 H_3EDTA^-	25	0.10	2.96	-117.57	[58]
H_3EDTA^-	1 H_2EDTA^{2-} + 1 H^+ ⇌ 1 H_3EDTA^-	25	0.10	3.04	-118.02	[63]
H_3EDTA^-	1 H_2EDTA^{2-} + 1 H^+ ⇌ 1 H_3EDTA^-	25	0.10	2.93	-117.40	[64]
H_3EDTA^-	1 H_2EDTA^{2-} + 1 H^+ ⇌ 1 H_3EDTA^-	25	0.10	3.07	-118.20	[65]
H_3EDTA^-	1 H_2EDTA^{2-} + 1 H^+ ⇌ 1 H_3EDTA^-	25	0.10	2.98	-117.68	[75]
H_3EDTA^-	1 H_2EDTA^{2-} + 1 H^+ ⇌ 1 H_3EDTA^-	25	0.12	3.17	-118.77	[66]
H_3EDTA^-	1 H_2EDTA^{2-} + 1 H^+ ⇌ 1 H_3EDTA^-	25	0.15	3.71	-121.85	[67]
H_3EDTA^-	1 H_2EDTA^{2-} + 1 H^+ ⇌ 1 H_3EDTA^-	25	0.20	2.90	-117.23	[68]
H_3EDTA^-	1 H_2EDTA^{2-} + 1 H^+ ⇌ 1 H_3EDTA^-	20	0.1	2.96	-117.57	[69]
H_3EDTA^-	1 H_2EDTA^{2-} + 1 H^+ ⇌ 1 H_3EDTA^-		0.1	2.96	-117.57	[70]
H_3EDTA^-	1 H_2EDTA^{2-} + 1 H^+ ⇌ 1 H_3EDTA^-	25	0.1	3.19	-118.89	[72]
H_3EDTA^-	1 H_2EDTA^{2-} + 1 H^+ ⇌ 1 H_3EDTA^-	25	0.1	3.20	-118.95	[72]
H_3EDTA^-	1 H_2EDTA^{2-} + 1 H^+ ⇌ 1 H_3EDTA^-	25	0.1	3.43	-120.26	[72]
H_3EDTA^-	1 H_2EDTA^{2-} + 1 H^+ ⇌ 1 H_3EDTA^-	25	0.15	3.19	-118.87	[4]
H_3EDTA^-	1 H_2EDTA^{2-} + 1 H^+ ⇌ 1 H_3EDTA^-	RT	0.1	3.09	-118.32	[73]
H_3EDTA^-	1 H_2EDTA^{2-} + 1 H^+ ⇌ 1 H_3EDTA^-	25	0.1	3.00	-117.81	[74]
H_3EDTA^-	1 H_2EDTA^{2-} + 1 H^+ ⇌ 1 H_3EDTA^-	25	0.10	2.98	-117.68	[59]
H_3EDTA^-	1 H_2EDTA^{2-} + 1 H^+ ⇌ 1 H_3EDTA^-	25	0.10	3.23	-119.11	[55]
H_3EDTA^-	1 H_2EDTA^{2-} + 1 H^+ ⇌ 1 H_3EDTA^-	25	0	3.00	-117.79	[71]
H_3EDTA^-	1 H_2EDTA^{2-} + 1 H^+ ⇌ 1 H_3EDTA^-	25	0.1	3.03	-117.98	[76]
H_3EDTA^-		25	0		-117.23	[77]
				mean	-118.24	
$H_4EDTA(aq)$	1 H_3EDTA^- + 1 H^+ ⇌ 1 $H_4EDTA(aq)$	25	0.10	2.19	-130.76	[57]
$H_4EDTA(aq)$	1 H_3EDTA^- + 1 H^+ ⇌ 1 $H_4EDTA(aq)$	25	0.10	2.39	-131.90	[60]

Appendix C. Data considered in the review of solution complex and mineral thermodynamic constants. Only species with more than one datum considered listed

Species	Equilibrium equation	T/ ºC	I	Corrected logK	$\Delta_f G_m^0$ / kJ mol^{-1}	Ref
$H_4EDTA(aq)$	1 H_3EDTA^- + 1 H^+ ⇌ 1 $H_4EDTA(aq)$	25	0.10	2.18	-130.70	[61]
$H_4EDTA(aq)$	1 H_3EDTA^- + 1 H^+ ⇌ 1 $H_4EDTA(aq)$	25	0.10	2.19	-130.76	[62]
$H_4EDTA(aq)$	1 H_3EDTA^- + 1 H^+ ⇌ 1 $H_4EDTA(aq)$	25	0.10	2.19	-130.76	[58]
$H_4EDTA(aq)$	1 H_3EDTA^- + 1 H^+ ⇌ 1 $H_4EDTA(aq)$	25	0.10	2.29	-131.33	[65]
$H_4EDTA(aq)$	1 H_3EDTA^- + 1 H^+ ⇌ 1 $H_4EDTA(aq)$	25	0.10	2.19	-130.76	[75]
$H_4EDTA(aq)$	1 H_3EDTA^- + 1 H^+ ⇌ 1 $H_4EDTA(aq)$	25	0.12	2.30	-131.39	[66]
$H_4EDTA(aq)$	1 H_3EDTA^- + 1 H^+ ⇌ 1 $H_4EDTA(aq)$	25	0.15	2.49	-132.47	[67]
$H_4EDTA(aq)$	1 H_3EDTA^- + 1 H^+ ⇌ 1 $H_4EDTA(aq)$	25	0.20	2.30	-131.39	[68]
$H_4EDTA(aq)$	1 H_3EDTA^- + 1 H^+ ⇌ 1 $H_4EDTA(aq)$	20	0.1	2.19	-130.76	[69]
$H_4EDTA(aq)$	1 H_3EDTA^- + 1 H^+ ⇌ 1 $H_4EDTA(aq)$	20	0.1	2.20	-130.82	[70]
$H_4EDTA(aq)$	1 H_3EDTA^- + 1 H^+ ⇌ 1 $H_4EDTA(aq)$	25	0.1	2.48	-132.36	[72]
$H_4EDTA(aq)$	1 H_3EDTA^- + 1 H^+ ⇌ 1 $H_4EDTA(aq)$	25	0.1	2.41	-131.96	[72]
$H_4EDTA(aq)$	1 H_3EDTA^- + 1 H^+ ⇌ 1 $H_4EDTA(aq)$	25	0.1	2.55	-132.76	[72]
$H_4EDTA(aq)$	1 H_3EDTA^- + 1 H^+ ⇌ 1 $H_4EDTA(aq)$	25	0.15	2.32	-131.48	[4]
$H_4EDTA(aq)$	1 H_3EDTA^- + 1 H^+ ⇌ 1 $H_4EDTA(aq)$	25	0.1	2.18	-130.65	[74]
$H_4EDTA(aq)$	1 H_3EDTA^- + 1 H^+ ⇌ 1 $H_4EDTA(aq)$	25	0.10	2.19	-130.76	[59]
$H_4EDTA(aq)$	1 H_3EDTA^- + 1 H^+ ⇌ 1 $H_4EDTA(aq)$	25	0.10	2.26	-131.16	[63]
$H_4EDTA(aq)$	1 H_3EDTA^- + 1 H^+ ⇌ 1 $H_4EDTA(aq)$	25	0.10	1.99	-129.62	[55]
$H_4EDTA(aq)$	1 H_3EDTA^- + 1 H^+ ⇌ 1 $H_4EDTA(aq)$	25	0	2.20	-130.79	[71]
$H_4EDTA(aq)$	1 H_3EDTA^- + 1 H^+ ⇌ 1 $H_4EDTA(aq)$	25	0.1	2.22	-130.88	[76]
$H_4EDTA(aq)$	1 H_3EDTA^- + 1 H^+ ⇌ 1 $H_4EDTA(aq)$	25	0.3		-131.51	[77]
				mean	-131.21	
H_5EDTA^+	1 $EDTA^{4-}$ + 5 H^+ ⇌ 1 H_5EDTA^+	25	0	23.46	-133.93	[78]
H_5EDTA^+	1 $H_4EDTA(aq)$ + 1 H^+ ⇌ 1 H_5EDTA^+	25	0.10	1.40	-139.20	[65]
H_5EDTA^+	1 $H_4EDTA(aq)$ + 1 H^+ ⇌ 1 H_5EDTA^+	37	0.15	1.55	-140.05	[79]
H_5EDTA^+	1 $H_4EDTA(aq)$ + 1 H^+ ⇌ 1 H_5EDTA^+	25	0.10	1.51	-139.83	[80]
H_5EDTA^+	1 $H_4EDTA(aq)$ + 1 H^+ ⇌ 1 H_5EDTA^+	20	0	1.62	-140.45	[81]
H_5EDTA^+	1 $H_4EDTA(aq)$ + 1 H^+ ⇌ 1 H_5EDTA^+	25	0.10	1.50	-139.77	[75]
H_5EDTA^+	1 $H_4EDTA(aq)$ + 1 H^+ ⇌ 1 H_5EDTA^+	20	0.1	1.55	-140.05	[82]

Appendix C. Data considered in the review of solution complex and mineral thermodynamic constants. Only species with more than one datum considered listed

Species	Equilibrium equation	T/ ºC	I	Corrected logK	$\Delta_f G_m^0$ / kJ mol^{-1}	Ref
				mean	-139.04	
H_6EDTA^{2+}	1 H_5EDTA^+ + 1 H^+ ⇌ 1 H_6EDTA^{2+}	25	0.10	-0.09	-138.50	[65]
H_6EDTA^{2+}	1 H_5EDTA^+ + 1 H^+ ⇌ 1 H_6EDTA^{2+}	20	0	0.92	-144.29	[81]
				mean	-141.40	
NaOH(aq)	1 Na^+ + 1 OH^- ⇌ 1 NaOH(aq)	25	0	-0.57	-415.92	[83]
NaOH(aq)	1 Na^+ + 1 OH^- ⇌ 1 NaOH(aq)	25	0	-0.70	-415.18	[84]
NaOH(aq)	1 Na^+ + 1 OH^- ⇌ 1 NaOH(aq)	25	0	0.10	-419.74	[75]
NaOH(aq)	1 Na^+ + 1 H_2O ⇌ 1 NaOH(aq) + 1 H^+	25	0	-14.08	-418.72	[85]
NaOH(aq)	1 Na^+ + 1 H_2O ⇌ 1 NaOH(aq) + 1 H^+	25	0	-14.79	-414.64	[41]
NaOH(aq)		25	0		-418.26	[9]
NaOH(aq)	1 Na^+ + 1 OH^- ⇌ 1 NaOH(aq)	25	0	-0.72	-415.06	[86]
				mean	-416.79	
NaCl(aq)	1 Na^+ + 1 Cl^- ⇌ 1 NaCl(aq)	25	0	-0.60	-389.75	[87]
NaCl(aq)	1 Na^+ + 1 Cl^- ⇌ 1 NaCl(aq)	25	0	-0.48	-390.43	[43]
NaCl(aq)	1 Na^+ + 1 Cl^- ⇌ 1 NaCl(aq)	25	0	-1.60	-384.04	[88]
NaCl(aq)	1 Na^+ + 1 Cl^- ⇌ 1 NaCl(aq)	25	0	-0.77	-388.77	[89]
NaCl(aq)	1 Na^+ + 1 Cl^- ⇌ 1 NaCl(aq)	25	0	-0.04	-392.94	[90]
NaCl(aq)	1 Na^+ + 1 Cl^- ⇌ 1 NaCl(aq)	25	0	-0.50	-390.32	[75]
NaCl(aq)	1 Na^+ + 1 Cl^- ⇌ 1 NaCl(aq)	25	0	-0.78	-388.73	[41]
NaCl(aq)	1 Na^+ + 1 Cl^- ⇌ 1 NaCl(aq)	25	0	-0.78	-388.72	[91]
NaCl(aq)		25	0		-389.00	[8]
				mean	-389.19	
$NaNO_3$(aq)	1 Na^+ + 1 NO_3^- ⇌ 1 $NaNO_3$(aq)	25	0	-0.55	-369.61	[75]
$NaNO_3$(aq)	1 Na^+ + 1 NO_3^- ⇌ 1 $NaNO_3$(aq)	25	0	-0.85	-367.90	[92]
$NaNO_3$(aq)	1 Na^+ + 1 NO_3^- ⇌ 1 $NaNO_3$(aq)	25	0	-1.22	-365.78	[93]
$NaNO_3$(aq)	1 Na^+ + 1 NO_3^- ⇌ 1 $NaNO_3$(aq)	25	0	-0.55	-369.61	[94]
$NaNO_3$(aq)	1 Na^+ + 1 NO_3^- ⇌ 1 $NaNO_3$(aq)	25	0	-0.57	-369.49	[95]

Appendix C. Data considered in the review of solution complex and mineral thermodynamic constants. Only species with more than one datum considered listed

Species	Equilibrium equation	T/ ºC	I	Corrected logK	$\Delta_f G_m^0$ / kJ mol^{-1}	Ref
				mean	-368.48	
$NaSO_4^-$	$1\ Na^+ + 1\ SO_4^{2-} \rightleftharpoons 1\ NaSO_4^-$	25	0.1	1.05	-1011.95	[96]
$NaSO_4^-$	$1\ Na^+ + 1\ SO_4^{2-} \rightleftharpoons 1\ NaSO_4^-$	25	0.1	1.01	-1011.72	[97]
$NaSO_4^-$	$1\ Na^+ + 1\ SO_4^{2-} \rightleftharpoons 1\ NaSO_4^-$	25	0	0.71	-1010.03	[98]
$NaSO_4^-$	$1\ Na^+ + 1\ SO_4^{2-} \rightleftharpoons 1\ NaSO_4^-$	25	0	0.65	-1009.67	[99]
$NaSO_4^-$	$1\ Na^+ + 1\ SO_4^{2-} \rightleftharpoons 1\ NaSO_4^-$	25	0	0.90	-1011.09	[100]
$NaSO_4^-$	$1\ Na^+ + 1\ SO_4^{2-} \rightleftharpoons 1\ NaSO_4^-$	25	0	0.72	-1010.07	[101]
$NaSO_4^-$	$1\ Na^+ + 1\ SO_4^{2-} \rightleftharpoons 1\ NaSO_4^-$	25	0	0.73	-1010.12	[75]
$NaSO_4^-$	$1\ Na^+ + 1\ SO_4^{2-} \rightleftharpoons 1\ NaSO_4^-$	25	0	0.82	-1010.64	[41]
$NaSO_4^-$	$1\ Na^+ + 1\ SO_4^{2-} \rightleftharpoons 1\ NaSO_4^-$	25	0	0.74	-1010.18	[85]
				mean	-1010.61	
$NaCO_3^-$	$1\ Na^+ + 1\ CO_3^{2-} \rightleftharpoons 1\ NaCO_3^-$	25	0	1.29	-797.22	[102]
$NaCO_3^-$	$1\ Na^+ + 1\ CO_3^{2-} \rightleftharpoons 1\ NaCO_3^-$	25	0	0.55	-792.99	[103]
$NaCO_3^-$	$1\ Na^+ + 1\ CO_3^{2-} \rightleftharpoons 1\ NaCO_3^-$	25	0	1.27	-797.10	[104]
$NaCO_3^-$	$1\ Na^+ + 1\ CO_3^{2-} \rightleftharpoons 1\ NaCO_3^-$	25	0	1.27	-797.10	[75]
$NaCO_3^-$	$1\ Na^+ + 1\ HCO_3^- \rightleftharpoons 1\ NaCO_3^- + 1\ H^+$	25	0	-9.81	-792.78	[41]
				mean	-795.44	
$NaHCO_3$(aq)	$1\ Na^+ + 1\ HCO_3^- \rightleftharpoons 1\ NaHCO_3$(aq)	25	0	0.12	-849.48	[87]
$NaHCO_3$(aq)	$1\ Na^+ + 1\ HCO_3^- \rightleftharpoons 1\ NaHCO_3$(aq)	25	0	0.16	-849.71	[103]
$NaHCO_3$(aq)	$1\ Na^+ + 1\ HCO_3^- \rightleftharpoons 1\ NaHCO_3$(aq)	25	0	-0.25	-847.37	[105]
$NaHCO_3$(aq)	$1\ Na^+ + 1\ HCO_3^- \rightleftharpoons 1\ NaHCO_3$(aq)	25	0	-0.25	-847.37	[75]
$NaHCO_3$(aq)	$1\ Na^+ + 1\ HCO_3^- \rightleftharpoons 1\ NaHCO_3$(aq)	25	0	0.15	-849.68	[41]
				mean	-848.72	
$NaPO_4^{2-}$	$1\ Na^+ + 1\ PO_4^{3-} \rightleftharpoons 1\ NaPO_4^{2-}$	25	0	1.43	-1295.61	[106]
$NaPO_4^{2-}$	$1\ Na^+ + 1\ PO_4^{3-} \rightleftharpoons 1\ NaPO_4^{2-}$	25	0	1.43	-1295.61	[75]
				mean	-1295.61	

Appendix C. Data considered in the review of solution complex and mineral thermodynamic constants. Only species with more than one datum considered listed

Species	Equilibrium equation	T/ ºC	I	Corrected logK	$\Delta_f G_m^0$ / kJ mol^{-1}	Ref
$NaHPO_4^-$	1 Na^+ + 1 PO_4^{3-} + 1 H^+ ⇌ 1 $NaHPO_4^-$	25	0	13.40	-1363.93	[106]
$NaHPO_4^-$	1 Na^+ + 1 HPO_4^{2-} ⇌ 1 $NaHPO_4^-$	25	0	0.85	-1362.79	[107]
$NaHPO_4^-$	1 Na^+ + 1 HPO_4^{2-} ⇌ 1 $NaHPO_4^-$	25	0	1.07	-1364.05	[75]
$NaHPO_4^-$	1 Na^+ + 1 HPO_4^{2-} ⇌ 1 $NaHPO_4^-$	25	0	0.92	-1363.19	[41]
				mean	-1363.49	
NaH_2PO_4(aq)	1 Na^+ + 1 PO_4^{3-} + 2 H^+ ⇌ 1 NaH_2PO_4(aq)	25	0	19.81	-1400.52	[106]
NaH_2PO_4(aq)	1 Na^+ + 1 $H_2PO_4^-$ ⇌ 1 NaH_2PO_4(aq)	25	0.7	-0.12	-1398.44	[108]
NaH_2PO_4(aq)	1 Na^+ + 1 $H_2PO_4^-$ ⇌ 1 NaH_2PO_4(aq)	25	0	0.30	-1400.82	[75]
				mean	-1399.92	
$Na_2PO_4^-$	2 Na^+ + 1 PO_4^{3-} ⇌ 1 $Na_2PO_4^-$	25	0	2.59	-1564.18	[106]
$Na_2PO_4^-$	1 Na^+ + 1 $NaPO_4^{2-}$ ⇌ 1 $Na_2PO_4^-$	25	0	1.16	-1564.18	[75]
				mean	-1564.18	
Na_2HPO_4(aq)	2 Na^+ + 1 PO_4^{3-} + 1 H^+ ⇌ 1 Na_2HPO_4(aq)	25	0	13.32	-1625.43	[106]
Na_2HPO_4(aq)	1 $Na_2PO_4^-$ + 1 H^+ ⇌ 1 Na_2HPO_4(aq)	25	0	10.73	-1625.43	[75]
				mean	-1625.43	
$NaCit^{2-}$	1 Na^+ + 1 Cit^{3-} ⇌ 1 $NaCit^{2-}$	25	0	1.43	-270.12	[109]
$NaCit^{2-}$	1 Na^+ + 1 Cit^{3-} ⇌ 1 $NaCit^{2-}$	25	0	1.34	-269.60	[110]
$NaCit^{2-}$	1 Na^+ + 1 Cit^{3-} ⇌ 1 $NaCit^{2-}$	25	0	1.41	-270.00	[111]
$NaCit^{2-}$	1 Na^+ + 1 Cit^{3-} ⇌ 1 $NaCit^{2-}$	25	0	1.47	-270.34	[74]
$NaCit^{2-}$	1 Na^+ + 1 Cit^{3-} ⇌ 1 $NaCit^{2-}$	25	0	1.67	-271.49	[112]
$NaCit^{2-}$	1 Na^+ + 1 Cit^{3-} ⇌ 1 $NaCit^{2-}$	25	0	1.54	-270.74	[87]
				mean	-270.38	
Na_2Cit^-	2 Na^+ + 1 Cit^{3-} ⇌ 1 Na_2Cit^-	25	0	2.55	-538.46	[112]
Na_2Cit^-	2 Na^+ + 1 Cit^{3-} ⇌ 1 Na_2Cit^-	25	0	2.48	-538.06	[87]
Na_2Cit^-	2 Na^+ + 1 Cit^{3-} ⇌ 1 Na_2Cit^-	25	0	2.38	-537.49	[2]
				mean	-538.00	

Appendix C. Data considered in the review of solution complex and mineral thermodynamic constants. Only species with more than one datum considered listed

Species	Equilibrium equation	T/ ºC	I	Corrected logK	$\Delta_f G_m^0$ / kJ mol^{-1}	Ref
$NaHCit^-$	1 Na^+ + 1 Cit^{3-} + 1 H^+ ⇌ 1 $NaHCit^-$	25	0	7.72	-306.02	[113]
$NaHCit^-$	1 Na^+ + 1 Cit^{3-} + 1 H^+ ⇌ 1 $NaHCit^-$	25	0	6.96	-301.68	[111]
$NaHCit^-$	1 Na^+ + 1 Cit^{3-} + 1 H^+ ⇌ 1 $NaHCit^-$	25	0	7.18	-302.94	[74]
$NaHCit^-$	1 Na^+ + 1 Cit^{3-} + 1 H^+ ⇌ 1 $NaHCit^-$	25	0	7.50	-304.76	[112]
$NaHCit^-$	1 Na^+ + 1 Cit^{3-} + 1 H^+ ⇌ 1 $NaHCit^-$	25	0	7.33	-303.79	[2]
				mean	-303.84	
$NaH_2Cit(aq)$	1 Na^+ + 1 Cit^{3-} + 2 H^+ ⇌ 1 $NaH_2Cit(aq)$	25	0	11.76	-329.08	[113]
$NaH_2Cit(aq)$	1 Na^+ + 1 Cit^{3-} + 2 H^+ ⇌ 1 $NaH_2Cit(aq)$	25	0	11.40	-327.02	[2]
				mean	-328.05	
$NaEDTA^{3-}$	1 Na^+ + 1 $EDTA^{4-}$ ⇌ 1 $NaEDTA^{3-}$	25	0	2.50	-276.22	[78]
$NaEDTA^{3-}$	1 Na^+ + 1 $EDTA^{4-}$ ⇌ 1 $NaEDTA^{3-}$	25	0	2.70	-277.36	[71]
$NaEDTA^{3-}$	1 Na^+ + 1 $EDTA^{4-}$ ⇌ 1 $NaEDTA^{3-}$	25	0.3	2.62	-276.88	[74]
$NaEDTA^{3-}$	1 Na^+ + 1 $EDTA^{4-}$ ⇌ 1 $NaEDTA^{3-}$	25	0.32	2.57	-276.60	[1]
$NaEDTA^{3-}$	1 Na^+ + 1 $EDTA^{4-}$ ⇌ 1 $NaEDTA^{3-}$		0.01	2.97	-278.90	[114]
$NaEDTA^{3-}$	1 Na^+ + 1 $EDTA^{4-}$ ⇌ 1 $NaEDTA^{3-}$	20	0.1	2.52	-276.34	[115]
$NaEDTA^{3-}$	1 Na^+ + 1 $EDTA^{4-}$ ⇌ 1 $NaEDTA^{3-}$	25	0.15	3.31	-280.84	[4]
$NaEDTA^{3-}$	1 Na^+ + 1 $EDTA^{4-}$ ⇌ 1 $NaEDTA^{3-}$	25	0.1	2.68	-277.25	[116]
$NaEDTA^{3-}$	1 Na^+ + 1 $EDTA^{4-}$ ⇌ 1 $NaEDTA^{3-}$	25	0.1	2.72	-277.48	[75]
				mean	-277.54	
$NaHEDTA^{2-}$	1 Na^+ + 1 $HEDTA^{3-}$ ⇌ 1 $NaHEDTA^{2-}$	25	0.1	2.44	-338.07	[75]
$NaHEDTA^{2-}$	1 Na^+ + 1 $HEDTA^{3-}$ ⇌ 1 $NaHEDTA^{2-}$	25	0.32	1.07	-330.25	[1]
$NaHEDTA^{2-}$	1 Na^+ + 1 $EDTA^{4-}$ + 1 H^+ ⇌ 1 $NaHEDTA^{2-}$	25	0.1	11.30	-326.44	[74]
$NaHEDTA^{2-}$	1 Na^+ + 1 $HEDTA^{3-}$ ⇌ 1 $NaHEDTA^{2-}$		0.01	0.24	-325.50	[114]
$NaHEDTA^{2-}$	1 Na^+ + 1 $EDTA^{4-}$ + 1 H^+ ⇌ 1 $NaHEDTA^{2-}$	25	0.15	14.12	-342.53	[4]
				mean	-332.56	
KCl(aq)	1 K^+ + 1 Cl^- ⇌ 1 KCl(aq)	25	0	-0.51	-410.82	[87]

Appendix C. Data considered in the review of solution complex and mineral thermodynamic constants. Only species with more than one datum considered listed

Species	Equilibrium equation	T/ ºC	I	Corrected logK	$\Delta_f G_m^0$ / kJ mol^{-1}	Ref
KCl(aq)	1 K^+ + 1 Cl^- ⇌ 1 KCl(aq)	25	0	-0.76	-409.39	[89]
KCl(aq)	1 K^+ + 1 Cl^- ⇌ 1 KCl(aq)	25	0	-0.10	-413.16	[90]
KCl(aq)	1 K^+ + 1 Cl^- ⇌ 1 KCl(aq)	25	0	-0.50	-410.87	[75]
KCl(aq)	1 K^+ + 1 Cl^- ⇌ 1 KCl(aq)	25	0	-0.42	-411.33	[87]
				mean	-411.11	
KSO_4^-	1 K^+ + 1 SO_4^{2-} ⇌ 1 KSO_4^-	25	0	0.84	-1031.31	[50]
KSO_4^-	1 K^+ + 1 SO_4^{2-} ⇌ 1 KSO_4^-	25	0	0.75	-1030.80	[99]
KSO_4^-	1 K^+ + 1 SO_4^{2-} ⇌ 1 KSO_4^-	25	0	0.96	-1031.99	[101]
KSO_4^-	1 K^+ + 1 SO_4^{2-} ⇌ 1 KSO_4^-	25	0	0.85	-1031.37	[75]
KSO_4^-	1 K^+ + 1 SO_4^{2-} ⇌ 1 KSO_4^-	25	0	0.85	-1031.37	[85]
KSO_4^-	1 K^+ + 1 SO_4^{2-} ⇌ 1 KSO_4^-	25	0	0.88	-1031.53	[41]
KSO_4^-		25	0		-1032.63	[8]
				mean	-1031.57	
KPO_4^{2-}	1 K^+ + 1 PO_4^{3-} ⇌ 1 KPO_4^{2-}	25	0	1.37	-1315.82	[106]
KPO_4^{2-}	1 K^+ + 1 PO_4^{3-} ⇌ 1 KPO_4^{2-}	25	0	1.43	-1316.16	[75]
KPO_4^{2-}	1 K^+ + 1 PO_4^{3-} ⇌ 1 KPO_4^{2-}	25	0	1.37	-1315.82	[6]
				mean	-1315.93	
$KHPO_4^-$	1 K^+ + 1 PO_4^{3-} + 1 H^+ ⇌ 1 $KHPO_4^-$	25	0	13.21	-1383.40	[106]
$KHPO_4^-$	1 K^+ + 1 HPO_4^{2-} ⇌ 1 $KHPO_4^-$	25	0	0.88	-1383.52	[75]
$KHPO_4^-$	1 K^+ + 1 HPO_4^{2-} ⇌ 1 $KHPO_4^-$	25	0	0.78	-1382.95	[41]
$KHPO_4^-$	1 K^+ + 1 PO_4^{3-} + 1 H^+ ⇌ 1 $KHPO_4^-$	25	0	13.23	-1383.52	[6]
				mean	-1383.35	
KH_2PO_4(aq)	1 K^+ + 1 PO_4^{3-} + 2 H^+ ⇌ 1 KH_2PO_4(aq)	25	0	19.79	-1420.96	[106]
KH_2PO_4(aq)	1 K^+ + 1 $H_2PO_4^-$ ⇌ 1 KH_2PO_4(aq)	25	0	0.30	-1421.37	[75]
KH_2PO_4(aq)	1 K^+ + 1 PO_4^{3-} + 2 H^+ ⇌ 1 KH_2PO_4(aq)	25	0	19.79	-1420.96	[6]
				mean	-1421.10	

Appendix C. Data considered in the review of solution complex and mineral thermodynamic constants. Only species with more than one datum considered listed

Species	Equilibrium equation	T/ ºC	I	Corrected logK	$\Delta_f G_m^0$ / kJ mol^{-1}	Ref
$K_2PO_4^-$	$2\ K^+ + 1\ PO_4^{3-} \rightleftharpoons 1\ K_2PO_4^-$	25	0	2.20	-1603.07	[106]
$K_2PO_4^-$	$1\ K^+ + 1\ KPO_4^{2-} \rightleftharpoons 1\ K_2PO_4^-$	25	0	0.83	-1603.18	[75]
$K_2PO_4^-$	$2\ K^+ + 1\ PO_4^{3-} \rightleftharpoons 1\ K_2PO_4^-$	25	0	2.20	-1603.07	[6]
				mean	-1603.11	
K_2HPO_4(aq)	$2\ K^+ + 1\ PO_4^{3-} + 1\ H^+ \rightleftharpoons 1\ K_2HPO_4$(aq)	25	0	13.44	-1667.23	[106]
K_2HPO_4(aq)	$1\ K_2PO_4^- + 1\ H^+ \rightleftharpoons 1\ K_2HPO_4$(aq)	25	0	11.24	-1667.26	[75]
K_2HPO_4(aq)	$2\ K^+ + 1\ PO_4^{3-} + 1\ H^+ \rightleftharpoons 1\ K_2HPO_4$(aq)	25	0	13.44	-1667.23	[6]
				mean	-1667.24	
$KCit^{2-}$	$1\ K^+ + 1\ Cit^{3-} \rightleftharpoons 1\ KCit^{2-}$	25	0	1.10	-288.79	[117]
$KCit^{2-}$	$1\ K^+ + 1\ Cit^{3-} \rightleftharpoons 1\ KCit^{2-}$	25	0	1.16	-289.13	[109]
$KCit^{2-}$	$1\ K^+ + 1\ Cit^{3-} \rightleftharpoons 1\ KCit^{2-}$	25	0	1.23	-289.53	[110]
$KCit^{2-}$	$1\ K^+ + 1\ Cit^{3-} \rightleftharpoons 1\ KCit^{2-}$	25	0	1.29	-289.87	[118]
$KCit^{2-}$	$1\ K^+ + 1\ Cit^{3-} \rightleftharpoons 1\ KCit^{2-}$	25	0	1.36	-290.27	[119]
$KCit^{2-}$	$1\ K^+ + 1\ Cit^{3-} \rightleftharpoons 1\ KCit^{2-}$	25	0	1.54	-291.30	[112]
$KCit^{2-}$	$1\ K^+ + 1\ Cit^{3-} \rightleftharpoons 1\ KCit^{2-}$	25	0	1.51	-291.13	[87]
$KCit^{2-}$	$1\ K^+ + 1\ Cit^{3-} \rightleftharpoons 1\ KCit^{2-}$	25	0	1.42	-290.62	[2]
				mean	-290.08	
K_2Cit^-	$2\ K^+ + 1\ Cit^{3-} \rightleftharpoons 1\ K_2Cit^-$	25	0	2.10	-577.01	[112]
K_2Cit^-	$2\ K^+ + 1\ Cit^{3-} \rightleftharpoons 1\ K_2Cit^-$	25	0	2.13	-577.18	[87]
K_2Cit^-	$2\ K^+ + 1\ Cit^{3-} \rightleftharpoons 1\ K_2Cit^-$	25	0	1.93	-576.04	[2]
				mean	-576.74	
$KHCit^-$	$1\ K^+ + 1\ Cit^{3-} + 1\ H^+ \rightleftharpoons 1\ KHCit^-$	25	0	6.56	-319.95	[118]
$KHCit^-$	$1\ K^+ + 1\ Cit^{3-} + 1\ H^+ \rightleftharpoons 1\ KHCit^-$	25	0	7.01	-322.52	[119]
$KHCit^-$	$1\ K^+ + 1\ Cit^{3-} + 1\ H^+ \rightleftharpoons 1\ KHCit^-$	25	0	7.30	-324.18	[112]
$KHCit^-$	$1\ K^+ + 1\ Cit^{3-} + 1\ H^+ \rightleftharpoons 1\ KHCit^-$	25	0	7.13	-323.21	[2]
				mean	-322.47	

Appendix C. Data considered in the review of solution complex and mineral thermodynamic constants. Only species with more than one datum considered listed

Species	Equilibrium equation	T/ ºC	I	Corrected logK	$\Delta_f G_m^0$ / kJ mol^{-1}	Ref
$KH_2Cit(aq)$	1 K^+ + 1 Cit^{3-} + 2 H^+ ⇌ 1 $KH_2Cit(aq)$	25	0	11.13	-346.04	[119]
$KH_2Cit(aq)$	1 K^+ + 1 Cit^{3-} + 2 H^+ ⇌ 1 $KH_2Cit(aq)$	25	0	11.30	-347.01	[2]
				mean	-346.53	
$KEDTA^{3-}$	1 K^+ + 1 $EDTA^{4-}$ ⇌ 1 $KEDTA^{3-}$	25	0	1.70	-292.21	[78]
$KEDTA^{3-}$	1 K^+ + 1 $EDTA^{4-}$ ⇌ 1 $KEDTA^{3-}$	25	0.1	1.66	-291.99	[74]
$KEDTA^{3-}$	1 K^+ + 1 $EDTA^{4-}$ ⇌ 1 $KEDTA^{3-}$	25	0.32	1.74	-292.42	[1]
$KEDTA^{3-}$	1 K^+ + 1 $EDTA^{4-}$ ⇌ 1 $KEDTA^{3-}$	25	0.15	2.56	-297.11	[4]
$KEDTA^{3-}$	1 K^+ + 1 $EDTA^{4-}$ ⇌ 1 $KEDTA^{3-}$	25	0.1	1.41	-290.56	[116]
$KEDTA^{3-}$	1 K^+ + 1 $EDTA^{4-}$ ⇌ 1 $KEDTA^{3-}$	25	0.1	1.66	-291.99	[75]
				mean	-292.71	
$KHEDTA^{2-}$	1 K^+ + 1 $HEDTA^{3-}$ ⇌ 1 $KHEDTA^{2-}$	25	0.32	0.27	-346.24	[1]
$KHEDTA^{2-}$	1 K^+ + 1 $EDTA^{4-}$ + 1 H^+ ⇌ 1 $KHEDTA^{2-}$	25	0.15	12.76	-355.33	[4]
				mean	-350.79	
KH_2EDTA^-	1 $KHEDTA^{2-}$ + 1 H^+ ⇌ 1 KH_2EDTA^-	25	0.1	4.39	-375.83	[75]
KH_2EDTA^-	1 $KHEDTA^{2-}$ + 1 H^+ ⇌ 1 KH_2EDTA^-	20	0.1	4.24	-374.98	[75]
KH_2EDTA^-	1 K^+ + 2 H^+ + 1 $EDTA^{4-}$ ⇌ 1 KH_2EDTA^-	25	0.15	20.13	-397.39	[4]
				mean	-382.73	
$MgOH^+$	1 Mg^{2+} + 1 H_2O ⇌ 1 $MgOH^+$ + 1 H^+	25	0	-11.68	-625.85	[120]
$MgOH^+$	1 Mg^{2+} + 1 OH^- ⇌ 1 $MgOH^+$	25	0	2.21	-625.21	[121]
$MgOH^+$	1 Mg^{2+} + 1 OH^- ⇌ 1 $MgOH^+$	25	0	1.60	-621.73	[122]
$MgOH^+$	1 Mg^{2+} + 1 OH^- ⇌ 1 $MgOH^+$	25	0	2.60	-627.44	[75]
$MgOH^+$	1 Mg^{2+} + 1 OH^- ⇌ 1 $MgOH^+$	25	0	2.45	-626.58	[50]
$MgOH^+$		25	0		-624.90	[9]
				mean	-625.28	
$MgCl^+$	1 Mg^{2+} + 1 Cl^- ⇌ 1 $MgCl^+$	25	0	0.49	-589.39	[123]
$MgCl^+$	1 Mg^{2+} + 1 Cl^- ⇌ 1 $MgCl^+$	25	0	0.60	-590.02	[75]

Appendix C. Data considered in the review of solution complex and mineral thermodynamic constants. Only species with more than one datum considered listed

Species	Equilibrium equation	T/ ºC	I	Corrected logK	$\Delta_f G_m^0$ / kJ mol^{-1}	Ref
$MgCl^+$	1 Mg^{2+} + 1 Cl^- ⇌ 1 $MgCl^+$	25	0.1	0.63	-590.19	[75]
$MgCl^+$	1 Mg^{2+} + 1 Cl^- ⇌ 1 $MgCl^+$	25	0	-0.13	-585.82	[41]
$MgCl^+$	1 Mg^{2+} + 1 Cl^- ⇌ 1 $MgCl^+$	25	0	0.57	-589.85	[124]
$MgCl^+$		25	0		-584.90	[8]
				mean	-588.36	
$MgSO_4$(aq)	1 Mg^{2+} + 1 SO_4^{2-} ⇌ 1 $MgSO_4$(aq)	20	0	2.21	-1211.99	[125]
$MgSO_4$(aq)	1 Mg^{2+} + 1 SO_4^{2-} ⇌ 1 $MgSO_4$(aq)	25	0	2.34	-1212.74	[126]
$MgSO_4$(aq)	1 Mg^{2+} + 1 SO_4^{2-} ⇌ 1 $MgSO_4$(aq)	25	0	2.23	-1212.11	[85]
$MgSO_4$(aq)	1 Mg^{2+} + 1 SO_4^{2-} ⇌ 1 $MgSO_4$(aq)	25	0	2.13	-1211.54	[127]
$MgSO_4$(aq)	1 Mg^{2+} + 1 SO_4^{2-} ⇌ 1 $MgSO_4$(aq)	25	0	2.24	-1212.17	[128]
$MgSO_4$(aq)	1 Mg^{2+} + 1 SO_4^{2-} ⇌ 1 $MgSO_4$(aq)	25	0	2.24	-1212.17	[88]
$MgSO_4$(aq)	1 Mg^{2+} + 1 SO_4^{2-} ⇌ 1 $MgSO_4$(aq)	25	0	2.23	-1212.11	[99]
$MgSO_4$(aq)	1 Mg^{2+} + 1 SO_4^{2-} ⇌ 1 $MgSO_4$(aq)	25	0	2.40	-1213.08	[129]
$MgSO_4$(aq)	1 Mg^{2+} + 1 SO_4^{2-} ⇌ 1 $MgSO_4$(aq)	25	0	2.26	-1212.28	[75]
$MgSO_4$(aq)	1 Mg^{2+} + 1 SO_4^{2-} ⇌ 1 $MgSO_4$(aq)	25	0	2.41	-1213.15	[41]
				mean	-1212.33	
$MgCO_3$(aq)	1 Mg^{2+} + 1 CO_3^{2-} ⇌ 1 $MgCO_3$(aq)	25	0	3.32	-1002.23	[130]
$MgCO_3$(aq)	1 Mg^{2+} + 1 CO_3^{2-} ⇌ 1 $MgCO_3$(aq)	25	0	2.98	-1000.31	[131]
$MgCO_3$(aq)	1 Mg^{2+} + 1 CO_3^{2-} ⇌ 1 $MgCO_3$(aq)	25	0	2.88	-999.71	[132]
$MgCO_3$(aq)	1 Mg^{2+} + 1 CO_3^{2-} ⇌ 1 $MgCO_3$(aq)	25	0	3.24	-1001.77	[103]
$MgCO_3$(aq)	1 Mg^{2+} + 1 CO_3^{2-} ⇌ 1 $MgCO_3$(aq)	25	0	3.40	-1002.68	[104]
$MgCO_3$(aq)	1 Mg^{2+} + 1 CO_3^{2-} ⇌ 1 $MgCO_3$(aq)	25	0	2.92	-999.94	[75]
$MgCO_3$(aq)	1 Mg^{2+} + 1 CO_3^{2-} ⇌ 1 $MgCO_3$(aq)	25	0	2.98	-1000.28	[75]
$MgCO_3$(aq)	1 Mg^{2+} + 1 HCO_3^- ⇌ 1 $MgCO_3$(aq) + 1 H^+	25	0	-7.35	-1000.27	[41]
$MgCO_3$(aq)		25	0		-999.64	[8]
				mean	-1000.76	
$MgHCO_3^+$	1 Mg^{2+} + 1 HCO_3^- ⇌ 1 $MgHCO_3^+$	25	0	1.23	-1049.24	[130]
$MgHCO_3^+$	1 Mg^{2+} + 1 HCO_3^- ⇌ 1 $MgHCO_3^+$	25	0	1.07	-1048.30	[131]

Appendix C. Data considered in the review of solution complex and mineral thermodynamic constants. Only species with more than one datum considered listed

Species	Equilibrium equation	T/ ºC	I	Corrected logK	$\Delta_f G_m^0$ / kJ mol^{-1}	Ref
$MgHCO_3^+$	1 Mg^{2+} + 1 HCO_3^- ⇌ 1 $MgHCO_3^+$	25	0	1.23	-1049.24	[103]
$MgHCO_3^+$	1 Mg^{2+} + 1 HCO_3^- ⇌ 1 $MgHCO_3^+$	25	0	0.95	-1047.64	[133]
$MgHCO_3^+$	1 Mg^{2+} + 1 HCO_3^- ⇌ 1 $MgHCO_3^+$	25	0	1.16	-1048.84	[105]
$MgHCO_3^+$	1 Mg^{2+} + 1 HCO_3^- ⇌ 1 $MgHCO_3^+$	25	0	1.01	-1047.99	[75]
$MgHCO_3^+$	1 Mg^{2+} + 1 CO_3^{2-} + 1 H^+ ⇌ 1 $MgHCO_3^+$	25	0	11.31	-1047.83	[134]
$MgHCO_3^+$	1 Mg^{2+} + 1 HCO_3^- ⇌ 1 $MgHCO_3^+$	25	0	1.04	-1048.13	[41]
				mean	-1048.40	
$MgPO_4^-$	1 Mg^{2+} + 1 PO_4^{3-} ⇌ 1 $MgPO_4^-$	25	0.15	3.34	-1499.91	[135]
$MgPO_4^-$	1 Mg^{2+} + 1 PO_4^{3-} ⇌ 1 $MgPO_4^-$	25	0.2	4.66	-1507.45	[136]
$MgPO_4^-$	1 Mg^{2+} + 1 HPO_4^{2-} ⇌ 1 $MgPO_4^-$ + 1 H^+	25	0	-5.73	-1518.64	[41]
$MgPO_4^-$	1 Mg^{2+} + 1 PO_4^{3-} ⇌ 1 $MgPO_4^-$	25	0	4.93	-1509.01	[6]
				mean	-1508.75	
$MgHPO_4$(aq)	1 Mg^{2+} + 1 PO_4^{3-} + 1 H^+ ⇌ 1 $MgHPO_4$(aq)	25	0.25	15.65	-1570.19	[137]
$MgHPO_4$(aq)	1 Mg^{2+} + 1 HPO_4^{2-} ⇌ 1 $MgHPO_4$(aq)	25	0.1	2.69	-1566.72	[138]
$MgHPO_4$(aq)	1 Mg^{2+} + 1 HPO_4^{2-} ⇌ 1 $MgHPO_4$(aq)	25	0	2.85	-1567.63	[11]
$MgHPO_4$(aq)	1 Mg^{2+} + 1 HPO_4^{2-} ⇌ 1 $MgHPO_4$(aq)	25	0	2.70	-1566.78	[139]
$MgHPO_4$(aq)	1 Mg^{2+} + 1 HPO_4^{2-} ⇌ 1 $MgHPO_4$(aq)	25	0.2	2.96	-1568.25	[136]
$MgHPO_4$(aq)	1 Mg^{2+} + 1 HPO_4^{2-} ⇌ 1 $MgHPO_4$(aq)	25	0	2.85	-1567.63	[140]
$MgHPO_4$(aq)	1 Mg^{2+} + 1 HPO_4^{2-} ⇌ 1 $MgHPO_4$(aq)	25	0	2.74	-1567.01	[141]
$MgHPO_4$(aq)	1 Mg^{2+} + 1 HPO_4^{2-} ⇌ 1 $MgHPO_4$(aq)	25	0	2.80	-1567.35	[75]
$MgHPO_4$(aq)	1 Mg^{2+} + 1 HPO_4^{2-} ⇌ 1 $MgHPO_4$(aq)	25	0	2.91	-1567.98	[41]
$MgHPO_4$(aq)	1 Mg^{2+} + 1 PO_4^{3-} + 1 H^+ ⇌ 1 $MgHPO_4$(aq)	25	0	15.15	-1567.34	[6]
				mean	-1567.69	
$MgH_2PO_4^+$	1 Mg^{2+} + 1 $H_2PO_4^-$ ⇌ 1 $MgH_2PO_4^+$	25	0	0.61	-1596.01	[11]
$MgH_2PO_4^+$	1 Mg^{2+} + 1 $H_2PO_4^-$ ⇌ 1 $MgH_2PO_4^+$	25	0.2	2.02	-1604.05	[136]
$MgH_2PO_4^+$	1 Mg^{2+} + 1 $H_2PO_4^-$ ⇌ 1 $MgH_2PO_4^+$	25	0	1.28	-1599.83	[140]
$MgH_2PO_4^+$	1 Mg^{2+} + 1 PO_4^{3-} + 2 H^+ ⇌ 1 $MgH_2PO_4^+$	25	0	21.24	-1602.10	[6]
				mean	-1600.50	

Appendix C. Data considered in the review of solution complex and mineral thermodynamic constants. Only species with more than one datum considered listed

Species	Equilibrium equation	T/ ºC	I	Corrected logK	$\Delta_f G_m^0$ / kJ mol^{-1}	Ref
$MgCit^-$	1 Mg^{2+} + 1 Cit^{3-} ⇌ 1 $MgCit^-$	25	0	4.65	-481.92	[142]
$MgCit^-$	1 Mg^{2+} + 1 Cit^{3-} ⇌ 1 $MgCit^-$	25	0	4.89	-483.29	[143]
$MgCit^-$	1 Mg^{2+} + 1 Cit^{3-} ⇌ 1 $MgCit^-$	25	0	4.53	-481.23	[144]
$MgCit^-$	1 Mg^{2+} + 1 Cit^{3-} ⇌ 1 $MgCit^-$	25	0	5.00	-483.92	[109]
$MgCit^-$	1 Mg^{2+} + 1 Cit^{3-} ⇌ 1 $MgCit^-$	25	0	4.91	-483.40	[145]
$MgCit^-$	1 Mg^{2+} + 1 Cit^{3-} ⇌ 1 $MgCit^-$	25	0	4.67	-482.03	[146]
$MgCit^-$	1 Mg^{2+} + 1 Cit^{3-} ⇌ 1 $MgCit^-$	25	0	4.90	-483.34	[147]
$MgCit^-$	1 Mg^{2+} + 1 Cit^{3-} ⇌ 1 $MgCit^-$	25	0	5.01	-483.97	[148]
$MgCit^-$	1 Mg^{2+} + 1 Cit^{3-} ⇌ 1 $MgCit^-$	25	0	4.93	-483.52	[149]
$MgCit^-$	1 Mg^{2+} + 1 Cit^{3-} ⇌ 1 $MgCit^-$	25	0	5.13	-484.66	[150]
$MgCit^-$	1 Mg^{2+} + 1 Cit^{3-} ⇌ 1 $MgCit^-$	25	0	4.66	-481.97	[151]
$MgCit^-$	1 Mg^{2+} + 1 Cit^{3-} ⇌ 1 $MgCit^-$	25	0	4.75	-482.49	[12]
$MgCit^-$	1 Mg^{2+} + 1 Cit^{3-} ⇌ 1 $MgCit^-$	25	0	4.85	-483.06	[152]
$MgCit^-$	1 Mg^{2+} + 1 Cit^{3-} ⇌ 1 $MgCit^-$	25	0	4.87	-483.17	[153]
$MgCit^-$	1 Mg^{2+} + 1 Cit^{3-} ⇌ 1 $MgCit^-$	25	0	4.92	-483.46	[154]
$MgCit^-$	1 Mg^{2+} + 1 Cit^{3-} ⇌ 1 $MgCit^-$	25	0	4.74	-482.43	[155]
$MgCit^-$	1 Mg^{2+} + 1 Cit^{3-} ⇌ 1 $MgCit^-$	25	0	4.79	-482.72	[10]
$MgCit^-$	1 Mg^{2+} + 1 Cit^{3-} ⇌ 1 $MgCit^-$	25	0	4.92	-483.46	[156]
$MgCit^-$	1 Mg^{2+} + 1 Cit^{3-} ⇌ 1 $MgCit^-$	25	0	4.70	-482.20	[135]
$MgCit^-$	1 Mg^{2+} + 1 Cit^{3-} ⇌ 1 $MgCit^-$	25	0	4.71	-482.26	[2]
				mean	-482.92	
MgHCit(aq)	1 Mg^{2+} + 1 Cit^{3-} + 1 H^+ ⇌ 1 MgHCit(aq)	25	0	8.79	-505.55	[144]
MgHCit(aq)	1 Mg^{2+} + 1 Cit^{3-} + 1 H^+ ⇌ 1 MgHCit(aq)	25	0	9.07	-507.15	[146]
MgHCit(aq)	1 Mg^{2+} + 1 Cit^{3-} + 1 H^+ ⇌ 1 MgHCit(aq)	25	0	9.07	-507.15	[148]
MgHCit(aq)	1 Mg^{2+} + 1 Cit^{3-} + 1 H^+ ⇌ 1 MgHCit(aq)	25	0	9.14	-507.55	[150]
MgHCit(aq)	1 Mg^{2+} + 1 Cit^{3-} + 1 H^+ ⇌ 1 MgHCit(aq)	25	0	8.97	-506.58	[157]
MgHCit(aq)	1 Mg^{2+} + 1 Cit^{3-} + 1 H^+ ⇌ 1 MgHCit(aq)	25	0	9.16	-507.66	[151]
MgHCit(aq)	1 Mg^{2+} + 1 Cit^{3-} + 1 H^+ ⇌ 1 MgHCit(aq)	25	0	9.00	-506.75	[152]
MgHCit(aq)	1 Mg^{2+} + 1 Cit^{3-} + 1 H^+ ⇌ 1 MgHCit(aq)	25	0	8.88	-506.06	[153]

Appendix C. Data considered in the review of solution complex and mineral thermodynamic constants. Only species with more than one datum considered listed

Species	Equilibrium equation	T/ ºC	I	Corrected logK	$\Delta_f G_m^0$ / kJ mol^{-1}	Ref
MgHCit(aq)	1 Mg^{2+} + 1 Cit^{3-} + 1 H^+ ⇌ 1 MgHCit(aq)	25	0	9.11	-507.38	[155]
MgHCit(aq)	1 Mg^{2+} + 1 Cit^{3-} + 1 H^+ ⇌ 1 MgHCit(aq)	25	0	9.18	-507.77	[10]
MgHCit(aq)	1 Mg^{2+} + 1 Cit^{3-} + 1 H^+ ⇌ 1 MgHCit(aq)	25	0	8.84	-505.83	[2]
				mean	-506.86	
MgH_2Cit^+	1 Mg^{2+} + 1 Cit^{3-} + 2 H^+ ⇌ 1 MgH_2Cit^+	25	0	12.43	-526.33	[146]
MgH_2Cit^+	1 Mg^{2+} + 1 Cit^{3-} + 2 H^+ ⇌ 1 MgH_2Cit^+	25	0	12.19	-524.96	[152]
MgH_2Cit^+	1 Mg^{2+} + 1 Cit^{3-} + 2 H^+ ⇌ 1 MgH_2Cit^+	25	0	12.71	-527.92	[10]
MgH_2Cit^+	1 Mg^{2+} + 1 Cit^{3-} + 2 H^+ ⇌ 1 MgH_2Cit^+	25	0	12.57	-527.13	[158]
				mean	-526.58	
$MgEDTA^{2-}$	1 Mg^{2+} + 1 $EDTA^{4-}$ ⇌ 1 $MgEDTA^{2-}$	25	0	10.60	-515.88	[78]
$MgEDTA^{2-}$	1 Mg^{2+} + 1 $EDTA^{4-}$ ⇌ 1 $MgEDTA^{2-}$	20	0.1	10.20	-513.60	[65]
$MgEDTA^{2-}$	1 Mg^{2+} + 1 $EDTA^{4-}$ ⇌ 1 $MgEDTA^{2-}$	20	0.1	10.24	-513.83	[69]
$MgEDTA^{2-}$	1 Mg^{2+} + 1 $EDTA^{4-}$ ⇌ 1 $MgEDTA^{2-}$	25	0.3	9.70	-510.75	[159]
$MgEDTA^{2-}$	1 Mg^{2+} + 1 $EDTA^{4-}$ ⇌ 1 $MgEDTA^{2-}$	20	0.1	12.55	-527.02	[160]
$MgEDTA^{2-}$	1 Mg^{2+} + 1 $EDTA^{4-}$ ⇌ 1 $MgEDTA^{2-}$	20	0.1	10.24	-513.83	[161]
$MgEDTA^{2-}$	1 Mg^{2+} + 1 $EDTA^{4-}$ ⇌ 1 $MgEDTA^{2-}$	25	0.1	10.36	-514.51	[162]
$MgEDTA^{2-}$	1 Mg^{2+} + 1 $EDTA^{4-}$ ⇌ 1 $MgEDTA^{2-}$	25	0	9.10	-507.32	[163]
$MgEDTA^{2-}$		25	0		-507.28	[164]
$MgEDTA^{2-}$	1 Mg^{2+} + 1 $EDTA^{4-}$ ⇌ 1 $MgEDTA^{2-}$	25	0.1	10.62	-516.00	[165]
$MgEDTA^{2-}$	1 Mg^{2+} + 1 $EDTA^{4-}$ ⇌ 1 $MgEDTA^{2-}$	20	0.1	10.24	-513.83	[166]
$MgEDTA^{2-}$	1 Mg^{2+} + 1 $EDTA^{4-}$ ⇌ 1 $MgEDTA^{2-}$	20	0	9.12	-507.43	[115]
$MgEDTA^{2-}$	1 Mg^{2+} + 1 $EDTA^{4-}$ ⇌ 1 $MgEDTA^{2-}$	25	0.1	10.51	-515.37	[75]
$MgEDTA^{2-}$	1 Mg^{2+} + 1 $EDTA^{4-}$ ⇌ 1 $MgEDTA^{2-}$	25	0.1	10.68	-516.34	[75]
$MgEDTA^{2-}$	1 Mg^{2+} + 1 $EDTA^{4-}$ ⇌ 1 $MgEDTA^{2-}$	25	0	10.60	-515.88	[167]
$MgEDTA^{2-}$	1 Mg^{2+} + 1 $EDTA^{4-}$ ⇌ 1 $MgEDTA^{2-}$	20	0.1	10.41	-514.80	[168]
$MgEDTA^{2-}$	1 Mg^{2+} + 1 $EDTA^{4-}$ ⇌ 1 $MgEDTA^{2-}$	20	0	9.12	-507.43	[169]
				mean	-513.59	
$MgHEDTA^-$	1 Mg^{2+} + 1 $EDTA^{4-}$ + 1 H^+ ⇌ 1 $MgHEDTA^-$	25	0	15.10	-541.57	[78]

Appendix C. Data considered in the review of solution complex and mineral thermodynamic constants. Only species with more than one datum considered listed

Species	Equilibrium equation	T/ ºC	I	Corrected logK	$\Delta_f G_m^0$ / kJ mol^{-1}	Ref
$MgHEDTA^-$	1 Mg^{2+} + 1 $HEDTA^{3-}$ ⇌ 1 $MgHEDTA^-$	20	0.1	3.57	-537.93	[161]
$MgHEDTA^-$	1 Mg^{2+} + 1 $HEDTA^{3-}$ ⇌ 1 $MgHEDTA^-$	20	0.1	3.57	-537.93	[166]
$MgHEDTA^-$	1 Mg^{2+} + 1 $HEDTA^{3-}$ ⇌ 1 $MgHEDTA^-$	25	0.1	5.29	-547.75	[75]
$MgHEDTA^-$	1 Mg^{2+} + 1 $HEDTA^{3-}$ ⇌ 1 $MgHEDTA^-$	20	0.1	5.14	-546.89	[75]
$MgHEDTA^-$	1 $MgEDTA^{2-}$ + 1 H^+ ⇌ 1 $MgHEDTA^-$	20	0.1	4.33	-538.31	[170]
				mean	-541.73	
$CaOH^+$	1 Ca^{2+} + 1 OH^- ⇌ 1 $CaOH^+$	25	0	1.15	-716.59	[15]
$CaOH^+$	1 Ca^{2+} + 1 OH^- ⇌ 1 $CaOH^+$	25	0.15	1.47	-718.41	[171]
$CaOH^+$	1 Ca^{2+} + 1 OH^- ⇌ 1 $CaOH^+$	25	0	1.30	-717.45	[172]
$CaOH^+$	1 Ca^{2+} + 1 OH^- ⇌ 1 $CaOH^+$	25	0	1.30	-717.45	[75]
$CaOH^+$	1 Ca^{2+} + 1 H_2O ⇌ 1 $CaOH^+$ + 1 H^+	25	0	-12.85	-716.60	[41]
$CaOH^+$	1 Ca^{2+} + 1 H_2O ⇌ 1 $CaOH^+$ + 1 H^+	25	0	-12.72	-717.34	[85]
$CaOH^+$		25	0		-717.20	[173]
				mean	-717.29	
$CaCl^+$	1 Ca^{2+} + 1 Cl^- ⇌ 1 $CaCl^+$	25	0	0.42	-686.42	[123]
$CaCl^+$	1 Ca^{2+} + 1 Cl^- ⇌ 1 $CaCl^+$	25	0	0.43	-686.48	[87]
$CaCl^+$	1 Ca^{2+} + 1 Cl^- ⇌ 1 $CaCl^+$	25	0.1	0.63	-687.62	[75]
$CaCl^+$	1 Ca^{2+} + 1 Cl^- ⇌ 1 $CaCl^+$	25	0	-0.70	-680.05	[41]
$CaCl^+$		25	0		-682.87	[8]
				mean	-684.69	
$CaNO_3^+$	1 Ca^{2+} + 1 NO_3^- ⇌ 1 $CaNO_3^+$	25	0.5	0.45	-666.16	[14]
$CaNO_3^+$	1 Ca^{2+} + 1 NO_3^- ⇌ 1 $CaNO_3^+$	25	0	0.60	-667.02	[100]
$CaNO_3^+$	1 Ca^{2+} + 1 NO_3^- ⇌ 1 $CaNO_3^+$	25	0	0.31	-665.37	[174]
$CaNO_3^+$	1 Ca^{2+} + 1 NO_3^- ⇌ 1 $CaNO_3^+$	25	0	0.50	-666.45	[75]
$CaNO_3^+$	1 Ca^{2+} + 1 NO_3^- ⇌ 1 $CaNO_3^+$	25	0	0.70	-667.60	[41]
$CaNO_3^+$	1 Ca^{2+} + 1 NO_3^- ⇌ 1 $CaNO_3^+$	25	0	0.70	-667.60	[87]
				mean	-666.70	

Appendix C. Data considered in the review of solution complex and mineral thermodynamic constants. Only species with more than one datum considered listed

$CaSO_4(aq)$	$1\ Ca^{2+} + 1\ SO_4^{2-} \rightleftharpoons 1\ CaSO_4(aq)$	25	0.1	2.25	-1309.65	[175]
$CaSO_4(aq)$	$1\ Ca^{2+} + 1\ SO_4^{2-} \rightleftharpoons 1\ CaSO_4(aq)$	25	0	2.31	-1310.00	[176]
$CaSO_4(aq)$	$1\ Ca^{2+} + 1\ SO_4^{2-} \rightleftharpoons 1\ CaSO_4(aq)$	25	0	2.23	-1309.54	[177]
$CaSO_4(aq)$	$1\ Ca^{2+} + 1\ SO_4^{2-} \rightleftharpoons 1\ CaSO_4(aq)$	25	0.2	2.56	-1311.42	[178]
$CaSO_4(aq)$	$1\ Ca^{2+} + 1\ SO_4^{2-} \rightleftharpoons 1\ CaSO_4(aq)$	25	0	2.43	-1310.68	[99]
$CaSO_4(aq)$	$1\ Ca^{2+} + 1\ SO_4^{2-} \rightleftharpoons 1\ CaSO_4(aq)$	25	0	2.31	-1310.00	[51]
$CaSO_4(aq)$	$1\ Ca^{2+} + 1\ SO_4^{2-} \rightleftharpoons 1\ CaSO_4(aq)$	25	0	2.27	-1309.77	[179]
$CaSO_4(aq)$	$1\ Ca^{2+} + 1\ SO_4^{2-} \rightleftharpoons 1\ CaSO_4(aq)$	25	0	2.35	-1310.22	[130]
$CaSO_4(aq)$	$1\ Ca^{2+} + 1\ SO_4^{2-} \rightleftharpoons 1\ CaSO_4(aq)$	25	0	2.36	-1310.28	[75]
$CaSO_4(aq)$	$1\ Ca^{2+} + 1\ SO_4^{2-} \rightleftharpoons 1\ CaSO_4(aq)$	25	0	2.11	-1308.86	[41]
$CaSO_4(aq)$	$1\ Ca^{2+} + 1\ SO_4^{2-} \rightleftharpoons 1\ CaSO_4(aq)$	25	0	2.30	-1309.94	[85]
$CaSO_4(aq)$		25	0		-1310.18	[8]
				mean	-1310.04	
$CaCO_3(aq)$	$1\ Ca^{2+} + 1\ CO_3^{2-} \rightleftharpoons 1\ CaCO_3(aq)$	25	0	3.20	-1098.97	[75]
$CaCO_3(aq)$	$1\ Ca^{2+} + 1\ CO_3^{2-} \rightleftharpoons 1\ CaCO_3(aq)$	25	0	4.44	-1106.05	[180]
$CaCO_3(aq)$	$1\ Ca^{2+} + 1\ CO_3^{2-} \rightleftharpoons 1\ CaCO_3(aq)$	25	0	3.20	-1098.97	[181]
$CaCO_3(aq)$	$1\ Ca^{2+} + 1\ CO_3^{2-} \rightleftharpoons 1\ CaCO_3(aq)$	25	0	3.15	-1098.69	[132]
$CaCO_3(aq)$	$1\ Ca^{2+} + 1\ CO_3^{2-} \rightleftharpoons 1\ CaCO_3(aq)$	25	0	3.10	-1098.40	[182]
$CaCO_3(aq)$	$1\ Ca^{2+} + 1\ CO_3^{2-} \rightleftharpoons 1\ CaCO_3(aq)$	25	0	4.48	-1106.28	[183]
$CaCO_3(aq)$	$1\ Ca^{2+} + 1\ CO_3^{2-} \rightleftharpoons 1\ CaCO_3(aq)$	25	0	3.20	-1098.97	[105]
$CaCO_3(aq)$	$1\ Ca^{2+} + 1\ HCO_3^{-} \rightleftharpoons 1\ CaCO_3(aq) + 1\ H^{+}$	25	0	-7.00	-1099.69	[41]
$CaCO_3(aq)$		25	0		-1100.50	[8]
				mean	-1100.72	
$CaHCO_3^{+}$	$1\ Ca^{2+} + 1\ HCO_3^{-} \rightleftharpoons 1\ CaHCO_3^{+}$	25	0	1.14	-1146.16	[180]
$CaHCO_3^{+}$	$1\ Ca^{2+} + 1\ HCO_3^{-} \rightleftharpoons 1\ CaHCO_3^{+}$	25	0	1.00	-1145.36	[181]
$CaHCO_3^{+}$	$1\ Ca^{2+} + 1\ HCO_3^{-} \rightleftharpoons 1\ CaHCO_3^{+}$	25	0	1.05	-1145.63	[41]
$CaHCO_3^{+}$	$1\ Ca^{2+} + 1\ HCO_3^{-} \rightleftharpoons 1\ CaHCO_3^{+}$	25	0	1.25	-1146.79	[183]
$CaHCO_3^{+}$	$1\ Ca^{2+} + 1\ HCO_3^{-} \rightleftharpoons 1\ CaHCO_3^{+}$	25	0	1.26	-1146.84	[105]
$CaHCO_3^{+}$	$1\ Ca^{2+} + 1\ HCO_3^{-} \rightleftharpoons 1\ CaHCO_3^{+}$	25	0	1.27	-1146.90	[75]
$CaHCO_3^{+}$	$1\ Ca^{2+} + 1\ H^{+} + 1\ CO_3^{2-} \rightleftharpoons 1\ CaHCO_3^{+}$	25	0	11.44	-1146.01	[40]
				mean	-1146.24	

Appendix C. Data considered in the review of solution complex and mineral thermodynamic constants. Only species with more than one datum considered listed

$CaPO_4^-$	$1\ Ca^{2+} + 1\ PO_4^{3-} \rightleftharpoons 1\ CaPO_4^-$	25	0	0.96	-1583.78	[16]
$CaPO_4^-$	$1\ Ca^{2+} + 1\ PO_4^{3-} \rightleftharpoons 1\ CaPO_4^-$	25	0.15	2.74	-1593.92	[135]
$CaPO_4^-$	$1\ Ca^{2+} + 1\ PO_4^{3-} \rightleftharpoons 1\ CaPO_4^-$	25	0	6.46	-1615.17	[184]
$CaPO_4^-$	$1\ Ca^{2+} + 1\ PO_4^{3-} \rightleftharpoons 1\ CaPO_4^-$	25	0	6.46	-1615.17	[6]
$CaPO_4^-$	$1\ Ca^{2+} + 1\ HPO_4^{2-} \rightleftharpoons 1\ CaPO_4^- + 1\ H^+$	25	0	-5.86	-1615.34	[41]
$CaPO_4^-$	$1\ Ca^{2+} + 1\ PO_4^{3-} \rightleftharpoons 1\ CaPO_4^-$	25	0	6.46	-1615.17	[78]
				mean	-1606.42	
$CaHPO_4(aq)$	$1\ Ca^{2+} + 1\ HPO_4^{2-} \rightleftharpoons 1\ CaHPO_4(aq)$	25	0.1	2.50	-1663.07	[138]
$CaHPO_4(aq)$	$1\ Ca^{2+} + 1\ HPO_4^{2-} \rightleftharpoons 1\ CaHPO_4(aq)$	25	0	2.54	-1663.29	[13]
$CaHPO_4(aq)$	$1\ Ca^{2+} + 1\ HPO_4^{2-} \rightleftharpoons 1\ CaHPO_4(aq)$	25	0.1	2.73	-1664.38	[175]
$CaHPO_4(aq)$	$1\ Ca^{2+} + 1\ HPO_4^{2-} \rightleftharpoons 1\ CaHPO_4(aq)$	25	0	2.41	-1662.55	[185]
$CaHPO_4(aq)$	$1\ Ca^{2+} + 1\ HPO_4^{2-} \rightleftharpoons 1\ CaHPO_4(aq)$	25	0	2.74	-1664.44	[184]
$CaHPO_4(aq)$	$1\ Ca^{2+} + 1\ HPO_4^{2-} \rightleftharpoons 1\ CaHPO_4(aq)$	25	0	2.66	-1663.98	[75]
$CaHPO_4(aq)$	$1\ Ca^{2+} + 1\ HPO_4^{2-} \rightleftharpoons 1\ CaHPO_4(aq)$	25	0	2.74	-1664.44	[41]
$CaHPO_4(aq)$	$1\ Ca^{2+} + 1\ PO_4^{3-} + 1\ H^+ \rightleftharpoons 1\ CaHPO_4(aq)$	25	0	15.03	-1664.09	[6]
				mean	-1663.78	
$CaH_2PO_4^+$	$1\ Ca^{2+} + 1\ H_2PO_4^- \rightleftharpoons 1\ CaH_2PO_4^+$	25	0	0.60	-1693.38	[185]
$CaH_2PO_4^+$	$1\ Ca^{2+} + 1\ H_2PO_4^- \rightleftharpoons 1\ CaH_2PO_4^+$	25	0	1.41	-1698.00	[184]
$CaH_2PO_4^+$	$1\ Ca^{2+} + 1\ H_2PO_4^- \rightleftharpoons 1\ CaH_2PO_4^+$	25	0	1.35	-1697.66	[75]
$CaH_2PO_4^+$	$1\ Ca^{2+} + 1\ PO_4^{3-} + 2\ H^+ \rightleftharpoons 1\ CaH_2PO_4^+$	25	0	20.97	-1697.99	[6]
				mean	-1696.76	
$CaCit^-$	$1\ Ca^{2+} + 1\ Cit^{3-} \rightleftharpoons 1\ CaCit^-$	25	0	4.85	-580.49	[186]
$CaCit^-$	$1\ Ca^{2+} + 1\ Cit^{3-} \rightleftharpoons 1\ CaCit^-$	25	0	4.67	-579.46	[142]
$CaCit^-$	$1\ Ca^{2+} + 1\ Cit^{3-} \rightleftharpoons 1\ CaCit^-$	25	0	4.60	-579.06	[187]
$CaCit^-$	$1\ Ca^{2+} + 1\ Cit^{3-} \rightleftharpoons 1\ CaCit^-$	25	0	4.84	-580.43	[188]
$CaCit^-$	$1\ Ca^{2+} + 1\ Cit^{3-} \rightleftharpoons 1\ CaCit^-$	25	0	4.90	-580.78	[189]
$CaCit^-$	$1\ Ca^{2+} + 1\ Cit^{3-} \rightleftharpoons 1\ CaCit^-$	25	0	4.60	-579.06	[190]
$CaCit^-$	$1\ Ca^{2+} + 1\ Cit^{3-} \rightleftharpoons 1\ CaCit^-$	25	0	4.68	-579.52	[191]
$CaCit^-$	$1\ Ca^{2+} + 1\ Cit^{3-} \rightleftharpoons 1\ CaCit^-$	25	0	4.64	-579.29	[192]
$CaCit^-$	$1\ Ca^{2+} + 1\ Cit^{3-} \rightleftharpoons 1\ CaCit^-$	25	0	5.00	-581.35	[193]
$CaCit^-$	$1\ Ca^{2+} + 1\ Cit^{3-} \rightleftharpoons 1\ CaCit^-$	25	0	4.60	-579.06	[109]

Appendix C. Data considered in the review of solution complex and mineral thermodynamic constants. Only species with more than one datum considered listed

$CaCit^-$	$1\ Ca^{2+} + 1\ Cit^{3-} \rightleftharpoons 1\ CaCit^-$	25	0	4.61	-579.12	[194]
$CaCit^-$	$1\ Ca^{2+} + 1\ Cit^{3-} \rightleftharpoons 1\ CaCit^-$	25	0	4.82	-580.32	[146]
$CaCit^-$	$1\ Ca^{2+} + 1\ Cit^{3-} \rightleftharpoons 1\ CaCit^-$	25	0	4.95	-581.06	[195]
$CaCit^-$	$1\ Ca^{2+} + 1\ Cit^{3-} \rightleftharpoons 1\ CaCit^-$	25	0	4.67	-579.46	[196]
$CaCit^-$	$1\ Ca^{2+} + 1\ Cit^{3-} \rightleftharpoons 1\ CaCit^-$	25	0	4.78	-580.09	[151]
$CaCit^-$	$1\ Ca^{2+} + 1\ Cit^{3-} \rightleftharpoons 1\ CaCit^-$	25	0	4.82	-580.32	[19]
$CaCit^-$	$1\ Ca^{2+} + 1\ Cit^{3-} \rightleftharpoons 1\ CaCit^-$	25	0	4.76	-579.98	[12]
$CaCit^-$	$1\ Ca^{2+} + 1\ Cit^{3-} \rightleftharpoons 1\ CaCit^-$	25	0	4.70	-579.63	[175]
$CaCit^-$	$1\ Ca^{2+} + 1\ Cit^{3-} \rightleftharpoons 1\ CaCit^-$	25	0	4.92	-580.89	[152]
$CaCit^-$	$1\ Ca^{2+} + 1\ Cit^{3-} \rightleftharpoons 1\ CaCit^-$	25	0	4.87	-580.60	[153]
$CaCit^-$	$1\ Ca^{2+} + 1\ Cit^{3-} \rightleftharpoons 1\ CaCit^-$	25	0	4.85	-580.49	[154]
$CaCit^-$	$1\ Ca^{2+} + 1\ Cit^{3-} \rightleftharpoons 1\ CaCit^-$	25	0	4.71	-579.69	[155]
$CaCit^-$	$1\ Ca^{2+} + 1\ Cit^{3-} \rightleftharpoons 1\ CaCit^-$	25	0	4.82	-580.32	[10]
$CaCit^-$	$1\ Ca^{2+} + 1\ Cit^{3-} \rightleftharpoons 1\ CaCit^-$	25	0	4.84	-580.43	[197]
$CaCit^-$	$1\ Ca^{2+} + 1\ Cit^{3-} \rightleftharpoons 1\ CaCit^-$	25	0	4.77	-580.03	[198]
$CaCit^-$	$1\ Ca^{2+} + 1\ Cit^{3-} \rightleftharpoons 1\ CaCit^-$	25	0	4.63	-579.23	[135]
$CaCit^-$	$1\ Ca^{2+} + 1\ Cit^{3-} \rightleftharpoons 1\ CaCit^-$	25	0	4.80	-580.20	[199]
$CaCit^-$	$1\ Ca^{2+} + 1\ Cit^{3-} \rightleftharpoons 1\ CaCit^-$	25	0	4.91	-580.83	[2]
				mean	-580.04	
$Ca(Cit)_2^{4-}$	$1\ Ca^{2+} + 2\ Cit^{3-} \rightleftharpoons 1\ Ca(Cit)_2^{4-}$	25	0	5.70	-585.34	[10]
$Ca(Cit)_2^{4-}$	$1\ Ca^{2+} + 2\ Cit^{3-} \rightleftharpoons 1\ Ca(Cit)_2^{4-}$	25	0	5.88	-586.37	[200]
				mean	-585.86	
CaHCit(aq)	$1\ Ca^{2+} + 1\ Cit^{3-} + 1\ H^+ \rightleftharpoons 1\ CaHCit(aq)$	25	0	9.66	-607.95	[188]
CaHCit(aq)	$1\ Ca^{2+} + 1\ Cit^{3-} + 1\ H^+ \rightleftharpoons 1\ CaHCit(aq)$	25	0	9.42	-606.58	[189]
CaHCit(aq)	$1\ Ca^{2+} + 1\ Cit^{3-} + 1\ H^+ \rightleftharpoons 1\ CaHCit(aq)$	25	0	9.46	-606.80	[191]
CaHCit(aq)	$1\ Ca^{2+} + 1\ Cit^{3-} + 1\ H^+ \rightleftharpoons 1\ CaHCit(aq)$	25	0	9.32	-606.00	[146]
CaHCit(aq)	$1\ Ca^{2+} + 1\ Cit^{3-} + 1\ H^+ \rightleftharpoons 1\ CaHCit(aq)$	25	0	9.18	-605.21	[157]
CaHCit(aq)	$1\ Ca^{2+} + 1\ Cit^{3-} + 1\ H^+ \rightleftharpoons 1\ CaHCit(aq)$	25	0	9.55	-607.32	[151]
CaHCit(aq)	$1\ Ca^{2+} + 1\ Cit^{3-} + 1\ H^+ \rightleftharpoons 1\ CaHCit(aq)$	25	0	9.26	-605.66	[152]
CaHCit(aq)	$1\ Ca^{2+} + 1\ Cit^{3-} + 1\ H^+ \rightleftharpoons 1\ CaHCit(aq)$	25	0	9.30	-605.89	[153]
CaHCit(aq)	$1\ Ca^{2+} + 1\ Cit^{3-} + 1\ H^+ \rightleftharpoons 1\ CaHCit(aq)$	25	0	9.16	-605.09	[154]
CaHCit(aq)	$1\ Ca^{2+} + 1\ Cit^{3-} + 1\ H^+ \rightleftharpoons 1\ CaHCit(aq)$	25	0	9.78	-608.63	[155]

Appendix C. Data considered in the review of solution complex and mineral thermodynamic constants. Only species with more than one datum considered listed

$CaHCit(aq)$	$1\ Ca^{2+} + 1\ Cit^{3-} + 1\ H^{+} \rightleftharpoons 1\ CaHCit(aq)$	25	0	9.31	-605.95	[10]
$CaHCit(aq)$	$1\ Ca^{2+} + 1\ Cit^{3-} + 1\ H^{+} \rightleftharpoons 1\ CaHCit(aq)$	25	0	9.23	-605.49	[2]
				mean	-606.38	
CaH_2Cit^{+}	$1\ Ca^{2+} + 1\ Cit^{3-} + 2\ H^{+} \rightleftharpoons 1\ CaH_2Cit^{+}$	25	0	12.64	-624.96	[146]
CaH_2Cit^{+}	$1\ Ca^{2+} + 1\ Cit^{3-} + 2\ H^{+} \rightleftharpoons 1\ CaH_2Cit^{+}$	25	0	12.63	-624.90	[152]
CaH_2Cit^{+}	$1\ Ca^{2+} + 1\ Cit^{3-} + 2\ H^{+} \rightleftharpoons 1\ CaH_2Cit^{+}$	25	0	12.71	-625.36	[10]
CaH_2Cit^{+}	$1\ Ca^{2+} + 1\ Cit^{3-} + 2\ H^{+} \rightleftharpoons 1\ CaH_2Cit^{+}$	25	0	12.57	-624.56	[158]
				mean	-624.94	
$Ca(HCit)_2^{2-}$	$1\ Ca^{2+} + 2\ Cit^{3-} + 2\ H^{+} \rightleftharpoons 1\ Ca(HCit)_2^{2-}$	25	0	19.53	-664.28	[188]
$Ca(HCit)_2^{2-}$	$1\ Ca^{2+} + 2\ Cit^{3-} + 2\ H^{+} \rightleftharpoons 1\ Ca(HCit)_2^{2-}$	25	0	18.44	-658.06	[12]
				mean	-661.17	
$CaEDTA^{2-}$	$1\ Ca^{2+} + 1\ EDTA^{4-} \rightleftharpoons 1\ CaEDTA^{2-}$	25	0	12.40	-623.59	[78]
$CaEDTA^{2-}$	$1\ Ca^{2+} + 1\ EDTA^{4-} \rightleftharpoons 1\ CaEDTA^{2-}$	25	0.1	12.65	-625.01	[175]
$CaEDTA^{2-}$	$1\ Ca^{2+} + 1\ EDTA^{4-} \rightleftharpoons 1\ CaEDTA^{2-}$	20	0.1	12.41	-623.64	[69]
$CaEDTA^{2-}$	$1\ Ca^{2+} + 1\ EDTA^{4-} \rightleftharpoons 1\ CaEDTA^{2-}$	25	0	11.00	-615.59	[201]
$CaEDTA^{2-}$	$1\ Ca^{2+} + 1\ EDTA^{4-} \rightleftharpoons 1\ CaEDTA^{2-}$	25	0.3	11.58	-618.91	[159]
$CaEDTA^{2-}$	$1\ Ca^{2+} + 1\ EDTA^{4-} \rightleftharpoons 1\ CaEDTA^{2-}$	25	0.1	12.45	-623.87	[60]
$CaEDTA^{2-}$	$1\ Ca^{2+} + 1\ EDTA^{4-} \rightleftharpoons 1\ CaEDTA^{2-}$	25	0.1	12.50	-624.16	[202]
$CaEDTA^{2-}$	$1\ Ca^{2+} + 1\ EDTA^{4-} \rightleftharpoons 1\ CaEDTA^{2-}$	20	0.1	12.57	-624.56	[203]
$CaEDTA^{2-}$	$1\ Ca^{2+} + 1\ EDTA^{4-} \rightleftharpoons 1\ CaEDTA^{2-}$	20	0.1	12.72	-625.41	[160]
$CaEDTA^{2-}$	$1\ Ca^{2+} + 1\ EDTA^{4-} \rightleftharpoons 1\ CaEDTA^{2-}$	25	0.1	12.29	-622.96	[204]
$CaEDTA^{2-}$	$1\ Ca^{2+} + 1\ EDTA^{4-} \rightleftharpoons 1\ CaEDTA^{2-}$	25	0.1	12.14	-622.10	[162]
$CaEDTA^{2-}$	$1\ Ca^{2+} + 1\ EDTA^{4-} \rightleftharpoons 1\ CaEDTA^{2-}$	25	0	11.00	-615.59	[163]
$CaEDTA^{2-}$	$1\ Ca^{2+} + 1\ EDTA^{4-} \rightleftharpoons 1\ CaEDTA^{2-}$	22	0.1	12.57	-624.56	[205]
$CaEDTA^{2-}$	$1\ Ca^{2+} + 1\ EDTA^{4-} \rightleftharpoons 1\ CaEDTA^{2-}$	25	0.1	12.42	-623.70	[165]
$CaEDTA^{2-}$	$1\ Ca^{2+} + 1\ EDTA^{4-} \rightleftharpoons 1\ CaEDTA^{2-}$	20	0.1	12.31	-623.07	[166]
$CaEDTA^{2-}$	$1\ Ca^{2+} + 1\ EDTA^{4-} \rightleftharpoons 1\ CaEDTA^{2-}$	25	0.1	12.37	-623.42	[75]
$CaEDTA^{2-}$	$1\ Ca^{2+} + 1\ EDTA^{4-} \rightleftharpoons 1\ CaEDTA^{2-}$	25	0.1	12.53	-624.33	[75]
				mean	-622.62	
$CaHEDTA^{-}$	$1\ Ca^{2+} + 1\ HEDTA^{3-} \rightleftharpoons 1\ CaHEDTA^{-}$	25	0.1	4.71	-641.87	[60]

Appendix C. Data considered in the review of solution complex and mineral thermodynamic constants. Only species with more than one datum considered listed

$CaHEDTA^-$	$1\ Ca^{2+} + 1\ HEDTA^{3-} \rightleftharpoons 1\ CaHEDTA^-$	20	0.1	4.80	-642.38	[161]
$CaHEDTA^-$	$1\ Ca^{2+} + 1\ HEDTA^{3-} \rightleftharpoons 1\ CaHEDTA^-$	20	0.1	4.80	-642.38	[166]
$CaHEDTA^-$	$1\ Ca^{2+} + 1\ HEDTA^{3-} \rightleftharpoons 1\ CaHEDTA^-$	25	0.1	4.39	-640.04	[75]
				mean	-641.67	
$Ca_2EDTA(aq)$	$2\ Ca^{2+} + 1\ EDTA^{4-} \rightleftharpoons 1\ Ca_2EDTA(aq)$		0.3	14.85	-1190.36	[206]
$Ca_2EDTA(aq)$	$1\ Ca^{2+} + 1\ CaEDTA^{2-} \rightleftharpoons 1\ Ca_2EDTA(aq)$	20	0.2	2.12	-1187.52	[18]
				mean	-1188.94	
UO_2OH^+		25	0		-1160.01	[207]
UO_2OH^+	$1\ UO_2^{2+} + 1\ H_2O \rightleftharpoons 1\ UO_2OH^+ + 1\ H^+$	25	0.1	-5.69	-1157.18	[208]
UO_2OH^+	$1\ UO_2^{2+} + 1\ H_2O \rightleftharpoons 1\ UO_2OH^+ + 1\ H^+$	25	0	-5.19	-1160.07	[209]
				mean	-1159.09	
$UO_2(OH)_2(aq)$	$1\ UO_2^{2+} + 2\ H_2O \rightleftharpoons 1\ UO_2(OH)_2(aq) + 2\ H^+$	25	0	-11.50	-1361.19	[210]
$UO_2(OH)_2(aq)$	$1\ UO_2^{2+} + 2\ H_2O \rightleftharpoons 1\ UO_2(OH)_2(aq) + 2\ H^+$	25	0		-1359.00	[211]
$UO_2(OH)_2(aq)$	$1\ UO_2OH^+ + 1\ H_2O \rightleftharpoons 1\ UO_2(OH)_2(aq) + 1\ H^+$	25	0.1	-6.49	-1359.18	[208]
				mean	-1359.79	
$UO_2(OH)_3^-$	$1\ UO_2^{2+} + 3\ H_2O \rightleftharpoons 1\ UO_2(OH)_3^- + 3\ H^+$	25	0	-20	-1549.81	[212]
$UO_2(OH)_3^-$		25	0		-1554.38	[207]
				mean	-1552.10	
$UO_2(OH)_4^{2-}$		25	0		-1712.75	[207]
$UO_2(OH)_4^{2-}$	$1\ U^{4+} + 6\ H_2O \rightleftharpoons 1\ UO_2(OH)_4^{2-} + 6\ H^+$	25	0	-44.50	-1698.69	[213]
				mean	-1705.72	
$(UO_2)_2(OH)_2^{2+}$	$2\ UO_2^{2+} + 2\ H_2O \rightleftharpoons 1\ (UO_2)_2(OH)_2^{2+} + 2\ H^+$	25	0.1	-5.92	-2345.56	[214]
$(UO_2)_2(OH)_2^{2+}$	$2\ UO_2^{2+} + 2\ H_2O \rightleftharpoons 1\ (UO_2)_2(OH)_2^{2+} + 2\ H^+$	25	0	-5.62	-2347.30	[207]
$(UO_2)_2(OH)_2^{2+}$	$2\ UO_2^{2+} + 2\ H_2O \rightleftharpoons 1\ (UO_2)_2(OH)_2^{2+} + 2\ H^+$	25	0	-5.51	-2347.93	[21]
$(UO_2)_2(OH)_2^{2+}$	$2\ UO_2^{2+} + 2\ H_2O \rightleftharpoons 1\ (UO_2)_2(OH)_2^{2+} + 2\ H^+$	25	0	-5.76	-2346.50	[209]
				mean	-2346.82	
$(UO_2)_3(OH)_5^+$	$3\ UO_2^{2+} + 5\ H_2O \rightleftharpoons 1\ (UO_2)_3(OH)_5^+ + 5\ H^+$	25	0	-15.55	-3954.59	[207]

Appendix C. Data considered in the review of solution complex and mineral thermodynamic constants. Only species with more than one datum considered listed

$(UO_2)_3(OH)_5^+$	$3\ UO_2^{2+} + 5\ H_2O \rightleftharpoons 1\ (UO_2)_3(OH)_5^+ + 5\ H^+$	25	0	-15.33	-3955.85	[21]
$(UO_2)_3(OH)_5^+$	$3\ UO_2^{2+} + 5\ H_2O \rightleftharpoons 1\ (UO_2)_3(OH)_5^+ + 5\ H^+$	25	0	-15.89	-3952.65	[209]
				mean	-3954.36	
$(UO_2)_3(OH)_7^-$		25	0		-4340.69	[207]
$(UO_2)_3(OH)_7^-$	$3\ UO_2^{2+} + 7\ H_2O \rightleftharpoons 1\ (UO_2)_3(OH)_7^- + 7\ H^+$	25	0	-32.70	-4330.98	[212]
$(UO_2)_3(OH)_7^-$	$3\ UO_2^{2+} + 7\ H_2O \rightleftharpoons 1\ (UO_2)_3(OH)_7^- + 7\ H^+$	25	0	-27.77	-4359.12	[21]
$(UO_2)_3(OH)_7^-$	$3\ UO_2^{2+} + 7\ H_2O \rightleftharpoons 1\ (UO_2)_3(OH)_7^- + 7\ H^+$	25	0	-29.26	-4350.62	[209]
				mean	-4345.35	
$UO_2HPO_4(aq)$		25	0		-2089.86	[207]
$UO_2HPO_4(aq)$	$1\ UO_2^{2+} + 1\ PO_4^{3-} + 1\ H^+ \rightleftharpoons 1\ UO_2HPO_4(aq)$	25	0	19.63	-2090.09	[212]
$UO_2HPO_4(aq)$	$1\ UO_2^{2+} + 1\ PO_4^{3-} + 1\ H^+ \rightleftharpoons 1\ UO_2HPO_4(aq)$	25	0	19.87	-2091.46	[215]
$UO_2HPO_4(aq)$	$1\ UO_2^{2+} + 1\ PO_4^{3-} + 1\ H^+ \rightleftharpoons 1\ UO_2HPO_4(aq)$	25	0	19.53	-2089.52	[215]
				mean	-2090.23	
$UO_2H_2PO_4^+$		25	0		-2108.31	[207]
$UO_2H_2PO_4^+$	$1\ UO_2^{2+} + 1\ PO_4^{3-} + 2\ H^+ \rightleftharpoons 1\ UO_2H_2PO_4^+$	25	0	22.82	-2108.30	[216]
$UO_2H_2PO_4^+$	$1\ UO_2^{2+} + 1\ PO_4^{3-} + 2\ H^+ \rightleftharpoons 1\ UO_2H_2PO_4^+$	25	0	22.89	-2108.70	[217]
$UO_2H_2PO_4^+$	$1\ UO_2^{2+} + 1\ PO_4^{3-} + 2\ H^+ \rightleftharpoons 1\ UO_2H_2PO_4^+$	25	0	22.60	-2107.04	[218]
$UO_2H_2PO_4^+$	$1\ UO_2^{2+} + 1\ PO_4^{3-} + 2\ H^+ \rightleftharpoons 1\ UO_2H_2PO_4^+$	25	0	23.20	-2110.47	[219]
$UO_2H_2PO_4^+$	$1\ UO_2^{2+} + 1\ PO_4^{3-} + 2\ H^+ \rightleftharpoons 1\ UO_2H_2PO_4^+$	25	0	23.02	-2109.44	[220]
$UO_2H_2PO_4^+$	$1\ UO_2^{2+} + 1\ PO_4^{3-} + 2\ H^+ \rightleftharpoons 1\ UO_2H_2PO_4^+$	25	0	22.58	-2106.93	[215]
$UO_2H_2PO_4^+$	$1\ UO_2^{2+} + 1\ PO_4^{3-} + 2\ H^+ \rightleftharpoons 1\ UO_2H_2PO_4^+$	25	0	22.31	-2105.39	[215]
				mean	-2108.07	
$UO_2(H_2PO_4)_2(aq)$		25	0		-3254.94	[207]
$UO_2(H_2PO_4)_2(aq)$	$1\ UO_2^{2+} + 2\ PO_4^{3-} + 4\ H^+ \rightleftharpoons 1\ UO_2(H_2PO_4)_2(aq)$	25	0	44.99	-3260.34	[216]
$UO_2(H_2PO_4)_2(aq)$	$1\ UO_2^{2+} + 2\ PO_4^{3-} + 4\ H^+ \rightleftharpoons 1\ UO_2(H_2PO_4)_2(aq)$	25	0	44.70	-3258.68	[218]
$UO_2(H_2PO_4)_2(aq)$	$1\ UO_2^{2+} + 2\ PO_4^{3-} + 4\ H^+ \rightleftharpoons 1\ UO_2(H_2PO_4)_2(aq)$	25	0	44.70	-3258.68	[219]
$UO_2(H_2PO_4)_2(aq)$	$1\ UO_2^{2+} + 2\ PO_4^{3-} + 4\ H^+ \rightleftharpoons 1\ UO_2(H_2PO_4)_2(aq)$	25	0	44.87	-3259.65	[220]
$UO_2(H_2PO_4)_2(aq)$	$1\ UO_2^{2+} + 2\ PO_4^{3-} + 4\ H^+ \rightleftharpoons 1\ UO_2(H_2PO_4)_2(aq)$	25	0	46.09	-3266.61	[215]
				mean	-3259.82	

Appendix C. Data considered in the review of solution complex and mineral thermodynamic constants. Only species with more than one datum considered listed

$Ca_2UO_2(CO_3)_3(aq)$	$2\ Ca^{2+} + 1\ UO_2^{2+} + 3\ CO_3^{2-} \rightleftharpoons 1\ Ca_2UO_2(CO_3)_3(aq)$	25	0	30.55	-3816.24	[17]
$Ca_2UO_2(CO_3)_3(aq)$	$2\ Ca^{2+} + 1\ UO_2^{2+} + 3\ CO_3^{2-} \rightleftharpoons 1\ Ca_2UO_2(CO_3)_3(aq)$	25	0	29.10	-3807.97	[221]
				mean	-3812.11	
UO_2Cit^-	$1\ UO_2^{2+} + 1\ Cit^{3-} \rightleftharpoons 1\ UO_2Cit^-$	21	0.1	7.99	-998.16	[222]
UO_2Cit^-	$1\ U^{4+} + 1\ Cit^{3-} + 2\ H_2O \rightleftharpoons 1\ UO_2Cit^- + 4\ H^+ + 2\ e^-$	25	0	0.89	-1009.22	[144]
UO_2Cit^-	$1\ U^{4+} + 1\ Cit^{3-} + 2\ H_2O \rightleftharpoons 1\ UO_2Cit^- + 4\ H^+ + 2\ e^-$	25	0	0.70	-1008.14	[223]
UO_2Cit^-	$1\ U^{4+} + 1\ Cit^{3-} + 2\ H_2O \rightleftharpoons 1\ UO_2Cit^- + 4\ H^+ + 2\ e^-$	25	0	-0.36	-1002.09	[224]
UO_2Cit^-	$1\ U^{4+} + 1\ Cit^{3-} + 2\ H_2O \rightleftharpoons 1\ UO_2Cit^- + 4\ H^+ + 2\ e^-$	25	0	-0.48	-1001.40	[225]
UO_2Cit^-	$1\ U^{4+} + 1\ Cit^{3-} + 2\ H_2O \rightleftharpoons 1\ UO_2Cit^- + 4\ H^+ + 2\ e^-$	25	0	-0.65	-1000.43	[226]
UO_2Cit^-	$1\ U^{4+} + 1\ Cit^{3-} + 2\ H_2O \rightleftharpoons 1\ UO_2Cit^- + 4\ H^+ + 2\ e^-$	25	0	0.61	-1007.62	[227]
UO_2Cit^-	$1\ U^{4+} + 1\ Cit^{3-} + 2\ H_2O \rightleftharpoons 1\ UO_2Cit^- + 4\ H^+ + 2\ e^-$	25	0	-0.03	-1003.97	[228]
				mean	-1003.88	
$UO_2HCit(aq)$	$1\ U^{4+} + 1\ Cit^{3-} + 2\ H_2O \rightleftharpoons 1\ UO_2HCit(aq) + 3\ H^+ + 2\ e^-$	25	0	2.36	-1017.61	[225]
$UO_2HCit(aq)$	$1\ U^{4+} + 1\ Cit^{3-} + 2\ H_2O \rightleftharpoons 1\ UO_2HCit(aq) + 3\ H^+ + 2\ e^-$	25	0	2.20	-1016.70	[226]
				mean	-1017.15	
$UO_2H_2Cit^+$	$1\ U^{4+} + 1\ Cit^{3-} + 2\ H_2O \rightleftharpoons 1\ UO_2H_2Cit^+ + 2\ H^+ + 2\ e^-$	25	0	5.31	-1034.45	[225]
$UO_2H_2Cit^+$	$1\ U^{4+} + 1\ Cit^{3-} + 2\ H_2O \rightleftharpoons 1\ UO_2H_2Cit^+ + 2\ H^+ + 2\ e^-$	25	0	3.82	-1025.94	[226]
				mean	-1030.20	
$(UO_2)_2(Cit)_2^{2-}$	$2\ U^{4+} + 2\ Cit^{3-} + 4\ H_2O \rightleftharpoons 1\ (UO_2)_2(Cit)_2^{2-} + 8\ H^+ + 4\ e^-$	25	0	3.55	-2028.54	[223]
$(UO_2)_2(Cit)_2^{2-}$	$2\ U^{4+} + 2\ Cit^{3-} + 4\ H_2O \rightleftharpoons 1\ (UO_2)_2(Cit)_2^{2-} + 8\ H^+ + 4\ e^-$	25	0	3.14	-2026.20	[224]
$(UO_2)_2(Cit)_2^{2-}$	$2\ U^{4+} + 2\ Cit^{3-} + 4\ H_2O \rightleftharpoons 1\ (UO_2)_2(Cit)_2^{2-} + 8\ H^+ + 4\ e^-$	25	0	1.76	-2018.33	[229]
$(UO_2)_2(Cit)_2^{2-}$	$2\ U^{4+} + 2\ Cit^{3-} + 4\ H_2O \rightleftharpoons 1\ (UO_2)_2(Cit)_2^{2-} + 8\ H^+ + 4\ e^-$	25	0	2.01	-2019.75	[230]
				mean	-2023.21	
UO_2EDTA^{2-}	$1\ UO_2^{2+} + 1\ EDTA^{4-} \rightleftharpoons 1\ UO_2EDTA^{2-}$	24	0.1	12.12	-1021.73	[80]
UO_2EDTA^{2-}	$1\ UO_2^{2+} + 1\ EDTA^{4-} \rightleftharpoons 1\ UO_2EDTA^{2-}$	25	0	13.00	-1026.76	[71]
UO_2EDTA^{2-}		25	0		-1027.79	[77]
				mean	-1025.43	
UO_2HEDTA^-	$1\ UO_2^{2+} + 1\ HEDTA^{3-} \rightleftharpoons 1\ UO_2HEDTA^-$	25	0.1	8.69	-1064.33	[231]

Appendix C. Data considered in the review of solution complex and mineral thermodynamic constants. Only species with more than one datum considered listed

UO_2HEDTA^-	$1\ UO_2^{2+} + 1\ HEDTA^{3-} \rightleftharpoons 1\ UO_2HEDTA^-$	25	0.15	9.24	-1067.45	[232]
UO_2HEDTA^-	$1\ UO_2^{2+} + 1\ HEDTA^{3-} \rightleftharpoons 1\ UO_2HEDTA^-$	25	0.1	8.61	-1063.87	[233]
UO_2HEDTA^-	$1\ UO_2^{2+} + 1\ EDTA^{4-} + 1\ H^+ \rightleftharpoons 1\ UO_2HEDTA^-$	25	0	20.20	-1067.85	[71]
UO_2HEDTA^-		25	0		-1060.60	[77]
UO_2HEDTA^-	$1\ UO_2^{2+} + 1\ HEDTA^{3-} \rightleftharpoons 1\ UO_2HEDTA^-$	25	0.1	8.19	-1061.48	[64]
UO_2HEDTA^-	$1\ UO_2^{2+} + 1\ HEDTA^{3-} \rightleftharpoons 1\ UO_2HEDTA^-$	25	0.1	8.69	-1064.33	[234]
				mean	-1064.27	
$UO_2(OH)HEDTA^{2-}$	$1\ UO_2HEDTA^- + 1\ H_2O \rightleftharpoons 1\ UO_2(OH)HEDTA^{2-} + 1\ H^+$	25	0.1	-6.05	-1266.88	[231]
$UO_2(OH)HEDTA^{2-}$	$1\ UO_2^{2+} + 1\ H_2O + 1\ EDTA^{4-} \rightleftharpoons 1\ UO_2(OH)HEDTA^{2-}$	25	0.1	12.37	-1260.29	[64]
$UO_2(OH)HEDTA^{2-}$	$1\ UO_2HEDTA^- + 1\ H_2O \rightleftharpoons 1\ UO_2(OH)HEDTA^{2-} + 1\ H^+$	25	0.15	-6.08	-1266.71	[232]
				mean	-1264.63	
Fe^{3+}	$1\ Fe^{2+} \rightleftharpoons 1\ Fe^{3+} + 1\ e^-$	25	0	-13.02	-17.25	[40]
Fe^{3+}		25	0		-17.25	[9]
				mean	-17.25	
$FeOH^+$	$1\ H_2O + 1\ Fe^{2+} \rightleftharpoons 1\ FeOH^+ + 1\ H^+$	25	0	-9.23	-276.02	[235]
$FeOH^+$	$1\ H_2O + 1\ Fe^{2+} \rightleftharpoons 1\ FeOH^+ + 1\ H^+$	25	0	-9.49	-274.54	[236]
$FeOH^+$	$1\ H_2O + 1\ Fe^{2+} \rightleftharpoons 1\ FeOH^+ + 1\ H^+$	25	0	-9.58	-274.02	[237]
$FeOH^+$	$1\ H_2O + 1\ Fe^{2+} \rightleftharpoons 1\ FeOH^+ + 1\ H^+$	25	0	-9.30	-275.62	[238]
$FeOH^+$	$1\ H_2O + 1\ Fe^{2+} \rightleftharpoons 1\ FeOH^+ + 1\ H^+$	25	0	-9.50	-274.48	[239]
$FeOH^+$	$1\ H_2O + 1\ Fe^{2+} \rightleftharpoons 1\ FeOH^+ + 1\ H^+$	25	0	-9.56	-274.14	[43]
$FeOH^+$	$1\ OH^- + 1\ Fe^{2+} \rightleftharpoons 1\ FeOH^+$	25	0	4.60	-275.04	[75]
$FeOH^+$		25	0		-275.70	[9]
$FeOH^+$	$1\ H_2O + 1\ Fe^{2+} \rightleftharpoons 1\ FeOH^+ + 1\ H^+$	25	0	-9.51	-274.42	[240]
$FeOH^+$		25	0		-270.80	[241]
				mean	-274.48	
$FeOH^{2+}$	$1\ Fe^{3+} + 1\ H_2O \rightleftharpoons 1\ FeOH^{2+} + 1\ H^+$	25	0	-2.10	-242.40	[242]
$FeOH^{2+}$	$1\ Fe^{3+} + 1\ H_2O \rightleftharpoons 1\ FeOH^{2+} + 1\ H^+$	25	0	-2.18	-241.94	[243]
$FeOH^{2+}$	$1\ Fe^{3+} + 1\ H_2O \rightleftharpoons 1\ FeOH^{2+} + 1\ H^+$	25	0.15	-2.57	-239.71	[244]
$FeOH^{2+}$	$1\ Fe^{3+} + 1\ H_2O \rightleftharpoons 1\ FeOH^{2+} + 1\ H^+$	25	0.1	-2.29	-241.32	[245]
$FeOH^{2+}$	$1\ Fe^{3+} + 1\ H_2O \rightleftharpoons 1\ FeOH^{2+} + 1\ H^+$	25	0.1	-2.35	-240.97	[246]

Appendix C. Data considered in the review of solution complex and mineral thermodynamic constants. Only species with more than one datum considered listed

$FeOH^{2+}$	$1\ Fe^{3+} + 1\ H_2O \rightleftharpoons 1\ FeOH^{2+} + 1\ H^+$	25	0.25	-2.13	-242.22	[247]
$FeOH^{2+}$	$1\ Fe^{3+} + 1\ H_2O \rightleftharpoons 1\ FeOH^{2+} + 1\ H^+$	25	0.004	-2.29	-241.31	[248]
$FeOH^{2+}$	$1\ Fe^{3+} + 1\ H_2O \rightleftharpoons 1\ FeOH^{2+} + 1\ H^+$	25	0.02	-2.25	-241.55	[248]
$FeOH^{2+}$	$1\ Fe^{3+} + 1\ H_2O \rightleftharpoons 1\ FeOH^{2+} + 1\ H^+$	25	0.5	-2.41	-240.62	[249]
$FeOH^{2+}$	$1\ Fe^{3+} + 1\ H_2O \rightleftharpoons 1\ FeOH^{2+} + 1\ H^+$	25	0.43	-2.19	-241.87	[250]
$FeOH^{2+}$	$1\ Fe^{3+} + 1\ H_2O \rightleftharpoons 1\ FeOH^{2+} + 1\ H^+$	25	0	-2.19	-241.89	[251]
$FeOH^{2+}$	$1\ Fe^{3+} + 1\ H_2O \rightleftharpoons 1\ FeOH^{2+} + 1\ H^+$	25	0.46	-2.16	-242.05	[252]
$FeOH^{2+}$	$1\ Fe^{3+} + 1\ H_2O \rightleftharpoons 1\ FeOH^{2+} + 1\ H^+$	25	0	-1.96	-243.20	[253]
$FeOH^{2+}$	$1\ Fe^{3+} + 1\ H_2O \rightleftharpoons 1\ FeOH^{2+} + 1\ H^+$	25	0	-2.46	-240.35	[254]
$FeOH^{2+}$	$1\ Fe^{3+} + 1\ H_2O \rightleftharpoons 1\ FeOH^{2+} + 1\ H^+$	25	0.4	-2.35	-240.96	[255]
$FeOH^{2+}$	$1\ Fe^{3+} + 1\ OH^- \rightleftharpoons 1\ FeOH^{2+}$	25	0	11.81	-241.88	[75]
$FeOH^{2+}$	$1\ Fe^{3+} + 1\ OH^- \rightleftharpoons 1\ FeOH^{2+}$	25	0.1	11.92	-242.48	[75]
$FeOH^{2+}$		25	0		-242.00	[9]
$FeOH^{2+}$	$1\ Fe^{3+} + 1\ H_2O \rightleftharpoons 1\ FeOH^{2+} + 1\ H^+$	25	0	-2.20	-241.83	[240]
$FeOH^{2+}$		25	0		-242.23	[241]
$FeOH^{2+}$	$1\ Fe^{3+} + 1\ H_2O \rightleftharpoons 1\ FeOH^{2+} + 1\ H^+$	25	0.5	-2.27	-241.42	[36]
				mean	-241.63	
$Fe(OH)_2(aq)$	$2\ H_2O + 1\ Fe^{2+} \rightleftharpoons 1\ Fe(OH)_2(aq) + 2\ H^+$	25	0	-20.35	-449.69	[43]
$Fe(OH)_2(aq)$	$2\ OH^- + 1\ Fe^{2+} \rightleftharpoons 1\ Fe(OH)_2(aq)$	25	0	7.50	-448.82	[75]
$Fe(OH)_2(aq)$		25	0		-449.49	[9]
$Fe(OH)_2(aq)$	$2\ H_2O + 1\ Fe^{2+} \rightleftharpoons 1\ Fe(OH)_2(aq) + 2\ H^+$	25	0	-20.61	-448.20	[240]
$Fe(OH)_2(aq)$		25	0		-447.43	[241]
				mean	-448.73	
$Fe(OH)_2^+$	$1\ Fe^{3+} + 2\ H_2O \rightleftharpoons 1\ Fe(OH)_2^+ + 2\ H^+$	20	0.1	-5.49	-460.16	[256]
$Fe(OH)_2^+$	$1\ Fe^{3+} + 2\ H_2O \rightleftharpoons 1\ Fe(OH)_2^+ + 2\ H^+$	20	0.05	-5.89	-457.93	[256]
$Fe(OH)_2^+$	$1\ Fe^{3+} + 2\ H_2O \rightleftharpoons 1\ Fe(OH)_2^+ + 2\ H^+$	25	0	-6.30	-455.57	[242]
$Fe(OH)_2^+$	$1\ Fe^{3+} + 2\ H_2O \rightleftharpoons 1\ Fe(OH)_2^+ + 2\ H^+$	25	0	-5.60	-459.56	[243]
$Fe(OH)_2^+$	$1\ Fe^{3+} + 2\ H_2O \rightleftharpoons 1\ Fe(OH)_2^+ + 2\ H^+$	25	0.15	-5.59	-459.61	[244]
$Fe(OH)_2^+$	$1\ FeOH^{2+} + 1\ H_2O \rightleftharpoons 1\ Fe(OH)_2^+ + 1\ H^+$	25	0	-4.70	-451.94	[254]
$Fe(OH)_2^+$	$1\ Fe^{3+} + 2\ OH^- \rightleftharpoons 1\ Fe(OH)_2^+$	25	0	23.40	-465.26	[75]
$Fe(OH)_2^+$		25	0		-459.46	[9]
$Fe(OH)_2^+$	$1\ Fe^{3+} + 2\ H_2O \rightleftharpoons 1\ Fe(OH)_2^+ + 2\ H^+$	25	0	-5.54	-459.91	[257]

Appendix C. Data considered in the review of solution complex and mineral thermodynamic constants. Only species with more than one datum considered listed

$Fe(OH)_2^+$		25	0		-459.50	[241]
				mean	-458.89	
$Fe(OH)_3^-$	$3\ H_2O + 1\ Fe^{2+} \rightleftharpoons 1\ Fe(OH)_3^- + 3\ H^+$	25	0	-32.24	-618.96	[43]
$Fe(OH)_3^-$	$3\ OH^- + 1\ Fe^{2+} \rightleftharpoons 1\ Fe(OH)_3^-$	25	0	13.00	-637.43	[75]
$Fe(OH)_3^-$		25	0		-612.65	[241]
				mean	-623.01	
$Fe(OH)_3(aq)$	$1\ Fe^{3+} + 3\ H_2O \rightleftharpoons 1\ Fe(OH)_3(aq) + 3\ H^+$	25	0	-14.30	-647.04	[242]
$Fe(OH)_3(aq)$	$1\ Fe^{2+} + 3\ H_2O \rightleftharpoons 1\ Fe(OH)_3(aq) + 3\ H^+ + 1\ e^-$	25	0	-25.58	-656.97	[40]
$Fe(OH)_3(aq)$	$1\ Fe^{3+} + 3\ H_2O \rightleftharpoons 1\ Fe(OH)_3(aq) + 3\ H^+$	25	0	-12.00	-660.17	[41]
$Fe(OH)_3(aq)$		25	0		-660.43	[9]
$Fe(OH)_3(aq)$	$1\ Fe^{3+} + 3\ H_2O \rightleftharpoons 1\ Fe(OH)_3(aq) + 3\ H^+$	25	0	-11.80	-661.31	[257]
$Fe(OH)_3(aq)$	$1\ Fe^{3+} + 3\ H_2O \rightleftharpoons 1\ Fe(OH)_3(aq) + 3\ H^+$	25	0	-12.92	-654.92	[258]
$Fe(OH)_3(aq)$	$1\ Fe^{3+} + 3\ H_2O \rightleftharpoons 1\ Fe(OH)_3(aq) + 3\ H^+$	25	0	-12.00	-660.17	[259]
$Fe(OH)_3(aq)$		25	0		-660.51	[241]
				mean	-657.69	
$Fe(OH)_4^{2-}$	$4\ H_2O + 1\ Fe^{2+} \rightleftharpoons 1\ Fe(OH)_4^{2-} + 4\ H^+$	25	0	-45.18	-782.24	[43]
$Fe(OH)_4^{2-}$	$4\ OH^- + 1\ Fe^{2+} \rightleftharpoons 1\ Fe(OH)_4^{2-}$	25	0	10.00	-777.53	[75]
$Fe(OH)_4^{2-}$		25	0		-775.87	[241]
				mean	-778.54	
$Fe(OH)_4^-$	$1\ Fe^{3+} + 4\ H_2O \rightleftharpoons 1\ Fe(OH)_4^- + 4\ H^+$	25	0	-22.30	-838.52	[242]
$Fe(OH)_4^-$	$1\ Fe^{2+} + 4\ H_2O \rightleftharpoons 1\ Fe(OH)_4^- + 4\ H^+ + 1\ e^-$	25	0	-34.62	-842.51	[40]
$Fe(OH)_4^-$	$1\ Fe^{3+} + 4\ OH^- \rightleftharpoons 1\ Fe(OH)_4^-$	25	0	34.40	-842.48	[75]
$Fe(OH)_4^-$	$1\ Fe^{3+} + 4\ H_2O \rightleftharpoons 1\ Fe(OH)_4^- + 4\ H^+$	25	0	-21.60	-842.51	[41]
$Fe(OH)_4^-$		25	0		-842.72	[9]
$Fe(OH)_4^-$		25	0		-845.59	[260]
$Fe(OH)_4^-$		25	0		-840.78	[261]
$Fe(OH)_4^-$	$1\ Fe^{3+} + 4\ H_2O \rightleftharpoons 1\ Fe(OH)_4^- + 4\ H^+$	25	0	-24.40	-826.53	[258]
$Fe(OH)_4^-$		25	0		-842.85	[241]
				mean	-840.50	

Appendix C. Data considered in the review of solution complex and mineral thermodynamic constants. Only species with more than one datum considered listed

$Fe_2(OH)_2^{4+}$	$2\ Fe^{3+} + 2\ H_2O \rightleftharpoons 1\ Fe_2(OH)_2^{4+} + 2\ H^+$	20	0.05	-2.79	-492.85	[256]
$Fe_2(OH)_2^{4+}$	$2\ Fe^{3+} + 2\ H_2O \rightleftharpoons 1\ Fe_2(OH)_2^{4+} + 2\ H^+$	25	0	-2.92	-492.11	[243]
$Fe_2(OH)_2^{4+}$	$2\ Fe^{3+} + 2\ H_2O \rightleftharpoons 1\ Fe_2(OH)_2^{4+} + 2\ H^+$	25	0.2	-3.46	-489.03	[262]
$Fe_2(OH)_2^{4+}$	$2\ Fe^{3+} + 2\ H_2O \rightleftharpoons 1\ Fe_2(OH)_2^{4+} + 2\ H^+$	25	0.1	-2.10	-496.79	[246]
$Fe_2(OH)_2^{4+}$	$2\ Fe^{3+} + 2\ OH^- \rightleftharpoons 1\ Fe_2(OH)_2^{4+}$	25	0	25.14	-492.44	[75]
				mean	-492.64	
$Fe_3(OH)_4^{5+}$	$3\ Fe^{2+} + 4\ H_2O \rightleftharpoons 1\ Fe_3(OH)_4^{5+} + 4\ H^+ + 3\ e^-$	25	0	-45.36	-964.34	[40]
$Fe_3(OH)_4^{5+}$	$3\ Fe^{3+} + 4\ OH^- \rightleftharpoons 1\ Fe_3(OH)_4^{5+}$	25	0	49.70	-964.31	[75]
				mean	-964.33	
$FeCl^+$	$1\ Fe^{2+} + 1\ Cl^- \rightleftharpoons 1\ FeCl^+$	25	0	-0.16	-221.87	[263]
$FeCl^+$	$1\ Fe^{2+} + 1\ Cl^- \rightleftharpoons 1\ FeCl^+$	25	0	0.14	-223.58	[40]
$FeCl^+$	$1\ Fe^{2+} + 1\ Cl^- \rightleftharpoons 1\ FeCl^+$	25	0	-0.20	-221.64	[75]
$FeCl^+$	$1\ Fe^{2+} + 1\ Cl^- \rightleftharpoons 1\ FeCl^+$	25	0	-0.16	-221.87	[41]
$FeCl^+$		25	0		-222.03	[8]
				mean	-222.20	
$FeCl^{2+}$	$1\ Fe^{3+} + 1\ Cl^- \rightleftharpoons 1\ FeCl^{2+}$	25	0.1	2.18	-160.88	[264]
$FeCl^{2+}$	$1\ Fe^{3+} + 1\ Cl^- \rightleftharpoons 1\ FeCl^{2+}$	20	0.4	1.07	-154.58	[265]
$FeCl^{2+}$	$1\ Fe^{3+} + 1\ Cl^- \rightleftharpoons 1\ FeCl^{2+}$	21	0.1	1.57	-157.40	[266]
$FeCl^{2+}$	$1\ Fe^{3+} + 1\ Cl^- \rightleftharpoons 1\ FeCl^{2+}$	25	0	0.70	-152.46	[267]
$FeCl^{2+}$	$1\ Fe^{3+} + 1\ Cl^- \rightleftharpoons 1\ FeCl^{2+}$	25	0.5	1.33	-156.07	[268]
$FeCl^{2+}$	$1\ Fe^{3+} + 1\ Cl^- \rightleftharpoons 1\ FeCl^{2+}$	20	0.15	1.32	-155.99	[269]
$FeCl^{2+}$	$1\ Fe^{3+} + 1\ Cl^- \rightleftharpoons 1\ FeCl^{2+}$	25	0	1.38	-156.34	[270]
$FeCl^{2+}$	$1\ Fe^{3+} + 1\ Cl^- \rightleftharpoons 1\ FeCl^{2+}$	25	0	0.54	-151.54	[271]
$FeCl^{2+}$	$1\ Fe^{3+} + 1\ Cl^- \rightleftharpoons 1\ FeCl^{2+}$	25	0	0.45	-151.05	[271]
$FeCl^{2+}$	$1\ Fe^{3+} + 1\ Cl^- \rightleftharpoons 1\ FeCl^{2+}$	25	0.5	1.22	-155.44	[272]
$FeCl^{2+}$	$1\ Fe^{3+} + 1\ Cl^- \rightleftharpoons 1\ FeCl^{2+}$	25	0.2	1.54	-157.28	[273]
$FeCl^{2+}$	$1\ Fe^{3+} + 1\ Cl^- \rightleftharpoons 1\ FeCl^{2+}$	25	0	1.48	-156.91	[274]
$FeCl^{2+}$	$1\ Fe^{2+} + 1\ Cl^- \rightleftharpoons 1\ FeCl^{2+} + 1\ e^-$	25	0	-11.52	-157.03	[275]
$FeCl^{2+}$	$1\ Fe^{3+} + 1\ Cl^- \rightleftharpoons 1\ FeCl^{2+}$	25	0	1.48	-156.91	[75]
$FeCl^{2+}$		25	0		-157.08	[8]
$FeCl^{2+}$	$1\ Fe^{3+} + 1\ Cl^- \rightleftharpoons 1\ FeCl^{2+}$	25	0	1.28	-155.77	[257]

Appendix C. Data considered in the review of solution complex and mineral thermodynamic constants. Only species with more than one datum considered listed

				mean	-155.80	
$FeCl_2^+$	$1\ FeCl^{2+} + 1\ Cl^- \rightleftharpoons 1\ FeCl_2^+$	25	0	0.65	-290.72	[274]
$FeCl_2^+$	$1\ Fe^{2+} + 2\ Cl^- \rightleftharpoons 1\ FeCl_2^+ + 1\ e^-$	25	0	-10.64	-293.27	[275]
$FeCl_2^+$	$1\ Fe^{3+} + 2\ Cl^- \rightleftharpoons 1\ FeCl_2^+$	25	0	2.13	-291.84	[75]
$FeCl_2^+$	$1\ Fe^{3+} + 2\ Cl^- \rightleftharpoons 1\ FeCl_2^+$	25	0	1.16	-286.30	[257]
$FeCl_2^+$	$1\ Fe^{3+} + 2\ Cl^- \rightleftharpoons 1\ FeCl_2^+$	25	0	0.65	-283.39	[258]
				mean	-289.11	
$FeCl_3(aq)$	$1\ FeCl_2^+ + 1\ Cl^- \rightleftharpoons 1\ FeCl_3(aq)$	25	0	-0.82	-415.64	[276]
$FeCl_3(aq)$	$1\ Fe^{3+} + 3\ Cl^- \rightleftharpoons 1\ FeCl_3(aq)$	25	0	1.12	-417.26	[50]
$FeCl_3(aq)$	$1\ FeCl_2^+ + 1\ Cl^- \rightleftharpoons 1\ FeCl_3(aq)$	25	0	-1.00	-414.61	[274]
				mean	-415.84	
$FeCl_4^-$	$1\ Fe^{3+} + 4\ Cl^- \rightleftharpoons 1\ FeCl_4^-$	25	0	-0.75	-537.85	[50]
$FeCl_4^-$	$1\ Fe^{2+} + 4\ Cl^- \rightleftharpoons 1\ FeCl_4^- + 1\ e^-$	25	0	-13.82	-537.55	[276]
$FeCl_4^-$	$1\ Fe^{3+} + 4\ Cl^- \rightleftharpoons 1\ FeCl_4^-$	25	0	-0.79	-537.61	[41]
				mean	-537.67	
$FeNO_3^{2+}$	$1\ Fe^{3+} + 1\ NO_3^- \rightleftharpoons 1\ FeNO_3^{2+}$	20	0.4	0.36	-130.11	[265]
$FeNO_3^{2+}$	$1\ Fe^{3+} + 1\ NO_3^- \rightleftharpoons 1\ FeNO_3^{2+}$	25	0	0.76	-132.38	[277]
$FeNO_3^{2+}$	$1\ Fe^{3+} + 1\ NO_3^- \rightleftharpoons 1\ FeNO_3^{2+}$	25	0	1.00	-133.75	[278]
$FeNO_3^{2+}$	$1\ Fe^{3+} + 1\ NO_3^- \rightleftharpoons 1\ FeNO_3^{2+}$	25	0	1.00	-133.75	[279]
$FeNO_3^{2+}$	$1\ Fe^{3+} + 1\ NO_3^- \rightleftharpoons 1\ FeNO_3^{2+}$	25	0	1.00	-133.75	[75]
				mean	-132.75	
$FeSO_4(aq)$	$1\ Fe^{2+} + 1\ SO_4^{2-} \rightleftharpoons 1\ FeSO_4(aq)$	25	0.06	3.45	-855.27	[280]
$FeSO_4(aq)$	$1\ Fe^{2+} + 1\ SO_4^{2-} \rightleftharpoons 1\ FeSO_4(aq)$	25	0	2.20	-848.13	[99]
$FeSO_4(aq)$	$1\ Fe^{2+} + 1\ SO_4^{2-} \rightleftharpoons 1\ FeSO_4(aq)$	25	0	2.25	-848.41	[40]
$FeSO_4(aq)$	$1\ Fe^{2+} + 1\ SO_4^{2-} \rightleftharpoons 1\ FeSO_4(aq)$	25	0	2.39	-849.21	[75]
				mean	-850.26	
$FeSO_4^+$	$1\ Fe^{3+} + 1\ SO_4^{2-} \rightleftharpoons 1\ FeSO_4^+$	20	0.4	3.45	-780.96	[265]
$FeSO_4^+$	$1\ Fe^{3+} + 1\ SO_4^{2-} \rightleftharpoons 1\ FeSO_4^+$	25	0	4.74	-788.31	[281]

Appendix C. Data considered in the review of solution complex and mineral thermodynamic constants. Only species with more than one datum considered listed

$FeSO_4^+$	$1\ Fe^{3+} + 1\ SO_4^{2-} \rightleftharpoons 1\ FeSO_4^+$	25	0.06	4.04	-784.30	[282]
$FeSO_4^+$	$1\ Fe^{3+} + 1\ SO_4^{2-} \rightleftharpoons 1\ FeSO_4^+$	25	0.5	3.52	-781.33	[283]
$FeSO_4^+$	$1\ Fe^{3+} + 1\ SO_4^{2-} \rightleftharpoons 1\ FeSO_4^+$	25	0.5	3.47	-781.08	[284]
$FeSO_4^+$	$1\ Fe^{3+} + 1\ SO_4^{2-} \rightleftharpoons 1\ FeSO_4^+$	25	0	4.04	-784.31	[278]
$FeSO_4^+$	$1\ Fe^{3+} + 1\ SO_4^{2-} \rightleftharpoons 1\ FeSO_4^+$	25	0	4.05	-784.37	[75]
$FeSO_4^+$	$1\ Fe^{3+} + 1\ SO_4^{2-} \rightleftharpoons 1\ FeSO_4^+$	25	0	4.27	-785.63	
				mean	-783.79	
$Fe(SO_4)_2^-$	$1\ Fe^{3+} + 2\ SO_4^{2-} \rightleftharpoons 1\ Fe(SO_4)_2^-$	25	0	6.11	-1540.13	[285]
$Fe(SO_4)_2^-$	$1\ FeSO_4^+ + 1\ SO_4^{2-} \rightleftharpoons 1\ Fe(SO_4)_2^-$	25	0	1.30	-1535.21	[278]
				mean	-1537.67	
$FeCO_3(aq)$	$1\ Fe^{2+} + 1\ CO_3^{2-} \rightleftharpoons 1\ FeCO_3(aq)$	25	0	5.45	-650.57	[24]
$FeCO_3(aq)$	$1\ Fe^{2+} + 1\ HCO_3^- \rightleftharpoons 1\ FeCO_3(aq) + 1\ H^+$	25	0	-5.60	-646.45	[41]
$FeCO_3(aq)$	$1\ Fe^{2+} + 1\ CO_3^{2-} \rightleftharpoons 1\ FeCO_3(aq)$	25	0	4.38	-644.47	[286]
$FeCO_3(aq)$	$1\ Fe^{2+} + 1\ CO_3^{2-} \rightleftharpoons 1\ FeCO_3(aq)$	25	0	5.45	-650.57	[257]
				mean	-648.02	
$FeHCO_3^+$	$1\ Fe^{2+} + 1\ CO_3^{2-} + 1\ H^+ \rightleftharpoons 1\ FeHCO_3^+$	25	0	11.43	-684.71	[75]
$FeHCO_3^+$	$1\ Fe^{2+} + 1\ HCO_3^- \rightleftharpoons 1\ FeHCO_3^+$	25	0	1.10	-684.69	[75]
$FeHCO_3^+$	$1\ Fe^{2+} + 1\ HCO_3^- \rightleftharpoons 1\ FeHCO_3^+$	25	0	2.72	-693.94	[41]
$FeHCO_3^+$	$1\ Fe^{2+} + 1\ HCO_3^- \rightleftharpoons 1\ FeHCO_3^+$	25	0	2.00	-689.83	[286]
$FeHCO_3^+$	$1\ Fe^{2+} + 1\ HCO_3^- \rightleftharpoons 1\ FeHCO_3^+$	25	0	1.47	-686.80	[257]
				mean	-687.99	
$Fe(CO_3)_2^{2-}$	$1\ Fe^{2+} + 2\ CO_3^{2-} \rightleftharpoons 1\ Fe(CO_3)_2^{2-}$	25	0	7.17	-1188.29	[24]
$Fe(CO_3)_2^{2-}$	$1\ Fe^{2+} + 2\ CO_3^{2-} \rightleftharpoons 1\ Fe(CO_3)_2^{2-}$	25	0	7.16	-1188.23	[257]
				mean	-1188.26	
$FeHPO_4(aq)$	$1\ Fe^{2+} + 1\ HPO_4^{2-} \rightleftharpoons 1\ FeHPO_4(aq)$	25	0	4.08	-1210.84	[27]
$FeHPO_4(aq)$	$1\ Fe^{2+} + 1\ HPO_4^{2-} \rightleftharpoons 1\ FeHPO_4(aq)$	25	0	3.60	-1208.10	[287]
$FeHPO_4(aq)$	$1\ Fe^{2+} + 1\ HPO_4^{2-} \rightleftharpoons 1\ FeHPO_4(aq)$	25	0	7.19	-1228.57	[288]
$FeHPO_4(aq)$	$1\ Fe^{2+} + 1\ HPO_4^{2-} \rightleftharpoons 1\ FeHPO_4(aq)$	25	0	2.46	-1201.60	[75]
				mean	-1212.28	

Appendix C. Data considered in the review of solution complex and mineral thermodynamic constants. Only species with more than one datum considered listed

$FeHPO_4^+$	$1\ Fe^{3+} + 1\ HPO_4^{2-} \rightleftharpoons 1\ FeHPO_4^+$	25	0	10.00	-1170.32	[26]
$FeHPO_4^+$	$1\ Fe^{3+} + 1\ HPO_4^{2-} \rightleftharpoons 1\ FeHPO_4^+$	25	0.1	10.24	-1171.69	[28]
$FeHPO_4^+$	$1\ Fe^{3+} + 1\ HPO_4^{2-} \rightleftharpoons 1\ FeHPO_4^+$	25	0.4	9.39	-1166.86	[289]
$FeHPO_4^+$	$1\ Fe^{3+} + 1\ HPO_4^{2-} \rightleftharpoons 1\ FeHPO_4^+$	25	0.5	9.46	-1167.26	[75]
				mean	-1169.03	
$FeH_2PO_4^+$	$1\ Fe^{2+} + 1\ H_2PO_4^- \rightleftharpoons 1\ FeH_2PO_4^+$	25	0	1.01	-1234.48	[27]
$FeH_2PO_4^+$	$1\ Fe^{2+} + 1\ H_2PO_4^- \rightleftharpoons 1\ FeH_2PO_4^+$	25	0	2.70	-1244.13	[287]
				mean	-1239.30	
$FeH_2PO_4^{2+}$	$1\ Fe^{3+} + 1\ H_2PO_4^- \rightleftharpoons 1\ FeH_2PO_4^{2+}$	25	0	4.00	-1177.23	[26]
$FeH_2PO_4^{2+}$	$1\ Fe^{3+} + 1\ H_2PO_4^- \rightleftharpoons 1\ FeH_2PO_4^{2+}$	25	0.4	4.03	-1177.41	[289]
$FeH_2PO_4^{2+}$	$1\ Fe^{3+} + 1\ H_2PO_4^- \rightleftharpoons 1\ FeH_2PO_4^{2+}$	25	0.4	4.07	-1177.64	[289]
$FeH_2PO_4^{2+}$	$1\ Fe^{3+} + 1\ H_2PO_4^- \rightleftharpoons 1\ FeH_2PO_4^{2+}$	25	0.5	4.05	-1177.53	[75]
				mean	-1177.45	
$Fe(H_2PO_4)_2(aq)$	$1\ Fe^{2+} + 2\ H_2PO_4^- \rightleftharpoons 1\ Fe(H_2PO_4)_2(aq)$	25	0	2.71	-2381.33	[27]
$Fe(H_2PO_4)_2(aq)$	$1\ Fe^{2+} + 2\ H_2PO_4^- \rightleftharpoons 1\ Fe(H_2PO_4)_2(aq)$	25	3	2.40	-2379.57	[75]
				mean	-2380.45	
$FeCit^-$	$1\ Fe^{2+} + 1\ Cit^{3-} \rightleftharpoons 1\ FeCit^-$	37	0.15	6.00	-125.80	[33]
$FeCit^-$	$1\ Fe^{2+} + 1\ Cit^{3-} \rightleftharpoons 1\ FeCit^-$	25	0.1	6.09	-126.33	[42]
$FeCit^-$	$1\ Fe^{2+} + 1\ Cit^{3-} \rightleftharpoons 1\ FeCit^-$	20	0.1	5.69	-124.05	[290]
$FeCit^-$	$1\ Fe^{2+} + 1\ Cit^{3-} \rightleftharpoons 1\ FeCit^-$	25	0	5.67	-123.93	[148]
				mean	-125.03	
FeCit(aq)	$1\ Fe^{3+} + 1\ Cit^{3-} \rightleftharpoons 1\ FeCit(aq)$	25	0.1	13.13	-92.18	[291]
FeCit(aq)	$1\ Fe^{3+} + 1\ Cit^{3-} \rightleftharpoons 1\ FeCit(aq)$	25	0.15	13.36	-93.48	[292]
FeCit(aq)	$1\ Fe^{3+} + 1\ Cit^{3-} \rightleftharpoons 1\ FeCit(aq)$	25	0.1	13.15	-92.28	[42]
FeCit(aq)	$1\ Fe^{3+} + 1\ Cit^{3-} \rightleftharpoons 1\ FeCit(aq)$	25	0.1	12.18	-86.75	[28]
FeCit(aq)	$1\ Fe^{3+} + 1\ H_3Cit(aq) \rightleftharpoons 1\ FeCit(aq) + 3\ H^+$	24	0.1	-1.17	-91.68	[293]
FeCit(aq)	$1\ Fe^{2+} + 1\ Cit^{3-} \rightleftharpoons 1\ FeCit(aq) + 1\ e^-$	25	0	0.61	-95.05	[294]
FeCit(aq)	$1\ Fe^{2+} + 1\ Cit^{3-} \rightleftharpoons 1\ FeCit(aq) + 1\ e^-$	25	0	0.66	-95.33	[295]

Appendix C. Data considered in the review of solution complex and mineral thermodynamic constants. Only species with more than one datum considered listed

$FeCit(aq)$	$1\ Fe^{2+} + 1\ Cit^{3-} \rightleftharpoons 1\ FeCit(aq) + 1\ e^-$	25	0	0.36	-93.62	[290]
$FeCit(aq)$	$1\ Fe^{2+} + 1\ Cit^{3-} \rightleftharpoons 1\ FeCit(aq) + 1\ e^-$	25	0	0.38	-93.73	[296]
				mean	-92.68	
$FeHCit(aq)$	$1\ Fe^{2+} + 1\ H_3Cit(aq) \rightleftharpoons 1\ FeHCit(aq) + 2\ H^+$	25	0	-4.55	-146.73	[34]
$FeHCit(aq)$	$1\ Fe^{2+} + 1\ Cit^{3-} + 1\ H^+ \rightleftharpoons 1\ FeHCit(aq)$	37	0.15	10.40	-150.91	[33]
$FeHCit(aq)$	$1\ Fe^{2+} + 1\ Cit^{3-} + 1\ H^+ \rightleftharpoons 1\ FeHCit(aq)$	25	0.1	10.13	-149.36	[42]
$FeHCit(aq)$	$1\ Fe^{2+} + 1\ HCit^{2-} \rightleftharpoons 1\ FeHCit(aq)$	20	0.1	3.51	-147.71	[290]
$FeHCit(aq)$	$1\ Fe^{2+} + 1\ Cit^{3-} + 1\ H^+ \rightleftharpoons 1\ FeHCit(aq)$	25	0	9.87	-147.90	[148]
$FeHCit(aq)$	$1\ Fe^{2+} + 1\ Cit^{3-} + 1\ H^+ \rightleftharpoons 1\ FeHCit(aq)$	25	0	10.00	-148.65	[12]
				mean	-148.54	
$FeHCit^+$	$1\ Fe^{3+} + 1\ Cit^{3-} + 1\ H^+ \rightleftharpoons 1\ FeHCit^+$	25	0.01	13.14	-92.24	[291]
$FeHCit^+$	$1\ Fe^{3+} + 1\ HCit^{2-} \rightleftharpoons 1\ FeHCit^+$	25	0.15	8.14	-99.80	[292]
$FeHCit^+$	$1\ Fe^{3+} + 1\ Cit^{3-} + 1\ H^+ \rightleftharpoons 1\ FeHCit^+$	25	0.1	14.32	-98.96	[42]
$FeHCit^+$	$1\ Fe^{2+} + 1\ Cit^{3-} + 1\ H^+ \rightleftharpoons 1\ FeHCit^+ + 1\ e^-$	25	0	0.94	-96.93	[297]
$FeHCit^+$	$1\ Fe^{2+} + 1\ Cit^{3-} + 1\ H^+ \rightleftharpoons 1\ FeHCit^+ + 1\ e^-$	25	0	0.88	-96.59	[295]
$FeHCit^+$	$1\ Fe^{2+} + 1\ Cit^{3-} + 1\ H^+ \rightleftharpoons 1\ FeHCit^+ + 1\ e^-$	25	0	0.94	-96.93	[298]
$FeHCit^+$	$1\ Fe^{2+} + 1\ Cit^{3-} + 1\ H^+ \rightleftharpoons 1\ FeHCit^+ + 1\ e^-$	25	0	1.48	-100.01	[299]
$FeHCit^+$	$1\ Fe^{2+} + 1\ Cit^{3-} + 1\ H^+ \rightleftharpoons 1\ FeHCit^+ + 1\ e^-$	25	0	1.28	-98.87	[12]
$FeHCit^+$	$1\ Fe^{2+} + 1\ Cit^{3-} + 1\ H^+ \rightleftharpoons 1\ FeHCit^+ + 1\ e^-$	25	0	1.37	-99.39	[37]
$FeHCit^+$	$1\ Fe^{2+} + 1\ Cit^{3-} + 1\ H^+ \rightleftharpoons 1\ FeHCit^+ + 1\ e^-$	25	0	1.26	-98.76	[296]
				mean	-97.85	
FeH_2Cit^+	$1\ Fe^{2+} + 1\ H_3Cit(aq) \rightleftharpoons 1\ FeH_2Cit^+ + 1\ H^+$	25	0	-1.61	-163.51	[34]
FeH_2Cit^+	$1\ Fe^{2+} + 1\ Cit^{3-} + 2\ H^+ \rightleftharpoons 1\ FeH_2Cit^+$	37	0.15	12.88	-165.07	[33]
FeH_2Cit^+	$1\ Fe^{2+} + 1\ Cit^{3-} + 2\ H^+ \rightleftharpoons 1\ FeH_2Cit^+$	25	0	12.83	-164.80	[295]
FeH_2Cit^+	$1\ Fe^{2+} + 1\ Cit^{3-} + 2\ H^+ \rightleftharpoons 1\ FeH_2Cit^+$	25	0	12.75	-164.34	[12]
				mean	-164.43	
$Fe(Cit)_2^{3-}$	$1\ Fe^{3+} + 2\ Cit^{3-} \rightleftharpoons 1\ Fe(Cit)_2^{3-}$	25	0.01	19.06	-126.03	[291]
$Fe(Cit)_2^{3-}$	$1\ Fe^{3+} + 2\ Cit^{3-} \rightleftharpoons 1\ Fe(Cit)_2^{3-}$	25	0.15	20.36	-133.44	[292]
$Fe(Cit)_2^{3-}$	$1\ Fe^{3+} + 2\ Cit^{3-} \rightleftharpoons 1\ Fe(Cit)_2^{3-}$	25	0.1	17.88	-119.28	[28]
$Fe(Cit)_2^{3-}$	$1\ Fe^{2+} + 2\ Cit^{3-} \rightleftharpoons 1\ Fe(Cit)_2^{3-} + 1\ e^-$	25	0	6.13	-126.56	[37]

Appendix C. Data considered in the review of solution complex and mineral thermodynamic constants. Only species with more than one datum considered listed

				mean	-126.33	
$Fe(HCit)_2^-$	$1\ Fe^{2+} + 2\ Cit^{3-} + 2\ H^+ \rightleftharpoons 1\ Fe(HCit)_2^- + 1\ e^-$	25	0	13.39	-168.00	[12]
$Fe(HCit)_2^-$	$1\ Fe^{2+} + 2\ Cit^{3-} + 2\ H^+ \rightleftharpoons 1\ Fe(HCit)_2^- + 1\ e^-$	25	0	13.31	-167.54	[37]
				mean	-167.77	
$FeOHCit^-$	$1\ Fe^{2-} + 1\ H_2O + 1\ Cit^{3-} \rightleftharpoons 1\ FeOHCit^- + 1\ H^+ + 1\ e^-$	25	0	-2.17	-316.32	[295]
$FeOHCit^-$	$1\ Fe^{2-} + 1\ H_2O + 1\ Cit^{3-} \rightleftharpoons 1\ FeOHCit^- + 1\ H^+ + 1\ e^-$	25	0	-2.60	-313.86	[42]
$FeOHCit^-$	$1\ Fe^{2-} + 1\ H_2O + 1\ Cit^{3-} \rightleftharpoons 1\ FeOHCit^- + 1\ H^+ + 1\ e^-$	25	0	-2.07	-316.89	[12]
$FeOHCit^-$	$1\ Fe^{2-} + 1\ H_2O + 1\ Cit^{3-} \rightleftharpoons 1\ FeOHCit^- + 1\ H^+ + 1\ e^-$	25	0	-2.87	-312.32	[300]
$FeOHCit^-$	$1\ Fe^{2-} + 1\ H_2O + 1\ Cit^{3-} \rightleftharpoons 1\ FeOHCit^- + 1\ H^+ + 1\ e^-$	25	0	-3.02	-311.47	[37]
$FeOHCit^-$	$1\ Fe^{2-} + 1\ H_2O + 1\ Cit^{3-} \rightleftharpoons 1\ FeOHCit^- + 1\ H^+ + 1\ e^-$	25	0	-2.27	-315.75	[296]
				mean	-314.44	
$Fe(OH)_2Cit^{2-}$	$1\ Fe^{2-} + 2\ H_2O + 1\ Cit^{3-} \rightleftharpoons 1\ Fe(OH)_2Cit^{2-} + 2\ H^+ + 1\ e^-$	25	0	-10.06	-508.42	[295]
$Fe(OH)_2Cit^{2-}$	$1\ Fe^{2-} + 2\ H_2O + 1\ Cit^{3-} \rightleftharpoons 1\ Fe(OH)_2Cit^{2-} + 2\ H^+ + 1\ e^-$	25	0	-10.00	-508.76	[12]
				mean	-508.59	
$Fe_2(OH)_2(Cit)_2^{2-}$	$2\ Fe^{2-} + 2\ H_2O + 2\ Cit^{3-} \rightleftharpoons 1\ Fe_2(OH)_2(Cit)_2^{2-} + 2\ H^+ + 2\ e^-$	25	0	-2.95	-640.57	[290]
$Fe_2(OH)_2(Cit)_2^{2-}$	$2\ Fe^{2-} + 2\ H_2O + 2\ Cit^{3-} \rightleftharpoons 1\ Fe_2(OH)_2(Cit)_2^{2-} + 2\ H^+ + 2\ e^-$	25	0	-2.74	-641.77	[32]
$Fe_2(OH)_2(Cit)_2^{2-}$	$2\ Fe^{2-} + 2\ H_2O + 2\ Cit^{3-} \rightleftharpoons 1\ Fe_2(OH)_2(Cit)_2^{2-} + 2\ H^+ + 2\ e^-$	25	0	-2.95	-640.57	[34]
				mean	-640.97	
$Fe_2(OH)_3(Cit)_2^{3-}$	$2\ Fe^{2-} + 3\ H_2O + 2\ Cit^{3-} \rightleftharpoons 1\ Fe_2(OH)_3(Cit)_2^{3-} + 3\ H^+ + 2\ e^-$	25	0	-8.47	-846.20	[32]
$Fe_2(OH)_3(Cit)_2^{3-}$	$2\ Fe^{2-} + 3\ H_2O + 2\ Cit^{3-} \rightleftharpoons 1\ Fe_2(OH)_3(Cit)_2^{3-} + 3\ H^+ + 2\ e^-$	25	0	-7.03	-854.42	[34]
				mean	-850.31	
$FeEDTA^{2-}$	$1\ Fe^{2+} + 1\ EDTA^{4-} \rightleftharpoons 1\ FeEDTA^{2-}$	25	0.1	16.66	-186.66	[301]
$FeEDTA^{2-}$	$1\ Fe^{2+} + 1\ EDTA^{4-} \rightleftharpoons 1\ FeEDTA^{2-}$	25	0.1	15.91	-182.38	[302]
$FeEDTA^{2-}$	$1\ Fe^{2+} + 1\ EDTA^{4-} \rightleftharpoons 1\ FeEDTA^{2-}$	20	0.1	15.92	-182.44	[161]
$FeEDTA^{2-}$	$1\ Fe^{2+} + 1\ EDTA^{4-} \rightleftharpoons 1\ FeEDTA^{2-}$	25	0.1	16.05	-183.18	[31]
$FeEDTA^{2-}$	$1\ Fe^{2+} + 1\ EDTA^{4-} \rightleftharpoons 1\ FeEDTA^{2-}$	20	0.1	16.05	-183.18	[166]
$FeEDTA^{2-}$	$1\ Fe^{2+} + 1\ EDTA^{4-} \rightleftharpoons 1\ FeEDTA^{2-}$	25	0.1	16.02	-183.01	[75]
$FeEDTA^{2-}$	$1\ Fe^{2+} + 1\ EDTA^{4-} \rightleftharpoons 1\ FeEDTA^{2-}$	25	0	16.00	-182.89	[78]

Appendix C. Data considered in the review of solution complex and mineral thermodynamic constants. Only species with more than one datum considered listed

				mean	-183.39	
$FeEDTA^-$	$1\ Fe^{3+} + 1\ EDTA^{4-} \rightleftharpoons 1\ FeEDTA^-$	25	0.1	27.53	-174.39	[76]
$FeEDTA^-$	$1\ Fe^{3+} + 1\ EDTA^{4-} \rightleftharpoons 1\ FeEDTA^-$	25	0.2	28.32	-178.91	[38]
$FeEDTA^-$	$1\ Fe^{3+} + 1\ EDTA^{4-} \rightleftharpoons 1\ FeEDTA^-$	20	0.1	27.68	-175.25	[303]
$FeEDTA^-$	$1\ Fe^{3+} + 1\ EDTA^{4-} \rightleftharpoons 1\ FeEDTA^-$	19	0.1	26.33	-167.54	[304]
$FeEDTA^-$	$1\ Fe^{3+} + 1\ EDTA^{4-} \rightleftharpoons 1\ FeEDTA^-$	20	0	24.23	-155.55	[39]
$FeEDTA^-$	$1\ Fe^{3+} + 1\ EDTA^{4-} \rightleftharpoons 1\ FeEDTA^-$	25	0.1	27.68	-175.25	[31]
$FeEDTA^-$	$1\ Fe^{3+} + 1\ EDTA^{4-} \rightleftharpoons 1\ FeEDTA^-$	20	0.1	27.68	-175.25	[305]
$FeEDTA^-$	$1\ Fe^{3+} + 1\ EDTA^{4-} \rightleftharpoons 1\ FeEDTA^-$	25	0.1	27.68	-175.25	[75]
				mean	-172.17	
$FeHEDTA^-$	$1\ FeEDTA^{2-} + 1\ H^+ \rightleftharpoons 1\ FeHEDTA^-$	25	0.1	2.49	-197.61	[301]
$FeHEDTA^-$	$1\ Fe^{2+} + 1\ HEDTA^{3-} \rightleftharpoons 1\ FeHEDTA^-$	20	0.2	9.32	-206.94	[38]
$FeHEDTA^-$	$1\ Fe^{2+} + 1\ HEDTA^{3-} \rightleftharpoons 1\ FeHEDTA^-$	25	0.1	7.51	-196.63	[302]
$FeHEDTA^-$	$1\ Fe^{2+} + 1\ HEDTA^{3-} \rightleftharpoons 1\ FeHEDTA^-$	20	0.1	8.90	-204.56	[161]
$FeHEDTA^-$	$1\ Fe^{2+} + 1\ HEDTA^{3-} \rightleftharpoons 1\ FeHEDTA^-$	20	0.1	8.90	-204.56	[166]
$FeHEDTA^-$	$1\ Fe^{2+} + 1\ HEDTA^{3-} \rightleftharpoons 1\ FeHEDTA^-$	25	0.1	8.86	-204.33	[75]
$FeHEDTA^-$	$1\ Fe^{2+} + 1\ EDTA^{4-} + 1\ H^+ \rightleftharpoons 1\ FeHEDTA^-$	25	0	19.06	-200.36	[78]
				mean	-202.14	
FeHEDTA(aq)	$1\ FeEDTA^- + 1\ H^+ \rightleftharpoons 1\ FeHEDTA(aq)$	20	0.1	1.42	-180.25	[303]
FeHEDTA(aq)	$1\ Fe^{3+} + 1\ HEDTA^{3-} \rightleftharpoons 1\ FeHEDTA(aq)$	19	0.1	16.53	-173.75	[304]
FeHEDTA(aq)	$1\ Fe^{3+} + 1\ HEDTA^{3-} \rightleftharpoons 1\ FeHEDTA(aq)$	20	0	15.26	-166.53	[39]
FeHEDTA(aq)	$1\ Fe^{3+} + 1\ HEDTA^{3-} \rightleftharpoons 1\ FeHEDTA(aq)$	20	0.1	18.14	-182.94	[305]
FeHEDTA(aq)	$1\ FeEDTA^- + 1\ H^+ \rightleftharpoons 1\ FeHEDTA(aq)$	25	0.1	1.52	-180.82	[75]
FeHEDTA(aq)	$1\ FeEDTA^- + 1\ H^+ \rightleftharpoons 1\ FeHEDTA(aq)$	25	0.1	1.52	-180.82	[306]
				mean	-177.52	
$Fe(OH)EDTA^{3-}$	$1\ FeEDTA^{2-} + 1\ OH^- \rightleftharpoons 1\ Fe(OH)EDTA^{3-}$	25	0.1	4.47	-366.13	[31]
$Fe(OH)EDTA^{3-}$	$1\ FeEDTA^{2-} + 1\ H2O \rightleftharpoons 1\ Fe(OH)EDTA^{3-} + 1\ H^+$	20	0.1	-9.72	-365.08	[305]
$Fe(OH)EDTA^{3-}$	$1\ FeEDTA^{2-} + 1\ OH^- \rightleftharpoons 1\ Fe(OH)EDTA^{3-}$	20	0.1	4.45	-366.01	[169]
				mean	-365.74	

Appendix C. Data considered in the review of solution complex and mineral thermodynamic constants. Only species with more than one datum considered listed

$Fe(OH)_2EDTA^{4-}$	$1\ Fe(OH)EDTA^{3-} + 1\ OH^- \rightleftharpoons 1\ Fe(OH)_2EDTA^{4-}$	25	0.1	3.45	-542.68	[31]
$Fe(OH)_2EDTA^{4-}$	$1\ Fe(OH)EDTA^{3-} + 1\ H_2O \rightleftharpoons 1\ Fe(OH)_2EDTA^{4-} + 1\ H^+$	20	0.1	-10.66	-542.03	[305]
				mean	-542.36	
$Fe(OH)EDTA^{2-}$	$1\ FeEDTA^- + 1\ H_2O \rightleftharpoons 1\ Fe(OH)EDTA^{2-} + 1\ H^+$	25	0.1	-7.84	-364.56	[76]
$Fe(OH)EDTA^{2-}$	$1\ FeEDTA^- + 1\ OH^- \rightleftharpoons 1\ Fe(OH)EDTA^{2-}$	20	0.1	6.28	-365.27	[303]
$Fe(OH)EDTA^{2-}$	$1\ Fe^{3+} + 1\ OH^- + 1\ EDTA^{4-} \rightleftharpoons 1\ Fe(OH)EDTA^{2-}$	20	0.1	36.37	-382.04	[307]
$Fe(OH)EDTA^{2-}$	$1\ FeEDTA^- + 1\ H_2O \rightleftharpoons 1\ Fe(OH)EDTA^{2-} + 1\ H^+$	25	0.1	-7.83	-364.62	[31]
$Fe(OH)EDTA^{2-}$	$1\ FeEDTA^- + 1\ H_2O \rightleftharpoons 1\ Fe(OH)EDTA^{2-} + 1\ H^+$	20	0.1	-7.92	-364.11	[305]
$Fe(OH)EDTA^{2-}$	$1\ FeEDTA^- + 1\ H_2O \rightleftharpoons 1\ Fe(OH)EDTA^{2-} + 1\ H^+$	25	0.1	-7.82	-364.68	[75]
				mean	-367.55	
$Fe(OH)_2EDTA^{3-}$	$1\ Fe(OH)EDTA^{2-} + 1\ OH^- \rightleftharpoons 1\ Fe(OH)_2EDTA^{3-}$	25	0.1	4.10	-548.17	[31]
$Fe(OH)_2EDTA^{3-}$	$1\ Fe(OH)EDTA^{2-} + 1\ H_2O \rightleftharpoons 1\ Fe(OH)_2EDTA^{3-} + 1\ H^+$	20	0.1	-10.06	-547.29	[305]
$Fe(OH)_2EDTA^{3-}$	$1\ Fe(OH)EDTA^{2-} + 1\ OH^- \rightleftharpoons 1\ Fe(OH)_2EDTA^{3-}$	20	0.1	4.11	-548.23	[169]
				mean	-547.90	
$Ca(OH)_2$, Portlandite	$1\ Ca^{2+} + 2\ OH^- \rightleftharpoons 1\ Ca(OH)_2$, Portlandite	25	0	-5.19	-837.62	[75]
$Ca(OH)_2$, Portlandite	$1\ Ca^{2+} + 2\ H_2O \rightleftharpoons 1\ Ca(OH)_2$, Portlandite $+ 2\ H^+$	25	0	-32.58	-841.14	[41]
$Ca(OH)_2$, Portlandite	$1\ Ca^{2+} + 2\ H_2O \rightleftharpoons 1\ Ca(OH)_2$, Portlandite $+ 2\ H^+$	25	0	-22.80	-896.94	[308]
$Ca(OH)_2$, Portlandite		25	0		-897.50	[309]
$Ca(OH)_2$, Portlandite		25	0		-898.41	[310]
				mean	-874.32	
$Ca_4H(PO_4)_3{\cdot}3H_2O$	$4\ Ca^{2+} + 3\ PO_4^{3-} + 1\ H^+ + 3\ H_2O \rightleftharpoons 1\ Ca_4H(PO_4)_3{\cdot}3H_2O$	25	0	47.08	-6267.85	[311]
$Ca_4H(PO_4)_3{\cdot}3H_2O$	$4\ Ca^{2+} + 3\ PO_4^{3-} + 1\ H^+ + 3\ H_2O \rightleftharpoons 1\ Ca_4H(PO_4)_3{\cdot}3H_2O$	25	0	46.9	-6266.82	[312]
$Ca_4H(PO_4)_3{\cdot}3H_2O$	$4\ Ca^{2+} + 3\ HPO_4^{2-} + 3\ H_2O \rightleftharpoons 1\ Ca_4H(PO_4)_3{\cdot}3H_2O + 2\ H^+$	25	0	9.93	-6267.30	[312]
				mean	-6267.32	
$Ca_5(PO_4)_3OH$, hydroxyapatite		25	0		-6338.3	[309]
$Ca_5(PO_4)_3OH$, hydroxyapatite	$5\ Ca^{2+} + 3\ PO_4^{3-} + 1\ OH^- \rightleftharpoons 1\ Ca_5(PO_4)_3OH$, hydroxyapatite	25	0	55.91	-6316.86	[313]
$Ca_5(PO_4)_3OH$, hydroxyapatite	$5\ Ca^{2+} + 3\ PO_4^{3-} + 1\ OH^- \rightleftharpoons 1\ Ca_5(PO_4)_3OH$, hydroxyapatite	25	0	57.8	-6327.65	[314]
$Ca_5(PO_4)_3OH$, hydroxyapatite	$5\ Ca^{2+} + 3\ PO_4^{3-} + 1\ OH^- \rightleftharpoons 1\ Ca_5(PO_4)_3OH$, hydroxyapatite	25	0	58.52	-6331.74	[315]

Appendix C. Data considered in the review of solution complex and mineral thermodynamic constants. Only species with more than one datum considered listed

				mean	-6328.64	
$CaCO_3$, Aragonite	1 Ca^{2+} + 1 CO_3^{2-} ⇌ 1 $CaCO_3$, Aragonite	25	0	8.30	-1128.08	[316]
$CaCO_3$, Aragonite	1 Ca^{2+} + 1 CO_3^{2-} ⇌ 1 $CaCO_3$, Aragonite	25	0	8.10	-1126.94	[317]
$CaCO_3$, Aragonite	1 Ca^{2+} + 1 CO_3^{2-} ⇌ 1 $CaCO_3$, Aragonite	25	0	8.22	-1127.63	[105]
$CaCO_3$, Aragonite	1 Ca^{2+} + 1 CO_3^{2-} ⇌ 1 $CaCO_3$, Aragonite	25	0	8.30	-1128.08	[75]
$CaCO_3$, Aragonite		25	0		-1128.30	[309]
$CaCO_3$, Aragonite		25	0		-1127.79	[310]
				mean	-1127.80	
$CaCO_3$, Calcite	1 Ca^{2+} + 1 CO_3^{2-} ⇌ 1 $CaCO_3$, Calcite	25	0	8.48	-1129.11	[180]
$CaCO_3$, Calcite	1 Ca^{2+} + 1 CO_3^{2-} ⇌ 1 $CaCO_3$, Calcite	25	0	8.48	-1129.11	[316]
$CaCO_3$, Calcite	1 Ca^{2+} + 1 CO_3^{2-} ⇌ 1 $CaCO_3$, Calcite	25	0	8.42	-1128.77	[181]
$CaCO_3$, Calcite	1 Ca^{2+} + 1 CO_3^{2-} ⇌ 1 $CaCO_3$, Calcite	25	0	8.46	-1128.98	[172]
$CaCO_3$, Calcite	1 Ca^{2+} + 1 CO_3^{2-} ⇌ 1 $CaCO_3$, Calcite	25	0	8.40	-1128.65	[318]
$CaCO_3$, Calcite	1 Ca^{2+} + 1 CO_3^{2-} ⇌ 1 $CaCO_3$, Calcite	25	0	8.21	-1127.58	[50]
$CaCO_3$, Calcite	1 Ca^{2+} + 1 CO_3^{2-} ⇌ 1 $CaCO_3$, Calcite	25	0	8.22	-1127.63	[319]
$CaCO_3$, Calcite	1 Ca^{2+} + 1 CO_3^{2-} ⇌ 1 $CaCO_3$, Calcite	25	0	8.31	-1128.14	[183]
$CaCO_3$, Calcite	1 Ca^{2+} + 1 CO_3^{2-} ⇌ 1 $CaCO_3$, Calcite	25	0	8.35	-1128.37	[105]
$CaCO_3$, Calcite	1 Ca^{2+} + 1 CO_3^{2-} ⇌ 1 $CaCO_3$, Calcite	25	0	8.48	-1129.11	[75]
$CaCO_3$, Calcite		25	0		-1129.07	[309]
$CaCO_3$, Calcite		25	0		-1128.30	[320]
$CaCO_3$, Calcite		25	0		-1128.84	[310]
$CaCO_3$, Calcite		25	0		-1128.81	[321]
				mean	-1128.61	
$CaHPO_4{\cdot}2H_2O$, brushite	1 Ca^{2+} + 1 HPO_4^{2-} + 2 H_2O ⇌ $CaHPO_4{\cdot}2H_2O$, brushite	25	0	6.55	-2160.46	[322]
$CaHPO_4{\cdot}2H_2O$, brushite	1 Ca^{2+} + 1 HPO_4^{2-} + 2 H_2O ⇌ $CaHPO_4{\cdot}2H_2O$, brushite	25	0	6.60	-2160.75	[107]
$CaHPO_4{\cdot}2H_2O$, brushite	1 Ca^{2+} + 1 HPO_4^{2-} + 2 H_2O ⇌ $CaHPO_4{\cdot}2H_2O$, brushite	25	0	6.59	-2160.69	[185]
				mean	-2160.63	
$CaMg(CO_3)_2$, Dolomite(Ordered)	1 Ca^{2+} + 1 Mg^{2+} + 2 CO_3^{2-} ⇌ 1 $CaMg(CO_3)_2$, Dolomite(Ordered)	25	0	17.09	-2161.53	[308]
$CaMg(CO_3)_2$,		25	0		-2161.70	[309]

Appendix C. Data considered in the review of solution complex and mineral thermodynamic constants. Only species with more than one datum considered listed

Dolomite(Ordered) $CaMg(CO_3)_2$,						
Dolomite(Ordered) $CaMg(CO_3)_2$,		25	0		-2162.35	[320]
Dolomite(Ordered) $CaMg(CO_3)_2$,		25	0		-2161.67	[310]
Dolomite(Ordered)		25	0		-2163.76	[321]
				mean	-2162.20	
$CaSO_4$, anhydrite	$1\ Ca^{2+} + 1\ SO_4^{2-} \rightleftharpoons 1\ CaSO_4$, anhydrite	25	0	4.27	-1321.15	[323]
$CaSO_4$, anhydrite	$1\ Ca^{2+} + 1\ SO_4^{2-} \rightleftharpoons 1\ CaSO_4$, anhydrite	25	0	4.36	-1321.70	[324]
$CaSO_4$, anhydrite	$1\ Ca^{2+} + 1\ SO_4^{2-} \rightleftharpoons 1\ CaSO_4$, anhydrite	25	0	4.27	-1321.18	[325]
$CaSO_4$, anhydrite	$1\ Ca^{2+} + 1\ SO_4^{2-} \rightleftharpoons 1\ CaSO_4$, anhydrite	25	0	4.31	-1321.39	[41]
$CaSO_4$, anhydrite	$1\ Ca^{2+} + 1\ SO_4^{2-} \rightleftharpoons 1\ CaSO_4$, anhydrite	25	0	4.36	-1321.70	[308]
$CaSO_4$, anhydrite		25	0		-1321.98	[309]
$CaSO_4$, anhydrite		25	0		-1321.70	[310]
$CaSO_4$, anhydrite	$1\ Ca^{2+} + 1\ SO_4^{2-} \rightleftharpoons 1\ CaSO_4$, anhydrite	25	0	4.36	-1321.70	[326]
$CaSO_4$, anhydrite	$1\ Ca^{2+} + 1\ SO_4^{2-} \rightleftharpoons 1\ CaSO_4$, anhydrite	25	0	4.19	-1320.73	[327]
				mean	-1321.47	
$CaSO_4 \cdot 2H_2O$, gypsum	$1\ Ca^{2+} + 1\ SO_4^{2-} + 2\ H_2O \rightleftharpoons 1\ CaSO_4 \cdot 2H_2O$, gypsum	25	0	4.60	-1797.33	[323]
$CaSO_4 \cdot 2H_2O$, gypsum	$1\ Ca^{2+} + 1\ SO_4^{2-} + 2\ H_2O \rightleftharpoons 1\ CaSO_4 \cdot 2H_2O$, gypsum	25	0	4.59	-1797.29	[324]
$CaSO_4 \cdot 2H_2O$, gypsum	$1\ Ca^{2+} + 1\ SO_4^{2-} + 2\ H_2O \rightleftharpoons 1\ CaSO_4 \cdot 2H_2O$, gypsum	25	0	4.52	-1796.89	[325]
$CaSO_4 \cdot 2H_2O$, gypsum	$1\ Ca^{2+} + 1\ SO_4^{2-} + 2\ H_2O \rightleftharpoons 1\ CaSO_4 \cdot 2H_2O$, gypsum	25	0	4.61	-1797.40	[75]
$CaSO_4 \cdot 2H_2O$, gypsum	$1\ Ca^{2+} + 1\ SO_4^{2-} + 2\ H_2O \rightleftharpoons 1\ CaSO_4 \cdot 2H_2O$, gypsum	25	0	4.48	-1796.68	[41]
$CaSO_4 \cdot 2H_2O$, gypsum	$1\ Ca^{2+} + 1\ SO_4^{2-} + 2\ H_2O \rightleftharpoons 1\ CaSO_4 \cdot 2H_2O$, gypsum	25	0	4.58	-1797.23	[308]
$CaSO_4 \cdot 2H_2O$, gypsum		25	0		-1797.36	[309]
$CaSO_4 \cdot 2H_2O$, gypsum		25	0		-1797.20	[310]
				mean	-1797.17	
$Fe(OH)_2$(s)	$1\ Fe^{2+} + 2\ OH^- \rightleftharpoons 1\ Fe(OH)_2$(s)	25	0	14.39	-488.14	[235]
$Fe(OH)_2$(s)	$1\ Fe^{2+} + 2\ OH^- \rightleftharpoons 1\ Fe(OH)_2$(s)	25	0	15.10	-492.20	[328]
$Fe(OH)_2$(s)	$1\ Fe^{2+} + 2\ OH^- \rightleftharpoons 1\ Fe(OH)_2$(s)	25	0	14.54	-489.00	[329]
$Fe(OH)_2$(s)	$1\ Fe^{2+} + 2\ OH^- \rightleftharpoons 1\ Fe(OH)_2$(s)	25	0	14.67	-489.74	[329]

Appendix C. Data considered in the review of solution complex and mineral thermodynamic constants. Only species with more than one datum considered listed

$Fe(OH)_2$(s)	1 Fe^{2+} + 2 OH^- ⇌ 1 $Fe(OH)_2$(s)	25	0	14.81	-490.54	[329]
$Fe(OH)_2$(s)	1 Fe^{2+} + 2 OH^- ⇌ 1 $Fe(OH)_2$(s)	25	0	14.43	-488.37	[75]
$Fe(OH)_2$(s)	1 Fe^{2+} + 2 H_2O ⇌ 1 $Fe(OH)_2$(s) + 2 H^+	25	0	-13.90	-486.48	[41]
				mean	-489.21	
$Fe(OH)_3$, ferrihydrite		25	0		-705.29	[241]
$Fe(OH)_3$, ferrihydrite	1 Fe^{3+} + 3 OH^- ⇌ 1 $Fe(OH)_3$, ferrihydrite	25	0	38.80	-710.38	[75]
$Fe(OH)_3$, ferrihydrite		25	0		-700.00	[257]
$Fe(OH)_3$, ferrihydrite		25	0		-705.50	[326]
$Fe(OH)_3$, ferrihydrite		25	0		-701.05	[330]
$Fe(OH)_3$, ferrihydrite		25	0		-692.07	[309]
				mean	-702.38	
Fe_2O_3, hematite		25	0		-744.30	[241]
Fe_2O_3, hematite	2 Fe^{3+} + 3 H_2O ⇌ 1 Fe_2O_3, hematite + 6 H^+	25	0	-0.11	-745.30	[41]
Fe_2O_3, hematite		25	0		-744.77	[260]
Fe_2O_3, hematite		25	0		-742.70	[326]
Fe_2O_3, hematite		25	0		-742.20	[330]
Fe_2O_3, hematite		25	0		-742.80	[309]
Fe_2O_3, hematite		25	0		-743.68	[320]
Fe_2O_3, hematite		25	0		-742.68	[310]
Fe_2O_3, hematite		25	0		-743.72	[321]
				mean	-743.57	
Fe_3O_4, magnetite		25	0		-1012.57	[241]
Fe_3O_4, magnetite		25	0		-1012.90	[309]
Fe_3O_4, magnetite		25	0		-1014.24	[320]
Fe_3O_4, magnetite		25	0		-1012.57	[310]
Fe_3O_4, magnetite		25	0		-1014.34	[321]
				mean	-1013.32	
$FeCO_3$, siderite	1 Fe^{2+} + 1 CO_3^{2-} ⇌ 1 $FeCO_3$, siderite	25	0	10.24	-677.92	[331]
$FeCO_3$, siderite	1 Fe^{2+} + 1 CO_3^{2-} ⇌ 1 $FeCO_3$, siderite	25	0	10.68	-680.43	[332]
$FeCO_3$, siderite	1 Fe^{2+} + 1 CO_3^{2-} ⇌ 1 $FeCO_3$, siderite	25	0	10.80	-681.11	[75]

Appendix C. Data considered in the review of solution complex and mineral thermodynamic constants. Only species with more than one datum considered listed

$FeCO_3$, siderite	1 Fe^{2+} + 1 CO_3^{2-} ⇌ 1 $FeCO_3$, siderite	25	0	10.89	-681.63	[308]
$FeCO_3$, siderite		25	0		-673.05	[309]
$FeCO_3$, siderite		25	0		-666.70	[310]
				mean	-676.80	
FeOOH, goethite		25	0		-485.30	[241]
FeOOH, goethite	1 Fe^{3+} + 3 OH^- ⇌ 1 FeOOH, goethite + 1 H_2O	25	0	41.50	-488.65	[75]
FeOOH, goethite	1 Fe^{3+} + 2 H_2O ⇌ 1 FeOOH, goethite + 3 H^+	25	0	-0.53	-488.48	[41]
FeOOH, goethite		25	0		-488.60	[257]
FeOOH, goethite		25	0		-488.60	[331]
FeOOH, goethite		25	0		-488.55	[309]
FeOOH, goethite		25	0		-488.55	[310]
				mean	-488.10	
$Mg(OH)_2$, Brucite	1 Mg^{2+} + 2 H_2O ⇌ 1 $Mg(OH)_2$, Brucite + 2 H^+	25	0	-16.30	-836.63	[41]
$Mg(OH)_2$, Brucite	1 Mg^{2+} + 2 H_2O ⇌ 1 $Mg(OH)_2$, Brucite + 2 H^+	25	0	-16.84	-833.53	[308]
$Mg(OH)_2$, Brucite		25	0		-833.51	[309]
$Mg(OH)_2$, Brucite		25	0		-834.87	[320]
$Mg(OH)_2$, Brucite		25	0		-833.51	[310]
$Mg(OH)_2$, Brucite		25	0		-834.55	[321]
				mean	-834.43	
$MgCO_3$, magnesite	1 Mg^{2+} + 1 CO_3^{2-} ⇌ 1 $MgCO_3$, magnesite	25	0	8.09	-1029.45	[333]
$MgCO_3$, magnesite	1 Mg^{2+} + 1 CO_3^{2-} ⇌ 1 $MgCO_3$, magnesite	25	0	7.46	-1025.86	[75]
$MgCO_3$, magnesite	1 Mg^{2+} + 1 HCO_3^- ⇌ 1 $MgCO_3$, magnesite + 1 H^+	25	0	-2.29	-1029.13	[41]
$MgCO_3$, magnesite		25	0		-1012.10	[309]
$MgCO_3$, magnesite		25	0		-1030.71	[320]
$MgCO_3$, magnesite		25	0		-1029.48	[310]
$MgCO_3$, magnesite		25	0		-1029.12	[321]
				mean	-1026.55	

1. Botts, J., A. Chashin, and H. Young, Biochemistry, 1965. **4**: p. 1788.
2. De Stefano, C., et al., Anal.Chim.Acta., 1999. **398**: p. 103-110.
3. Fisher, F.H., J. Soln. Chem., 1975. **4**: p. 237-240.
4. Chen, M. and R. Reid, Can.J.Chem., 1993. **71**: p. 763.
5. Dickson, A.G. and M. Whitfield, *An ion-association model for estimating acidity constants (at 25 °C and 1 atm total pressure) in electrolyte mixtures related to seawater.* An ion-association model for estimating acidity constants (at 25 °C and 1 atm total pressure) in electrolyte mixtures related to seawater, 1981. **10**: p. 315-333.
6. De Stefano, C., et al., *Equilibrium studies in natural fluids: Interactions of PO43-, P2O74- and P3O105- with the major constituents of sea water.* Chemical Speciation and Bioavailability, 1998. **10**: p. 19-26.
7. Fisher, F.H. and A.P. Fox, *LiSO4-, RbSO4-, CsSO4-, and (NH4)SO4- ion pairs in aqueous solutions at pressures up to 2000 atm.* Journal of Solution Chemistry, 1978. **7**: p. 561-570.
8. Sverjensky, D.A., E.L. Shock, and H.C. Helgeson, Geochimica et Cosmochimica Acta, 1997. **61**(7): p. 1359-1412.
9. Shock, E.L., et al., Geochimica et Cosmochimica Acta., 1997. **61**(5): p. 907-950.
10. Blaquiere, C. and G. Berthon, Inorg.Chim.Acta., 1987. **135**: p. 179.
11. Ciavatta, L., M. Iuliano, and R. Porto, Ann.Chim.(Rome), 1994. **84**: p. 95.
12. May, P.M., P.W. Linder, and D.R. Williams, *Computer simulation of metal-ion equilibria in biofluids: Models for the low-molecular weight complex distribution of calcium(II), magnesium(II), manganese(II), iron(III), copper(II), zinc(II), and lead(II) ions in human blood plasma.* Journal of the Chemical Society, Dalton Transactions., 1977: p. 588-595.
13. Ciavatta, L., M. Iuliano, and R. Porto, Ann.Chim.(Rome), 1991. **81**: p. 243.
14. Fedorov, V., et al., Zh.Neorg.Khim., 1974. **19**: p. 1746(E:950).
15. Guiomar, M., M. Lito, and A. Covington, J.Solution Chem., 1998. **27**: p. 925.
16. Porto, R., Ann.Chim.(Rome),, 1995. **85**: p. 55.
17. Bernhard, G., et al., *Uranyl(VI) carbonate complex formation: Validation of the Ca2UO2(CO3)3(aq) species.* Radiochim. Acta, 2001. **89**: p. 511-518.
18. Leyden, D. and J. Whidley, Anal.Chim.Acta., 1968. **42**: p. 271.
19. Ramamoorthy, S. and P.G. Manning, *Equilibrium studies of solutions containing Al[3+]. Ca[2+] or Cd[2+] and cysteine, orthophosphate and a carboxylic acid.* Journal of Inorganic and Nuclear Chemistry, 1975. **34**: p. 3443-3448.
20. Comarmond, J. and P.L. Brown, *The hydrolysis of uranium(VI) in sulfate media.* Radiochimica acta, 2000(In press).
21. Palmer, D.A. and C. Nguyen-Trung, *Aqueous uranyl complexes. 3. Potentiometric measurements of the hydrolysis of uranyl(VI) ion at 25°C.* Journal of Solution Chemistry, 1995. **24**: p. 1281-1291.
22. Hummel, W., *Organic complexation of Radionuclides in cement pore water: A case study*. 1993, Paul Scherrer Institut: Villigen, Switzerland.
23. Geipel, G., et al., *Uranium(VI) sulfate complexation studied by time-resolved laser-induced fluorescence spectroscopy (TRLFS).* Radiochimica Acta, 1996. **75**: p. 199-204.
24. Bruno, J., P. Wersin, and W. Stumm, Geochim.Cosmo.Acta., 1992. **56**: p. 1139.
25. Kotlyarova, I., N. Skorik, and V. Kumok, Zh.Neorg.Khim., 1977. **22**: p. 2582.
26. Ciavatta, L. and M. Iuliano, Ann.Chim.(Rome), 1995. **85**: p. 235.
27. Ciavatta, L., M. Iuliano, and R. Porta, Ann.Chim.(Rome), 1992. **82**(121): p. 447-463.
28. Ramamoorthy, S. and P. Manning, Inorg.Nucl.Chem.Lett., 1974. **10**: p. 109.
29. Filatova, L., Zh.Neorg.Khim., 1974. **19**: p. 3335.
30. Stipp, S.L., Environmental Science and Technology, 1990. **24**: p. 699-706.
31. Skochdopole, R. and S. Chaberek, J.Inorg.Nucl.Chem., 1959. **11**: p. 222.
32. Sal'nikov, Y.I. and N.E. Zhuravleva, Russian Journal of Inorganic Chemistry, 1986. **31**: p. 1078-1080.

33. Amico, P., et al., Inorg.Chim.Acta., 1979. **36**: p. 1.
34. Glebov, A., et al., Zh.Neorg.Khim., 1990. **35**: p. 2290.
35. Khoe, G. and R. Robins, J.Chem.Soc.,Dalton Trans., 1988: p. 2015.
36. Salvado, V., et al. *The hydrolysis of Fe(III) in NaNO3 0.5 M aqueous solutions*. in *Spanish-Italian and Mediterranean Basin Congress (SIMEC'94)*. 1994. S'agaro, Spain.
37. Ribas, X., V. Salvado, and M. Valiente, Journal of Chemical Research, 1989. **332**: p. 2533-2553.
38. Borggaard, O., Acta Chem.Scand., 1972. **26**: p. 393.
39. Beck, M. and S. Gorog, J.Inorg.Nucl.Chem., 1960. **12**: p. 353.
40. Nordstrom, D.K., et al., *Revised chemical equilibrium data for major water-mineral reactions and their limitations.*, in *Chemical Modelling of Aqueous Systems II*, R.L. Bassett, Editor. 1990, American Chemical Society: Washington D.C. p. 398-413.
41. Van der Lee, J., *CHESS database*. 1999.
42. Field, T.B., J.L. McCourt, and W.A.E. McBryde, *Composition and stability of iron and copper citrate complexes in aqueous solution.* Canadian Journal of Chemistry., 1974. **52**(3119).
43. Markich, S.J. and P.L. Brown, *Thermochemical data (log K) for environmentally-relevent elements.* 1999, ANSTO Environment Division: Menai, NSW, Australia. p. 131.
44. Maffia, M. and A. Meirelles, J.Chem.Eng.Data., 2001. **46**: p. 582.
45. Borkowski, M., G. Choppin, and R. Moore, Inorg.Chim.Acta., 2000. **298**: p. 141.
46. Barron, D., S. Buti, and J. Barbosa, Phys.Chem.Chem.Phys., 1999. **1**: p. 295.
47. De Robertis, A., C. De Stefano, and C. Foti, J.Chem.Eng.Data., 1999. **44**: p. 262.
48. Petkovic, D., J.Chem.Soc.,Dalton Trans., 1982: p. 2425.
49. Robinson, R. and R. Bates, Anal.Chem., 1971. **43**: p. 969.
50. Helgeson, H., Am.J.Sci., 1969. **267**: p. 729.
51. Helgeson, H., J.Phys.Chem., 1967. **71**: p. 3121.
52. Davis, W. and H. De Bruin, J.Inorg.Nucl.Chem., 1964. **26**: p. 1069.
53. Hood, G. and C. Reilly, J.Chim.Phys., 1960. **32**: p. 127.
54. McKay, H., Trans.Faraday Society, 1956. **52**: p. 1568.
55. Aizawa, S., T. Natsume, and K. Hatano, Inorg.Chim.Acta, 1996. **248**: p. 215.
56. Sun, Y., C. Anderson, and T. Pajeau, J.Med.Chem., 1996. **39**: p. 458.
57. Letkeman, P. and A. Martell, Inorg.Chem., 1979. **18**: p. 1284.
58. Eberle, S. and U. Wede, J.Inorg.Nucl.Chem., 1970. **32**: p. 109.
59. Frausto da Silva, J. and M. Simoes, Talanta, 1968. **15**: p. 609.
60. Anderegg, G. and N. Podder, J.Coord.Chem., 1975. **4**: p. 267.
61. Bauman, E., J.Inorg.Nucl.Chem., 1974. **36**: p. 1827.
62. Felcman, J. and J. da Silva, Talanta, 1983. **30**: p. 565.
63. Wikberg, H. and A. Ringbom, Suomen Kem., 1968. **B41**: p. 177.
64. Overvoll, A. and W. Lund, Anal.Chim.Acta., 1982. **143**: p. 153.
65. Anderegg, G., IUPAC Chemical Data Series, 1978. **14**.
66. Rajan, K., et al., J.Inorg.Biochem., 1981. **14**: p. 339.
67. Svetlova, I. and N. Dobrynina, Zh.Neorg.Khim., 1989. **34**: p. 52.
68. Avdeef, A., D. Kearney, and J. Brown, Anal.Chem.(USA), 1982. **54**: p. 2322.
69. Novak, V., et al., Chem.Zvesti, 1978. **32**: p. 19.
70. Sirotkova, L. and M. Kalina, Chem.Zvesti, 1981. **35**: p. 339.
71. Falck, W.E., D. Read, and J.B. Thomas, *CHEMVAL2: Thermodynamic Database.* 1996, CEC Report EUR 16897.
72. Kumar, K. and C. Chang, Inorg.Chem., 1994. **33**: p. 3567.
73. Turner, D. and M. dos Santos, Anal.Chim.Acta., 1992. **258**: p. 259.
74. Daniele, P., C. Rigano, and S. Sammartano, Anal.Chem.(USA), 1985. **57**: p. 2956.

75. Martell, A.E., R.M. Smith, and R.J. Motekaitis, *NIST Critically Selected Stability Constants of Metal Complexes*. 2001, NIST Standard Reference Data: Gaithersburg, MD. USA.
76. Delgado, R., S. Quintino, and M. Teixeira, J.Chem.Soc.,Dalton Trans., 1997(55).
77. Pokrovsky, O.S., et al., *Interaction of Neptunyl(V) and Uranyl(VI) with EDTA in NaCl Media: Experimental study and Pitzer Modeling.* Radiochim. Acta., 1998. **80**: p. 23-29.
78. Allison, J.D., D.S. Brown, and Novo-Gradac, *MINTEQA2/PRODEFA2, A Geochemical Assessment Model for Environmental Systems: Version 3.0 User's Manual*. 1991, U.S. Environmental Protection Agency: Athens, GA.
79. Arena, G., Ann.Chim.(Rome), 1979. **68**: p. 535.
80. Krot, N., N. Ermolaev, and A. Gelman, Zh.Neorg.Khim., 1962. **7**: p. 1062.
81. Beck, M. and S. Gorog, Analyst, 1959. **48**: p. 90.
82. Matsumura, K., N. Nakasuka, and M. Tanaka, Inorganic Chemistry, 1987. **26**: p. 1419.
83. Gimblett, F. and C. Monk, Trans.Faraday Society, 1954. **50**: p. 965.
84. Bell, R. and J. Prue, J.Chem.Soc., 1949: p. 362.
85. De Robertis, A., et al., *Equilibrium studies in natural fluids: A chemical speciation model for the major constituents of sea water.* Chemical Speciation and Bioavailability, 1994. **6**: p. 65-84.
86. Ho, P. and D.A. Palmer, J. Soln. Chem., 1996. **25**: p. 711-729.
87. De Robertis, A., P. Di Giacomo, and C. Foti, Anal.Chim.Acta, 1995. **300**: p. 45.
88. Hanna, E., A. Pethybridge, and J. Prue, Electrochim.Acta., 1971. **16**: p. 677.
89. Paterson, R., S. Jalota, and H. Dunsmore, J.Chem.Soc.(A), 1971: p. 2116.
90. Chiu, Y. and R. Fuoss, J.Phys.Chem., 1968. **72**: p. 4123.
91. Shock, E.L., et al., J. Chem. Soc. Faraday Trans., 1992. **88**: p. 803-826.
92. Solovkin, A., Zh.Fiz.Khim., 1974. **48**: p. 2655.
93. Riddell, J., D. Lockwood, and D. Irish, Can.J.Chem., 1972. **50**: p. 2951.
94. Justice, M., R. Bury, and J. Justice, Electrochim.Acta,, 1971. **16**: p. 687.
95. Bury, R., M. Justice, and J. Justice, Compt.Rend., 1969. **268**(C): p. 670.
96. De Stefano, C., et al., J.Chem.Res., 1988: p. 372.
97. Isaev, I., V. Leontev, and e. al, Zh.Neorg.Khim., 1983. **28**: p. 3013(1709).
98. Martynova, O., L. Vasina, and S. Pozdnyakova, Dokl.Akad.Nauk SSSR,, 1974. **217**: p. 1080.
99. Izatt, R., et al., J.Chem.Soc.(A), 1969. **45**: p. 47.
100. Masterton, W. and L. Berka, J.Phys.Chem., 1966. **70**: p. 1924.
101. Jenkins, I. and C. Monk, J.Am.Chem.Soc., 1950. **72**: p. 2695.
102. Capewell, S., G. Hefter, and P. May, J.Solution Chem., 1998. **27**: p. 865.
103. Nakayama, F., J.Chem.Eng.Data, 1971. **16**: p. 178.
104. Garrels, R., M. Thompson, and R. Siever, Am.J.Sci., 1961. **259**: p. 24.
105. Garrels, R. and M. Thompson, Am.J.Sci., 1962. **260**: p. 57.
106. Daniele, P., A. de Robertis, and C. de Stefano, J.Solution Chem., 1991. **20**: p. 495.
107. Patel, P., T. Gregory, and W. Brown, P Patel,T Gregory,W Brown; J.Res.Nat.Bur.Stand.,78,A675 (1974), 1974. **78**: p. A675.
108. Migneault, D. and R. Force, J.Solution Chem., 1988. **17**: p. 987.
109. Walser, M., *Ion association. V. Dissociation constants for complexes of citrate with sodium, potassium, calcium and magnesium ions.* Journal of Physical Chemistry, 1961. **65**: p. 159-161.
110. Rechnitz, G.A. and S.B. Zamochnick, *Application of cation-sensitive glass electrodes to the study of alkali metal complexes. II.* Talanta, 1964. **11**: p. 1061-1065.
111. Cucinotta, V., et al., *The formation of proton and alkali-metal complexes with ligands of biological interest in aqueous solution. Potentiometric and PMR investigation of Li+, Na+, K+, Rb+, Cs+ and NH4+ complexes with citrate.* Inorganica Chimica Acta, 1981. **56**: p. L45-L47.

112. Daniele, P.G., et al., *Studies on polyfunctional O-ligands. Formation thermodynamics of simple and mixed alkali metal complexes with citrate at different ionic strengths in aqueous solution.* J. Chem. Res., 1990. **S**: p. 300-301.
113. Arena, G., et al., *The formation of proton and alkali-metal complexes with ligands of biological interest in aqueous solution . Part 1. Potentiometric and calorimetric investigation of H+ and Na+ complexes with citrate, tartrate and malate.* Thermochimica Acta, 1980. **36**: p. 329-342.
114. Palaty, V., Can.J.Chem., 1963. **41**: p. 18.
115. Schwarzenbach, G. and H. Ackermann, Helv.Chim.Acta, 1947. **30**: p. 1798.
116. Watters, J. and O. Schupp, J.Inorg.Nucl.Chem., 1968. **30**: p. 3359.
117. Bates, R.G. and G.D. Pinching, *Resolution of the dissociation constants of citric acid at 0 to 50 °C, and determination of certain related thermodynamic functions.* Journal of the American Chemical Society, 1949. **71**: p. 1274-1283.
118. Daniele, P.G., C. Rigano, and S. Sammartano, *The formation of proton and alkali-metal complexes with ligands of biological interest in aqueous solution, Potentiometric study of the H+-K+-citrate system at 37 °C and 0.03 < I < 1.0.* Annali di Chimica (Rome), 1980. **70**: p. 119-130.
119. Daniele, P.G., et al., *Calcium-malonate complexes in aqueous solution. Thermodynamic parameters and their ionic strength dependence.* Thermochimica Acta, 1984. **72**: p. 305-322.
120. Palmer, D. and D. Wesolowski, J.Solution Chem., 1997. **26**: p. 217.
121. Mcgee, K. and P. Hostetler, Am.J.Sci., 1975. **275**: p. 304.
122. Dyrssen, D. and I. Hansson, Marine Chem., 1972. **1**: p. 137.
123. De Robertis, A. and C. De Stefano, Ann.Chim.(Rome), 1998. **88**: p. 103.
124. De Robertis, A., et al., *Ion association of Cl- with Na+, K+, Mg2+ and Ca2+ in aqueous solution at 10 ≤ T ≤ 45 °C and 0 ≤ I ≤ 1 mol-1. A literature data analysis.* Thermochimica Acta, 1987. **155**: p. 241-248.
125. Tsierkezos, N. and I. Molinou, J.Chem.Eng.Data., 2000. **45**: p. 819.
126. Emara, M., C. Lin, and G. Atkinson, Bull.Soc.Chim.Fr., 1980. **1**: p. 173.
127. Katayama, S., Bull.Chem.Soc.Jpn., 1973. **46**: p. 106.
128. Inada, I., K. Shimizu, and J. Osugi, Rev.Phys.Chem.Japan., 1972. **42**(1).
129. Marshall, W., J.Phys.Chem., 1967. **71**(3584).
130. Le Guyader, M., G. Dorange, and A. Marchand, Bull.Soc.Chim.Fr., 1985. **1**: p. 636.
131. Siebert, R. and P. Hostetler, Am.J.Sci., 1977. **277**: p. 697.
132. Reardon, E. and D. Langmuir, Am.J.Sci., 1974. **274**: p. 599.
133. Hostetler, P., J.Phys.Chem., 1963. **67**: p. 720.
134. Falck, W.E., *Critical Evaluation of the CHEMVAL Thermodynamic Database with Respect to its contents and Relevance to Radioactive Waste Disposal at Sellafield and Dounreay.* 1992, United Kingdom Department of Environment and Commission of the European Communities: Luxembourg.
135. Glab, S., et al., Anal.Chim.Acta,, 1993. **273**: p. 493-497.
136. Linder, P. and J. Little, Talanta, 1985. **32**: p. 83.
137. Iotta, S., et al., NMR in Biomedicine., 1996. **9**: p. 24.
138. Saha, A., N. Saha, and J. Ji, J.Biol.Inorg.Chem., 1996. **1**: p. 231.
139. Hershey, J., M. Fernandez, and F. Millero, J.Solution Chem., 1989. **18**: p. 875.
140. Verbeeck, R., P. de Bruyne, and e. al, Inorg.Chem., 1984. **23**: p. 1922.
141. Phillips, R., P. George, and R. Rutman, J.Biol.Chem., 1969. **244**: p. 3330.
142. Hastings, A.B., et al., Journal of Biological Chemistry, 1934. **107**: p. 351-370.
143. Nordbo, R., Skandinavisches Archiv fur Physiologie, 1938. **80**: p. 341-347.
144. Li, N.C., A. Lindenbaum, and J.M. White, Journal of Inorganic and Nuclear Chemistry, 1959. **12**: p. 122-128.
145. Watanabe, S., et al., Journal of Biochemistry (Tokyo), 1963. **54**: p. 17-24.

146. Campi, E., et al., Journal of Inorganic and Nuclear Chemistry, 1964. **26**: p. 553-564.
147. Pattnaik, R.K. and S. Pani, Journal of the Indian Chemical Society, 1965. **42**: p. 527-530.
148. Tate, S.S., A.K. Grzybowski, and S.P. Datta, Journal of the Chemical Society, 1965: p. 3905-3912.
149. Blair, J.M., European Journal of Biochemistry, 1969. **8**: p. 287-291.
150. Grzybowski, A.K., S.S. Tate, and S.P. Datta, Journal of the Chemical Society A, 1970: p. 241-245.
151. Field, T.B., et al., Analytica Chimica Acta, 1975. **74**: p. 101-106.
152. Pearce, K.N., Australian Journal of Chemistry, 1980. **33**: p. 1511-1517.
153. Amico, P., et al., Ann.Chim.(Rome), 1982. **72**: p. 1.
154. Hirokawa, T. and Y. Kiso, Journal of Chromatography, 1982. **248**: p. 342-362.
155. Rizkalla, E.N., M.S. Antonious, and S.S. Anis, Inorganica Chimica Acta, 1985. **96**: p. 171-178.
156. Ghandour, M.A., et al., Journal of Indian Chemical Society, 1988. **65**: p. 716-718.
157. Meyer, J.L., Analytical Biochemistry, 1974. **62**: p. 295-300.
158. Butina, E.A., et al., Izvestiya Vysshikh Uchebnykh Zavedenii Pishchevaya Tekhnologiya, 1992. **2**: p. 52-53.
159. Vasil'ev, V.P. and A.K. Belonogova, Zh.Neorg.Khim., 1976. **21**: p. 1225.
160. Jokl, V. and J. Majer, Chem.Zvesti, 1965. **19**: p. 249-281.
161. Anderegg, G., Helv. Chim. Acta., 1964. **47**: p. 1801.
162. Bohigian, T. and A. Martell. 1960, US Comm.Con. p. 1823.
163. Jordan, J. and T. Alleman, Anal.Chem., 1957. **29**: p. 9.
164. Martell, A., Rec.Trav.Chim., 1956. **75**: p. 781.
165. Sarma, B. and P. Ray, J.Indian Chem.Soc., 1956. **33**: p. 841.
166. Schwarzenbach, G., R. Gut, and G. Anderegg, Helv. Chim. Acta., 1954. **37**: p. 937.
167. Morel, F.M.M. and J.G. Herring, *Principles and applications of aquatic chemistry*. 1993, New York: John Wiley and sons Inc.
168. Irving, H.M.N.H. and R. Parkins, J. Inorg. Nucl. Chem., 1966. **28**: p. 1629.
169. Kotrly, S. and L. Sucha, *Handbook of Chemical Equilibria in Analytical Chemistry*. 1985, Chichester: Ellis Horwood.
170. Schwarzenbach, G., H. Senn, and G. Anderegg, Helv. Chim. Acta., 1957. **40**: p. 1886.
171. Daniele, P., A. De Robertis, and e. al, Ann.Chim.(Rome), 1983. **73**: p. 619.
172. Martynova, O., L. Vasina, and e. al., Dokl.Akad.Nauk SSSR, 1972. **202**: p. 1337(E:173).
173. Shock, E.L., 2000.
174. Vasilev, V., V. Vasileva, and e. al., Izv.VUZ.Khim., 1963. **6**: p. 339.
175. Craggs, A., G. Moody, and J. Thomas, Analyst, 1979. **104**: p. 961.
176. Ainsworth, R., J.Chem.Soc.,Faraday Trans.I, 1973. **69**: p. 1028.
177. Sung-Tsuen, L. and G. Nancollas, J.Crystal Growth, 1970. **6**: p. 281.
178. Dyrssen, D., E. Ivanova, and K. Aren, Vestnik Moskov Univ., 1969. **24**(1): p. 41.
179. Nakayama, F. and B. Rasnick, Anal.Chem., 1967. **39**: p. 1022.
180. Le Guyader, M., G. Dorange, and e. al., Bull.Soc.Chim.Fr., 1983. **1**: p. 203.
181. Jacobson, R. and D. Langmuir, Geochim.Cosmo.Acta., 1974. **38**: p. 301.
182. Lafon, G., Geochim.Cosmo.Acta,, 1970. **34**: p. 935.
183. Nakayama, F., Soil Sci., 1968. **106**: p. 429.
184. Chughtai, A., R. Marshall, and G. Nancollas, J.Phys.Chem., 1968. **72**: p. 208.
185. Gregory, T., E. Moreno, and W. Brown, J.Res.Nat.Bur.Stand., 1970. **74**: p. 461.
186. Bejerrum, N. and A. Unmack, Danske Videnskabernes Selskabernes, Mathematisk-Fysiske Meddelelser, 1929. **9**(1).
187. Joseph, N.R., Journal of Biological Chemistry, 1946. **164**: p. 529-541.
188. Heinz, E., Biochemische Zeitschrift, 1951. **321**: p. 314-342.
189. Davies, C.W. and B.E. Hoyle, Journal of the Chemical Society, 1953: p. 4134-4136.
190. Schubert, J., Journal of the American Chemical Society, 1954. **76**: p. 3442-3444.

191. Davies, C.W. and B.E. Hoyle, Journal of the Chemical Society, 1955: p. 1038.
192. Lefebvre, J., Journal de Chimie Physique et de Physico-Chimie Biologique, 1957. **54**: p. 581-600.
193. Pattnaik, R.K. and S. Pani, Journal of the Indian Chemical Society, 1961. **38**: p. 379-384.
194. Matushima, Y., Chemical and Pharmaceutical Bulletin, 1963. **11**: p. 566-570.
195. Rechnitz, G.A. and T.M. Hseu, Anal.Chem., 1969. **41**: p. 111-115.
196. Rumbaut, N.A., Bulletin des Societes Chimiques Belges, 1971. **80**: p. 63-71.
197. Singh, R., et al., J.Chem.Eng.Data., 1991. **36**: p. 52-54.
198. Glab, S., A. Hulanicki, and U. Nowicka, Talanta, 1992. **39**: p. 1555-1559.
199. Mironov, V.E., et al., Russian Journal of Inorganic Chemistry, 1996. **41**: p. 268-269.
200. Ashby, R.A. and R.J. Sleet, Clinica Chimica Acta, 1992. **210**: p. 157-165.
201. Moyers, E. and J. Fritz, Anal.Chem., 1977. **49**: p. 418.
202. Hansen, E. and J. Ruzicka, Talanta, 1973. **20**: p. 1105.
203. Anderegg, G. and S. Malik, Helv. Chim. Acta., 1970. **53**: p. 564-577.
204. Anon, Chem.Soc.Spec.Publ. no.17, 1964.
205. Schwarzenbach, G. and G. Anderegg, Helv. Chim. Acta., 1957. **40**: p. 1773.
206. Matorina, N. and N. Safonova, Zh.Neorg.Khim., 1960. **5**: p. 151.
207. Grenthe, I., et al., *Chemical Thermodynamics of Uranium*. 1992, Amsterdam: North-Holland. 716.
208. Choppin, G.R. and J.N. Mathur, *Hydrolysis of Actinyl(VI) Cations.* Radiochimica Acta., 1991. **52/53**: p. 25-28.
209. De Stefano, C., et al., *Dependence on ionic strength of the hydrolysis constants for dioxouranium(VI) in NaCl(aq) and NaNO3(aq), at pH < 6 and t =25 ºC.* J. Chem. Eng. Data., 2002. **47**: p. 533-538.
210. Silva, R.J., *Mechanisms for the retardation of uranium(VI) migration.* Mat.Res. Cos. Symp. Proc., 1992. **257**: p. 323.
211. Lemire, R.J. and P.R. Tremaine, *Uranium and Plutonium Equilibria in aqueous solutions to 200 °C.* J. Chem. Eng. Data., 1980. **25**: p. 361-370.
212. Sandino, A. and J. Bruno, *The solubility of (UO2)3(PO4)2.4H2O(s) and the formation of U(VI) phosphate complexes: Their influence in uranium speciation in natural waters.* Geochim. Cosmochim. Acta, 1992. **56**: p. 4135.
213. Baston, G.M.N., et al., *The solubility of Uranium in Cementitious Near-Field Chemical Conditions.* 1993, United Kingdom Atomic Energy Authority: Oxford.
214. Meinrath, G., *Direct spectroscopic speciation of schoepite phase equilibria.* Journal of Radioanalytical and Nuclear Chemistry, 1998. **232**(1-2): p. 179-188.
215. Brendler, V., et al., *Complexation in the system UO2[2+]/PO4[3-]/OH[-]: Potentiometric and Spectroscopic Investigations at very low ionic strengths.* Radiochimica Acta, 1996. **74**: p. 75-80.
216. Baes, C.F.J., *A spectrophotometric investigation of uranyl phosphate complex formation in perchloric acid solution.* J. Phys. Chem., 1956. **60**: p. 878.
217. Thamer, B., *Spectrophotometric and solvent-extraction studies of uranyl phosphate complexes.* J. Am. Chem. Soc., 1957. **79**: p. 4298.
218. Marcus, Y. *Anion exchange of metal complexes: The uranyl phosphate system*. in *2nd UN International Conf. on the peaceful use of atomic energy*. 1958. Geneva.
219. Markovic, M. and N. Pavkovic, *Solubility and equilibrium constants of uranyl in phosphate solutions.* Inor. Chem., 1983. **22**: p. 978.
220. Mathur, J.N., *Complexation and thermodynamics of the uranyl ion with phosphate.* Polyhedron, 1991. **10**: p. 47.
221. Kalmykov, S.N. and G.R. Choppin, Radiochimica Acta., 2000. **88**: p. 603-606.
222. Lenhart, J.J., et al., *Uranium(VI) complexation with citric, humic and fulvic acids.* Radiochim. Acta., 2000. **88**: p. 345-353.

223. Feldman, I., C.A. North, and H.B. Hunter, Journal of Physical Chemistry, 1960. **64**: p. 1224-1230.
224. Rajan, K.S. and A.E. Martell, Inorganic Chemistry, 1965. **4**: p. 462-469.
225. Ohyoshi, E., J. Oda, and A. Ohyoshi, Bulletin of the Chemical Society of Japan, 1975. **48**: p. 227-229.
226. Vanura, P. and L. Kuca, Collection of Czechoslovak Chemical Communications, 1980. **45**: p. 41-53.
227. Hamed, M.M.A., et al., Journal of Chemical Engineering Data, 1994. **39**: p. 565-567.
228. Bronikowski, M., et al., *UO2+ and NpO2+ complexation with citrate in brine solutions.*, in *Actinide Speciation in High Ionic Strength Media*, R.e. al., Editor. 1999, Kluwer Academic/Plenum Publishers. p. 177-185.
229. Markovits, G., P. Klotz, and L. Newman, Inorganic Chemistry, 1972. **11**: p. 2405-2408.
230. Sircar, J.K., Zeitschrift fuer Physikalische Chemie (Leipzig), 1984. **265**: p. 330-336.
231. Frausto da Silva, J. and M. Simoes, J.Inorg.Nucl.Chem., 1970. **32**: p. 1313.
232. Bhat, T. and M. Krishnamurthy, J.Inorg.Nucl.Chem., 1964. **26**: p. 587.
233. Stary, J., Collec.Czech.Chem.Commun., 1960. **25**: p. 2630.
234. Anderegg, G., *Critical survey of stability constants of EDTA complexes*. IUPAC Chemical data series, 14. 1977, Oxford: Pergamon Press.
235. Johnson, G. and J. Bauman, Inorg.Chem., 1978. **17**: p. 2774.
236. Mesmer, R., Inorg.Chem., 1971. **10**: p. 857.
237. Mesmer, R. 1970.
238. Sweeton, F. and C. Baes, J.Chem.Thermodyn., 1970. **2**: p. 479.
239. Morozumi, T. and F. Posey, Denki Kagaku, 1967. **35**: p. 633.
240. Millero, F.J., Geochimica Cosmochimica Acta, 1992. **56**: p. 3123-3132.
241. Beverskog, B. and I. Puigdomenech, Corrosion Science, 1996. **38**(12): p. 2121-2135.
242. Liu, X. and F. Millero, Geochim Cosmo Acta, 1999. **63**: p. 3487.
243. Daniele, P., et al., Talanta, 1994. **41**: p. 1577.
244. El-Ezaby, M., et al., Inorg.Chim.Acta., 1986. **123**: p. 53.
245. Yakubov, H., V. Shcherbakova, and e. al, Zh.Neorg.Khim., 1982. **27**: p. 1203.
246. Knight, S.R. and R. Sylva, J.Inorg.Nucl.Chem., 1975. **37**: p. 779.
247. Behar, B. and G. Stein, Isr.J.Chem., 1969. **7**: p. 827.
248. Turner, R. and K. Miles, Can.J.Chem., 1957. **35**: p. 1002.
249. Wilson, A. and H. Taube, J.Am.Chem.Soc., 1952. **74**: p. 3509.
250. Barb, W., et al., Trans.Faraday Society, 1951. **47**: p. 591.
251. Siddall, T. and W. Vosburgh, J.Am.Chem.Soc., 1951. **73**: p. 4270.
252. Olson, A. and T. Simonson, J.Chim.Phys., 1949. **17**(348): p. 1322.
253. Lindstrand, F., Sv.Kem.Tidskr., 1944. **56**: p. 251.
254. Lamb, A. and A. Jacques, J.Am.Chem.Soc., 1938. **60**: p. 1215.
255. Bray, W. and A. Hershey, J.Am.Chem.Soc., 1934. **56**: p. 1889.
256. Djurdjevic, P., M. Stankov, and J. Odovik, Polyhedron, 2000. **19**: p. 1085.
257. Millero, F.J., W. Yao, and J.A. Aicher, J. Mar. Chem, 1995. **50**: p. 21-39.
258. Byrne, R.H. and D.R. Kester, Mar. Chem., 1976. **4**: p. 255-274.
259. Baes, C.F. and R.E. Mesmer, *Iron*, in *The Hydrolysis of cations*, R.E. Mesmer, Editor. 1976, Wiley: New York. p. 226-237.
260. Diakonov, I.I., et al., Geochimica et Cosmochimica Acta., 1999. **63**(15): p. 2247-2261.
261. Ziemniak, S.E., M.E. Jones, and K.E.S. Combs, J. Soln. Chem., 1995. **24**: p. 837-877.
262. Yakovlev, Y., F. Kulba, and e. al, Zh.Neorg.Khim., 1978. **23**: p. 411.
263. Heinrich, C. and T. Seward, Geochim.Cosmo.Acta., 1990. **54**: p. 2207.
264. El-Ayaan, U., et al., J.Chem.Soc.,Dalton Trans., 1997: p. 2813.
265. Feng, Q. and H. Waki, Polyhedron, 1988. **7**: p. 291.
266. Yourchenko, E., G. Kolonin, and e. al, Zh.Neorg.Khim., 1976. **21**: p. 3050.
267. Levanon, H., G. Stein, and Z. Luz, J.Chem.Phys., 1970. **53**: p. 876.

268. Rowley, J. and N. Sutin, J.Phys.Chem., 1970. **74**: p. 2043.
269. Fordham, A., Australian J.Chem., 1969. **22**: p. 1111.
270. Vasilev, V. and G. Lobanov, Zh.Fiz.Khim., 1967. **41**: p. 1969.
271. Woods, W., P. Gallagher, and E. King, Inorg.Chem., 1962. **1**: p. 55-61.
272. Sutin, N., J. Rowley, and R. Dodson, J.Phys.Chem., 1961. **65**: p. 1248.
273. White, J., P. Kelly, and N. Li, J.Inorg.Nucl.Chem., 1961. **16**: p. 337.
274. Rabinowitch, E. and W. Stockmayer, J.Am.Chem.Soc., 1942. **64**(335).
275. Tagirov, B.R., et al., Chemical Geology, 2000. **162**: p. 193-219.
276. Bjerrum, J. and I. Lukes, Acta Chem.Scand., 1986. **A40**: p. 31.
277. Horne, R., B. Myers, and G. Frysinger, Inorg.Chem., 1964. **3**: p. 452.
278. Mattoo, B., Z.Phys.Chem.,(Frankfurt), 1959. **19**: p. 156.
279. Sykes, K., J.Chem.Soc., 1952. **124**.
280. Maryanov, B., Zh.Anal.Khim., 1972. **27**: p. 2099.
281. Nicolaeva, N. and L. Tsvelodub, Zh.Neorg.Khim., 1975. **20**: p. 3033.
282. Sidorenko, V. and V. Gordienko, Zh.Anal.Khim., 1969. **24**(3): p. 315.
283. Willix, R., Trans.Faraday Society, 1963. **59**: p. 1315.
284. Davis, G. and W. Smith, Can.J.Chem., 1962. **40**: p. 1836.
285. Bachmann, K. and K. Lieser, Ber.Buns.Phys.Chem., 1963. **67**: p. 802-810.
286. Parkhurst, D.L. and C.A.J. Appelo, *Users guide to Phreeqc (version 2) - a computer program for speciation, batch-reaction, one-dimensional transport, and inverse geochemical calculations*. 1999, U.S. Department of the interior, U.S. Geological survey: Denver, Colorado. p. 312.
287. Nriagu, J., Geochim.Cosmo.Acta., 1972. **36**: p. 459.
288. Lahiri, S. and S. Aditya, J.Indian Chem.Soc., 1964. **41**(517).
289. Galal-Gorchev, H. and W. Stumm, J.Inorg.Nucl.Chem., 1963. **25**: p. 567.
290. Timberlake, C., J.Chem.Soc., 1964: p. 5078.
291. Chen, Q., X. Zhang, and L. Hepler, Can.J.Chem., 1993. **71**: p. 937.
292. Martin, R., J.Inorg.Biochem., 1986. **28**: p. 181.
293. Warner, R. and I. Weber, J.Am.Chem.Soc., 1953. **75**: p. 5086.
294. Bertin-Batch, C., Annals die Chimie, France, 1952. **7**: p. 481-531.
295. Hamm, R.E., C.M. Shull, and D.M. Grant, J.Am.Chem.Soc., 1954. **76**: p. 2111-2114.
296. Trunova, E.K., et al., Ukranian Journal of Chemistry, 1993. **59**: p. 1-5.
297. Lanford, O.E. and J. Quinan, Journal of the Chemical Society, 1948. **70**: p. 2900-2903.
298. Kostromina, N.A., N.V. Beloshitskii, and V.F. Romanov, Soviet Journal of Coordination Chemistry, 1975. **1**: p. 1144-1148.
299. Vanura, P. and L. Kuca, Collection of Czechoslovak Chemical Communications, 1978. **43**: p. 1460-1475.
300. Manzurola, E., et al., J.Chem.Soc.,Faraday Trans.I, 1989. **85**: p. 373-379.
301. Clark, N. and A. Martell, Inorg.Chem., 1988. **27**: p. 1297.
302. Brunetti, A., G. Nancollas, and P. Smith, J.Am.Chem.Soc., 1969. **91**: p. 4680.
303. Bottari, E. and G. Anderegg, Helv. Chim. Acta., 1967. **50**: p. 2349.
304. Zhirnova, N., K. Astakhov, and S. Barkov, Zh.Fiz.Khim., 1967. **41**: p. 366.
305. Schwarzenbach, G. and J. Heller, Helv.Chim. Acta., 1951. **34**: p. 576.
306. Taliaferro, C.H., R.J. Motekaitis, and A.E. Martell, Inorganic Chemistry, 1984. **23**: p. 1188.
307. Stary, J., Anal.Chim.Acta., 1963. **28**: p. 132.
308. Appelo, C.A.J. and D. Postma, *Geochemistry, groundwater and pollution*. 1996, Rotterdam: A.A. Balkema.
309. Drever, J.I., *The Geochemistry of Natural Waters*. 1997, New Jersey: Prentice-Hall. 436.
310. Robie, R.A., B.S. Hemingway, and J.R. Fisher, *Thermodynamic Properties of Minerals & Related Substances at 298.15K and 1 Bar (105 Pascals) Pressure and at Higher*

Temperatures. 1978, U.S. Geological Survey, United States Government Printing Office: Washington.
311. Christoffersen, J., et al., *A contribution to the understanding of the formation of calcium phosphates.* J. Cryst. Growth., 1989. **94**: p. 767-777.
312. Moreno, E., W. Brown, and G. Osborn, Proc.Soil Sci.Soc.Amer., 1960. **24**: p. 94-99.
313. Farr, T., TVA Chem.Eng.Rept., 1950. **8**(26): p. 52.
314. Clark, J., Can.J.Chem., 1955. **33**: p. 1696.
315. McDowell, H., T.M. Gregory, and W.E. Brown, *Solubility of Ca5(PO4)3OH in the system Ca(OH)2 - H3PO4 - H2O at 5, 15, 25, and 37°C.* J. Res. Nat. Bur. Stand., 1977. **81A**: p. 273-281.
316. Sass, E., J. Morse, and F. Millero, Am.J.Sci., 1983. **283**: p. 218.
317. Broecker, W. and T. Takahashi, J.Geophys.Res., 1966. **71**: p. 1575.
318. Langmuir, D., Geochim.Cosmo.Acta., 1971. **35**: p. 1023.
319. Khodakovskii, I., B. Ryzhenko, and G. Naumov, Geokhim., 1968: p. 1486.
320. Berman, R.G., J. Petrology, 1988. **29**: p. 445-522.
321. Berman, R.G., T.H. Brown, and H.J. Greenwood, *An internally consistent thermodynamic data base for minerals in the system Na2O-K2O-CaO-MgO-FeO-Fe2O3-Al2O3-SiO2-TiO2-H2O-CO2.*, Atomic Energy of Canada Ltd.
322. Bennett, A. and F. Adams, Soil Sci.Soc.Am.J., 1976. **40**: p. 39.
323. Raju, K. and G. Atkinson, J.Chem.Eng.Data., 1990. **35**: p. 361.
324. Langmuir, D. and D. Melchior, Geochim.Cosmo.Acta., 1985. **49**: p. 2423.
325. Yeatts, L. and W. Marshall, J.Phys.Chem., 1969. **73**: p. 81.
326. Stumm, W. and J.J. Morgan, *Aquatic Chemistry, Chemical Equilibria and Rates in Natural Waters*. 3rd ed. 1996, New York: John Wiley & Sons, Inc.
327. Read, D. and T.W. Broyd, *Recent progress in testing chemical equilibrium models: the CHEMVAL project.* Radiochim. Acta., 1991. **52**: p. 453.
328. Leussing, D. and I. Kolthoff, J.Am.Chem.Soc., 1953. **75**: p. 2476.
329. Murata, K., J.Soc.Chem.Ind.Japan, 1932. **35**(suppl.): p. 523.
330. Bard, A.J., R. Parsons, and J. Jordan, *Standard Potentials in Aqueous Solution*. 1985, New York: Dekker.
331. Singer, P. and W. Stumm, J.Am.Water Workers Assn., 1970. **62**: p. 198.
332. Kelley, K. and C. Anderson, Bur.Mines,Bull., 1935. **384**.
333. Christ, C. and P. Hostetler, Am.J.Sci., 1970. **268**: p. 439.

THE EFFECTS OF DATABASE PARAMETER UNCERTAINTY ON URANIUM (VI) EQUILIBRIUM CALCULATIONS

FRANK H. DENISON AND JACQUELINE GARNIER-LAPLACE*

Laboratoire de Radioécologie et Ecotoxicologie, Institut de Radioprotection et Sûreté Nucléaire, CE Cadarache, Bât. 186, BP 3, 13115 St-Paul-Lez-Durance cedex, France

Tel : +33 4 42 25 37 33

Fax : +33 4 42 25 64 44

*Corresponding author: jacqueline.garnier-laplace@irsn.fr
same address

Accepted for publication in Geochimica Cosmochimica Acta.

1. ABSTRACT

The propagation of database parameter uncertainty has been assessed for aqueous and mineral equilibrium calculations of uranium by Monte Carlo and quasi-Monte Carlo simulations in simple inorganic solution compositions. The concentration output distributions of individual chemical species varies greatly depending on the solution composition modelled. The relative uncertainty for a particular species is generally reduced in regions of solution composition for which it is predicted to be dominant, due to the asymptotic behaviour imposed by the mass balance constraint where the species concentration approaches the total element concentration. The relative uncertainties of minor species, in regions where another species comprising one or several of the same components is predicted to be dominant with a high probability, also appear to be reduced slightly. Composition regions where two or several species are equally important tend to produce elevated uncertainties for related minor species, although the uncertainties of the major species themselves tend to be reduced. The non-linear behaviour of the equilibrium systems can lead to asymmetric or bimodal output distributions; this is particularly evident close to equivalence points or solubility boundaries. Relatively conservative estimates of input uncertainty can result in considerable output uncertainty due to both the complexity of uranium solution chemistry and the system interdependencies. The results of this study suggest that for some modelling scenarios, "classical" speciation calculations based on mean value estimates of the thermodynamic values may result in predictions of a relatively low probability compared to an approach that considers the effects of uncertainty propagation.

2. INTRODUCTION

Aqueous speciation modelling is a widely used interdisciplinary activity encompassing, amongst others, the fields of numerical mathematics, chemistry, geochemistry, hydrology and ecotoxicology. Speciation studies, both analytical and modelling approaches, are central to modern geochemistry and other fields such as ecotoxicology. They have been successfully applied to a wide range of systems to elucidate the processes underpinning water quality, transport/retention phenomena (Van der Lee and De Windt, 2001) and bioavailability or toxicity of contaminants to the biota (Paquin et al. 2002). Although analytical techniques to determine speciation are improving, it is often not practicable or possible to directly measure the activities of individual solution species, particularly at the low concentrations of environmental interest. Therefore predictive geochemical speciation models are employed to estimate the distribution of the total metal concentration through its various possible species (i.e. solution and surface complexes or mineral phases).

Equilibrium solution speciation has been extensively studied, and a robust comprehensive theoretical framework based on equilibrium thermodynamic principles has been developed. As for all mathematical models the predictive ability is limited by both the conceptual uncertainties in the model formulation and the quality of the data supplied to the model, including both the modelling scenario and the model constants (Ekberg, 1999). Within the context of geochemical modelling to calculate the distribution of the various chemical species of an element in the aqueous phase, conceptual uncertainties such as the inclusion or omission of chemical species and the veracity of the chosen chemical models (e.g. for activity-concentration relationships and the assumption of system equilibrium) will generally result in a systematic bias, although the vector of bias may vary depending on the particular modelling scenario. In addition to the potential uncertainty in the structural model of the system of interest, there is a degree of uncertainty inherent in the analytical measurement of the required

thermodynamic data that will result in uncertainty in the model predictions. Obviously, all of these statements are also applicable to the modelling of the distribution of an element between solid and liquid phases.

Quality assessment should be an integral part of the application of computer modelling to environmental problems and a number of authors have underlined the significant variations in existing thermodynamic data (OECD-NEA, 1996; Unsworth et al. 2002). However with a few exceptions (Ekberg, 1999; Nitzsche et al. 2000; Tebes-Stevens et al. 2001; Smith et al. 1999; Criscenti et al. 1996 and Cabaniss, 1999), systematic approaches to investigate the effects of this inherent uncertainty have not been applied. A variety of speciation codes are widely available which apply one of two distinct, but thermodynamically related, techniques to calculate equilibria in aqueous systems: Gibbs free energy minimisation methods or the more commonly applied equilibrium constant method. Both of these approaches require a reliable and consistent database of accurate thermodynamic values appropriate to the domain of application to be provided to the model in some form. Databases that are sufficiently coherent to be applied to a wide range of different systems are large, typically containing data for several thousand chemical species, which creates an obvious potential for the introduction of errors and uncertainty. It has long been recognised that considerable differences exist between different database compilations, and inter-comparison exercises have frequently resulted in widely differing results. These differences are sometimes the result of errors introduced by data reduction or conversion (Serkiz et al. 1996) but more generally due to a lack of consistency in the compilation. Literature values frequently give small confidence limits, if any are given, however when a number of determinations are compared, much greater differences are found than these intervals would indicate. This variability arises from a number of causes including inconsistent treatment of the chemical system and systematic errors of the applied method. Additionally, as noted by Nitzsche et al. (2000), the

requirements for accuracy and precision of data in speciation modelling databases are normally much higher than those that were demanded for the original application.

It is obvious that there is inherent uncertainty in the application of speciation modelling, even in conditions where the conceptual model formulation is ideal. Normally, modelling is performed using only single values of the thermodynamic data contained in the database. This approach does not permit any estimation of the uncertainty associated with the model predictions. Ideally, each thermodynamic value may be characterised by its expectation value and an assigned uncertainty depending on the extent and quality of the available data. The propagation of these input uncertainty distributions can lead to very different species concentration output distributions (Cabaniss, 1997). Consideration of this uncertainty propagation should be integral to the application of speciation modelling to environmental studies, including both the interpretation of acquired data and the predictive modelling for transport, bioavailability or toxicity studies for the studied element.

The objective of this work is to investigate the effect of database parameter uncertainty, using realistic estimates for the expectation and uncertainty values, on the output concentration distributions for the aqueous speciation modelling of uranium in very simple inorganic solution compositions. Uranium was selected as the element of interest due to the existence of generally high quality thermodynamic data resulting from the OECD-NEA review work and subsequent studies and its relatively complex solution chemistry to highlight the potential for uncertainty propagation. The calculations were performed using Monte Carlo (MC) and quasi-Monte Carlo (QMC) methods, assuming mutually independent Gaussian distributions for the parameter uncertainty. Although derivative methods of predicting uncertainty exist (Cabaniss, 1997) and are considerably faster than Monte Carlo methods, the requirement of linear combination of the parameter uncertainties was not satisfied for the speciation of uranium, and so this method was not applied. The number of runs required in order to provide

acceptably small parameter estimate errors was investigated for a number of descriptive parameters. The potential of the different sampling strategies of quasi-Monte Carlo methods to improve efficiency over the Monte Carlo method was also assessed. Finally, recommendations are provided for the proper use of chemical speciation models, considering the effects of uncertain thermodynamic data.

3. METHODOLOGY

The modelling scenarios selected for the study were deliberately very simple with restricted ranges of solution compositions. The effects of varying the partial pressure of CO_2 ($0 - 10^{-2}$ atm.) and the total concentration of phosphate ($0 - 10^{-3}$ mol dm^{-3}) were both investigated in the pH range 4 – 9. The presence of a non-complexing electrolyte of 10^{-2} mol dm^{-3} was included in all scenarios to maintain a constant ionic strength.

To assess the effects of database uncertainty on model output, realistic values for all the database constants and their uncertainties are required. To realise this, a comprehensive database was compiled, based mainly on the OECD-NEA data reviews (Grenthe et al. 1992) and modified where more recent data have become available. New literature data were added following the NEA recommended procedures as closely as possible and the equilibrium constants were reduced to standard molar Gibbs energy of formation values for the calculation of uncertainty values. To eliminate error amplification due to this data reduction the uncertainty values were calculated relative to a set of basis species adapted to the solution compositions rather than the NEA elemental reference states. The thermodynamic data together with the uncertainties as single standard deviation values are given in Table 1.

The chemical equilibrium program CHESS (Van der Lee, 1998) was used to perform all speciation calculations using the truncated-Davies model of activity-correction, the modified Newton-Raphson error criterion set to 10^{-10} and suppressing the formation of mineral phases. To study the uncertainty propagation Monte Carlo simulations of 10,000 runs were

performed, each run drawing input thermodynamic data from independent normal distributions of given mean value and standard deviation for each equilibrium equation. For the Monte Carlo simulations the input thermodynamic data were generated using the Box-Muller (Box and Muller, 1958) algorithm, supplied with uniform variates by the "Mersenne Prime Twister" random number generator MT19937 of Matsumoto and Nishimura (1998). For the quasi-Monte Carlo simulations the samples were generated from a Sobol (1967) low discrepancy sequence point set, transformed to Gaussian variates by Moro's algorithm (1995). Simulations performed using samples generated from low discrepancy sequences are theroetically more efficient than simulations using random sampling, i.e. the sample size required to obtain a sufficiently good representation of the output distribution is theoretically smaller. A program was written in C using functions from the GNU-GSL (Galassi et al. 2002) to provide input data files, extract the required data from the output files and perform statistical analyses on the output distributions.

The probabilistic errors of the parameter estimations were calculated by a jackknife estimate of variance (Efron and Tibshirani, 1993) σ^2 given by:

$$\sigma^2 = \frac{n-1}{n}\sum_{i=1}^{n}\left(p_i - \overline{p}\right)^2$$

where n is the number of data, $\overline{p}$ is the estimated parameter and p_i is the parameter recalculated n times omitting the ith datum.

4. RESULTS AND DISCUSSION

4.1. Evaluation of simulation input parameter distributions.

The generated input parameter distributions for both the MC and QMC methods were evaluated by the Kolmogorov-Smirnov test (Knuth, 1981) and were acceptably Gaussian for n = 100 or greater. The maximum difference between the distributions' mean and the assigned mean values of the equilibrium reactions given in table 1 was *ca.* 2 and 0.8 % for $n = 100$, dropping to 0.2 and 0.02 % for $n = 10^4$ for the MC and the QMC methods respectively.

4.2. Probabilistic error of the parameter estimates for the uranium species output distributions.

The value of n that was required to obtain acceptable estimates of the output distributions depended on: the solution composition, the output species and the parameter(s) of interest. The coefficient of variance of the jackknife σ estimates for a number of different statistical parameters was calculated for different n values between 10^2 and 10^4 for both the MC and QMC methods, for various different solution compositions. Some representative results of the jackknife σ estimates are shown in figure 1, for a solution composition of: total uranium concentration 10^{-6} mol dm^{-3}, pH 6, pCO_2 3.10^{-4} atm. in a hypothetically non-complexing electrolyte of 10^{-2} mol dm^{-3}. The coefficient of variance of the MC and QMC estimates of the mean values for the output distributions of the species UO_2^{2+}, UO_2OH^+, $UO_2(OH)_2(aq)$, $UO_2(OH)_3^-$ and $UO_2(CO_3)_2^{2-}$ are shown. The results show the expected reduction in the probabilistic error of the MC mean estimates as the value of n increases; the error has probabilistic order $O\left(n^{-1/2}\right)$. No improvement in the error bound was found by using the QMC instead of the MC method in this range of n, although the convergence of the error bound was often more regular. The theoretical advantage of using a low-discrepancy sequence for the QMC method is that the asymptotic error bound rate is superior to that of the MC method for

a fixed dimension, *s*, if *n* is sufficiently large i.e. $O\left(n^{-1}\log^{s} n\right)$. However, for reasonably large values of *s,* the value of *n* required to ensure that the QMC error bound is smaller than that of the MC can be very large and hence of little practical advantage (L'Ecuyer and Lemieux, 2002) as appears to be the case here. The error bounds of other statistical parameters of the distributions, such as the standard deviation, higher moments or quantiles are greater than those of the mean values, sometimes very much so. The value of *n* required to obtain acceptable estimates of some parameters for some (usually minor) species can be prohibitively large. However in the case of UO_2^{2+} for the conditions investigated (pH 5 – 8, pCO_2 0 – 10^{-2} atm., $[UO_2]_T$ = 10^{-6} mol dm^{-3}), the maximum error bound of the jackknife estimates of standard deviation for the mean, median, standard deviation and a number of arbitrary quantiles was *ca.* 10 % of the parameter value for $n = 10^3$, dropping to *ca.* 2 % for $n = 10^4$. This demonstrates the principal limitation of the MC methods, i.e. it is not possible to determine a priori the value of *n* required to provide acceptable estimates of the output distributions, additionally the value of *n* can vary greatly depending on the particular modelling scenario and output species of interest. In cases where the value of *n* required is large, alternative strategies to improve the sampling efficiency of the parameter space could be advantageous.

4.3. Concentration output distributions.

Just as the concentrations of individual solution species of uranium can change dramatically for quite small changes in the solution composition, so can the forms of the output distributions. The output distributions are generally not Gaussian (or log Gaussian) and the forms of the distributions (dispersion, skewness, kurtosis) can change significantly on changing the solution composition. This is best shown by the skewness values, a measure of the distribution's asymmetry calculated from the third moment of the data. Symmetrical distributions have a small skewness value, whilst asymmetric distributions have large either

positive or negative values. Figure 2 shows MC estimates of the skewness values of the output distributions of four species as a function of pH and for several different values of pCO_2. One consequence of these asymmetric distributions is that summarising the distributions using parametric statistical functions can be misleading. Additionally, the distribution mean value estimates are often significantly different from the mean-value database calculations. This suggests that "classical" speciation calculations based on mean value estimates of the thermodynamic values may result in predictions of a relatively low probability compared to an approach that considers the effects of uncertainty propagation.

4.4. The effect of solution composition on the output distributions.

To investigate the effects of changing solution composition on the concentration output distributions and the relative uncertainties of model predictions, three parameters that strongly influence the speciation of uranium were selected and varied within realistic ranges. All calculations were performed using the MC method with $n = 10^4$, total uranyl concentration was fixed at 10^{-6} mol dm^{-3}, the ionic strength was maintained constant by including a hypothetically non-complexing electrolyte of 10^{-2} mol dm^{-3} and the formation of solid phases was suppressed. Typical output distributions are shown for selected species at several pH values and a CO_2 partial pressure of 3.10^{-4} atm. in figure 3, the areas under the probability density curves are unity. The distributions for each species can vary considerably between different pH values, and the concentration distributions for some species can cover several orders of magnitude. To summarise the effect of database uncertainty on the relative uncertainty of output concentrations as a function of varying solution composition, inter-quantile ranges normalised with respect to the distribution mean were calculated. Figure 4 shows the effect of varying pH and pCO_2 on the inter-decile (Q0.1 – Q0.9) distribution intervals as a percentage of the mean for the species UO_2^{2+} and $UO_2(CO_3)_2^{2-}$. Figure 5 shows the effect of varying pH and phosphate concentration on the species UO_2^{2+} and

UO_2HPO_4(aq). In all cases, the relative uncertainty varies considerably as a function of the solution composition. In general, in solution compositions for which the mean-value database predicts a species to be dominant, the output uncertainty of that species is relatively low compared to other composition regions. This can be seen for the species UO_2^{2+} at low pH and phosphate concentration, the species UO_2HPO_4(aq) at moderately high phosphate concentrations and low pH and also for the local minima of the species $UO_2(CO_3)_2^{2-}$. The dominant species predicted by the mean-value database for the region of pH values between 7 and 8 and pCO_2 values between 10^{-4} and 10^{-2} atm. changes from the species $(UO_2)_2CO_3(OH)_3^-$ to $UO_2(CO_3)_2^{2-}$ to $UO_2(CO_3)_3^{4-}$ on increasing pH and pCO_2; the relative uncertainties of all three of these species exhibit local minima in the regions where they are predicted to be dominant with a high probability. The relative uncertainties of minor species, in regions where another species comprising one or several of the same components is predicted to be dominant with a high degree of certainty, also appear to be reduced slightly (e.g. the behaviour of the relative uncertainty of UO_2^{2+} in the region of pH and pCO_2 where the dominant uranyl species changes). Similarly, equivalence points between two species dominant in different regions tend to produce elevated uncertainties for related minor species, although the uncertainties of the major species themselves tend to be reduced. This type of behaviour has been observed before, for example simulations of base titration's of simple acids performed by Cabaniss (1997) produced large uncertainties in the pH output distributions near to the equivalence points, the distributions being bimodal with minima at or close to the equivalence points.

4.5. Effect on solubility equilibria.

The effect of database uncertainty on calculations involving equilibrium with a solid phase was investigated, by performing simulations involving equilibrium with $UO_3{\cdot}2H_2O$(s) (schoepite). Total uranyl concentration was fixed at 10^{-2} mol dm^{-3} and a range of solution

compositions varying both pH and pCO_2 were modelled. Calculations using the mean-value database indicated that an equivalence point between the solid and aqueous uranium fractions, at atmospheric pCO_2, is located at a pH value of *ca.* 8.7. As stated earlier, composition regions near to equivalence points are often sensitive to parameter uncertainty and this was again found to be the case. Because the total uranyl concentration was constrained, the output distributions of the total aqueous uranium concentration close to the equivalence point are bimodal, as the concentration output distribution approaches the total concentration constraint. Figure 6 shows the output distributions of the total aqueous uranium concentration at pH 8.7 and three CO_2 partial pressures close to the equivalence point. The distributions cover over an order of magnitude in concentration and obviously predictions of dissolved uranium concentrations under these sensitive conditions would be quite uncertain. A contour plot of the probability densities as a function of the pH at atmospheric pCO_2 is shown in figure 7, again the concentration distributions are broadly spread over a large range of pH values with bimodal concentration distributions in some regions of solution composition. A discontinuity at elevated pH near to the dissolution boundary can be clearly seen.

4.6. Processing time.

The principal limitation of the Monte Carlo and quasi-Monte Carlo methods is the time required to perform the simulations. The choice of the program CHESS was decided by these concerns, due to its superior computational speed compared to other available programs. The method of coupling the program written to perform the simulations and calculate the statistical parameters of the output distributions with CHESS was decided by the ease of development and was not very efficient, however the processing time required for the presented simulations was not prohibitive. For example a simulation of $n = 10^4$ samples took approximately 5 seconds using an AMD Athlon 1700+ processor. There is considerable scope to reduce processing time by either improving the method of coupling the two programs, or

integrating the Monte Carlo and speciation codes. However the application of the Monte Carlo approach to some speciation modelling applications, such as reactive transport modelling, will obviously be constrained by the processing time. Attempts to reduce the number of runs required to obtain acceptable parameter estimates were not successful for the considered scenarios. The use of a low discrepancy sequence and also Latin Hypercube sampling (results not presented) did not reduce the error of the parameter estimates compared to the Monte Carlo method, however these different sampling strategies may be more successful when applied to different scenarios. If the modelled system is suitable then the derivative method of estimating the uncertainty proposed by Cabaniss (1997) would be preferred due to the greatly reduced processing requirements. Large ranges of input conditions used together with the randomised parameter values can lead to convergence problems in the modified Newton-Raphson algorithm of CHESS. Judicious selection of the scenario basis species was sufficient to overcome this problem for the scenarios presented.

5. CONCLUSIONS

Uncertainty is inherent in the application of geochemical speciation modelling and this is especially the case where there is uncertainty regarding the model formulation, for example the chemical equilibrium model, the assumption of equilibrium conditions and the models used to describe concentration-activity relationships as well as the model constants. Only this second aspect has been investigated in this study, and it is clear that there is the potential for very considerable uncertainty in model predictions from this alone. Model output is only as reliable as the input data and the magnitude and consequences of this uncertainty is specific to the modelling scenario. Due to the very large number of potential applications it is difficult to generalise what the impact of the uncertainty will be. The results of this study illustrate the importance of very high quality thermodynamic data to minimise the effects of uncertainty propagation.

This study is, by necessity, of limited scope and based on a number of simplifying assumptions. The mean and uncertainty values assigned to the thermodynamic parameters are obviously of fundamental importance to the results, as is the assumption of independent Gaussian distributions. For a truly coherent database compilation this assumption of mutual independence will be invalid for certain combinations of inter-dependant parameters, for example the successive hydrolysis products of uranium. However establishing the correlation relationships between different input parameters would be a very significant task. The quality of available databases is highly variable, and there are few that approach the ideal of being both internally consistent and sufficiently coherent to be applied to a wide range of different systems. Hence, although the assumption of mutual independence may be theoretically limited, it is probably justified for many databases in routine use. The issue of uncertainty needs to be considered in all stages of the modelling process to enable valid estimates of a model's predictive ability for a particular scenario, from the experiments performed to determine the chemical equilibrium model and parameter constants to the application of the model. The application of uncertainty and sensitivity analyses to the interpretation of experimental data would serve a number of useful purposes. These include a more robust probabilistic interpretation of the chemical system (and avoidance of the temptation to obtain perfect model fits with the particular database employed by proposing increasingly elaborate chemical systems). Obviously physical evidence for the existence of the proposed species is always to be preferred. Sensitivity analysis can lead to the establishment of inter-parameter relationships, which can subsequently be used to both improve uncertainty estimates for the model applications, and also facilitate the maintenance of database consistency. Uncertainty and sensitivity analysis of modelling scenarios can provide information about which parameters are the most sensitive for a particular scenario and allow better targeting of data

gathering requirements, although frequently the most sensitive parameters are intuitive with a good understanding of the chemical system.

The focus of this work has been the uncertainty of uranium equilibrium calculations, which was motivated by its environmental relevance and the availability of high quality data reviews. However the aqueous speciation of uranium is complex compared to many other elements, undergoing very large changes over relatively small ranges of solution composition with a considerable number of species that may be significant for various ranges of solution composition. The complexity of uranium aqueous speciation leads to elevated propagation of uncertainties due to the interdependencies of the system (or conversely to a higher requirement for input parameter precision to obtain an acceptable level of output uncertainty). Less complex systems can be expected to result in reduced propagation of input uncertainty, although in particular composition regions, for example near to equivalence points or solubility boundaries, relatively elevated output uncertainties can still be expected.

6. REFERENCES

Baston G. M. N., Brownsword M., Cross J. E., Hobley J., Moreton A. D., Smith-Briggs J. K. and Thomason H. P. (1993) The solubility of Uranium in Cementitious Near-Field Chemical Conditions. United Kingdom Atomic Energy Authority: Oxford.

Box G. E. P. and Muller M. E. (1958) A note on the generation of random normal deviates. *Ann. Math. Stat.* **29**, 610-611.

Brendler V., Geipel G., Bernhard G. and Nitsche, H. (1996) Complexation in the system UO2[2+]/PO4[3-]/OH[-]: Potentiometric and Spectroscopic Investigations at very low ionic strengths. *Radiochimica Acta*. **74**, 75-80.

Cabaniss S. E. (1997) Propagation of uncertainty in aqueous equilibrium calculations: non-gaussian output distribution. *Anal.Chem*. **69,** 3658-3664.

Cabaniss S. E. (1999) Uncertainty propagation in geochemical calculations: non-linearity in solubility equilibria. *Applied Geochemistry*. **14,** 255-262.

Choppin G. R. and Mathur J. N. (1991) Hydrolysis of Actinyl(VI) Cations. *Radiochimica Acta.* **52/53,** 25-28.

Criscenti L.J., Laniak G. F. and Erikson R. L. (1996) Propagation of uncertainty through geochemical code calculations. *Geochim.Cosmo.Acta*. **60**(19). 3551-3568.

De Stefano C., Gianguzza A., Leggio T. and Sammartano S. (2002) Dependence on ionic strength of the hydrolysis constants for dioxouranium(VI) in NaCl(aq) and NaNO3(aq), at pH < 6 and t =25 ºC. *J. Chem. Eng. Data*. **47**. 533-538.

L'Ecuyer P. and Lemieux C. (2002) Recent Advances in Randomized Quasi-Monte Carlo Methods. In *Modelling Uncertainty: An Examination of its Theory, Methods, and Applications* (eds. M. Dror, P. L'Ecuyer, and F. Szidarovszki). Kluwer Academic. pp. 419-474.

Efron B. and Tibshirani R. J. (1993) An introduction to the Bootstrap. Monographs on Statistics and Applied Probability. Vol. 57. Chapman and Hall, London.

Ekberg C. (1999) Sensitivity analysis and simulation uncertainties in predictive geochemical modelling. Freiberg on-line geoscience http://www.geo.tu-freiberg.de/fog

Galassi M. (2002) GNU Scientific Library. Free Software Foundation, Cambridge, MA, USA.

Grenthe I., Fuger J., Konings R. J. M., Lemire R. J., Muller A. B., Nguyen-Trung C. and Wanner H.(1992) Chemical Thermodynamics of Uranium. North-Holland, Amsterdam.

Grenthe I., Puigdomenech I., Sandino M. C. A. and Rand, M. H. (1995) Corrections to the Uranium NEA-TDB review. In *Chemical Thermodynamics of Americium*, (eds. Silva R. J. *et. al.*) North-Holland, Amsterdam. pp. 347-374.

Knuth, D. E. (1981). Seminumerical Algorithms, 2nd ed., vol 2 of The Art of Computer Programming. Reading, MA. USA., Addison-Wesley.

Lemire R. J. and Tremaine P. R. (1980) Uranium and Plutonium Equilibria in aqueous solutions to 200 °C. *J. Chem. Eng. Data.* **25**. 361-370.

Mathur J. N., (1991) Complexation and thermodynamics of the uranyl ion with phosphate. *Polyhedron*. **10**. 47.

Matsumoto M. and Nishimura T. (1998) Mersenne Twister. A 623-dimensionally equidistributed uniform pseudo-random number generator. ACM Transactions on Modelling and Computer Simulation, Special issue on Uniform Random Number Generation.

Meinrath G. (1998) Direct spectroscopic speciation of schoepite phase equilibria. *Journal of Radioanalytical and Nuclear Chemistry*. **232**(1-2). 179-188.

Moro B. (1995) "The Full Monte", in Over the Rainbow. Developments in Exotic Options and Complex Swaps (ed. R. Jarrow). RISK Publications.

Nitzsche O., Meinrath G. and Merkel B. (2000) Database uncertainty as a limiting factor in reactive transport prognosis. *Journal of Contaminant Hydrology*. **44**. 223-237.

OECD-NEA (1996) Survey of Thermodynamic and Kinetic Databases. Organisation for Economic Co-operation and Development, Nuclear Energy Authority, Paris. p. 39.

Palmer, D. A and Nguyen-Trung C. (1995) Aqueous uranyl complexes. 3. Potentiometric measurements of the hydrolysis of uranyl(VI) ion at 25°C. *Journal of Solution Chemistry*. **24**. 1281-1291.

Paquin P. *et. al*. (2002) The biotic ligand model: a historical overview. Comparative Biochemistry and Physiology Part C: Toxicology & Pharmacology. **133**(1-2). 3-35.

Sandino A. and Bruno J. (1992) The solubility of $(UO_2)_3(PO_4)_2.4H_2O$(s) and the formation of U(VI) phosphate complexes: Their influence in uranium speciation in natural waters. *Geochim. Cosmochim. Acta*. **56**. 4135.

Serkiz S.M. *et. al.* (1996) Correcting errors in the thermodynamic database for the equilibrium speciation model MINTEQA2. *Water Research*. **30**(8). 1930-1933.

Silva R.J. (1992) Mechanisms for the retardation of uranium(VI) migration. *Mat.Res. Cos. Symp. Proc*. **257**. 323.

Smith D.S., Adams, N. W. H. and Kramer, J. R. (1999) Resolving uncertainty in chemical speciation determinations. *Geochim.Cosmo.Acta.* **63**(19/20). 3337-3347.

Sobol I.M. (1967) The distribution of points in a cube and the approximate evaluation of integrals. *U.S.S.R Comput. Math. and Math. Phys*. **7**. 86-112.

Tebes-Stevens C.L., Espinoza F. and Valocchi A. J. (2001) Evaluating the sensitivity of a subsurface multicomponent reactive transport model with respect to transport and reaction parameters. *Journal of Contaminant Hydrology*. **52**. 3-27.

Unsworth E. R., Jones P. (2002). The effect of thermodynamic data on computer model predictions of uranium speciation in natural water systems. *Journal of Environmental Monitoring* **4**(4). 528-532.

Van der Lee J. and De Windt L. (2001) Present state and future directions of modeling of geochemistry in hydrogeological systems. *Journal of Contaminant Hydrology*. **47**(2-4). 265-282.

Van der Lee J. (1998) Thermodynamic and mathematical concepts of Chess.École des Mines de Paris, Paris.

Table 1. Selected thermodynamic data (mean log equilibrium constants and their associated standard deviation values) for the system H_2O-UO_2^{2+}-CO_2-PO_4^{3-} at I = 0 and 25 ºC

Reaction	Log K	σ	References
$1\ H_2O \rightleftharpoons 1\ OH^- + 1\ H^+$	-14.00	0.005	a
$1\ HCO_3^- + 1\ H^+ \rightleftharpoons 1\ CO_2\,(g) + 1\ H_2O$	7.83	0.01	a
$1\ HCO_3^- + 1\ H^+ \rightleftharpoons 1\ CO_2\,(aq) + 1\ H_2O$	6.35	0.026	a
$1\ HCO_3^- \rightleftharpoons 1\ CO_3^{2-} + 1\ H^+$	-10.33	0.036	a
$1\ HPO_4^{2-} \rightleftharpoons 1\ PO_4^{3-} + 1\ H^+$	-12.35	0.14	a
$1\ HPO_4^{2-} + 1\ H^+ \rightleftharpoons 1\ H_2PO_4^-$	7.21	0.14	a
$1\ HPO_4^{2-} + 2\ H^+ \rightleftharpoons 1\ H_3PO_4\,(aq)$	9.35	0.14	a
$1\ UO_2^{2+} + 1\ H_2O \rightleftharpoons UO_2OH^+ + 1\ H^+$	-5.36	0.22	a, b, c
$1\ UO_2^{2+} + 2\ H_2O \rightleftharpoons UO_2(OH)_2(aq) + 2\ H^+$	-11.75	0.46	b, d, e, f
$1\ UO_2^{2+} + 3\ H_2O \rightleftharpoons UO_2(OH)_3^- + 3\ H^+$	-19.6	0.46	a, g
$1\ UO_2^{2+} + 4\ H_2O \rightleftharpoons UO_2(OH)_4^{2-} + 4\ H^+$	-34.23	1.7	a, h
$2\ UO_2^{2+} + 1\ H_2O \rightleftharpoons 1\ (UO_2)_2OH^{3+} + 1\ H^+$	-2.7	0.60	a
$2\ UO_2^{2+} + 2\ H_2O \rightleftharpoons (UO_2)_2(OH)_2^{2+} + 2\ H^+$	-5.7	0.29	a, c, i, j
$3\ UO_2^{2+} + 4\ H_2O \rightleftharpoons 1\ (UO_2)_3(OH)_4^{2+} + 4\ H^+$	-11.9	0.50	a
$3\ UO_2^{2+} + 5\ H_2O \rightleftharpoons (UO_2)_3(OH)_5^+ + 5\ H^+$	-15.59	0.40	a, c, j
$3\ UO_2^{2+} + 7\ H_2O \rightleftharpoons (UO_2)_3(OH)_7^- + 7\ H^+$	-30.18	2.0	a, c, g, j
$4\ UO_2^{2+} + 7\ H_2O \rightleftharpoons 1\ (UO_2)_4(OH)_7^+ + 7\ H^+$	-21.9	0.81	a
$1\ UO_2^{2+} + 1\ HCO_3^- \rightleftharpoons 1\ UO_2CO_3\,(aq) + 1\ H^+$	-0.65	0.16	a
$1\ UO_2^{2+} + 2\ HCO_3^- \rightleftharpoons 1\ UO_2(CO_3)_2^{2-} + 2\ H^+$	-3.71	0.18	a
$1\ UO_2^{2+} + 3\ HCO_3^- \rightleftharpoons 1\ UO_2(CO_3)_3^{4-} + 3\ H^+$	-9.38	0.19	a
$3\ UO_2^{2+} + 6\ HCO_3^- \rightleftharpoons 1\ (UO_2)_3(CO_3)_6^{6-} + 6\ H^+$	-7.96	0.72	a
$2\ UO_2^{2+} + 1\ HCO_3^- + 3\ H_2O \rightleftharpoons 1\ (UO_2)_2CO_3(OH)_3^- + 4\ H^+$	-11.18	0.40	a
$3\ UO_2^{2+} + 1\ HCO_3^- + 3\ H_2O \rightleftharpoons 1\ (UO_2)_3O(OH)_2(HCO_3)^+ + 4\ H^+$	-9.67	0.54	a
$11\ UO_2^{2+} + 6\ HCO_3^- + 12\ H_2O \rightleftharpoons 1\ (UO_2)_{11}(CO_3)_6(OH)_{12}^{2-} + 18\ H^+$	-25.54	2.0	a
$1\ UO_2^{2+} + 1\ HPO_4^{2-} \rightleftharpoons 1\ UO_2PO_4^- + 1\ H^+$	0.88	0.22	a
$1\ UO_2^{2+} + 1\ HPO_4^{2-} \rightleftharpoons UO_2HPO_4(aq)$	7.3	0.24	a, g, k
$1\ UO_2^{2+} + 1\ HPO_4^{2-} + 1\ H^+ \rightleftharpoons UO_2H_2PO_4^+$	10.43	0.34	a, k, l
$1\ UO_2^{2+} + 1\ HPO_4^{2-} + 2\ H^+ \rightleftharpoons 1\ UO_2H_3PO_4^{2+}$	10.11	0.22	a
$1\ UO_2^{2+} + 2\ HPO_4^{2-} + 2\ H^+ \rightleftharpoons UO_2(H_2PO_4)_2(aq)$	20.2	0.88	a, k, l
$1\ UO_2^{2+} + 2\ HPO_4^{2-} + 3\ H^+ \rightleftharpoons 1\ UO_2(H_2PO_4)(H_3PO_4)^+$	20.35	0.33	a
$1\ UO_2^{2+} + 3\ H_2O \rightleftharpoons 1\ UO_3.2H_2O_{(s)} + 2\ H^+$	-4.81	0.15	a

[a] Grenthe et al, 1992; [b] Choppin and Mathur, 1991; [c] De Stefano et al, 2002; [d] Silva, 1992; [e] Lemire and Tremaine, 1980; [f] Grenthe et al, 1995; [g] Sandino and Bruno; [h] Baston et al, 1993; [i] Meinrath, 1998; [j] Palmer and Nguyen-Trung, 1995; [k] Brendler et al, 1996; [l] Mathur, 1991.

Figure 1. Coefficient of variance of distribution mean estimates by the MC and QMC methods for selected output species. $[UO_2^{2+}]_T = 10^{-6}$ mol dm^{-3}, pH = 6, $pCO_2 = 3.10^{-4}$ atm.

Figure 2. Skewness of selected output distributions as a function of pH and at several CO_2 partial pressures

Figure 3. Probability density functions of concentration output distributions from $n = 10^4$ Monte Carlo simulations at four pH values and a pCO_2 of 3.10^{-4} atm.

Figure 4. Relative uncertainty of output concentrations of selected species as a function of pH and pCO_2.

Figure 5. Relative uncertainty of output concentrations of selected species as a function of pH and phosphate concentration.

Figure 6. Probability density functions of the total aqueous uranium fraction in equilibrium with schoepite at pH 8.7 and three different CO_2 partial pressures.

Figure 7. Contour plot of the probability density function of the total aqueous uranium fraction in equilibrium with schoepite as a function of pH at a CO_2 partial pressure of 1 atm.

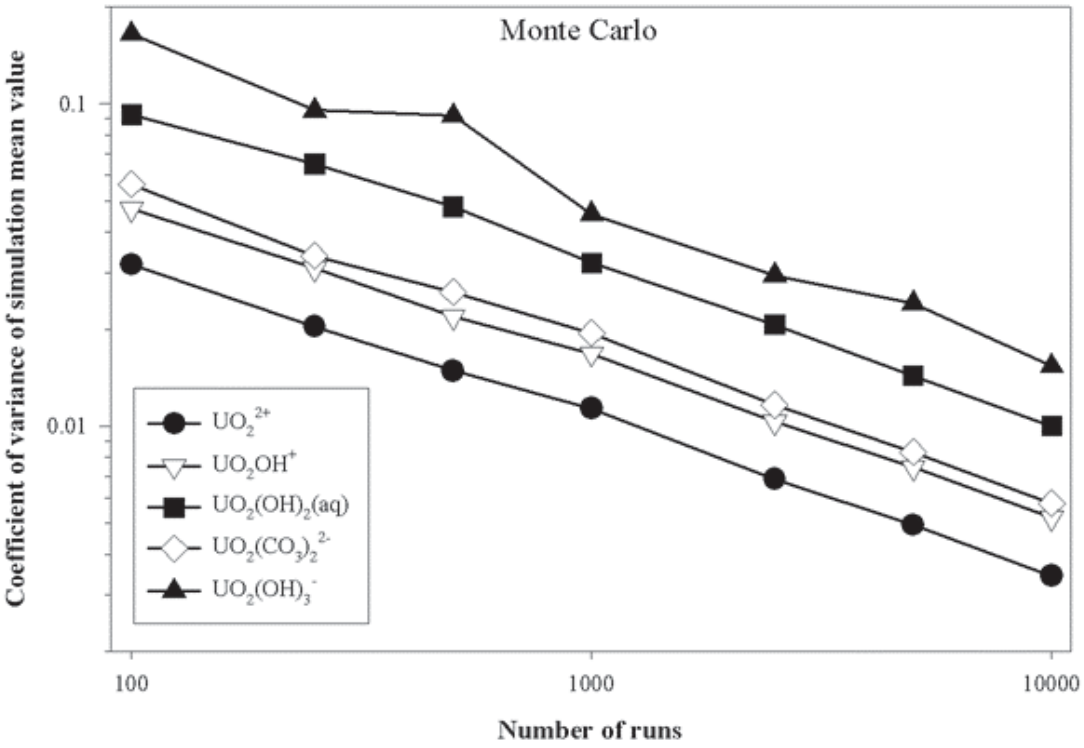
Monte Carlo
Coefficient of variance of simulation mean value
0.1
0.01
100
1000
10000
Number of runs
UO2 2+
UO2OH+
UO2(OH)2(aq)
UO2(CO3)2 2-
UO2(OH)3-

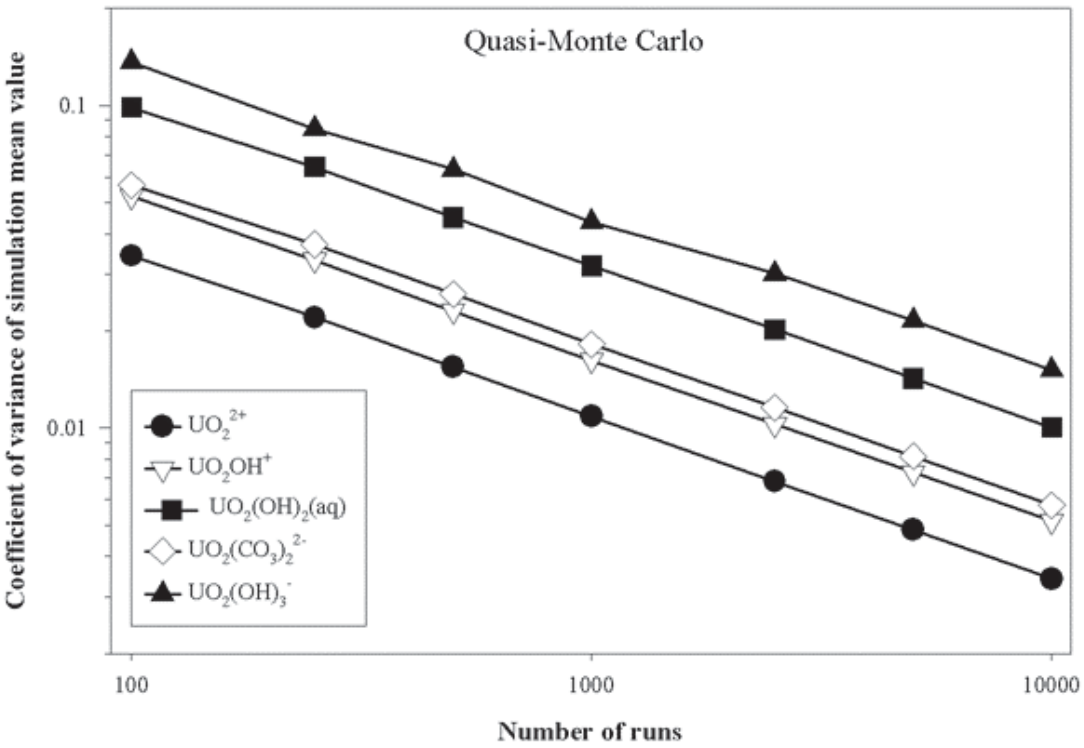
Quasi-Monte Carlo
Coefficient of variance of simulation mean value
0.1
0.01
100
1000
10000
Number of runs
UO2 2+
UO2OH+
UO2(OH)2(aq)
UO2(CO3)2 2-
UO2(OH)3-

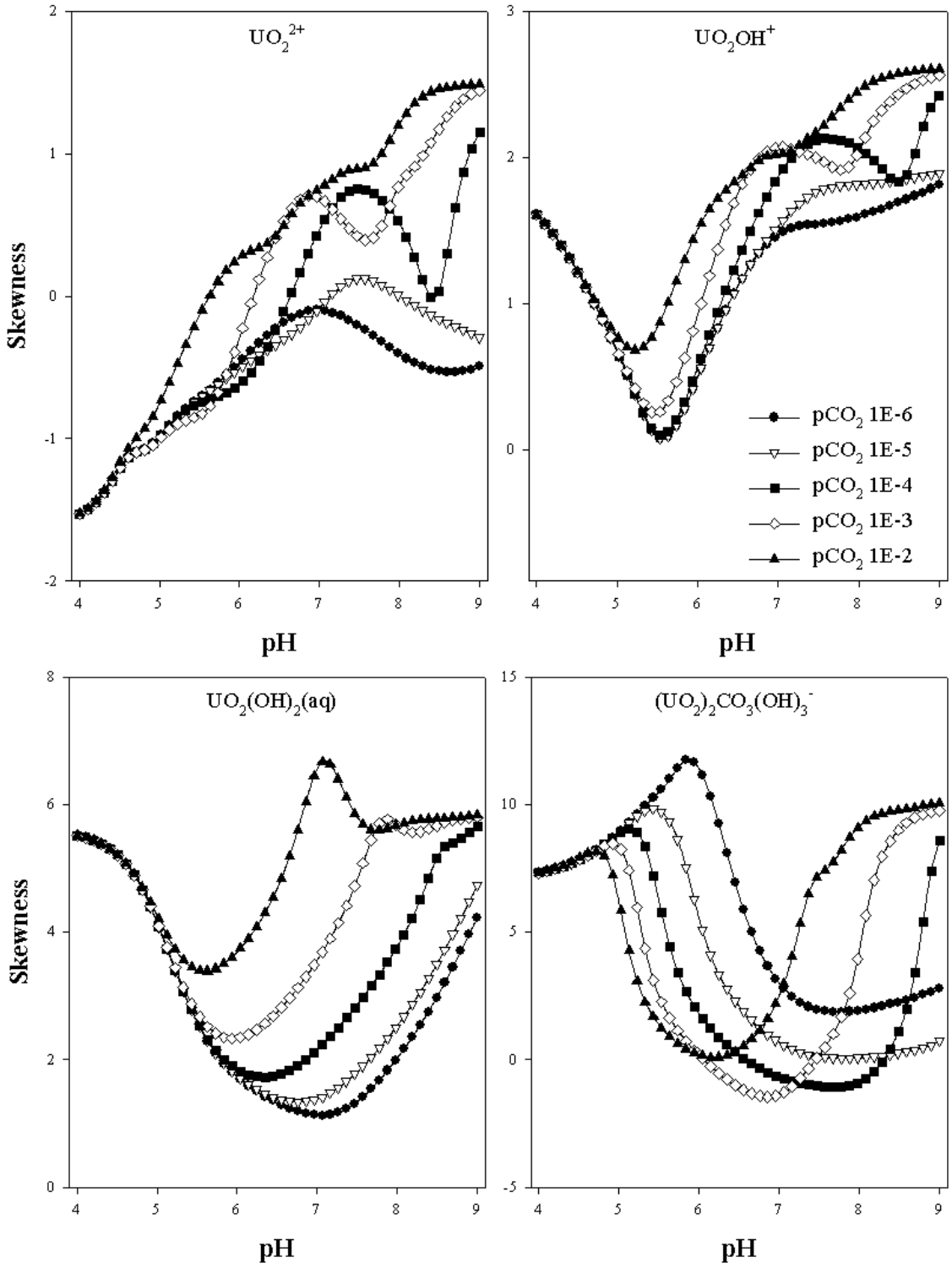
UO_2^{2+}
UO_2OH^+
$UO_2(OH)_2(aq)$
$(UO_2)_2CO_3(OH)_3^-$
Skewness
pH
pCO_2 1E-6
pCO_2 1E-5
pCO_2 1E-4
pCO_2 1E-3
pCO_2 1E-2

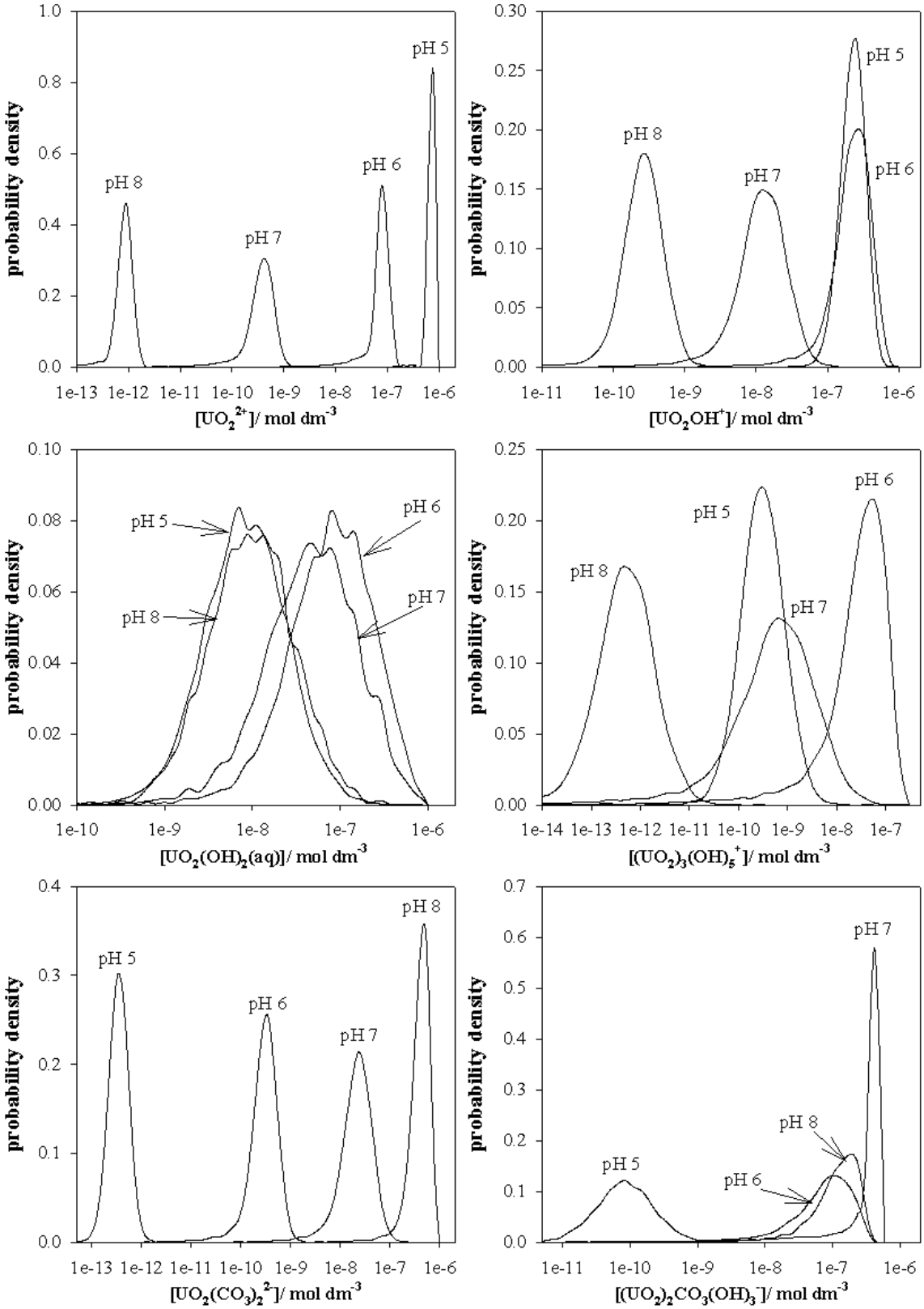
probability density
pH 8
pH 7
pH 6
pH 5
[UO2 2+]/ mol dm-3
[UO2OH+]/ mol dm-3
[UO2(OH)2(aq)]/ mol dm-3
[(UO2)3(OH)5+]/ mol dm-3
[UO2(CO3)2 2-]/ mol dm-3
[(UO2)2CO3(OH)3-]/ mol dm-3

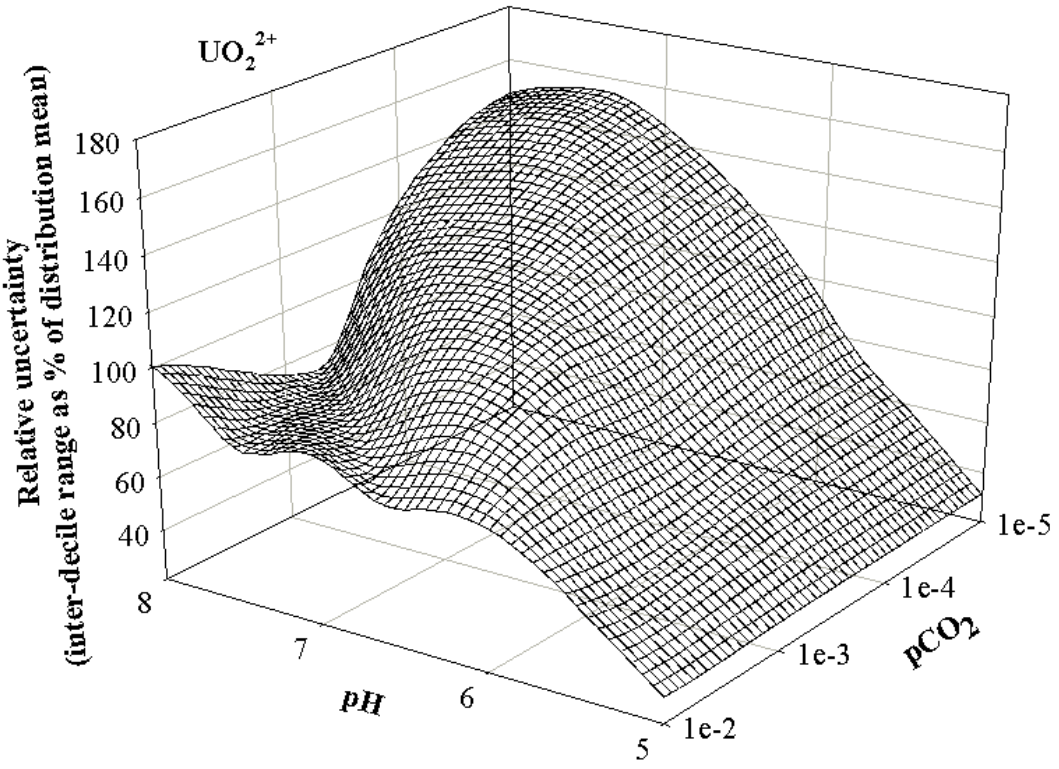
UO_2^{2+}
Relative uncertainty
(inter-decile range as % of distribution mean)
180
160
140
120
100
80
60
40
8
7
6
5
pH
1e-2
1e-3
1e-4
1e-5
pCO2

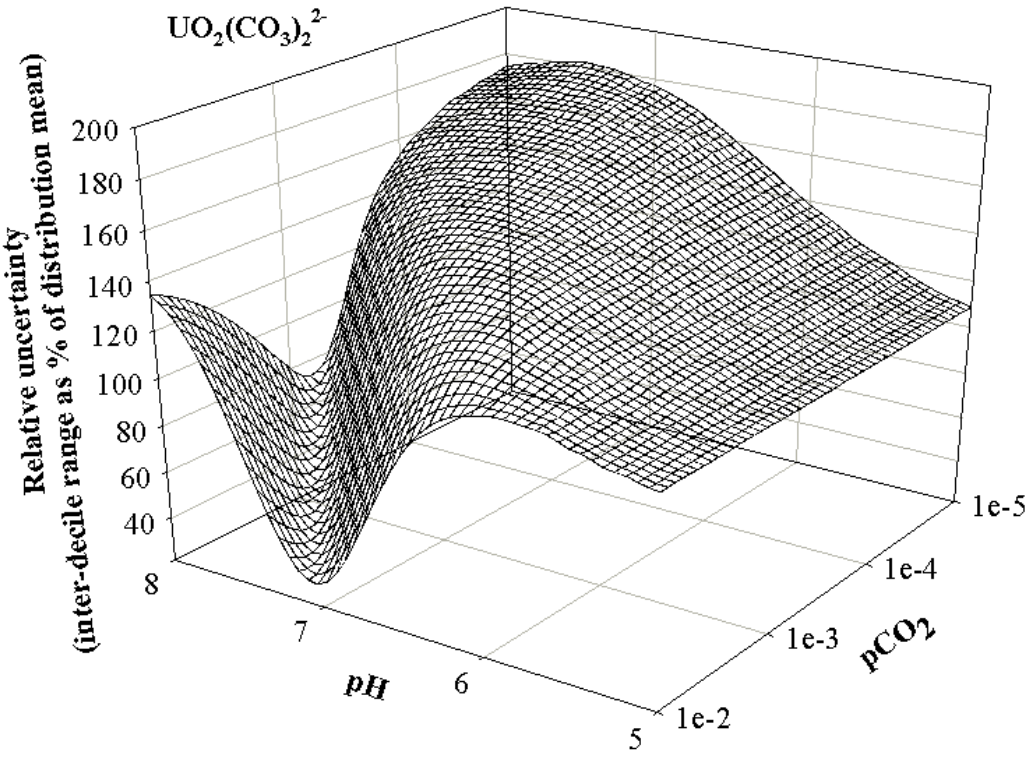
$UO_2(CO_3)_2^{2-}$
Relative uncertainty
(inter-decile range as % of distribution mean)
200
180
160
140
120
100
80
60
40
8
7
6
5
pH
1e-2
1e-3
1e-4
1e-5
pCO2

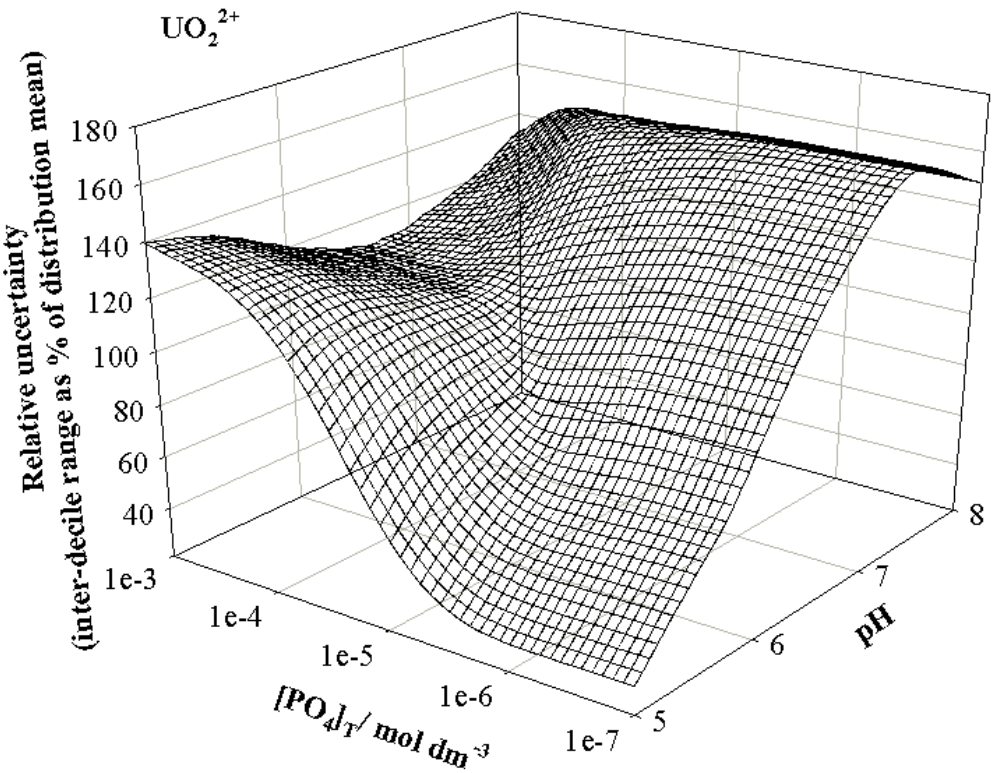
UO_2^{2+}
Relative uncertainty
(inter-decile range as % of distribution mean)
180
160
140
120
100
80
60
40
1e-3
1e-4
1e-5
1e-6
1e-7
$[PO_4]_T$/ mol dm^{-3}
5
6
7
8
pH

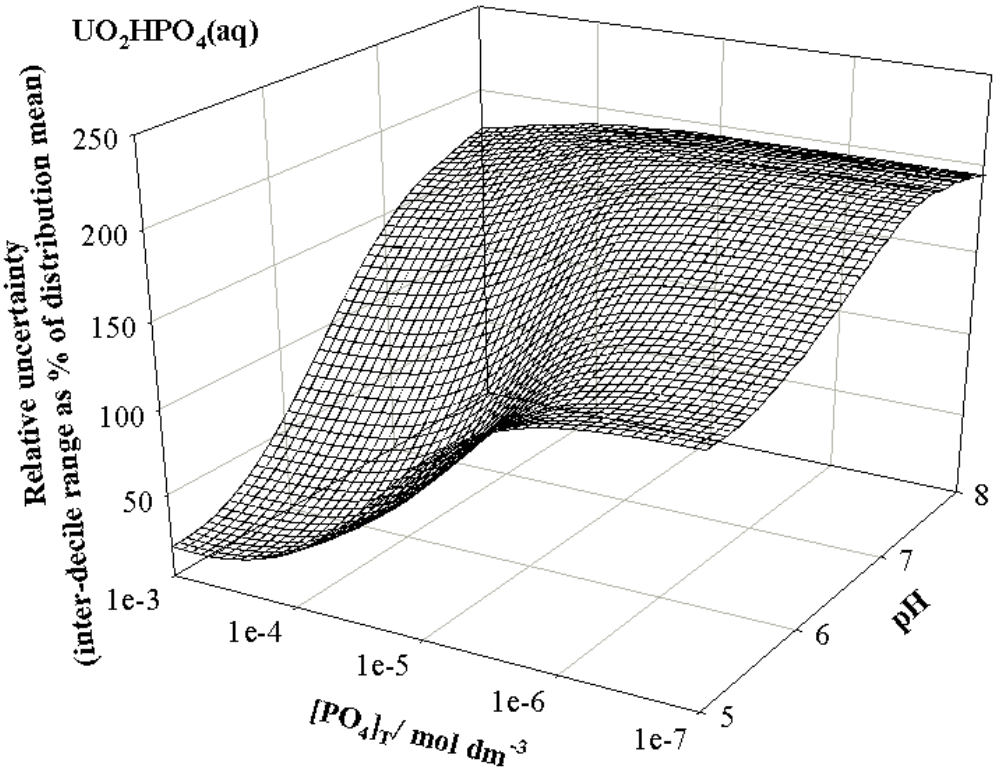
UO_2HPO_4(aq)
Relative uncertainty
(inter-decile range as % of distribution mean)
250
200
150
100
50
1e-3
1e-4
1e-5
1e-6
1e-7
$[PO_4]_T$/ mol dm^{-3}
5
6
7
8
pH

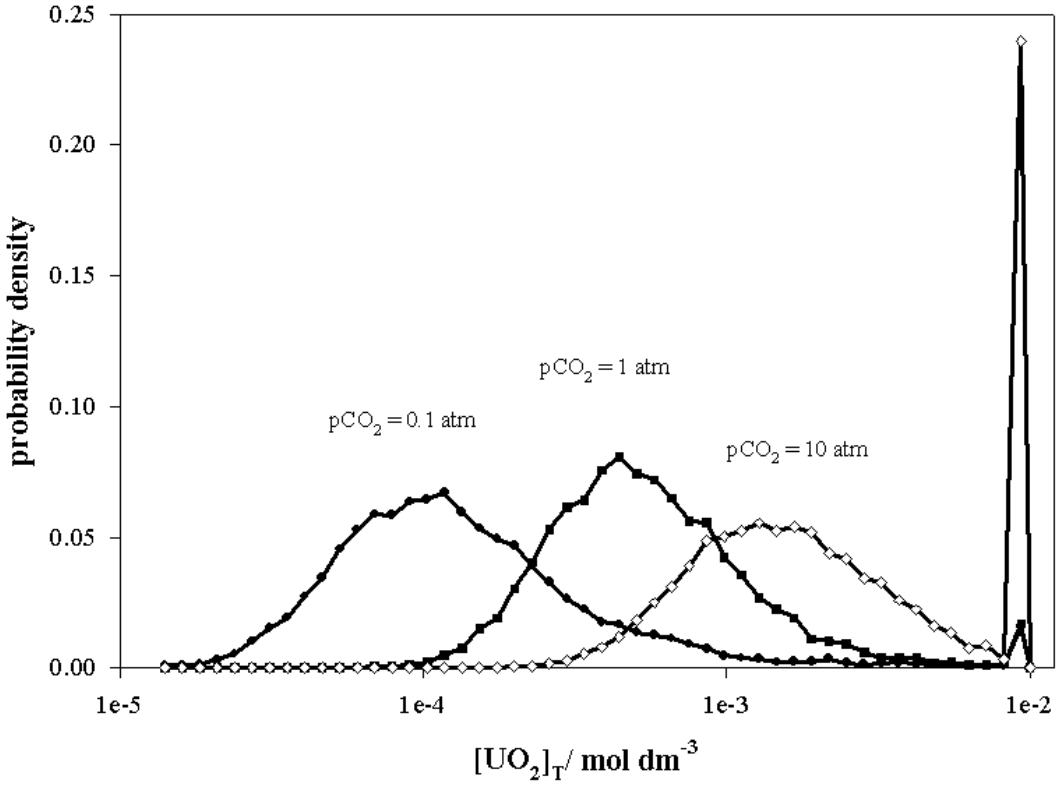
0.25
0.20
0.15
0.10
0.05
0.00
probability density
pCO2 = 1 atm
pCO2 = 0.1 atm
pCO2 = 10 atm
1e-5
1e-4
1e-3
1e-2
[UO2]T/ mol dm-3

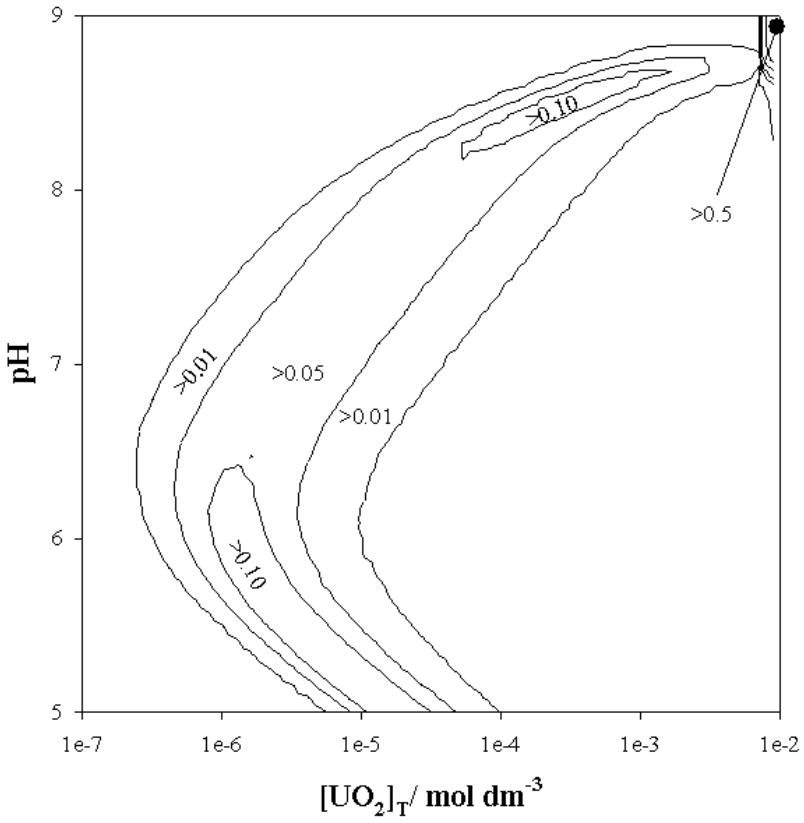
9
8
7
6
5
pH
1e-7
1e-6
1e-5
1e-4
1e-3
1e-2
[UO2]T/ mol dm-3
>0.10
>0.5
>0.01
>0.05
>0.01
>0.10

SETAC PRESS

Environmental Toxicology and Chemistry, Vol. 23, No. 5, pp. 1108–1114, 2004

Printed in the USA
0730-7268/04 $12.00 + .00

VALVE CLOSURE RESPONSE TO URANIUM EXPOSURE FOR A FRESHWATER BIVALVE (*CORBICULA FLUMINEA*): QUANTIFICATION OF THE INFLUENCE OF pH

ELODIE FOURNIER,*† DAMIEN TRAN,† FRANCIS DENISON,† JEAN-CHARLES MASSABUAU,‡ and JACQUELINE GARNIER-LAPLACE†

†Laboratoire de Radioécologie et Ecotoxicologie, Institut de Radioprotection et de Sûreté Nucléaire Bât 186, BP 3, 13115 Saint-Paul-Lez-Durance Cedex, France

‡UMR 5805, Laboratoire d'Ecophysiologie et Ecotoxicologie des Systèmes Aquatiques, Université Bordeaux 1 et CNRS, Place du Docteur Peyneau, 33120, Arcachon, France

(*Received* 10 *December* 2002; *Accepted* 14 *October* 2003)

Abstract—Laboratory experiments were carried out to analyze the first valve closure response of a freshwater bivalve (*Corbicula fluminea*) exposed to uranium during a 5-h period. Experiments were performed in a well-defined artificial water at two pH values, 5.5 and 6.5, with a noninvasive method of valve recording. Sensitivity thresholds, based on percentage of bivalve that close their valves in a given time, were determined. Response thresholds depended on the total uranium concentration, integration time of response (fast responses could only be observed for the highest concentrations), and pH. The bivalve is much more sensitive to total uranium concentration at pH 5.5 than pH 6.5. The minimal sensitivity threshold determined, expressed as the uranium concentration inducing the valve closure of 50% of the bivalves, was 0.05 μmol/L at pH 5.5 after 5 h of exposure. Moreover, higher concentrations of the free ion UO_2^{2+} are required at pH 5.5 than at pH 6.5 to illicit the same response. Two hypotheses can be proposed, that UO_2^{2+} is not the only detected species or that competition exists between H^+ and UO_2^{2+} for binding sites.

Keywords—*Corbicula fluminea* Uranium Valve movement pH Speciation

INTRODUCTION

Uranium is a naturally occurring heavy metal, a member of the actinide series, that is widely distributed throughout the environment. Its concentrations in terrestrial and aquatic ecosystems may be increased in connection with various anthropogenic contributions, originating from uses throughout the different stages of the nuclear fuel cycle (mines and waste storage sites in particular), agricultural use (phosphate-based fertilizers), research laboratories, and military use of depleted uranium [1]. The environmental geochemistry of uranium is characterized by mobility in zones with high oxidation–reduction potential (U(VI)), such as natural watercourses, but also reductive immobilization and precipitation in zones with low oxidation–reduction potential (U(IV)) [2].

The methodology for efficient monitoring of freshwater quality includes the use of bioindicators, which alleviates a number of problems associated with the analysis of trace pollutants in water or sediments and gives a direct indication of their bioavailability to the biocenosis. The possible organisms for use as trace pollutant indicators include bivalve species, for example, the Asiatic clam *Corbicula fluminea*, which is ubiquitous and abundant throughout the majority of European waterways. This species already has been used for biomonitoring purposes within aquatic ecosystems to assess early changes in water and sediment quality by measuring exposure or the induced biological effects, such as accumulation of contaminants within the soft bodies [3–5], biochemical perturbations [6,7], or behavioral changes [8–10]. In the last decades, a number of studies have dealt with the development of a biosensor technique based on the detection of abnormalities in valve movement behavior of the bivalves as an early response when exposed to toxic concentrations of metals [8,11–13]. Bivalves are filter feeders, and their feeding-induced ventilatory activity (obviously associated with an opened valve state) is a primary limiting step that controls the water flow rate through the body and hence the delivery of contaminants. For bivalves, the ability to rapidly detect the presence of uranium is evidently a key adaptation to protect the organism against metal toxicity. Markich et al. [13], when using the freshwater bivalve *Velesunio angasi*, showed that the valve movement behavior is a quantifiable and rapid endpoint for assessing the toxicity of uranium exposures. They demonstrated that the sensitivity of *V. angasi* to uranium increased when the pH decreased from 6.0 to 5.0, but they also found that the free-ion activity model (FIAM) failed to describe the studied uranium–organism interactions at more than one pH.

In this study, we applied a noninvasive valvometric method [14] to record valve movement behavior of *C. fluminea* exposed to uranium at two pH values (5.5 and 6.5). The aims of this work were twofold: to study the first valve closure response of *C. fluminea* and to assess the relevancy of using this endpoint as a biological early warning system of uranium presence in freshwaters. Two main ecotoxicological endpoints were determined: the delay required to obtain a significant response and the detected uranium concentration in water, that is, the sensitivity threshold to uranium for *C. fluminea*. Additionally, the valve closure response was related to the aqueous speciation of uranium in the water used, and the consistency with the FIAM is discussed.

* To whom correspondence may be addressed (elodie.fournier@irsn.fr).

Presented at the 12th Annual Meeting, SETAC Europe, Vienna, Austria, May 12–16, 2002.

Table 1. Nominal and measured ion concentrations in the synthetic water used during the experiments. Results are presented as mean values ± standard errors (n = 33)

Ions (mmol/L)	Control	pH 5.5	pH 6.5
K^+	0.50	0.61 ± 0.01	0.74 ± 0.01
Na^+	0.25	0.51 ± 0.03	0.36 ± 0.03
Mg^{2+}	0.50	0.54 ± 0.01	0.52 ± 0.01
Ca^{2+}	1.50	1.53 ± 0.01	1.51 ± 0.03
Cl^-	3.00	3.49 ± 0.05	3.58 ± 0.04
NO_3^-	0.75	0.75 ± 0.01	0.77 ± 0.01
SO_4^{2-}	0.50	0.50 ± 0.01	0.51 ± 0.01
HCO_3^-		1×10^{-3}[a]	18×10^{-3}[a]

[a] Corresponds to the simulated values predicted by J-Chess software [15] under the assumption of equilibrium with the atmosphere.

MATERIALS AND METHODS

Animal collection and maintenance

Specimens of *C. fluminea* were collected manually from River Saint-Seurin sur l'Isle (France). On arrival at the laboratory (Marine Biological Station, Arcachon, France) a few hours after collection, a homogeneous group of clams (n = 165) was constituted with a mean anteroposterior shell length of 27.50 ± 0.08 mm (mean ± standard error), corresponding to a mean wet weight of 0.68 ± 0.01 g for the whole soft body. They were maintained at 20°C in a polyvinyl chloride tank (83 × 83 × 20 cm) filled with aerated tap water over washed quartz sand (SILAQ, Mios, France) in which the animals could move freely, burrow, and hide. Animals were fed daily with a suspension of unicellular algae (*Scenedesmus subspicatus*; total density 2×10^5 cells/ml within the tank just after the addition). One half of the volume of water was changed once a week. Mortality was negligible (<3%) during the one-month maintenance period before the beginning of acclimation and experiments. This species previously has been maintained in our laboratory facilities up to three years without noticeable mortality.

Experimental water composition

Experiments were performed at two pH values (5.5 and 6.5) in a synthetic water air-equilibrated by air-bubbling. The composition of the water is given on Table 1. Alkalinity was calculated with J-Chess software [15]. Each unit was continuously supplied with algae (to give a cell density of 1.35×10^5 cells/ml within the experimental unit) via a peristaltic pump (Gilson, Villiers-Le-Bel, France). The pH was regulated by addition of HCl (0.1 mol/L) via a second peristaltic pump under the control of a pH stat (CONSORT R301, Illkirch, Belgium). The tanks were bubbled with air to improve algal mixing and gas–water equilibration and to control the physiological respiratory state of the bivalves.

Animal equipment and experimental units

Just before the 7-d experimental period, bivalves were equipped with impedance electrodes. This minimally perturbing technique with emphasis on stress problems in bivalves and experimental design was detailed by Tran et al. [14]. Briefly, to permit the natural and unhindered movement of each individual in the sand substrate, light platinum electrodes (20 mg each, 3 mm diameter) were glued (Loctite 431, Manutan, Gonesse, France) to each valve. Measurement of the distance between the two electrodes was performed by a purpose-built computer-based data acquisition system (LAB PC 1200, National Instrument, Austin, TX, USA) and LAB VIEW software (National Instrument). For each test condition, five equipped bivalves were maintained in each of three identical experimental units (15 individuals total). Tran et al. [14] demonstrated that 15 is a sufficient number to precisely estimate responses of *C. fluminea* and that our experimental conditions allow a fairly efficient replicability independent of time. The units consisted of glass tanks lined with alimentary plastic (PLASTILUZ, Bordeaux, France), containing 500 ml of washed quartz sand (SILAQ) as substrate and 3 L of synthetic water under flow-through conditions (complete water renewal every 36 h).

Exposure protocol

Five nominal uranium concentrations (0.25, 0.5, 0.75, 1.0, and 2.0 μmol/L) were studied at pH 6.50 ± 0.06 and six concentrations (0.1, 0.25, 0.50, 0.75, 1.0, and 2.0 μmol/L) were studied at pH = 5.50 ± 0.05. Before commencing the exposures, the valve movement behavior of *C. fluminea* was monitored over a 24-h period to obtain reference data that permitted calculation of the closure response of the bivalves in uncontaminated conditions. The exposure started at 11:00 AM by stopping the water renewal and adding an appropriate volume of a uranyl nitrate solution ($UO_2(NO_3)_2 \cdot 6H_2O$; stock solution 5 mmol/L; Fluka, Buchs, Switzerland) brought to neutral pH by addition of potassium hydroxide. Air bubbling was continued in the tanks to improve uranium mixing and maintain water oxygenation. The effects of uranium on the valve closure response were studied during the following 5 h (i.e., from 11:00 AM to 4:00 PM). The bivalves were not fed for the 24-h period before uranium exposure, as well as during exposure, to minimize uranium–algae interactions.

Chemical analyses

Water samples were taken hourly during the acclimatization and exposure periods. The water samples (acidified to 2% [v/v] HNO_3 for cation determinations) were analyzed for major ion concentrations (ion chromatography, detection limits of ~10 μmol/L; Dionex DX-120, Sunnyvale, CA, USA). Uranium concentrations were determined by inductively coupled plasma–optical emission spectrometry (limit of detection uranium at 10 nmol/L; optima 4300 DV, Perkin-Elmer, Norwalk, CT, USA). All water samples were refrigerated at 4°C in darkness before analysis.

Geochemical speciation modeling for uranium in solution

Because of the lack of practicable techniques to directly measure individual uranium chemical species in solution, the thermodynamic geochemical speciation code J-Chess [15] was used to predict the speciation of uranium in the water used. A consistent database was compiled from the Organization for Economic Cooperation and Development–Nuclear Energy Agency thermochemical database [16], modified to include more recent data. The literature review was critically compiled by Denison [17]. The input parameters for J-Chess were based on measured physicochemical data (temperature, pH, and ion concentrations, as mentioned in Table 1), and all calculations, including alkalinity, were constrained to a fixed input pH (5.5 or 6.5) for the artificial water at the equilibrium with the atmosphere.

Evaluation of valve activity response of the individuals and statistical analyses

The first valve closure event of an individual after commencing the exposure was considered a response to the presence of uranium. The percentage of individuals exhibiting a response to each uranium concentration during a given integration time of response (ITR) was calculated.

A logistic regression model [18] was used to fit sigmoidal relationships between the percentage (p) of reacting bivalves (n = 15) for each experimental condition and the nominal concentration of uranium in water (expressed in μmol/L). This type of model is applicable to dichotomous variables (0, no reaction; 1, reaction) as follows

$$\text{logit}(p/100) = B0 \log(ECp) + B1 \quad (1)$$

where B0 and B1 are the estimated parameters for which statistical significance was tested at $p = 0.05$ and EC is the effect concentration (nominal concentration of uranium in water). The adequacy of the logistic model was evaluated with a likelihood test ratio [19]. From the fitted sigmoidal concentration–response curves, a series of effect concentrations (ECp; expressed in uranium at μmol/L) ranging from EC20 through to EC80 were calculated for *C. fluminea* exposed to uranium. In addition, the endpoint EC50 quantifying the sensitivity of the bivalve to uranium as a function of the ITR (expressed in min) selected for the data analysis has been modeled according to the following equation:

$$EC50 = EC0 + ae^{-b\ ITR} \quad (2)$$

where a and b are estimated parameters. The effect of pH was tested with the Mann–Whitney test at a significance of p = 0.05.

Statistical analyses were performed with the software SigmaStat® for Windows (Ver 2.0, SPSS Science, Chicago, IL, USA). For the regressions, all estimated parameters are presented with the standard error of estimation (± standard error).

RESULTS

Water chemistry and uranium concentrations

A summary of measured data is given in Table 1. Major ion concentrations were similar between the two regulated pH conditions (5.5 and 6.5), except for K^+ and Na^+ concentrations. The difference between the mean measured concentrations and the nominal value for these two cations was respectively +22% (pH 5.5) and +48% (pH 6.5) for K^+, and +104% (pH 5.5) and +44% (pH 6.5) for Na^+. The difference between measured uranium concentration at the beginning of the experimental phase and expected nominal concentration was less than 10% for all conditions.

Uranium aqueous speciation

Uranium aqueous species distributions were predicted by J-Chess simulations for the experimental conditions, that is, in synthetic air-equilibrated water at pH 5.5 and 6.5 for total uranium concentrations ranging from 0.1 μmol/L to 2 μmol/L. The predicted speciation of uranium is complex and is highly dependent on pH and total uranium concentration. At pH 5.5, UO_2^{2+} and UO_2OH^+ were the dominant species and contributed to 80% of total uranium (Fig. 1a). At pH 6.5, UO_2^{2+} was predicted to be a minor species (1.5%). The ternary uranyl species $(UO_2)_2CO_3(OH)_3^-$ was predicted to be the dominant species at pH 6.5 (35–60%), whereas at pH 5.5, it contributed less than 1%. The relative contribution of the ternary uranyl species to the total uranium concentration in water increased with the total uranium concentration (Fig. 1b).

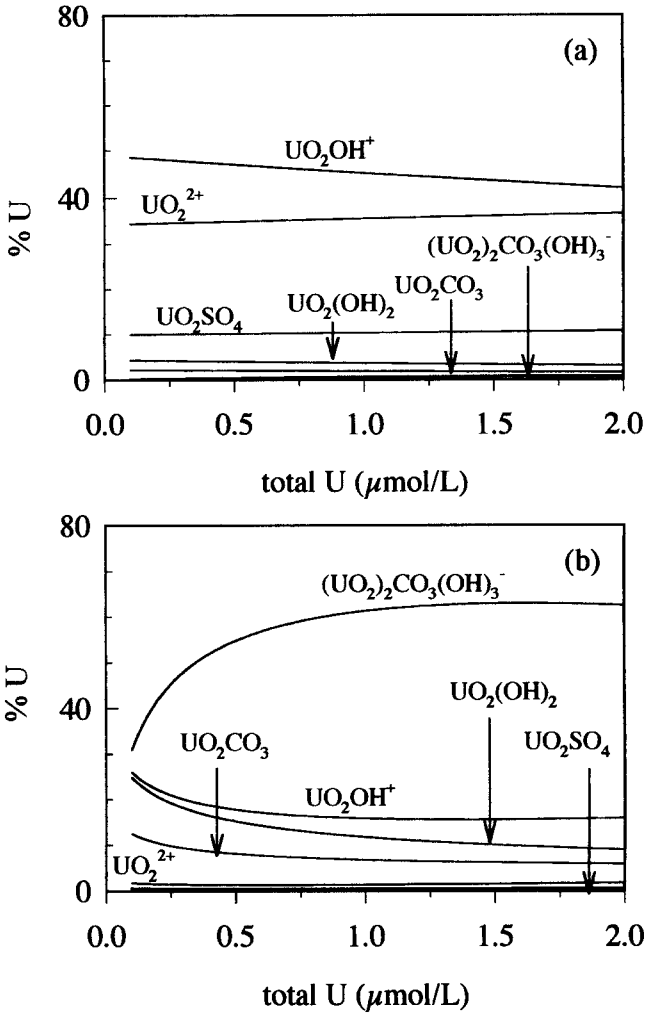

Fig. 1. Contribution of each aqueous chemical species of uranium (U) to the total concentration of the metal (expressed in percent) in the synthetic water used and for the two pH conditions (**a**) pH 5.5 and (**b**) pH 6.5. Values were predicted with J-Chess software [15] associated with a critically revised thermodynamic database. A uranyl species only was represented on the diagram if its contribution was more than 1% to the total uranium concentration for at least one of the two pH conditions.

Uranium water concentration–response relationships

For all experimental conditions, the 5-h duration exposure of clams to uranium resulted in a significant valve closure response in comparison with the behavioral pattern observed without any addition of metal (i.e., less than the inductively coupled plasma–optical emission spectrometry limit of detection). To demonstrate the effect of uranium concentration at the two pH values studied, the percentage of bivalves that reacted when using ITR in the range 10 to 300 min is presented as a function of the uranium exposure concentration in Figure 2. For both pH values studied, the percentage of reacting bivalves increased with increasing uranium concentration. For example, at pH 6.5, after a 10-min exposure period, the percentage of bivalves that reacted increased from approximately 25% at 0.25 μmol/L to approximately 75% at 1 μmol/L. More-

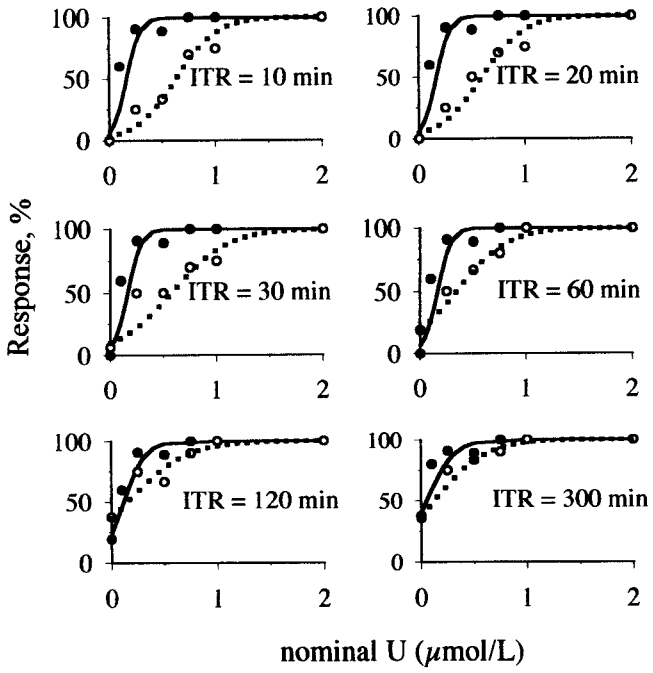

Fig. 2. Uranium (U) concentration–response curves for the valve closure of *Corbicula fluminea* exposed to uranium in the synthetic water at two pH values, as a function of the integration time of response (ITR) selected for the data treatment. A logistic regression model (Eqn. 1) was fitted to experimental data series for the two pH conditions (pH 5.5, solid line for model and black circles for empirical data, and pH 6.5, dotted line for model and white circles for empirical data).

over, for a given uranium concentration, the percentage of reacting bivalves depended strongly on the ITR period used, increasing markedly with increasing ITR. For example, at pH 6.5 and a uranium concentration of 0.5 μmol/L, the percentage of reacting bivalves increased from 30 to 80% on increasing the ITR from 10 to 300 min. The effect of the ITR was less important at pH 5.5 than at pH 6.5. *Corbicula fluminea* appeared to be much more sensitive to uranium concentration at pH 5.5 than at pH 6.5. For example, after a 10-min exposure period at 0.5 μmol/L, 30% of the 15 studied bivalves have reacted at pH 6.5 compared to 100% at pH 5.5.

The relationship between the series of the calculated effect concentrations and ITR selected for analysis is presented in Table 2. The ECp estimated values tended to decrease for increasing ITR. Statistical data that accompany the values (standard errors) offer a basis for appreciating the quality of the model's parameter adjustment. The selected model fits the experimental data for both pH conditions. For a given ITR, the sensitivity of *C. fluminea* to uranium was highly dependent on pH and was much higher at pH 5.5 than at pH 6.5. For example, EC50 corresponding to a 10-min exposure period was four times lower for pH 5.5 (0.17 μmol/L) than for pH 6.5 (0.63 μmol/L). However, for a 300-min ITR, the difference in sensitivity was less important, with only a factor of 2.6 (EC50 equal to 0.05 and 0.13 μmol/L for pH 5.5 and 6.5, respectively).

Relationship between EC50 and ITR

The relationship between EC50 and ITR is summarized in Figure 3. At pH 6.5, the sensitivity of the clams strongly increased with increasing ITR. The EC50 rapidly decreased during the two first hours of exposure, from 0.80 μmol/L after a 5-min exposure period, to reach a plateau at 0.15 μmol/L at 180 min. This plateau corresponded to the minimal uranium concentration in the water used that could be detected by *C. fluminea* at pH 6.5. At pH 5.5, the change of EC50 with the ITR clearly appeared to be less important, and the sensitivity is remarkably important even for the shortest ITR. For example, after 5 min of exposure, the sensitivity of *C. fluminea* at pH 5.5 is uranium at 0.20 μmol/L compared to 0.08 μmol/L for a 300-min exposure period.

Table 2. Total dissolved uranium concentration (in μmol/L) that induced the valve closure response for percent (p) of the bivalves (effect concentration [ECp]) according to the integration time of response (ITR) selected for analysis at pH 5.5 and pH 6.5. The parameters B0 and B1 correspond to the estimated parameters (means ± standard errors) obtained when fitting a logistic regression model (logit(p/100) = B0 log(ECp) + B1) to experimental data series[a]

ITR (min)	B0 ± SE	B1 ± SE	EC20 (μmol/L)	EC50 (μmol/L)	EC80 (μmol/L)
		pH 5.5			
10	−2.68 ± 0.67	16.19 ± 3.98	0.08	0.17	0.25
20	−2.68 ± 0.67	16.19 ± 3.98	0.08	0.17	0.25
30	−2.68 ± 0.67	16.19 ± 3.98	0.08	0.17	0.25
60	−2.68 ± 0.67	16.19 ± 3.98	0.08	0.17	0.25
120	−1.76 ± 0.48	12.31 ± 3.19	<	0.12	0.26
300	−0.42 ± 0.35	7.79 ± 2.57	<	0.05	0.23
		pH 6.5			
10	−3.41 ± 1.06	5.39 ± 1.63	0.38	0.63	0.89
20	−3.11 ± 0.95	5.22 ± 1.53	0.33	0.60	0.86
30	−2.23 ± 0.70	3.86 ± 1.17	0.22	0.58	0.94
60	−1.46 ± 0.56	4.25 ± 1.23	0.02	0.35	0.67
120	−1.34 ± 0.55	4.96 ± 1.42	<	0.16	0.53
300	−0.53 ± 0.48	4.20 ± 1.42	<	0.13	0.46

[a] SE = standard error; < = below detection limits.

Relationship between valve closure response and UO_2^{2+} concentration

Figure 4 represents EC50 expressed in μmol/L of the concentration of the uranyl free ion species versus the ITR. *Corbicula fluminea* clearly appeared to be more sensitive to uranyl ion at pH 6.5 than at pH 5.5 within the range of the selected ITRs (5–300 min). The concentration of UO_2^{2+} corresponding

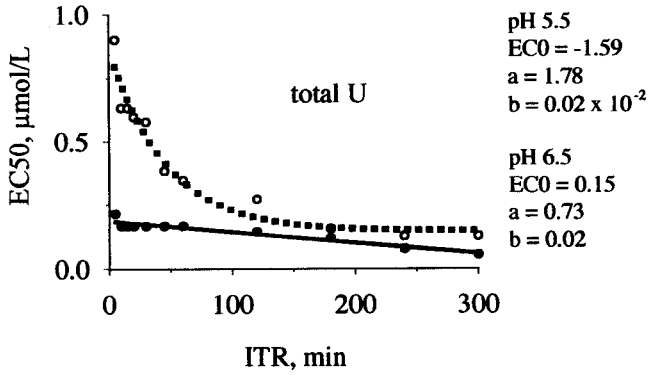

Fig. 3. Sensitivity threshold to uranium (U), expressed as effective concentration (EC50), that is, the concentration of total uranium in water (in μmol/L) inducing a valve-closure reaction for 50% of the bivalves under experimental conditions, versus the integration time of response (ITR) selected for the analysis. A regression model (Eqn. 2) was fitted to experimental data for the two pH conditions (pH 5.5, solid line and black circles, and pH 6.5, dotted line and white circles).

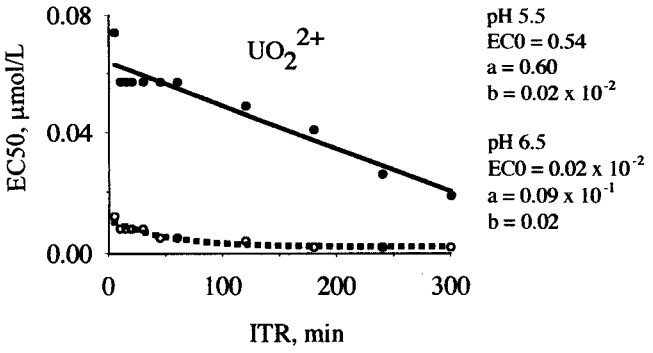

Fig. 4. Sensitivity threshold to the uranyl free ion, expressed as effective concentration (EC50), that is, the activity of uranyl ion (UO_2^{2+}) in water (in µmol/L) inducing a valve-closure reaction for 50% of the bivalves under experimental conditions, versus the integration time of response (ITR) selected for the analysis. A regression model (Eqn. 2) was fitted to experimental data for the two pH conditions (pH 5.5, solid line and black circles, and pH 6.5, dotted line and white circles).

to EC50 was approximately 10 times higher at pH 5.5 than at pH 6.5 (e.g., EC50 equal to 0.021 µmol/L [UO_2^{2+}] at pH 5.5 compared to 0.002 µmol/L [UO_2^{2+}] at pH 6.5).

DISCUSSION

Minimal sensitivity threshold for uranium and C. fluminea

Our results demonstrate a clear effect of uranium on valve closure response of *C. fluminea*. *Corbicula fluminea* was able to detect and to respond early to increasing uranium concentration by closing its valves. For the two pH values (5.5 and 6.5), the intensity of the response for the bivalve depended on both the uranium concentration and the integration time selected to carry out the data analysis. *Corbicula fluminea* appeared to be more sensitive at pH 5.5 than at pH 6.5, reaching EC50 values as low as 0.05 µmol/L (12 µg/L) of total uranium at pH 5.5 for a 300-min ITR. This value corresponded to the minimal sensitivity threshold that was evidenced during the experiments in the present synthetic water. To our knowledge, no detection threshold for uranium and *C. fluminea* has been described in the literature. Markich et al. [13] determined the valve movement response of a tropical freshwater species *V. angasi* in terms of the duration of valve opening to increasing concentration of total uranium in a synthetic water under conditions of varying pH from 5.0 to 6.0. For pH 5.5, the sensitivity of this species for uranium was quantified by a uranium water concentration of 163 µg/L (0.68 µmol/L, which is 14 times our threshold value) that induced a 50% reduction in the duration of valve opening for a 48-h exposure period. However, comparison with those results is limited because of experimental differences such as the composition of the synthetic water, the bivalve species, the temperature, the valvometry technique (free bivalves for our study vs glue-fixed organisms) and the use in the present study of different ITR for the data analysis. The same valvometry technique was used by Tran et al. [14] to determine bivalve sensitivity to cadmium exposure. Tran et al. [14] calculated an EC50 value for cadmium of 0.14 µmol/L for an ITR of 300 min. This value is three times the presently determined threshold of 0.05 µmol/L for uranium. However, note that it was obtained for different ion composition of water, at 15°C and pH 7.8, in comparison to the present experimental conditions at 20°C and 5.5 for this study.

Influence of pH on valve closure response and role of uranium speciation

Corbicula fluminea was 2.5-fold more sensitive to total uranium concentration after an integration time of 300 min at pH 5.5 (EC50 = 0.05 µmol/L) than at pH 6.5 (EC50 = 0.13 µmol/L). These results are consistent with those from Markich et al. [13], who reported that *V. angasi* was more sensitive at low pH. The sensitivity to uranium after a 48-h exposure period increased when pH decreased, from 634 µg/L (2.7 µmol/L) at pH 6.0 to 117 µg/L (0.49 µmol/L) at pH 5.0. For the two studies, the delay to obtain a significant response for the bivalves exposed to a given total uranium concentration diminished as pH decreased. Furthermore, our results showed that without uranium in the water column, the spontaneous valve closure reaction was independent of pH. This finding joins the results from Markich et al. [13], who gave evidence that the valve movement behavior of *V. angasi* under their experimental conditions and without adding any pollutant does not significantly differ between pH 5.0 and 6.0. Our results suggested that hydronium ions did not modify the biological response. Therefore, the difference of the sensitivity to uranium between pH 5.5 and 6.5 could be related to the aqueous speciation of uranium, which undergoes tremendous changes within a pH range of 4 to 8 and in the presence of ligands commonly found in natural waters (carbonate, phosphate, hydroxide, and natural organic matter, not taken into account within these preliminary sets of experiments). According to the FIAM, metal uptake but also toxicity normally vary as a function of the concentration of the free-metal ion in solution [20]. Under conditions of varying pH, the FIAM fails to explain the observed difference in sensitivity; the EC50 values calculated in function of the simulated free-ion concentrations are very significantly different for the two pH values (Fig. 4). Concerning our water composition, the activity of UO_2^{2+} increased markedly by a factor 30 when pH decreases from 6.5 to 5.5 (Fig. 1). The EC50 values expressed in terms of [UO_2^{2+}] are approximately 10 times higher whatever the ITR at pH 5.5 compared to pH 6.5. Because EC50 is not directly proportional to [UO_2^{2+}], other chemical species are suggested to contribute to the physiological response of the bivalves. A number of exceptions to the FIAM have been reported in the literature when varying pH, such as those reported for uranium toxicity (valve movement response) toward the bivalve *V. angasi* by Markich et al. [13]. Increasing pH from 5.0 to 6.0 decreased uranium toxicity; however, this amelioration could not be solely related to the decrease in [UO_2^{2+}] within this range. Markich et al. [13] concluded that both UO_2^{2+} and the first hydrolysis product of uranyl (UO_2OH^+) could be responsible. Indeed, three potential mechanisms to explain the reduction in the sensitivity to total uranium for the valve closure response of *C. fluminea* when pH increases from 5.5 to 6.5 may be suggested: increasing formation of uranyl inorganic complexes in water that reduces metal binding to the membrane and therefore reduces metal detection, formation of biological ligand surface complexes of uranium with other species than UO_2^{2+}, and competition between H^+ and UO_2^{2+} for cell surface binding sites that are physiologically active within the induction of the valve movement. According to the FIAM or its derivative, the biological ligand model, this surface complexation is the first interaction with the organism necessary to induce a biological response and competition is assumed to occur between the toxic metal and cations (e.g., H^+) for binding sites on the biotic

ligand [21,22]. Within this conceptual model, a competition between H^+ and UO_2^{2+} for receptor sites may explain discrepancies observed under different pH exposure conditions. At pH 5.5, where H^+ activity is higher, a higher UO_2^{2+} concentration could be necessary to induce the same physiological effect (expressed as EC50). Moreover, the higher Na^+ activity measured in water at pH 5.5 also may induce a more important competition.

Franklin et al. [23] also found an influence of pH on the chronic toxicity of uranium when using the green alga *Chlorella vulgaris*. They reported that increasing pH from 5.7 to 6.5 worsens uranium toxicity (EC50 from growth inhibition bioassays of uranium at 328 nmol/L down to 185 nmol/L). However, it is difficult to compare the sensitivity for different test organisms and different biological endpoints, especially for uranium, for which aqueous speciation is so sensitive to water quality parameters (e.g., pH, hardness, alkalinity, and dissolved organic matter).

CONCLUSION

At pH 5.5 and pH 6.5, *C. fluminea* is able to detect and rapidly respond to increasing uranium concentrations by closing its shell. The valve closure responses in terms of their kinetics and intensity depend on the uranium concentration and on the ITR. For short ITRs (5 min < ITR < 120 min), the sensitivity thresholds are relatively high (EC50 equal to uranium at 0.17 μmol/L and 0.63 μmol/L for ITR of 10 min at pH 5.5 and 6.5, respectively). However, for longer ITRs (>120 min), the detection by *C. fluminea* became increasingly sensitive (EC50 equal to uranium at 0.05 μmol/L and 0.13 μmol/L at pH 5.5 and 6.5, respectively, for an ITR of 300 min). Sensitivity obviously also depends on pH, with a 2.6-fold increase for EC50 when pH decreases from 6.5 to 5.5. Apparent inconsistency with the FIAM for the valve closure response of the bivalve to uranium exposure requires further investigations, while complexifying the well-defined composition of the artificial water and testing the influence of other major parameters of the water quality (e.g., hardness, alkalinity, and dissolved organic matter). Under our experimental conditions (e.g., 20°C, normoxia, and acidic synthetic freshwater), the minimal uranium concentration detectable with *C. fluminea* is 0.05 μmol/L (12 μg/L) at pH 5.5. Knowledge of the influence of water quality criteria on uranium toxicity is required to be able to derive protection guidelines for uranium concentration in freshwaters.

In freshwaters, background levels for uranium concentration range from 0.02 to 6 μg/L [24]. Near uranium mining sites, where pH is often acid, uranium concentrations may reach hundreds of micrograms per liter. Within this framework, the method presented in this paper could be employed in the field, as an alarm system of degradation of water quality for the receiving waters from uranium mine wastewaters. At pH 5.5, an increase in the uranium concentration to a high level (>0.5 μmol/L) should be detected in less than 10 min, whereas an increase to a low level of uranium (<0.1 μmol/L) should be detected in 4 h.

Acknowledgement—We thank C. Adam and G. Durrieu for their helpful discussion and comments. The technical aspect of the valvometer device was developed by P. Ciret. The technical assistance of I. Cavalié and V. Camilleri for uranium measurements also was greatly appreciated. This work is part of the ENVIRHOM program funded by the Institute for Radioprotection and Nuclear Safety.

REFERENCES

1. Colle C, Garnier-Laplace J, Roussel-Debet S, Adam C, Baudin JP. 2001. Comportement de l'uranium dans l'environnement. In Métivier H, ed, *L'Uranium de l'Environnement à l'Homme*. EDP Sciences, Les Ulis, France, pp 187–211.
2. Ragnarsdottir KV, Charlet L. 2000. Uranium behaviour in natural environments. In Cotter-Howells JJ, Batcherder M, Campbell L, Valsami-Jones E, eds, *Environmental Mineralogy: Microbial Interactions, Antropogenic Influences, Contaminated Lands and Waste Management*, Series 9. Mineralogical Society of Great Britain and Ireland, London, UK, pp 333–377.
3. Andres S, Baudrimont M, Lapaquellerie Y, Ribeyre F, Maillet N, Latouche C, Boudou A. 1999. Field transplantation of the freshwater bivalve *Corbicula fluminea* along a polymetallic contamination gradient (River Lot, France): I. Geochemical characteristics of the sampling sites and cadmium and zinc bioaccumulation kinetics. *Environ Toxicol Chem* 18:2462–2471.
4. Baudrimont M, Andres S, Metivaud J, Lapaquellerie Y, Maillet N, Latouche C, Ribeyre F, Boudou A. 1999. Field transplantation of the freshwater bivalve *Corbicula fluminea* along a polymetalllic contamination gradient (River Lot, France): II. Metallothionein response to metal exposure. *Environ Toxicol Chem* 18: 2472–2477.
5. Gunther AJ, Davis JA, Hardin DD, Gold J, Bell D, Crick JR, Scelfo GM, Sericano J, Stephenson M. 1999. Long-term bioaccumulation monitoring with transplanted bivalves in the San Francisco estuary. *Mar Pollut Bull* 38:170–181.
6. Doyotte A, Cossu C, Jacquin MC, Babut M, Vasseur P. 1997. Antioxidant enzymes, glutathione and lipid peroxidation as relevant biomarkers of experimental or field exposure in the gills and the digestive gland of the freshwater bivalve *Unio tumidus*. *Aquat Toxicol* 39:93–110.
7. Cossu C, Doyotte A, Jacquin MC, Babut M, Exinger A, Vasseur P. 1997. Glutathione reductase, selenium-dependent glutathione peroxidase, glutathione levels, and lipid peroxidation in freshwater bivalves, *Unio tumidus*, as biomarkers of aquatic contamination in field studies. *Ecotoxicol Environ Saf* 38:122–131.
8. Kramer KJM, Jenner HA, Zwart D. 1989. The valve movement response of mussels: A tool in biological monitoring. *Hydrobiologia* 188/189:433–443.
9. Sluyts H, Van Hoof F, Cornet A, Paulussen J. 1996. A dynamic new alarm system for use in biological early warning systems. *Environ Toxicol Chem* 15:1317–1323.
10. Sloff W, De Zwart D, Marquenie JM. 1983. Detection limits of a biological monitoring system for chemical water pollution based on mussel activity. *Bull Environ Contam Toxicol* 30:400–405.
11. Ham KD, Peterson MJ. 1994. Effect of fluctuating low-level chlorine concentrations on valve-movement behavior of the asiatic clam (*Corbicula fluminea*). *Environ Toxicol Chem* 13: 493–498.
12. Borcherding J. 1994. The "*Dreissena*-monitor" improved evaluation of dynamic limits for the establishment of alarm-thresholds during toxicity tests and for continuous water control. In Hill IA, Heimbach F, Leeuwangh P, Matthiessen P, eds, *Freshwater Field Test for Hazard Assessment of Chemicals*. Lewis, Boca Raton, FL, USA, pp 477–484.
13. Markich SJ, Brown PL, Jeffree RA, Lim RP. 2000. Valve movement responses of *Velesunio angasi* (Bivalvia: Hyriidae) to manganese and uranium: An exception to the free ion activity model. *Aquat Toxicol* 51:155–175.
14. Tran D, Ciret P, Ciutat A, Durrieu G, Massabuau JC. 2003. Estimation of potential and limits of bivalve closure response to detect contaminants: Application to cadmium. *Environ Toxicol Chem* 22:914–920.
15. Van der Lee J. Thermodynamic and mathematical concepts of Chess. Technical Report LMH/RD/98/39. GIG–Ecole des Mines de Paris, Fontainebleau, France.
16. Grenthe I, Fuger J, Konings RJM, Lemire R, Muller R, Nguyen-Trung C, Wanner H. 1992. *Chemical Thermodynamics of Uranium*. Nuclear Energy Agency, Organization for Economic Cooperation and Development, Amsterdam, The Netherlands.
17. Denison F. Application of chemical speciation modelling to uranium toxicity and bioavailability studies: Compilation of a coherent database for simple experimental systems and an inves-

tigation of the effect of database uncertainty on model predictions. SERLAB-02-41. Technical report. Institute of Nuclear Protection and Safety, Cadarache, France.
18. Gourieroux C, Monfort A. 1981. Asymptotic properties of the maximum likelihood estimator in dichotomous logistic regression models. *J Econometr* 17:83–97.
19. Beer M. 2001. Asymptotic properties of the maximum likelihood estimator in dichotomous logistic regression models. PhD thesis. University of Fribourg, Fribourg, Switzerland.
20. Campbell PGC. 1995. Interaction between trace metals and aquatic organisms: A critique of the free-ion activity model. In Tessier A, Turner DR, eds, *Metal Speciation and Bioavailability in Aquatic Systems*. John Wiley, New York, NY, USA, pp 45–102.
21. De Schamphelaere KAC, Janssen CR. 2002. A biotic ligand model predicting acute copper toxicity to *Daphnia magna*: The effects of calcium, magnesium, sodium, potassium and pH. *Environ Sci Technol* 36:48–54.
22. Heijerick DC, De Schamphelaere KAC, Janssen CR. 2002. Biotic ligand model development predicting Zn toxicity to the alga *Pseudokirchneriella subcapitata*: Possibilities and limitations. *Comp Biochem Physiol C Comp Pharmacol Toxicol* 133:207–218.
23. Franklin NM, Stauber JL, Markich SJ, Lim RP. 2000. pH-Dependent toxicity of copper and uranium to a tropical freshwater alga (*Chlorella*). *Aquat Toxicol* 48:275–289.
24. Bonin B, Blanc PL. 2001. L'uranium dans le milieu naturel, des origines jusqu'à la mine. In Métivier H, ed, *L'Uranium de l'Environnement à l'Homme*. EDP Sciences, Les Ulis, France, pp 7–41.